

Recent advancements in the dental biomaterials applied in various diagnostic, restorative, regenerative and therapeutic procedures

Edited by

Mohammad Khursheed Alam, Kumar Chandan Srivastava,
Mohd Fadhli Khamis and Adam Husein

Published in

Frontiers in Bioengineering and Biotechnology
Frontiers in Materials



FRONTIERS EBOOK COPYRIGHT STATEMENT

The copyright in the text of individual articles in this ebook is the property of their respective authors or their respective institutions or funders. The copyright in graphics and images within each article may be subject to copyright of other parties. In both cases this is subject to a license granted to Frontiers.

The compilation of articles constituting this ebook is the property of Frontiers.

Each article within this ebook, and the ebook itself, are published under the most recent version of the Creative Commons CC-BY licence. The version current at the date of publication of this ebook is CC-BY 4.0. If the CC-BY licence is updated, the licence granted by Frontiers is automatically updated to the new version.

When exercising any right under the CC-BY licence, Frontiers must be attributed as the original publisher of the article or ebook, as applicable.

Authors have the responsibility of ensuring that any graphics or other materials which are the property of others may be included in the CC-BY licence, but this should be checked before relying on the CC-BY licence to reproduce those materials. Any copyright notices relating to those materials must be complied with.

Copyright and source acknowledgement notices may not be removed and must be displayed in any copy, derivative work or partial copy which includes the elements in question.

All copyright, and all rights therein, are protected by national and international copyright laws. The above represents a summary only. For further information please read Frontiers' Conditions for Website Use and Copyright Statement, and the applicable CC-BY licence.

ISSN 1664-8714
ISBN 978-2-83251-393-4
DOI 10.3389/978-2-83251-393-4

About Frontiers

Frontiers is more than just an open access publisher of scholarly articles: it is a pioneering approach to the world of academia, radically improving the way scholarly research is managed. The grand vision of Frontiers is a world where all people have an equal opportunity to seek, share and generate knowledge. Frontiers provides immediate and permanent online open access to all its publications, but this alone is not enough to realize our grand goals.

Frontiers journal series

The Frontiers journal series is a multi-tier and interdisciplinary set of open-access, online journals, promising a paradigm shift from the current review, selection and dissemination processes in academic publishing. All Frontiers journals are driven by researchers for researchers; therefore, they constitute a service to the scholarly community. At the same time, the *Frontiers journal series* operates on a revolutionary invention, the tiered publishing system, initially addressing specific communities of scholars, and gradually climbing up to broader public understanding, thus serving the interests of the lay society, too.

Dedication to quality

Each Frontiers article is a landmark of the highest quality, thanks to genuinely collaborative interactions between authors and review editors, who include some of the world's best academicians. Research must be certified by peers before entering a stream of knowledge that may eventually reach the public - and shape society; therefore, Frontiers only applies the most rigorous and unbiased reviews. Frontiers revolutionizes research publishing by freely delivering the most outstanding research, evaluated with no bias from both the academic and social point of view. By applying the most advanced information technologies, Frontiers is catapulting scholarly publishing into a new generation.

What are Frontiers Research Topics?

Frontiers Research Topics are very popular trademarks of the *Frontiers journals series*: they are collections of at least ten articles, all centered on a particular subject. With their unique mix of varied contributions from Original Research to Review Articles, Frontiers Research Topics unify the most influential researchers, the latest key findings and historical advances in a hot research area.

Find out more on how to host your own Frontiers Research Topic or contribute to one as an author by contacting the Frontiers editorial office: frontiersin.org/about/contact

Recent advancements in the dental biomaterials applied in various diagnostic, restorative, regenerative and therapeutic procedures

Topic editors

Mohammad Khursheed Alam — Al Jouf University, Saudi Arabia

Kumar Chandan Srivastava — Al Jouf University, Saudi Arabia

Mohd Fadhli Khamis — Universiti Sains Malaysia Health Campus, Malaysia

Adam Husein — Universiti Sains Malaysia Health Campus, Malaysia

Citation

Alam, M. K., Srivastava, K. C., Khamis, M. F., Husein, A., eds. (2023).

Recent advancements in the dental biomaterials applied in various diagnostic, restorative, regenerative and therapeutic procedures. Lausanne: Frontiers Media SA.
doi: 10.3389/978-2-83251-393-4

Table of contents

05	Editorial: Recent advancements in the dental biomaterials applied in various diagnostic, restorative, regenerative, and therapeutic procedures Mohammad Khursheed Alam, Kumar Chandan Srivastava, Mohd Fadhli Khamis and Adam Husein
08	Effect of Magnesium-Based Coatings on Titanium or Zirconia Substrates on Bone Regeneration and Implant Osseointegration- A Systematic Review Ahmad H Almeahmadi
23	Hierarchical Intrafibrillarly Mineralized Collagen Membrane Promotes Guided Bone Regeneration and Regulates M2 Macrophage Polarization Yaowei Xuan, Lin Li, Muzhi Ma, Junkai Cao and Zhen Zhang
37	Effects of Plant Extracts on Dentin Bonding Strength: A Systematic Review and Meta-Analysis Shikai Zhao, Fang Hua, Jiarong Yan, Hongye Yang and Cui Huang
50	Effect of Different Concentrations of Silver Nanoparticles on the Quality of the Chemical Bond of Glass Ionomer Cement Dentine in Primary Teeth Faisal Mohammed Abed, Sunil Babu Kotha, Haneen AlShukairi, Fatmah Nasser Almotawah, Rwan Abdulali Alabdulaly and Sreekanth Kumar Mallineni
59	Graphene-Based Nanomaterials for Dental Applications: Principles, Current Advances, and Future Outlook Xiaojing Li, Xin Liang, Yanhui Wang, Dashan Wang, Minhua Teng, Hao Xu, Baodong Zhao and Lei Han
80	Comparative Evaluation of Stress Acting on Abutment, Bone, and Connector of Different Designs of Acid-Etched Resin-Bonded Fixed Partial Dentures: Finite Element Analysis Saquib Ahmed Shaikh, Punith Rai, Sami Aldhuwayhi, Sreekanth Kumar Mallineni, Krishnapalli Lekha, Angel Mary Joseph, Vardharaj Vinutha Kumari and Roseline Meshramkar
93	Case Report: Combining Molar Interradicular Osteotomy With Immediate Implant Placement: A Three-Year Case-Series Study Adel S. Alagl and Marwa Madi
101	Application of Amorphous Calcium Phosphate Agents in the Prevention and Treatment of Enamel Demineralization Jiarong Yan, Hongye Yang, Ting Luo, Fang Hua and Hong He
111	Zinc Oxide Nanoparticles: A Review on Its Applications in Dentistry C Pushpalatha, Jithya Suresh, VS Gayathri, SV Sowmya, Dominic Augustine, Ahmed Alamoudi, Bassam Zidane, Nassreen Hassan Mohammad Albar and Shankargouda Patil

- 120 **Impact of Frontier Development of Alveolar Bone Grafting on Orthodontic Tooth Movement**
Yilan Miao, Yu-Cheng Chang, Nipul Tanna, Nicolette Almer, Chun-Hsi Chung, Min Zou, Zhong Zheng and Chenshuang Li
- 129 **The Anticariogenic Efficacy of Nano Silver Fluoride**
C. Pushpalatha, K. V. Bharkhavy, Arshiya Shakir, Dominic Augustine, S. V. Sowmya, Hammam Ahmed Bahammam, Sarah Ahmed Bahammam, Nassreen Hassan Mohammad Albar, Bassam Zidane and Shankargouda Patil
- 138 **Modified Mineral Trioxide Aggregate—A Versatile Dental Material: An Insight on Applications and Newer Advancements**
C. Pushpalatha, Vismaya Dhareshwar, S. V. Sowmya, Dominic Augustine, Thilla Sekar Vinothkumar, Apathsakayan Renugalakshmi, Amal Shaiban, Ateet Kakti, Shilpa H. Bhandi, Alok Dubey, Amulya V. Rai and Shankargouda Patil



OPEN ACCESS

EDITED AND REVIEWED BY
Hasan Uludag,
University of Alberta, Canada

*CORRESPONDENCE
Mohammad Khursheed Alam,
✉ dralam@gmail.com

SPECIALTY SECTION
This article was submitted to
Biomaterials,
a section of the journal
Frontiers in Bioengineering and
Biotechnology

RECEIVED 05 December 2022
ACCEPTED 12 December 2022
PUBLISHED 09 January 2023

CITATION
Alam MK, Srivastava KC, Khamis MF and
Husein A (2023), Editorial: Recent
advancements in the dental
biomaterials applied in various
diagnostic, restorative, regenerative,
and therapeutic procedures.
Front. Bioeng. Biotechnol. 10:1116208.
doi: 10.3389/fbioe.2022.1116208

COPYRIGHT
© 2023 Alam, Srivastava, Khamis and
Husein. This is an open-access article
distributed under the terms of the
[Creative Commons Attribution License](#)
(CC BY). The use, distribution or
reproduction in other forums is
permitted, provided the original
author(s) and the copyright owner(s) are
credited and that the original
publication in this journal is cited, in
accordance with accepted academic
practice. No use, distribution or
reproduction is permitted which does
not comply with these terms.

Editorial: Recent advancements in the dental biomaterials applied in various diagnostic, restorative, regenerative, and therapeutic procedures

Mohammad Khursheed Alam^{1*}, Kumar Chandan Srivastava¹,
Mohd Fadhli Khamis² and Adam Husein^{2,3}

¹College of Dentistry, Jouf University, Sakaka, Saudi Arabia, ²School of Dental Sciences, Universiti Sains Malaysia, Kota Bharu, Kelantan, Malaysia, ³College of Dental Medicine, University of Sharjah, Sharjah, United Arab Emirates

KEYWORDS

nanodentistry, silver nanoparticles, dental implant surface coating, osseointegration, guided bone regeneration, graphene, stem cell, modified MTA

Editorial on the Research Topic

Recent advancements in the dental biomaterials applied in various diagnostic, restorative, regenerative and therapeutic procedures

Recent advancements in the dental biomaterials applied in various diagnostic, restorative, regenerative, and therapeutic procedures

In recent times, dentistry has evolved in many directions at a very rapid pace. These advancements can be witnessed in every aspect of dentistry, including diagnosis, investigation, and therapeutic approaches, such as restorative, reparative, regenerative, and rehabilitative techniques. With improvements in investigative methodologies such as micro-computed tomography, scanning electron microscopy, spectroscopy, quantitative real-time polymerase chain reaction (PCR), cell line culture, immunohistochemistry, and laser scanning confocal microscopy (LSCM), the field's understanding of diseases in terms of their etiopathogenesis and the available responses in the form of treatments have improved tremendously. Furthermore, nanotechnology has also contributed to a revolution taking place in various areas of the sciences, such as molecular biology, chemistry, and engineering. Dentistry is no exception to this: a vast amount of research is ongoing in this area, with existing dental biomaterials being modified to improve their physical, mechanical, and biological properties. Additionally, with the expanding need for treatment, new biomaterials are even being developed, while alterations to existing

materials, such as restorative cements and obturating materials, are being improvised to overcome the shortcomings of their mechanical or chemical properties. There is demand for the development or improvisation of rehabilitating materials, such as dental implant surfaces and guided regeneration membranes, in order to make them more biocompatible, or to provide them with antibacterial properties or a cellular inductive nature.

In this Research Topic, a wide range of research papers have been published, discussing various aspects of the dental material sciences and taking the form of original research articles, narrative reviews, mini reviews, and case reports.

In a systematic review, [Almehmadi](#) compared the impact of titanium or zirconia implant surfaces coated with magnesium (Mg) to that of non-coated surfaces in terms of the success of implants. Based on the eligibility criteria and PICO statement, a total of 14 *in vitro* and animal studies were considered. Within the limitations of the review in terms of heterogeneity, the results of the *in vitro* studies showed an improvement in cell behavior, increased expression of various osteogenic markers such as alkaline phosphatase, and evidence of antibacterial properties in the case of the Mg-coated surfaces. The results of the animal studies also supported the use of Mg-coated surfaces, with these cases displaying characteristics such as high bone fill, enhanced bone-implant contact, and new bone formation.

In another systematic review and meta-analysis, [Zhao et al.](#) compared dental adhesives incorporating various plant extracts to adhesives without such additives in terms of their immediate strength of bonding with dentine. Furthermore, they also explored the difference in dentine strength between cases with and without the use of plant extracts as primers. Lastly, they also studied the influence of different types of plant extract and their use at varying concentrations. In consideration of the inclusion and exclusion criteria, a search strategy was devised that included all possible keywords. A total of 30 *in vitro* studies were considered for qualitative analysis, whereas 14 studies were analyzed quantitatively. It was concluded that there is a statistically significant improvement in immediate dentine-adhesive strength when adhesives with plant extracts are used. Additionally, improvement can be observed when plant extracts are used as primers. Among the plant extracts, 10% proanthocyanidine emerged as the most promising primer for improvement of the immediate bonding strength.

A original study by [Xuan et al.](#) aimed to compare a novel hierarchical intrafibrillarly mineralized collagen membrane (HIMCM) with the conventional therapeutic options for guided bone regeneration, such as collagen membrane and extrafibrillarly mineralized collagen. The newly fabricated membrane displayed superior physical properties (such as hydrophilicity and tensile strength) and chemical properties compared to the traditional options, and thus was found to mimic the microstructure of bone closely. Furthermore, HIMCM impregnated with bone marrow mesenchymal stem cells displayed enhanced signs of bone regeneration, such as

proliferation and eventually differentiation into cells with a clear osteogenic fate. Additionally, in an animal experiment, the HIMCM was found to successfully fill a large surgical defect with bone analogous to neighboring bone in terms of density and architecture.

Another original piece of research by [Abed et al.](#) involved a comparative analysis of the chemical bond between glass ionomer cement (GIC) and the dentine of primary dentation, in which silver nanoparticles in three different concentrations (namely .2, .4, and .6%) were added to the GIC. The bond strength was enhanced by the addition of these nanoparticles, even at a low concentration of .4%.

Nanotechnology is a very promising avenue of research in the dental biomaterial sciences, and many relevant research and review papers have been published in this Research Topic. [Li et al.](#) describe the details of research relating to graphene-based materials in a review paper. Graphene is a carbon-based nanomaterial and its derivatives possess excellent properties, such as biocompatibility, stimulation of cell differentiation, and anti-bacterial activity, which mean that it has various applications in dentistry. To mention a few, these include teeth whitening, adhesives, cements, coatings for dental implants, and tissue engineering, including bone and dental pulp. Yet another review, by [Pushpalatha et al.](#), discusses a versatile dental material, namely mineral trioxide aggregate (MTA). The paper describes the advantages of this material and its varied applications in dentistry. Additionally, the authors discuss the downsides of MTA, such as long setting time, discoloration, mud-like consistency, and poor handling characteristics; these have prompted new advancements, leading to the development of modified MTA. This subsequently developed material succeeds in overcoming the downsides of MTA and has better properties, such as improved setting time, enhanced compressive strength, microhardness, antibacterial activity, biocompatibility, regenerative ability, and suitability for local drug delivery.

Essentially, the aim of this Research Topic was to aggregate and disseminate work relating to current concepts and trends in dentistry, including but not limited to its diagnostic, restorative, and regenerative aspects. In addition to collecting and publicizing these developments, this Research Topic also attempts to bring multidisciplinary researchers together under a common roof. Furthermore, it also furnishes researchers and clinicians across the globe with an opportunity to share their innovative research and their perspectives on technological advancements in dentistry and how these can make a difference to patients' quality of life. Lastly, this Research Topic will ignite the interest of a global readership in this Research Topic and stimulate further research ideas among them, as well as enhancing readers' interest in this domain and assisting them in planning out their future research. This Research Topic covers the theme *via* all forms of research paper, including systematic reviews,

meta-analyses, original research, narrative scoping reviews, and case series.

Author contributions

MA and KS contributed equally to the conceptualization and writing. All authors contributed to the article and approved the submitted version.

Acknowledgments

The editors thank all authors and reviewers for their outstanding contributions to this Frontiers Research Topic.

Conflict of interest

The authors declare that the research was conducted in the absence of any commercial or financial relationships that could be construed as a potential conflict of interest.

Publisher's note

All claims expressed in this article are solely those of the authors and do not necessarily represent those of their affiliated organizations, or those of the publisher, the editors and the reviewers. Any product that may be evaluated in this article, or claim that may be made by its manufacturer, is not guaranteed or endorsed by the publisher.



Effect of Magnesium-Based Coatings on Titanium or Zirconia Substrates on Bone Regeneration and Implant Osseointegration- A Systematic Review

Ahmad H Almeahmadi*

Faculty of Dentistry, Oral Biology Department, King Abdulaziz University, Jeddah, Saudi Arabia

OPEN ACCESS

Edited by:

Kumar Chandan Srivastava,
Al Jouf University, Saudi Arabia

Reviewed by:

Shivasakthy Manivasakan,
Sri Balaji Vidyapeeth University, India

Ritika Bhambhani,
Guru Nanak Institute of Dental
Sciences and Research, India

*Correspondence:

Ahmad H Almeahmadi
ahalmehmadi@kau.edu.sa

Specialty section:

This article was submitted to
Biomaterials,
a section of the journal
Frontiers in Materials

Received: 06 August 2021

Accepted: 19 October 2021

Published: 01 November 2021

Citation:

Almeahmadi AH (2021) Effect of
Magnesium-Based Coatings on
Titanium or Zirconia Substrates on
Bone Regeneration and Implant
Osseointegration- A
Systematic Review.
Front. Mater. 8:754697.
doi: 10.3389/fmats.2021.754697

Magnesium (Mg) is an essential trace element that has a significant role in the human body through its effects on bone metabolism. It has various applications in orthopaedics and dentistry and the interest of this systematic review lies in its potential role as a dental implant surface coating. The dental implants can fail at different stages starting with its osseointegration phase to the restorative stage in the oral cavity. The biological loss of bone integration to the implant surface has been classified as one of the primary reasons for dental implant failure. There have been numerous strategies that have been shown to compensate this reason for implant failure, among which are the dental implant surface coatings. These coatings have been shown to improve the enhance the adhesion as well as the process of osseointegration. There are numerous studies in the existing literature that have analyzed the effects of Mg-based coatings on cellular as well as biological processes in bone-implant integration. A systematic search of various databases yielded 175 articles, of which 14 *in vitro* and experimental animal studies that analyzed the effect of Mg-based coatings and compared it to other coatings or no surface coatings were included in this systematic review. The main outcomes of this systematic review have been cellular behavior, osseointegration, and osteogenic markers and the effects of Mg-based coatings in these parameters have been highlighted in this review.

Keywords: magnesium, dental implant surface coating, osseointegration, osteogenic markers, hydroxyapatite

INTRODUCTION

Titanium (Ti) and its alloys have become the mainstay biomaterials for dental implants for their mechanical properties and excellent biocompatibility. But, these metals can get corroded in a biological environment and toxic reactions may occur (Tschernitschek et al., 2005; Niinomi, 2008). Zirconia (Zir) implants were extensively used for their increased corrosion resistance, good biocompatibility, favorable esthetic and good mechanical properties. Even though both materials have load-bearing applications with their unique properties, the main challenge in implant dentistry remains to be osseointegration. Dental implants of both metal and ceramic materials are prone to failure due to insufficient integration to bone. It may result in the formation of a fibrous tissue or weak bone formation that may cause infections or unstable implants prone to surgical removal (Best et al., 2008; Liang et al., 2007; Brohede et al., 2009).

In present day implantology, osseointegration is well-researched and predictable but it is also reliant on the case selection and the surgical procedure or loading protocol based on the stage of failure despite the successful clinical outcomes of dental implants (Albrektsson, 1998). The literature suggests that there are two mechanisms by which surface modifications on implants can influence osseointegration and they include: 1) biomechanical interlocking where there is bone growth into the rough surface of the implant and 2) biochemical interaction and bonding at the tissue-implant junction (Albrektsson and Wennerberg, 2004). For enhanced osseointegration, three factors have to be considered and they include 1) Improving macro-retentive features in dental implants such as screw/thread design or solid body press fit, and sintered bead technologies, 2) Improving micro-retentive features such as “surface roughness” of the implant to favor cellular and molecular mechanisms for bone growth along the implant surface, and 3) Surface modification that results in a topography favorable for the differentiation of cells that enable an osseous interface on the surface of implants (Stanford, 2008).

Surface coatings on titanium and zirconia dental implants offer the best approach to improving the rate of implant-bone integration and enhancing adhesion to other materials in restorations. It offers dual benefits with improved micromechanical retention and alteration of the surface chemistry for activation of biological processes that favor bone growth (Ying Kei Lung, 2017). There are various techniques that can be used to generate a surface coating on dental implants and they include plasma spraying, sol-gel processing, grit blasting, sand blasting with acid etching, laser etching, ion implantation and sputtering. There is consistent research with both plasma spraying and acid etching techniques (Jemat et al., 2015). Some of the materials that can be coated on the implant surface include hydroxyapatite (HA), ceramics, calcium phosphate, bioactive glass, and fluoride. Grit blasting and sol-gel techniques promote adhesion to restoration whereas materials like bioactive glass and HA promote osseointegration (Lung and Matinlinna, 2012; CattaniLorente et al., 2010; Hench, 2002; Darimont et al., 2002). The downside of materials like bioactive glass and HA include poor mechanical strength, brittleness, and bacterial infections around implants, so the quest for newer biomaterials is on the rise with research targets on materials having antibacterial activity, improving osseointegration outcomes that in turn can translate into long-term clinical success (Ying Kei Lung, 2017).

The alteration of implant surface chemical characteristics comprises a more significant approach in improving the biological activity of dental implants and trace elements like calcium, zinc, silicon, magnesium, and strontium have been commonly used as surface coatings for dental implants (Sawada et al., 2013; Hass et al., 2012; Yu et al., 2013; Park et al., 2010; Shi et al., 2012). Various studies have shown their positive influence on osteoblastic activity and enhance bone growth along with improved bone healing (Boanini et al., 2010; Castellani et al., 2011; Hoppe et al., 2011). Magnesium (Mg) is the fourth most abundant cation in the human body and

with the total physiologic Mg, half of it being stored in mineralized bone tissue (Staiger et al., 2006). Magnesium has been shown to play a critical role in bone metabolism and it can interact with integrins on the surface of osteoblasts, thereby promoting its cell stability and adhesion properties (Zreiqat et al., 2002; Yamasaki et al., 2002).

There are numerous studies in the existing literature that have shown the effects of magnesium coatings on titanium or zirconia implants but there is a lack of a systematic approach towards the reporting of its properties with respect to cell bioactivity, osseointegration, or bone regeneration. Thus, the aim of this systematic review was to collate the evidence on magnesium coatings on titanium or zirconia implants, comparisons with conventional or no surface coatings, and to analyze its effects on outcomes like cell behavior, osseointegration, and markers of osteogenesis.

MATERIALS AND METHODS

According to the Preferred Reporting Items for Systematic Reviews and Meta Analyses (PRISMA) guidelines, the focused question was constructed in the Population Intervention Control Outcomes (PICO) format and it was What is the effect of magnesium-based coatings in Ti or Zir implants on osseointegration, bioactivity, and markers of osteogenesis.

Literature Search

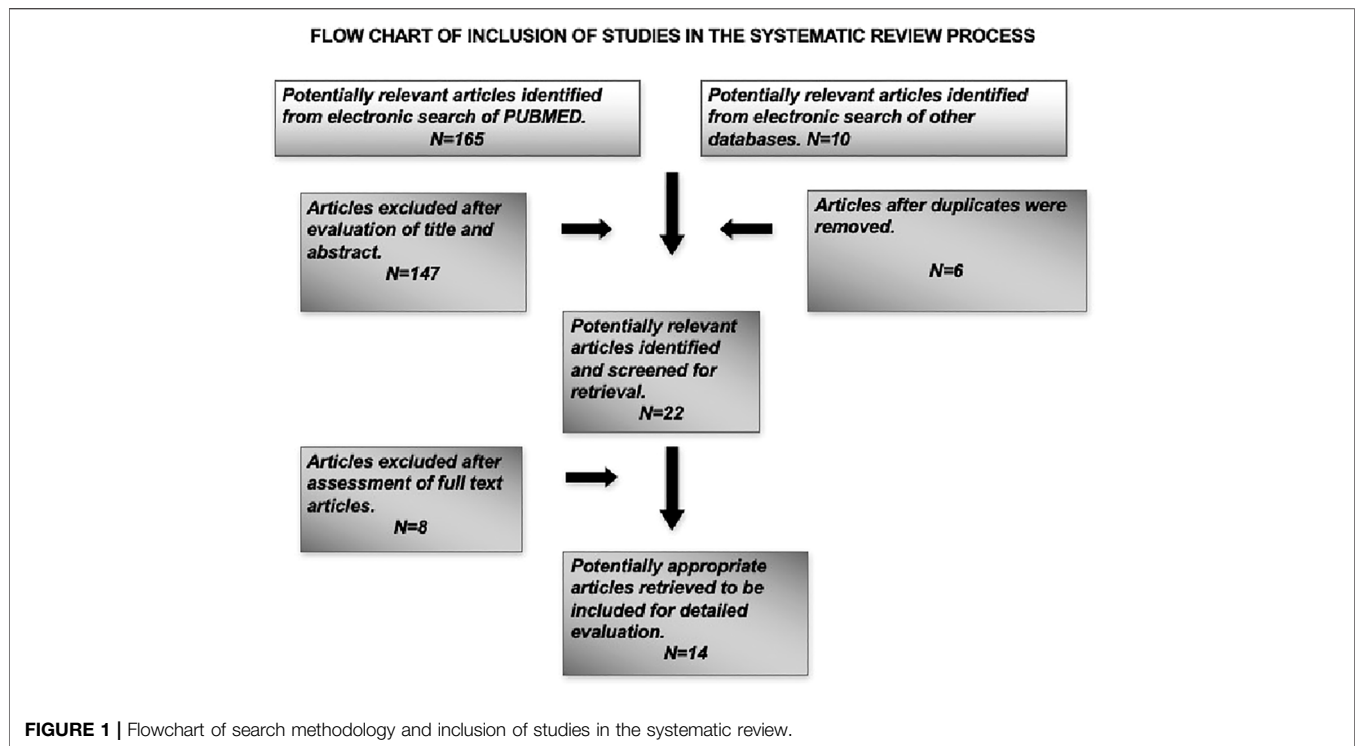
A combination of keywords like “dental implant”, “magnesium”, “implant coatings, and “osseointegration” were used in an electronic search in databases like Pubmed/Medline, Embase, Google Scholar, and Cochrane library. The search was performed using the PICO format and it was performed individually for the keywords and combined with “and” and “or” terms.

Pubmed/Medline: Search: (dental implant) or (titanium implant) or (zirconia implant) or (Ti dental implant) or (dental implant surface coating) or (surface coating) and (magnesium) or (magnesium oxide) or (magnesium carbonate) or (magnesium fluoride) or (magnesium based surface coating) and (ceramics) or (bioactive glass) or (fluoride) or (ceramics) or (hydroxyapatite) or (calcium phosphate) and (cell adhesion) or (cell proliferation) or (cell differentiation) or (bioactivity) or (osteoblast) or (fibroblast) or (osseointegration)

A manual search was performed to include articles that were relevant to the topic of the systematic review. The bibliographies from the full-texts of the articles were manually searched for relevant articles to be included in this review. The search timeline included articles where the focus question was addressed and it was between the years 2000 and 2019.

Eligibility Criteria

This systematic review aimed to analyze the effects of magnesium-based implant coatings on osseointegration and bone regeneration at cellular level, so animal and *in vitro* studies were included in the search along with studies that were conducted in humans that had observed the desired



outcomes. Only articles published in English language were included in this review. The exclusion criteria included articles which had no relevance to dentistry and only to orthopedic applications, reviews, and letters to the editor. Also, articles that observed the outcome measures in non-titanium materials like magnesium implants and the coatings were excluded from this review. The focused question was used to analyze the included studies and the relevant information on outcome measures were extracted. A flowchart has been depicted on the search methodology employed in this systematic review (Figure 1).

Data Extraction

Two independent reviewers (XX, YY) conducted the literature search employing the keywords and MeSh terms, following which the articles were analyzed based on the eligibility criteria. If there was disagreement on the inclusion of certain articles, a discussion was held to resolve it. In instances where a study did not report raw data relevant to the outcome measures, the data was extracted from either the tables or graphical representations in the study. The corresponding authors were contacted to solve doubts or provide missing information relevant to the systematic review. The data extraction tables have been attached (Supplementary file).

Risk of Bias Assessment of Included Studies

The quality assessment for each animal study was carried out using the SYRCLE's RoB tool that has 10 items and two independent authors (XX, YY) performed risk assessment

across the following categories: Sequence generation, allocation concealment, blinding of investigators and outcome assessors, random housing for animals, selective reporting of outcome measures, addressing incomplete outcome, and other potential risks for bias. The risk was categorized either as "high-risk", "low-risk" or "unclear risk" (Hooijmans et al., 2014). A third independent author (ZZ) resolved any disagreements on risk assessment with a discussion. In the existing literature, there are no tools or indices for the validation of *in vitro* studies and the risk of bias is quite low due to its position in the hierarchy of evidence-based dentistry (Richards, 2009).

RESULTS

Search Results

The systematic search of the literature yielded a total of 175 articles of which 22 articles were identified to be satisfying the eligibility criteria. The manual search of relevant journals and bibliography yielded two articles that were included in this systematic review. Some articles were excluded after full text assessment and a total of 14 articles were included for evaluation in this review. Among the included articles, nine were *in vitro* studies (Gorrieri et al., 2006; Jiang et al., 2014; Mihailescu et al., 2016; Onder et al., 2018; Pardun et al., 2015; Park et al., 2013; Won et al., 2017; Yu et al., 2017; Xie et al., 2009), four experimental animal models (Sul et al., 2006; Cho et al., 2010; Li et al., 2014; Tao et al., 2016) and one study was part animal model and part *in vitro* design (Zhao et al., 2013). The characteristics and the main outcome measures of the included studies have been shown in (Table 1).

TABLE 1 | Characteristics and Main outcome of Included Studies.

S. NO	Author and year	Type of study	Type of implant	Surface coating	Osteogenic markers and cell bioactivity	Histometric/micro-ct analysis
1	Gorrieri et al. (2006)	<i>In vitro</i>	1. Rectangular Ti test specimens (13 × 4 × 0.5 mm) 2. Ti implants (13 × 4 × 1 mm) 3. Ti mini implants (11 × 3 mm)	Calcium magnesium carbonate- Sand blasting	Alkaline phosphatase activity assay- increased in sandblasted implants but not significant Fluorescence phalloidin staining Sand-blasted surface: MG63 osteoblast-like cell exhibit spindle-shaped morphology with irregular surface. Actin expression was localized suggestive of migration front No sandblasting: Polygonal morphology with prevalent actin sub-membrane expression	
2	Sul et al. (2006)	Animal study- New Zealand White Rabbits (n = 10)	1. Control group- Machine turned implants (n = 10) 2. Test group- Magnesium ion-incorporated oxidised implants (n = 10)	Magnesium oxide- Micro-arc oxidation process		Osseointegration speed between 3 and 6 weeks: Test Mg implants- 2.5 Ncm/week Control Machine turned implants- 2.0 Ncm/week (p-value<0.005)
3	Cho et al. (2010)	Animal study- New Zealand White Rabbits (n = 24)	1. Control- Screw-type RBM implant (8.3 × 3.8 mm) (n = 24) 2. 3 Test groups- Differential Mg ion dosage a. Mg-1 (Concn-9.24%) (n = 24) b. Mg-2 (Concn-10.13%) (n = 24) c. Mg-3 (Concn-11.74%) (n = 24)	Resorbable blasting materials (RBM)- Hydroxyapatite, Beta-tricalcium phosphate		Removal Torque value: Mg-1 implants higher RTQ value when compared to Mg-2 and control implants. (p < 0.05) Bone-Implant contact values: Highest- Mg-1 (36.1 ± 12.3%) Lowest-Mg-2 (26.2% ± 10.1%) (p < 0.05) Bone Fill Area: Mg-1 (74.1 ± 12.3%) Mg-2 (58.1 ± 24.1%) Mg-3 (72.4 ± 11%) Control (63.3 ± 18.3%) (p < 0.05) New bone formation: Mg-1 (510.8 ± 167.2 μm) Other groups (330–370 μm) (p = 0.109)
4	Jiang et al. (2014)	<i>In- vitro</i>	1. Commercially pure Grade 2 Ti plates a. Mg30 (30 min plasma immersion) b. Mg 60 (60 min plasma immersion)	Magnesium- Plasma immersion ion-implantation method	Rat bone marrow mesenchymal stem cells Cell morphology and proliferation Cells exhibited spindle-shaped morphology with actin filaments showing improved spread on Mg-treated Ti surface, especially in Mg 60 group ALP activity Increased activity in Mg-treated surfaces and it was significantly higher in Mg60 group Highest expression of Osteocalcin (OCN) and Osteopontin (OPN) in Mg60 group Western blot analysis Protein expression of ALP, OCN, and OPN was highest in Mg60 group compared to other groups Upregulation of osteogenic differentiation-related genes like ALP, OPN, and OCN.	

(Continued on following page)

TABLE 1 | (Continued) Characteristics and Main outcome of Included Studies.

S. NO	Author and year	Type of study	Type of implant	Surface coating	Osteogenic markers and cell bioactivity	Histometric/micro-ct analysis
5	Li et al. (2014)	Animal study- Ovariectomized rats ($n = 18$)	1. Rod-shaped Ti implants (12×1.1 mm) ($n = 36$) and Ti discs (Diameter-9 mm) ($n = 12$) a. Magnesium-incorporated HA (MgHA) coating b. HA coating	MgHA) and HA coating on implant using Sol-gel-dip-coating method		Bone Area ratio a. MgHA = 36.76% b. HA = 27.26% ($p < 0.01$) Bone implant contact a. MgHA = 52.57% b. HA = 34.06% ($p < 0.01$) Micro-CT analysis Trabecular bone architecture and osseointegration was significantly improved with MgHA compared to HA group
6	Mihailescu et al. (2016)	<i>In vitro</i> study	1. Bovine derived HA (BHA) coating 2. BHA:MgF2 3. BHA:MgO	MgF2 or MgO- Pulsed laser deposition	Epithelial cells type 2 (HeP-2). Cell viability: Human Genes of arrestin beta 1 (ARRB1), mannosidase alpha class 2B (MAN2B1), and transient receptor potential channel 1 (TRPC1) expression increased in the following order: BHA > BHA:MgF2 > BHA:MgO. Antimicrobial activity BHA:MgO and BHA: MgF2 exhibit 4 times higher anti-bacterial activity against the tested strains: <i>Enterococcus</i> sp. <i>Candida albicans</i> <i>Micrococcus</i> sp	
7	Onder et al. (2018)	<i>In vitro</i> study	1. Titanium Grade II plates a. Low (Mg < 10 at%; MgL b. High (Mg > 10 at%; MgL 2. Ti plates 3. Ti nitride plates	Mg- Arc-PVD technique	Rat bone-marrow-derived stem cells Cell proliferation: All surfaces supported cell attachment and proliferation and it was observed on day 1, 5, and 8. Cell numbers increased on all the surfaces for first 5 days. At day 8, cell numbers decreased in Ti and TiN, whereas it continued to remain constant or increased for magnesium doped Ti implants Collagen deposition: More Type I collagen was deposited on TiN and Mg-doped implants (Low). The deposition decreased when Mg content was increased. ALP activity At day 5, activity was lowest with Ti implants and highest on Mg-doped Ti implants (Low). Mg-doped Ti implants (High) ALP activity was significantly lower than that of the low counterpart at day 5 Cell density and mineralization: Higher on Mg containing surfaces. Calcium deposition: Was higher with Mg-containing surfaces	

(Continued on following page)

TABLE 1 | (Continued) Characteristics and Main outcome of Included Studies.

S. NO	Author and year	Type of study	Type of implant	Surface coating	Osteogenic markers and cell bioactivity	Histometric/micro-ct analysis
8	Pardun et al. (2015)	<i>In vitro</i> study	1. Yttria-stabilized zirconia and HA incorporated with MgO or MgF2 2. TZCP, Thermanox-Reference samples	MgO or MgF2-Wet powder spraying	Human osteoblasts (HOB) Cell proliferation: Higher in Mg-coatings with constant increase of formazan over 9 days. Reference samples had the lowest activity Cell differentiation: ALP activity was increased in all samples and it was reduced in TZCP and increased in Thermanox. Cell growth, morphology, and spreading. TZCP- round morphology Thermanox- Flat and extensively spread. Mg-containing coating- Flat cells and spread extensively. Highest cell viability, ALP activity, and cell number in Thermanox. Similar results in Mg-containing surfaces	
9	Park et al. (2013)	<i>In-vitro</i>	1. Titanium-Grade II discs (12 mm, 25 mm diameter/ 1 mm thickness) a. TiS- Non-coated Ti surface b. Ti-Mg- Ti coated with Mg c. Ti-MgHA- Ti surface coated with Mg and HA.	Mg coating- Direct current magnetron sputtering. MgHA- Radiofrequency magnetron sputtering	Mouse MC3T3-E1 cells Cell proliferation: Ti-Mg and Ti-MgHA had higher proliferation rate of 112 and 124% respectively when compared to Ti-S ($p > 0.05$) ALP activity: Cells on Ti-Mg and Ti-MgHA showed 50–60% higher ALP activity than those on Ti-S ($p < 0.05$) Osteogenic markers: Bone sialoprotein (BSP)- mRNA expression increased 1.8 and 2.1-fold in Ti-Mg and Ti-MgHA respectively. Osteocalcin (OCN) mRNA expression increased 1.5 and 1.4-fold in Ti-Mg and Ti-MgHA respectively BSP and OCN expression more than Ti-S surface Extracellular matrix: COL-I gene: There was expression of this gene in both Ti-Mg and Ti-MgHA surfaces	
10	Tao et al. (2016)	Animal study- Sprague Dawley rats (n = 50) a. Ovariectomy (n = 45) b. Sham operation (n=5)	1. Titanium implants (20 × 1 mm) a. Pure HA coating b. HA incorporated with 10% Zinc, Mg, and Strontium. i) ZnHA ii) MgHA iii) SrHA	Electrochemical deposition for coatings		MicroCT Bone volume/total volume: Sr-HA = 40.2 ± 2 . Mg-HA = 30.3 ± 1.5 Zn-HA = 28.6 ± 1.2 HA = 23.8 ± 1.2 Bone area ratio: At 12 weeks, Increased by Sr-HA = 1.51 fold Mg-HA = 1.28 fold Zn-HA = 1.23 fold Compared to HA ($p < 0.05$) Bone implant contact: At 12 weeks, Increased by Sr-HA = 1.81 fold Mg-HA = 1.61 fold Zn-HA = 1.54 fold Compared to HA ($p < 0.05$)

(Continued on following page)

TABLE 1 | (Continued) Characteristics and Main outcome of Included Studies.

S. NO	Author and year	Type of study	Type of implant	Surface coating	Osteogenic markers and cell bioactivity	Histometric/micro-ct analysis
11	Won et al. (2017)	<i>In vitro</i> study	1. Titanium Surfaces a. Resorbable Blast Media (RBM) b. Ca-ion implanted surface c. Mg-ion implanted surface	Plasma immersion ion implantation method	Human bone marrow Mesenchymal stem cells (hBM-MSC) Cell attachment morphology Mg-ion implanted surface- Flattened morphology with wide extracellular membrane bridge compared to RBM. Ca ion-implanted surface- More extended filopodia compared to RBM and Mg-ion implanted surface Cell proliferation Cell proliferation on all surfaces significantly increased but there was no difference between three surfaces Osteogenic differentiation RUNX-2-Higher expression in Mg-ion implanted surface COL-Type I: Higher expression in Mg-ion implanted surface OCN: Lower in Ca-ion implanted surface compared to RBM and Mg-ion implanted surface ALP activity: Higher in RBM surface	
12	Xie et al. (2009)	<i>In vitro</i> study	1. Titanium alloy cylinders (25.4 × 25.4 mm) (n = 2) a. Magnesium silicate (MS) coating. b. Grit blasted and roughened-HA	MS coating- Plasma spraying method	Canine bone marrow stem cells Cell adhesion and morphology Polygonal shape with cytoplasmic processes adhering to coated surface. They spread to reach larger sizes on the coating with compact bodies and short cellular extensions. Cells were closely adherent to coated surface Cell proliferation Number of cells increased with culture time and similar to that of HA coating ALP activity Remained high whereas HA coating surface began to decrease. MSC's on MS coating had higher differentiation level compared to those of HA.	
13	Yu et al. (2016)	<i>In vitro</i> study	1. Titanium plates (10 × 10 × 1 mm; 20 × 20 × 1 mm) 2. Titanium cylinders (2 × 7 mm) a. Zn/Mg PIII b. Zn-PIII c. Mg-PIII d. Ti	Zn/Mg ion co-implanted Ti- Plasma ion implantation method	Rat bone marrow Mesenchymal stem cells (BMSC's): Cell density and morphology: Increased cell density and filopodia extension in Zn/Mg PIII→ can promote initial adhesion and spreading. Zn/Mg PIII→ Can upregulate integrin-alpha1 and integrin-beta1 than ZnPIII and MgPIII.	

(Continued on following page)

TABLE 1 | (Continued) Characteristics and Main outcome of Included Studies.

S. NO	Author and year	Type of study	Type of implant	Surface coating	Osteogenic markers and cell bioactivity	Histometric/micro-ct analysis
					Cell viability: Higher with Zn/MgPIII. Osteogenic markers: RUNX-2, OCN, OPN, ALP was higher with Zn/MgPIII. Concomitant protein levels of ALP, OCN were significantly enhanced than other three surfaces. Human Umbilical Vein Endothelial cells (HUVECs) Zn/MgPIII and MgPIII improved the viability of HUVECs	
					Zn/MgPIII Increased expression of VEGF (Vasular endothelial growth factor) and KDR (kinase domain receptor) with increased protein expression of Hypoxia-inducible factor (HIF-1 α)	
					Antibacterial: P gingivalis, F nucleatum, Strep. Mutans. Zn/MgPIII and ZnPIII surfaces had the highest inhibitory rates with bacteria counting method compared to MgPIII. ($p < 0.01$)	
14	Zhao et al. (2013)	<i>In vitro</i> study and Animal study New Zealand White Rabbits ($n = 15$)	1. Screw titanium implants (8×4.1 mm) ($n = 30$) 2. Titanium plates (25 mm \times 1.5 mm) ($n = 12$); ($10 \times 10 \times 1$ mm) ($n = 72$) a. EDHA coatingb. EDMHA coating	Pure hydroxyapatite (EDHA) or Mg-substituted HA (EDMHA)-Electrochemical deposition	Mouse MC3T3-E1 preosteoblasts Cell growth Significantly more viable cells were found on EDMHA coated surface than EDHA ($p = 0.02$) at 7 days of culture ALP activity EDMHA group: 0.78 ± 0.13 nmol/ μ g/h EDHA 0.41 ± 0.1 nmol/ μ g/h ($p = 0.004$) OCN levels EDMHA group: 116.42 ± 7.64 ng/mg EDHA 94.7 ± 13.1 ng/mg ($p = 0.004$)	Bone implant contact (%) At 2 weeks: EDMHA group: 61.77 ± 8.53 EDHA: 44.17 ± 12.35 ($p = 0.086$) Bone area (%) At 2 weeks: EDMHA group: 40.30 ± 10.67 EDHA: 38.39 ± 23.25 ($p = 0.831$)

In vitro Studies

The *in vitro* studies included in this systematic review observed the effects of various magnesium-based coating like calcium magnesium carbonate, magnesium fluoride (MgF₂), magnesium oxide (MgO), magnesium silicate, HA incorporated with Mg or MgO, zinc and magnesium co-implanted titanium surface, along with effects of varying concentrations of Mg on osseointegration or bone regeneration. The cell lines used in the *in vitro* studies include human, canine, and rat bone marrow mesenchymal stem cells (hBM-MSCs, cBMSCs, rBMSCs), MG-63 osteoblast-like cells, MC3T3-E1, Hep-2 epithelial cells, and human umbilical vein endothelial cells (HUVECs) (Gorrieri et al., 2006; Jiang et al., 2014; Mihailescu et al., 2016; Onder et al., 2018; Pardun et al., 2015; (Park et al., 2013; Won et al., 2017; Yu et al., 2017; Xie et al., 2009; Zhao et al., 2013). The results of the *in vitro* studies have been

summarized in (Table 2) and analysis of individual outcomes have been explained below.

Cellular Morphology

A total of six out of ten included *in vitro* studies observed the effect of Mg-based coatings on the cellular morphology of either pre-osteoblasts or bone marrow mesenchymal stem cells. The cells were either spindle-shaped or flattened in morphology with filopodia extensions and actin localization for the promotion of initial adhesion and spreading (Gorrieri et al., 2006; Jiang et al., 2014; Pardun et al., 2015; Won et al., 2017; Yu et al., 2017). An exception was the study conducted by Xie et al., where the observed cells were polygonal in shape with compact bodies and short cellular extensions (Xie et al., 2009).

TABLE 2 | Summary of results of *in vitro* studies observed for main outcome measures in Magnesium-based coatings.

S. No	Author, year/ Cell type	Type of coating	Cell morphology	Cell proliferation	Osteogenic markers						Collagen COL-1	Anti-bacterial activity
					ALP	OCN	OPN	BSP	ARB-1/ MAN2B1	RUNX-2		
1	Gorrieri et al. (2006)/MG63-Osteoblast like cells	Calcium Mg carbonate	Spindle-shaped and actin expression was localized	-	↑	-	-	-	-	-	-	-
2	Jiang et al. (2014)/rBMSCs	Mg30 Mg60*	Spindle-shaped Spindle-shaped with actin filaments	- -	↑ ↑	- ↑	- ↑	- -	- -	- -	- -	- -
3	Mihailescu et al. (2016)/Hep-2 epithelial cells	BHA MgF2* BHA MgO	- -	- -	- -	- -	- -	- -	↑ ↑	- -	- -	↑ ↑
4	Onder et al. (2018)/rBMSCs	Low Mg%* High Mg%	- -	↑ ↑	↑ ↑	- -	- -	- -	- -	- -	↑ ↑	- -
5	Pardun et al. (2015)/Human Osteoblast	MgO MgF2	Flat cells and spread extensively Flat cells and spread extensively	↑ ↑	↑ ↑	- -	- -	- -	- -	- -	- -	- -
6	Park et al. (2013)/MC3T3-E1 cells	Ti-Mg Ti-MgHA*	- -	↑ ↑	↑ ↑	↑ ↑	- -	↑ ↑	- -	- -	↑ ↑	- -
7	Won et al. (2017)/hBM-MSCs	Mg-ion implanted surface	Flattened cells with wide extracellular membrane bridge	↑	↑	↑	-	-	-	↑	↑	-
8	Xie et al. (2009)/cBMSCs	Mg silicate	Polygonal shape with compact bodies and short cellular extension	↑	↑	-	-	-	-	-	-	-
9	Yu et al. (2016)/rBMSCs	Zn-MgPill* MgPill	Increased cell density and filopodia extension promoting initial adhesion and spreading Increased cell density and filopodia extension promoting initial adhesion and spreading	↑ ↑	↑ ↑	↑ ↑	↑ ↑	- -	- -	↑ ↑	- -	↑ ↑
10	Zhao et al. (2013)/MC3T3-E1 cells	EDMHA	-	↑	↑	↑	-	-	-	-	-	-

Cellular Proliferation

In this systematic review, a total of seven out of ten included studies observed the effect of Mg-based coatings on cellular proliferation and found that there was a substantial increase in proliferation in the studied cell-lines. The surface coatings include MgO, MgF2, MgHA, Mg-ions, Zn-Mg co-implanted, and magnesium silicate. There was a relatively higher increase in surface coatings that include MgHA, Low Mg concentration, and Zn-Mg co-implanted surfaces when compared to their respective control groups (Onder et al., 2018; Pardun et al., 2015; Park et al., 2013; Won et al., 2017; Yu et al., 2017; Xie et al., 2009; Zhao et al., 2013).

Osteogenic Markers

All the included studies in the systematic review observed the expression of osteogenic markers using polymerase chain reaction and the markers include: 1) alkaline phosphatase

(ALP), osteocalcin (OCN), Osteopontin (OPN), bone sialoprotein (BSP), arrestin beta-1 (ARB-1), mannosidase alpha class-2B (MAN2B-1), and runt-related transcription factor-2 (RUNX-2). The observed osteogenic markers were significantly elevated with the Mg-based coatings analyzed in the respective studies (Gorrieri et al., 2006; Jiang et al., 2014; Mihailescu et al., 2016; Onder et al., 2018; Pardun et al., 2015; Park et al., 2013; Won et al., 2017; Yu et al., 2017; Xie et al., 2009; Zhao et al., 2013).

Collagen Deposition

In three *in vitro* studies, the deposition of collagen type-I was significantly increased with Ti-Mg, MgHA, Mg-ion implanted surfaces with varying concentrations. There was significant increase with Low Mg% (9.24%) when compared to High Mg %, and also in Mg-HA group on comparison with Ti-Mg group (Onder et al., 2018; Park et al., 2013; Won et al., 2017).

Anti-Bacterial Activity

Two *in vitro* studies observed the anti-bacterial effect of Mg-based coatings with one study examining bovine-derived HA (BHA) with MgO or MgF₂ and the other study observing Mg and Zn-Mg co-implanted Ti surfaces. Yu et al., showed that Zn-Mg co-implanted surfaces had the highest antibacterial effect against microbes like *Porphyromonas gingivalis*, *Fusobacterium nucleatum*, and *Streptococcus mutans* when compared to only Mg-incorporated surfaces (Yu et al., 2017). Mihailescu et al., observed that both BHA:MgO and BHA:MgF₂ had 4 times higher inhibitory activity against strains of *Enterococcus* sp, *Micrococcus* sp, and *Candida albicans* (Mihailescu et al., 2016).

Animal Experiments

In the animal-model experimental study conducted by Sul et al., on NZ white rabbits, the osseointegration speed was compared between Mg-ion incorporated oxidized implants and non-coated machine turned implants. There was highly significant difference in the speeds between the test and Mg-ion groups at 3 and 6 weeks with p -value < 0.005 and also notable differences in the strengths favoring the Mg-ion group during the same follow-up intervals (Sul et al., 2006). Cho et al., observed the effects of differential concentrations of Mg-ions as surface coating and observed that Mg-1 implants (Mg concentration-9.24%) had the highest removal torque values (RTQ) when compared to the other groups as well as the highest bone-implant contact (BIC) values, bone fill area, and new bone formation when compared to the other groups in the study (Cho et al., 2010).

The other animal studies ($n = 3$) observed the incorporation of Mg to hydroxyapatite (HA) on titanium surfaces either using sol-gel-dip coating method or electrochemical deposition (Li et al., 2014); (Tao et al., 2016); (Zhao et al., 2013). In all the studies, the control group was pure HA coating whereas one study compared Mg-based coating with HA incorporated with other elements like Zinc (Zn) and Strontium (Sr) (Tao et al., 2016). The analyzed results observed that bone area ratio and BIC values were significantly higher for Mg-HA coating when compared to pure HA titanium surface (Li et al., 2014); (Tao et al., 2016); (Zhao et al., 2013). A micro-CT analysis also observed that trabecular bone structure and osseointegration was significantly improved with Mg-HA coating Li et al., 2014; Tao et al., 2016; Zhao et al., 2013). Li et al., observed during biomechanical testing that Mg-HA coating increased the interfacial shear strength and maximum push-out force when compared to HA coatings (Li et al., 2014). Tao et al., observed some slightly improved results with Sr-HA when compared to Mg-HA in terms of BIC values, bone volume, and bone area ratio (Tao et al., 2016). The summary of results from the animal studies have been tabulated in (Table 3).

Risk of Bias Assessment

In this systematic review, all experimental animal studies were subjected to SYRCL's RoB tool for assessing the risk of bias. For each domain in the risk assessment tool, the risk of bias for each study has been summarized in (Figure 2). The 10 risks of bias items belonging to the risk assessment tool have been presented as percentages for all the included experimental studies

(Figure 3). The studies presented with relatively higher risk of bias for random sequence generation, allocation concealment and blinding whereas the randomization and blinding of outcome assessments, selective reporting of outcome data, and other potential bias were poorly described in the studies. A significantly lower risk of bias was observed for reporting of baseline characteristics and reporting of incomplete outcome data among the included studies.

DISCUSSION

One of the essential trace elements for both animals and humans is Mg due to its influence on physiologic activities and bone metabolism. The deficiency of Mg in the diet can cause reduced bone mass and deranges the mineral and bone metabolic pathways in rats (Rude et al., 2006). In the ideal scenario, biomaterials must influence the proliferation and differentiation of the targeted cell types to stimulate formation of functional tissue (Sader et al., 2009). In the existing literature, there have been studies that show the positive effect of Mg incorporation into Ti implants with stimulated bone formation and osseointegration (Revell et al., 2004; Pang et al., 2014). There are some lacunae in research that can show the cumulative effects of Mg as surface coating on dental implants. Thus, in this systematic review, the focused question was the effect of various Mg-based coatings on Ti or Zir implants in terms of cell behavior, osteogenic markers, and on the process of osseointegration.

A total of 14 studies of both *in vitro* and experimental animal model design were included in this review based on the eligibility criteria. The results from the animal models were based on histologic or micro-CT analysis and observations were made in relation to bone-related parameters and osseointegration. It was shown that Mg-based coatings significantly increased the BIC values, bone area ratio, and bone volumes as well as improved speed of osseointegration and higher RTQ values (Sul et al., 2006; Cho et al., 2010; Li et al., 2014; Tao et al., 2016; Zhao et al., 2013). The process of osseointegration is reflected based on the evolution of bone growth and integration in the peri-implant tissues (Yu et al., 2016). It is well known that bone formation and integration are quantitatively measured in terms of BIC and bone area and BIC values are known to have a strong association with the strength of the bone-implant surface (Yu et al., 2016; Zhou et al., 2008). It is pivotal to note the superior bone contact observed in Mg-based coatings on Ti/Zir surfaces when compared to other observed surface coatings such as Resorbable Blasting Materials (RBM-HA, Beta-tricalcium phosphate), HA, ZnHA or groups with no implant surface coating (Sul et al., 2006; Cho et al., 2010; Li et al., 2014; Tao et al., 2016; Zhao et al., 2013).

The role of BMSCs (osteoblast precursor) and osteoblast cells cannot be emphasized more as their initial adhesion and subsequent proliferation can have a direct effect on cellular functionality and the process of osseointegration (Jiang et al., 2013). From the *in vitro* studies, it was observed that the cells were flattened or spindle-shaped with cellular extensions that facilitate

TABLE 3 | Summary of results of animal models observed for main outcome measures.

S. NO	Author	Materials	Groups	Surface coating	MICRO-CT/HISTOMETRIC analysis
1	Sul et al. (2006)	Animal study- New Zealand White Rabbits ($n = 10$)	1. Control group- Machine turned implants ($n = 10$) 2. Test group- Magnesium ion-incorporated oxidised implants ($n = 10$)	Magnesium oxide- Micro-arc oxidation process	Osseointegration speed between 3 and 6 weeks: Test Mg implants- 2.5 Ncm/week Control Machine turned implants- 2.0 Ncm/week (p -value<0.005)
2	Cho et al. (2010)	Animal study- New Zealand White Rabbits ($n = 24$)	1. Control- Screw-type RBM implant (8.3×3.8 mm) ($n = 24$) Resorbable blasting materials (RBM)- Hydroxyapatite, Beta-tricalcium phosphate 2. Test groups- Differential Mg ion dosage a. Mg-1 (Concn-9.24%) ($n = 24$) b. Mg-2 (Concn-10.13%) ($n = 24$) c. Mg-3 (Concn-11.74%) ($n = 24$)	Mg-Plasma Source Ion Implantation Method	Removal Torque value: Mg-1 implants higher RTQ value when compared to Mg-2 and control implants. ($p < 0.05$) Bone-Implant contact values: Highest-Mg-1 ($36.1 \pm 12.3\%$) Lowest-Mg-2 ($26.2\% \pm 10.1\%$) ($p < 0.05$) Bone Fill Area: Mg-1 ($74.1 \pm 12.3\%$) Mg-2 ($58.1 \pm 24.1\%$) Mg-3 ($72.4 \pm 11\%$) Control ($63.3 \pm 18.3\%$) ($p < 0.05$) New bone formation: Mg-1 ($510.8 \pm 167.2 \mu\text{m}$) Other groups ($330\text{--}370 \mu\text{m}$) ($p = 0.109$)
3	Li et al. (2014)	Animal study- Ovariectomized rats ($n = 18$)	1. Rod-shaped Ti implants (12×1.1 mm) ($n = 36$) and Ti discs (Diameter-9mm) ($n = 12$) a. Magnesium-incorporated HA (MgHA) coating b. HA coating	MgHA) and HA coating on implant using Sol-gel-dip-coating method	Bone Area ratio c. MgHA = 36.76% d. HA = 27.26% ($p < 0.01$) Bone implant contact c. MgHA = 52.57% d. HA = 34.06% ($p < 0.01$) Micro-CT analysis Trabecular bone architecture and osseointegration was significantly improved with MgHA compared to HA group
4	Tao et al. (2016)	Animal study- Sprague Dawley rats ($n = 50$) c. Ovariectomy ($n = 45$) d. Sham operation ($n = 5$)	1. Titanium implants (20×1 mm) a. Pure HA coating b. HA incorporated with 10% Zinc, Mg, and Strontium. i) ZnHA ii) MgHA iii) SrHA	Electrochemical deposition for coatings	MicroCT Bone volume/total volume Sr-HA = 40.2 ± 2.4 Mg-HA = 30.3 ± 1.5 Zn-HA = 28.6 ± 1.2 HA = 23.8 ± 1.2 Bone area ratio At 12 weeks, Increased by Sr-HA = 1.51 fold Mg-HA = 1.28 fold Zn-HA = 1.23 fold Compared to HA ($p < 0.05$) Bone implant contact At 12 weeks, Increased by Sr-HA = 1.81 fold Mg-HA = 1.61 fold Zn-HA = 1.54 fold Compared to HA ($p < 0.05$)
5	Zhao et al. (2013)	<i>In vitro</i> study and Animal study New Zealand White Rabbits ($n = 15$)	1. Screw titanium implants (8×4.1 mm) ($n = 30$) 2. Titanium plates ($25 \text{ mm} \times 1.5 \text{ mm}$) ($n = 12$); ($10 \times 10 \times 1 \text{ mm}$) ($n = 72$) a. EDHA coating b. EDMHA coating	Pure hydroxyapatite (EDHA) or Mg-substituted HA (EDMHA)- Electrochemical deposition	Bone implant contact (%) At 2 weeks EDMHA group: 61.77 ± 8.53 EDHA 44.17 ± 12.35 ($p = 0.086$) Bone area (%) At 2 weeks EDMHA group: 40.30 ± 10.67 EDHA 38.39 ± 23.25 ($p = 0.831$)

adhesion and spreading on Mg-containing surfaces (Gorrieri et al., 2006; Jiang et al., 2014; Pardun et al., 2015; Won et al., 2017; Yu et al., 2017). The presence of actin filaments in spindle-shaped cells

was suggestive of the migratory attitude of the osteoblasts. The polygonal shape with cytoplasmic processes enabled the cells to spread to reach larger sizes on the coating and they were found to

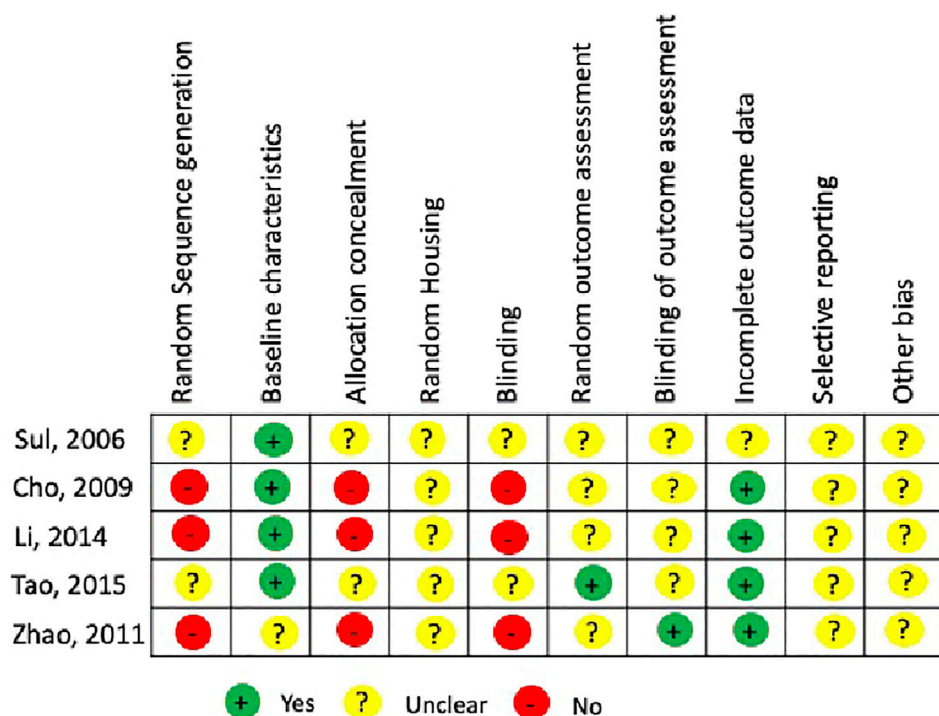


FIGURE 2 | Risk assessment using SYRCLE RoB tool for individual animal experimental studies included in the systematic review.

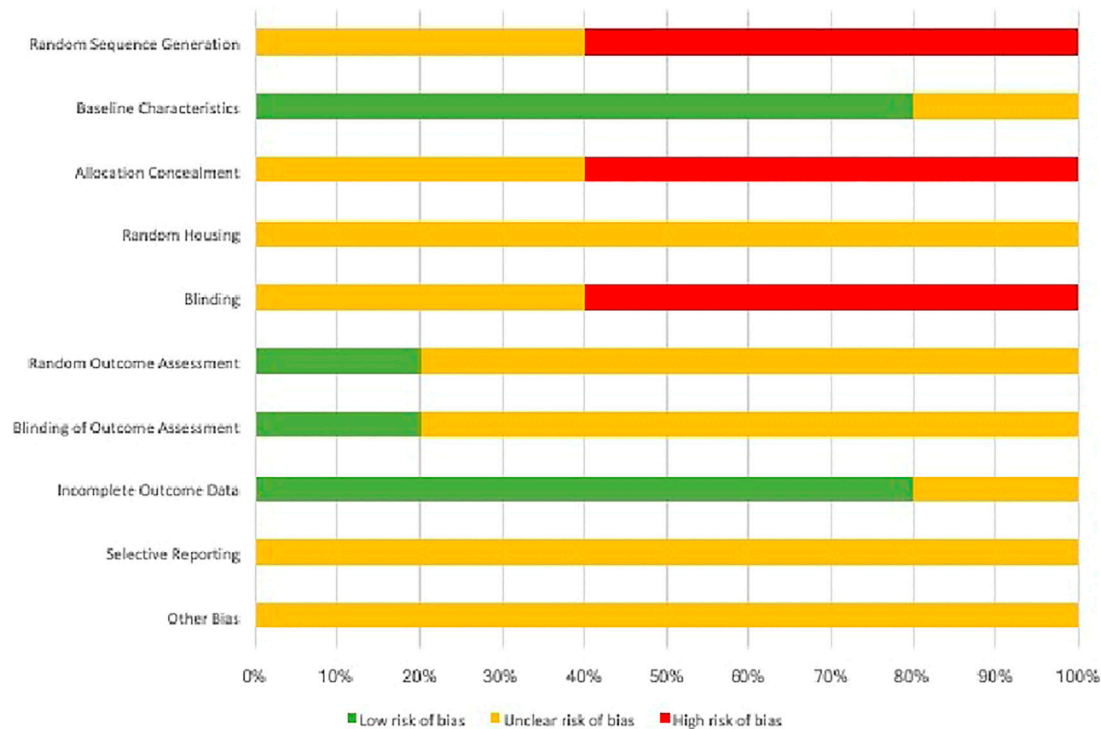


FIGURE 3 | Cumulative risk assessment of the included studies in the systematic review using individual items in SYRCLE RoB tool.

be closely adherent to the coating (Gorrieri et al., 2006; Xie et al., 2009). Also, it was observed that there was increased cellular proliferation and cell viability with increased levels of osteogenic markers such as ALP, OCN, OPN, BSP, RUNX-2 etc influenced by the presence of Mg in the implant surface coating (Gorrieri et al., 2006; Jiang et al., 2014; Mihailescu et al., 2016; Onder et al., 2018; Pardun et al., 2015; Park et al., 2013; Won et al., 2017; Yu et al., 2017; Xie et al., 2009; Zhao et al., 2013). There was also increased deposition of Type-I collagen which is an essential component of the extracellular matrix and increased Ca deposition that can contribute to bone mineralization (Onder et al., 2018; Park et al., 2013; Won et al., 2017).

The success of dental implants is not only dependent on osseointegration but on the disruption of the microbial biofilm that can affect the health of the peri-implant tissues. Various organisms like *Prevotella intermedia*, *Porphomonas gingivalis*, *Actinobacillus actinomycetemcomitans* have been identified as etiological factors that can result in peri-implantitis where there is a pathological loss of peri-implant supporting tissues (Leonhardt et al., 1999; Schmidlin et al., 2013). This has warranted research towards newer and effective strategies on antibacterial surface coatings to prevent microbial adhesion and colonization on dental implants (Holban et al., 2014). Two studies in this systematic review observed the anti-bacterial effect of Mg-based coatings and there was significantly higher inhibitory effect with these coatings on microbes like *P. gingivalis*, *F. nucleatum*, *S. mutans*, *Micrococcus* sp, *Enterococcus* sp, and *Candida albicans* (Mihailescu et al., 2016; Yu et al., 2017). But, the results of the study conducted by Yu et al., suggested that the Zn portion of Zn/Mg co-implanted surface could have contributed to the inhibitory effect because of Zn ions being established in the suppression of microbial adhesion and production of reactive oxygen species that are detrimental to the oral anaerobes (Yu et al., 2017). The study conducted by Mihailescu et al., suggested that BHA:MgO or BHA:MgF₂ have anti-biofilm properties based on the hypothesis that these coatings exhibited bactericidal properties by killing cells during or after the contact with the coated surfaces (Mihailescu et al., 2016).

The potential limitation in this systematic review could be that the studies belong to the lower level of evidence (animal-model and *in vitro* design) and the quality assessment of the included studies revealed that there could be many potential sources of bias. The included studies had considerable heterogeneity and in most of the animal studies, the steps of randomization and blinding were not performed and some studies did not clearly explain the

experimental protocol which is a potential confounding factor. The potential bias existing in these studies could have contributed to the positive outcomes obtained in it. There is a heterogeneity among the included studies in methodology, but the corresponding authors of the studies have been contacted for clarification or for providing any missing information relevant to performing to this review. Some disadvantages noted with Mg alloys include less corrosion resistance, lesser elastic modulus, but none has been identified yet with Mg coatings (Chakraborty Banerjee et al., 2019). But, from this systematic review, it is clear that there is a positive effect with Mg-based coatings on osteogenic activity and osseointegration in dental implants and these results could be ascertained as preliminary as the data was extracted mainly from *in vitro* and experimental animal models. However, future research should be targeted with more well-designed and non-biased clinical studies that focus on confirming these lab-oriented results.

CONCLUSION

From this systematic review of literature, the results from the *in vitro* studies show that Mg-based coatings improve the cellular behavior in terms of morphology and proliferation with increased expression of osteogenic markers and considerable antimicrobial activity. From the animal studies, it can be deduced that there was higher bone fill and BIC values with significant new bone formation. Even though the results are promising, there is considerable heterogeneity among the included studies, so clinical trials are warranted to provide compelling observations for outcomes that determine the long-term clinical success of dental implants.

DATA AVAILABILITY STATEMENT

The raw data supporting the conclusions of this article will be made available by the authors, without undue reservation.

AUTHOR CONTRIBUTIONS

Designing the search, analyzing the studies, analyzing results, writing manuscript and approval.

REFERENCES

- Albrektsson, T. (1998). *Hard Tissue Response. Handbook of Biomaterial Properties*. Boston, MA: Springer, 500–512. doi:10.1007/978-1-4615-5801-9_29
- Albrektsson, T., and Wennerberg, A. (2004). Oral Implant Surfaces: Part 1--review Focusing on Topographic and Chemical Properties of Different Surfaces and *In Vivo* Responses to Them. *Int. J. Prosthodont.* 17 (5), 536–543.
- Best, S. M., Porter, A. E., Thian, E. S., and Huang, J. (2008). Bioceramics: Past, Present and for the Future. *J. Eur. Ceram. Soc.* 28 (7), 1319–1327. doi:10.1016/j.jeurceramsoc.2007.12.001
- Boanini, E., Gazzano, M., and Bigi, A. (2010). Ionic Substitutions in Calcium Phosphates Synthesized at Low Temperature. *Acta Biomater.* 6 (6), 1882–1894. doi:10.1016/j.actbio.2009.12.041
- Brohede, U., Zhao, S., Lindberg, F., Mihranyan, A., Forsgren, J., Strømme, M., et al. (2009). A Novel Graded Bioactive High Adhesion Implant Coating. *Appl. Surf. Sci.* 255 (17), 7723–7728. doi:10.1016/j.apsusc.2009.04.149
- Castellani, C., Lindtner, R. A., Hausbrandt, P., Tschegg, E., Stanzl-Tschegg, S. E., Zanon, G., et al. (2011). Bone-Implant Interface Strength and Osseointegration: Biodegradable Magnesium Alloy Versus Standard Titanium Control. *Acta Biomater.* 7 (1), 432–440. doi:10.1016/j.actbio.2010.08.020
- Cattani Lorente, M., Scherrer, S. S., Richard, J., Demellayer, R., Amez-Droz, M., and Wiskott, H. W. A. (2010). Surface Roughness and EDS Characterization of

- a Y-TZP Dental Ceramic Treated With the Cojet Sand. *Dental Mater.* 26 (11), 1035–1042. doi:10.1016/j.dental.2010.06.005
- Chakraborty Banerjee, P., Al-Saadi, S., Choudhary, L., Harandi, S. E., and Singh, R. (2019). Magnesium Implants: Prospects and Challenges. *Materials*. 12 (1), 136. doi:10.3390/ma12010136
- Cho, L.-R., Kim, D.-G., Kim, J.-H., Byon, E.-S., Jeong, Y.-S., and Park, C.-J. (2010). Bone Response of Mg Ion-Implanted Clinical Implants with the Plasma Source Ion Implantation Method. *Clin. Oral Implants Res.* 21, 848. doi:10.1111/j.1600-0501.2009.01862.x
- Darimont, G. L., Cloots, R., Heinen, E., Seidel, L., and Legrand, R. (2002). *In Vivo* Behaviour of Hydroxyapatite Coatings on Titanium Implants: a Quantitative Study in the Rabbit. *Biomaterials*. 23 (12), 2569–2575. doi:10.1016/s0142-9612(01)00392-1
- Gorrieri, O., Fini, M., Kyriakidou, K., Zizzi, A., Mattioli-Belmonte, M., Castaldo, P., et al. (2006). *In Vitro* Evaluation of Bio-Functional Performances of Ghimas Titanium Implants. *Int. J. Artif. Organs*. 29 (10), 1012–1020. doi:10.1177/039139880602901012
- Hass, J. L., Garrison, E. M., Wicher, S. A., Knapp, B., Bridges, N., Mclroy, D., et al. (2012). Synthetic Osteogenic Extracellular Matrix Formed by Coated Silicon Dioxide Nanosprings. *J. Nanobiotechnology*. 10 (1), 6. doi:10.1186/1477-3155-10-6
- Hench, L. L. (2002). Third-Generation Biomedical Materials. *Science*. 295 (5557), 1014–1017. doi:10.1126/science.1067404
- Holban, A.-M., Bleotu, C., Chifiriuc, M. C., Bezirtoglou, E., and Lazar, V. (2014). Role of *Pseudomonas Aeruginosa* Sensing (QS) Molecules on the Viability and Cytokine Profile of Human Mesenchymal Stem Cells. *Virulence*. 5 (2), 303–310. doi:10.4161/viru.27571
- Hooijmans, C. R., Rovers, M. M., de Vries, R. B., Leenaars, M., Ritskes-Hoitinga, M., and Langendam, M. W. (2014). SYRCLE's Risk of Bias Tool for Animal Studies. *BMC Med. Res. Methodol.* 14 (1), 14–43. doi:10.1186/1471-2288-14-43
- Hoppe, A., Güldal, N. S., and Boccaccini, A. R. (2011). A Review of the Biological Response to Ionic Dissolution Products From Bioactive Glasses and Glass-Ceramics. *Biomaterials*. 32 (11), 2757–2774. doi:10.1016/j.biomaterials.2011.01.004
- Jemat, A., Ghazali, M. J., Razali, M., and Otsuka, Y. (2015). Surface Modifications and Their Effects on Titanium Dental Implants. *Biomed. Res. Int.* 2015, 1–11. doi:10.1155/2015/791725
- Jiang, X., Wang, G., Li, J., Zhang, W., Xu, L., Pan, H., et al. (2014). Magnesium Ion Implantation on a Micro/Nanostructured Titanium Surface Promotes its Bioactivity and Osteogenic Differentiation Function. *Int. J. Nanomedicine*. 8, 2387. doi:10.2147/ijn.s58357
- Jiang, X., Zhang, w., Li, z., Ling Xu, L., Yuqin Jin, Y., et al. (2013). Effects of a Hybrid Micro/nanorod Topography-Modified Titanium Implant on Adhesion and Osteogenic Differentiation in Rat Bone Marrow Mesenchymal Stem Cells. *Int J Nanomedicine*. 8, 257. doi:10.2147/ijn.s39357
- Leonhardt, A., Renvert, S., and Dahlén, G. (1999). Microbial Findings at Failing Implants. *Clin. Oral Implants Res.* 10 (5), 339–345. doi:10.1034/j.1600-0501.1999.100501.x
- Li, X., Li, Y., Liao, Y., Li, J., Zhang, L., and Hu, J. (2014). The Effect of Magnesium-Incorporated Hydroxyapatite Coating on Titanium Implant Fixation in Ovariectomized Rats. *Int. J. Oral Maxillofac. Implants*. 29 (1), 196–202. doi:10.11607/jomi.2893
- Liang, H., Wan, Y. Z., He, F., Huang, Y., Xu, J. D., Li, J. M., et al. (2007). Bioactivity of Mg-Ion-Implanted Zirconia and Titanium. *Appl. Surf. Sci.* 253 (6), 3326–3333. doi:10.1016/j.apsusc.2006.07.038
- Lung, C. Y. K., and Matinlinna, J. P. (2012). Aspects of Silane Coupling Agents and Surface Conditioning in Dentistry: An Overview. *Dental Mater.* 28 (5), 467–477. doi:10.1016/j.dental.2012.02.009
- Mihailescu, N., Stan, G. E., Duta, L., Chifiriuc, M. C., Bleotu, C., Sopronyi, M., et al. (2016). Structural, Compositional, Mechanical Characterization and Biological Assessment of Bovine-Derived Hydroxyapatite Coatings Reinforced With MgF₂ or MgO for Implants Functionalization. *Mater. Sci. Eng. C*. 59, 863–874. doi:10.1016/j.msec.2015.10.078
- Niinomi, M. (2008). Mechanical Biocompatibilities of Titanium Alloys for Biomedical Applications. *J. Mech. Behav. Biomed. Mater.* 1 (1), 30–42. doi:10.1016/j.jmbbm.2007.07.001
- Onder, S., Calikoglu-Koyuncu, A. C., Kazmanli, K., Urgen, M., Kok, F. N., and Torun-Kose, G. (2018). Magnesium Doping on TiN Coatings Affects Mesenchymal Stem Cell Differentiation and Proliferation Positively in a Dose-Dependent Manner. *Biomed Mater Eng.* 29 (4), 427–438. doi:10.3233/bme-181000
- Pang, K.-M., Lee, J.-W., Lee, J.-Y., Lee, J.-B., Kim, S.-M., Kim, M.-J., et al. (2014). Clinical Outcomes of Magnesium-Incorporated Oxidised Implants: a Randomised Double-Blind Clinical Trial. *Clin. Oral Impl. Res.* 25 (5), 616–621. doi:10.1111/clr.12091
- Pardun, K., Treccani, L., Volkmann, E., Streckbein, P., Heiss, C., Gerlach, J. W., et al. (2015). Magnesium-containing Mixed Coatings on Zirconia for Dental Implants: Mechanical Characterization and *In Vitro* Behavior. *J. Biomater. Appl.* 30 (1), 104–118. doi:10.1177/0885328215572428
- Park, J.-W., Kim, H.-K., Kim, Y.-J., Jang, J.-H., Song, H., and Hanawa, T. (2010). Osteoblast Response and Osseointegration of a Ti-6Al-4V alloy Implant Incorporating Strontium. *Acta Biomater.* 6 (7), 2843–2851. doi:10.1016/j.actbio.2010.01.017
- Park, K.-D., Lee, B.-A., Piao, X.-H., Lee, K.-K., Park, S.-W., Oh, H.-K., et al. (2013). Effect of Magnesium and Calcium Phosphate Coatings on Osteoblastic Responses to the Titanium Surface. *J. Adv. Prosthodont.* 5 (4), 402. doi:10.4047/jap.2013.5.4.402
- Revell, P., Damien, E., Zhang, X., Evans, P., and Howlett, C. (2004). The Effect of Magnesium Ions on Bone Bonding to Hydroxyapatite Coating on Titanium alloy Implants. *Key Eng. Mat.* 254, 447–450. doi:10.4028/www.scientific.net/KEM.254-256.447
- Richards, D. (2009). GRADING - Levels of Evidence. *Evid. Based Dent.* 10 (1), 24–25. doi:10.1038/sj.ebd.6400636
- Rude, R. K., Gruber, H. E., Norton, H. J., Wei, L. Y., Frausto, A., and Kilburn, J. (2006). Reduction of Dietary Magnesium by Only 50% in the Rat Disrupts Bone and Mineral Metabolism. *Osteoporos. Int.* 17 (7), 1022–1032. doi:10.1007/s00198-006-0104-3
- Sader, M. S., LeGeros, R. Z., and Soares, G. A. (2009). Human Osteoblasts Adhesion and Proliferation on Magnesium-Substituted Tricalcium Phosphate Dense Tablets. *J. Mater. Sci. Mater. Med.* 20 (2), 521–527. doi:10.1007/s10856-008-3610-3
- Sawada, R., Kono, K., Isama, K., Haishima, Y., and Matsuoka, A. (2013). Calcium-Incorporated Titanium Surfaces Influence the Osteogenic Differentiation of Human Mesenchymal Stem Cells. *J. Biomed. Mater. Res.* 101A (9), 2573–2585. doi:10.1002/jbm.a.34566
- Schmidlin, P. R., Müller, P., Attin, T., Wieland, M., Hofer, D., and Guggenheim, B. (2013). Polyspecies Biofilm Formation on Implant Surfaces With Different Surface Characteristics. *J. Appl. Oral Sci.* 21 (1), 48–55. doi:10.1590/1678-7757201302312
- Shi, X., Nakagawa, M., Kawachi, G., Xu, L., and Ishikawa, K. (2012). Surface Modification of Titanium by Hydrothermal Treatment in Mg-Containing Solution and Early Osteoblast Responses. *J. Mater. Sci. Mater. Med.* 23 (5), 1281–1290. doi:10.1007/s10856-012-4596-4
- Staiger, M. P., Pietak, A. M., Huadmai, J., and Dias, G. (2006). Magnesium and its Alloys as Orthopedic Biomaterials: A Review. *Biomaterials*. 27 (9), 1728–1734. doi:10.1016/j.biomaterials.2005.10.003
- Stanford, C. (2008). Surface Modifications of Dental Implants. *Aust. Dental J.* 53 (s1), S26–S33. doi:10.1111/j.1834-7819.2008.00038.x
- Sul, Y.-T., Jeong, Y., Johansson, C., and Albrektsson, T. (2006). Oxidized, Bioactive Implants Are Rapidly and Strongly Integrated in Bone. Part 1 - Experimental Implants. *Clin. Oral Implants Res.* 17 (5), 521–526. doi:10.1111/j.1600-0501.2005.01230.x
- Tao, Z.-S., Zhou, W.-S., He, X.-W., Liu, W., Bai, B.-L., Zhou, Q., et al. (2016). A Comparative Study of Zinc, Magnesium, Strontium-Incorporated Hydroxyapatite-Coated Titanium Implants for Osseointegration of Osteopenic Rats. *Mater. Sci. Eng. C*. 62, 226–232. doi:10.1016/j.msec.2016.01.034
- Tschernitschek, H., Borchers, L., and Geurtsen, W. (2005). Nonalloyed Titanium as a Bioinert Metal-Aa Review. *Quintessence Int.* 36 (7–8), 523–530.
- Won, S., Huh, Y.-H., Cho, L.-R., Lee, H.-S., Byon, E.-S., and Park, C. J. (2017). Cellular Response of Human Bone Marrow Derived Mesenchymal Stem Cells to Titanium Surfaces Implanted With Calcium and Magnesium Ions. *Tissue Eng. Regen. Med.* 14 (2), 123–131. doi:10.1007/s13770-017-0028-3

- Xie, Y., Zhai, W., Chen, L., Chang, J., Zheng, X., and Ding, C. (2009). Preparation and *In Vitro* Evaluation of Plasma-Sprayed Mg₂SiO₄ Coating on Titanium alloy. *Acta Biomater.* 5 (6), 2331–2337. doi:10.1016/j.actbio.2009.03.003
- Yamasaki, Y., Yoshida, Y., Okazaki, M., Shimazu, A., Uchida, T., Kubo, T., et al. (2002). Synthesis of Functionally Graded MgCO₃ Apatite Accelerating Osteoblast Adhesion. *J. Biomed. Mater. Res.* 62 (1), 99–105. doi:10.1002/jbm.10220
- Ying Kei Lung, C. (2017). Surface Coatings of Titanium and Zirconia. *Adv. Mater. Sci. [Internet]* 2 (2), 1. doi:10.15761/ams.1000124
- Yu, J., Li, K., Zheng, X., He, D., Ye, X., and Wang, M. (2013). *In Vitro* and *In Vivo* Evaluation of Zinc-Modified Ca-Si-Based Ceramic Coating for Bone Implants. *PLoS ONE*. 8 (3), e57564. doi:10.1371/journal.pone.0057564
- Yu, Y., Ding, T., Xue, Y., and Sun, J. (2016). Osteoinduction and Long-Term Osseointegration Promoted by Combined Effects of Nitrogen and Manganese Elements in High Nitrogen Nickel-Free Stainless Steel. *J. Mater. Chem. B*. 4 (4), 801–812. doi:10.1039/c5tb02190a
- Yu, Y., Jin, G., Xue, Y., Wang, D., Liu, X., and Sun, J. (2017). Multifunctions of Dual Zn/Mg Ion Co-Implanted Titanium on Osteogenesis, Angiogenesis and Bacteria Inhibition for Dental Implants. *Acta Biomater.* 49, 590–603. doi:10.1016/j.actbio.2016.11.067
- Zhao, S.-f., Jiang, Q.-h., Peel, S., Wang, X.-x., and He, F. m. (2013). Effects of Magnesium-Substituted Nanohydroxyapatite Coating on Implant Osseointegration. *Clin. Oral Impl. Res.* 24, 34–41. doi:10.1111/j.1600-0501.2011.02362.x
- Zhou, Y., Jiang, T., Qian, M., Zhang, X., Wang, J., Shi, B., et al. (2008). Roles of Bone Scintigraphy and Resonance Frequency Analysis in Evaluating Osseointegration of Endosseous Implant. *Biomaterials*. 29 (4), 461–474. doi:10.1016/j.biomaterials.2007.10.021
- Zreiqat, H., Howlett, C. R., Zannettino, A., Evans, P., Schulze-Tanzil, G., Knabe, C., et al. (2002). Mechanisms of Magnesium-Stimulated Adhesion of Osteoblastic Cells to Commonly Used Orthopaedic Implants. *J. Biomed. Mater. Res.* 62 (2), 175–184. doi:10.1002/jbm.10270

Conflict of Interest: The author declares that the research was conducted in the absence of any commercial or financial relationships that could be construed as a potential conflict of interest.

Publisher's Note: All claims expressed in this article are solely those of the authors and do not necessarily represent those of their affiliated organizations, or those of the publisher, the editors and the reviewers. Any product that may be evaluated in this article, or claim that may be made by its manufacturer, is not guaranteed or endorsed by the publisher.

Copyright © 2021 Almehmadi. This is an open-access article distributed under the terms of the Creative Commons Attribution License (CC BY). The use, distribution or reproduction in other forums is permitted, provided the original author(s) and the copyright owner(s) are credited and that the original publication in this journal is cited, in accordance with accepted academic practice. No use, distribution or reproduction is permitted which does not comply with these terms.



Hierarchical Intrafibrillarly Mineralized Collagen Membrane Promotes Guided Bone Regeneration and Regulates M2 Macrophage Polarization

Yaowei Xuan^{1,2}, Lin Li^{1,2}, Muzhi Ma³, Junkai Cao^{2*} and Zhen Zhang^{3*}

¹Medical School of Chinese PLA, Beijing, China, ²Department of Stomatology, The First Medical Centre, Chinese PLA General Hospital, Beijing, China, ³Department of Oral and Maxillofacial-Head and Neck Oncology, Shanghai Ninth People's Hospital, Shanghai Jiao Tong University School of Medicine, College of Stomatology, Shanghai Jiao Tong University, National Center for Stomatology, National Clinical Research Center for Oral Diseases, Shanghai Key Laboratory of Stomatology, Shanghai, China

OPEN ACCESS

Edited by:

Mohd Fadhi Khamis,
Universiti Sains Malaysia Health
Campus, Malaysia

Reviewed by:

Intan Ruspita,
Gadjah Mada University, Indonesia
Ahmad Azlina,
Universiti Sains Malaysia Health
Campus, Malaysia

*Correspondence:

Zhen Zhang
zz_zhang0101@163.com
Junkai Cao
caojk301@163.com

Specialty section:

This article was submitted to
Biomaterials,
a section of the journal
Frontiers in Bioengineering and
Biotechnology

Received: 22 September 2021

Accepted: 23 December 2021

Published: 26 January 2022

Citation:

Xuan Y, Li L, Ma M, Cao J and Zhang Z
(2022) Hierarchical Intrafibrillarly
Mineralized Collagen Membrane
Promotes Guided Bone Regeneration
and Regulates M2
Macrophage Polarization.
Front. Bioeng. Biotechnol. 9:781268.
doi: 10.3389/fbioe.2021.781268

Mineralized collagen has been introduced as a promising barrier membrane material for guided bone regeneration (GBR) due to its biomimetic nanostructure. Immune interaction between materials and host significantly influences the outcome of GBR. However, current barrier membranes are insufficient for clinical application due to limited mechanical or osteoimmunomodulatory properties. In this study, we fabricated hierarchical intrafibrillarly mineralized collagen (HIMC) membrane, comparing with collagen (COL) and extrafibrillarly mineralized collagen (EMC) membranes, HIMC membrane exhibited preferable physicochemical properties by mimicking the nanostructure of natural bone. Bone marrow mesenchymal stem cells (BMSCs) seeded on HIMC membrane showed superior proliferation, adhesion, and osteogenic differentiation capacity. HIMC membrane induced CD206+Arg-1+ M2 macrophage polarization, which in turn promoted more BMSCs migration. In rat skull defects, HIMC membrane promoted the regeneration of new bone with more bone mass and more mature bone architecture. The expression levels of Runx2 and osterix and CD68 + CD206 + M2 macrophage polarization were significantly enhanced. HIMC membrane provides an appropriate osteoimmune microenvironment to promote GBR and represents a promising material for further clinical application.

Keywords: mineralized collagen membrane, osteoimmunomodulation, macrophage polarization, guided bone regeneration, nanostructure

INTRODUCTION

Regeneration of periodontal tissue is a challenging step in the treatment of periodontitis, especially the regeneration of lost bone tissue. Guided bone regeneration (GBR) refers to the application of barrier membranes to block the ingrowth of gingival epithelium and connective tissue while also inducing the deposition of extracellular matrix, to maximize the repair and regeneration at the periodontal bone tissue (Aprile et al., 2020). The ideal barrier membranes for GBR should possess appropriate characteristics, such as low toxicity, superior biocompatibility, initial mechanical properties, suitable degradation rate, and surface characteristics conducive to cell attachment (Liu et al., 2016). However, among existing barrier materials for GBR, most absorbable membranes lack mechanical properties to maintain the space long enough for bone

regeneration, whereas non-absorbable membranes do not degrade and require a second operation for their removal. Thus, both types of membranes are insufficient for clinical application (Zhou et al., 2021).

The fabrication of mineralized collagen materials using biomimetic technology represents a promising approach for GBR due to mimicking the microstructural organization of natural bone. However, hydroxyapatite (HA) crystallites randomly stacked around the collagen fibrils in previously fabricated extrafibrillarly mineralized collagen (EMC), failing to provide an ordered microstructure. Therefore, EMC can offer only analogous chemical composition to native bone but not the same surface appearance and nanostructure of bone extracellular matrix (Kane and Ma, 2013; Hu et al., 2016). In contrast, hierarchical intrafibrillarly mineralized collagen (HIMC), which presents a surface that is highly similar to the natural bone matrix based on a hierarchical combination of collagen and HA, shows superior option for GBR applications (Liu et al., 2016). Both cell and animal studies have verified the excellent osteogenic induction potential and bone regeneration capacity of HIMC material (Liu et al., 2014; Sun et al., 2016; Zhang et al., 2019).

However, most previous studies of biomaterials for bone regeneration emphasized the physical properties and their direct influence on osteocytes, or they focused on materials that induced no response to the immune system to achieve “immune safety”. Through advances in the understanding of osteobiology, immune response was found to be generally activated during interaction between biomaterials and the host. Accordingly, the local microenvironment, especially the immune microenvironment, plays a key role in the regulation of osteogenesis (Schmidt-Bleek et al., 2014; Lin et al., 2021). Macrophages are important components of the immune response to biomaterials and are characterized by high plasticity. M1 macrophages are activated during classic inflammatory response and stimulate the secretion of pro-inflammatory cytokines like interleukin (IL)-6 and tumor necrosis factor alpha (TNF- α) to enhance osteoclast activity and bone resorption. Conversely, M2 macrophages exhibit anti-inflammatory properties and promote bone formation via the production of bone morphogenetic protein-2 and other osteogenic markers (Freytes et al., 2013; Wynn and Vannella, 2016). The ratio and transition of M1/M2 macrophages are considered important indicators of the local immune environment (Yu et al., 2016). Different types of biomaterials, such as collagen (COL) membrane, hydrogel, and biological coating have been shown to regulate macrophage polarization and thereby influence bone regeneration (Chu et al., 2017; Zhang R. et al., 2018; Tanaka et al., 2019). However, the effects of HIMC membrane on immune environment and macrophages comparing with conventional COL and EMC membrane remain relatively undetermined (Shi et al., 2018).

In this study, we investigated whether HIMC membrane can regulate macrophage polarization based on the biomimetic nanostructure. The novelty of the present study lies in the investigation of the osteogenic induction capacity and osteoimmunomodulatory properties elicited by HIMC membrane used for GBR both *in vitro* and *in vivo*. First,

HIMC membrane was fabricated, and the physicochemical properties were investigated in comparison to COL and EMC membranes. Moreover, we further explored the osteogenic effectiveness and osteoimmunomodulatory capacity of HIMC membrane using bone marrow-derived mesenchymal stem cells (BMSCs) and rat critical-sized skull defect models, to provide an important experimental basis for further testing the clinical potential of HIMC membrane for GBR.

MATERIALS AND METHODS

Fabrication of Membranes

According to the method of Cui et al. (Sun et al., 2016), hierarchical self-assembled nano-hydroxyapatite (nHA) was guided to nucleate among collagen molecules via a biomimetic mineralization process, resulting in the formation of HIMC membranes (Liao et al., 2004; Lian et al., 2013; Xu et al., 2016). Briefly, nHA was chemically synthesized from calcium salt, sodium hydroxide, and phosphoric acid. By regulating the mineralization process, collagen and HA can be hierarchically self-assembled. EMC membranes were synthesized using a previously described conventional crystallization method (Hu et al., 2016). COL membranes were prepared by dissolving type I collagen in dilute hydrochloric acid and, after adjustment of the pH, applying centrifugal vacuum drying. For *in vitro* experiments, the membranes were manufactured as round samples with diameters of 12 and 30 mm. For *in vivo* study, square samples with side lengths of 9 mm were fabricated.

Characterization of Membranes

Scanning Electron Microscopy

The surface topographies of HIMC, COL, and EMC membranes were surveyed by scanning electron microscopy (Inspect F, FEI, Eindhoven, Netherlands). The samples were fixed with 2.5% glutaraldehyde (pH 7.4) at 4°C for 24 h, rinsed three times with phosphate-buffered saline (PBS), dehydrated in gradient ethanol solutions (30–100%), and dried at critical-point. Then, the samples were gold sputter-coated and viewed under SEM.

Fourier Transform Infrared Spectroscopy

We employed FTIR (Thermo Nicolet, United States) to investigate the molecular structure and composition of the prepared HIMC, COL, and EMC membranes by analyzing the characteristic absorption peaks of functional groups.

Measurement of Mechanical Properties

Five samples of each material were prepared with dimensions of 10 mm \times 15 mm \times 0.15 mm for tensile strength measurements, and the effective tensile length was 10 mm. We utilized a universal mechanical testing machine (3367; Instron, Norwood, MA) to acquire the stress–strain curves and tensile strength results, with the crosshead speed at 1 mm/min.

Water Contact Angle Measurements

The static contact angle between the surface of each membrane type and a water drop was determined using an optical

instrument ($n = 3$). Four different droplet points were measured on images taken with a CCD camera to assess the hydrophilicity of each membrane type.

In Vitro Study

Cell Culture

The isolation, culture, and identification of rat BMSCs followed the previous study (Zhang Z. et al., 2018). We purchased RAW 264.7 cells from the Cell Resource Center (IBMS, CAMS/PUMC), and the cells were cultured in Dulbecco's modified Eagle medium (DMEM, Hyclone) containing 10% fetal bovine serum (FBS) in the environment of 37°C humidified incubator with 5% CO₂.

Cell Proliferation Assay

The proliferation of BMSCs seeded on different membranes was estimated using the CCK-8 assay. The membranes were sterilized by ultraviolet light overnight prior to cell seeding. BMSCs (5×10^4 per well) were added over the membranes in 24-well plates (BD Biosciences, Franklin Lakes, NJ, United States). After culture for 1, 3, and 5 days, 50 µl CCK-8 solution (Sigma-Aldrich, United States) was added to each well and incubated for 4 h. Then, the absorbance at 450 nm in each well was detected using a microplate reader (Rayto RT-6000, United States).

Cell Adhesion and Morphology

The adhesion and morphology of BMSCs on different membranes were evaluated by SEM and laser scanning confocal microscopy (LSCM) after culture for 24 h. The SEM procedure was the same as described above. For LSCM imaging, BMSCs on the membranes were immunostained to reveal the F-actin cytoskeleton and nucleus. We applied 4% paraformaldehyde to fix the cells, then 0.25% Triton X-100 was applied to permeabilize them, followed by blocking with 1% bovine serum albumin. Anti-F-actin antibody for cytoskeletal protein staining (green) and DAPI for nuclear staining (blue) were used. Representative LSCM images were taken (Olympus, Japan).

BMSCs Osteogenic Differentiation

Alkaline Phosphatase Assay

ALP assay of BMSCs on membranes was detected after osteogenic culture for 14 days. After removing the medium and rinsing three times with PBS, reagents were added following the instructions of the ALP assay kit (Sigma-Aldrich, United States). Finally, ALP staining was conducted and photographed. ALP activity was detected by transferring 50 µl of each sample to a 96-well plate, and the absorbance at 520 nm was measured with an automatic microplate reader.

Alizarin Red Staining

Calcium depositions of BMSCs on membranes for 21 days were evaluated by ARS. The samples were fixed in 4% paraformaldehyde after removal of the medium. Deionized water was used to rinse the samples three times and then the staining was performed with 2% ARS solution at room temperature for 20 min. The samples were washed again several times before calcium salt depositions were observed

and photographed under an optical microscope. Dye release was quantified with a spectrophotometer at 562 nm.

Quantitative Real-Time PCR

We conducted qRT-PCR to evaluate the mRNA expression levels of osteogenic differentiation markers in BMSCs grown on the membranes after 3 days. Total RNA extraction, cDNA synthesis, and qRT-PCR procedure were performed as previously reported (Zhang Z. et al., 2018). Relative mRNA expression levels were calculated by the $2^{-\Delta\Delta C_t}$ method. The primers used for qRT-PCR are presented in **Table 1**.

Western Blot

Total proteins were obtained from BMSCs after 3 days in culture using radioimmunoprecipitation assay (RIPA) lysis buffer (Beyotime, China). Then 30 µg protein lysate samples were separated by 8–15% sodium dodecyl sulfate-polyacrylamide gel electrophoresis (SDS-PAGE) before transfer to polyvinylidene difluoride (PVDF) membranes. Then the PVDF membranes were incubated overnight at 4°C with primary antibodies including COL1 (AF7001, dilution: 1:200, Affinity Biosciences, United States), OCN (DF12303, dilution: 1:100, Affinity Biosciences, United States), OPN (ab63856, dilution: 1:1,000, Abcam, United States), and GAPDH (ab9484, dilution: 1:200, Abcam, United States). Horseradish peroxidase-conjugated goat anti-rabbit secondary antibody (S0001, dilution: 1:2,000, Affinity Biosciences, United States) was added for incubation for 1 h at room temperature. Finally, enhanced chemiluminescence reagents (Millipore, United States) were utilized to visualize the immunocomplexes.

Macrophage Polarization Status

Flow Cytometry

RAW 264.7 cells (1×10^6 per well) were seeded on 6-well plates on different membranes. After 24 h, the cells were collected and resuspended in 100 µl binding buffer. M1 macrophage marker CD86 and the M2 marker CD206 antibodies (Biolegend, San Diego, CA, United States) were incubated for 30 min, flow cytometry (Beckman Coulter, Brea, CA, United States) and FlowJo software (TreeStar, United States) were utilized to analyze the cell clusters.

qRT-PCR

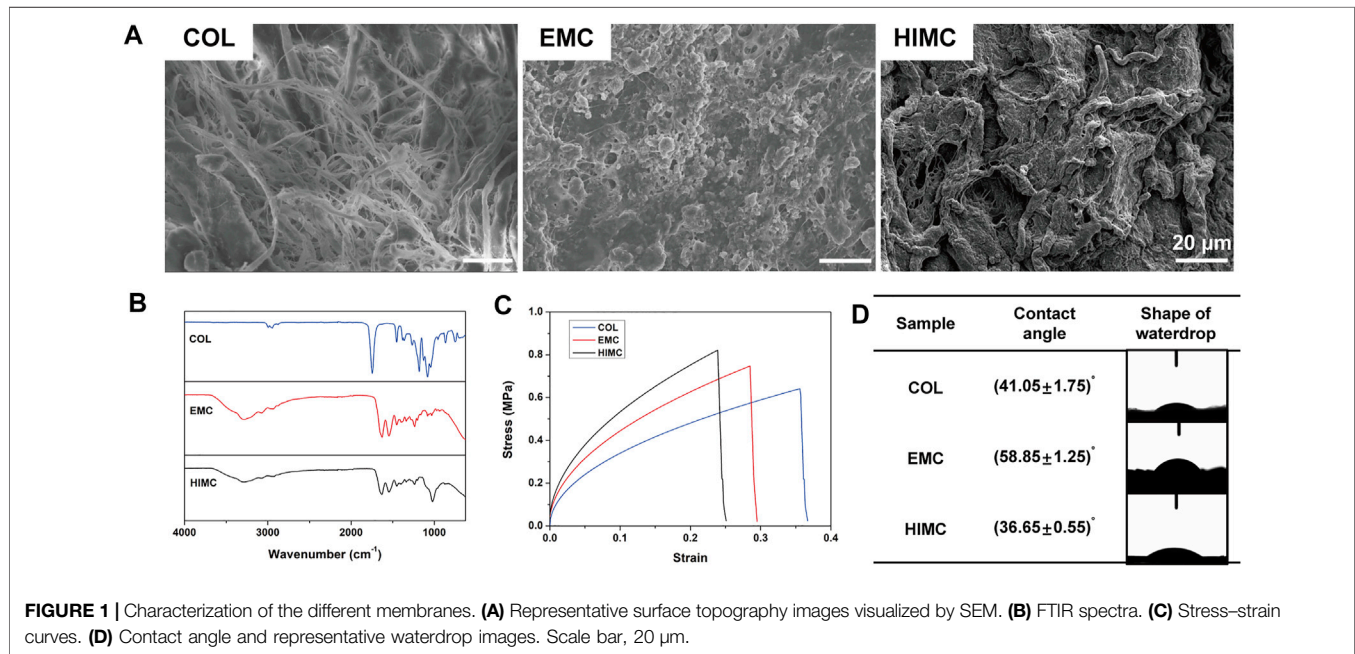
Total RNA was extracted from RAW 264.7 cells cultured for 24 h. The mRNA expression levels of the CD86, iNOS, CD206, and Arg-1 were analyzed by qRT-PCR. The primers used for qRT-PCR are shown in **Table 1**.

Transwell Migration Assay

The effect of macrophage polarization in response to different membranes on BMSCs migration was investigated by Transwell migration assay. First, conditioned medium was prepared by immersing 500 mg of each material in 50 ml α -MEM for 48 h. In the upper Transwell chamber, BMSCs were seeded, and RAW 264.7 cells were cultured in the lower. After overnight, the medium in the lower chamber was replaced with the material-conditioned medium. After 24 h of incubation, 4%

TABLE 1 | Sequences of primers used for qRT-PCR.

Gene	Forward primer sequence (5'–3')	Reverse primer sequence (5'–3')
GAPDH	TGTATCTGTTGTGGATCTGA	TTGCTGTTGAAGTCGCAGGAG
COL	AGAACAGCGTAGCCT	TCCGGTGTGACTCGT
OCN	GGACCTCTCTCTGCTCACTCTG	ACCTTACTGCCCTCCTGCTTGG
OPN	TGGCAGTGGTTTGCTTTTGC	TGTGGTCATGGCTTTCATTG
CD86	TAAGCAAGGATACCCGAAAC	AGAATACACACAATGGTCATATT
CD206	AGACGAAATCCCGCTACGG	CACCCATTGCAAGGCATC
Arg-1	CTCCAAGCCAAGCCCATAGAG	AGGGGCTGTCATTGGGGACATC
iNOS	AGACCCAGTGCCCTGCTTT	CACCAAGGTCATGCGGCT



paraformaldehyde was used for 30 min to fix the cells in the upper chamber. Then, the cells were stained with a crystal violet solution for observation and counting of the migrated BMSCs under an optical microscope.

In Vivo Study

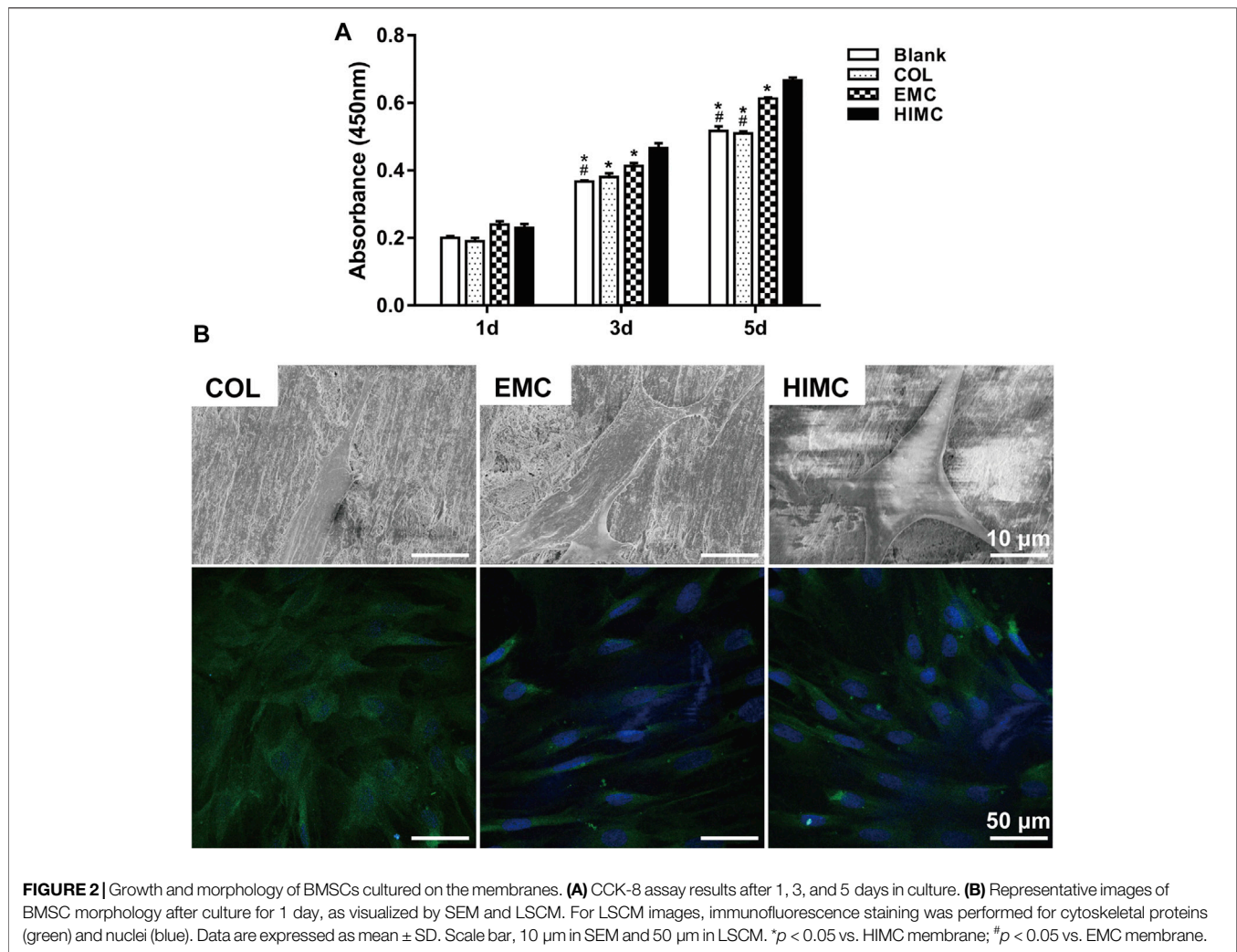
Rat Critical-Sized Skull Defect Model and GBR Process

Eight-week-old male Sprague–Dawley rats were given adaptive feeding for 2 weeks in a standard environment. All animal experiments were designed and executed in accordance with the Guidelines for Animal Health and Use of the National Institutes of Health and authorized by the Ethics Committee for Animal Experiments of Shanghai Jiao Tong University, Shanghai, China. After intraperitoneal injection of Zoletil (50 mg/kg, Virbac, France), the rats were anesthetized, followed by routine disinfection, hair removal, and incision. With the sagittal suture as the midline, circular bone drills with a 5 mm diameter were used to fabricate two symmetrical round defects on the parietal bone of rats (**Figure 5A**).

A total of 45 rats with bilateral skull defect area were randomly allocated into groups: negative control group, sham surgery group, COL group, EMC group, and HIMC membrane group. The membranes used to cover the defects were 9 mm \times 9 mm square shape (2 mm beyond the defect edge), and in the negative control group, no membrane was placed in the defect area. For the sham surgery group, only the scalp was cut without the creation of a cranial defect. Cefazolin (10 mg/kg) was given to prevent infection for 3 days after the operation.

Micro-Computed Tomography Evaluation

For μ -CT, 20 rats with bilateral cranial defects were randomly allocated into four groups ($n = 10$ in each group). At 12 weeks post-surgery, the rats were sacrificed with excess Zoletil and the skull samples were fixed with 4% paraformaldehyde for 5 days. The samples were examined with a μ -CT system (Scanco Medical, Bassersdorf, Switzerland) under 70 kV voltage, 114 mA electric current, and 700 ms integration time. Considering the diameter and depth of the defect, we constructed a cylindrical profile to scan all materials and newly regenerated bone regions. For each



sample, 150 consecutive cross-sections including the entire defect were collected. The image analysis software of the μ -CT 80 system was employed to calculate the ratio of bone volume to total tissue volume (BV/TV).

Histological Evaluation

Hematoxylin and Eosin Staining

After μ -CT scanning, these samples were collected and decalcified with 15% ethylene diamine tetraacetic acid (EDTA) for 3 weeks ($n = 10$ in each group), then gradually dehydrated, soaked in paraffin, and embedded. Next, the tissues were sliced into 5 μ m-thick sections for HE staining. We used a stereoscopic microscope (Eclipse E600, Nikon, Tokyo, Japan) to obtain images. The proportion of new bone regenerated was calculated using Image-Pro Plus (7.0 version, Media Cybernetics, Rockville, MD).

Immunohistochemical Staining

For IHC staining, there were 25 rats divided into five groups ($n = 10$ in each group). The expression of osteogenic markers and macrophage polarization markers was detected after 2 weeks post-surgery. Sections were prepared as described above.

Primary antibodies were added for incubation overnight including runt-related transcription factor 2 (Runx2, ab192256, dilution: 1:200, Abcam, Cambridge, MA, United States) and osterix (osx, ab22552, dilution: 1:200, Abcam, United States) as well as the macrophage polarization markers, pan marker CD68 (ab125212, dilution: 1:200, Abcam, United States), M1 marker iNOS (ab15323, dilution: 1:100, Abcam, United States), and M2 marker CD206 (ab64693, dilution: 1:200, Abcam, United States). The sections were then incubated with secondary antibody for 1 h and stained with DAB. Finally, the nuclei were stained with hematoxylin. The stained sections were visualized and photographed under an optical microscope (Leica DMI 6000B Microsystems, Wetzlar, Germany). Four non-overlapping fields were randomly selected under 40x microscope for each section, and the number of nuclear-stained cells in the fields was considered positive staining cells.

Statistical Analysis

All quantitative values are expressed as mean \pm standard deviation ($\bar{x} \pm SD$). GraphPad Prism Software (Version 7.0,

Inc., La Jolla, CA, United States) and SPSS 23.0 statistics software (IBM Corp, Armonk, NY, United States) were employed. Data analyses were performed with one-way analysis of variance (ANOVA) and Tukey's multiple-comparisons test. The distribution normality of all datasets was evaluated by Shapiro-Wilk test. p values <0.05 (two-sides) were considered statistically significant.

RESULTS

Comparison of the Physicochemical Properties of the HIMC, COL, and EMC Membranes

The microstructure of each material was observed by SEM. The HIMC membrane was structurally ordered and exhibited nanomorphology similar to the natural bone surface with a large surface roughness. The COL membrane exhibited a relatively smooth structure with no obvious protrusions. A coarse texture with nHA clusters stacked randomly around the fibers was observed on an EMC membrane (Figure 1A).

The functional chemical groups of the materials were detected by FTIR (Figure 1B). The spectra for all materials included peaks for amide I band (C=O bond, $1580\text{--}1720\text{ cm}^{-1}$) and amide II band (N=H bond, 1540 cm^{-1}), which are the representative peaks of collagen. The presence of a phosphate vibration zone at $900\text{--}1200\text{ cm}^{-1}$ in the spectra for HIMC membranes represented mineralized particles.

The stress-strain curves obtained from the tensile testing showed that HIMC, EMC, and COL membranes exhibited similar deformation patterns (Figure 1C). The maximum tensile strength of HIMC was greater than that of the other membranes, and that of EMC was greater than that of COL.

Water contact angle measurements demonstrated the hydrophilicity of the three membrane types (Figure 1D). The contact angle appeared to be smallest on the HIMC membrane and largest on the EMC, indicating that the HIMC membrane was the most hydrophilic material, followed by COL and EMC. The difference in the contact angles was significant between the HIMC and EMC membranes and between the COL and EMC membranes, but not between the HIMC and COL membranes.

Comparison of BMSCs Proliferation and Adhesion on HIMC, COL, and EMC Membranes

The proliferation of BMSCs seeded on the HIMC, COL, and EMC membranes was compared using the CCK-8 assay (Figure 2A). On the first day of culture, no significant difference in absorbance at 450 nm was observed between the groups. Cell growth was not inhibited on all materials over time. On Day 3 and Day 5, significantly higher absorbance value was detected for the HIMC membrane group compared to the COL and EMC groups, showing that BMSCs seeding on HIMC membrane proliferated better than the others.

The morphology of BMSCs seeded on different membranes was visualized by SEM (Figure 2B). The BMSCs adhered to the HIMC membrane surface showed a polygonal shape with many large pseudopods extending outward. The BMSCs on the COL surface exhibited a thin spindle shape and lacked obvious pseudopod protrusion. Even fewer pseudopods that appeared small and thin presented on the BMSCs seeding on the EMC membrane.

The cytoskeletal organization within BMSCs seeded on different materials was observed by LSM (Figure 2B). On COL membrane, BMSCs showed disordered cell fibers, with the cytoskeletal proteins oriented in different directions. On the EMC membrane, BMSCs had a fusiform shape, with elongated intracellular fibers, thin actin fibrils, and few branching points. In BMSCs on the HIMC membrane surface, the collagen fibers were tightly and thickly arranged, as seen in highly bifurcated osteoblasts, with a fine filamentous base and thick stress fiber formation.

Comparison of BMSCs Osteogenic Differentiation on HIMC, COL, and EMC Membranes

The osteogenic differentiation outcomes of BMSCs on different membranes were evaluated. BMSCs were cultured on different membranes for 14 and 21 days, and ALP and ARS were evaluated. For ALP activity assay, blue staining was more obviously observed on the HIMC membrane compared with COL and EMC membranes on Day 14 (Figure 3A). After 21 days in culture, ARS for calcium nodules presented densely red nodules among BMSCs on HIMC membranes, with fewer nodules on the EMC and COL membranes (Figure 3A). Semi-quantitative analysis of the results indicated the observed differences were statistically significant, the HIMC membrane distinctly enhanced the osteogenic capacity of BMSCs in terms of ALP and ARS (Figures 3B,C).

The mRNA and protein expression levels of osteogenic markers were measured in BMSCs cultured on different membranes for 3 days using qRT-PCR and Western blot analyses. BMSCs grown on HIMC membrane exhibited higher mRNA expression levels of the *COL1*, *OCN*, and *OPN* compared with BMSCs cultured on COL or EMC membranes (Figure 3D). ALP and *COL1* are early markers of osteogenesis, whereas *OCN* and *OPN* are expressed later in the osteogenic differentiation process. The results for protein expression obtained from Western blot were consistent with the qRT-PCR results (Figures 3E,F). Protein expression levels in the early (*COL1*) and late (*OCN* and *OPN*) osteogenic process were enhanced in BMSCs seeded on HIMC membranes compared with those in BMSCs seeded on COL and EMC membranes.

Comparison of Macrophage Polarization and Consequent BMSCs Migration on HIMC, COL, and EMC Membranes

To investigate the immunoregulatory characteristics of HIMC membrane, we exposed RAW 264.7 cells to HIMC, COL, and

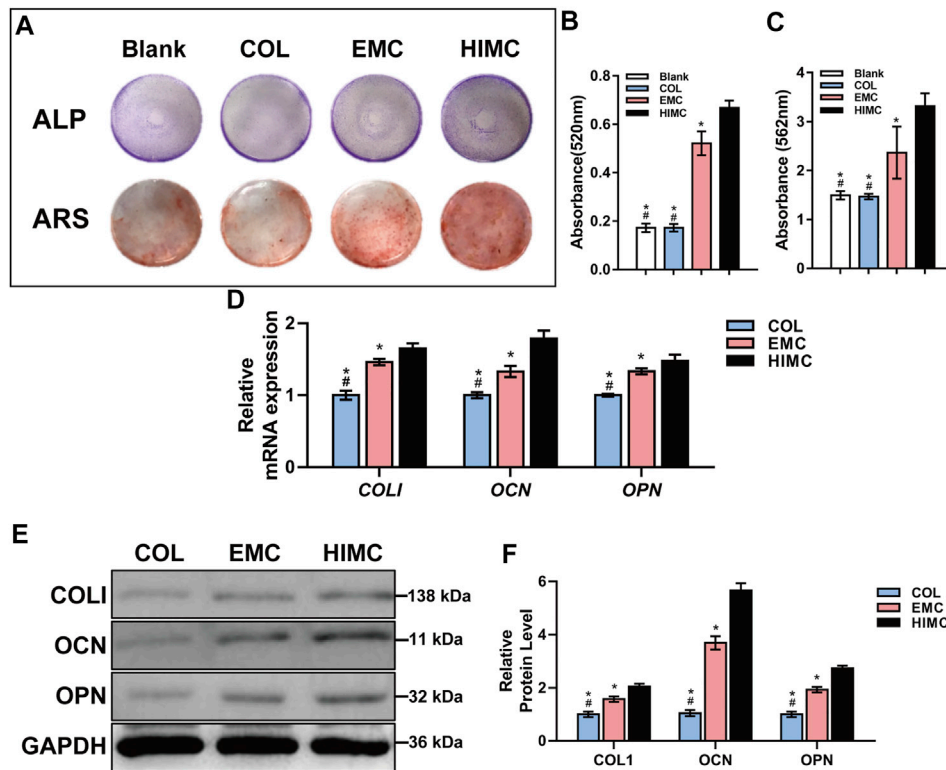


FIGURE 3 | Osteogenic differentiation capacity of BMSCs cultured on different membranes. **(A)** ALP staining and ARS. **(B)** Semi-quantitative results of ALP activity assay for absorbance at 520 nm. **(C)** Absorbance at 562 nm for ARS. **(D)** mRNA expression levels of *COL1*, *OCN*, and *OPN* as measured by qRT-PCR. **(E)** Protein expression levels of *COL1*, *OCN*, *OPN*, and *GAPDH* as quantified by Western blot. **(F)** Gray-scale analysis of Western blots. Data are expressed as mean \pm S.D. * $p < 0.05$ vs. HIMC membrane; # $p < 0.05$ vs. EMC membrane.

EMC membrane. Flow cytometric analysis was performed to identify M1 and M2 macrophage types after culture on different materials, based on the proportion of $CD86^+$ and $CD206^+$ cells (**Figures 4A,B**). The percentages of $CD206^+$ macrophages among different groups were 52.94% with HIMC membrane, 31.95% with EMC, and 19.31% with COL, and from these results, the percentage of M2 macrophages in the HIMC membranes group was remarkably higher. The percentages of $CD86^+$ macrophages were 8.96% with HIMC membrane, 59.67% with EMC, and 46% with COL, indicating that fewer macrophages in the HIMC group showed M1 polarization. Therefore, with the presence of more M2 macrophages and fewer M1 macrophages, the HIMC membrane was associated with the largest M2/M1 macrophage ratio among the three tested materials.

The relative mRNA expression levels of *CD86*, *iNOS* (M1 polarization markers), *CD206*, and *Arg-1* (M2 polarization markers) in RAW 264.7 cells exposed to different membranes were detected by qRT-PCR (**Figure 4C**). Compared with the levels in the other two groups, the expression levels of *CD86* and *iNOS* in the HIMC membrane group were greatly reduced, and *CD206* and *Arg-1* were notably increased. These results were similar to those from flow cytometric analysis, and macrophages on the HIMC membrane showed more M2 polarization.

Next, we studied the effects of different materials on interaction between BMSCs and macrophages (**Figure 4D**).

First, macrophages were stimulated by conditioned medium containing leached materials from the different membranes, and then macrophages and BMSCs were co-cultured in Transwell chambers for 24 h. In this assay, the number of BMSCs that migrated from the upper to the lower layer was statistically greater in the HIMC membrane group than the COL membrane group (**Figure 4E**), although no difference was detected between the EMC and HIMC groups.

Comparison of Bone Regeneration in Critical-Sized Skull Defect Model Covered With HIMC, COL, or EMC Membranes

To assess the osteogenic ability of HIMC membrane *in vivo* GBR model, we prepared critical-sized skull defects in rats and then covered the defects with different membranes (**Figure 5A**). μ -CT scanning was performed at 12 weeks post-surgery (**Figure 5B**). In the HIMC membranes group, nearly mature bone structure filled most of the defect area, and the density of the newly formed bone was analogous to that of the surrounding bone tissue. Bits of new bone were regenerated at the defect edges of the COL membrane group. In the EMC group, the defect area was reduced, and a network with a low-density shadow had formed in some areas. By comparison, in the negative control group which defects were not covered with membranes, the bone defect surface appeared round

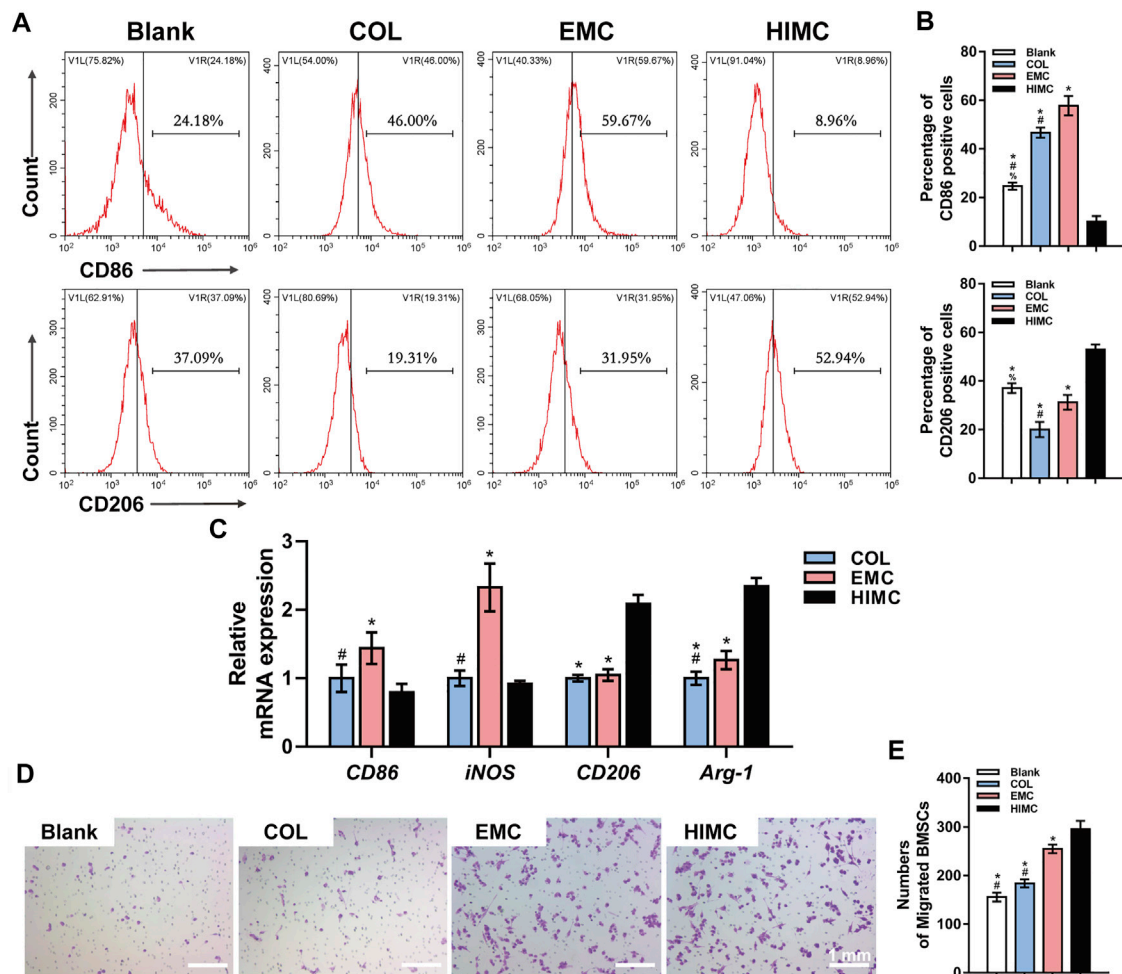


FIGURE 4 | Macrophage polarization and BMSC migration in response to different membranes. **(A)** Representative peak plots of CD86⁺ (M1 polarization) and CD206⁺ (M2 polarization) macrophage ratios examined by flow cytometry. **(B)** Percentages of CD86⁺ and CD206⁺ cells. **(C)** mRNA expression levels of M1 polarization genes (*CD86*, *iNOS*) and M2 (*CD206*, *Arg-1*) in macrophages as measured by qRT-PCR. **(D)** Crystal violet staining of Transwell inserts for detection of BMSC migration induced by macrophages. **(E)** Quantification of BMSC migration. Data are expressed as mean \pm SD. Scale bar, 1 mm. * $p < 0.05$ vs. HIMC membrane; # $p < 0.05$ vs. COL membrane.

and smooth, with little new bone tissue presented at the defect edge and no obvious mineralized structures were observed. Quantitative evaluation of the μ -CT images discovered that the ratio of BV/TV in the HIMC membrane group (0.4818 ± 0.0574) was statistically higher than those in the EMC (0.3627 ± 0.0436 ; $p < 0.05$) and the COL group (0.1252 ± 0.0196 ; $p < 0.05$; **Figure 5C**).

HE staining of the harvested skull defect area produced results consistent with the those from μ -CT imaging (**Figure 5B**). The HIMC membrane group showed newly formed mineralized bone with a higher density of bone trabecula and more mature structures as well as a significantly reduced defect area, compared with the other groups. In the stained section from the HIMC membrane group, abundant osteocytes and new bone distributed from the edge of the defect to the center, and a typical bone marrow cavity structure could be seen. In contrast, staining of the new bone in the COL group and the EMC group showed a

lower trabecular density, with new bone found only at the defect edge. In the negative control group, the defect area was predominantly fibrous tissue with no evidence of new bone formation. The semi-quantitative analysis results of the percentage of new bone based on HE staining images are presented in **Figure 5D**. The new bone percentage in the HIMC membrane group ($39 \pm 4.43\%$) was remarkably higher than those in the EMC membrane ($26.83 \pm 2.74\%$; $p < 0.05$) and the COL membrane group ($16.12 \pm 2.6\%$; $p < 0.05$).

IHC staining was performed to assess the performance of two transcription factors related to osteogenesis, Runx2 and Osx, in the bone defect area (**Figure 6A**). HIMC membrane samples contained more positive cells that highly expressed Runx2 and Osx, whereas a small number of positively stained cells were found in the samples from the COL and EMC groups. No significant positive staining was observed in either the negative control or the sham group. Semi-quantitative analysis of the IHC

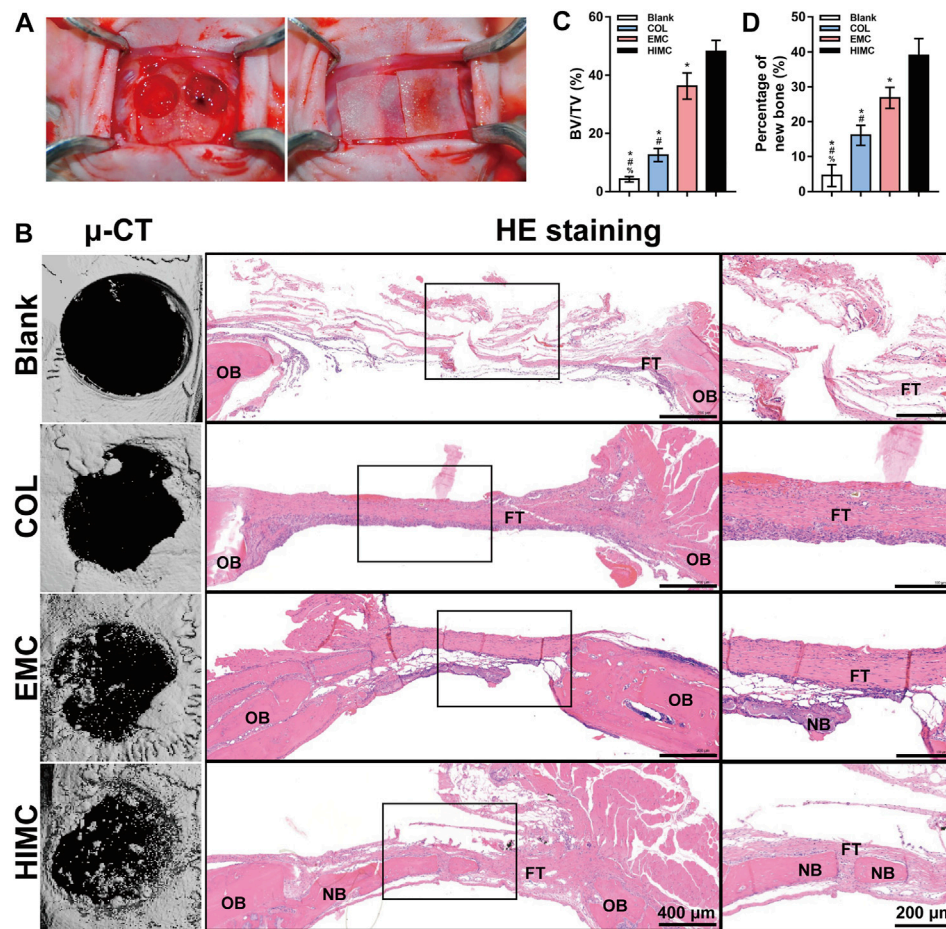


FIGURE 5 | Bone regeneration in rat critical-sized skull defect models covered with the different membranes. **(A)** Rat critical-sized cranial defect models. **(B)** Representative μ -CT images, HE staining images, and $\times 40$ magnification images of the regions outlined by black rectangles at 12 weeks post-surgery. **(C)** Quantitative analysis of new BV relative to the TV on the basis of μ -CT. **(D)** Semi-quantitative analysis of the percentages of new bone in the defect according to HE staining. Data are expressed as mean \pm SD. Scale bar, 400 μ m (20 \times) and 200 μ m (40 \times). * p < 0.05 vs. HIMC membrane; # p < 0.05 vs. EMC membrane; % p < 0.05 vs. COL membrane.

staining images presented statistical differences between the groups (Figure 6B).

Comparison of Macrophage Polarization in Critical-Sized Skull Defect Model

To evaluate the osteoimmunomodulatory properties of the HIMC membrane in the bone defect area, we examined the polarization status of macrophages by IHC staining (Figure 7A). CD68 is a pan marker for *in situ* macrophages. CD68⁺ cells were observed in samples from all groups except the sham group, indicating that macrophages played a role in the response to the materials in the bone defect. Macrophage phenotype was examined by IHC staining for M1 (iNOS) and M2 (CD206) markers. More iNOS⁺ cells were stained in the EMC group, in a pattern consistent with CD68⁺ cells, revealing that most of the macrophages in the defects covered with EMC membrane possessed the M1 phenotype. Fewer iNOS⁺ cells were observed in the samples from the COL group and the HIMC

membrane groups. On the other hand, we observed the largest number of CD206⁺ cells on the HIMC membrane group, further confirming the dominant effect of M2 macrophages in the defects covered with the HIMC membrane. The results of semi-quantitative analysis of the percentage of positive cells on IHC-stained images are presented in Figure 7B.

DISCUSSION

Biomimetic mineralized materials have been widely applied in studies of tissue and organ regeneration, and the prepared membranes have shown some ability to promote GBR (Fillingham and Jacobs, 2016; Yu et al., 2020). However, previous EMC material was commonly characterized by irregular HA deposition. Compared with EMC, the HIMC membrane was shown to more successfully simulate the nanostructure of natural bone through intrafibrillar mineralization and have a better ability to induce osteogenesis

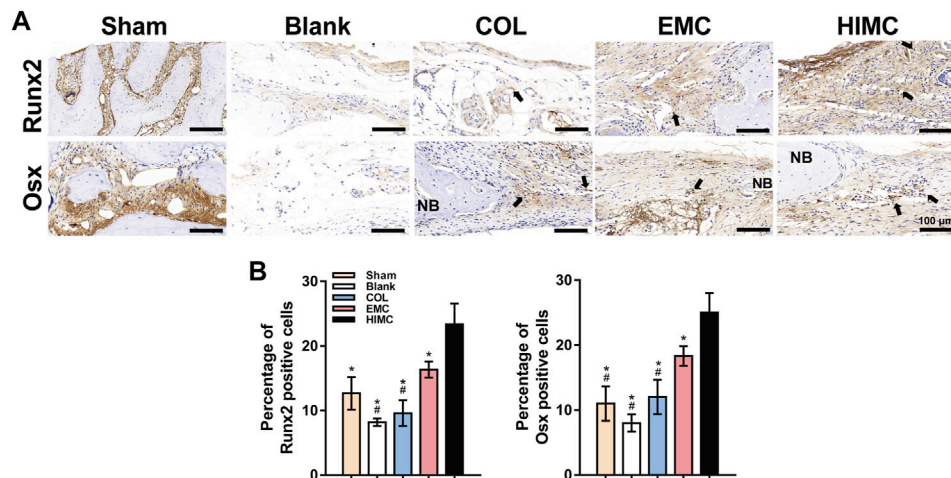


FIGURE 6 | Representative images of IHC staining for osteogenesis markers in the defect region of different groups at 2 weeks post-surgery. Positively stained cells are indicated by arrows. **(A)** Runx2 and Osx expression in defect tissues. **(B)** Semi-quantification of the positive cells. Data are expressed as mean \pm SD. Scale bar, 100 μ m. * p < 0.05 vs. HIMC membrane; # p < 0.05 vs. EMC membrane; % p < 0.05 vs. COL membrane.

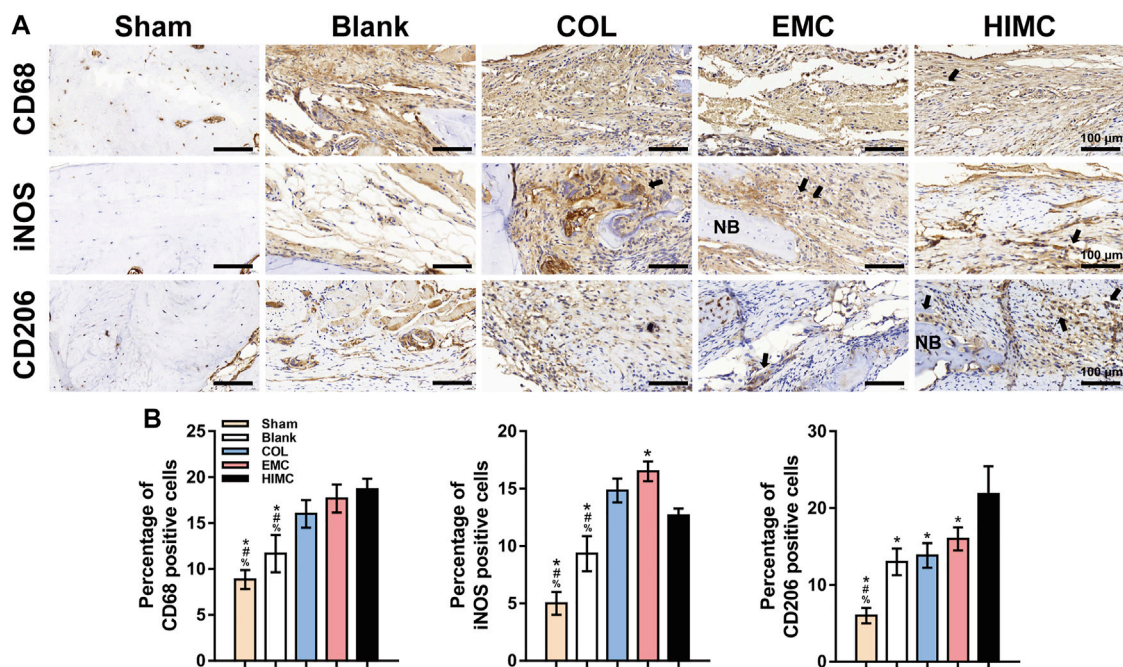


FIGURE 7 | IHC staining for macrophage polarization markers in the defect region of different groups at 2 weeks post-surgery. Positively stained cells are indicated by arrows. **(A)** Pan marker CD68, M1 marker iNOS, and M2 marker CD206 expression in defect tissues. **(B)** Semi-quantification of the positive cells. Data are expressed as mean \pm SD. Scale bar, 100 μ m. * p < 0.05 vs. HIMC membrane; # p < 0.05 vs. EMC membrane; % p < 0.05 vs. COL membrane.

(Liu et al., 2016; Wang et al., 2019). According to the previous research, intrafibrillar mineralization is the main structural source of the biomechanical properties of bone and affects the biological activity of relevant cell types (Balooch et al., 2008). In the present study, we fabricated HIMC membranes with a composite structure consisting of collagen and HA to guide bone regeneration. Compared with EMC and COL, the HIMC

membrane exhibited a clear structure and coarse surface on SEM, with regular interspersed rigid nHA and flexible collagen, providing superior strength similar to that of natural bone. Tensile testing results also showed that the HIMC membrane exhibited less strain under the same stress compared with EMC and COL. On FTIR spectra reflecting the chemical composition and mineral spatial distribution of the materials, the typical peaks

for collagen and phosphate were observed for the HIMC membrane. Water contact angle measurements suggested that the HIMC membrane was more hydrophilic and, thus, was more conducive to interaction between the membrane material and host fluids and cells upon implantation.

To evaluate the potential value of the HIMC membrane for promoting GBR, we first observed the behaviors of BMSCs seeded on different materials *in vitro*. The composition of biomaterials is known to affect cell morphology and adhesion (Ayala et al., 2011; Perez and Ginebra, 2013). BMSCs cultured on the HIMC membrane showed greater proliferation potential and better adhesion and morphology compared with those cultured on EMC or COL. SEM further showed that BMSCs extended large pseudopods on the HIMC membrane surface, whereas little expansion was observed on the other materials. A highly branched actin cytoskeleton and the formation of stress fibers are thought to be highly associated with the differentiation of stem cells along the osteogenic lineage, moreover promote the intracellular signal transduction (Mathieu and Lobo, 2012; Müller et al., 2013; Fu et al., 2016). Our immunofluorescence staining results confirmed that cell fibers within the BMSCs adhered to the HIMC membrane were thick and densely arranged, which may make for BMSCs osteogenic differentiation.

Next, we verified the osteogenic induction capacity of the HIMC membrane through *in vitro* and *in vivo* experiments. The outcomes of our research consistently proved that interaction with HIMC membrane up-regulated the osteogenesis-related genes and proteins in BMSCs during both the early and the late stages of osteogenesis. ARS also showed more calcium deposition and mineralized nodules among BMSCs adhered to the HIMC membrane *in vitro*. In the rat model of critical-sized skull defect, μ -CT and histological staining showed that by 12 weeks after application, the HIMC membrane within the defect had been essentially replaced by new bone tissue, which was not observed in defects filled with EMC or COL. Together the results of this study indicated that the HIMC membrane significantly promoted more bone regeneration and supported the GBR process both *in vivo* and *in vitro*.

Bone defect repair is a dynamic physiological process, and prior to osteogenesis and angiogenesis, the early inflammatory response of immune cells to biomaterials is a major determinant of treatment outcome (Franz et al., 2011). After implantation of biomaterials within a bone defect, osteocytes and immune cells partake a mutual microenvironment (Vishwakarma et al., 2016). As the central regulator of cellular activity within the bone defect area, the immune microenvironment, especially the macrophages affect the efficacy of biomaterial therapy. Previous research has proven that the M1 and M2 phenotype macrophages participate in the early inflammatory response and later bone wound healing, respectively, and that the M2/M1 ratio reflects the response of the local immune microenvironment (Ma et al., 2015; Wood et al., 2019).

CD86 is a costimulatory receptor necessary for T cell activation. CD206, also known as mannose receptor C type 1 (MRC1), is a cell-surface protein abundantly present on macrophages. As for macrophages, CD86 is normally expressed on M1 subtype, while CD206 is expressed on M2

(Barros et al., 2013; Fuchs et al., 2016). Our flow cytometric analysis showed that the rates of CD86⁺ (M1) and CD206⁺ (M2) macrophages exposed to HIMC membrane were 8.96 and 52.94%, which corresponded to the highest percentage of M2 macrophages and the highest M2/M1 ratio. mRNA expression analysis also revealed lower M1 expression and higher M2 expression of cells seeded on the HIMC membrane, further indicating that the macrophages exhibited more M2 polarization on the HIMC membrane. Otherwise, CD163 has also been suggested as an M2 marker, but more recently was shown that CD163 is an M2 marker only in combination with the transcription factor cMaf, thus CD163 cannot be considered as an M2 polarization marker when used alone (Barros et al., 2013). CD68 is a protein found in the granules of macrophages, which is used to co-label cells positive for a certain marker after IHC or *in situ* hybridization to prove they are macrophages (Gordon et al., 2014). Our results from IHC staining of skull defect samples were consistent with those from flow cytometry and qRT-PCR analyses, the HIMC membrane induced more CD68 + CD206 + macrophages polarization. In summary, these data concluded that the HIMC membrane induced more M2 phenotype macrophages both *in vivo* and *in vitro*. Zhou et al. previously reported pro-inflammatory response and damaged lysosomes on macrophages in EMC. Large HA particles impair the normal structure of cells, which may explain why EMC induced more M1 polarization (Jin et al., 2019). Therefore, ordered nHA particles on the HIMC membrane may create a better anti-inflammatory environment.

During normal fracture healing, pro-inflammatory M1 macrophages gradually transform into anti-inflammatory M2 macrophages, which corresponds to the regression of inflammation and the initiation of the osteogenesis process (Schlundt et al., 2018; Zhang et al., 2019). The transformation from M1 to M2 macrophages also contributes to the recruitment of MSCs and the consequent osteogenesis differentiation (Gibon et al., 2016; Weitzmann and Ofotokun, 2016). We investigated the effects of immune microenvironments including macrophages and different materials on the migration of BMSCs via Transwell experiments. Results showed that the HIMC membrane induced migration of the highest number of BMSCs, indicating that the HIMC membrane immune microenvironment may be better capable of recruiting MSCs. Moreover, M2 macrophages on the HIMC membrane express crucial genes to promote BMSCs differentiation such as interleukin (IL)-4 (Jin et al., 2019; Mahon et al., 2020). On another hand, scaffolds loaded with IL-4 for the purpose of promoting M1 to M2 polarization showed promising outcomes in fracture repair models, further demonstrating the beneficial effect of M2 in bone regeneration (Schlundt et al., 2018). To sum up, these findings demonstrated that the HIMC membrane acted not only on MSCs directly, but also more importantly affected the process of osteogenesis by regulating macrophage polarization.

The osteoimmunomodulatory effects of biomaterials are also significantly affected by the physicochemical properties of the materials, like the surface morphology, porosity, and hardness (Chen et al., 2018; Sadowska et al., 2018; Li et al., 2020). The

concept of “nano-bone immunoregulation” proposed by Xiao et al. emphasizes the adjustment of the chemistry and morphology of a nanostructure surface in order to influence the immune response in bone regeneration applications (Karageorgiou and Kaplan, 2005; Chen et al., 2017; Yu et al., 2018). The HIMC membrane prepared in the present study had a coarser surface and BMSCs showed better adhesion and extension on this membrane. These structural features were found to effectively promote the growth and osteogenic differentiation of BMSCs. In addition, the macrophages exhibit greater contact with the increasing roughness of biomaterials. Thus, cell adhesion, migration, proliferation, and differentiation can be directly influenced by precisely controlled changes in the topography of the biomaterial surface. The underlying mechanism involves the effects of physicochemical interactions, kinetics, and thermodynamic exchanges between nanotopography and biological systems on macrophage morphology and the transfer of physicochemical signals from outside to inside a cell to activate a variety of biological reactions (Chen et al., 2017). Therefore, rationally designed nanomaterials offer a promising strategy for enhancing bone regeneration and osteoimmunomodulatory efficacy.

To date, many studies have explored the modification of mineralized collagen materials. One strategy involves adding inorganic components to achieve dopant-induced osteogenesis, and collagen has been loaded or coated with HA modified with metal ions, like magnesium (Yu et al., 2018), silver, gold (Kumar et al., 2019), and zinc (Tiffany et al., 2019). The presence of these metal ions with the biomaterial creates a micro-current effect, which synergistically affects osteogenesis and immune microenvironment (Cai et al., 2017). Overall, the research to date indicates that composite materials with functional modifications are the direction in future biomaterials development. Meanwhile, the next generation of biomaterials for GBR, the design paradigm should shift from physical structures to bioactive structures with osteoimmunomodulatory properties.

The present study has limitations to consider. The concrete data involving osteogenic effects and macrophages polarization of the HIMC membrane remains unclear. The molecular mechanism by which HIMC membrane promotes macrophage polarization is also needed to elucidate. Further investigation will be required in the future.

REFERENCES

- Aprile, P., Letourneur, D., and Simon-Yarza, T. (2020). Membranes for Guided Bone Regeneration: A Road from Bench to Bedside. *Adv. Healthc. Mater.* 9 (19), 2000707. doi:10.1002/adhm.202000707
- Ayala, R., Zhang, C., Yang, D., Hwang, Y., Aung, A., Shroff, S. S., et al. (2011). Engineering the Cell-Material Interface for Controlling Stem Cell Adhesion, Migration, and Differentiation. *Biomaterials* 32 (15), 3700–3711. doi:10.1016/j.biomaterials.2011.02.004
- Balooch, M., Habelitz, S., Kinney, J. H., Marshall, S. J., and Marshall, G. W. (2008). Mechanical Properties of Mineralized Collagen Fibrils as Influenced by Demineralization. *J. Struct. Biol.* 162 (3), 404–410. doi:10.1016/j.jsb.2008.02.010
- Barros, M. H. M., Hauck, F., Dreyer, J. H., Kempkes, B., and Niedobitek, G. (2013). Macrophage Polarisation: an Immunohistochemical Approach for Identifying

CONCLUSION

Based on our findings, the HIMC membrane provided a favorable immune microenvironment for M2 macrophage polarization and osteogenic differentiation of BMSCs by mimicking the composition and nanostructure of natural bone. As a result, the HIMC membrane promotes bone regeneration and plays osteoimmunomodulatory effects, and hence represents a promising membrane material for GBR.

DATA AVAILABILITY STATEMENT

The original contributions presented in the study are included in the article/**Supplementary Material**, further inquiries can be directed to the corresponding authors.

ETHICS STATEMENT

The animal study was reviewed and approved by the Ethics Committee for Animal Experiments of Shanghai Jiao Tong University, Shanghai, China.

AUTHOR CONTRIBUTIONS

All authors listed have made a substantial, direct, and intellectual contribution to the work and approved it for publication.

FUNDING

This work was funded by National Key R&D Program of China (2020YFC2008900).

SUPPLEMENTARY MATERIAL

The Supplementary Material for this article can be found online at: <https://www.frontiersin.org/articles/10.3389/fbioe.2021.781268/full#supplementary-material>

M1 and M2 Macrophages. *PLoS one* 8 (11), e80908. doi:10.1371/journal.pone.0080908

- Cai, X., Han, B., Liu, Y., Tian, F., Liang, F., and Wang, X. (2017). Chlorhexidine-Loaded Amorphous Calcium Phosphate Nanoparticles for Inhibiting Degradation and Inducing Mineralization of Type I Collagen. *ACS Appl. Mater. Inter.* 9 (15), 12949–12958. doi:10.1021/acsami.6b14956
- Chen, Z., Bachhuka, A., Wei, F., Wang, X., Liu, G., Vasilev, K., et al. (2017). Nanotopography-based Strategy for the Precise Manipulation of Osteoimmunomodulation in Bone Regeneration. *Nanoscale* 9 (46), 18129–18152. doi:10.1039/c7nr05913b
- Chen, Z., Chen, L., Liu, R., Lin, Y., Chen, S., Lu, S., et al. (2018). The Osteoimmunomodulatory Property of a Barrier Collagen Membrane and its Manipulation via Coating Nanometer-Sized Bioactive Glass to Improve Guided Bone Regeneration. *Biomater. Sci.* 6 (5), 1007–1019. doi:10.1039/c7bm00869d

- Chu, C., Deng, J., Sun, X., Qu, Y., and Man, Y. (2017). Collagen Membrane and Immune Response in Guided Bone Regeneration: Recent Progress and Perspectives. *Tissue Eng. B: Rev.* 23 (5), 421–435. doi:10.1089/ten.TEB.2016.0463
- Fillingham, Y., and Jacobs, J. (2016). Bone Grafts and Their Substitutes. *Bone Jt. J.* 98-B, 6–9. doi:10.1302/0301-620x.98b.36350
- Franz, S., Rammelt, S., Scharnweber, D., and Simon, J. C. (2011). Immune Responses to Implants - a Review of the Implications for the Design of Immunomodulatory Biomaterials. *Biomaterials* 32 (28), 6692–6709. doi:10.1016/j.biomaterials.2011.05.078
- Freytes, D. O., Kang, J. W., Marcos-Campos, I., and Vunjak-Novakovic, G. (2013). Macrophages Modulate the Viability and Growth of Human Mesenchymal Stem Cells. *J. Cel. Biochem.* 114 (1), 220–229. doi:10.1002/jcb.24357
- Fu, Y., Liu, S., Cui, S.-J., Kou, X.-X., Wang, X.-D., Liu, X.-M., et al. (2016). Surface Chemistry of Nanoscale Mineralized Collagen Regulates Periodontal Ligament Stem Cell Fate. *ACS Appl. Mater. Inter.* 8 (25), 15958–15966. doi:10.1021/acsami.6b04951
- Fuchs, A.-K., Syrovets, T., Haas, K. A., Loos, C., Musyanovych, A., Mäiländer, V., et al. (2016). Carboxyl- and Amino-Functionalized Polystyrene Nanoparticles Differentially Affect the Polarization Profile of M1 and M2 Macrophage Subsets. *Biomaterials* 85, 78–87. doi:10.1016/j.biomaterials.2016.01.064
- Gibon, E., Lu, L., and Goodman, S. B. (2016). Aging, Inflammation, Stem Cells, and Bone Healing. *Stem Cell Res Ther* 7, 44. doi:10.1186/s13287-016-0300-9
- Gordon, S., Plüddemann, A., and Martinez Estrada, F. (2014). Macrophage Heterogeneity in Tissues: Phenotypic Diversity and Functions. *Immunol. Rev.* 262 (1), 36–55. doi:10.1111/imr.12223
- Hu, C., Zilm, M., and Wei, M. (2016). Fabrication of Intrafibrillar and Extrafibrillar Mineralized Collagen/apatite Scaffolds with a Hierarchical Structure. *J. Biomed. Mater. Res.* 104 (5), 1153–1161. doi:10.1002/jbm.a.35649
- Jin, S.-S., He, D.-Q., Luo, D., Wang, Y., Yu, M., Guan, B., et al. (2019). A Biomimetic Hierarchical Nanointerface Orchestrates Macrophage Polarization and Mesenchymal Stem Cell Recruitment to Promote Endogenous Bone Regeneration. *ACS nano* 13 (6), 6581–6595. doi:10.1021/acsnano.9b00489
- Kane, R., and Ma, P. X. (2013). Mimicking the Nanostructure of Bone Matrix to Regenerate Bone. *Mater. Today* 16 (11), 418–423. doi:10.1016/j.mattod.2013.11.001
- Karageorgiou, V., and Kaplan, D. (2005). Porosity of 3D Biomaterial Scaffolds and Osteogenesis. *Biomaterials* 26 (27), 5474–5491. doi:10.1016/j.biomaterials.2005.02.002
- Kumar, V. B., Khajuria, D. K., Karasik, D., and Gedanken, A. (2019). Silver and Gold Doped Hydroxyapatite Nanocomposites for Enhanced Bone Regeneration. *Biomed. Mater.* 14 (5), 055002. doi:10.1088/1748-605X/ab28e4
- Li, J., Zhang, Y.-J., Lv, Z.-Y., Liu, K., Meng, C.-X., Zou, B., et al. (2020). The Observed Difference of Macrophage Phenotype on Different Surface Roughness of Mineralized Collagen. *Regenerative Biomater.* 7 (2), 203–211. doi:10.1093/rb/rbz053
- Lian, K., Lu, H., Guo, X., Cui, F., Qiu, Z., and Xu, S. (2013). The Mineralized Collagen for the Reconstruction of Intra-articular Calcaneal Fractures with Trabecular Defects. *Biomater* 3 (4), e27250. doi:10.4161/biom.27250
- Liao, S. S., Cui, F. Z., Zhang, W., and Feng, Q. L. (2004). Hierarchically Biomimetic Bone Scaffold Materials: Nano-HA/collagen/PLA Composite. *J. Biomed. Mater. Res.* 69B (2), 158–165. doi:10.1002/jbm.b.20035
- Lin, Z., Shen, D., Zhou, W., Zheng, Y., Kong, T., Liu, X., et al. (2021). Regulation of Extracellular Bioactive Cations in Bone Tissue Microenvironment Induces Favorable Osteoimmune Conditions to Accelerate *In Situ* Bone Regeneration. *Bioactive Mater.* 6 (8), 2315–2330. doi:10.1016/j.bioactmat.2021.01.018
- Liu, Y., Liu, S., Luo, D., Xue, Z., Yang, X., Gu, L., et al. (2016). Hierarchically Staggered Nanostructure of Mineralized Collagen as a Bone-Grafting Scaffold. *Adv. Mater.* 28 (39), 8740–8748. doi:10.1002/adma.201602628
- Liu, Y., Luo, D., Liu, S., Fu, Y., Kou, X., Wang, X., et al. (2014). Effect of Nanostructure of Mineralized Collagen Scaffolds on Their Physical Properties and Osteogenic Potential. *J. Biomed. nanotechnol* 10 (6), 1049–1060. doi:10.1166/jbn.2014.1794
- Ma, J., Liu, R., Wang, X., Liu, Q., Chen, Y., Valle, R. P., et al. (2015). Crucial Role of Lateral Size for Graphene Oxide in Activating Macrophages and Stimulating Pro-inflammatory Responses in Cells and Animals. *ACS nano* 9 (10), 10498–10515. doi:10.1021/acsnano.5b04751
- Mahon, O. R., Browe, D. C., Gonzalez-Fernandez, T., Pitacco, P., Whelan, I. T., Von Euw, S., et al. (2020). Nano-particle Mediated M2 Macrophage Polarization Enhances Bone Formation and MSC Osteogenesis in an IL-10 Dependent Manner. *Biomaterials* 239, 119833. doi:10.1016/j.biomaterials.2020.119833
- Mathieu, P. S., and Lobo, E. G. (2012). Cytoskeletal and Focal Adhesion Influences on Mesenchymal Stem Cell Shape, Mechanical Properties, and Differentiation Down Osteogenic, Adipogenic, and Chondrogenic Pathways. *Tissue Eng. Part B: Rev.* 18 (6), 436–444. doi:10.1089/ten.TEB.2012.0014
- Müller, P., Langenbach, A., Kaminski, A., and Rychly, J. (2013). Modulating the Actin Cytoskeleton Affects Mechanically Induced Signal Transduction and Differentiation in Mesenchymal Stem Cells. *PLoS one* 8 (7), e71283. doi:10.1371/journal.pone.0071283
- Perez, R. A., and Ginebra, M.-P. (2013). Injectable Collagen/ α -Tricalcium Phosphate Cement: Collagen-mineral Phase Interactions and Cell Response. *J. Mater. Sci. Mater. Med.* 24 (2), 381–393. doi:10.1007/s10856-012-4799-8
- Sadowska, J. M., Wei, F., Guo, J., Guillem-Marti, J., Ginebra, M.-P., and Xiao, Y. (2018). Effect of Nano-Structural Properties of Biomimetic Hydroxyapatite on Osteoimmunomodulation. *Biomaterials* 181, 318–332. doi:10.1016/j.biomaterials.2018.07.058
- Schlundt, C., El Khassawna, T., Serra, A., Dienelt, A., Wendler, S., Schell, H., et al. (2018). Macrophages in Bone Fracture Healing: Their Essential Role in Endochondral Ossification. *Bone* 106, 78–89. doi:10.1016/j.bone.2015.10.019
- Schmidt-Bleek, K., Schell, H., Lienau, J., Schulz, N., Hoff, P., Pfaff, M., et al. (2014). Initial Immune Reaction and Angiogenesis in Bone Healing. *J. Tissue Eng. Regen. Med.* 8 (2), 120–130. doi:10.1002/term.1505
- Shi, X.-D., Chen, L.-W., Li, S.-W., Sun, X.-D., Cui, F.-Z., and Ma, H.-M. (2018). The Observed Difference of RAW264.7 Macrophage Phenotype on Mineralized Collagen and Hydroxyapatite. *Biomed. Mater.* 13 (4), 041001. doi:10.1088/1748-605X/aab523
- Sun, Y., Wang, C.-Y., Wang, Z.-Y., Cui, Y., Qiu, Z.-Y., Song, T.-X., et al. (2016). Test in Canine Extraction Site Preservations by Using Mineralized Collagen Plug with or without Membrane. *J. Biomater. Appl.* 30 (9), 1285–1299. doi:10.1177/0885328215625429
- Tanaka, R., Saito, Y., Fujiwara, Y., Jo, J.-i., and Tabata, Y. (2019). Preparation of Fibrin Hydrogels to Promote the Recruitment of Anti-inflammatory Macrophages. *Acta Biomater.* 89, 152–165. doi:10.1016/j.actbio.2019.03.011
- Tiffany, A. S., Gray, D. L., Woods, T. J., Subedi, K., and Harley, B. A. C. (2019). The Inclusion of Zinc into Mineralized Collagen Scaffolds for Craniofacial Bone Repair Applications. *Acta Biomater.* 93, 86–96. doi:10.1016/j.actbio.2019.05.031
- Vishwakarma, A., Bhise, N. S., Evangelista, M. B., Rouwkema, J., Dokmeci, M. R., Ghaemmaghami, A. M., et al. (2016). Engineering Immunomodulatory Biomaterials to Tune the Inflammatory Response. *Trends Biotechnol* 34 (6), 470–482. doi:10.1016/j.tibtech.2016.03.009
- Wang, J., Qu, Y., Chen, C., Sun, J., Pan, H., Shao, C., et al. (2019). Fabrication of Collagen Membranes with Different Intrafibrillar Mineralization Degree as a Potential Use for GBR. *Mater. Sci. Eng. C* 104, 109959. doi:10.1016/j.msec.2019.109959
- Weitzmann, M. N., and Ofotokun, I. (2016). Physiological and Pathophysiological Bone Turnover - Role of the Immune System. *Nat. Rev. Endocrinol.* 12 (9), 518–532. doi:10.1038/nrendo.2016.91
- Wood, M. J., Leckenby, A., Reynolds, G., Spiering, R., Pratt, A. G., Rankin, K. S., et al. (2019). Macrophage Proliferation Distinguishes 2 Subgroups of Knee Osteoarthritis Patients. *JCI insight* 4 (2), e125325. doi:10.1172/jci.insight.125325
- Wynn, T. A., and Vannella, K. M. (2016). Macrophages in Tissue Repair, Regeneration, and Fibrosis. *Immunity* 44 (3), 450–462. doi:10.1016/j.immuni.2016.02.015
- Xu, S.-J., Qiu, Z.-Y., Wu, J.-J., Kong, X.-D., Weng, X.-S., Cui, F.-Z., et al. (2016). Osteogenic Differentiation Gene Expression Profiling of hMSCs on Hydroxyapatite and Mineralized Collagen. *Tissue Engineering. Part. A.* 22, 170–181. doi:10.1089/ten.tea.2015.0237
- Yu, L., Rowe, D. W., Perera, I. P., Zhang, J., Suib, S. L., Xin, X., et al. (2020). Intrafibrillar Mineralized Collagen-Hydroxyapatite-Based Scaffolds for Bone

- Regeneration. *ACS Appl. Mater. Inter.* 12 (16), 18235–18249. doi:10.1021/acsami.0c00275
- Yu, Q., Wang, C., Yang, J., Guo, C., and Zhang, S. (2018). Mineralized collagen/Mg-Ca alloy Combined Scaffolds with Improved Biocompatibility for Enhanced Bone Response Following Tooth Extraction. *Biomed. Mater.* 13 (6), 065008. doi:10.1088/1748-605X/aadb47
- Yu, T., Zhao, L., Huang, X., Ma, C., Wang, Y., Zhang, J., et al. (2016). Enhanced Activity of the Macrophage M1/M2 Phenotypes and Phenotypic Switch to M1 in Periodontal Infection. *J. Periodontol.* 87 (9), 1092–1102. doi:10.1902/jop.2016.160081
- Zhang, R., Liu, X., Xiong, Z., Huang, Q., Yang, X., Yan, H., et al. (2018). The Immunomodulatory Effects of Zn-Incorporated Micro/nanostructured Coating in Inducing Osteogenesis. *Artif. Cell nanomedicine, Biotechnol.* 46, 1123–1130. doi:10.1080/21691401.2018.1446442
- Zhang, Z., Li, Z., Zhang, C., Liu, J., Bai, Y., Li, S., et al. (2018). Biomimetic Intrafibrillar Mineralized Collagen Promotes Bone Regeneration via Activation of the Wnt Signaling Pathway. *Int. J. Nanomedicine* 13, 7503–7516. doi:10.2147/ijn.S172164
- Zhang, Z., Zhang, S., Li, Z., Li, S., Liu, J., and Zhang, C. (2019). Osseointegration Effect of Biomimetic Intrafibrillarly Mineralized Collagen Applied Simultaneously with Titanium Implant: A Pilot In Vivo Study. *Clin. Oral Impl Res.* 30 (7), 637–648. doi:10.1111/clr.13449
- Zhou, T., Chen, S., Ding, X., Hu, Z., Cen, L., and Zhang, X. (2021). Fabrication and Characterization of Collagen/PVA Dual-Layer Membranes for Periodontal Bone Regeneration. *Front. Bioeng. Biotechnol.* 9, 630977. doi:10.3389/fbioe.2021.630977

Conflict of Interest: The authors declare that the research was conducted in the absence of any commercial or financial relationships that could be construed as a potential conflict of interest.

Publisher's Note: All claims expressed in this article are solely those of the authors and do not necessarily represent those of their affiliated organizations, or those of the publisher, the editors, and the reviewers. Any product that may be evaluated in this article, or claim that may be made by its manufacturer, is not guaranteed or endorsed by the publisher.

Copyright © 2022 Xuan, Li, Ma, Cao and Zhang. This is an open-access article distributed under the terms of the Creative Commons Attribution License (CC BY). The use, distribution or reproduction in other forums is permitted, provided the original author(s) and the copyright owner(s) are credited and that the original publication in this journal is cited, in accordance with accepted academic practice. No use, distribution or reproduction is permitted which does not comply with these terms.



Effects of Plant Extracts on Dentin Bonding Strength: A Systematic Review and Meta-Analysis

Shikai Zhao^{1†}, Fang Hua^{2,3†}, Jiarong Yan¹, Hongye Yang^{1,4*} and Cui Huang^{1,4*}

¹The State Key Laboratory Breeding Base of Basic Science of Stomatology (Hubei-MOST) and Key Laboratory for Oral Biomedical Ministry of Education, School and Hospital of Stomatology, Wuhan University, Wuhan, China, ²Department of Orthodontics, Center for Evidence-Based Stomatology, School and Hospital of Stomatology, Wuhan University, Wuhan, China, ³Division of Dentistry, School of Medical Sciences, Faculty of Biology, Medicine and Health, Manchester Academic Health Science Centre, University of Manchester, Manchester, United Kingdom, ⁴Department of Prosthodontics, School and Hospital of Stomatology, Wuhan University, Wuhan, China

OPEN ACCESS

Edited by:

Kumar Chandan Srivastava,
Al Jouf University, Saudi Arabia

Reviewed by:

Monica Yamauti,
Hokkaido University, Japan
Joanna Mystkowska,
Bialystok University of Technology,
Poland

*Correspondence:

Hongye Yang
yanghongye@whu.edu.cn
Cui Huang
huangcui@whu.edu.cn

[†]These authors have contributed
equally to this work

Specialty section:

This article was submitted to
Biomaterials,
a section of the journal
Frontiers in Bioengineering and
Biotechnology

Received: 15 December 2021

Accepted: 31 January 2022

Published: 24 February 2022

Citation:

Zhao S, Hua F, Yan J, Yang H and
Huang C (2022) Effects of Plant
Extracts on Dentin Bonding Strength:
A Systematic Review and Meta-
Analysis.
Front. Bioeng. Biotechnol. 10:836042.
doi: 10.3389/fbioe.2022.836042

Objective: To systematically review *in vitro* studies that evaluated the effects of plant extracts on dentin bonding strength.

Materials and Methods: Six electronic databases (PubMed, Embase, VIP, CNKI, Wanfang and The Cochrane Library) were searched from inception to September 2021 in accordance with the Preferred Reporting Items for Systematic Reviews (PRISMA). *In vitro* studies that compared the performance of dental adhesives with and without the plant extracts participation were included. The reference lists of the included studies were manually searched. Two researchers carried out study screening, data extraction and risk of bias assessment, independently and in duplicate. Meta-analysis was conducted using Review Manager 5.3.

Results: A total of 62 studies were selected for full-text analysis. 25 articles used the plant extracts as primers, while five added the plant extracts into adhesives. The meta-analysis included 14 articles of *in vitro* studies investigating the effects of different plant extract primers on dentin bonding strength of etch-and-rinse and self-etch adhesives, respectively. The global analysis showed statistically significant difference between dental adhesives with and without plant extract primers. It showed that the immediate bond strength of dental adhesives was improved with the application of plant extract primers.

Conclusion: The application of proanthocyanidin (PA) primers have positive effect on the *in vitro* immediate bonding strength of dental adhesives irrespective of etch-and-rinse or self-etch modes.

Keywords: dentin, bonding, plant extracts, natural crosslinkers, adhesives, primers

INTRODUCTION

Dentin bonding is the foundation of esthetic restoration (Drummond, 2008). Nowadays, manufacturers claim that dental adhesive system has already developed to the eighth generation (Taneja et al., 2017). However, irrespective of acceptable immediate bonds, the long-term bonding strength of these adhesives is inadequate (Deligeorgi et al., 2001; Hass et al., 2016a). As a result, nearly half of esthetic restorations cannot serve for more than 10 years, and dentists have to spend 60% of

working hours to replace them (Mjor et al., 2000; Deligeorgi et al., 2001). Thus, the improvement of long-term bond strength is still a puzzle that needs to be solved.

Unsatisfactory long-term dentin bonds are usually attributed to two reasons: The degradation of dentin collagen within the hybrid layer; and the emergence of secondary caries at the interface (Brackett et al., 2011). A reasonable strategy to solve these problems is to modify contemporary dental adhesives with different additives, such as chlorhexidine, nano-silver, carbon nanotube and amorphous calcium phosphate (Carrilho et al., 2007; Borges et al., 2013; Zhang et al., 2013; Alkhatheeri et al., 2015). Amongst these additives, plant extracts attracted great attention due to their biological safety and functional versatility (Gotti et al., 2015; Yang et al., 2017; Yu et al., 2017). Many articles have reported the advantages of natural plant extracts, including their capability to stabilize dentin collagen (La et al., 2009), and to inhibit MMPs (Du et al., 2012; Yang et al., 2016) and microbes (Kaul et al., 1985; Rigano et al., 2007). Therefore, many researchers have been attempting to dope plant extracts into adhesives or provide a separate plant extract primer to achieve high antibiotic property and improved long-term bond strength (La et al., 2009; Borges et al., 2013; Gotti et al., 2015; Yang et al., 2017).

However, the combination of different adhesives with different plant extracts may produce unpredictable results, and different concentration of plant extract primer may have different bonding performance (Macedo et al., 2009; Islam et al., 2014). Previous studies have tested a limited amount of plant extracts, using different experimental designs, with contradictory conclusions. Thus, a comprehensive overview summarizing the effect of all existing plant extracts on dental adhesives will be helpful for dental clinicians and relevant researchers.

The objectives of this study are to systematically review the *in vitro* studies that evaluated adhesive-dentin bond strength with or without plant extracts participation and to compare different plant extracts in terms of bond strength. The hypotheses are: no difference exists in the bond strengths when modifying the adhesives with plant extracts; no difference exists in the bond strengths when plant extract primers are used; no difference exists in the bond strength when using different concentrations of plant extracts.

MATERIALS AND METHODS

Criteria for Considering Studies for This Review

Inclusion Criteria

- Studies that added plant extracts to dental adhesives or used plant extract as primers.
- Studies that compared the performance of dental adhesives with and without the participation of plant extracts.
- *In vitro* studies that evaluated the bond strength of dental adhesives.

Exclusion criteria

Reviews, clinical trials or case reports.

Search Strategy

A systematic electronic search was conducted by two independent reviewers (SZ and HY) using nine databases (PubMed, Embase, Web of Science, Cochrane Library, VIP, CNKI, Wanfang, OpenGrey literature and ProQuest Dissertation Abstracts) from inception to September 2021 to identify articles related to plant extracts and dental bonding. The search terms were a combination of subject terms and free-text terms (**Appendix Table A1**).

When multiple publications about the same intervention were identified, the most informative and relevant article was selected for inclusion.

Data Collection and Analysis

Selection of Studies

Article titles and abstracts were independently screened by two authors (SZ and HY). The authors conducted a second review when the inclusion criteria were met. The abstracts were examined by two review authors (SZ and HY) independently using the same inclusion criteria. If there were disagreements, the abstract would be assessed by the third author (FH). Then full text of all potentially relevant studies were retrieved and independently assessed in duplicate by two review authors (SZ and HY). Any disagreement regarding the eligibility of the included studies was resolved through discussion with the third reviewer.

Data Extraction and Management

Data extraction was performed independently by two authors (SZ and HY). The demographic data, plant extracts used, plant extract concentration, bonding systems, as well as outcomes were recorded (**Table 1**). If any information was missing, we contacted the corresponding authors *via* email.

Quality Assessment

Two reviewers (SZ and HY) independently assessed the risk of bias of the included studies with the assessment instrument used in a previous systematic review of *in vitro* studies (Sarkis-Onofre et al., 2014). Quality assessment parameters included randomized teeth, teeth free of caries or restoration, operation following the manufacturer's instructions, given sample size, and the bonding procedures were performed by a single operator with or without blinding. The article would be given a "Yes" on the parameter if it was reported and performed appropriately in the article; and a "No" if it was not mentioned or not performed properly. Articles were classified into three levels of risk of bias according to the number of parameters that scored "Yes": high (≤ 2 parameters), medium (3-4 parameters), and low (5-6 parameters) (**Table 2**).

Statistical Analysis

Meta-analysis was conducted using Review Manager 5.3. Each possible comparison of the bond strength of dental adhesives with or without plant extracts participation was undertaken. In order to minimize the heterogeneity, only *in vitro* studies comparing the same plant extracts with the same concentration was included

TABLE 1 | Characteristics of the included studies.

First author	Year	Country	Publication	Plant extracts	Action modes	Plant extracts concentration	Dental adhesives	Outcome
Albuquerque N	2019	Brazil	Oper Dent	EGCG	Adhesive	0.1% w/v	Single Bond 2 (3M ESPE, St. Paul, MN, United States)	MTBS
Yang H	2017	China	SCI REP	Quercetin	Adhesive	100, 500 and 1,000 µg/ml	Single Bond 2	MTBS
Yu HH	2017	China	Materials (Basel)	EGCG, EGCG-3Me	Adhesive	200, 400, and 600 µg/ml	Single Bond 2	MTBS
Gotti VB	2015	Brazil	J Adhes Dent	Quercetin	Adhesive	5 wt%	Single Bond 2; Clearfil SE Bond (Kuraray Noritake Dental; Tokyo, Japan); Easy Bond (3M ESPE, St. Paul, MN, United States)	MTBS
Du X	2012	China	J Dent	EGCG	Adhesive	100, 200, and 300 µg/ml	Single Bond 2	MTBS
Peng W	2020	China	Materials Science and Engineering C	Resveratrol	Primer	1, 10, and 20 µg/ml	Single Bond Universal	MTBS
Zhang Z	2020	China	Dental Materials	EGCG	Primer	0.01%, 0.1%, 1%	Single Bond Universal	MTBS
Landmayer K	2020	Brazil	J Prosthet Dent	EGCG; Proanthocyanidin (PA)	Primer	EGCG at 400 µM; 10% PA	Single Bond 2	MTBS
Dávila-Sánchez A	2020	Chile	Dent Mater	Quercetin; Hesperidin; Rutin; Naringin; Proanthocyanidin	Primer	0.065	Single Bond Universal	MTBS
de Siqueira FSF	2020	Brazil	Clin Oral Investig	Proanthocyanidin	Primer	0.065	Prime and Bond Elect (Dentsply Sirona, Milford, DE, United States); Single Bond Universal; Tetric n-Bond Universal (Ivoclar Vivadent AG, Schaan, Liechtenstein)	MTBS
Yi L	2019	China	J Dent	Baicalin	Primer	0.01%, 0.05%, and 1% w/v	Single Bond Universal	MTBS
Albuquerque N	2019	Brazil	Oper Dent	EGCG	Primer	0.1% EGCG; or 1% PLGA/EGCG	Single Bond 2	MTBS
Costa CAG	2019	Brazil	J Adhes Dent	EGCG	Primer	0.1% EGCG; or 2% CHX	Clearfil SE Bond	MTBS
Fialho MPN	2019	Brazil	J Mech Behav Biomed Mater	EGCG	Primer	0.02%; 0.2%; 0.5%	Single Bond 2	MTBS
Li J	2018	China	Oper Dent	Baicalin	Primer	0.1, 0.5, 2.5, and 5.0 µg/ml	Single Bond 2	MTBS
Porto ICCM	2018	Brazil	Eur J Oral Sci	Quercetin; Resveratrol	Primer	100, 250, 500, or 1,000 µg ml, a mixture of quercetin and resveratrol (3:1, 1:1, 1:3; vol:vol)	Single Bond Universal	MTBS
Bacelar-Sá R	2017	Brazil	Braz Dent J	Proanthocyanidin	Primer	0.065	Single Bond Universal; Prime and Bond Elect; All-Bond 3 (Bisco Inc., Schaumburg, IL, United States); G-Aenial (GC Corp., Tokyo, Japan)	MTBS
Li K	2017	China	RSC Adv	Quercetin	Primer	0.1, 0.5, and 1 wt%	Single Bond 2	MTBS
Zheng P	2017	China	Sci Rep	Proanthocyanidin	Primer	0.05	Single Bond 2	MTBS
Zhou J	2016	China	Dent Mater	Grape seed extract	Primer	5 mass%	Single Bond 2	MTBS
Hass V	2016	Brazil	Dent Mater	Proanthocyanidin	Primer	6.5 wt%	Single Bond Plus; Tetric N-Bond	MTBS
Yang H	2016	United States	J Dent	EGCG	Primer	0.02% and 0.1%	Single Bond 2	MTBS
Zheng P	2015	China	Oper Dent	Grape seed extract	Primer	0.0005	OptiBond FL (Kerr, Scafati, Italy); Clearfil SE Bond	MTBS
Islam MS	2014	Japan	Dent Mater	Proanthocyanidin; Hesperidin	Primer	0.5%, 1%, 2%, 5% of hesperidin (HPN) or 0.5% of proanthocyanidins (PA)	Clearfil SE Bond	MTBS
Liu RR	2014	China	Int J Oral Sci	Proanthocyanidin	Primer	10% or 15%	Single Bond 2	MTBS
Santiago SL	2013	Brazil	J Adhes Dent	EGCG	Primer	0.02%, 0.1%, or 0.5% w/v	Single Bond 2	MTBS
Broyles AC	2013	United States	J Prosthodont	Grape seed extract	Primer	0.065	RelyX Unicem (3M ESPE, St. Paul, MN, United States); G-Cem self-adhesive cements (GC America, Alsip, IL)	MTBS

(Continued on following page)

TABLE 1 | (Continued) Characteristics of the included studies.

First author	Year	Country	Publication	Plant extracts	Action modes	Plant extracts concentration	Dental adhesives	Outcome
Liu RR	2012	China	Zhonghua Kou Qiang Yi Xue Za Zhi	Proanthocyanidin	Primer	0.15	Single Bond 2	MTBS
Macedo GV	2009	United States	J Dent Res	Grape seed extract	Primer	0.065	Single Bond 2; One Step Plus (Bisco, Schaumburg, IL, United States)	MTBS
Al-Ammar A	2009	United States	J Biomed Mater Res B Appl Biomater	Grape seed extract; Genipin	Primer	6.5% GSE; 0.5% GE	One Step Plus; Single Bond Plus	MTBS

Abbreviation: EGCG, epigallocatechin-3-gallate; EGCG-3Me, epigallocatechin-3-O-(3-O-methyl)-gallate; GSE, grape seed extract; GE, genipin.

TABLE 2 | Risk of bias of the studies considering aspects reported in the Materials and Methods section.

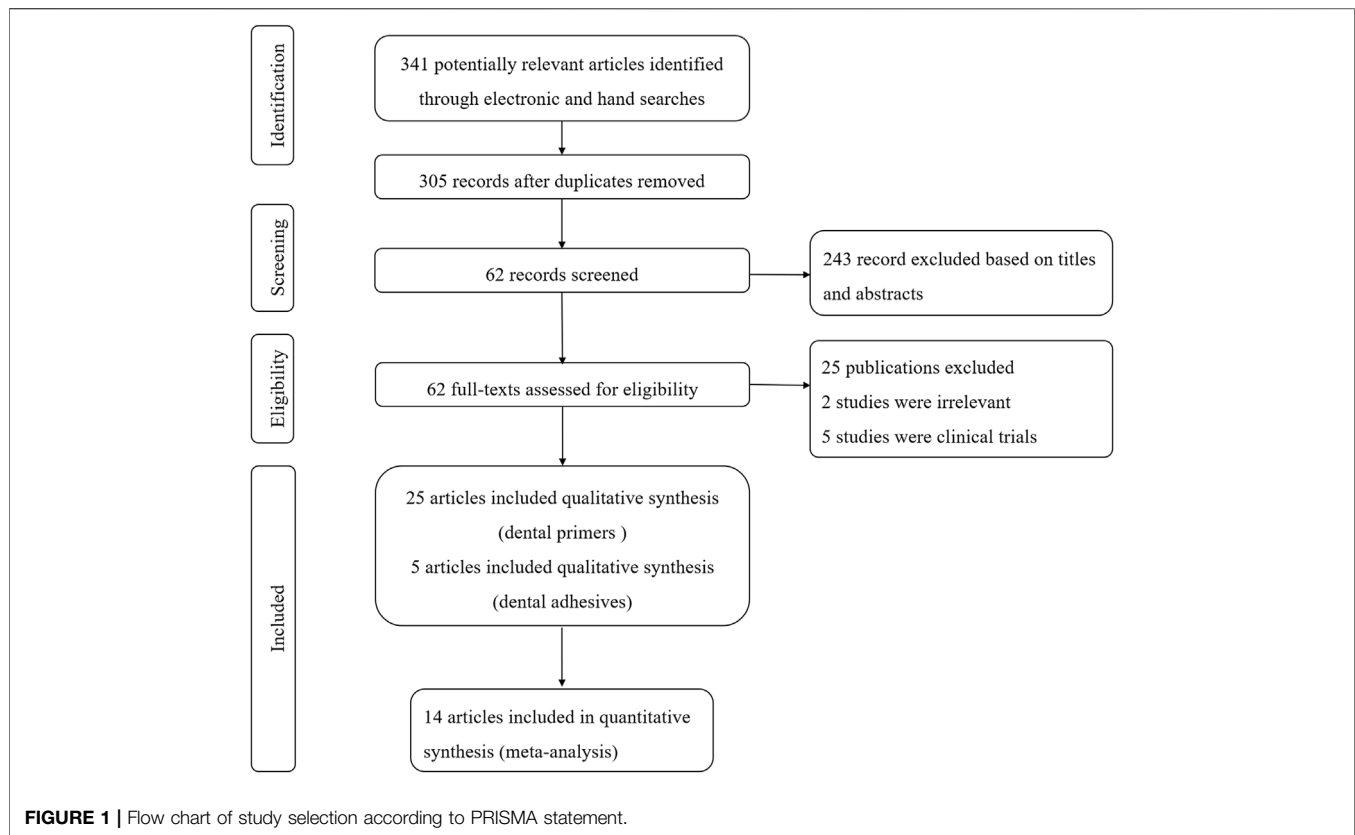
Study	Year	Random	Caries	Adhesive	Sample	Operator	Blind	Risk
Peng W	2020	Y	Y	Y	Y	Y	N	Low
Zhang Z	2020	Y	N	Y	Y	Y	N	Medium
Landmayer K	2020	N	Y	Y	Y	N	N	Medium
Dávila-Sánchez A	2020	Y	Y	Y	Y	Y	N	Low
de Siqueira FSF	2020	Y	Y	Y	Y	Y	N	Low
Albuquerque N	2019	Y	Y	Y	Y	N	N	Medium
Yi L	2019	Y	Y	Y	Y	Y	N	Low
Albuquerque N	2019	N	Y	Y	Y	N	N	Medium
Costa CAG	2019	Y	Y	Y	Y	N	N	Medium
Fialho MPN	2019	N	Y	Y	Y	Y	N	Medium
Li J	2018	Y	Y	Y	Y	N	N	Medium
Porto ICCM	2018	Y	Y	Y	Y	N	N	Medium
Yang H	2017	Y	Y	Y	Y	N	N	Medium
Yu HH	2017	Y	Y	Y	Y	N	N	Medium
Bacelar-Sá R	2017	N	Y	Y	Y	N	N	Medium
Li K	2017	Y	Y	Y	Y	N	N	Medium
Zheng P	2017	N	Y	Y	Y	N	N	Medium
Zhou J	2016	N	Y	Y	Y	N	N	Medium
Hass V	2016	N	Y	Y	Y	N	N	Medium
Yang H	2016	N	Y	Y	Y	Y	N	Medium
Gotti VB	2015	Y	N	Y	Y	N	N	Medium
Zheng P	2015	Y	Y	Y	Y	N	N	Medium
Islam MS	2014	N	Y	Y	Y	N	N	Medium
Liu RR	2014	Y	Y	Y	Y	N	N	Medium
Santiago SL	2013	N	Y	Y	Y	N	N	Medium
Broyles AC	2013	Y	Y	Y	Y	N	N	Medium
Du X	2012	Y	N	Y	Y	N	N	Medium
Liu RR	2012	Y	Y	Y	Y	N	N	Medium
Macedo GV	2009	Y	Y	Y	Y	N	N	Medium
Al-Ammar A	2009	Y	Y	Y	Y	N	N	Medium

in the global analysis. The mean difference with 95% confidence interval (CI) was calculated and $p \leq 0.05$ was considered significant. Statistical heterogeneity was assessed using the modified chi-square test (Cochran's Q), which indicates heterogeneity when $p > 0.1$, and I^2 test, which indicates heterogeneity when its values is greater than 50%. Random-effect model was used in the analysis. The publication bias was to be assessed if more than ten studies were included in a meta-analysis. Sensitivity analysis was also performed by sequentially excluding each study if there were sufficient studies (≥ 10).

RESULTS

Search Strategy and Characteristics

The initial search yielded 341 articles, out of which, 36 articles were eliminated after screening of titles and removal of duplicates. After abstract screening, 243 articles were excluded. A resultant sample of 62 articles was carried forward to the next stage, in which full-text copies were scrutinized. Finally, a total of 30 studies were systematically reviewed, in which 5 studies added plant extracts into adhesives and 25 studies used plant extract solution as primers (**Figure 1**). Twenty-nine articles were in



English and 1 were in Chinese. There are nine types of plant extracts and 15 types of adhesives involved (Table 1).

Risk of Bias

Most of the 30 studies (86.7%) exhibited a medium risk of bias, except for four (13.3%) with a low risk of bias. All of the studies used the adhesive according to the manufacturer's instructions and described sample size calculation, but none of the studies reported blinding. A total of 20 studies (66.7%) reported random assignment of teeth, and 27 studies (90%) used teeth free of caries. Only seven studies (23.3%) reported adhesive procedure performed by a single operator. The results are described in Figure 2 and Table 2.

Meta-Analysis

In the studies included in the meta-analysis, we only choose the data of interest. Only commercial adhesives were included, and the studies used experimental adhesives were excluded (Epasinghe et al., 2012). The effect of plant extracts on bonding strength may be related to different bonding modes such as self-etch or etch-and-rinse (Macedo et al., 2009; Bacelar-Sa et al., 2017). Hence, the disparity of the bond strength of different plant extracts in self-etch or etch-and-rinse adhesives was compared. Because aging methods were highly heterogeneous (i.e., water storage, saliva storage and PH cycling), it was not considered in the meta-analysis (Deng et al., 2014).

Due to the fact that different concentrations of plant extracts were used, only those with the same concentration were taken into meta-analysis. Of the 30 studies, data from 14 papers in which

plant extract solution serve as primers underwent meta-analysis. The results of the meta-analysis are shown in Figures 3–5.

Etch-and-Rinse Bond Strength (Plant Extract Primers)

The first analysis (etch-and rinse adhesive with or without plant extract primers) was performed, and the different concentration of plant extracts were the subgroups. A total of 29 datasets were selected, while 14 studies were included (Figure 3), with the following results: Q-test $p < 0.00001$, $I^2 = 95\%$ and overall effect $p = 0.0007$. Test for subgroup differences: Q-test $p = 0.02$ and $I^2 = 69.7\%$, which showed that the data of subgroups were consistent.

The data of subgroup using 0.1% EGCG as primer showed no statistically significant differences compared with control group (Z-test: $p > 0.05$). However, the result of proanthocyanidin (PA) showed that the experimental groups had significant higher bond strengths than the control groups, with overall effect $p < 0.05$. For primers with 5% PA and 6.5% PA, the result in the Q-test was both $p < 0.01$ and $I^2 = 98\%$, $I^2 = 91\%$, separately. However, the result of 10% PA in the Q-test was $p > 0.05$ and $I^2 = 0\%$. The results of the meta-analysis are shown in Figure 3.

Self-Etch Bond Strength (Plant Extract Primers)

For the second analysis (self-etch adhesive with or without plant extract primers), 10 data sets were selected, with four studies

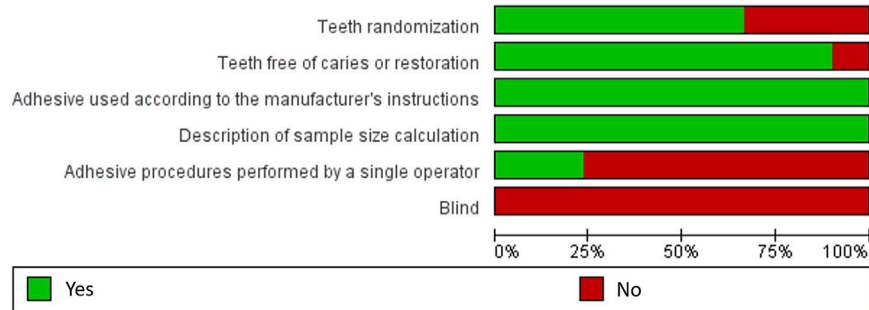


FIGURE 2 | Risk of bias graph judgements about each risk of bias item presented as percentages across all included studies.

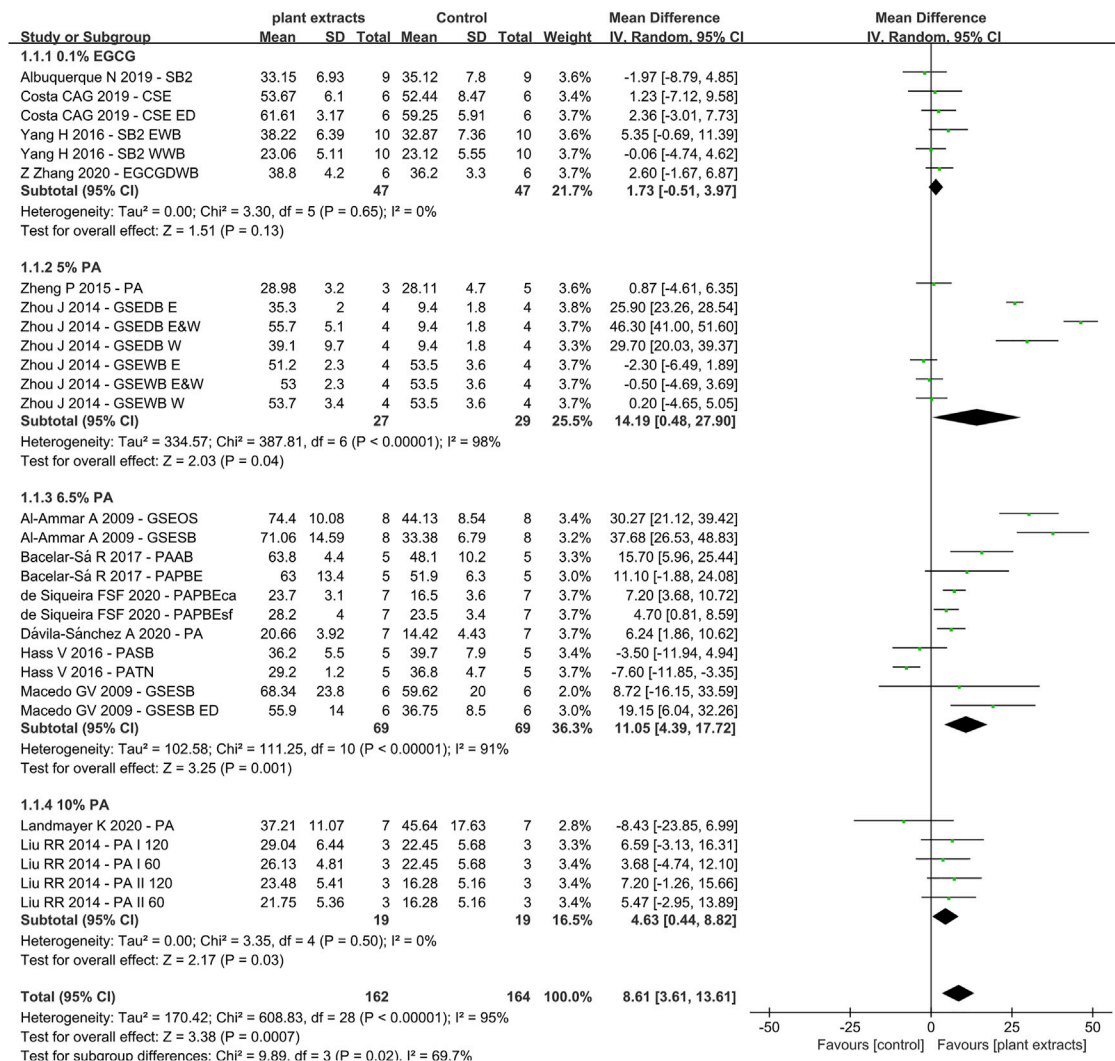


FIGURE 3 | Forest Plot—plant extract primers: etch-and-rinse immediate bond strength.

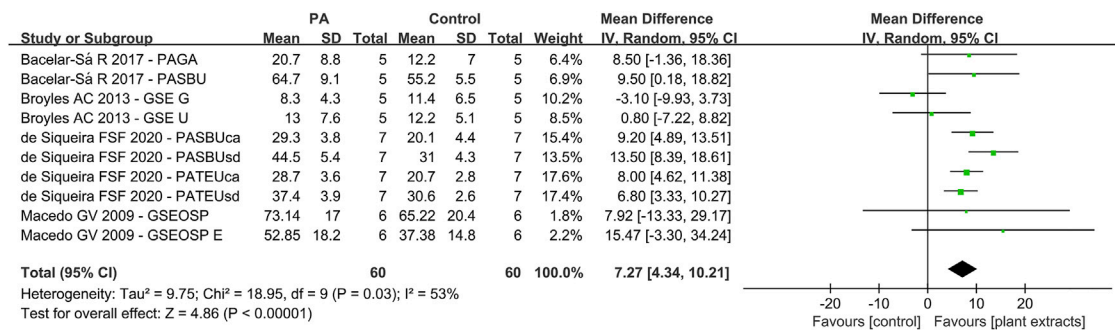


FIGURE 4 | Forest Plot—plant extract primers: self-etch immediate bond strength.

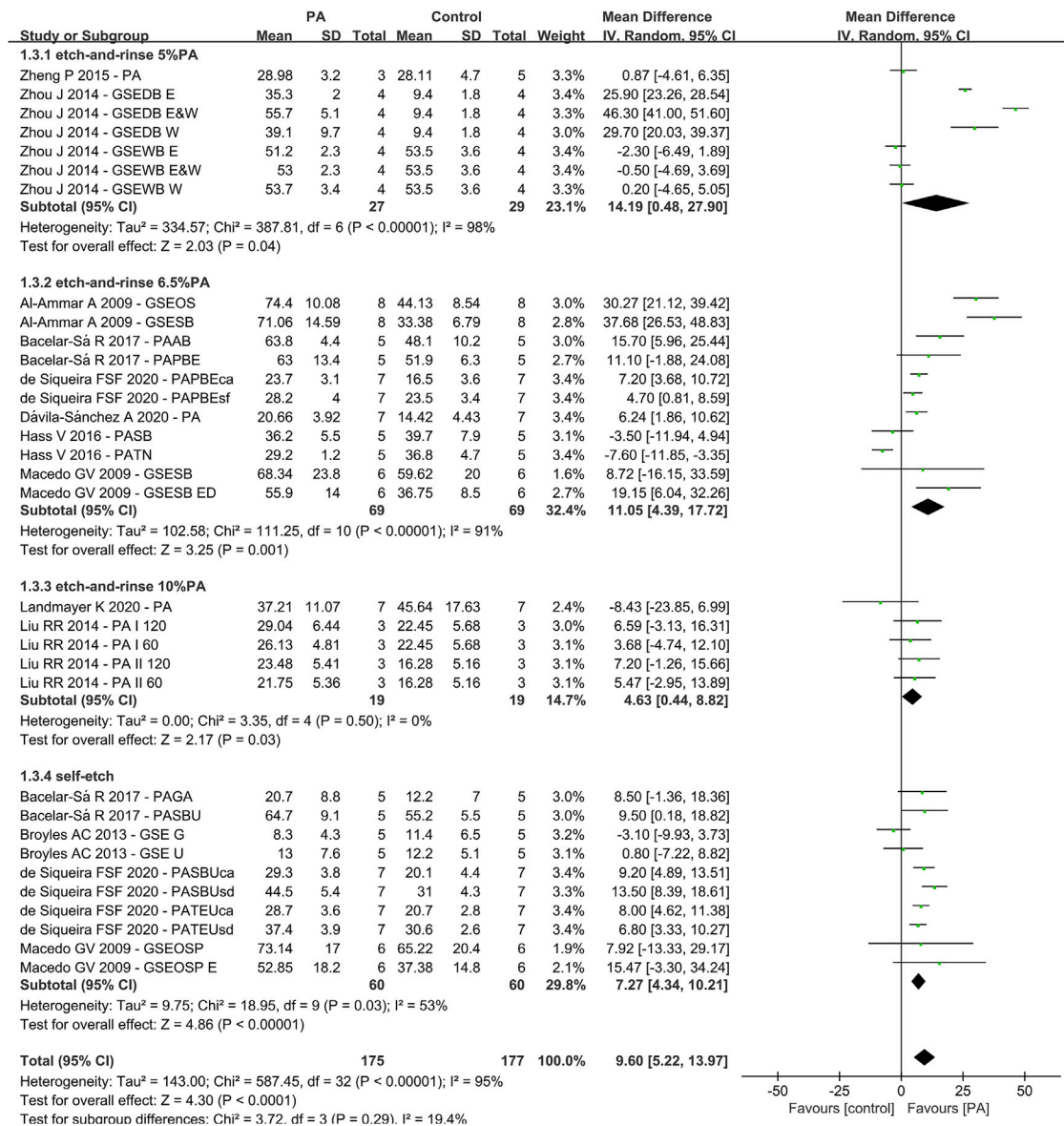


FIGURE 5 | Forest Plot—proanthocyanidin (PA) primers

included (Figure 4). The results were as followings: Q-test $p < 0.05$ and $I^2 = 53\%$. The global analysis showed statistically significant difference ($p < 0.05$).

Primers With Vs Without Proanthocyanidin

For the third analysis (primers with or without PA), 11 studies and 33 datasets were included (Figure 5). The difference between control and experimental groups were statistically significant (Q-test: $p < 0.01$, $I^2 = 95\%$ and Z-test: $p < 0.05$). The differences in the test for subgroups (primers with different concentration of PA) showed the following values: chi-squared = 3.72, $df = 3$ ($p = 0.29$) and $I^2 = 19.4\%$. The meta-analysis results are shown in Figure 5.

DISCUSSION

This systematic review is the first to verify the effects of plant extracts on dentin bonding strength from *in vitro* studies. Thorough database research was conducted, and data were extracted and integrated in tables. Each study was designed and performed on the basis of their own parameters (plant extract types, action modes, concentration, dental adhesives and indicators), as listed in Table 1. Nine different plant extracts were added into 15 types of adhesives or served as primers. Out of the 30 studies, the data from 14 were selected for further evaluation.

As shown in Table 1, there were different commercial adhesives used. We had undertaken several measures to avoid the discrepancy. Firstly, the details of the adhesives were listed, such as commercial name, manufacturer, and place of production. Secondly, the articles that used experimental adhesives were excluded in the present study. Thirdly, 19 of 30 included studies chose the same one commercial adhesive, Single Bond 2(3M ESPE, St. Paul, MN, United States). Furthermore, all included studies set the control group which did not add plant extracts into adhesives or serve as primers. All these strategies were helpful to eliminate the disturbance of different adhesives on research results to the utmost extent. Furthermore, the included studies all reported the manufacturers and details of plant extracts, such as resveratrol powder (Sigma-Aldrich, St. Louis, MO, United States), and the pureness of this product was listed as $\geq 99\%$ (HPLC).










Since plant extract was introduced, its effectiveness in crosslinking and biocompatibility has drawn a lot of attention. Different plant extracts were investigated, listing as follows: proanthocyanidin (PA), epigallocatechin-3-gallate (EGCG), quercetin (QUE), resveratrol (RSV), baicalein (BAI), hesperidin (HES), rutin (RUT) and naringin (NAR). Firstly, despite the chemical structure differences, they all belong to plant polyphenol, which possesses antioxidant and anti-inflammatory properties. These effects are mainly derived from phenolic hydroxyl groups in polyphenols (Leopoldini et al., 2011). The highly-hydroxylated structures make them capable of forming insoluble complexes with carbohydrates and proteins (Bravo, 1998; Teixeira et al., 2002). The major force that stabilizes the plant-extract-protein complexes is hydrogen bonding between phenolic hydroxyl and peptide carbonyl (Hagerman and Butler,

1980a; Hagerman and Butler, 1980b), which is strengthened by alkyl substitution on the amide nitrogen adjacent to the carbonyl (Cannon, 1955). Therefore, the mechanical properties of collagen complex would be increased (Yang et al., 2016). Secondly, plant extracts, such as baicalein and resveratrol, can inhibit the activity of peptidases directly or indirectly by changing the catalytic domain (Mazzoni et al., 2018) or crosslinking with noncollagenous proteins regulating peptidases (Breschi et al., 2010; Cova et al., 2011). Thirdly, many plant extracts, like baicalein, are commonly used in herbal medicines to treat bacterial and viral infections. They show remarkable antimicrobial effects on different bacteria including *Escherichia coli*, *P. cuspidatum* and *S. mutans* (Song et al., 2006; Duan et al., 2007; Zeng et al., 2008; Chinnam et al., 2010; Jang et al., 2014). The mechanisms are not clear yet, but it might be attributed to the inhibition of the cellular growth (Paulo et al., 2010).

One of the most studied plant extracts is proanthocyanidin (PA), also known as grape seed extracts (GSE) (Al-Ammar et al., 2009; Macedo et al., 2009; Liu et al., 2012; Broyles et al., 2013; Liu et al., 2014; Islam et al., 2014; Zheng et al., 2015; Zhou et al., 2016; Hass et al., 2016b; Bacelar-Sa et al., 2017; Zheng and Chen, 2017; de Siqueira et al., 2020; Ds et al., 2020; Landmayer et al., 2020). It is a condensed tannins extracted from *Vitis vinifera* grapes, which has been reported to contain 79.6% polyphenols (Aguiar et al., 2014). PA is composed of flavon-3-ol subunits, catechin, epicatechin and epicatechin-3-O-gallate and linked through C4-C8 (Cavaliere et al., 2010). These components are responsible for their properties such as free-radical scavenging capacity, high affinity for protein, antioxidant potential and capacity to enhance the mechanical properties of collagen (Castellan et al., 2010; Leme-Kraus et al., 2017). Epasinghe et al. (2012) reported that incorporation of less than 3% proanthocyanidin into dental adhesive can reduce nanoleakage without comprising 24 h adhesive-dentin bond strength. The meta-analysis of the PA primer effects on bonding showed a significant positive effect compared with the control group, irrespective of the concentrations or the type of adhesive used (Al-Ammar et al., 2010; Macedo et al., 2009; Liu et al., 2014; Wiegand et al., 2015; Zhou et al., 2016; Hass et al., 2016a; Bacelar-Sa et al., 2017; Ds et al., 2020; Landmayer et al., 2020; Siqueira et al., 2020). However, the results of 5 and 6.5% PA primer revealed a heterogeneity of 98% and 91% (Figure 3). The reason might be attributed to different bonding techniques such as dry bonding and wet bonding (Zhou et al., 2016). For 10% PA primer, the bonding strength shows statistically significant elevation with no heterogeneity (Liu et al., 2014; Landmayer et al., 2020). Although the heterogeneity varies from group to group, the subgroup analysis revealed no significant differences, which also prove the effectiveness of PA primer.

Another important plant extract being intensely investigated is epigallocatechin-3-gallate (EGCG) (Du et al., 2012; Santiago et al., 2013; Yang et al., 2016; Yu et al., 2017; Albuquerque et al., 2019; Costa et al., 2019; Fialho et al., 2019; Landmayer et al., 2020; Zhang et al., 2020). It is one of the flavanols in tea, also known as catechins (Tachibana, 2011). As a representative component of green tea, it cannot be found in any plants except *C. sinensis* (L.) Kuntze (Tachibana, 2011). EGCG consists of a meta-5,7-dihydroxyl-substituted A ring and trihydroxy phenol structures

TABLE 3 | Physical and chemical properties of the plant extracts and their possible effects on immediate bonding strength.

Plant extracts	Molecular formula	Mol. Weight (g/mol)	Number of hydroxyphenyl radicals	Effects on immediate bonding strength
Proanthocyanidin	C ₃₀ H ₂₆ O ₁₃	594.5	7	
Epigallocatechin gallate	C ₂₂ H ₁₈ O ₁₁	458.4	8	
Quercetin	C ₁₅ H ₁₀ O ₇	302.2	5	
Resveratrol	C ₁₄ H ₁₂ O ₃	228.2	3	
Baicalein	C ₁₅ H ₁₀ O ₅	270.2	3	
Genipin	C ₁₁ H ₁₄ O ₅	226.2	2	
Hesperidin	C ₂₈ H ₃₄ O ₁₅	610.6	2	
Rutin	C ₂₇ H ₃₀ O ₁₆	610.5	4	
Naringin	C ₂₇ H ₃₂ O ₁₄	580.5	2	

Green = evident; Yellow = unclear; Red = not recommended.

on both the B and D rings (Peter et al., 2017). The polyphenolic structure makes EGCG good donors for hydrogen bonding (Yang et al., 2009). Thus, it has shown the ability to bring various health benefits, like anti-metastasis, anti-inflammatory and antioxidant effects (Mukhtar and Ahmad, 2000; Mereles and Hunstein, 2011; Suzuki and Isemura, 2013). The similarity of chemical structure with other flavanols like PA makes it capable of enhancing the mechanical strength of collagen. The addition of EGCG directly into adhesives has been proven to preserve the bond strength after different ageing methods (Du et al., 2012; Yu et al., 2017; Albuquerque et al., 2019). The result of EGCG primer showed no negative influence on immediate bond strength (Zhang et al., 2020). The lack of data and various ageing methods make it impossible to do meta-analysis on aged bond strength. However, plenty of articles showed EGCG primer can improve the bond stability (Landmayer et al., 2020; Zhang et al., 2020). Furthermore, Yu et al. (2017) created a derivative of EGCG, called EGCG-3Me, which can enhance the bond stability, inhibited *S.mutans* adhesion and hinder its growth.

There are other plant extracts included in this systematic review: quercetin (QUE) (Gotti et al., 2015; Yang et al., 2017; Ds et al., 2020), resveratrol (RSV) (Porto et al., 2018; Peng et al., 2020), baicalein (BAI) (J. Li et al., 2018; Yi et al., 2019), genipin (GEN) (Al-Ammar et al., 2009), hesperidin (HES) (Islam et al., 2014; Ds et al., 2020), rutin (RUT) (Ds et al., 2020), and naringin (NAR) (Ds et al., 2020). The molecular formula, mass and number of hydroxyphenyl radicals are listed in Table 3. The data are inadequate to perform meta-analysis.

As natural crosslinkers, there are many factors influencing the crosslinking process. For instance, 1) the molecule size; 2) the number of molecules available in the solution; 3) the solubility index of the

molecule and its influence on the miscibility of the vehicle for its application in dentin; 4) the number and type of reactive sites of the molecule; 5) the characteristics of the dentin (Ds et al., 2020).

It is a paradox that the bigger molecules usually have more reactive sites that can enhance the crosslinking effect, but their ability to dissolve and diffuse would be lower than smaller ones. Moreover, the type of molecules in grape seed extracts are complex, with monomers, oligomers and polymers existing at the same time (Bravo, 1998). The size of the oligomers and polymers were larger, which makes it more difficult to diffuse into dentin tubules. According to the results of included studies, we concluded the possible effects of different plant extracts on immediate bonding strength and classified them into different colors: green means the effects on improving bonding strength were evident; yellow means more studies in need; red means probable adverse effects (Table 3).

The plant extracts are normally recognized as plant polyphenols, which encompass a wide variety of molecules that contain at least one aromatic ring with one or more hydroxyl groups (Ferrazzano et al., 2011). Although they were extracted from different plants, the similarity in their chemical structure makes it possible for them to all possess properties like antioxidation and anti-bacterium. To begin with, the highly-hydroxylated structures make them capable of forming complexes with proteins, especially proline-rich proteins in dental collagen (Bravo, 1998). This fortified crosslinking interaction helps enhance the mechanical strength of dental bonding (Yang et al., 2017; Yi et al., 2019; Peng et al., 2020). Furthermore, the polyphenolic compounds could coordinate with metal ions and compete with peptidases such as MMPs for the catalytic domain in collagen (Mazzoni et al., 2018). As a

result, the enzymatic hydrolysis of hybrid layer collagen would be impeded and the adhesive-dentin interface stability would be maintained (Epasinghe et al., 2012; Yang et al., 2016; Yang et al., 2017). Besides, the plant polyphenols were considered metabolites involved in the chemical defense of plants and possess the ability to inhibit bacteria (Ferrazzano et al., 2011). There is plenty of evidence supporting the inhibition of cariogenic bacteria by phenolic compounds. The mechanisms of polyphenols against bacteria like *S. mutans* may include affecting cell membrane permeability, inhibiting protein synthesis, blocking ATP synthesis and inhibiting bacterial metabolism (Chinnam et al., 2010; Xie et al., 2015). Lastly, as natural crosslinkers, the plant polyphenols are non-toxic compared to synthetic compounds like chlorhexidine and glutaraldehyde. They can protect cells by inhibiting oxidative stress-induced DNA damage, lipid peroxidation and protein oxidation (Kang et al., 2012). To conclude, all these *in vitro* studies demonstrated that the plant extracts, consisting of polyphenols, can enhance mechanical strength of dentin collagen, maintain dentin-adhesive stability, inhibit cariogenic bacteria and resist adhesive-induced cytotoxicity.

Although plant extracts have shown plenty of advantages, there are still a large variety of aspects to be explored, such as solvent, treatment time and concentrations. First, theoretically, the effect of plant extracts would increase with the concentration. However, the solubility of the compounds were not great (Bravo, 1998). Zhang et al. (2020) reported EGCG with dimethyl sulfoxide as a solvent can exert synergistic effect on dentin-adhesive interface stability. Second, the treatment time varies from one to another. Genipin is reported to have a slow rate of cross-linking induction that the mechanical strength increased only after 40 h treatment (Bedran-Russo et al., 2007). Third, the effect of different concentration on bonding is complex. It has been shown more than 3% PA added into adhesive directly can exert adverse effect on bonding (Epasinghe et al., 2012). More studies are needed to determine the suitable solvent, treatment time and concentrations of plant extracts.

As mentioned in this review, plant extracts are actually polyphenols, which possess phenolic hydroxyl groups and aromatic rings (Ferrazzano et al., 2011). Therefore, their solubility in solvents such as ethanol are high, due to their similar chemical structure like hydroxyl groups. Furthermore, the interactions between plant extract (eg. PA) and collagen can be disrupted by detergents of hydrogen bond-weakening solvents, suggesting that PA-collagen complex formation involves primarily hydrogen bonding between the protein amide carbonyl and the phenolic hydroxyl (Hagerman and Klucher, 1986). Ethanol, on the other hand, stimulate PA and collagen interactions (Bo et al., 2010). There is no evidence that the interaction is concentration-dependent.

REFERENCES

- Aguar, T. R., Vidal, C. M. P., Phansalkar, R. S., Todorova, I., Napolitano, J. G., Mcalpine, J. B., et al. (2014). Dentin Biomodification Potential Depends on
- The present study showed the changes in dentin bond strength after adding plant extracts into adhesives or serving as primers. Although strict selection was performed to minimize heterogeneity, the data of several subgroups remained high heterogeneous. There are three reasons for heterogeneity: 1. Different adhesive brands; 2. Different bonding modes (etch-and-rinse or self-etch); 3. Different dentin material (normal or eroded dentin). Also, several authors failed to report important details, such as whether the same operator performed the bonding steps of all specimens. These factors may help explain the high heterogeneity in *in vitro* experiments.
- ## CONCLUSIONS
- Plant extracts have positive effects on the immediate microtensile bond strength of the adhesive-dentin interface. Meta-analysis demonstrated that the use of proanthocyanidin (PA) primer, especially at the concentration of 10%, had statistically significant effect on the immediate dentin bonding strength. Considerable heterogeneity existed among the different adhesive brands, bonding modes and dentin materials used, which limited the meta-analysis approach. Further clinical research is needed to confirm the effect of plant extracts on bond strength *in vivo*.
- ## DATA AVAILABILITY STATEMENT
- The original contributions presented in the study are included in the article/Supplementary Material, further inquiries can be directed to the corresponding authors.
- ## AUTHOR CONTRIBUTIONS
- The conception and design of the study were performed by HY and CH. Literature retrieving and studies selection were performed by SZ and JY. Quality evaluation was carried out by CH and JY. Mathematical modeling and meta-analysis were conducted by FH and SZ. Results analysis and interpretation were undertaken by HY and SZ. The manuscript was drafted by HY and SZ. All authors read and approved the final manuscript.
- ## FUNDING
- This work was financially supported by National Natural Science Foundation of China (81701012), Youth Clinical Research Fund of Chinese Stomatological Association (CSA-B2018-01).
- Polyphenol Source. *J. Dent. Res.* 93 (4), 417–422. doi:10.1177/0022034514523783
- Al-Ammar, A., Drummond, J. L., and Bedran-Russo, A. K. (2010). The Use of Collagen Cross-Linking Agents to Enhance Dentin Bond Strength. *J. Biomed. Mater. Res. B Appl. Biomater.* 91 (1), 419–424. doi:10.1002/jbm.b.31417

- Al-Ammar, A., Drummond, J. L., and Bedran-Russo, A. K. (2009). The Use of Collagen Cross-Linking Agents to Enhance Dentin Bond Strength. *J. Biomed. Mater. Res.* 91B (1), 419–424. doi:10.1002/jbm.b.31417
- Albuquerque, N., Neri, J. R., Lemos, M., Yamauti, M., de Sousa, F., and Santiago, S. (2019). Effect of Polymeric Microparticles Loaded with Catechin on the Physicochemical Properties of an Adhesive System. *Oper. Dent.* 44 (4), E202–E211. doi:10.2341/18-112-L
- Alkathheeri, M. S., Palasuk, J., Eckert, G. J., Platt, J. A., and Bottino, M. C. (2015). Halloysite Nanotube Incorporation into Adhesive Systems-Effect on Bond Strength to Human Dentin. *Clin. Oral Invest.* 19 (8), 1905–1912. doi:10.1007/s00784-015-1413-8
- Bacelar-Sá, R., Giannini, M., Ambrosano, G. M. B., and Bedran-Russo, A. K. (2017). Dentin Sealing and Bond Strength Evaluation of Hema-free and Multi-Mode Adhesives to Biomodified Dentin. *Braz. Dent. J.* 28 (6), 731–737. doi:10.1590/0103-6440201701522
- Bedran-Russo, A. K. B., Pereira, P. N. R., Duarte, W. R., Drummond, J. L., and Yamauchi, M. (2007). Application of Crosslinkers to Dentin Collagen Enhances the Ultimate Tensile Strength. *J. Biomed. Mater. Res.* 80B (1), 268–272. doi:10.1002/jbm.b.30593
- Bo, H., Jaurequi, J., Bao, W. T., and Nimni, M. E. (2010). Proanthocyanidin: a Natural Crosslinking Reagent for Stabilizing Collagen Matrices. *J. Biomed. Mater. Res. A* 65A.
- Borges, B. C. D., Catelan, A., Sasaki, R. T., Ambrosano, G. M. B., Reis, A. F., and Aguiar, F. H. B. (2013). Effect of the Application of a Casein Phosphopeptide-Amorphous Calcium Phosphate (CPP-ACP) Paste and Adhesive Systems on Bond Durability of a Fissure Sealant. *Odontology* 101 (1), 52–59. doi:10.1007/s10266-012-0062-5
- Brackett, M. G., Li, N., Brackett, W. W., Sword, R. J., Qi, Y. P., Niu, L. N., et al. (2011). The Critical Barrier to Progress in Dentine Bonding with the Etch-And-Rinse Technique. *J. Dentistry* 39 (3), 238–248. doi:10.1016/j.jdent.2010.12.009
- Bravo, L. (1998). Polyphenols: Chemistry, Dietary Sources, Metabolism, and Nutritional Significance. *Nutr. Rev.* 56 (11), 317–333. doi:10.1111/j.1753-4887.1998.tb01670.x
- Breschi, L., Mazzoni, A., Nato, F., Carrilho, M., Visintini, E., Tjäderhane, L., et al. (2010). Chlorhexidine Stabilizes the Adhesive Interface: a 2-year *In Vitro* Study. *Dental Mater.* 26 (4), 320–325. doi:10.1016/j.dental.2009.11.153
- Broyles, A. C., Pavan, S., and Bedran-Russo, A. K. (2013). Effect of Dentin Surface Modification on the Microtensile Bond Strength of Self-Adhesive Resin Cements. *J. Prosthodont.* 22 (1), 59–62. doi:10.1111/j.1532-849X.2012.00890.x
- Cannon, C. G. (1955). The Interactions and Structure of the -CONH- Group in Amides and Polyamides. *Microchimica Acta* 43 (2-3), 555–588. doi:10.1007/bf01235027
- Carrilho, M. R. O., Carvalho, R. M., de Goes, M. F., di Hipólito, V., Geraldini, S., Tay, F. R., et al. (2007). Chlorhexidine Preserves Dentin Bond *In Vitro*. *J. Dent Res.* 86 (1), 90–94. doi:10.1177/154405910708600115
- Castellan, C. S., Pereira, P. N., Grande, R. H. M., and Bedran-Russo, A. K. (2010). Mechanical Characterization of Proanthocyanidin-Dentin Matrix Interaction. *Dental Mater.* 26 (10), 968–973. doi:10.1016/j.dental.2010.06.001
- Cavaliere, C., Foglia, P., Gubbiotti, R., Sacchetti, P., Samperi, R., and Laganà, A. (2010). Rapid-resolution Liquid Chromatography/mass Spectrometry for Determination and Quantitation of Polyphenols in Grape Berries. *Rapid Commun. Mass. Spectrom.* 22 (20), 3089–3099. doi:10.1002/rcm.3705
- Chinnam, N., Dadi, P. K., Sabri, S. A., Ahmad, M., Kabir, M. A., and Ahmad, Z. (2010). Dietary Bioflavonoids Inhibit *Escherichia coli* ATP Synthase in a Differential Manner. *Int. J. Biol. Macromolecules* 46 (5), 478–486. doi:10.1016/j.ijbiomac.2010.03.009
- Costa, C. A. G., Passos, V. F., Neri, J. R., Mendonça, J. S., and Santiago, S. L. (2019). Effect of Metalloproteinase Inhibitors on Bond Strength of a Self-Etching Adhesive on Erosively Demineralized Dentin. *J. Adhes. Dent.* 21 (4), 337–344. doi:10.3290/j.jad.a42930
- Cova, A., Breschi, L., Nato, F., Ruggeri, A., Jr., Carrilho, M., Tjäderhane, L., et al. (2011). Effect of UVA-Activated Riboflavin on Dentin Bonding. *J. Dent Res.* 90 (12), 1439–1445. doi:10.1177/0022034511423397
- de Siqueira, F. S. F., Hilgemberg, B., Araujo, L. C. R., Hass, V., Bandeca, M. C., Gomes, J. C., et al. (2020). Improving Bonding to Eroded Dentin by Using Collagen Cross-Linking Agents: 2 Years of Water Storage. *Clin. Oral Invest.* 24 (2), 809–822. doi:10.1007/s00784-019-02918-9
- Deligeorgi, V., Mjör, I. A., and Wilson, N. H. (2001). An Overview of Reasons for the Placement and Replacement of Restorations. *Prim. Dental Care* os8 (1), 5–11. doi:10.1308/135576101771799335
- Deng, D., Yang, H., Guo, J., Chen, X., Zhang, W., and Huang, C. (2014). Effects of Different Artificial Ageing Methods on the Degradation of Adhesive-Dentine Interfaces. *J. Dentistry* 42 (12), 1577–1585. doi:10.1016/j.jdent.2014.09.010
- Drummond, J. L. (2008). Degradation, Fatigue, and Failure of Resin Dental Composite Materials. *J. Dent Res.* 87 (8), 710–719. doi:10.1177/154405910808700802
- DS, A., Mfgb, C., Jpb, D., Mbd, E., Bh, D., Ss, F., et al. (2020). Influence of Flavonoids on Long-Term Bonding Stability on Caries-Affected Dentin - ScienceDirect. *Dental Mater.* 36 (9), 1151–1160. doi:10.1016/j.dental.2020.05.007
- Du, X., Huang, X., Huang, C., Wang, Y., and Zhang, Y. (2012). Epigallocatechin-3-gallate (EGCG) Enhances the Therapeutic Activity of a Dental Adhesive. *J. Dentistry* 40 (6), 485–492. doi:10.1016/j.jdent.2012.02.013
- Duan, C., Matsumura, S., Kariya, N., Nishimura, M., and Shimono, T. (2007). *In Vitro* antibacterial Activities of Scutellaria Baicalensis Georgi against Cariogenic Bacterial. *Pediatr. Dental J.* 17 (1), 58–64. doi:10.1016/s0917-2394(07)70096-4
- Epasinghe, D. J., Yiu, C. K. Y., Burrow, M. F., Tay, F. R., and King, N. M. (2012). Effect of Proanthocyanidin Incorporation into Dental Adhesive Resin on Resin-Dentine Bond Strength. *J. Dentistry* 40 (3), 173–180. doi:10.1016/j.jdent.2011.11.013
- Ferrazzano, G., Amato, I., Ingenito, A., Zarrelli, A., Pinto, G., and Pollio, A. (2011). Plant Polyphenols and Their Anti-cariogenic Properties: a Review. *Molecules* 16 (2), 1486–1507. doi:10.3390/molecules16021486
- Fialho, M. P. N., Hass, V., Nogueira, R. P., França, F. M. G., Turssi, C. P., Basting, R. T., et al. (2019). Effect of Epigallocatechin-3-Gallate Solutions on Bond Durability at the Adhesive Interface in Caries-Affected Dentin. *J. Mech. Behav. Biomed. Mater.* 91, 398–405. doi:10.1016/j.jmbbm.2018.11.022
- Gotti, V. B., Feitosa, V. P., Sauro, S., Correr-Sobrinho, L., Leal, F. B., Stansbury, J. W., et al. (2015). Effect of Antioxidants on the Dentin Interface Bond Stability of Adhesives Exposed to Hydrolytic Degradation. *J. Adhes. Dent* 17 (1), 35–44. doi:10.3290/j.jad.a33515
- Hagerman, A. E., and Klucher, K. M. (1986). Tannin-protein Interactions. *Prog. Clin. Biol. Res.* 213 (3), 67–76.
- Hagerman, A. E., and Butler, L. G. (1980a). Condensed Tannin Purification and Characterization of Tannin-Associated Proteins. *J. Agric. Food Chem.* 28 (5), 947–952. doi:10.1021/jf60231a011
- Hagerman, A. E., and Butler, L. G. (1980b). Determination of Protein in Tannin-Protein Precipitates. *J. Agric. Food Chem.* 28 (5), 944–947. doi:10.1021/jf60231a010
- Hass, V., Luque-Martinez, I., Muñoz, M. A., Reyes, M. F., Abuna, G., Sinhoret, M. A., et al. (2016a). The Effect of Proanthocyanidin-Containing 10% Phosphoric Acid on Bonding Properties and MMP Inhibition. *Dent Mater.* 32 (3), 468–475. doi:10.1016/j.dental.2015.12.007
- Hass, V., Luque-Martinez, I. V., Gutierrez, M. F., Moreira, C. G., Gotti, V. B., Feitosa, V. P., et al. (2016b). Collagen Cross-Linkers on Dentin Bonding: Stability of the Adhesive Interfaces, Degree of Conversion of the Adhesive, Cytotoxicity and *In Situ* MMP Inhibition. *Dental Mater.* 32 (6), 732–741. doi:10.1016/j.dental.2016.03.008
- Islam, M. S., Hiraishi, N., Nassar, M., Yiu, C., Otsuki, M., and Tagami, J. (2014). Effect of Hesperidin Incorporation into a Self-Etching Primer on Durability of Dentin Bond. *Dental Mater.* 30 (11), 1205–1212. doi:10.1016/j.dental.2014.08.371
- Jang, E.-J., Cha, S.-M., Choi, S.-M., and Cha, J.-D. (2014). Combination Effects of Baicalein with Antibiotics against Oral Pathogens. *Arch. Oral Biol.* 59 (11), 1233–1241. doi:10.1016/j.archoralbio.2014.07.008
- Kang, K. A., Zhang, R., Piao, M. J., Chae, S., Kim, H. S., Park, J. H., et al. (2012). Baicalein Inhibits Oxidative Stress-Induced Cellular Damage via Antioxidant Effects. *Toxicol. Ind. Health* 28 (5), 412–421. doi:10.1177/0748233711413799
- Kaul, T. N., Middleton, E., Jr., and Ogra, P. L. (1985). Antiviral Effect of Flavonoids on Human Viruses. *J. Med. Virol.* 15 (1), 71–79. doi:10.1002/jmv.1890150110
- La, V. D., Howell, A. B., and Grenier, D. (2009). Cranberry Proanthocyanidins Inhibit MMP Production and Activity. *J. Dent Res.* 88 (7), 627–632. doi:10.1177/0022034509339487
- Landmayer, K., Liberatti, G. A., Farias-Neto, A. M., Wang, L., Honório, H. M., and Franciconi-Dos-Rios, L. F. (2020). Could Applying Gels Containing Chlorhexidine, Epigallocatechin-3-Gallate, or Proanthocyanidin to Control Tooth Wear Progression Improve Bond Strength to Eroded Dentin. *J. Prosthet Dent* 124 (6), 798–e7. doi:10.1016/j.prosdent.2020.05.032
- Leme-Kraus, A. A., Aydin, B., Vidal, C. M., Phansalkar, R. M., Nam, J. W., Mcalpine, J., et al. (2017). Biostability of the Proanthocyanidins-Dentin Complex and Adhesion Studies. *J. Dent Res.* 96 (4), 412–406. doi:10.1177/0022034516680586

- Leopoldini, M., Russo, N., and Toscano, M. (2011). The Molecular Basis of Working Mechanism of Natural Polyphenolic Antioxidants. *Food Chem.* 125 (2), 288–306. doi:10.1016/j.foodchem.2010.08.012
- Li, J., Chen, B., Hong, N., Wu, S., and Li, Y. (2018). Effect of Baicalein on Matrix Metalloproteinases and Durability of Resin-Dentin Bonding. *Oper. Dent.* 43 (4), 426–436. doi:10.2341/17-097-L
- Li, K., Yang, H., Yan, H., Sun, Y., Chen, X., Guo, J., et al. (2017). Quercetin as a Simple but Versatile Primer in Dentin Bonding. *Rsc Adv.* 7, 36392–36402. doi:10.1039/c7ra07467k
- Liu, R.-R., Fang, M., Zhang, L., Tang, C.-F., Dou, Q., and Chen, J.-H. (2014). Anti-proteolytic Capacity and Bonding Durability of Proanthocyanidin-Biomodified Demineralized Dentin Matrix. *Int. J. Oral Sci.* 6 (3), 168–174. doi:10.1038/ijos.2014.22
- Liu, R. R., Fang, M., Zhao, S. J., Li, F., Shen, L. J., and Chen, J. H. (2012). The Potential Effect of Proanthocyanidins on the Stability of Resin-Dentin Bonds against thermal Cycling. *Zhonghua Kou Qiang Yi Xue Za Zhi* 47 (5), 268–272. doi:10.3760/cma.j.issn.1002-0098.2012.05.004
- Macedo, G. V., Yamauchi, M., and Bedran-Russo, A. K. (2009). Effects of Chemical Cross-Linkers on Caries-Affected Dentin Bonding. *J. Dent. Res.* 88 (12), 1096–1100. doi:10.1177/0022034509351001
- Mazzoni, A., Angeloni, V., Comba, A., Maravic, T., Cadenaro, M., Tezvergil-Mutluay, A., et al. (2018). Cross-linking Effect on Dentin Bond Strength and MMPs Activity. *Dental Mater.* 34 (2), 288–295. doi:10.1016/j.dental.2017.11.009
- Mereles, D., and Hunstein, W. (2011). Epigallocatechin-3-gallate (EGCG) for Clinical Trials: More Pitfalls Than Promises. *Ijms* 12 (9), 5592–5603. doi:10.3390/ijms12095592
- Mjör, I. A., Moorhead, J. E., and Dahl, J. E. (2000). Reasons for Replacement of Restorations in Permanent Teeth in General Dental Practice. *Int. Dental J.* 50 (6), 361–366. doi:10.1111/j.1875-595x.2000.tb00569.x
- Mukhtar, H., and Ahmad, N. (2000). Tea Polyphenols: Prevention of Cancer and Optimizing Health. *Am. J. Clin. Nutr.* 71 (6 Suppl. 1), 1698S–1702S. doi:10.1093/ajcn/71.6.1698S
- Paulo, S. L., Ferreira, S., and Gallardo, E. F. (2010). Antimicrobial Activity and Effects of Resveratrol on Human Pathogenic Bacteria. *WORLD JOURNAL MICROBIOLOGY BIOTECHNOLOGY* 53 (6), 716–723. doi:10.1007/s11274-010-0325-7
- Peng, W., Yi, L., Wang, Z., Yang, H., and Huang, C. (2020). Effects of Resveratrol/ethanol Pretreatment on Dentin Bonding Durability. *Mater. Sci. Eng. C* 114, 111000. doi:10.1016/j.msec.2020.111000
- Peter, B., Bosze, S., and Horvath, R. (2017). Biophysical Characteristics of Proteins and Living Cells Exposed to the green tea Polyphenol Epigallocatechin-3-Gallate (EGCG): Review of Recent Advances from Molecular Mechanisms to Nanomedicine and Clinical Trials. *Eur. Biophys. J.* 46 (1), 1–24. doi:10.1007/s00249-016-1141-2
- Porto, I. C. C. M., Nascimento, T. G., Oliveira, J. M. S., Freitas, P. H., Haimeur, A., and França, R. (2018). Use of Polyphenols as a Strategy to Prevent Bond Degradation in the Dentin-Resin Interface. *Eur. J. Oral Sci.* 126 (2), 146–158. doi:10.1111/eos.12403
- Rigano, D., Formisano, C., Basile, A., Lavitola, A., Senatore, F., Rosselli, S., et al. (2007). Antibacterial Activity of Flavonoids and Phenylpropanoids from *Marrubium Globosum* ssp. *Libanoticum*. *Phytother. Res.* 21 (4), 395–397. doi:10.1002/ptr.2061
- Santiago, S. L., Osorio, R., Neri, J. R., Carvalho, R. M., and Toledano, M. (2013). Effect of the Flavonoid Epigallocatechin-3-Gallate on Resin-Dentin Bond Strength. *J. Adhes. Dent.* 15 (6), 535–540. doi:10.3290/j.jad.a29532
- Sarkis-Onofre, R., Skupien, J., Cenci, M., Moraes, R., and Pereira-Cenci, T. (2014). The Role of Resin Cement on Bond Strength of Glass-Fiber Posts Luted into Root Canals: a Systematic Review and Meta-Analysis of *In Vitro* Studies. *Oper. Dent.* 39 (1), E31–E44. doi:10.2341/13-070-LIT
- Siqueira, F., Hilgemberg, B., Araujo, L., Hass, V., Bandeca, M. C., Gomes, J. C., et al. (2020). Improving Bonding to Eroded Dentin by Using Collagen Cross-Linking Agents: 2years of Water Storage. *Clin. Oral Investig.* 24 (2), 809–822. doi:10.1007/s00784-019-02918-9
- Song, J.-H., Kim, S.-K., Chang, K.-W., Han, S.-K., Yi, H.-K., and Jeon, J.-G. (2006). *In Vitro* Inhibitory Effects of Polygonum Cuspidatum on Bacterial Viability and Virulence Factors of Streptococcus Mutans and Streptococcus Sobrinus. *Arch. Oral Biol.* 51 (12), 1131–1140. doi:10.1016/j.archoralbio.2006.06.011
- Suzuki, Y., and Isemura, M. (2013). Binding Interaction between (-)-epigallocatechin Gallate Causes Impaired Spreading of Cancer Cells on Fibrinogen. *Biomed. Res.* 34 (6), 301–308. doi:10.2220/biomedres.34.301
- Tachibana, H. (2011). Green tea Polyphenol Sensing. *Proc. Jpn. Acad. Ser. B: Phys. Biol. Sci.* 87 (3), 66–80. doi:10.2183/pjab.87.66
- Taneja, S., Kumari, M., and Bansal, S. (2017). Effect of Saliva and Blood Contamination on the Shear Bond Strength of Fifth-, Seventh-, and Eighth-Generation Bonding Agents: An *In Vitro* Study. *J. Conserv. Dent.* 20 (3), 157–160. doi:10.4103/0972-0707.218310
- Teixeira, F., Pollock, M., Karim, A., and Jiang, Y. (2002). Use of Antioxidants for the Prophylaxis of Cold-Induced Peripheral Nerve Injury. *Mil. Med.* 167 (9), 753–755. doi:10.1093/milmed/167.9.753
- Wiegand, A., Zheng, P., and Zaruba, M. T. (2015). Effect of Different Matrix Metalloproteinase Inhibitors on Microtensile Bond Strength of an Etch-And-Rinse and a Self-Etch Adhesive to Dentin. *Oper. Dent.* 40(1):80–86. doi:10.2341/13-162-L
- Xie, Y., Yang, W., Tang, F., Chen, X., and Ren, L. (2014). Antibacterial Activities of Flavonoids: Structure-Activity Relationship and Mechanism. *Cmc* 22 (1), 132–149. doi:10.2174/0929867321666140916113443
- Yang, C. S., Wang, X., Lu, G., and Picinich, S. C. (2009). Cancer Prevention by tea: Animal Studies, Molecular Mechanisms and Human Relevance. *Nat. Rev. Cancer* 9 (6), 429–439. doi:10.1038/nrc2641
- Yang, H., Guo, J., Deng, D., Chen, Z., and Huang, C. (2016). Effect of Adjunctive Application of Epigallocatechin-3-Gallate and Ethanol-Wet Bonding on Adhesive-Dentin Bonds. *J. Dentistry* 44, 44–49. doi:10.1016/j.jdent.2015.12.001
- Yang, H., Li, K., Yan, H., Liu, S., Wang, Y., and Huang, C. (2017). High-performance Therapeutic Quercetin-Doped Adhesive for Adhesive-Dentin Interfaces. *Sci. Rep.* 7 (1), 8189. doi:10.1038/s41598-017-08633-3
- Yi, L., Yu, J., Han, L., Li, T., Yang, H., and Huang, C. (2019). Combination of Baicalein and Ethanol-Wet-Bonding Improves Dentin Bonding Durability. *J. Dentistry* 90, 103207. doi:10.1016/j.jdent.2019.103207
- Yu, H.-H., Zhang, L., Yu, F., Li, F., Liu, Z.-Y., and Chen, J.-H. (2017). Epigallocatechin-3-gallate and Epigallocatechin-3-O-(3-O-Methyl)-Gallate Enhance the Bonding Stability of an Etch-And-Rinse Adhesive to Dentin. *Materials* 10 (2), 183. doi:10.3390/ma10020183
- Zeng, Z., Qian, L., Cao, L., Tan, H., Huang, Y., Xue, X., et al. (2008). Virtual Screening for Novel Quorum Sensing Inhibitors to Eradicate Biofilm Formation of *Pseudomonas aeruginosa*. *Appl. Microbiol. Biotechnol.* 79 (1), 119–126. doi:10.1007/s00253-008-1406-5
- Zhang, K., Li, F., Imazato, S., Cheng, L., Liu, H., Arola, D. D., et al. (2013). Dual Antibacterial Agents of Nano-Silver and 12-methacryloyloxydodecylpyridinium Bromide in Dental Adhesive to Inhibit Caries. *J. Biomed. Mater. Res.* 101B (6), 929–938. doi:10.1002/jbm.b.32898
- Zhang, Z., Yu, J., Yao, C., Yang, H., and Huang, C. (2020). New Perspective to Improve Dentin-Adhesive Interface Stability by Using Dimethyl Sulfoxide Wet-Bonding and Epigallocatechin-3-Gallate. *Dental Mater.* 36 (11), 1452–1463. doi:10.1016/j.dental.2020.08.009
- Zheng, P., and Chen, H. (2017). Evaluate the Effect of Different Mmps Inhibitors on Adhesive Physical Properties of Dental Adhesives, Bond Strength and Mmp Substrate Activity. *Sci. Rep.* 7 (1), 4975. doi:10.1038/s41598-017-04340-1
- Zheng, P., Zaruba, M., Attin, T., and Wiegand, A. (2015). Effect of Different Matrix Metalloproteinase Inhibitors on Microtensile Bond Strength of an Etch-And-Rinse and a Self-Etching Adhesive to Dentin. *Oper. Dent.* 40 (1), 80–86. doi:10.2341/13-162-L
- Zhou, J., Chiba, A., Scheffel, D. L. S., Hebling, J., Agee, K., Tagami, J., et al. (2016). Cross-linked Dry Bonding: A New Etch-And-Rinse Technique. *Dental Mater.* 32 (9), 1124–1132. doi:10.1016/j.dental.2016.06.014

Conflict of Interest: The authors declare that the research was conducted in the absence of any commercial or financial relationships that could be construed as a potential conflict of interest.

Publisher's Note: All claims expressed in this article are solely those of the authors and do not necessarily represent those of their affiliated organizations, or those of the publisher, the editors and the reviewers. Any product that may be evaluated in this article, or claim that may be made by its manufacturer, is not guaranteed or endorsed by the publisher.

Copyright © 2022 Zhao, Hua, Yan, Yang and Huang. This is an open-access article distributed under the terms of the Creative Commons Attribution License (CC BY). The use, distribution or reproduction in other forums is permitted, provided the original author(s) and the copyright owner(s) are credited and that the original publication in this journal is cited, in accordance with accepted academic practice. No use, distribution or reproduction is permitted which does not comply with these terms.

APPENDIX

Table A1 | Search strategy used for PubMed (from inception to September 2021).

	Search terms
#1	Epigallocatechin gallate OR epigallocatechin-3-gallate OR epigallocatechin-3-O-gallate OR "EGCG cpd" OR epigallo-catechin gallate
#2	Quercetin[MeSH]
#3	Genipin
#4	Proanthocyanidins[MeSH] OR "condensed tannin*" OR "anthocyanidin polymer*" OR procyanidin*
#5	Naringenin
#6	Hesperidin[MeSH] OR "hesperetin 7 rhamnoglucoside" OR "hesperetin 7 rutinoside"
#7	"Crosslinking agent*" OR "cross link"
#8	Plant extracts[MeSH]
#9	#1 OR #2 OR #3 OR #4 OR #5 OR #6 OR #7 OR #8
#10	Dental cements[MeSH] OR "dental adhesive*" OR "luting agent*" OR dentistry [MeSH]
#11	Bond* AND strength
#12	#9 AND #10 AND #11



Effect of Different Concentrations of Silver Nanoparticles on the Quality of the Chemical Bond of Glass Ionomer Cement Dentine in Primary Teeth

Faisal Mohammed Abed^{1,2}, Sunil Babu Kotha^{2,3*}, Haneen AlShukairi², Fatmah Nasser Almotawah², Rwan Abdulali Alabdulaly⁴ and Sreekanth Kumar Mallineni^{5,6*}

¹Ministry of Health Specialized Dental Center, King Fahd General Hospital, Madinah, Saudi Arabia, ²Department of Preventive Dentistry, College of Dentistry, Riyadh Elm University (REU), Riyadh, Saudi Arabia, ³Department of Pediatric and Preventive Dentistry, Sharad Pawar Dental College and Hospital, Datta Meghe Institute of Medical Sciences (Deemed to be University), Wardha, India, ⁴Dental Intern, College of Dentistry, King Saud University, Riyadh, Saudi Arabia, ⁵Department of Preventive Dental Sciences, College of Dentistry, Majmaah University, Al-Majmaah, Saudi Arabia, ⁶Center for Transdisciplinary Research (CFTR), Saveetha Institute of Medical and Technical Sciences, Saveetha Dental College, Saveetha University, Chennai, India

OPEN ACCESS

Edited by:

Mohammad Khursheed Alam,
Al Jouf University, Saudi Arabia

Reviewed by:

Arlette Setiawan,
Universitas Padjadjaran, Indonesia
Daniel Carreno,
Pontificia Universidad Católica de
Chile, Chile

*Correspondence:

Sunil Babu Kotha
sunil.babu1606@gmail.com
sunil.babu@riyadh.edu.sa
Sreekanth Kumar Mallineni
drmallineni@gmail.com
s.mallineni@mu.edu.sa

Specialty section:

This article was submitted to
Biomaterials,
a section of the journal
Frontiers in Bioengineering and
Biotechnology

Received: 16 November 2021

Accepted: 01 February 2022

Published: 07 March 2022

Citation:

Abed FM, Kotha SB, AlShukairi H,
Almotawah FN, Alabdulaly RA and
Mallineni SK (2022) Effect of Different
Concentrations of Silver Nanoparticles
on the Quality of the Chemical Bond of
Glass Ionomer Cement Dentine in
Primary Teeth.
Front. Bioeng. Biotechnol. 10:816652.
doi: 10.3389/fbioe.2022.816652

Background: The nanotechnologies have been applied for dental restorative materials manufacturing such as glass ionomer cement, composites, tooth regeneration, and endodontic sealers. The study aimed to investigate the chemical bond of conventional glass ionomer cement and to evaluate the addition of different concentrations of silver nanoparticles (AgNPs) on the quality of the chemical bond of glass ionomer cement to primary dentin.

Methods: Silver nanoparticle (AgNP) powder was added in concentrations of 0.2, 0.4, and 0.6% to the conventional powder of GIC Fuji II. Then, the powder was added to the liquid and mixed with the recommended powder/liquid ratio of 3.6:1 g. The Fourier-transform infrared spectra (FTIR) of teeth with 0.2%, 0.4%, and 0.6% w/w of silver nanoparticles in GIC fills and the control tooth were obtained. The conventional glass ionomer was used as a control group. The control and the plain silver tooth were subjected to FTIR analysis using an ATR–FTIR spectrophotometer (ThermoFisher Scientific, Waltham, MA, United States) with zinc selenide (ZnSe) ATR crystal (attenuated total reflection) and OPUS v7.5 software. All spectra were recorded in the range of 500–3,500 cm⁻¹ in the transmission mode with an ATR module.

Results: The AgNPs added at 0.2, 0.4, and 0.6% concentration to GIC provided some information in the context of bond interaction with the dentin. Various bond peaks were seen for calcium, carbonate, phosphate, and amide. In our study, only the amide and phosphate were generated. The amide peaks were almost similar to the control, 0.2%, 0.4%, and 0.6%, with the peaks in the range of 1250–1650 cm⁻¹. There was a clear shift in

Abbreviations: Ag, silver; AgNO₃, silver nitrate; AgNPs, silver nanoparticles; Al₂O₃, aluminum oxide; ATR, attenuated total reflection; Bis-GMA, bisphenol A-glycidyl methacrylate; CaF₂, calcium fluoride; CaO, calcium oxide; COPD, chronic obstructive pulmonary disease; FTIR, Fourier-transform infrared spectroscopy; GIC, glass ionomer cement; HA, hydroxyapatite; HEMA, hydroxyethyl methacrylate; ISO, International Organization of Standardization; NaBo₄, sodium perborate; NPs, nanoparticles; P₂O₅, phosphorus pentoxide; PAA, polyacrylic acid; *S. aureus*, *Staphylococcus aureus*; SiO₂, silicon dioxide; SiOH, silanol; ZnSe, zinc selenide.

the phosphate peak from the control, 0.2, and 0.4%, which was about 1050 cm^{-1} , whereas for 0.6%, there was a clear shift from 1050 cm^{-1} to 880 cm^{-1} .

Conclusion: GIC supplemented with AgNPs showed that a concentration above 0.4% of AgNPs altered the bond quality in dentin interaction. In conclusion, adding AgNPs at a minimal level improves the mechanical properties and maintains the same bond quality as GIC.

Keywords: bond strength, silver nanoparticles, bonding, glass ionomer, primary teeth

INTRODUCTION

The glass ionomer cement (GIC) was first discovered by Wilson and Kent (1972). It has been widely used for restorations, liners and bases, pit and fissure sealants, luting materials, core buildups, and orthodontic bracket adhesives (Cibim et al., 2017). GIC's shortcomings are little fracture toughness, little wear resistance, and formal dissolution on water sorption that might lead to the growth of secondary caries, bacteria, and in the end, failure of the restoration (Garcia-Contreras et al., 2015). Furthermore, GICs have good biocompatibility, a low thermal expansion coefficient, and fluoride-releasing properties (Garcia-Contreras et al., 2015).

The secondary caries was reported as being the primary reason for the failure of GICs because the fluoride release was not enough to inhibit bacterial growth (Xie et al., 2011). The primary cause for caries and cariopathogenic biofilm development can be adhesion to the tooth surface by specific oral bacteria (Garcia et al., 2016). It can occur after a minimally invasive technique that would leave caries-affected tissues behind, thus resulting in elevation of the probability of residual bacteria on the prepared teeth cavities (Doozandeh et al., 2015). Furthermore, bacteria might invade tooth restoration interfaces throughout service when microleakage occurs in that region (Jowkar et al., 2019). Accordingly, a restoration may be affected by secondary caries that results from the growth of bacterial colonies, notably *Streptococcus mutans*, beneath the restorations (Kasraei et al., 2014).

For minimizing secondary caries failure, additional filler was introduced to improve the antibacterial and mechanical properties of the GICs without any interference with their bond strength and fluoride-releasing properties (Xu and Burgess, 2003; Garcia-Contreras et al., 2015). Nanotechnology is the science of producing functional structures and materials that range from 0.1 to 100 nm utilizing different physical and chemical processes. The developments of nanocomposites was the first attempt in the restorative dentistry field to use nanoparticles (NPs). This attempt has enabled scientists to develop nanoparticle-enriched GICs (Mitra et al., 2003). The nanotechnologies were applied for dental restorative materials manufacturing such as glass ionomer cement (i.e., nano-ionomers), composites (i.e., nanocomposites), tooth regeneration, and endodontic sealers (Mitra et al., 2011). The vital contribution from nanodental materials can be considered to be identifying oral health-related disorders via enhanced management and diagnosis of dental problems via bionanomaterials (Maman et al., 2018). Silver can be used in

elementary and ionized forms such as nanoparticles or silver zeolites (Monteiro et al., 2012; Padovani et al., 2015; Köroğlu et al., 2016; Crystal and Niederman, 2019). A silver alloy powder was formerly added to a restorative glass ionomer cement to make a metal reinforced GIC, which is more complex and more substantial. A silver powder was sintered to glass at high temperatures to obtain cermet cement. It has been claimed that such silver-sintered powder could improve abrasion resistance and durability (Simmons, 1983; McLean et al., 1994).

Silver nanoparticle incorporation into GIC powder could reduce biofilm formations that would not significantly affect the mechanical and physical properties. In one study, silver nanoparticles were not firmly bonded to the matrix. They did not significantly improve the mechanical properties, which could be due to their nanosize, which allowed dispersion between and around polymer chains (Köroğlu et al., 2016; El-Wassefy et al., 2018; Crystal and Niederman, 2019). Incorporating silver nanoparticles into glass ionomer cements significantly enhanced the material's wear resistance. The main improvement after adding silver nanoparticles was abrasion resistance and radio-opacity to the glass ionomer cement (McKinney et al., 1988; Xie et al., 2000). Fourier-transform infrared spectroscopy (FTIR) qualitative analysis can provide wave modes of molecules, assessed via the sample optical absorptions bands, which can be thought of as the fingerprints of specific molecules that provide accurate data on chemical changes inside a material. The latter being evaluated has suggested potential changes in absorption bands and/or new bands (Yamakami et al., 2018). Thus, there is evidence from previous studies about the advantages of adding silver nanoparticles (AgNPs), which show increased mechanical and antibacterial properties. Still, there are no studies on the quality of the bond interaction of silver nanoparticles (AgNPs) with dentin. The study aimed to investigate the chemical bond of conventional glass ionomer, evaluate the addition of silver nanoparticles (AgNPs) to traditional glass ionomer cement (GIC), and assess the effect of different concentrations of silver nanoparticles (AgNPs) on the quality of the chemical bond of glass ionomer cement to primary dentin.

METHODOLOGY

Materials

GC Fuji II [powder 15 g: 95% by weight alumino-fluoro-silicate glass with 5% polyacrylic acid powder, liquid 8 g (6.4 ml): 50 percent distilled water, 40 percent polyacrylic acid, and 10 percent



FIGURE 1 | (A) GC Fuji II powder and liquid; **(B)** silver nanoparticle (AgNP) powder used for making samples; **(C)** mixed GIC powder and silver nanoparticle (AgNP) powder with different concentrations 0.2, 0.4, and 0.6%; **(D)** electronic weighing scale used for measuring the weight of the GIC powder and other substance(s); **(E)** Fourier-transform infrared spectroscopy (FTIR).

polybasic carboxylic acid (GC, Tokyo, Japan)] and silver nanoparticles (AgNPs) (<100 μm in size) from Sigma Aldrich (St. Louis, MO, United States, Lot # MKBN3581V).

Ethical Approval

The proposal was registered with the research center of Riyadh Elm University (FPGRP/43835007/334), and ethical approval was obtained from the Institutional Review Board of the institution.

Preparation of Samples

In this *in vitro* study, a conventional GIC (GC Fuji II, GC Corporation, Tokyo, Japan) (f) and silver nanoparticle powders (AgNPs) <100 nm particle size (Sigma-Aldrich, St. Louis, MO, United States) (**Figure 1**) were purchased. The SNP powder was weighed carefully using a weighing machine with an accuracy of ± 0.0001 g Precisa (360A, Livingston, U.K) (**Figure 1**), and three concentrations were obtained: 0.2, 0.4, and 0.6% (w/w). The GIC specimens were divided into four groups for each test: GIC without silver nanoparticles (AgNPs) ($n = 10$), GIC with 0.2% silver nanoparticles (AgNPs) ($n = 10$), GIC with 0.4% silver nanoparticles (AgNPs) ($n = 10$), and GIC with 0.6% AgNPs ($n = 10$) (**Figure 3**). The materials were mixed with a powder/liquid P/L ratio of 2.6:1 g and were prepared following the manufacturer's instructions.

Preparation of Group(s)

The extracted teeth were collected from an operating room and dental clinic. The teeth were carefully examined to ensure the absence of debris. For 1 month, the teeth were stored in a 0.1% thymol solution with 0.9% isotonic sodium chloride (5°C) until the beginning of the experiment. We used a diamond separating disc (Edenta ISO No. 806.104.355.514.220, Switzerland; 15,000 rotations/min) at a slow-speed handpiece with continuous water cooling, perpendicular to the tooth's long axis, and sectioned approximately 2.0 mm of the tissue along with the cusps without exposing the pulp (Porenczuk et al., 2016). The 40 teeth were categorized into four groups with an equal distribution that includes group 1 (apply GIC on dentin as the control group), group 2 (apply GIC with silver nanoparticles (AgNPs) (0.2%) on dentin), group 3 (apply GIC with silver nanoparticles (AgNPs) (0.4%) on dentin), and group 4 (apply GIC with silver nanoparticles (AgNPs) (0.6%) on dentin). For the preparation of the control group, the ratio of powder and liquid was taken as per the manufacturers' instructions, and they were mixed on a glossy paper pad. Subsequently, all the samples were prepared for FTIR.

Analysis of the Mechanical Interaction

Fourier-transform infrared spectroscopy (FTIR) (**Figure 1**) provides the vibrational modes of the molecules, evaluated by

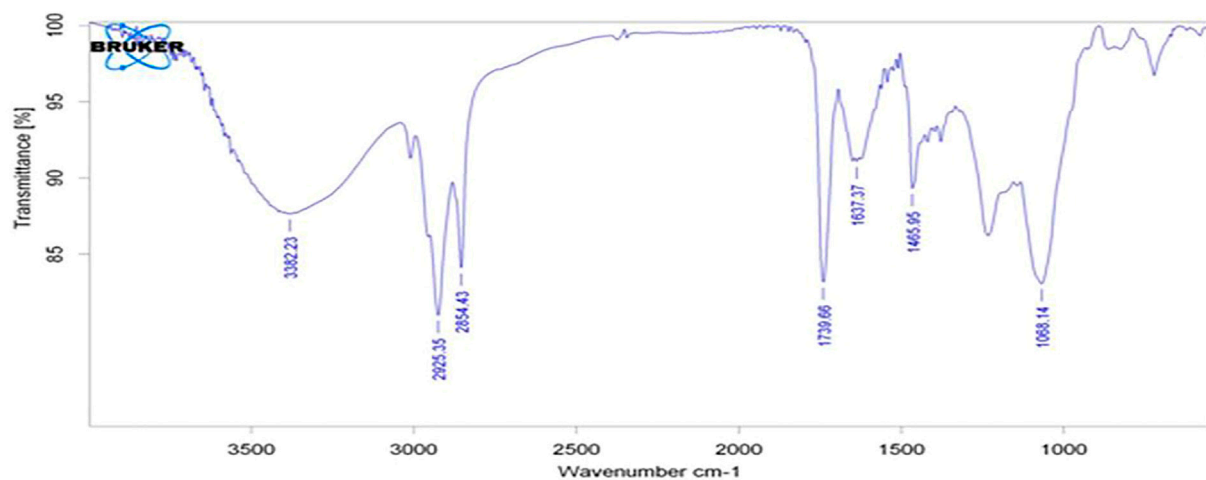


FIGURE 2 | Bioactive evaluation of silver nanoparticles.

the optical absorption bands of the sample, which are considered the fingerprints of specific molecules, enabling precise information about chemical changes in the material, the latter being assessed based on the possible changes in absorption bands and/or the appearance of new bands (Larkin, 2011). Teeth with 0.2%, 0.4%, and 0.6% w/w of silver nanoparticles and GIC, the control tooth, and plain silver were subjected to FTIR analysis using an ATR-FTIR spectrophotometer (Thermo Fisher Scientific, Waltham, MA, United States) with zinc selenide (ZnSe) ATR crystals (attenuated total reflection) and OPUS v7.5 software. All spectra were recorded in the range of 500–3,500 cm^{-1} in the transmission mode with an ATR module. The FTIR vibration range mode wavenumber was from 500 to 3500 cm^{-1} . The FTIR analysis of GIC showed a similar interaction with the dentin compared to the GIC, with 0.2 and 0.4% AgNPs. These vibrational groups were part of the cross-linking reaction and aging time. In addition, the FTIR spectra showed the vibration of Ag in molecular water associated at the range of 3300 cm^{-1} . The vibration band then shifted to 880 cm^{-1} . This band was related to the bonding structure present in the GIC sample with 0.6%. The other band existing at $\sim 1,550 \text{ cm}^{-1}$ referred to the formation of the asymmetric COOH band from the PAA.

Statistical Analysis

Only descriptive analysis was carried out, and statistical analysis was not performed in this study due to the qualitative characteristics of the data resulting from FTIR (Yamakami et al., 2018).

RESULTS

The results of the bioactive evaluation of silver nanoparticle cement, carried out by Fourier-transform infrared spectroscopy, are shown in **Figure 2**. The GIC had various peaks, of which v1, v2, v3, v4, and v5 with 1068 cm^{-1} , 1365 cm^{-1} , 1456 cm^{-1} , 1637 cm^{-1} , and 1740 cm^{-1} , respectively,

were significant. The results of the bioactive evaluation of glass ionomer cement, carried out by Fourier-transform infrared spectroscopy, are shown in **Figure 3**. The GIC had various peaks, of which v1, v2, v3, v4, and v5 with 1050 cm^{-1} , 1,365 cm^{-1} , 1,412 cm^{-1} , 1490 cm^{-1} , and 1556 cm^{-1} , respectively, were significant. The GIC with silver nanoparticles (AgNPs) 0.2% had various peaks, of which v1, v2, v3, v4, and v5 with 1,048 cm^{-1} , 1,368 cm^{-1} , 1,410 cm^{-1} , 1492 cm^{-1} , and 1561 cm^{-1} , respectively, were significant. The results of the bioactive evaluation of glass ionomer cement and silver nanoparticles (AgNPs) 0.2% with dentin, carried out by Fourier-transform infrared spectroscopy, are shown in **Figure 4**.

The results of the bioactive evaluation of glass ionomer cement with silver nanoparticles (AgNPs) 0.4% with dentin, carried out by Fourier-transform infrared spectroscopy, are shown in **Figure 5**. The GIC with silver nanoparticles (AgNPs) 0.4% had various peaks, of which v1, v2, v3, v4, v5 with 1,045 cm^{-1} , 1,360 cm^{-1} , 1,418 cm^{-1} , 1,485 cm^{-1} , and 1,548 cm^{-1} , respectively, were significant. The GIC with silver nanoparticles (AgNPs) 0.6% had various peaks, of which v1, v2, v3, v4, and v5 with 8,080 cm^{-1} , 1,365 cm^{-1} , 1,408 cm^{-1} , 1,493 cm^{-1} , and 1,565 cm^{-1} , respectively, were significant. The results of the bioactive evaluation of glass ionomer cement with silver nanoparticles (AgNPs) 0.6% with dentin, carried out by Fourier-transform infrared spectroscopy, are shown in **Figure 6**. The results of the bioactive evaluation of dentin performed by Fourier-transform infrared spectroscopy are shown in **Table 1**. The dentin had various peaks, of which v1, v2, v3, and v4, with 1040 cm^{-1} , 1242 cm^{-1} , 1546 cm^{-1} , and 1655 cm^{-1} , respectively, were significant.

DISCUSSION

The present study has been carried out to investigate the effect of the bonding interaction of AgNP incorporation into GIC onto the dentin surface. Three concentrations (0.2, 0.4, and 0.6%) were added, with the control being the GIC. This study showed a

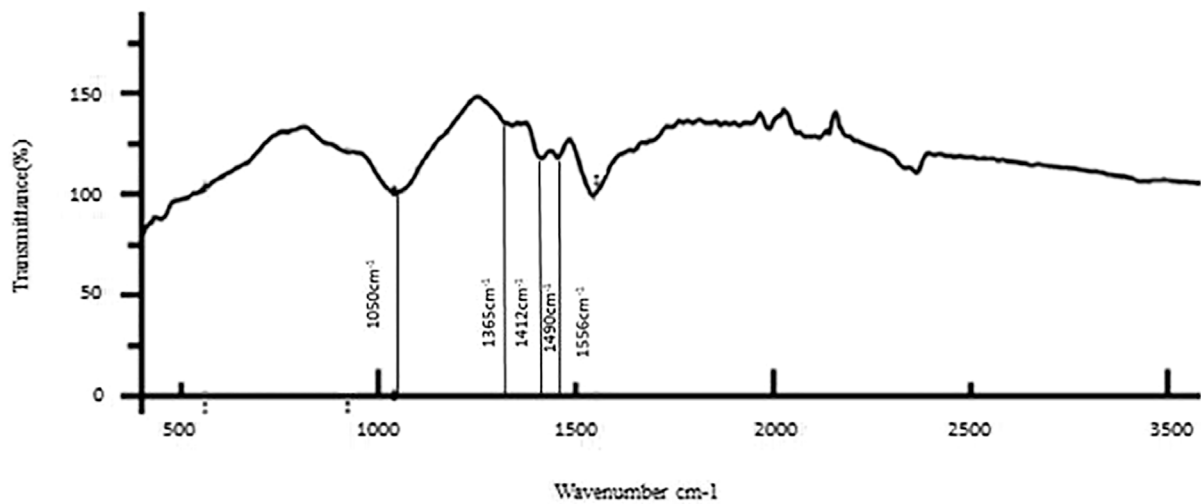


FIGURE 3 | Bioactive evaluation of glass ionomer cement (GIC) with dentin.

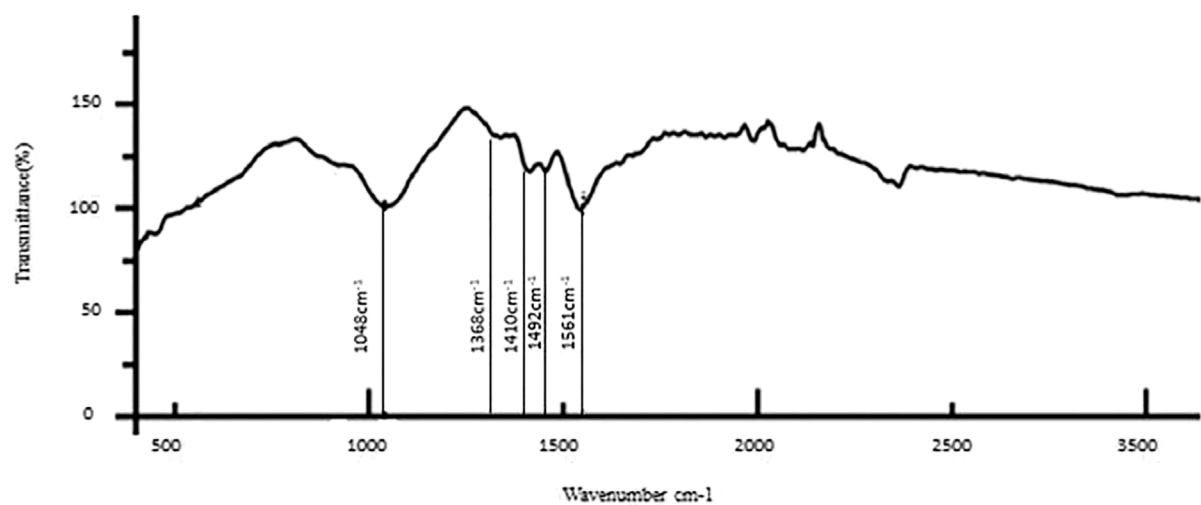


FIGURE 4 | Bioactive evaluation of glass ionomer cement (GIC) and silver nanoparticles (AgNPs) 0.2% sample with dentin.

greater variation of the transmission bands after the increased addition of silver nanoparticles, indicating a change in bond interaction with the dentin. Pure GIC has the disadvantage of less wear resistance, and it cannot withstand the masticatory forces. The common reason for the low resistance of GIC to fracture is the presence of voids in the cement matrix, which are formed by the inclusion of air during cement mixing. These voids may act as stress raisers and concentrators and eventually weaken the mechanical properties of the set cement (Kent, 1973; Elsaka et al., 2011; Liu et al., 2014). Many practitioners use this restoration due to the major advantage of its fluoride-releasing property (Xu and Burgess, 2003). The manufacturers also release many combinations to improve the mechanical properties without losing the fluoride release.

Recent studies suggest that the voids tend to be filled with nanoparticles incorporated into GIC (Elsaka et al., 2011; Gjorgievska et al., 2015). In this process of experimentation, a limited number of studies were carried out incorporating SNP with GIC (Paiva et al., 2018; Jowkar et al., 2019). Jowkar and co-workers (2019) used the addition of 0.1 and 0.2% of AgNPs to GIC in their study and concluded that the higher concentration of 0.2% showed a significant improvement in mechanical properties (surface hardness, flexural strength, compressive strength, and micro-shear bond strength to dentin). Paiva and co-workers (2018) concluded that a higher concentration of silver (0.5% by mass) in the matrix of nano-Ag-GIC allowed viable net setting time and increased the compressive strength of the experimental cement by 32%. The addition of AgNPs increased the mechanical

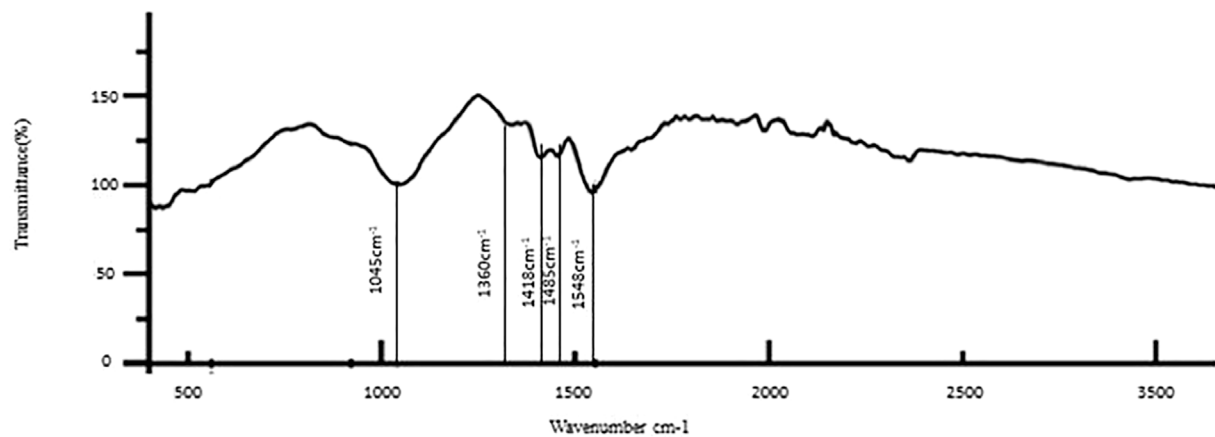


FIGURE 5 | Bioactive evaluation of glass ionomer cement (GIC) and silver nanoparticles (AgNPs) 0.4% sample with dentin.

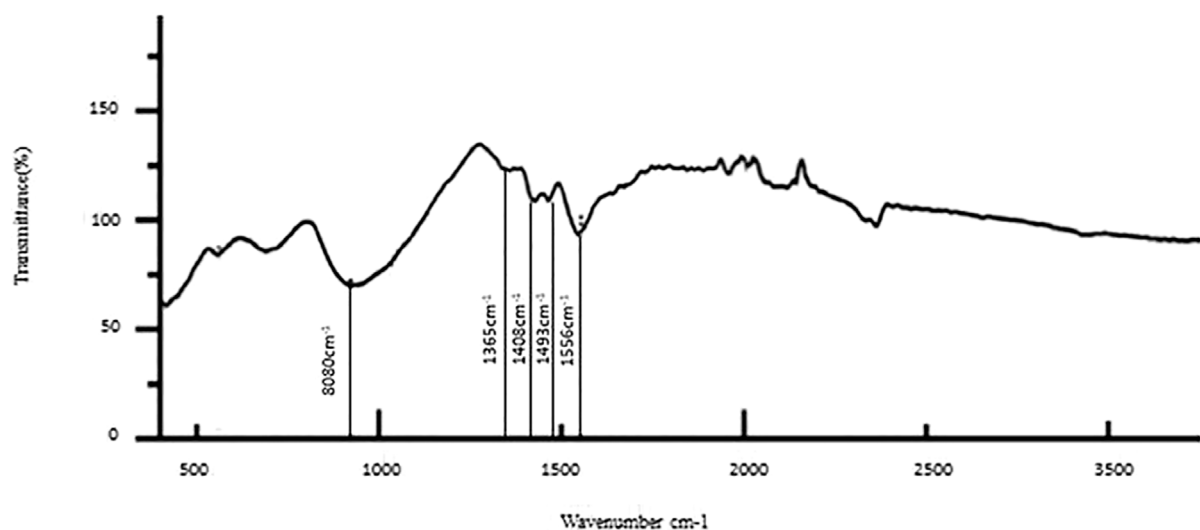


FIGURE 6 | Bioactive evaluation of glass ionomer cement (GIC) and silver nanoparticles (AgNPs) 0.6% sample with dentin.

properties of the GIC and improved the antibacterial property in arresting the caries (Padovani et al., 2015; Raggio et al., 2016; Paiva et al., 2018; Nuvvula and Mallineni, 2019).

The small sizes of the silver nanoparticles incorporated into GIC and the improved packing of particles within the matrix of the set cement may explain the improvement of the flexural and compressive strengths of the AgNP-containing GIC. Incorporating AgNPs into GIC may also result in a broader particle size distribution range. Therefore, these small silver nanoparticles can occupy the empty spaces between the larger glass particles and provide an additional bonding site for the polyacrylic polymer (Moshaverinia et al., 2008; Moshaverinia et al., 2010). Considering all these factors, we completed novel research on how various concentrations of AgNPs would change the interaction of GIC and AgNPs with the dentin. Several studies (Paiva et al., 2018; Jowkar et al., 2019) have shown that any

concentration less than 0.5% AgNPs with GIC improved the mechanical properties. Hence, our study added more than 0.5% AgNPs, that is, 0.6% AgNPs as one of the groups along with 0.2 and 0.4%.

The present study aimed to examine the quality of the bonding interaction without changing the ideal bond quality achieved with GIC. However, the study focused on the exchanges that occurred when the cement was brought into contact with dentin. It is essential to differentiate between short-term and long-term interactions. Short-term interactions occur when the freshly prepared glass ionomer cement is brought into contact with dentin. They correspond to the rapid inter-diffusions between the dentin elements and the glass ionomer cement when the cement is not entirely set. These inter-diffusions enable the GIC to adhere to dentin. This ceases once the cement has been developed completely. Long-term interactions correspond to

TABLE 1 | Wave numbers of dentin by Fourier-transform infrared spectroscopy.

Tissue	Amide I	Amide II	Amide III	Phosphate
Dentin	1,655	1,546	1,242	1,040

the slow diffusion of some elements of the glass ionomer cement through dentin. They can be caused by water in the buccal environment (Sennou et al., 1999).

This quality of binding of any restorative material to dentin is achieved through various methods such as FTIR (Paiva et al., 2018; Yamakami et al., 2018; Jowkar et al., 2019), Raman spectroscopy (Larkin, 2011; Yamakami et al., 2018), infrared spectroscopy (Larkin, 2011), and X-ray photoelectron spectroscopy (Sennou et al., 1999). Devaraj and co-workers (2013) reported that the FTIR spectra of silver nanoparticles exhibited prominent peaks at $2,927\text{ cm}^{-1}$, $1,631\text{ cm}^{-1}$, and $1,383\text{ cm}^{-1}$. Similar peaks were evident in the present study with little variation, showing various peaks, such as ν_1 , ν_2 , ν_3 , ν_4 , and ν_5 with $1,068\text{ cm}^{-1}$, $1,365\text{ cm}^{-1}$, $1,456\text{ cm}^{-1}$, $1,637\text{ cm}^{-1}$, and $1,740\text{ cm}^{-1}$, respectively. FTIR of the dentin surface showed several amide peaks (amide I, amide II, and amide III) in the range between $1,250$ and $1,650\text{ cm}^{-1}$, and the phosphate intensity ranged slightly over $1,000\text{ cm}^{-1}$ (Table 1). These results are similar to Spencer et al. (2005); Cao et al. (2014). Lin and co-workers (2001) reported two different absorption bands at $2,200\text{ cm}^{-1}$ and $2,015\text{ cm}^{-1}$ in the spectrum. Lopes and co-workers (2018) suggested a reaction in the organic matrix or between the organic matrix and minerals, resulting in a different peak.

The phosphate bonds were more peculiar with four vibrational modes: ν_1 , ν_2 , ν_3 , and ν_4 . All these modes were infrared radiography active and observed in dentin. In the present study, a single intense ν_3 band was observed at about $1,046\text{ cm}^{-1}$. The ν_3 band overlapped with the ν_1 band, the first one of greater intensity (Nelson and Featherstone, 1982). The phosphate ν_1 band was present at 960 cm^{-1} . The phosphate ν_4 band was observed at in 660 cm^{-1} and 520 cm^{-1} and was a sharp, well-defined band (Rehman and Bonfield, 1997). Last, a soft phosphate ν_2 band was observed in the region of 470 cm^{-1} (Bachmann et al., 2003). In the present study, AgNPs were added at 0.2, 0.4, and 0.6% concentration to GIC and provided evidence for the context of bond interaction with the dentin. There was a clear shift evident in the phosphate peak for control, 0.2%, and 0.4%, which was around $1,050\text{ cm}^{-1}$, while for 0.6%, there was a clear shift from $1,050\text{ cm}^{-1}$ to 880 cm^{-1} , which was evident in the present study. Various bond peaks were seen for calcium, carbonate, phosphate, and amide. In our study, only the amide and phosphate groups significantly generated peaks. The amide peaks were similar to the control, 0.2%, 0.4%, and 0.6%, ranging from $1,250$ to $1,650\text{ cm}^{-1}$. This shows that there was a change in the interaction of bonding. We found a change in bond quality when AgNPs increased to 0.6% in the present study.

Limitations

The statistical analysis was not carried out in the present study, based on the study and descriptive analysis carried out by Yamakami et al. (2018), and this is also considered one of the potential limitations. It was an *in vitro* study, and we cannot assess what would happen in a clinical setting. Second, we used GIC GC Fuji II in the study, and variations may occur using other types of GIC. FTIR does not offer the high spatial resolution capabilities of different techniques such as micro-Raman spectroscopy (approx. $1\text{ }\mu\text{m}$). However, FTIR has the advantage that IR spectra, with an acceptable signal/noise ratio, can be collected from areas measuring several hundred square micrometers in a matter of minutes.

Recommendations

We warrant further research to examine the addition of other substances to GIC and their effect on the bond strength of this material. *In vitro* studies already have good evidence, but we suggest *in vivo* studies to improve the quality of the restorations in a clinical condition.

CONCLUSION

The descriptive analysis in the present study showed that any concentration beyond 0.4% of AgNPs altered the bond quality with dentin interaction. In conclusion, adding AgNPs to a minimum improves the mechanical properties and maintains the same bond quality as GIC.

DATA AVAILABILITY STATEMENT

The raw data supporting the conclusion of this article will be made available by the authors, without undue reservation.

AUTHOR CONTRIBUTIONS

FA and SK were involved in data collection. FA, SK, and RA were involved in analysis. HA and SK developed the concept. FA, SK, HA, FA, and SM wrote the first draft. FA, SK, HA, FA, RA, and SM were involved in reviewing and editing the manuscript. All authors have read and agreed to the published version of the manuscript.

ACKNOWLEDGMENTS

The authors would like to thank Dr. Sharat Chandra Pani, Division of Paediatric Dentistry and Orthodontics, Schulich School of Medicine and Dentistry, University of Western Ontario, London, Canada, for his support on this work.

REFERENCES

- Bachmann, L., Diebold, R., Hibst, R., and Zezell, D. M. (2003). Infrared Absorption Bands of Enamel and Dentin Tissues from Human and Bovine Teeth. *Appl. Spectrosc. Rev.* 38, 1–14. doi:10.1081/asr-120017479
- Cao, Y., Liu, W., Ning, T., Mei, M. L., Li, Q.-L., Lo, E. C. M., et al. (2014). A Novel Oligopeptide Simulating Dentine Matrix Protein 1 for Biomimetic Mineralization of Dentine. *Clin. Oral Invest.* 18 (3), 873–881. doi:10.1007/s00784-013-1035-y
- Cibim, D. D., Saito, M. T., Giovani, P. A., Borges, A. F. S., Pecorari, V. G. A., Gomes, O. P., et al. (2017). Novel Nanotechnology of TiO₂ Improves Physical-Chemical and Biological Properties of Glass Ionomer Cement. *Int. J. Biomater.* 2017, 7123919. doi:10.1155/2017/7123919
- Crystal, Y. O., and Niederman, R. (2019). Evidence-Based Dentistry Update on Silver Diamine Fluoride. *Dental Clin. North America* 63 (1), 45–68. doi:10.1016/j.cden.2018.08.011
- Devaraj, P., Kumari, P., Aarti, C., and Renganathan, A. (2013). Synthesis and Characterization of Silver Nanoparticles Using Cannonball Leaves and Their Cytotoxic Activity against MCF-7 Cell Line. *J. nanotechnology* 2013, 598328. doi:10.1155/2013/598328
- Doozandeh, M., Mirmohammadi, M., and Mirmohammadi, M. (2015). The Simultaneous Effect of Extended Etching Time and Casein Phosphopeptide-Amorphous Calcium Phosphate Containing Paste Application on Shear Bond Strength of Etch-And-Rinse Adhesive to Caries-Affected Dentin. *J. Contemp. Dent Pract.* 16, 794–799. doi:10.5005/jp-journals-10024-1759
- El-Wassefy, N. A., El-Mahdy, R. H., and El-Kholany, N. R. (2018). The Impact of Silver Nanoparticles Integration on Biofilm Formation and Mechanical Properties of Glass Ionomer Cement. *J. Esthet Restor Dent* 30, 146–152. doi:10.1111/jerd.12353
- Elsaka, S. E., Hamouda, I. M., and Swain, M. V. (2011). Titanium Dioxide Nanoparticles Addition to a Conventional Glass-Ionomer Restorative: Influence on Physical and Antibacterial Properties. *J. Dentistry* 39 (9), 589–598. doi:10.1016/j.jdent.2011.05.006
- Garcia, I. M., Leitune, V. C. B., Balbinot, G. D. S., Samuel, S. M. W., and Collares, F. M. (2016). Influence of Niobium Pentoxide Addition on the Properties of Glass Ionomer Cements. *Acta Biomater. Odontologica Scand.* 2 (1), 138–143. doi:10.1080/23337931.2016.1239182
- Garcia-Contreras, R., Scougall-Vilchis, R. J., Contreras-Bulnes, R., Sakagami, H., Morales-Luckie, R. A., and Nakajima, H. (2015). Mechanical, Antibacterial and Bond Strength Properties of Nano-Titanium-Enriched Glass Ionomer Cement. *J. Appl. Oral Sci.* 23, 321–328. doi:10.1590/1678-775720140496
- Gjorgievska, E., Van Tendeloo, G., Nicholson, J. W., Coleman, N. J., Slipper, I. J., and Booth, S. (2015). The Incorporation of Nanoparticles into Conventional Glass-Ionomer Dental Restorative Cements. *Microsc. Microanal. Microsc. Microanal.* 21 (2), 21392392–21406406. doi:10.1017/S1431927615000057
- Jowkar, Z., Jowkar, M., and Shafiei, F. (2019). Mechanical and Dentin Bond Strength Properties of the Nanosilver Enriched Glass Ionomer Cement. *J. Clin. Exp. Dent* 11, e275–e281. doi:10.4317/jced.55522
- Kasraei, S., Sami, L., Hendi, S., Alikhani, M. Y., Rezaei-Soufi, L., and Khamverdi, Z. (2014). Antibacterial Properties of Composite Resins Incorporating Silver and Zinc Oxide Nanoparticles on *Streptococcus mutans* and *Lactobacillus*. *Restor. Dent. Endod.* 39 (2), 109–114. doi:10.5395/rde.2014.39.2.109
- Kent, B. E., Lewis, B. G., and Wilson, A. D. (1973). The Properties of a Glass Ionomer Cement. *Br. Dent J.* 135, 322–326. doi:10.1038/sj.bdj.4803083
- Köroğlu, A., Şahin, O., Kürkçüoğlu, I., Dede, D. Ö., Özdemir, T., and Hazer, B. (2016). Silver Nanoparticle Incorporation Effect on Mechanical and Thermal Properties of Denture Base Acrylic Resins. *J. Appl. Oral Sci.* 24 (6), 590–596.
- Larkin, P. (2011). *Infrared and Raman Spectroscopy: Principles and Spectral Interpretation*. Amsterdam: Elsevier.
- Lin, C., Lee, B., Lin, F., Kok, S., and Lan, W. (2001). Phase, Compositional, and Morphological Changes of Human Dentin after Nd:YAG Laser Treatment. *J. Endodontics* 27 (6), 389–393. doi:10.1097/00004770-200106000-00004
- Liu, Y., Yao, X., Liu, Y. W., and Wang, Y. (2014). A Fourier Transform Infrared Spectroscopy Analysis of Carious Dentin from Transparent Zone to normal Zone. *Caries Res.* 48 (4), 320–329. doi:10.1159/000356868
- Lopes, C. M. C. D. F., Galvan, J., Chibinski, A. C. R., and Wambier, D. S. (2018). Fluoride Release and Surface Roughness of a New Glass Ionomer Cement: Glass Carbomer. *Rev. Odontol. UNESP* 47, 1–6. doi:10.1590/1807-2577.06717
- Maman, P., Nagpal, M., Gilhotra, R. M., and Aggarwal, G. (2018). Nano Era of Dentistry-An Update. *Curr. Drug Deliv.* 15 (2), 186–204. doi:10.2174/1567201814666170825155201
- McKinney, J. E., Antonucci, J. M., and Rupp, N. W. (1988). Wear and Microhardness of a Silver-Sintered Glass-Ionomer Cement. *J. Dent Res.* 67, 831–835. doi:10.1177/00220345880670050701
- McLean, J. W., Nicholson, J. W., and Wilson, A. D. (1994). Proposed Nomenclature for Glass-Ionomer Dental Cements and Related Materials. *Quintessence Int.* 25, 587–589.
- Mitra, S. B., Oxman, J. D., Falsafi, A., and Ton, T. T. (2011). Fluoride Release and Recharge Behavior of a Nano-Filled Resin-Modified Glass Ionomer Compared with that of Other Fluoride Releasing Materials. *Am. J. Dent* 24, 372–378.
- Mitra, S. B., Wu, D., and Holmes, B. N. (2003). An Application of Nanotechnology in Advanced Dental Materials. *J. Am. Dental Assoc.* 134, 1382–1390. doi:10.14219/jada.archive.2003.0054
- Monteiro, D. R., Gorup, L. F., Takamiya, A. S., De Camargo, E. R., Filho, A. C. R., and Barbosa, D. B. (2012). Silver Distribution and Release from an Antimicrobial Denture Base Resin Containing Silver Colloidal Nanoparticles. *J. Prosthodont.* 21, 7–15. doi:10.1111/j.1532-849x.2011.00772.x
- Moshaverinia, A., Ansari, S., Moshaverinia, M., Roohpour, N., Darr, J. A., and Rehman, I. (2008). Effects of Incorporation of Hydroxyapatite and Fluoroapatite Nanobioceramics into Conventional Glass Ionomer Cements (GIC). *Acta Biomater.* 4, 432–440. doi:10.1016/j.actbio.2007.07.011
- Moshaverinia, A., Brantley, W. A., Chee, W. W. L., Rohpour, N., Ansari, S., Zheng, F., et al. (2010). Measure of Microhardness, Fracture Toughness and Flexural Strength of N-Vinylcaprolactam (NVC)-containing Glass-Ionomer Dental Cements. *Dental Mater.* 26, 1137–1143. doi:10.1016/j.dental.2010.08.002
- Nelson, D. G., and Featherstone, J. D. (1982). Preparation, Analysis, and Characterization of Carbonated Apatites. *Calcif Tissue Int.* 34 Suppl 2 (Suppl. 2), S69–S81.
- Nuvvula, S., and Mallineni, S. K. (2019). Silver Diamine Fluoride in Pediatric Dentistry. *J. South. Asian Assoc. Pediatr. Dent* 2 (2), 73–80. doi:10.5005/jp-journals-10077-3024
- Padovani, G. C., Feitosa, V. P., Sauro, S., Tay, F. R., Durán, G., Paula, A. J., et al. (2015). Advances in Dental Materials through Nanotechnology: Facts, Perspectives and Toxicological Aspects. *Trends Biotechnol.* 33, 621–636. doi:10.1016/j.tibtech.2015.09.005
- Paiva, L., Fidalgo, T. K. S., Da Costa, L. P., Maia, L. C., Balan, L., Anselme, K., et al. (2018). Antibacterial Properties and Compressive Strength of New One-step Preparation Silver Nanoparticles in Glass Ionomer Cements (NanoAg-GIC). *J. Dentistry* 69, 102–109. doi:10.1016/j.jdent.2017.12.003
- Porenczuk, A., Firlej, P., Szczepańska, G., Kolenda, A., and Olczak-Kowalczyk, D. (2016). The Laboratory Comparison of Shear Bond Strength and Microscopic Assessment of Failure Modes for a Glass-Ionomer Cement and Dentin Bonding Systems Combined with Silver Nanoparticles. *Acta Bioeng. Biomech.* 18, 59–70.
- Raggio, D. P., Tedesco, T. K., Calvo, A. F. B., and Braga, M. M. (2016). Do glass Ionomer Cements Prevent Caries Lesions in Margins of Restorations in Primary Teeth? *J. Am. Dental Assoc.* 147, 177–185. doi:10.1016/j.adaj.2015.09.016
- Rehman, I., and Bonfield, W. (1997). Characterization of Hydroxyapatite and Carbonated Apatite by Photo Acoustic FTIR Spectroscopy. *J. Mater. Sci. Mater. Med.* 8, 1–4. doi:10.1023/a:1018570213546
- Simmons, J. J. (1983). The Miracle Mixture. Glass Ionomer and Alloy Powder. *Tex. Dent. J.* 100 (10), 6–12.
- Sennou, H. E., Lebugle, A. A., and Grégoire, G. L. (1999). X-ray Photoelectron Spectroscopy Study of the Dentin-Glass Ionomer Cement Interface. *Dental Mater.* 15 (4), 229–237. doi:10.1016/s0109-5641(99)00036-6
- Spencer, P., Wang, Y., Katz, J. L., and Misra, A. (2005). Physicochemical Interactions at the Dentin/adhesive Interface Using FTIR Chemical Imaging. *J. Biomed. Opt.* 10, 031104. doi:10.1117/1.1914844

- Wilson, A. D., and Kent, B. E. (1972). A New Translucent Cement for Dentistry. The Glass Ionomer Cement. *Br. Dent J.* 132, 133–135. doi:10.1038/sj.bdj.4802810
- Xie, D., Brantley, W. A., Culbertson, B. M., and Wang, G. (2000). Mechanical Properties and Microstructures of Glass-Ionomer Cements. *Dental Mater.* 16 (2), 129–138. doi:10.1016/s0109-5641(99)00093-7
- Xie, D., Weng, Y., Guo, X., Zhao, J., Gregory, R. L., and Zheng, C. (2011). Preparation and Evaluation of a Novel Glass-Ionomer Cement with Antibacterial Functions. *Dental Mater.* 27 (5), 487–496. doi:10.1016/j.dental.2011.02.006
- Xu, X., and Burgess, J. O. (2003). Compressive Strength, Fluoride Release and Recharge of Fluoride-Releasing Materials. *Biomaterials* 24, 2451–2461. doi:10.1016/s0142-9612(02)00638-5
- Yamakami, S. A., Ubaldini, A. L. M., Sato, F., Medina Neto, A., Pascotto, R. C., and Baesso, M. L. (2018). Study of the Chemical Interaction between a High-Viscosity Glass Ionomer Cement and Dentin. *J. Appl. Oral Sci.* 26, e20170384. doi:10.1590/1678-7757-2017-0384

Conflict of Interest: The authors declare that the research was conducted in the absence of any commercial or financial relationships that could be construed as a potential conflict of interest.

Publisher's Note: All claims expressed in this article are solely those of the authors and do not necessarily represent those of their affiliated organizations, or those of the publisher, the editors, and the reviewers. Any product that may be evaluated in this article, or claim that may be made by its manufacturer, is not guaranteed or endorsed by the publisher.

Copyright © 2022 Abed, Kotha, AlShukairi, Almotawah, Alabdulaly and Mallineni. This is an open-access article distributed under the terms of the Creative Commons Attribution License (CC BY). The use, distribution or reproduction in other forums is permitted, provided the original author(s) and the copyright owner(s) are credited and that the original publication in this journal is cited, in accordance with accepted academic practice. No use, distribution or reproduction is permitted which does not comply with these terms.



Graphene-Based Nanomaterials for Dental Applications: Principles, Current Advances, and Future Outlook

Xiaojing Li^{1†}, Xin Liang^{2†}, Yanhui Wang¹, Dashan Wang¹, Minhua Teng¹, Hao Xu¹, Baodong Zhao^{1*} and Lei Han^{2*}

¹Department of Oral Implantology, The Affiliated Hospital of Qingdao University, Qingdao, China, ²College of Chemistry and Pharmaceutical Sciences, Qingdao Agricultural University, Qingdao, China

OPEN ACCESS

Edited by:

Mohammad Khursheed Alam,
Al Jouf University, Saudi Arabia

Reviewed by:

Marco Tatullo,
University of Bari Medical School, Italy
Naseer Ahmed,
Universiti Sains Malaysia (USM),
Malaysia

*Correspondence:

Baodong Zhao
zbd315@sina.com
Lei Han
hanlei@qau.edu.cn

[†]These authors have contributed
equally to this work

Specialty section:

This article was submitted to
Biomaterials,
a section of the journal
Frontiers in Bioengineering and
Biotechnology

Received: 29 October 2021

Accepted: 08 February 2022

Published: 10 March 2022

Citation:

Li X, Liang X, Wang Y, Wang D,
Teng M, Xu H, Zhao B and Han L
(2022) Graphene-Based
Nanomaterials for Dental Applications:
Principles, Current Advances, and
Future Outlook.
Front. Bioeng. Biotechnol. 10:804201.
doi: 10.3389/fbioe.2022.804201

With the development of nanotechnology, nanomaterials have been used in dental fields over the past years. Among them, graphene and its derivatives have attracted great attentions, owing to their excellent physicochemical property, morphology, biocompatibility, multi-differentiation activity, and antimicrobial activity. In our review, we summarized the recent progress about their applications on the dentistry. The synthesis methods, structures, and properties of graphene-based materials are discussed. Then, the dental applications of graphene-based materials are emphatically collected and described. Finally, the challenges and outlooks of graphene-based nanomaterials on the dental applications are discussed in this paper, aiming at inspiring more excellent studies.

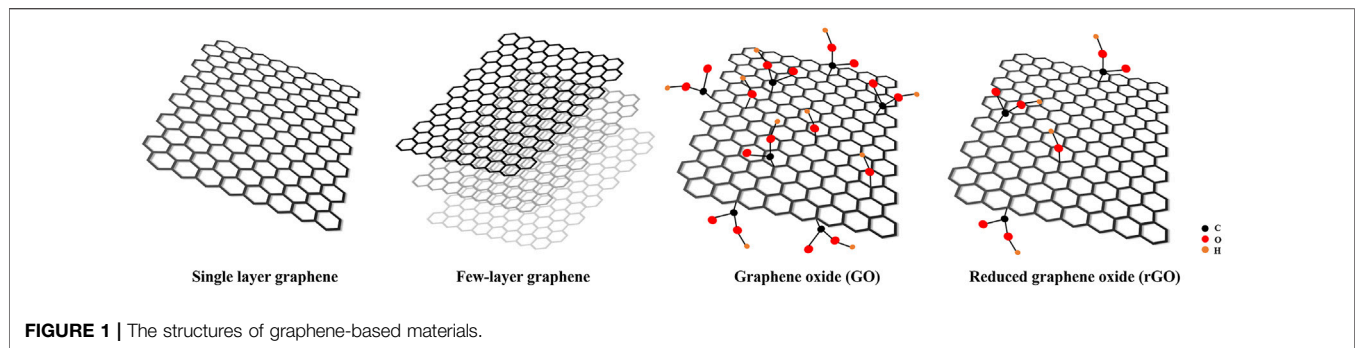
Keywords: graphene, graphene oxide, dentistry, dental implants, osseointegration, bone regeneration, dental prosthesis

INTRODUCTION

Oral health is quite important because it can deeply affect human health and quality of life (Lamster, 2021). However, World Health Organization (WHO) had reported that over 70% world's population suffered the dental-related diseases in 2016 (Gordon and Donoff, 2016). At the 74th World Health Assembly of WHO in 2021, oral health has been highly concerned (Lamster, 2021). The main common oral diseases include dental caries, periodontal diseases, tooth loss, and oral cancer. Nowadays, maintaining oral health is challenging. Although, many techniques and methods have been adopted to treat oral diseases, yet there was no ideal method. To improve these methods, many kinds of biomaterials have been applied.

Tissue defects (especially bone defect) caused by traumas, infections, or tumors are one of the most common diseases in dental field (Liu et al., 2020). Currently, many efforts have been taken to repair tissue defects. Moreover, the regeneration of dental-like tissues were harder than tissues like bone, and muscle, because cementum regeneration is slow and pulp regeneration is hard. Besides, the regeneration of alveolar bone is relative active and rapid (Riccardo et al., 2018). Tissue engineering is commonly considered as a superior treatment strategy, where scaffolds played a vital role. Nowadays, most commercial biomaterials lack osteoinductive properties, which are very important for bone regeneration (Wu et al., 2017). Therefore, it is vital and urgent to discover an osteoinductive biomaterial for bone reconstruction.

In the field of dentistry, dental implants have been widely applied to restore the missing teeth due to their various advantages. It is well known that osseointegration is the gold standard for successful dental implantation. Titanium and its alloy have been applied as dental implant materials because of



its good biocompatibility, mechanical properties, and so on. Except for all its merits, titanium implants also have failures due to the poor osseointegration. Therefore, it is important to improve the performance of titanium dental implants, and modifications of dental implant surfaces played an important role (Steflik et al., 1999). Various biomaterials have been widely applied to enhance the osteogenic properties of dental implants. In addition, the peri-implantitis is also the main failure reason for dental implants (Hideaki et al., 2019). Therefore, it is of great importance to explore new excellent antibacterial surfaces of dental implant.

Nanomaterials have showed wonderful performances in improving the strength and resist wear of tooth fillers and sealants. Moreover, nanomaterials also performed excellent antimicrobial properties in the application of restorative materials (Sharan et al., 2017). Owing to the above advantages, outstanding nanomaterials are widely applied in the dental fields of restorative materials, adhesives, cements, primers, and so on.

Among various nanomaterials, graphene, as a promising two-dimensional (2D) carbon-based nanomaterial, is the thinnest and strongest material. In 2004, it was first isolated by Novoselov and Geim using mechanical exfoliation with a sticky tape and they won the Nobel Prize in 2010 (Novoselov et al., 2004). Graphene-based materials could be divided into four categories: single-layer graphene, few-layered graphene, graphene oxide (GO) and reduced graphene oxide (rGO) (Figure 1) (Bei et al., 2019). Owing to perfect physical properties, well electrical conductivity, and excellent biocompatibility, graphene and its derivative have attracted much attention in the field of medicine and biomedical fields. Moreover, graphene and its derivatives have also aroused great attentions in the field of dentistry and tissue engineering, dental implant coatings, bone cements, resin additives, and tooth whitening.

During the past 20 years, significant advances have been achieved in regulating properties of graphene and its derivatives, elucidating their underlying mechanisms, and broadening potential applications. Up to now, there are more than 2,942 studies related to graphene-based materials for dental applications. Although numerous excellent reviews have been published, most of those reviews were mainly focused on certain specific aspect. Therefore, a comprehensive review is needed to summarize and analyze all the progress, especially the achievements from more than 2,271 research papers published

in the past 5 years (Figure 2). Such an analysis is necessary to help researchers to better understand graphene-based materials. To highlight the recent progress, various types, performance, and the applications of graphene-based materials such as graphene, GO, and rGO are summarized in this review. Finally, the challenges and future perspectives of graphene-based materials are also discussed. The purpose of this review aimed at summarizing the dental application of graphene-based materials and proposing the challenges and prospects.

SYNTHESIS AND STRUCTURE OF GRAPHENE AND ITS DERIVATIVE

Graphene, as a promising one-atom thick, 2D carbon-based nanomaterial, is currently the thinnest and strongest material. GO and rGO are the two main derivatives of graphene. Graphene and its derivatives have similar structures but different functional groups, which could lead to the differences in the physical and chemical properties. In this part, the synthesis and structure of graphene and its derivatives will be discussed.

Synthesis and Structure of Graphene

In 2004, the Novoselov and Geim group firstly isolated graphene by mechanical exfoliation method with a sticky tape (Novoselov et al., 2004). Graphene made up of sp^2 hybridized carbon atoms arranged in honeycombed lattice, and the structure of graphene is composed of six-membered rings stacked in parallel shape with no chemical groups on the surface of graphene (Zhang et al., 2019). Graphene aroused great interest, owing to its high mechanical strength, large surface area, good conductivity, and so on (Du et al., 2020).

Graphene from mechanical exfoliation has high purity and low defect, yet the yield is very low. To enhance the yield of graphene, many synthesis methods have been developed. There are two main synthesis approaches: top-down approach and bottom-up approach (Huang et al., 2012; Liao et al., 2018). On the one hand, the bottom-up approach includes the direct synthesis of graphene from the carbon materials, such as chemical vapor deposition (CVD) methods, graphitization of carbon-containing substrates by high temperature annealing, solid-phase deposition (Guo et al., 2009; Xiao et al., 2011). On the other hand, the top-down approach involves micromechanical cleavage, chemical exfoliation of GO followed by reduction treatment, and liquid-phase exfoliation.

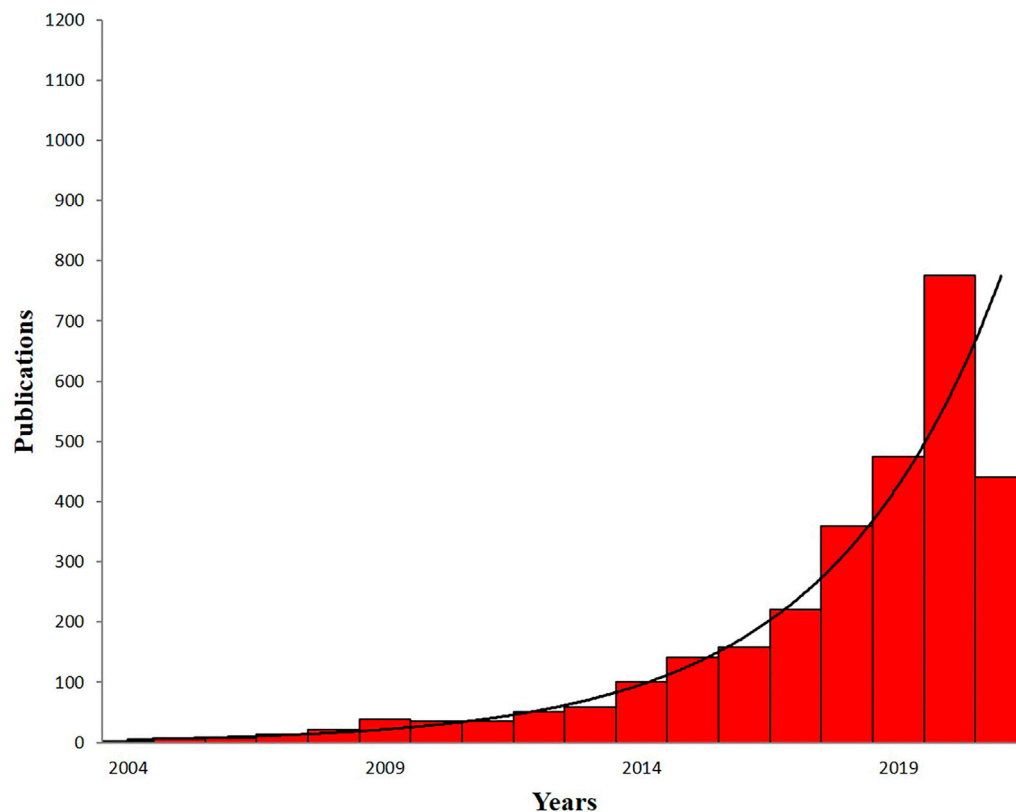


FIGURE 2 | The numbers of published papers on the application of graphene-based materials in dental field by the end of June 2021. Data are from PubMed.

Mechanical Exfoliation

In 2004, Geim group firstly obtained monolayer graphene by mechanical exfoliation method (Novoselov et al., 2004). The mechanical exfoliation of graphene is realized with a sticky tape from graphite crystals. Then, the tape was treated with specific solvents (such as acetone), and then, graphene was desorbed and harvested (Phaedon and Christos, 2012). Although the resulting graphene was highly pure without any chemical groups and defects, the yield was very low (Phaedon and Christos, 2012).

Liquid-Phase Exfoliation

Liquid-phase exfoliation is a good technique for a small scale of synthesis of graphene. First, graphite suspension is prepared in an organic solvent to weaken the van der Waals forces between the graphite layers. The graphite was then stripped into graphene sheets by ultrasound at a certain voltage. After further centrifugation, large quantities of single and multilayer graphene were obtained (Ghughe et al., 2016). The graphene is pure but small, and the number of layer is uncontrollable. Moreover, the use of surfactants and organic solvents leads to environmental pollution. The residual surfactants are difficult to remove in the process of exfoliation graphene. N,N-dimethyl-form amide (DMF), N-methyl-2-pyrrolidone (NMP), and dichlorobenzene (DCB) are the most frequently used organic

solvents. However, they are toxic and detrimental to cells (Liao et al., 2018).

Chemical Vapor Deposition

CVD, one of the most successful approaches, has been widely employed for the low-cost and high-yield preparation of high-quality monolayer or few-layer graphene, where a large area monolayer graphene film formed on the metal (Ming et al., 2014). As for the synthesis process, methane, ethane, or propane is pyrolyzed at high temperature to form carbon onto the metal foils, such as Cu, Ni, Fe, Pt, and Ru. Then, the graphene film formed from free carbon atoms (Liao et al., 2018).

Chemical Exfoliation

Among various methods, chemical methods are one of the most productive ways in the synthesis of graphene-based materials. GO is firstly obtained by the Hummers method, which involves stirring or ultrasonic reaction of graphite with sulfuric acid, sodium nitrate, and potassium permanganate in water. Then, GO is kept at 1,000°C to exfoliate GO. GO is then reduced to rGO with reducing agents. Finally, rGO is converted to graphene by thermal or chemical treatments. However, it is difficult to remove all the oxygen-containing molecules in the GO. Besides, the long processing times and the toxic gases such as NO₂ and N₂O₄ are also adverse factors during the synthesis progress.

Epitaxial Graphene

Epitaxial graphene could be fabricated on the SiC wafers under ultra-high vacuum and high temperatures. During the process, Si atoms on the surface of SiC wafers are sublimated and carbon domains are stayed on the SiC wafer surface, eventually forming graphene (Norimatsu and Kusunoki, 2014). However, because of the simultaneously growth of graphene in different position, the as-prepared graphene is not homogenous compared to other exfoliation methods.

In addition, Nickel diffusion approach is also a good alternative to SiC crystals. Nickel has a lattice structure similar to graphene with a thin nickel layer evaporated onto a SiC crystal. Being heated, the carbon diffuses through nickel layer and forms a graphene layer on the surface. The above methods make it easier to detach graphene layer from SiC crystal (Park and Ruoff, 2009).

GO exfoliation is also involved in other method such as laser ablation, anodic bonding, and photoexfoliation (Ansari et al., 2019). Laser ablation is the use of laser energy to peel graphene. In addition, the density of laser plays an important role in dominating the thickness and quality of graphene flakes (Kazemizadeh and Malekfar, 2017). Moreover, electrochemical exfoliation of graphite could obtain graphene nanosheets (Liu et al., 2008).

Synthesis and Structure of GO

GO, achieved by the oxidation of graphene, presented various reactive oxygen functional groups (e.g., hydroxyl, carboxyl, and epoxy groups) located on the basal plane and the edges of GO, which are beneficial to combine different biomolecules such as proteins and drugs. The function of the above groups aims at interacting with proteins in the form of covalent, electrostatic, and hydrogen bonding. Considering the structure of GO, the amount of carbon atoms in GO has declined to 40%–60%, which are replaced with oxygen atoms. Therefore, GO displays the hydrophilic property. Although GO has shown more hydrophilic than graphene, GO displays defective structure, poor insulating property, and mechanical property (Reina et al., 2017).

The most well-known method of GO synthesis was proposed by Hummers and Offeman in 1958, in which graphite was oxidized by potassium permanganate and sulfuric acid (Hummers and Offeman, 1958). In the Hummers method, NaNO_3 and KMnO_4 , as oxidants, were dissolved in concentrated H_2SO_4 to oxidize graphite. However, the Hummers method has the drawbacks of generation of toxic gas such as NO_2 and N_2O_4 , residual nitrate (Yu et al., 2016). To solve this problem, Kovtyukhova et al. used $\text{K}_2\text{S}_2\text{O}_8$ and P_2O_5 to peroxide the graphite (Kovtyukhova et al., 1999). The mixture was then thermally isolated and cooled at room temperature for 6 h. Then, the mixture was rinsed with water until neutral pH. Finally, GO was obtained by the Hummers method. GO with high degree of oxidation was obtained by the oxidation of KMnO_4 and NaNO_3 . In addition, Marcano et al. used KMnO_4 rather than NaNO_3 from the Hummers method. In addition, a mixture of $\text{H}_2\text{SO}_4/\text{H}_3\text{PO}_4$ was further used to enhance the effect of oxidization (Marcano et al., 2010). The modified method showed many advantages, such as high yields, no generation

of toxic gas, and the controlled temperature. As we know, oxidization is the most important factor for fabricating the GO. Furthermore, Li et al. fabricated a high quality of GO with a green method within 1 h (Peng et al., 2015). The abovementioned improved method obtained a large-scale of graphene by using a strong oxidant K_2FeO_4 without producing heavy metals and toxic gases.

Synthesis and Structure of rGO

rGO is mainly acquired by the reduction of GO. After reduction, the structures and properties of rGO have been greatly changed. Many oxygen-containing groups are removed from GO, and the sp^2 structure of GO was restored to some extent, achieving a low carbon to oxygen ration (Lazauskas et al., 2018). As a result, the electrical conductivity is significantly enhanced. However, the conductivity of rGO is still inferior to graphene because of the residual oxygen and defects structure during the synthesis of GO.

The rGO could be obtained by the reduction of GO with different reduction conditions such as chemical reduction, thermal reduction, photochemical production, photothermal reduction, biological reduction, and electrochemical reduction (Cote et al., 2009; Guo et al., 2009; He et al., 2011; Mao et al., 2010; Williams et al., 2008; Yin et al., 2010). Among them, chemical reduction of GO is the most widely used technique to synthesize rGO with hydrazine, ascorbic acid, and bovine serum albumin (BSA) as reducing agents (Phaedon and Christos, 2012) (Rai et al., 2020) (Liu et al., 2010). Hydrazine is widely used in the chemical reduction of GO, but it is toxic and detrimental to cells. To overcome the limitations of these toxic-reducing agents, various green reduction agents have been investigated. For example, Cherian et al. used ascorbic acid as a reducing agent and stirred for 2 h in 95°C water bath to produce high-yielding black rGO (Cherian et al., 2019). Except for chemical reduction, thermal reduction of GO is employed under vacuum inert or other conditions suitable for reduction between 300°C and $2,000^\circ\text{C}$ (Pei and Cheng, 2012; Wang et al., 2017). Photothermal reduction of GO can also be produced using laser with wavelengths under 390 nm (Lazauskas et al., 2018). Moreover, Li et al. reported that microwave heating could be used for the reduction of rGO in microwave ovens (Li et al., 2010).

DENTISTRY-RELATED PROPERTY OF GRAPHENE AND ITS DERIVATIVES

Biocompatibility and Cytotoxicity

To develop the application of graphene-based materials in dentistry, it is necessary to evaluate the biocompatibility and cytotoxicity of graphene-based materials (Olteanu et al., 2015). Many researchers have been discussed the cytotoxicity of graphene and its derivatives. Up to date, the affected factors involved concentrations, surface functionalization, and so on.

Many studies have shown a dose-dependent effect on the biocompatibility and toxicity of graphene and its derivatives. Some researchers showed that the toxicity of GO to fibroblast cells was little when the concentration of GO was lower than $20\text{ }\mu\text{g/ml}$ (Kan et al., 2011). Whereas, the cytotoxicity of GO

increased when the concentration was up to 50 µg/ml. Wang et al. investigated the cytotoxicity of GO in mice and the results demonstrated a dose-dependent toxic behaviors *in vivo* (Wang et al., 2011). When the concentrations of GO were 0.1 and 0.2 mg, there was no toxicity was detected. With the increase concentration to 0.4 mg, chronic toxicity was observed in mice.

Some studies have also focused on the effect of surface functionalization on cytotoxicity. Diana et al. investigated the cytotoxicity of GO, nitrogen-doped graphene (N-Gr), and thermally reduced GO (TRGO) on human dental follicle stem cells and analyzed the involved specific mechanism (Olteanu et al., 2015). The result showed the lowest cytotoxicity of GO and the highest cytotoxicity of TRGO. However, Malgorzata et al. also compared the viability of leukocytes with GO, rGO, and rGO-PEG (Podolska et al., 2020). The results showed that there was no significant difference in the viability of leukocytes at the concentration of 50 µg/ml, indicating that the surface functionalization had no effect on the cell viability.

When the biomaterials were implanted to the tissue, the inflammation would be provoked by the protein interactions. During this process, many factors such surface charge, topography, and chemical compositions were involved and affected the resorption of protein. Besides, many molecules also played an important role in the process of inflammation such as betaines (D'Onofrio et al., 2019). Moreover, the tissue inflammation caused by graphene-based materials should be attracted on much attention. Eriberto et al. had reported that titanium nanoparticles released from dental implants could cause the chronic inflammation on the soft and bone tissue around the dental implants (Bressan et al., 2019).

Therefore, when using graphene-based nanomaterials as the coatings of dental implants and so on, we should also focused on its effect on the surrounding tissue inflammation. In the study of Rosa et al., they confirmed that friction during the dental implants emplaces when the loads is over 400 mN (Rosa et al., 2021). However, they also investigated that graphene nanocoatings did not activate the high expression of inflammatory markers such as TNF-α from macrophages. Of course, more and more studies should be done to prove this result.

Stimulation of Cell Differentiation

Ideal biomaterials in the tissue engineering show the ability to induce the adherence, proliferation, and differentiation of cells. Many *in vitro* studies have shown that graphene and its derivatives showed the multi-differentiation ability such as osteogenic differentiation and regeneration of dental pulp.

Many studies have proved that graphene-based materials have the potential in promoting the osteogenic differentiation of various cells including MC3T3-E1, bone marrow mesenchymal stem cells (BMSCs), periodontal ligament stem cells (PDLs), dental pulp stem cells (DPSCs), etc. (Lee, Shin, and Lee et al., 2015a; Norahan et al., 2019; Xie et al., 2016; Zhou et al., 2016). The osteogenic differentiation of graphene, GO, and rGO has all been tested in different forms and synthesis methods. DPSCs, PDLs, dental follicle progenitor cells (DFPCs), and BMSCs are used to induce the osteogenic

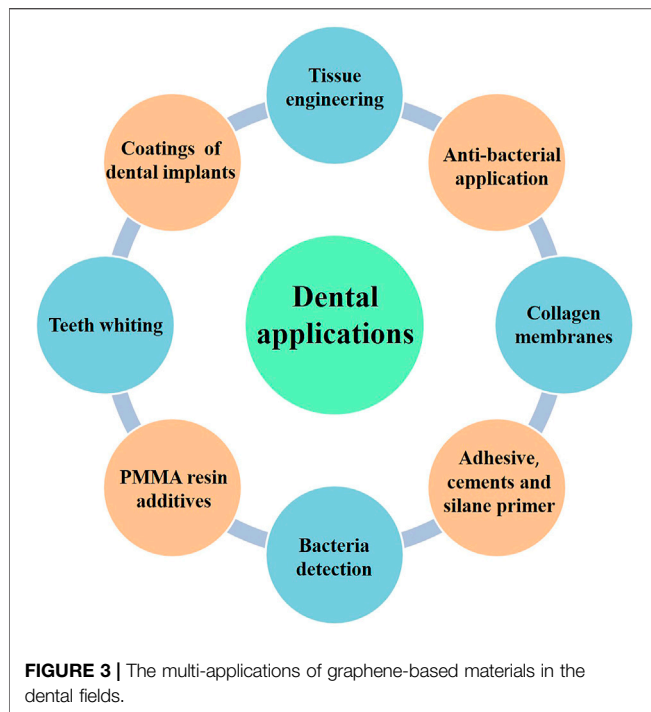
differentiation. For example, Han et al. prepared a monolayer graphene on copper foils by CVD method and studied the ability to induce the osteogenic differentiation of DPSCs (Xie et al., 2016). The results showed that osteogenic genes and proteins runt-related transcription factor 2 (RUNX2), osteocalcin (OCN), and collagen (COL) were upregulated on graphene, after the culture of 14 and 28 days. Erika et al. fabricated GO-coated COL sponge scaffolds and evaluated the ability of bone formation in tooth extraction socket (Nishida et al., 2016). After the GO scaffolds were implanted into the tooth extraction sockets of dogs, the radiological density and histological results showed that the GO promoted bone formation was fourfold compared with the control. To further investigate the osteogenic ability of rGO, Lee et al. constructed rGO coating on the HAP composites, which confirmed the osteogenic effect of rGO on human mesenchymal stem cells (hMSCs), the improved mineralization of calcium and phosphate and enhanced ALP activity (Lee et al., 2015b, Shin, and Jin et al., 2015).

To investigate the ability of graphene-based materials on the dental pulp regeneration, some researchers had focused on the neurogenic differentiation of graphene-based nanomaterials. For example, Seonwoo et al. prepared nanofibers (NFs) with electrospinning technique by incorporated with rGO and polycaprolactone (PCL) and investigated their enhanced neurogenesis of DPSCs (Seonwoo et al., 2018). The results showed that NFs with rGO showed high expression of Tuj-1 (the early marker of neurogenesis) and NeuN (the late marker of neurogenesis).

Scaffolds are an important part in the bone tissue engineering. Similarly, periodontal tissue engineering also required scaffolds to achieve an ideal therapy for periodontitis. Kawamoto et al. studied the GO modified COL sponge scaffold and evaluated the regeneration of periodontal tissue *in vivo* (Kohei et al., 2018). The rat cranial defect model was constructed, and the results showed that the new formed bone in the GO scaffolds was more than that of the control. To stimulate the therapy of periodontitis in human, the class II furcation defects of dog were conducted. CT results showed that the radiopacity of GO scaffolds was obviously increased. In addition, the histological results showed that more new formed alveolar bone was found and the furcation defect was filled without severe root resorption. More interestingly, periodontal ligament-like and cementum-like tissues were also occurred, showing an ideal therapy effect.

Antibacterial Property

As an excellent biomaterial in dentistry, low cytotoxicity and multi-differentiation ability are necessary. Except for these, antibacterial property cannot be ignored. The antibacterial effect of graphene-based materials was firstly discovered by Hu et al. (Hu et al., 2010). Then, more and more researchers had confirmed the antibacterial effect. For example, Gholibegloo et al. found that the bacterial survival rate of *S. mutans* treated with GO, GO-carnosine (GO-Car), and GO-Car/hydroxyapatite (HAP) can decrease by 67%, 86.4%, and 78.2%, respectively (Gholibegloo et al., 2018). Many composites had been



fabricated to study its antibacterial property, and some researchers fabricated the graphene-based materials into glass ionomer cements (GICs), polymethyl methacrylate (PMMA), and dental adhesive (Bregnocchi et al., 2017; Lee J.-H. et al., 2018; Sun et al., 2018).

DENTAL APPLICATIONS OF GRAPHENE-BASED MATERIALS

With the improved synthesis methods, expanded types of graphene-based materials, and engineered properties, various applications have been collected and discussed as follows (Figure 3). In addition, a main summary of graphene-based materials used in the dental field is given in Table 1.

Tissue Engineering

Tissue engineering is widely used in the repair and regeneration of various defects caused by tumors, traumas, infections, and so on. It is well known that the scaffolds provide a platform for the attachment, proliferation, and differentiation of different stem cells in the tissue engineering. Many researchers proved that graphene-based materials were suitable for fabricating or coating for scaffolds in the tissue engineering.

TABLE 1 | The graphene-based materials used in the main study of dental fields.

Applications	Types of graphene	Properties	Application types	References
Bone tissue engineering	Graphene/HA Monolayer graphene rGO/BCP rGO/HA Silk fibroin/GO/BMP-2 GO/chitosan	Biomimetic mineralization Osteogenic differentiation Osteogenic differentiation Mineralization Osteogenic differentiation Osteogenic differentiation	Scaffolds Coatings Coatings Scaffolds Scaffolds Scaffolds	Fan et al. (2014) Xie et al. (2016) Jeong-Woo et al. (2017) Lee et al. (2015b) Wu et al. (2019) Amiryaghoubi et al. (2020)
Dental pulp regeneration	Graphene dispersion NFs/rGO/PCL GO	Neural differentiation Neural differentiation Osteogenic differentiation Odontogenic differentiation	Scaffolds Scaffolds Scaffolds	Jelena et al. (2018) Seonwoo et al. (2018) Vinicius et al. (2016)
Periodontal tissue regeneration	3D collagen sponge/GO Silk-fibroin/GO	Osteogenic differentiation periodontal ligament-like tissue regeneration Cementum-like tissue regeneration Osteogenic differentiation Cementoblast differentiation	Scaffolds Scaffolds	Kohei et al. (2018) Vera-Sánchez et al. (2016)
Dental implant and abutment	Single-layer graphene sheets GO/CS/HA GO rGO/Dex rGO nanosheets GO/Minocycline hydrochloride (MH) GO/Ag	Osteogenic differentiation Osteogenic differentiation Osteogenic differentiation Osteogenic differentiation Osteogenic differentiation Antibacterial property Antibacterial property	Coatings Coatings Coatings Coatings Coatings Coatings Coatings	Ming et al. (2018) Suo et al. (2018) Zhou et al. (2016) Jung et al. (2015) Lu et al. (2020) Qian et al. (2018) Jin et al. (2017)
Collagene mmember	GO	Roughness and stiffness Osteogenic differentiation Inflammation effect	Coatings	Marco et al. (2017)

TABLE 2 | The abbreviations and full name used in this paper.

Abbreviations	Full name
WHO	World health organization
GO	Graphene oxide
rGO	Reduced graphene oxide
CVD	Chemical vapor deposition
DMF	N,N-dimethyl-form amide
NMP	N-methyl-2-pyrrolidone
DCB	Dichlorobenzene
BSA	Bovine serum albumin
N-Gr	Nitrogen-doped graphene
TRGO	Thermally reduced graphene oxide
BMSCs	Bone marrow mesenchymal stem cells
PDLCS	Periodontal ligament stem cells
DPSCs	Dental pulp stem cells
DFPCs	Dental follicle progenitor cells
RUNX2	Proteins runt-related transcription factor 2
OCN	Osteocalcin
COL	Collagen
hMSCs	Human mesenchymal stem cells
NFs	Nanofibers
PCL	Polycaprolactone
GICs	Glass ionomer cements
HAp	Hydroxyapatite
BCP	Biphasic calcium phosphate
EMFs	Electromagnetic fields
SCPAs	Stem cells of apical papilla
GNPs	Graphene nanoplatelets
FG	Fluorinated graphene
PMMA	Polymethyl methacrylate
nGO	Graphene oxide nanosheets
hGFs	Human gingival fibroblasts
hASCs	Human adipose-derived stem cells
hBMSCs	Human bone marrow mesenchymal stem cells
Dex	Dexamethasone
MH	Minocycline hydrochloride
H ₂ O ₂	Hydrogen peroxide
PDT	Photodynamic therapy
IL-8	Interleukin-8
WSL	White spot lesion
BAG	Bioactive glass
GBR	Guided bone regeneration
GTR	Guided tissue regeneration
AMOX	Amoxicillin
SRP	Solid rigid polyurethane

Bone Tissue Engineering

Many studies confirmed that graphene-based materials can promote the osteogenic differentiation of various cells including osteogenic cells such as MC3T3-E1 and stem cells such as BMSCs, PDLCS, and DPSCs. As for bone tissue engineering, graphene-based materials could be used in various forms (such as composite powers, scaffolds, and surface coatings) (Yong et al., 2018).

Many studies have reported that graphene could stimulate different types of stem cells to form osteoblasts. Fan et al. reported that graphene/HAp composite sheet displayed good biomimetic mineralization (Fan et al., 2014). The similar osteogenic differentiation has been proved by Xie et al. (Xie et al., 2016). They prepared monolayer graphene with CVD and further evaluated the degree of mineralization and expression of osteogenic genes and proteins. They found that graphene

induced RUNX2 and OCN expression and stimulated high expression of OPN and OCN in DPSCs. Moreover, Li et al. showed that graphene could induce the higher expression of osteogenic-related genes (OCN, OPN, BMP-2, and Runx2) compared with the control (Li et al., 2015). In addition, the enhanced osteogenic effect had also been confirmed by the high OCN expression at the protein level.

To confirm the osteogenic differentiation of rGO, some researchers had fabricated rGO coatings and composites (Norahan et al., 2019). Kim et al. successfully fabricated rGO coating on the biphasic calcium phosphate (BCP) (Jeong-Woo et al., 2017). The results showed that the regeneration of new bone volume was higher in the rGO groups compared with the control (Figures 4–6). Except for coatings, composites are also the new strategy to confirm the osteogenic property of rGO. Lee and his colleges also constructed the rGO composites with HAPs to further prove the promoted osteogenic properties of rGO (Lee et al., 2015a). The results showed that rGO/HAP composites at 10 µg/ml induced more calcium deposits at day 14 and 21, whereas the rGO group induced more calcium deposition at day 21. The rGO/HAP composite group also showed more mineralized bone nodules than the control at day 28 in von Kossa staining. Interestingly, Lim et al. creatively studied the synergistic effect of electromagnetic fields (EMFs) and reduced rGO on the osteogenic, neurogenic, and audiogenic differentiation of hMSCs (Lim et al., 2016). The ALP activity showed that rGO + PEMF group showed the highest ALP expression after incubation of 7 days.

To confirm the osteogenic differentiation of GO, diverse functionalizations of GO had been done such as scaffolds and nanosheets. As used for the scaffolds, Wu et al. modified the silk fibroin scaffold with GO-functionalized BMP-2 peptide. The results showed that the expression of OPN and COL-1 was upregulated by GO-P24 both in the osteogenic medium and non-osteogenic medium, demonstrating the synergistic effects of GO and BMP-2 (Wu et al., 2019). The experiment *in vivo* also confirmed the above results. Then, Azadian et al. also successfully fabricated the polyvinylidene fluoride (PVDF)–polyvinylalcohol (PVA)–GO scaffold and evaluated the ALP activity, calcium contents assays, and expression of osteogenic gene markers (Azadian et al., 2020). After 7 and 14 days, ALP expression and calcium content in PVDF-PVA group were higher than the other groups and PVDF-PVA-GO group, which also achieved the highest expression of Col-1, Runx2, and OCN in hiPSCs for 7 and 14 days. Besides, GO coatings are also constructed to prove the osteogenic property of GO. Recently, Amiryaghoubi and his co-workers reported a new injectable hydrogel composed with GO and chitosan (CS) as stem cells scaffolds for bone regeneration. According to the results, GO improved the mechanical properties of hydrogel and achieved an excellent performance in bone tissue engineering (Amiryaghoubi et al., 2020). Besides, Wei et al. testified the effect of pristine GO nanosheets on the proliferation and osteogenic ability of BMSCs by two biomimetic cell culture methods (Wei et al., 2017). When the concentration of GO nanosheets was 10 µg/ml, the proliferation of BMSCs with both seeding methods was inhibited at 3 days. Nowadays, phosphorene is a new 2D nanomaterials, which attracted great attentions after graphene (Tatullo et al., 2019a). The properties of phosphorene

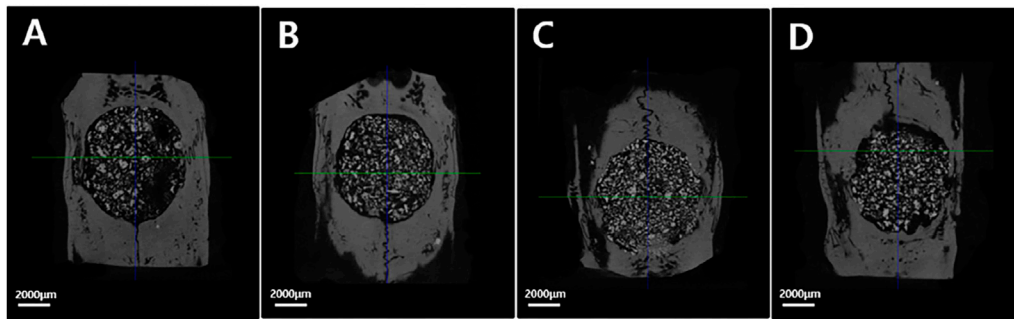


FIGURE 4 | The micro-CT images of different groups. (A) Control group; (B) rGO2 group; (C) rGO4 group; (D) rGO6 group (Jeong-Woo et al., 2017). Open access, 2017, Jeong-Woo Kim.

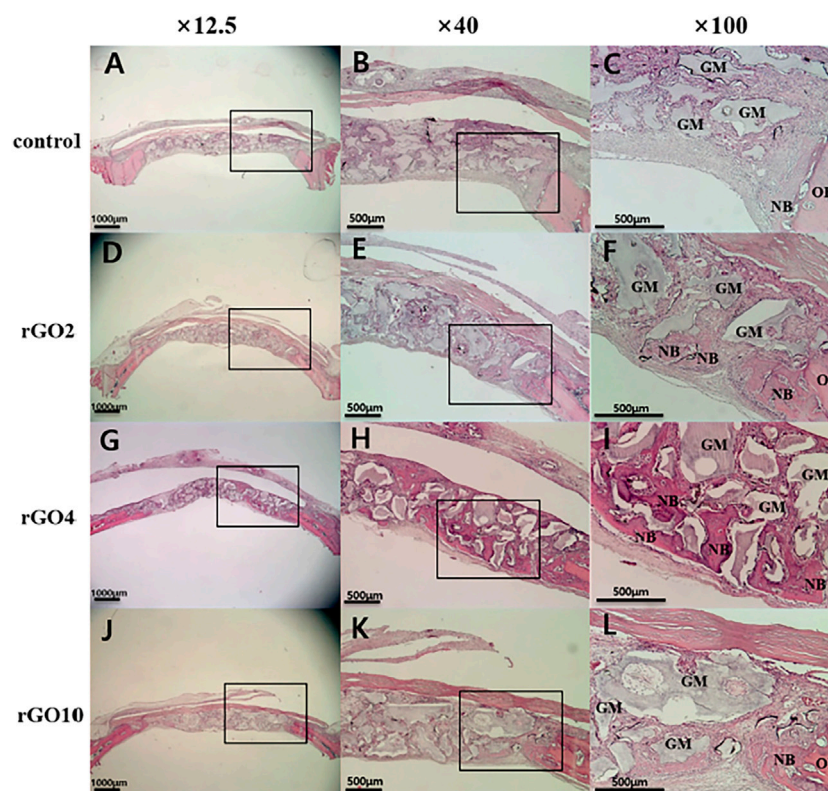


FIGURE 5 | Histological images of specimens at 2 weeks after surgery. Black box is the interest area. (A–C) Control group; (D–F) rGO2 group; (G–I) rGO4 group; (J–L) rGO10 group. NB, new bone; OB, old bone; GM, bone graft material (Jeong-Woo et al., 2017). Open access, 2017, Jeong-Woo Kim.

were quite similar to graphene-based materials, and they had wonderful biodegradability and biocompatibility compared with graphene-based materials. Liu et al. also investigated the synergistic effect of GO and phosphorene on the osteogenic differentiation (Liu et al., 2019).

Dental Pulp Regeneration

The neural and odontogenic differentiation induced by graphene-based materials were also observed. Graphene dispersion can be

applied on the neural differentiation of stem cells of apical papilla (SCPAs) (Jelena et al., 2018). A good neuron-like cell bodies with long process were found in the graphene dispersion group. The graphene dispersion group showed high expression of NF-M and β III-tubulin and showed strong β III-tubulin and NeuN immuno-reactivity 7 days after nerve induction, indicating that graphene enhanced the neural differentiation of SCPAs.

To intensify the neural differentiation of graphene-based materials, Seonwoo et al. prepared a NFs incorporated with

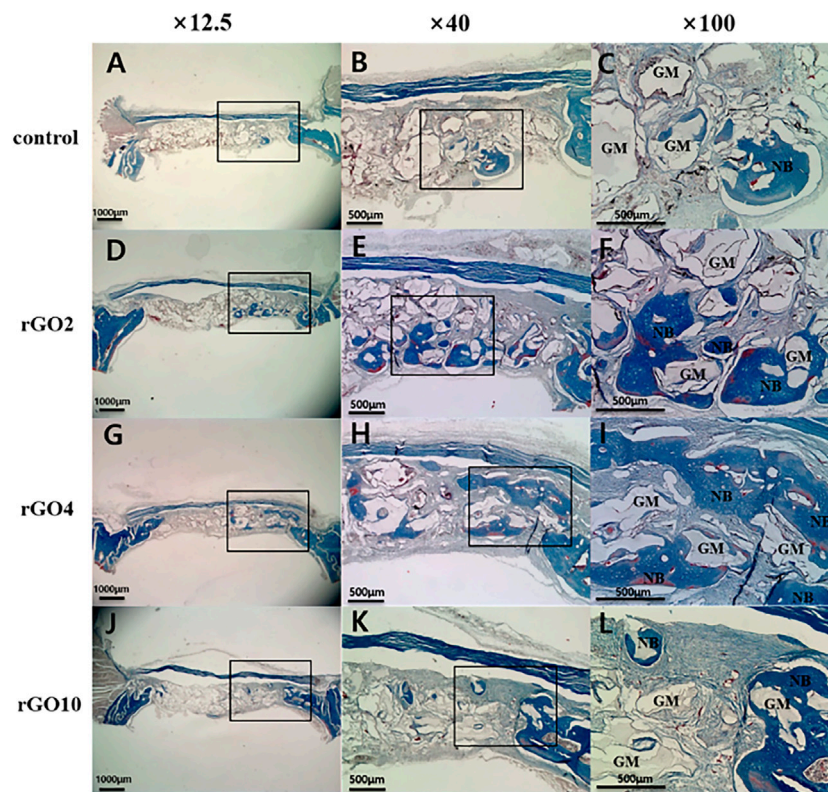


FIGURE 6 | Histological images of specimen at 8 weeks after surgery with Masson's trichrome staining. Black box is the interest area. (A–C) Control group; (D–F) rGO2 group; (G–I) rGO4 group; (J–L) rGO10 group. NB, new bone; OB, old bone; GM, bone graft material (Jeong-Woo et al., 2017). Open access, 2017, Jeong-Woo Kim.

rGO and PCL by electrospinning technique and investigated the enhanced neurogenesis of DPSCs (Seonwoo et al., 2018). The results showed that NFs with 0.1% and 1% rGO exhibited high expression of Tuj-1 and NeuN, whereas NFs with higher rGO concentration only achieved intense expression of NeuN on days 3 and 7. To prove the neural differentiation of GO, Rosa et al. investigated the effect of GO on the differentiation of DPSCs (Vinicius et al., 2016). Except for the high expression of Runx2 and OCN, GO also significantly upregulated DMP-1 and DSPP with the odontogenic differentiation of DPSCs.

Periodontal Tissue Regeneration

As we know, periodontitis is an inflammatory disease with dramatic destruction in periodontal tissue such as periodontal ligament, alveolar bone, and cementum. With the deterioration of periodontitis, the tooth faced the fate of losing, which led to many functional disorders. Therefore, it is quite urgent to regenerate and appealed many researchers. Compared with graphene and rGO, GO showed the hydrophilic surface and good dispersibility, which facilitated the absorption of some related proteins. Kawamoto et al. conducted 3D COL sponge scaffold with GO dispersion (Kohei et al., 2018). The histometric analysis showed that new formed bone in the GO group was, respectively, 2.7- and 2.3-fold greater than the control. In *in vivo* experiment, more new alveolar bone was found and filled the furcation defect. Even

more interestingly, periodontal ligament-like, cementum-like tissue was also observed in the GO group (Figures 7, 8). To investigate the related mechanisms, Vera-Sánchez et al. had fabricated the GO and silk-fibroin composites and evaluated their osteogenic differentiation and cementoblast differentiation (Vera-Sánchez et al., 2016). The results of RT-PCR showed that the cementum related genes PTPLA/CAP and CEMP1 were highly expressed after incubating for 10 days. They further ascertained the cementoblast differentiation by evaluating the expression of cementum-related protein CEMP1 on days 10.

Adhesives, Cements and Silane Primer

Adhesives and cements are two kinds of common materials in the dental restorations. Although they showed the advantages of aesthetic effect and high hardness, the problems of high polymerization shrinkage and bad antibacterial property limited their development. Silane primer played an important role in the bonding of zirconia.

Owing to various advantages of graphene-based materials, it has been applied to reinforce the properties of adhesive materials (Farooq et al., 2021). Graphene nanoplatelets (GNPs) are usually prepared as fillers of polymer dental adhesives because of the antimicrobial and antibiofilm activity. The nanocomposites filled with GNPs have been shown to effectively inhibit the active of *S. mutans* cells without compromising the bonding properties

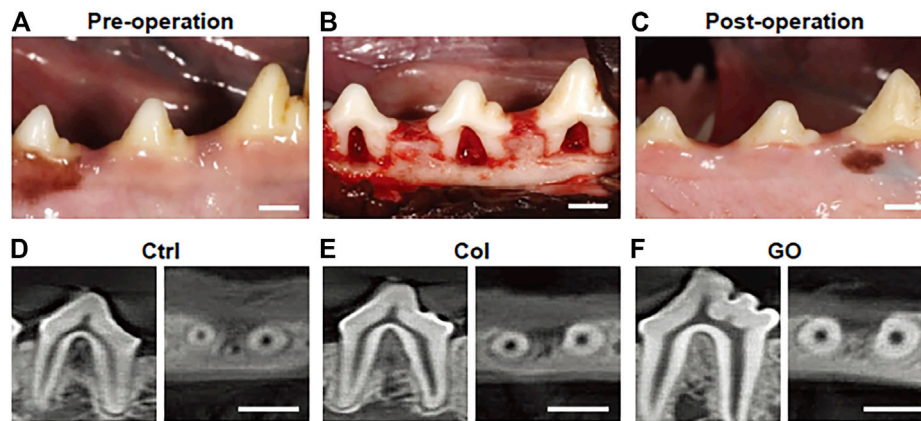


FIGURE 7 | The photographs and CT images of class II furcation defects of dog. **(A)** Pre-operation; **(B)** class II furcation defects in the surgery; **(C)** postoperation; **(D–F)** CT images after 4 weeks surgery. **(D)** No implantation group; **(E)** collagen scaffold group; **(F)** GO scaffold group (Kohei et al., 2018). Free full-text article, 2018, Kohei Kawamoto.

(Bregnocchi et al., 2017). Therefore, GNPs may be an ideal filler for dental adhesives, whose antibiofilm activity did not reduce mechanical performances.

When graphene nanosheets were added to two kinds of calcium silicate cements in powder form of different proportions, GNP–cement composites do well in shortening the bonding time and increasing the hardness of both cements. However, the bonding properties of one cement named Endocem Zr (ECZ) were impaired significantly, indicating that the addition of GNPs may improve the physico-mechanical properties of materials but not ideal for all materials in terms of bonding properties (Nileshkumar et al., 2017). Unlike gray GNPs, bright white fluorinated graphene (FG) may be a better filler in dentistry. FG has been used to the modification of GICs, presenting great advantages on the mechanical, tribological, and antibacterial properties. Compared with traditional GICs, the composites not only increase the Vickers micro hardness and compression strength but also decrease the friction coefficient. In the antibacterial properties, the GIC/FG composites achieve good antibacterial properties against *Staphylococci aureus* and *Streptococcus mutans* (Sun et al., 2018).

Considering the bonding properties of resin composites to ZrO_2 , silane primers formed adhesive layer show the poorest mechanical properties (Fallahzadeh et al., 2017). Therefore, the corporation of GO sheets into the silane primers may be a good choice to improve the mechanical properties of the adhesive layer. The results showed that the addition of GO sheets significantly increased the shear bond strength between resin composite and ZrO_2 , improved the surface roughness, and slightly increased the water contact angle (Khan et al., 2019). Therefore, graphene-base materials are ideal filler for adhesive, cements, and silane primers with proper materials.

Polymethyl Methacrylate Resin

PMMA resin has been used in prosthetic dentistry, especially complete and removable partial dentures over the past 80 years

(Bacali et al., 2019), possessing many advantages such as easy manufacturing process, low cost, low modulus of elasticity, easy repair, and good aesthetics. However, the limitations of PMMA such as low mechanical properties, large polymerization shrinkage, and the poor inhibition of biofilms formation still exist (Bahra et al., 2013; Gad et al., 2019; Matsuo et al., 2015; Ruse and Sadoun, 2014). Recently, the graphene family has exhibited good mechanical and desirable antibacterial properties in different forms in other fields. Because of the mechanical effect of graphene on PMMA, Azevedo et al. has achieved the definitive maxillary full-arch rehabilitation by incorporating GO into the PMMA resin (Azevedo et al., 2019). After 8 months later, there were no mechanical, aesthetic, and other complications found, indicating that the addition of GO to PMMA resin would be a good choice for prosthetic rehabilitation. Bacali et al. reported PMMA with graphene-silver nanoparticles (Gr-Ag), and the mechanical properties, hydrophilic abilities, and the morphology of the composites were further evaluated (Bacali et al., 2019). The results showed that the compression parameters, bending, and tensile strength of the Gr-Ag fillers were significantly higher than the pure PMMA group, indicating that the addition of Gr-Ag improved the mechanical properties of PMMA resin. Moreover, Bacali and his co-workers also assessed the antibacterial properties of Gr-Ag-modified PMMA (Bacali et al., 2020), and the results confirmed that Gr-Ag-modified groups showed higher inhibition effect in all Gram-negative strain, *Staphylococcus aureus*, *E. coli*, and *Streptococcus mutans* (Bacali et al., 2020). In conclusion, graphene-based materials may be an ideal filler to promote the physical-mechanical and antibacterial properties of PMMA.

Meanwhile, graphene oxide nanosheets (nGO) have been used to improve the antimicrobial-adhesive effects of PMMA resin by Lee and his co-workers (Lee SM. et al., 2018). The immediate antimicrobial-adhesive effects showed that nGO-incorporated groups exhibited stronger antimicrobial effect against *C. albicans*, *E. coli*, *S. aureus*, and *S. mutans* after 1 h of

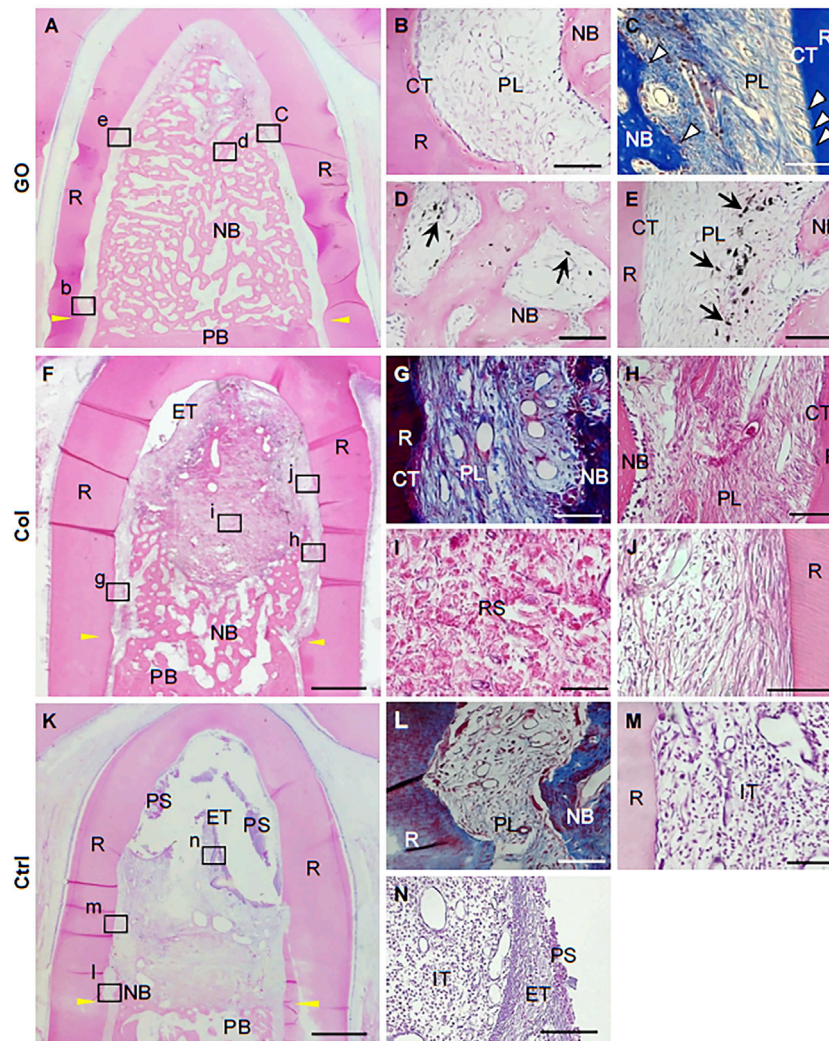


FIGURE 8 | Histological images after GO scaffold implantation into class II furcation defects of dog. **(A–E)** GO scaffold group; **(F–J)** collagen scaffolds group; **(K–N)** no implantation group. **(A)** Periodontal ligament-like tissue, cementum-like tissue, and alveolar bone with Sharpey's fiber. **(B–E)** High magnification of the black box areas **(B–E)** in **(A)**. **(G–J)** High magnification of the black box areas **(G–J)** in **(F)**. **(K–N)** High magnification of the black box areas **(L–N)** in **(K)** (Kohei et al., 2018). Free full-text article, 2018, Kohei Kawamoto.

attachment than only PMMA group except for 0.5% nGO-incorporated group against *E. coli* and *S. mutans*. Furthermore, PMMA with 2% nGO showed greater anti-adhesion effects than the PMMA resin after culturing for 28 days of *C. albicans*, indicating that the hydrophilicity of PMMA could be improved by the incorporation of nGO. Bacali et al. evaluated the antibacterial activity, cytotoxicity, monomer release, and mechanical properties of PMMA resin by adding graphene-Ag nanoparticles (G-AgNp) (Bacali et al., 2020). The results showed that G-AgNp-containing group displayed good antibacterial effects on both Gram-positive and Gram-negative strain and exhibited better antibacterial effect on Gram-positive strain *Staphylococcus aureus* than PMMA. Besides, Gram-negative strain *E. coli* also was sensitive to G-AgNp. Therefore, graphene family proved to be promising filler mixed with PMMA in antibacterial applications.

Coatings for Dental Implants and Abutments

Titanium and its alloys have been widely used in dental implants, owing to their various advantages such as good biocompatibility, high mechanical property, and corrosion resistance (Fe Ridoun et al., 2017; Jeong et al., 2017; Xie et al., 2014). However, implant failure still occurs. Because of the poor osseointegration and peri-implantitis of titanium and its alloys (Berglundh et al., 2019; Smeets et al., 2014; Kordbacheh et al., 2019). Therefore, many surface modifications by graphene-based materials have been used to improve the bioactivities of titanium and its alloys (Barfeie et al., 2015; Chouirfa et al., 2018; Li et al., 2009; Souza et al., 2019).

It is well known that the osseointegration is the gold standard of the success of dental implants. Therefore, the new bone

formation between dental implants and bone tissues is of great significance. In regard to the superior osteogenic differentiation of graphene in bone tissue engineering, they also attracted much attention in the modification of dental implant. Park et al. reviewed that the strategies of graphene-based modifications could be mainly divided into four categories: 1) a layer-by-layer assembly; 2) PMMA-mediated method; 3) electrophoretic deposition; and 4) APTES-induced method (Park et al., 2017).

To promote the osteogenic properties, many researchers have made many efforts. Gu et al. successfully constructed single-layer graphene sheets on the titanium substrates by PMMA-mediated method (Ming et al., 2018). The result showed that graphene sheets exhibited superior adhesion and proliferation properties of human gingival fibroblasts (hGFs), human adipose-derived stem cells (hASCs), and human BMSCs (hBMSCs) compared with the control. The osteogenic differentiation of hASCs and hBMSCs was also improved by graphene sheets. Otherwise, the above study recommended that PMMA treated at 160°C for 2 h enhanced the adhesion strength between graphene and titanium. Meanwhile, Suo et al. successfully constructed a homogeneous GO/CS/HAp composites on Ti substrates by electrophoretic deposition, improving the osteogenic property of Ti substrates *in vitro* and osseointegration *in vivo* (Suo et al., 2018). Besides, some other researchers have tried the APTES inducement to fabricate the graphene coatings (Jung et al., 2015; Lu et al., 2020; Zhou et al., 2016). Zhou et al. modified the Ti substrates with 3-APTES and then immersed it in the GO solution for 24 h (Zhou et al., 2016). PDLCs were used to evaluate the cell attachment, morphology, proliferation, and osteogenic differentiation *in vitro*. All the results indicated that GO coating showed a positive effect on improving the bioactivity of PDLCs. Jung and his colleges prepared a dexamethasone (Dex)-loaded rGO coating on Ti13Nb13Zr (MPCr-TNZ) multipass rolled titanium alloy surface by using the spin coating technology after pretreatment with APTES, showing a stable long-term release behaviors of Dex (Jung et al., 2015). A possible mechanism is π - π stacking. In conclusion, the Dex-loaded rGO-MPCr-TNZ achieved an enhanced proliferation and facilitated differentiation of MC3T3-E1 cells into osteoblasts. Besides, an implantation of a prototype dental implant was modified with Dex-loaded rGO to an artificial bone block, demonstrating the feasibility of the stable surface modification for further clinical applications. Recently, Lu and his coworkers ascertained the improved osteogenic effect of rGO nanosheets on the surface of titanium (Lu et al., 2020). Compared with the control, rGO groups achieved more growth factors absorption especially BMP-2, IGF, and TGF- β . Moreover, rGO-modified group displayed a more stretch cell cytoskeleton and excellent osteogenic differentiation of BMSCs. In conclusion, graphene-based material is a good candidate for dental implant surface modification material, which can improve the osseointegration of implants with proper methods.

Moreover, the excellent antibacterial activity of graphene also captured a tremendous interest in dental implant surface coatings. It is generally accepted that the failures of dental implants are still the occurrence of bacterial infections. Therefore, the titanium surface antibacterial modification is

very necessary. Qian et al. reported an electrostatically prepared GO coating that loaded the Minocycline hydrochloride (MH) on titanium (Qian et al., 2018). According to the results, GO-modified surface could prohibit the growth of *Staphylococcus aureus*, *Streptococcus mutans*, and *Escherichia coli*. Whereas MH-loaded GO coating showed superior antibacterial property with the synergistic effect of GO and MH, which were contact-killing and release-killing. Jin et al. prepared GO film and Ag nanoparticles on the titanium substrates by electroplating and ultraviolet reduction methods (Jin et al., 2017). In addition, GO-Ag-Ti composite exhibited a prominent antibacterial activity to *S. mutans* and *P. gingivalis* compared with the Ti substrate. Therefore, it can be inferred that graphene-based materials showed outstanding antibacterial activity when combined with proper materials.

Besides the titanium dental implants, zirconia has also been used for dental implant materials (Priyadarsini et al., 2017). To improve its inert properties, many surface modifications have been used. Graphene shows obvious merit in zirconia implant surface modifications (Cho and Ko, 2013; Schunemann et al., 2019). Li et al. reported a zirconia/graphene (ZrO₂/GNs) composites, which were coated on the surface of zirconia by an atmosphere plasma spray technique (Li et al., 2014). The results indicated that ZrO₂/GNs composites showed the excellent wear resistance and zirconia's tribological behavior.

Peri-implantitis has become a common disease that threatened the survival rates of dental implants. Many strategies have been adopted to avoid the happening of peri-implantitis (Jansäker et al., 2010; Koldstad et al., 2018). Abutments are also an important part of implant system, and medicated abutments may be a good option for preventing the peri-implantitis. Qian et al. successfully fabricated a MH-loaded GO coating on the dental implant abutment and further evaluated the antibacterial activities and the adhesive ability of gingival fibroblasts with beagle dogs model (Qian et al., 2019). The results showed that MH/GO/Ti group achieved least bone loss, which could be negligible, whereas Ti and MH/Ti groups showed more bone loss by micro-CT analysis. Histological analysis showed that there were fewer neutrophils and more osteocytes in the MH/GO/Ti group than in the Ti and MH/Ti groups. Therefore, it can be inferred that MH-loaded GO films on abutment surfaces may be a superior option for prohibiting the progress of peri-implantitis in the future.

Teeth Whitening

As we know, hydrogen peroxide (H₂O₂) has been widely utilized for in-office whitening for a long time. The H₂O₂ molecules can penetrate deep the teeth and carry out the bleaching process. However, the relative high concentrations of H₂O₂ caused some side effects such as tooth sensitivity and gingival irritation (Carey and Clifton, 2014; Kwon and Wertz, 2015). Therefore, many improved strategies have been made to accelerate the tooth whitening and decrease the side effects. Su et al. reported a cobalt (Co)/tetraphenylporphyrin (TPP)/rGO nanocomposite, which showed better tooth-whitening efficacy stained with dyes, tea, and betel nuts compared with the H₂O₂ only (I-Hsuan et al., 2016). In addition, H₂O₂ produces an extremely

short lifetime of the active free radical. Therefore, to achieve a good bleaching effect, H_2O_2 must first penetrate into the teeth and quickly produce active free radicals. However, the Co/TPP/rGO nanocomposite can be used as a catalyst to produce more reactions between the staining molecules and H_2O_2 , which accelerate the bleaching process. In summary, graphene-based materials are a promising catalyst for tooth whitening application with proper types and concentrations.

Antibacterial Property

Bacterial biofilms formation plays an important role in the development of dental caries, periodontitis, and peri-implantitis (Berglundh et al., 2019; He et al., 2015; Kulshrestha et al., 2014; Slots, 2017; Ucja et al., 2017). Traditionally, antibiotics have been used for controlling the biofilms formation, whereas they faced a serious problem of antibiotic resistance, owing to the abuse of antibiotics. Many new methods for inhibiting the biofilms formation were explored. The antibacterial effect of graphene-based materials was firstly discovered by Hu et al. (Hu et al., 2010). Nowadays, more and more researchers have confirmed its effect in a various form.

Photodynamic therapy (PDT) is known as an alternative method for treatment of periodontitis and peri-implantitis. Pourhajibagher et al. investigated the effect of graphene quantum dot (GQD)–curcumin (Cur) on the perio-pathogen biofilms combined with PDT (Pourhajibagher et al., 2019). The production of reactive oxygen species (ROS) by GOD-Cur-PDT showed a dose-dependent tendency. In addition, the expression of *A. actinomycetemcomitans rcpA* gene, *P. gingivalis fimA* gene, and *P. intermedia inpA* gene was, respectively, reduced by 8.1-, 9.6-, and 11.8-fold. To improve the ICG photodynamic effect, Gholibegloo et al. fabricated the ICG-loaded GO, GO-Car, or GO-Car/HAp nanocomposites and investigated the antibacterial effect of *S. mutans* in planktonic forms and biofilms (Gholibegloo et al., 2018). Compared with the control group, GO, GO-Car, and GO-Car/HAp group decreased the survival of bacteria to 67%, 86.4%, and 78.2%, respectively. In preventing the biofilm formation of *S. mutans*, GO-Car group acquired the best effect. When treated with aPDT, the GO, GO-Car, and GO-Car/HAp group suppressed the biofilm formation up to 1.4%, 63.8%, and 56.8%, respectively. Then, the expression of *S. mutans gtfB* gene was decreased 6.0-, 9.0-, and 7.9-fold in GO, GO-Car, and GO-Car/HAp group, respectively, when without irradiation. Akbari et al. constructed the nano-GO (NGO)–ICG composite to enhance the efficiency of ICG (Akbari et al., 2017). The results showed that the NGO-ICG group achieved a significant decrease in the count of *E. faecalis* and significantly suppressed the formation of *E. faecalis* biofilms.

Besides, some researchers fabricated the graphene-based materials into GICs, PMMA, and dental adhesives to improve the physical properties and antibacterial ability (Bregnocchi et al., 2017; Lee J.-H. et al., 2018; Sun et al., 2018). Interestingly, Sun et al. evaluated the antibacterial effect of GIC/FG composites on *S. aureus* and *S. mutans*, showing that the highest antibacterial ability of FG (4 wt%) for *S. aureus* and *S. mutans* was 88.1% and 85.3%, respectively (Sun et al., 2018). Lee et al. constructed an nGO-PMMA and achieved a sustained antibacterial effect against

C. albicans over 28 days (Lee SM. et al., 2018). Bregnocchi et al. added the GNP into the dental adhesive with different content and 0.2% GNP group, showing a significant decrease on the *S. mutans* (Bregnocchi et al., 2017).

Jin et al. studied the antibacterial effect of Ti-GO-Ag *in vitro* and *in vivo* (Jin et al., 2019). The GO group significantly suppressed the bacterial activity of *S. mutans* and *P. gingivalis* with the increasing concentration after 24 h. Zhao et al. confirmed the antibacterial activity of GO on *S. mutans* (Zhao et al., 2020). Ioannidis et al. synthesized the Ag-GO composites, showing obviously decreased bacterial activity (Ioannidis et al., 2019). Qiu et al. testified that GO had excellent antibacterial properties against *S. aureus* and *E. coli* (Jiajun et al., 2017). Potential mechanisms were further analyzed, including nanoknives, wrapping or trapping, and ROS production. rGO was also used as an antimicrobial agent in suppressing *S. mutans* by Wu et al. (Wu et al., 2018).

Inhibition of the Growth of Fungal

Peri-implantitis is a common reason for the failure of dental implant. In addition, *Candida albicans* was found in the 31% peri-implantitis sites, which quickly attracted much attention (Schwarz et al., 2015). The species of *Candida albicans* in peri-implantitis patients were five times more than the health individuals (Alrabiah et al., 2019; Alsahhaf et al., 2019). Moreover, owing to the high resistant property of *Candida albicans*, the antifungal treatments are usually failure. The modification of dental implant coatings is a good method to prevent the formation of biofilms. Agarwalla et al. constructed a graphene nanocoating for twice (TiGD) and five times (TiGV) to evaluate the inhibition properties of *Candida albicans* biofilms (Agarwalla et al., 2020). According to XTT reduction assay, TiGD and TiGV group showed a lower absorbance compared with the control. Then, the colony-forming unit assay that displayed less viable yeast units on the TiGD and TiGV groups at all time points, indicating the inhibition effect of graphene on the fungal biofilm formations.

Biosensor for Biomarker Detection From Saliva

Dental disease diagnosis can reduce the mortality rates of some serious diseases and improve the quality of life of patients. Owing to its superior electrical and mechanical ability, graphene-based materials are widely used on dental disease diagnosis (Goldoni et al., 2021).

Detection of Bacterial and Viral Markers

In 2012, Mannoor et al. made the first graphene nano-sensors on tooth enamel (Mannoor et al., 2012). They fabricated a graphene sensing element with wireless readout coil attached to the silk fibroin and then transferred onto tooth enamel. The specific biological recognition was acquired by self-assembling AMP-graphene peptides onto the graphene. The reduction of electrical resistance displayed the binding of a single *E. coli* on the bare graphene nanosensor. The AMP-modified graphene nanosensor that showed a strong connection between peptides

and bacteria realized the detection and wireless remote monitoring of *Helicobacter pylori* in saliva. Gandouzi et al. build an electrochemical platform using rGO and gold nanoparticles, and the sensor showed high sensitivity to the markers (Islem et al., 2019). To diagnosis of periodontal disease in early stage, Lee et al. developed a sandwich-type biosensors to detect the human odontogenic ameloblast-associated protein (ODAM) (Wu et al., 2017). Checkin et al. fabricated an rGO/MoS₂ glassy carbon electrode for detecting the human papillomavirus type 16 (HPV-16), showing the high stability and storage performance (Chekin et al., 2018).

Detection of Drugs

Saliva is a body fluid that could be used to monitor the drugs and other harmful substances. The biosensor is a good way to detect the analytes of drugs and harmful substances. Graphene-based materials are applying to fabricate the portable biosensors. For example, Mohamed and his coworkers constructed a bio-sensing platform for detecting two drugs: the benzocaine and the antipyrine. To increase the selectivity of biosensor, they decorated the GO sheets with metal nanoparticles, achieving the high reproducibility and good selectivity (Mohamed et al., 2017). Parate and his coworkers modified the electrochemical biosensors with graphene to monitor the byproducts of smoke and tobacco with a wide linear range of 1–100 nM and the sensitivity of 1.89 μ A/decade (Parate et al., 2019).

Detection of Cancer Markers

Early diagnosis of disease is especially important for patients. Biomarker is a biological molecule which indicated the incidence of disease such as infections and cancers (Henry and Hayes, 2012). The overexpression of interleukin-8 (IL-8) has been reported to indicate the tumor progression in the oral cancer. Verma and his colleges fabricated a biosensor with rGO-modified ITO glass modified with rGO and then coated with Au NPs to detect IL-8 in saliva (Verma et al., 2017). The biosensor showed a high reproducibility and a long-term stability. After 3 months of dry storage, the retainment of biosensor is 94.3%. The performance of the biosensor was 91.8% even after 4 months of dry storage. To improve the performance of the biosensors, they also modified the GO with zinc oxide reduction and functionalized with IL-8 antibodies, showing that the sensitivity of the biosensor increased and the reproducibility was low with a RSD of 3.2% (Verma and Singh, 2019).

Owing to its excellent electrical properties, graphene-based appliances are reckoned as the gold standard in the biosensor fields. Nowadays, borophene has the similar anisotropic property with graphene (Tatullo et al., 2019b and Zavan et al., 2019). Song et al. had reported that, if the combination with borophene, graphene, and hydrogel in proper way, then it will improve the effect of implantable and wearable biosensors (Song et al., 2017). Therefore, when graphene combined with proper 2D nanomaterials, the efficiency of biosensors will be improved significantly. This may be also a good tendency in the development of graphene-based biosensors before the final clinical usage.

Prevention of Enamel and Dentin From Demineralization

White spot lesion (WSL) is one of the most common side effects of orthodontic treatment, which is caused by enamel surface demineralization (Bishara and Ostby, 2008; Nam et al., 2019). Therefore, it is of great significance to overcome WSL in the process of orthodontic treatment. Nowadays, many researchers are focusing on the studying of new bonding agent composites to prevent enamel demineralization caused by bacteria. Owing to the prominent antibacterial activity of GO, Lee and his colleges added GO to a bioactive glass (BAG) (Lee J.-H. et al., 2018). With the increase of GO concentrations, the length of anti-demineralization of the GO group increased. Besides, GO-containing groups also showed superior antibacterial effect after 24 and 48 h. The anti-demineralization mechanism of the composites may be attributed to the synergic effect of antibacterial effect of GO and the ion-releasing effect of BAG. In conclusion, GO is a promising addition in the anti-demineralization of enamel in proper style.

Dental caries and dental erosion were associated with the demineralization of dentin, which caused by acids from bacteria, food, and environments, leading to dentin hypersensitivity and pain (Addy, 2005). Nizami et al. synthesized five different functionalized GO nanocomposites and evaluated the biological and prevention of demineralization effects (Nizami et al., 2020). Compared with the control, the dentin slices coated with GO-Ag, GO-Ag-CaF₂, and GO-CaF₂ all exhibited superior prevention of decalcification. Besides, GO-Ag and GO-Ag-CaF₂ group showed better antibacterial activity compared with other groups, which may be related to the synergic effect of GO and Ag. Moreover, the color variation of f-GO coatings on the dentin surface is negligible, showing that GO is a promising dentin anti-demineralization resistant material.

Collagen Membranes

COL membrane has been widely used in guided bone regeneration (GBR) and guided tissue regeneration (GTR) as barrier membrane to hinder the soft tissue invasion of new bone (Chu et al., 2017a, Deng, and Sun et al., 2017; Elgali et al., 2017; Wessing et al., 2018). Although COL membrane has many good properties such as facilitated manipulation and less surgical intervention, it still needs various modifications to improve the biocompatibility (Chu et al., 2017b, Deng, and Hou et al., 2017). Marco et al. enriched the COL membranes with GO *via* a non-covalent functionalization by the interaction between oxygenated carbon functional parts and COL through hydrogen bonding (Marco et al., 2017). The membranes enriched with GO displayed lower deformability, increased roughness, and higher stiffness. The stability of GO in the COL membranes was evaluated, and there was no obvious GO dissolution found in the bulk solution compared with the control. After cultured on membranes with 2 and 10 μ g/ml GO for 3 days, the cell proliferations of hGFs were significantly higher than the control. With regard to the inflammatory response, the secretion of IL-6 and PGE2 showed significantly lower in cells cultured on the GO-coated membranes at day 3 compared with the control.

When it comes to DPSCs, Radunovic et al. confirmed the superior cell proliferations on the GO-coated membranes at days 14 and 28 (Li et al., 2015). Meanwhile, the expression of BMP2 on the GO-coated membranes showed higher at days 3 and 7, whereas the expression of RUNX2 and SP7 on the GO-coated membranes showed augmented after 21 and 28 days when compared with the uncoated membrane. Moreover, LDH assay also confirmed that there was no cytotoxicity of GO coating on the COL membrane. Although GO displayed superior effect on the cell growth, osteogenic differentiation, and inflammation response on the COL membrane, more studies *in vitro* and *in vivo* also needed to testify their definitive effect.

Drug Delivery

There is close interaction between bacteria and dental caries, and endodontic and periodontal diseases. Several groups of bacteria that require a common antibacterial strategy are usually involved. Amoxicillin (AMOX) is a kind of broad-spectrum antibiotic that is the first-choice antibiotic in the treatment of endodontic infection in Asian and European countries. In the conditional paste, the dose is not accurately controlled (Nan, 2016). Drug carrier can realize the gradual releasing of antibiotic drugs to easily achieve effective drug concentrations in the infected site. Trusek et al. found that GO had the potential in acting as a drug carrier especially in the therapy of dental inflammation (Trusek and Kijak, 2021). They linked the AMOX to GO using a peptide linker, which is Leu-Leu-Gly and then dispersed in the hydrogel. AMOX was released by enzymatic hydrolysis, showing the effective release of AMOX and the inhibition of bacteria strain growth.

CHALLENGES AND PERSPECTIVE

Graphene-based materials, the promising candidate for dentistry materials, have been widely used in dentistry research, owing to its cell differentiation and antibacterial property. This review summarized recent advances in expanding the types of graphene-based materials and the studies about dentistry-related properties, deepening the understanding of categories of graphene-based materials. Compared with other related studies, it displayed a quite comprehensive and detailed review about the great achievements in dental applications such as bone tissue engineering, coatings for dental implants, antibacterial properties, and COL membranes. Except for the usage in the tissue engineering, dental implant coatings, COL membrane, and adhesive, we also focused on some new fields such as drug delivery, prevention of enamel and dentin from demineralization, biosensor for oral biomarker detection, and inhibition of the growth of fungal. For the application of graphene nanomaterials in the biosensor, it could be used to detect bacterial and viral markers, drugs, and cancer markers. With the development of the application of graphene in dentistry, there are still some challenges remaining to be tackled until the final commercialized (Figure 9).

The Long-Term Cytotoxicity *in Vivo*

The excellent biomaterials should have a good biocompatibility without long-term cytotoxicity *in vitro* and *in vivo*. Because of the

limited understanding of graphene and its derivatives, a major challenge in clinical applications is the uncertainty of its cytotoxicity *in vitro* and *in vivo* and its potential mechanisms. Up to date, there is not an agreement on the cytotoxicity and potential hazards of graphene-based materials according to various studies. The factors that involved in the cytotoxicity include concentrations, surface functionalization, types of graphene family and synthetic methods, and the layer numbers. Many studies have focused on the dose dependent effect on the cytotoxicity, yet there is still no agreement for the upper limit concentration (Duch et al., 2011). When it comes to the mechanisms of cytotoxicity, ROS may play a critical role in it. When it comes to the synthetic methods, graphene films with CVD method were reckoned to be biocompatible without obvious cytotoxicity. However, when the graphene is dispersed in solution, the cytotoxicity of cells may increase, which may be caused by the accumulation or the sharp-edge penetration into the cells. Therefore, we expect to see more and more studies for long-term biocompatibility *in vivo* and *in vitro*.

The Method to Solve the Biodegradation

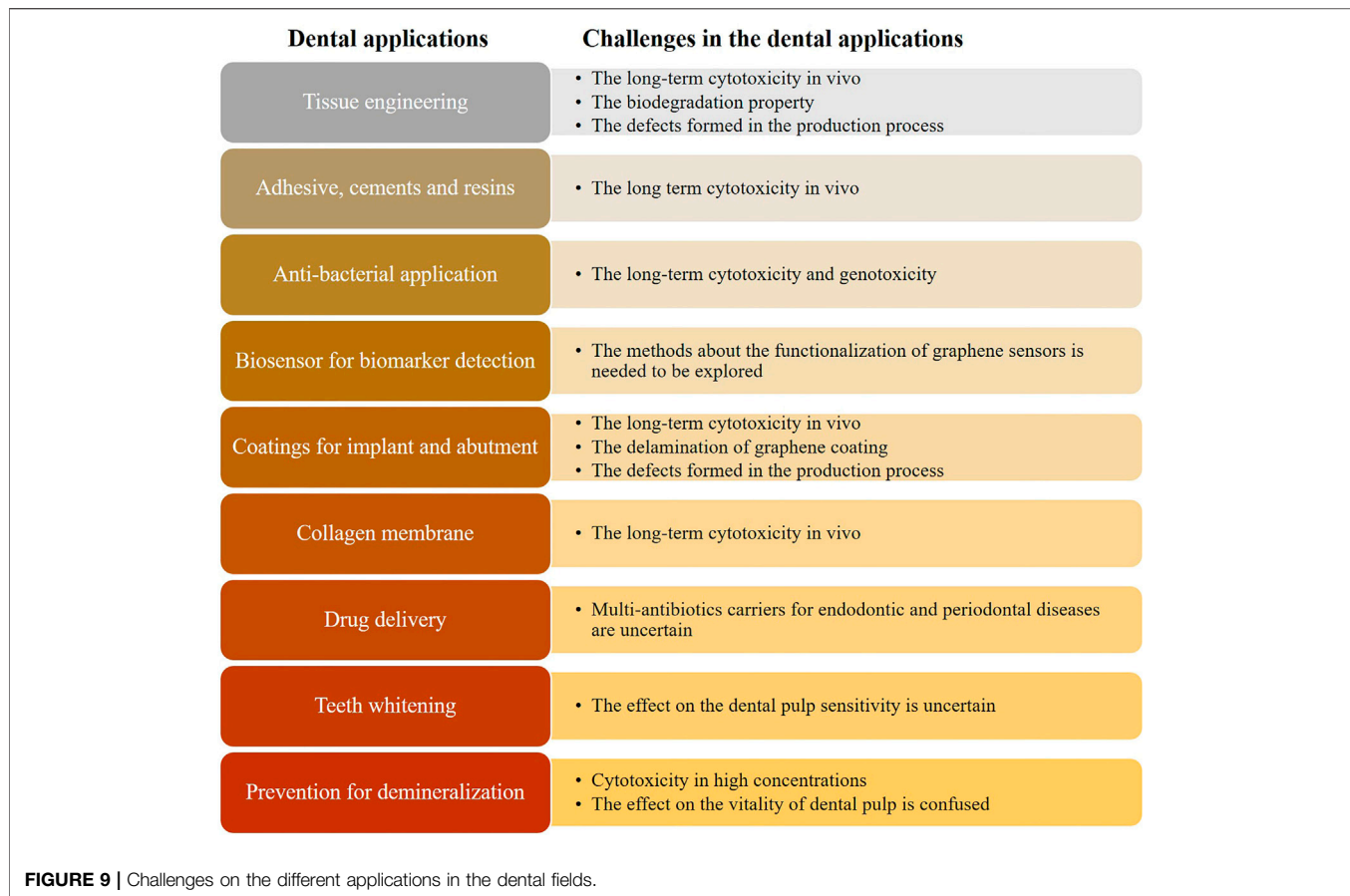
Another challenge of graphene-based materials is biodegradation, especially in the tissue engineering. With the formation of new tissue, the ideal biomaterial should be free of any toxic products. Up to date, there are limited literatures related to the biodegradation of graphene-based materials. Therefore, graphene-based material as an ideal biomaterial should be considered and explored to solve this problem.

The Defects Formed During the Production Process

Although the graphene used in the current study is a controlled and uncontaminated defect-free sample, the synthesis quality still should be highly examined when it was used in the clinic. Actually, the formed variety of unpredictable defects is mainly due to the differences in the synthesis methods. Once the defects occurred, the properties such as susceptibility and electronic structure will be changed (Riccardo et al., 2018). Therefore, the study of controlling the formation of defects during the graphene synthesis would be a big challenge but rewarding research areas.

Disturb the Cell Cycle

Little of the current studies are focused on the effect of GO on the cell cycle. Nowadays, Hashemi et al. innovatively focused on the effect of GO on the cell cycle (Hashemi et al., 2020). In the process of cell division, the synthesis of DNA is an important process. Certain mutagenic materials may cause the increased DNA synthesis in the S phase of cell cycle. In the study of Hashemi et al., GO increased the synthesis of DNA according to some underlying mechanisms such as damaged DNA, ROS production, and the double-strand breaks in the DNA. Cell apoptosis in mGO and nGO were greater, displaying a concentration and size-dependent effect. According to the result of cell cycle, there is a block occurred in the G₂/M phase in the GO groups. Thus, the



effect of GO on the cell cycle should be carefully considered and explored before the final clinical use.

The Delamination of Graphene Coatings

Although graphene has many advantages in the dental field, its clinical translation still needs to be carefully considered. Graphene-based materials had been used as coatings mostly in tissue engineering and dental implants surfaces. When used as the dental implant coatings, friction could cause the delamination of carbon-based coatings on the titanium with the loads over 400 mN (Rosa et al., 2021). Rosa et al. reported that there was no significant difference between the solid rigid polyurethane (SRP) and the control following the integrity of graphene nanocoatings by stimulating in the SRP and pig maxilla. However, there was a 35% decrease in the coverage area in ROI C from the bone group. Therefore, the delamination of graphene should be considered carefully (Agarwalla et al., 2019; Ming et al., 2018). How to improve the bonding strength of graphene-based materials and substrates is a question needed to be carefully investigated. Up to date, the methods of graphene-based materials coatings on the titanium surfaces are mainly based on the physical methods such as spin-coating techniques and layer-by-layer self-assembly methods. There are still technical difficulties in the chemical combinations with graphene and titanium. Compared with the chemical methods, the physical combination is weak and unstable. Therefore, the delamination of graphene coatings is a risk factor when used as

coatings. Some researchers had reported that titanium nanoparticles released from dental implants could cause the chronic inflammation on the soft and bone tissue around the dental implants. Therefore, when used graphene-based nanomaterials as coatings of dental implants, we should focus on the delamination of graphene coatings on the surrounding tissue inflammation.

The Improved Methods About the Functionalization of Graphene Sensors

When used as a biosensor, the large surface of graphene-based nanomaterial provided good adhesive conformability and the functionalization of graphene could be achieved by AMP-graphene peptide for biological recognition. However, there are different kinds of bacteria in the mouth. Therefore, more strategies should be made to recognize more bacteria, and the methods for the functionalization of graphene biosensor are quite important.

Single-Antibiotic Carrier for Endodontic and Periodontal Diseases

GO had been successfully used as a drug carrier for AMOX, which is a broad-spectrum antibiotic and could be used to control dental infections. However, the limitation is that whether two or more different drugs could be carried simultaneously is not sure and more studies are needed.

Eventually, graphene and its derivatives will be of great interest for a long time in the dental field. Although there are some limitations in the real clinical usage of dentistry, graphene, as a more reliable and more friendly biomaterial, can prompt more effective dental treatments in the near future.

The Unfavorable Antibacterial Effect on the Polymicrobial Biofilms

Although there are many studies focused on the antibacterial effect of graphene-based materials on the single strain of bacteria or monoclonal biofilm, yet no study revealed the antibacterial effect on the mature polymicrobial biofilms. On the basis of the above limitations, there is still a long way before the final clinical usage of graphene-based materials in the dental fields.

CONCLUSION

All acronyms and abbreviation used in the text are explained in Table 2. Just as we know, there are many advantages of graphene-based materials for the dental fields. However,

many challenges also existed and need to be solved. All in all, we should confirm that the usage of graphene-based nanomaterials in dental fields deserved to be deeply studied and it can bring a quite new dental treatment concept in the near future.

AUTHOR CONTRIBUTIONS

XL and XLi contributed equally to this review paper. LH, BZ, and XL conceived the content of paper. XL, LH, and XLi wrote the paper. YW, DW, HX, and MT took part in the collecting some related papers. XL draw all the flow charts. All authors reviewed and commented on the manuscript.

FUNDING

This work was financially supported by National Natural Science Foundation of China (Grant No. 21705087) and Research Foundation for Distinguished Scholars of Qingdao Agricultural University (663-1117015).

REFERENCES

- Addy, M. (2005). Tooth Brushing, Tooth Wear and Dentine Hypersensitivity - Are They Associated? *Int. Dental J.* 55 (4 Suppl. 1), 261–267. doi:10.1111/j.1875-595x.2005.tb00063.x
- Agarwalla, S. V., Ellepola, K., Costa, M. C. F. d., Fachine, G. J. M., Morin, J. L. P., Castro Neto, A. H., et al. (2019). Hydrophobicity of Graphene as a Driving Force for Inhibiting Biofilm Formation of Pathogenic Bacteria and Fungi. *Dental Mater.* 35 (3), 403–413. doi:10.1016/j.dental.2018.09.016
- Agarwalla, S. V., Ellepola, K., Silikas, N., Castro Neto, A., Seneviratne, C. J., and Rosa, V. (2021). Persistent Inhibition of *Candida Albicans* Biofilm and Hyphae Growth on Titanium by Graphene Nanocoating. *Dental Mater.* 37 (2), 370–377. doi:10.1016/j.dental.2020.11.028
- Akbari, T., Pourhajabagher, M., Hosseini, F., Chiniforush, N., Gholibegloo, E., Khoobi, M., et al. (2017). The Effect of Indocyanine green Loaded on a Novel Nano-Graphene Oxide for High Performance of Photodynamic Therapy against *Enterococcus faecalis*. *Photodiagnosis Photodynamic Ther.* 20, 148–153. doi:10.1016/j.pdpdt.2017.08.017
- Alp, G., Johnston, W. M., and Yilmaz, B. (2019). Optical Properties and Surface Roughness of Prepolymerized Poly(methyl Methacrylate) Denture Base Materials. *The J. Prosthetic Dentistry* 121 (2), 347–352. doi:10.1016/j.prosdent.2018.03.001
- Alrabiah, M., Alshagroud, R. S., Alsahhaf, A., Almojaly, S. A., Abduljabbar, T., and Javed, F. (2019). Presence of *Candida* Species in the Subgingival Oral Biofilm of Patients with Peri-implantitis. *Clin. Implant Dent Relat. Res.* 21 (4), 781–785. doi:10.1111/cid.12760
- Alsahhaf, A., Al-Aali, K. A., Alshagroud, R. S., Alshiddi, I. F., Alrahlah, A., Abduljabbar, T., et al. (2019). Comparison of Yeast Species in the Subgingival Oral Biofilm of Individuals with Type 2 Diabetes and Peri-implantitis and Individuals with Peri-implantitis without Diabetes. *J. Periodontol.* 90 (12), 1383–1389. doi:10.1002/JPER.19-0091
- Amiryaghoubi, N., Noroozi Pesyan, N., Fathi, M., and Omid, Y. (2020). Injectable Thermosensitive Hybrid Hydrogel Containing Graphene Oxide and Chitosan as Dental Pulp Stem Cells Scaffold for Bone Tissue Engineering. *Int. J. Biol. Macromolecules* 162, 1338–1357. doi:10.1016/j.jbiomac.2020.06.138
- Ansari, M. O., Gauthaman, K., Essa, A., Bencherif, S. A., and Memic, A. (2019). Graphene and Graphene-Based Materials in Biomedical Applications. *Cmc* 26 (38), 6834–6850. doi:10.2174/0929867326666190705155854
- Azadian, E., Arjmand, B., Ardeshirylajimi, A., Hosseinzadeh, S., Omid, M., and Khojasteh, A. (2020). Polyvinyl Alcohol Modified Polyvinylidene Fluoride-graphene Oxide Scaffold Promotes Osteogenic Differentiation Potential of Human Induced Pluripotent Stem Cells. *J. Cel. Biochem.* 121 (5-6), 3185–3196. doi:10.1002/jcb.29585
- Azevedo, L., Antonaya-Martin, J., Molinero-Mourelle, P., and del Rio-Highsmith, J. (2019). Improving PMMA Resin Using Graphene Oxide for a Definitive Prosthodontic Rehabilitation - a Clinical Report. *J. Clin. Exp. Dent* 11, 670–674. doi:10.4317/jced.55883
- Bacali, C., Badea, M., Moldovan, M., Sarosi, C., Nastase, V., Baldea, I., et al. (2019). The Influence of Graphene in Improvement of Physico-Mechanical Properties in PMMA Denture Base Resins. *Materials* 12 (14), 2335. doi:10.3390/ma12142335
- Bacali, C., Baldea, I., Moldovan, M., Carpa, R., Olteanu, D. E., Filip, G. A., et al. (2020). Flexural Strength, Biocompatibility, and Antimicrobial Activity of a Polymethyl Methacrylate Denture Resin Enhanced with Graphene and Silver Nanoparticles. *Clin. Oral Invest.* 24 (4), 2713–2725. doi:10.1007/s00784-019-03133-2
- Barfeie, A., Wilson, J., and Rees, J. (2015). Implant Surface Characteristics and Their Effect on Osseointegration. *Br. Dent J.* 218 (5), E9. doi:10.1038/sj.bdj.2015.171
- Bei, H., Yang, Y., Zhang, Q., Tian, Y., Luo, X., Yang, M., et al. (2019). Graphene-Based Nanocomposites for Neural Tissue Engineering. *Molecules* 24 (4), 658. doi:10.3390/molecules24040658
- Berglundh, T., Jepsen, S., Stadlinger, B., and Terheyden, H. (2019). Peri-implantitis and its Prevention. *Clin. Oral Impl Res.* 30 (2), 150–155. doi:10.1111/clr.13401
- Bishara, S. E., and Ostby, A. W. (2008). White Spot Lesions: Formation, Prevention, and Treatment. *Semin. Orthod.* 14 (3), 174–182. doi:10.1053/j.sodo.2008.03.002
- Bregnocchi, A., Zanni, E., Uccelletti, D., Marra, F., Cavallini, D., De Angelis, F., et al. (2017). Graphene-based Dental Adhesive with Anti-biofilm Activity. *J. Nanobiotechnol.* 15 (1), 89. doi:10.1186/s12951-017-0322-1
- Bressan, E., Ferroni, L., Gardin, C., Bellin, G., Sbricoli, L., Sivoella, S., et al. (2019). Metal Nanoparticles Released from Dental Implant Surfaces: Potential Contribution to Chronic Inflammation and Peri-Implant Bone Loss. *Materials* 12 (12), 2036. doi:10.3390/ma12122036
- Carey, C. M., and Clifton, M. (2014). Tooth Whitening: What We Now Know. *J. Evid. Based Dental Pract.* 14, 70–76. doi:10.1016/j.jebdp.2014.02.006
- Chekin, F., Bagga, K., Subramanian, P., Jijie, R., Singh, S. K., Kurungot, S., et al. (2018). Nucleic Aptamer Modified Porous Reduced Graphene oxide/MoS2

- Based Electrodes for Viral Detection: Application to Human Papillomavirus (HPV). *Sensors Actuators B: Chem.* 262, 991–1000. doi:10.1016/j.snb.2018.02.065
- Cherian, R. S., Sandeman, S., Ray, S., Savina, I. N., J., A., and P. V., M. (2019). Green Synthesis of Pluronic Stabilized Reduced Graphene Oxide: Chemical and Biological Characterization. *Colloids Surf. B: Biointerfaces* 179, 94–106. doi:10.1016/j.colsurfb.2019.03.043
- Cho, B. H., and Ko, W. B. (2013). Preparation of Graphene-ZrO₂ Nanocomposites by Heat Treatment and Photocatalytic Degradation of Organic Dyes. *J. Nanosci. Nanotech.* 13 (11), 7625–7630. doi:10.1166/jnn.2013.7819
- Chouirfa, H., Bouloussa, H., Migonney, V., and Falentin-Daudré, C. (2019). Review of Titanium Surface Modification Techniques and Coatings for Antibacterial Applications. *Acta Biomater.* 83, 37–54. doi:10.1016/j.actbio.2018.10.036
- Chu, C., Deng, J., Hou, Y., Xiang, L., Wu, Y., Qu, Y., et al. (2017a). Application of PEG and ECGG Modified Collagen-Base Membrane to Promote Osteoblasts Proliferation. *Mater. Sci. Eng. C* 76, 31–36. doi:10.1016/j.msec.2017.02.157
- Chu, C., Deng, J., Sun, X., Qu, Y., and Man, Y. (2017b). Collagen Membrane and Immune Response in Guided Bone Regeneration: Recent Progress and Perspectives. *Tissue Eng. B: Rev.* 23 (5), 421–435. doi:10.1089/ten.teb.2016.0463
- Cote, L. J., Cruz-Silva, R., and Huang, J. (2009). Flash Reduction and Patterning of Graphite Oxide and its Polymer Composite. *J. Am. Chem. Soc.* 131 (31), 11027–11032. doi:10.1021/ja902348g
- D'Onofrio, N., Balestrieri, A., Neglia, G., Monaco, A., Tatullo, M., Casale, R., et al. (2019). Antioxidant and Anti-inflammatory Activities of Buffalo Milk δ -Valerobetaine. *J. Agric. Food Chem.* 67 (6), 1702–1710. doi:10.1021/acs.jafc.8b07166
- Du, Z., Wang, C., Zhang, R., Wang, X., and Li, X. (2020). Applications of Graphene and its Derivatives in Bone Repair: Advantages for Promoting Bone Formation and Providing Real-Time Detection, Challenges and Future Prospects. *Ijn* 15, 7523–7551. doi:10.2147/IJN.S271917
- Dubey, N., Rajan, S. S., Bello, Y. D., Min, K.-S., and Rosa, V. (2017). Graphene Nanosheets to Improve Physico-Mechanical Properties of Bioactive Calcium Silicate Cements. *Materials* 10 (6), 606. doi:10.3390/ma10060606
- Duch, M. C., Budinger, G. R. S., Liang, Y. T., Soberanes, S., Urich, D., Chiarella, S. E., et al. (2011). Minimizing Oxidation and Stable Nanoscale Dispersion Improves the Biocompatibility of Graphene in the Lung. *Nano Lett.* 11 (12), 5201–5207. doi:10.1021/nl202515a
- Dybowska-Sarapuk, L., Kotela, A., Krzemiński, J., Wróblewska, M., Marchel, H., Romaniec, M., et al. (2017). Graphene Nanolayers as a New Method for Bacterial Biofilm Prevention: Preliminary Results. *J. Aoac Int.* 100 (4), 900–904. doi:10.5740/jaoacint.17-0164
- El Bahra, S., Ludwig, K., Samran, A., Freitag-Wolf, S., and Kern, M. (2013). Linear and Volumetric Dimensional Changes of Injection-Molded PMMA Denture Base Resins. *Dental Mater.* 29 (11), 1091–1097. doi:10.1016/j.dental.2013.07.020
- Elgali, I., Omar, O., Dahlin, C., and Thomsen, P. (2017). Guided Bone Regeneration: Materials and Biological Mechanisms Revisited. *Eur. J. Oral Sci.* 125 (5), 315–337. doi:10.1111/eos.12364
- Fallahzadeh, F., Safarzadeh-Khosroshahi, S., and Atai, M. (2017). Dentin Bonding Agent with Improved Bond Strength to Dentin through Incorporation of Sepiolite Nanoparticles. *J. Clin. Exp. Dent* 9 (6), e738–e742. doi:10.4317/jced.53722
- Fan, Z., Wang, J., Wang, Z., Ran, H., Li, Y., Niu, L., et al. (2014). One-pot Synthesis of Graphene/hydroxyapatite Nanorod Composite for Tissue Engineering. *Carbon* 66, 407–416. doi:10.1016/j.carbon.2013.09.016
- Farooq, I., Ali, S., Al-Saleh, S., Al-Hamdan, E. M., Al-Refai, M. H., Abduljabbar, T., et al. (2021). Synergistic Effect of Bioactive Inorganic Fillers in Enhancing Properties of Dentin Adhesives-A Review. *Polymers* 13 (13), 2169. doi:10.3390/polym13132169
- Gandouzi, I., Tertis, M., Cernat, A., Saidane-Mosbahi, D., Ilea, A., Cristea, C., et al. (2019). A Nanocomposite Based on Reduced Graphene and Gold Nanoparticles for Highly Sensitive Electrochemical Detection of pseudomonas Aeruginosa through its Virulence Factors. *Materials* 12 (7), 1180. doi:10.3390/ma12071180
- Gholibegloo, E., Karbasi, A., Pourhajibagher, M., Chiniforush, N., Ramazani, A., Akbari, T., et al. (2018). Carnosine-graphene Oxide Conjugates Decorated with Hydroxyapatite as Promising Nanocarrier for ICG Loading with Enhanced Antibacterial Effects in Photodynamic Therapy against Streptococcus Mutans. *J. Photochem. Photobiol. B: Biol.* 181, 14–22. doi:10.1016/j.jphotobiol.2018.02.004
- Ghuge, A. D., Shirode, A. R., and Kadam, V. J. (2017). Graphene: A Comprehensive Review. *Cdt* 18 (6), 724–733. doi:10.2174/1389450117666160709023425
- Goldoni, R., Farronato, M., Connelly, S. T., Tartaglia, G. M., and Yeo, W.-H. (2021). Recent Advances in Graphene-Based Nanobiosensors for Salivary Biomarker Detection. *Biosens. Bioelectron.* 171, 112723. doi:10.1016/j.bios.2020.112723
- Gordon, S. C., and Donoff, R. B. (2016). Problems and Solutions for Interprofessional Education in north American Dental Schools. *Dental Clin. North America* 60 (4), 811–824. doi:10.1016/j.cden.2016.05.002
- Gu, M., Liu, Y., Chen, T., Du, F., Zhao, X., Xiong, C., et al. (2014). Is Graphene a Promising Nano-Material for Promoting Surface Modification of Implants or Scaffold Materials in Bone Tissue Engineering? *Tissue Eng. Part B: Rev.* 20 (5), 477–491. doi:10.1089/ten.TEB.2013.0638
- Guazzo, R., Gardin, C., Bellin, G., Sbricoli, L., Ferroni, L., Ludovichetti, F., et al. (2018). Graphene-Based Nanomaterials for Tissue Engineering in the Dental Field. *Nanomaterials* 8 (5), 349. doi:10.3390/nano8050349
- Guo, H.-L., Wang, X.-F., Qian, Q.-Y., Wang, F.-B., and Xia, X.-H. (2009). A green Approach to the Synthesis of Graphene Nanosheets. *ACS Nano* 3 (9), 2653–2659. doi:10.1021/nn900227d
- Hashemi, E., Akhavan, O., Shamsara, M., Ansari Majd, S., Sanati, M. H., Daliri Joupri, M., et al. (2020). Graphene Oxide Negatively Regulates Cell Cycle in Embryonic Fibroblast Cells. *Ijn* 15, 6201–6209. doi:10.2147/IJN.S260228
- He, J., Zhu, X., Qi, Z., Wang, C., Mao, X., Zhu, C., et al. (2015). Killing Dental Pathogens Using Antibacterial Graphene Oxide. *ACS Appl. Mater. Inter.* 7 (9), 5605–5611. doi:10.1021/acsami.5b01069
- He, Q., Wu, S., Gao, S., Cao, X., Yin, Z., Li, H., et al. (2011). Transparent, Flexible, All-Reduced Graphene Oxide Thin Film Transistors. *ACS Nano* 5 (6), 5038–5044. doi:10.1021/nn201118c
- Henry, N. L., and Hayes, D. F. (2012). Cancer Biomarkers. *Mol. Oncol.* 6 (2), 140–146. doi:10.1016/j.molonc.2012.01.010
- Hideaki Hirooka Stefanand Renvert (2019). Diagnosis of Periimplant Disease. *Implant Dent* 28 (2), 144–149. doi:10.1097/ID.0000000000000868
- Hu, W., Peng, C., Luo, W., Lv, M., Li, X., Li, D., et al. (2010). Graphene-based Antibacterial Paper. *ACS Nano* 4 (7), 4317–4323. doi:10.1021/nn101097v
- Huang, X., Qi, X., Boey, F., and Zhang, H. (2012). Graphene-based Composites. *Chem. Soc. Rev.* 41 (2), 666–686. doi:10.1039/c1cs15078b
- Hummers, W. S., and Offeman, R. E. (1958). Preparation of Graphitic Oxide. *J. Am. Chem. Soc.* 208, 1334–1339. doi:10.1021/ja01539a017
- I-Hsuan Yu-PinLeeChen-FuWangand Lai-Hao (2016). Evaluating a Cobalt-Tetraphenylporphyrin Complex, Functionalized with a Reduced Graphene Oxide Nanocomposite, for Improved Tooth Whitening. *J. Esthet Restor Dent* 28 (5), 321–329. doi:10.1111/jerd.12240
- Ioannidis, K., Niazi, S., Mylonas, P., Mannocci, F., and Deb, S. (2019). The Synthesis of Nano Silver-Graphene Oxide System and its Efficacy against Endodontic Biofilms Using a Novel Tooth Model. *Dental Mater.* 35 (11), 1614–1629. doi:10.1016/j.dental.2019.08.105
- Jelena, S., Bosko, T., Nadja, N., Jasna, V., Radmila, P., Rados, G., et al. (2018). Differentiation of Stem Cells from Apical Papilla into Neural Lineage Using Graphene Dispersion and Single Walled Carbon Nanotubes. *J. Biomed. Mater. Res.* 106 (10), 2653–2661. doi:10.1002/jbm.a.36461
- Jeong, W.-S., Kwon, J.-S., Lee, J.-H., Uhm, S.-H., Ha Choi, E., and Kim, K.-M. (2017). Bacterial Attachment on Titanium Surfaces Is Dependent on Topography and Chemical Changes Induced by Nonthermal Atmospheric Pressure Plasma. *Biomed. Mater.* 12 (4), 045015. doi:10.1088/1748-605X/aa734e
- Jin, J., Fei, D., Zhang, Y., and Wang, Q. (2019). Functionalized Titanium Implant in Regulating Bacteria and Cell Response. *Ijn* 14, 1433–1450. doi:10.2147/IJN.S193176
- Jin, J., Zhang, L., Shi, M., Zhang, Y., and Wang, Q. (2017). Ti-GO-Ag Nanocomposite: The Effect of Content Level on the Antimicrobial Activity and Cytotoxicity. *Ijn* 12, 4209–4224. doi:10.2147/IJN.S134843
- Jung, H. S., Lee, T., Kwon, I. K., Kim, H. S., Hahn, S. K., and Lee, C. S. (2015). Surface Modification of Multipass Caliber-Rolled Ti alloy with Dexamethasone-Loaded Graphene for Dental applicationsResearch Support, Non-U.S. Gov't]. *ACS Appl. Mater. InterfacesACS Appl. Mater. Inter.* 7 (18), 9598–9607. doi:10.1021/acsami.5b03431

- Kazemizadeh, F., and Malekfar, R. (2018). One Step Synthesis of Porous Graphene by Laser Ablation: A New and Facile Approach. *Physica B: Condensed Matter* 530, 236–241. doi:10.1016/j.physb.2017.11.052
- Khan, A. A., Al-Khureif, A. A., Saadaldin, S. A., Mohamed, B. A., Musaibah, A. S. O., Divakar, D. D., et al. (2019). Graphene Oxide-based Experimental Silane Primers Enhance Shear Bond Strength between Resin Composite and Zirconia. *Eur. J. Oral Sci.* 127 (6), 570–576. doi:10.1111/eos.12665
- Kim, J.-W., Shin, Y., Lee, J.-J., Bae, E.-B., Jeon, Y.-C., Jeong, C.-M., et al. (2017). The Effect of Reduced Graphene Oxide-Coated Biphasic Calcium Phosphate Bone Graft Material on Osteogenesis. *Ijms* 18 (8), 1725. doi:10.3390/ijms18081725
- Kohei, K., Hirofumi, M., Erika, N., Saori, M., Akihito, K., Akito, T., et al. (2018). Characterization and Evaluation of Graphene Oxide Scaffold for Periodontal Wound Healing of Class II Furcation Defects in Dog. *Int. J. Nanomed.* 13, 2365–2376. doi:10.2147/IJN.S163206
- Koldsland, O. C., Wohlfahrt, J. C., and Aass, A. M. (2018). Surgical Treatment of Peri-Implantitis: Prognostic Indicators of Short-Term Results. *J. Clin. Periodontol.* 45 (1), 100–113. doi:10.1111/jcpe.12816
- Kordbacheh, C. K., Finkelstein, J., and Papapanou, P. N. (2019). Peri-implantitis Prevalence, Incidence Rate, and Risk Factors: A Study of Electronic Health Records at a U.S. Dental School. *Clin. Oral Impl. Res.* 30 (4), 306–314. doi:10.1111/clr.13416
- Kovtyukhova, N. I., Ollivier, P. J., Martin, B. R., Mallouk, T. E., Chizhik, S. A., Buzaneva, E. V., et al. (1999). Layer-by-Layer Assembly of Ultrathin Composite Films from Micron-Sized Graphite Oxide Sheets and Polycations. *Chem. Mater.* 11 (3), 771–778. doi:10.1021/cm981085u
- Kulshrestha, S., Khan, S., Meena, R., Singh, B. R., and Khan, A. U. (2014). A Graphene/zinc Oxide Nanocomposite Film Protects Dental Implant Surfaces against cariogenic *Streptococcus Mutans*. *Biofouling* 30 (9–10), 1281–1294. doi:10.1080/08927014.2014.983093
- Kwon, S. R., and Wertz, P. W. (2015). Review of the Mechanism of Tooth Whitening. *J. Esthet. Restor. Dent* 27 (5), 240–257. doi:10.1111/jerd.12152
- Lamster, I. B. (2021). The 2021 WHO Resolution on Oral Health. *Int. Dental J.* 71 (4), 279–280. doi:10.1016/j.identj.2021.06.003
- Lazauskas, A., Marcinauskas, L., and Andrulevicius, M. (2018). Photothermal Reduction of Thick Graphene Oxide Multilayer Films via Direct Laser Writing: Morphology, Structural and Chemical Properties. *Superlattices and Microstructures* 122, 36–45. doi:10.1016/j.spmi.2018.08.024
- Lee, J.-H., Jo, J.-K., Kim, D.-A., Patel, K. D., Kim, H.-W., and Lee, H.-H. (2018a). Nano-graphene Oxide Incorporated into PMMA Resin to Prevent Microbial Adhesion. *Dental Mater.* 34 (4), e63–e72. doi:10.1016/j.dental.2018.01.019
- Lee, J. H., Shin, Y. C., Jin, O. S., Kang, S. H., Hwang, Y.-S., Park, J.-C., et al. (2015a). Reduced Graphene Oxide-Coated Hydroxyapatite Composites Stimulate Spontaneous Osteogenic Differentiation of Human Mesenchymal Stem Cells. *Nanoscale* 7 (27), 11642–11651. doi:10.1039/c5nr01580d
- Lee, J. H., Shin, Y. C., Lee, S.-M., Jin, O. S., Kang, S. H., Hong, S. W., et al. (2015b). Enhanced Osteogenesis by Reduced Graphene Oxide/Hydroxyapatite Nanocomposites. *Sci. Rep.* 5, 18833. doi:10.1038/srep18833
- Lee, S. M., Yoo, S. Y., Kim, I. R., Park, B. S., Son, W. S., Ko, C. C., et al. (2018b). Enamel Anti-demineralization Effect of Orthodontic Adhesive Containing Bioactive Glass and Graphene Oxide: An *In-Vitro* Study. *Materials (Basel)* 11 (9), 1728. doi:10.3390/ma11091728
- Li, H., Xie, Y., Li, K., Huang, L., Huang, S., Zhao, B., et al. (2014). Microstructure and Wear Behavior of Graphene Nanosheets-Reinforced Zirconia Coating. *Ceramics Int.* 40 (8), 12821–12829. doi:10.1016/j.ceramint.2014.04.136
- Li, J., Wang, G., Geng, H., Zhu, H., Zhang, M., Di, Z., et al. (2015). CVD Growth of Graphene on NiTi alloy for Enhanced Biological Activity. *ACS Appl. Mater. Inter.* 7 (36), 19876–19881. doi:10.1021/acsami.5b06639
- Li, Q.-L., Huang, N., Chen, J., Wan, G., Zhao, A., Chen, J., et al. (2009). Anticoagulant Surface Modification of Titanium via Layer-By-Layer Assembly of Collagen and Sulfated Chitosan Multilayers. *J. Biomed. Mater. Res.* 89A (3), 575–584. doi:10.1002/jbm.a.31999
- Li, Z., Yao, Y., Lin, Z., Moon, K.-S., Lin, W., and Wong, C. (2010). Ultrafast, Dry Microwave Synthesis of Graphene Sheets. *J. Mater. Chem.* 20 (23), 4781. doi:10.1039/c0jm00168f
- Liao, C., Li, Y., and Tjong, S. (2018). Graphene Nanomaterials: Synthesis, Biocompatibility, and Cytotoxicity. *Ijms* 19 (11), 3564. doi:10.3390/ijms19113564
- Lim, K.-T., Seonwoo, H., Choi, K. S., Jin, H., Jang, K.-J., Kim, J., et al. (2016). Pulsed-Electromagnetic-Field-Assisted Reduced Graphene Oxide Substrates for Multidifferentiation of Human Mesenchymal Stem Cells. *Adv. Healthc. Mater.* 5 (16), 2069–2079. doi:10.1002/adhm.201600429
- Liu, J., Fu, S., Yuan, B., Li, Y., and Deng, Z. (2010). Toward a Universal "adhesive Nanosheet" for the Assembly of Multiple Nanoparticles Based on a Protein-Induced Reduction/Decoration of Graphene Oxide. *J. Am. Chem. Soc.* 132 (21), 7279–7281. doi:10.1021/ja100938r
- Liu, L.-N., Zhang, X.-H., Liu, H.-H., Li, K.-H., Wu, Q.-H., Liu, Y., et al. (2020). Osteogenesis Differences Around Titanium Implant and in Bone Defect between Jaw Bones and Long Bones. *J. Craniofac. Surg.* 31 (8), 2193–2198. doi:10.1097/SCS.00000000000006795
- Liu, N., Luo, F., Wu, H., Liu, Y., Zhang, C., and Chen, J. (2008). One-Step Ionic-Liquid-Assisted Electrochemical Synthesis of Ionic-Liquid-Functionalized Graphene Sheets Directly from Graphite. *Adv. Funct. Mater.* 18, 1518–1525. doi:10.1002/adfm.200700797
- Liu, X., Miller, A. L., Park, S., George, M. N., Waletzki, B. E., Xu, H., et al. (2019). Two-Dimensional Black Phosphorus and Graphene Oxide Nanosheets Synergistically Enhance Cell Proliferation and Osteogenesis on 3D Printed Scaffolds. *ACS Appl. Mater. Inter.* 11 (26), 23558–23572. doi:10.1021/acsami.9b04121
- Lu, J., Sun, J., Zou, D., Song, J., and Yang, S. (2020). Graphene-Modified Titanium Surface Enhances Local Growth Factor Adsorption and Promotes Osteogenic Differentiation of Bone Marrow Stromal Cells. *Front. Bioeng. Biotechnol.* 8, 621788. doi:10.3389/fbioe.2020.621788
- Mannoor, M. S., Tao, H., Clayton, J. D., Sengupta, A., Kaplan, D. L., Naik, R. R., et al. (2012). Graphene-based Wireless Bacteria Detection on Tooth Enamel. *Nat. Commun.* 3, 763. doi:10.1038/ncomms1767
- Mao, S., Lu, G., Yu, K., Bo, Z., and Chen, J. (2010). Specific Protein Detection Using Thermally Reduced Graphene Oxide Sheet Decorated with Gold Nanoparticle-Antibody Conjugates. *Adv. Mater.* 22 (32), 3521–3526. doi:10.1002/adma.201000520
- Marcano, D. C., Kosynkin, D. V., Berlin, J. M., Sinitskii, A., Sun, Z., Slesarev, A., et al. (2010). Improved Synthesis of Graphene Oxide. *ACS Nano* 4 (8), 4806–4814. doi:10.1021/nn1006368
- Marco, P. D., Zara, S., Colli, M. D., Radunovic, M., Lazović, V., Ettorre, V., et al. (2017). Graphene Oxide Improves the Biocompatibility of Collagen Membranes in an *In Vitro* Model of Human Primary Gingival Fibroblasts. *Biomed. Mater.* 12 (5), 055005. doi:10.1088/1748-605X/aa7907
- Matsuo, H., Suenaga, H., Takahashi, M., Suzuki, O., Sasaki, K., and Takahashi, N. (2015). Deterioration of Polymethyl Methacrylate Dentures in the Oral Cavity. *Dent. Mater. J.* 34 (2), 234–239. doi:10.4012/dmj.2014-089
- Miyaji, H., Kato, A., Takita, H., Iwanaga, T., Momose, T., Ogawa, K., et al. (2016). Graphene Oxide Scaffold Accelerates Cellular Proliferative Response and Alveolar Bone Healing of Tooth Extraction Socket. *Ijn* 11, 2265–2277. doi:10.2147/IJN.S104778
- Ming, G., Lv, L., Feng, D., Niu, T., Tong, C., Xia, D., et al. (2018). Effects of thermal Treatment on the Adhesion Strength and Osteoinductive Activity of Single-Layer Graphene Sheets on Titanium Substrates. *Sci. Rep.* 8 (1), 8141. doi:10.1038/s41598-018-26551-w
- Mohamed, M. A., Atty, S. A., Merey, H. A., Fattah, T. A., Foster, C. W., and Banks, C. E. (2017). Titanium Nanoparticles (TiO₂)/graphene Oxide Nanosheets (GO): An Electrochemical Sensing Platform for the Sensitive and Simultaneous Determination of Benzocaine in the Presence of Antipyrine. *Analyst* 142 (19), 3674–3679. doi:10.1039/c7an01101f
- Nam, H.-J., Kim, Y.-M., Kwon, Y. H., Kim, I.-R., Park, B.-S., Son, W.-S., et al. (2019). Enamel Surface Remineralization Effect by Fluorinated Graphite and Bioactive Glass-Containing Orthodontic Bonding Resin. *Materials* 12 (8), 1308. doi:10.3390/ma12081308
- Nan, A. (2016). Miscellaneous Drugs, Materials, Medical Devices and Techniques. *Side Effects Drugs Annu.* 38, 523–532. doi:10.1016/bs.seda.2016.09.002
- Nizami, M. Z. I., Nishina, Y., Yamamoto, T., Shinoda-Ito, Y., and Takashiba, S. (2020). Functionalized Graphene Oxide Shields Tooth Dentin from Decalcification. *J. Dent. Res.* 99 (2), 182–188. doi:10.1177/0022034519894583
- Norahan, M. H., Amroon, M., Ghahremanzadeh, R., Rabiee, N., and Baheiraei, N. (2019). Reduced Graphene Oxide: Osteogenic Potential for Bone Tissue Engineering. *IET nanobiotechnol.* 13 (7), 720–725. doi:10.1049/iet-nbt.2019.0125

- Norimatsu, W., and Kusunoki, M. (2014). Epitaxial Graphene on SiC{0001}: Advances and Perspectives. *Phys. Chem. Chem. Phys.* 16 (8), 3501–3511. doi:10.1039/c3cp54523g
- Novoselov, K. S., Geim, A. K., Morozov, S. V., Jiang, D., Zhang, Y., Dubonos, S. V., et al. (2004). Electric Field Effect in Atomically Thin Carbon Films. *Science* 306 (5696), 666–669. doi:10.1126/science.1102896
- Olteanu, D., Filip, A., Socaci, C., Biris, A. R., Filip, X., Coros, M., et al. (2015). Cytotoxicity Assessment of Graphene-Based Nanomaterials on Human Dental Follicle Stem Cells. *Colloids Surf. B: Biointerfaces* 136, 791–798. doi:10.1016/j.colsurfb.2015.10.023
- Parate, K., Karunakaran, C., and Claussen, J. C. (2019). Electrochemical Cotinine Sensing with a Molecularly Imprinted Polymer on a Graphene-Platinum Nanoparticle Modified Carbon Electrode towards Cigarette Smoke Exposure Monitoring. *Sensors Actuators B: Chem.* 287, 165–172. doi:10.1016/j.snb.2019.02.032
- Park, C., Park, S., Lee, D., Choi, K. S., Lim, H.-P., and Kim, J. (2017). Graphene as an Enabling Strategy for Dental Implant and Tissue Regeneration. *Tissue Eng. Regen. Med.* 14 (5), 481–493. doi:10.1007/s13770-017-0052-3
- Park, S., and Ruoff, R. S. (2009). Chemical Methods for the Production of Graphenes. *Nat. Nanotech* 4 (4), 217–224. doi:10.1038/nnano.2009.58
- Parnia, F., Yazdani, J., Javaherzadeh, V., and Maleki Dizaj, S. (2017). Overview of Nanoparticle Coating of Dental Implants for Enhanced Osseointegration and Antimicrobial Purposes. *J. Pharm. Pharm. Sci.* 20 (0), 148–160. doi:10.18433/J3GP6G
- Pei, S., and Cheng, H.-M. (2012). The Reduction of Graphene Oxide. *Carbon* 50 (9), 3210–3228. doi:10.1016/j.carbon.2011.11.010
- Peng, L., Xu, Z., Liu, Z., Wei, Y., Sun, H., Li, Z., et al. (2015). An Iron-Based green Approach to 1-h Production of Single-Layer Graphene Oxide. *Nat. Commun.* 6, 5716. doi:10.1038/ncomms6716
- Phaedon, A., and Christos, D. (2012). Graphene: Synthesis and Applications. *Mater. Today* 15, 83–97. doi:10.1016/S1369-7021(12)70044-5
- Podolska, M. J., Barras, A., Alexiou, C., Frey, B., Gaip, U., Boukherroub, R., et al. (2020). Graphene Oxide Nanosheets for Localized Hyperthermia-Physicochemical Characterization, Biocompatibility, and Induction of Tumor Cell Death. *Cells* 9 (3), 776. doi:10.3390/cells9030776
- Pourhajibagher, M., Parker, S., Chiniforush, N., and Bahador, A. (2019). Photocatalytic Triggering via Semiconductor Graphene Quantum Dots by Photochemical Doping with Curcumin versus Perio-Pathogens Mixed Biofilms. *Photodiagnosis Photodynamic Ther.* 28, 125–131. doi:10.1016/j.pdpdt.2019.08.025
- Priyadarsini, S., Mukherjee, S., and Mishra, M. (2018). Nanoparticles Used in Dentistry: A Review. *J. Oral Biol. Craniofac. Res.* 8, 58–67. doi:10.1016/j.jobcr.2017.12.004
- Qian, W., Qiu, J., and Liu, X. (2019). Minocycline Hydrochloride-loaded Graphene Oxide Films on Implant Abutments for Peri-implantitis Treatment in Beagle Dogs. *J. Periodontol.* 91 (6), 792–799. doi:10.1002/JPER.19-0285
- Qian, W., Qiu, J., Su, J., and Liu, X. (2018). Minocycline Hydrochloride Loaded on Titanium by Graphene Oxide: An Excellent Antibacterial Platform with the Synergistic Effect of Contact-Killing and Release-Killing. *Biomater. Sci.* 6 (2), 304–313. doi:10.1039/c7bm00931c
- Qiu, J., Geng, H., Wang, D., Qian, S., Zhu, H., Qiao, Y., et al. (2017). Layer-Number Dependent Antibacterial and Osteogenic Behaviors of Graphene Oxide Electrophoretic Deposited on Titanium. *ACS Appl. Mater. Inter.* 9 (14), 12253–12263. doi:10.1021/acsami.7b00314
- Rai, V. K., Mahata, S., Kashyap, H., Singh, M., and Rai, A. (2020). Bio-reduction of Graphene Oxide: Catalytic Applications of (Reduced) GO in Organic Synthesis. *Cos* 17 (3), 164–191. doi:10.2174/1570179417666200115110403
- Reina, G., González-Domínguez, J. M., Criado, A., Vázquez, E., Bianco, A., and Prato, M. (2017). Promises, Facts and Challenges for Graphene in Biomedical Applications. *Chem. Soc. Rev.* 46 (15), 4400–4416. doi:10.1039/c7cs00363c
- Roos-Jansäker, A.-M., Renvert, S., and Egelberg, J. (2003). Treatment of Peri-Implant Infections: A Literature Review. *J. Clin. Periodontol.* 30 (6), 467–485. doi:10.1034/j.1600-051X.2003.00296.x
- Rosa, V., Malhotra, R., Agarwalla, S. V., Morin, J. L. P., Luong-Van, E. K., Han, Y. M., et al. (2021). Graphene Nanocoating: High Quality and Stability upon Several Stressors. *J. Dent. Res.* 100 (10), 1169–1177. doi:10.1177/00220345211024526
- Ruse, N. D., and Sadoun, M. J. (2014). Resin-composite Blocks for Dental CAD/CAM Applications. *J. Dent. Res.* 93 (12), 1232–1234. doi:10.1177/0022034514553976
- Schünemann, F. H., Galárraga-Vinueza, M. E., Magini, R., Fredel, M., Silva, F., Souza, J. C. M., et al. (2019). Zirconia Surface Modifications for Implant Dentistry. *Mater. Sci. Eng. C* 98, 1294–1305. doi:10.1016/j.msec.2019.01.062
- Schwarz, F., Becker, K., Rahn, S., Hegewald, A., Pfeffer, K., and Henrich, B. (2015). Real-time PCR Analysis of Fungal Organisms and Bacterial Species at Peri-Implantitis Sites. *Int. J. Implant Dent* 1 (1), 1–7. doi:10.1186/s40729-015-0010-6
- Seonwoo, H., Jang, K.-J., Lee, D., Park, S., Lee, M., Park, S., et al. (2018). Neurogenic Differentiation of Human Dental Pulp Stem Cells on Graphene-Polycaprolactone Hybrid Nanofibers. *Nanomaterials* 8 (7), 554. doi:10.3390/nano8070554
- Sharan, J., Singh, S., Lale, S. V., Mishra, M., Koul, V., and Kharbanda, O. P. (2017). Applications of Nanomaterials in Dental Science: A Review. *J. Nanosci Nanotechnol* 17 (4), 2235–2255. doi:10.1166/jnn.2017.13885
- Shin, Y. C., Song, S.-J. Song, Jeong, S. J., Kim, B., Kwon, I. K., Hong, S. W., et al. (2018). Graphene-Based Nanocomposites as Promising Options for Hard Tissue Regeneration. *Adv. Exp. Med. Biol.* 1078, 103–117. doi:10.1007/978-981-13-0950-2_6
- Slots, J. (2017). Periodontitis: Facts, Fallacies and the Future. *Periodontol.* 2000 75 (1), 7–23. doi:10.1111/prd.12221
- Smeets, R., Henningsen, A., Jung, O., Heiland, M., Hammächer, C., and Stein, J. M. (2014). Definition, Etiology, Prevention and Treatment of Peri-Implantitis - a Review. *Head Face Med.* 10, 34. doi:10.1186/1746-160x-10-34
- Song, H. S., Kwon, O. S., Kim, J.-H., Conde, J., and Artzi, N. (2017). 3D Hydrogel Scaffold Doped with 2D Graphene Materials for Biosensors and Bioelectronics. *Biosens. Bioelectron.* 89 (Pt 1), 187–200. doi:10.1016/j.bios.2016.03.045
- Souza, J. C. M., Sordi, M. B., Kanazawa, M., Ravindran, S., Henriques, B., Silva, F. S., et al. (2019). Nano-scale Modification of Titanium Implant Surfaces to Enhance Osseointegration. *Acta Biomater.* 94, 112–131. doi:10.1016/j.actbio.2019.05.045
- Steflik, D. E., Corpe, R. S., Young, T. R., Sisk, A. L., and Parr, G. R. (1999). The Biologic Tissue Responses to Uncoated and Coated Implanted Biomaterials. *Adv. Dent Res.* 13 (1), 27–33. doi:10.1177/08959374990130011101
- Sun, L., Yan, Z., Duan, Y., Zhang, J., and Liu, B. (2018). Improvement of the Mechanical, Tribological and Antibacterial Properties of Glass Ionomer Cements by Fluorinated Graphene. *Dental Mater.* 34 (6), e115–e127. doi:10.1016/j.dental.2018.02.006
- Suo, L., Jiang, N., Wang, Y., Wang, P., Chen, J., Pei, X., et al. (2018). The Enhancement of Osseointegration Using a Graphene Oxide/chitosan/hydroxyapatite Composite Coating on Titanium Fabricated by Electrophoretic Deposition. *J. Biomed. Mater. Res.* 107 (3), 635–645. doi:10.1002/jbm.b.34156
- Tatullo, M., Genovese, F., Aiello, E., Amantea, M., Makeeva, I., Zavan, B., et al. (2019a). Phosphorene Is the New Graphene in Biomedical Applications. *Materials* 12 (14), 2301. doi:10.3390/ma12142301
- Tatullo, M., Zavan, B., Genovese, F., Codisotti, B., Makeeva, I., Rengo, S., et al. (2019b). Borophene Is a Promising 2D Allotropic Material for Biomedical Devices. *Appl. Sci.* 9 (17), 3446. doi:10.3390/app9173446
- Trusek, A., and Kijak, E. (2021). Drug Carriers Based on Graphene Oxide and Hydrogel: Opportunities and Challenges in Infection Control Tested by Amoxicillin Release. *Materials* 14 (12), 3182. doi:10.3390/ma14123182
- Vera-Sánchez, M., Aznar-Cervantes, S., Jover, E., García-Bernal, D., Oñate-Sánchez, R. E., Hernández-Romero, D., et al. (2016). Silk-fibroin and Graphene Oxide Composites Promote Human Periodontal Ligament Stem Cell Spontaneous Differentiation into Osteo/cementoblast-like Cells. *Stem Cell Development* 25 (22), 1742–1754. doi:10.1089/scd.2016.0028
- Verma, S., Singh, A., Shukla, A., Kaswan, J., Arora, K., Ramirez-Vick, J., et al. (2017). Anti-IL8/AuNPs-rGO/ITO as an Immunosensing Platform for Noninvasive Electrochemical Detection of Oral Cancer. *ACS Appl. Mater. Inter.* 9 (33), 27462–27474. doi:10.1021/acsami.7b06839
- Verma, S., and Singh, S. P. (2019). Non-invasive Oral Cancer Detection from Saliva Using Zinc Oxide-Reduced Graphene Oxide Nanocomposite Based Bioelectrode. *MRS Commun.* 9 (4), 1227–1234. doi:10.1557/mrc.2019.138
- Vinicius, Rosa, Han, Nileshkumar, Dubey, et al. (2016). Graphene Oxide-Based Substrate: Physical and Surface Characterization, Cytocompatibility and Differentiation Potential of Dental Pulp Stem Cells. *Dental Mater.* 32 (8), 1019–1025. doi:10.1016/j.dental.2016.05.008

- Wang, G., Qian, F., Saltikov, C. W., Jiao, Y., and Li, Y. (2011). Microbial Reduction of Graphene Oxide by *Shewanella*. *Nano Res.* 4 (6), 563–570. doi:10.1007/s12274-011-0112-2
- Wang, K., Ruan, J., Song, H., Zhang, J., Wo, Y., Guo, S., et al. (2011). Biocompatibility of Graphene Oxide. *Nanoscale Res. Lett.* 6 (1), 8. doi:10.1007/s11671-010-9751-6
- Wang, Y., Chen, Y., Lacey, S. D., Xu, L., Xie, H., Li, T., et al. (2018). Reduced Graphene Oxide Film with Record-High Conductivity and Mobility. *Mater. Today* 21, 186–192. doi:10.1016/j.mattod.2017.10.008
- Wei, C., Liu, Z., Jiang, F., Zeng, B., Huang, M., and Yu, D. (2017). Cellular Behaviours of Bone Marrow-Derived Mesenchymal Stem Cells towards Pristine Graphene Oxide Nanosheets. *Cell Prolif* 50 (5), e12367. doi:10.1111/cpr.12367
- Wessing, B., Lettner, S., and Zechner, W. (2018). Guided Bone Regeneration with Collagen Membranes and Particulate Graft Materials: A Systematic Review and Meta-Analysis. *Int. J. Oral Maxillofac. Implants* 33 (1), 87–100. doi:10.11607/jomi.5461
- Williams, G., Seger, B., and Kamat, P. V. (2008). TiO₂-Graphene Nanocomposites. UV-Assisted Photocatalytic Reduction of Graphene Oxide. *ACS Nano* 2 (7), 1487–1491. doi:10.1021/nn800251f
- Wu, J., Zheng, A., Liu, Y., Jiao, D., Zeng, D., Wang, X., et al. (2019). Enhanced Bone Regeneration of the Silk Fibroin Electrospun Scaffolds through the Modification of the Graphene Oxide Functionalized by BMP-2 Peptide. *Ijn* 14, 733–751. doi:10.2147/IJN.S187664
- Wu, R., Zhao, Q., Lu, S., Fu, Y., Yu, D., and Zhao, W. (2018). Inhibitory Effect of Reduced Graphene Oxide-Silver Nanocomposite on Progression of Artificial Enamel Caries. *J. Appl. Oral Sci.* 27, e20180042. doi:10.1590/1678-7757-2018-0042
- Wu, X., Ding, S.-J., Lin, K., and Su, J. (2017). A Review on the Biocompatibility and Potential Applications of Graphene in Inducing Cell Differentiation and Tissue Regeneration. *J. Mater. Chem. B* 5 (17), 3084–3102. doi:10.1039/c6tb03067j
- Xiao, N., Dong, X., Song, L., Liu, D., Tay, Y., Wu, S., et al. (2011). Enhanced Thermopower of Graphene Films with Oxygen Plasma Treatment. *ACS Nano* 5 (4), 2749–2755. doi:10.1021/nn2001849
- Xie, H., Chua, M., Islam, I., Bentini, R., Cao, T., Viana-Gomes, J. C., et al. (2017). CVD-grown Monolayer Graphene Induces Osteogenic but Not Odontoblastic Differentiation of Dental Pulp Stem Cells. *Dental Mater.* 33 (1), e13–e21. doi:10.1016/j.dental.2016.09.030
- Xie, Y., Li, H., Zhang, C., Gu, X., Zheng, X., and Huang, L. (2014). Graphene-reinforced Calcium Silicate Coatings for Load-Bearing Implants. *Biomed. Mater.* 9 (2), 025009. doi:10.1088/1748-6041/9/2/025009
- Yin, Z., Sun, S., Salim, T., Wu, S., Huang, X., He, Q., et al. (2010). Organic Photovoltaic Devices Using Highly Flexible Reduced Graphene Oxide Films as Transparent Electrodes. *ACS Nano* 4 (9), 5263–5268. doi:10.1021/nn1015874
- Yu, H., Zhang, B., Bulin, C., Li, R., and Xing, R. (2016). High-efficient Synthesis of Graphene Oxide Based on Improved Hummers Method. *Sci. Rep.* 6, 36143. doi:10.1038/srep36143
- Zhang, Y., Wan, Q., and Yang, N. (2019). Recent Advances of Porous Graphene: Synthesis, Functionalization, and Electrochemical Applications. *Small* 15 (48), 1903780. doi:10.1002/smll.201903780
- Zhao, M., Shan, T., Wu, Q., and Gu, L. (2020). The Antibacterial Effect of Graphene Oxide on *Streptococcus Mutans*. *J. Nanosci Nanotechnol* 20 (4), 2095–2103. doi:10.1166/jnn.2020.17319
- Zhou, Q., Yang, P., Li, X., Liu, H., and Ge, S. (2016). Bioactivity of Periodontal Ligament Stem Cells on Sodium Titanate Coated with Graphene Oxide. *Sci. Rep.* 6 (1), 19343. doi:10.1038/srep19343

Conflict of Interest: The authors declare that the research was conducted in the absence of any commercial or financial relationships that could be construed as a potential conflict of interest.

Publisher's Note: All claims expressed in this article are solely those of the authors and do not necessarily represent those of their affiliated organizations or those of the publisher, the editors, and the reviewers. Any product that may be evaluated in this article, or claim that may be made by its manufacturer, is not guaranteed or endorsed by the publisher.

Copyright © 2022 Li, Liang, Wang, Wang, Teng, Xu, Zhao and Han. This is an open-access article distributed under the terms of the Creative Commons Attribution License (CC BY). The use, distribution or reproduction in other forums is permitted, provided the original author(s) and the copyright owner(s) are credited and that the original publication in this journal is cited, in accordance with accepted academic practice. No use, distribution or reproduction is permitted which does not comply with these terms.



Comparative Evaluation of Stress Acting on Abutment, Bone, and Connector of Different Designs of Acid-Etched Resin-Bonded Fixed Partial Dentures: Finite Element Analysis

Saquib Ahmed Shaikh¹, Punith Rai², Sami Aldhuwayhi¹, Sreekanth Kumar Mallineni^{3,4*}, Krishnapalli Lekha², Angel Mary Joseph¹, Vardharaj Vinutha Kumari¹ and Roseline Meshramkar²

OPEN ACCESS

Edited by:

Kumar Chandan Srivastava,
Al Jouf University, Saudi Arabia

Reviewed by:

Srinivasulu Sakamuri,
Narayana Dental College and Hospital,
India
Marina Belfer,
Peoples' Friendship University of
Russia, Russia

*Correspondence:

Sreekanth Kumar Mallineni
s.mallineni@mu.edu.sa
drmallineni@gmail.com

Specialty section:

This article was submitted to
Biomaterials,
a section of the journal
Frontiers in Bioengineering and
Biotechnology

Received: 20 October 2021

Accepted: 22 February 2022

Published: 26 April 2022

Citation:

Shaikh SA, Rai P, Aldhuwayhi S,
Mallineni SK, Lekha K, Joseph AM,
Kumari VV and Meshramkar R (2022)
Comparative Evaluation of Stress
Acting on Abutment, Bone, and
Connector of Different Designs of Acid-
Etched Resin-Bonded Fixed Partial
Dentures: Finite Element Analysis.
Front. Bioeng. Biotechnol. 10:798988.
doi: 10.3389/fbioe.2022.798988

¹Department of Prosthodontics, College of Dentistry, Majmaah University, Majmaah, Saudi Arabia, ²Department of Prosthodontics, SDM Dental College, Dharwad, India, ³Department of Preventive Dental Science, College of Dentistry, Majmaah University, Majmaah, Saudi Arabia, ⁴Center for Transdisciplinary Research (CFTR), Saveetha Institute of Medical and Technical Sciences, Saveetha Dental College, Saveetha University, Chennai, India

Background: Finite element analysis (FEA) is one of the best methods for evaluating the stress distribution of restorations, such as fixed partial dentures. The development of resin cement has transformed prosthesis bonding and retention properties. Resin-bonded fixed partial dentures (RBFPD) have been considered minimally invasive treatment options for the prosthetic rehabilitation of single missing teeth.

Objectives: The aim of this study was to evaluate the stress load and distribution in four different designs of acid-etched RBFPDs using FEA.

Materials and Methods: The designs included standard tooth preparation principles and additional features. The first premolar and first molar abutments replaced the missing second premolar. Designs 1, 2, 3, and 4 included (1) lingual wings and occlusal rests; (2) wings and proximal slices; (3) wings, rests, and grooves; and (4) wings, rests, grooves, and occlusal coverage. The prepared models were restored with RBFPDs. A load of 100 N was applied to the central groove of the pontic to simulate occlusal forces. The materials used in the models were considered to be isotropic, homogeneous, and linearly elastic. FEA was used to reveal stresses acting on the abutment, bone, and connector in all prosthesis designs.

Results: The stresses transmitted to the abutment and bones were lowest for design 3, using wings, rests, and grooves. The stresses acting on the connector were the weakest in design 2. The stresses transmitted to the abutment and bone were highest in designs 1 and 4. The stresses transmitted to the connector were highest in design 3.

Conclusion: The wings, rests, and grooves design is possibly the ideal and conservative tooth preparation design to receive a posterior RBFPD. This design transmits less stress to

the abutments and less bone resorption in the FEA. It is most likely to be successful in the clinical provision and ensures the longevity of the prosthesis.

Keywords: finite element analysis, resin-bonded, partial denture, stresses, prosthodontic

INTRODUCTION

Conventional resin-bonded fixed partial dentures (RBFDPs) offer a limited treatment option for prosthetic rehabilitation of a single edentulous space. With the advent of more contemporary designs and retention aids, RBFDPs can be incorporated into a broader range of edentulous positions (Tanaka et al., 2019). These include smaller-sized anterior teeth and premolars. The success of etched-cast RBFDPs is mainly dependent on tooth preparation (Arora et al., 2014). Various researchers have proposed designs with varying claims for enhancing retention and resistance form (Lin et al., 2005; Tanoue, 2016; Acharya et al., 2021). The standard preparations have wings and occlusal rests on the abutment teeth, while other patterns reportedly have proximal slices, grooves, and extensive coverage on occlusal surfaces. Nevertheless, clinicians have no general agreement about which design is best suited for a long-lasting service of RBFDPs (Lin et al., 2005). The conservative designs of RBFDP result in an excellent stress concentration in the abutment because of its geometry; the maximum stresses in restoration are known to be concentrated around the connector region (Tanoue, 2016). Excessive stress on the periodontal ligament leads to the resorption of supporting bone and weakening of the abutment teeth, leading to the restoration's failure (Acharya et al., 2021). It becomes imperative to evaluate the stresses acting on the abutment, bone, and connector in various tooth preparation designs to determine the most suitable combination for enhancing the retention and clinical longevity of RBFDPs (Tanoue, 2016).

Finite element analysis (FEA) is a powerful tool to analyze the designed engineering parts for their strength. The developed features must be robust in design and sustainable against all kinds of loading conditions and work satisfactorily during their design life. For example, backhoe excavators work in severe working environments with cyclic operations. During the design stage, it is imperative to examine the strength of the various parts of the backhoe excavator for the maximum breakout force condition. This can be achieved through performing the FEA of all the parts of the backhoe excavator attachment. However, it is not enough to provide components with a safe design based on strength only, and it should also be light in weight, reliable, and economical. Structural weight optimization is the best solution to obtain the parts with reduced weight without compromising their strength. FEA is a quick and low-cost method to investigate stress distribution and strain patterns of complex restorations such as fixed partial dentures (FPDs) (Medina-Galvez et al., 2021). Many studies have compared the functional behavior of three-unit RBFDPs, two-unit cantilevered RBFDPs (Lin et al., 2005; Tanoue, 2016), and cantilevered RBFDPs (Acharya et al., 2021; Medina-Galvez et al., 2021). The three-dimensional assessments of the abutment teeth are necessary to accomplish more significant treatment

outcomes using an RBFDP. Based on the three-dimensional information, clinicians would choose the types of frameworks, such as three- or two-unit RBFDPs supporting the tooth (abutment) axis, periodontal structure, and the possible preparation area. Few published studies reported using FEA in prosthodontics (Botelho, 2000; Zalkind et al., 2003; Aversa et al., 2009; Silva et al., 2009; Anweigi et al., 2020; Medina-Galvez et al.,

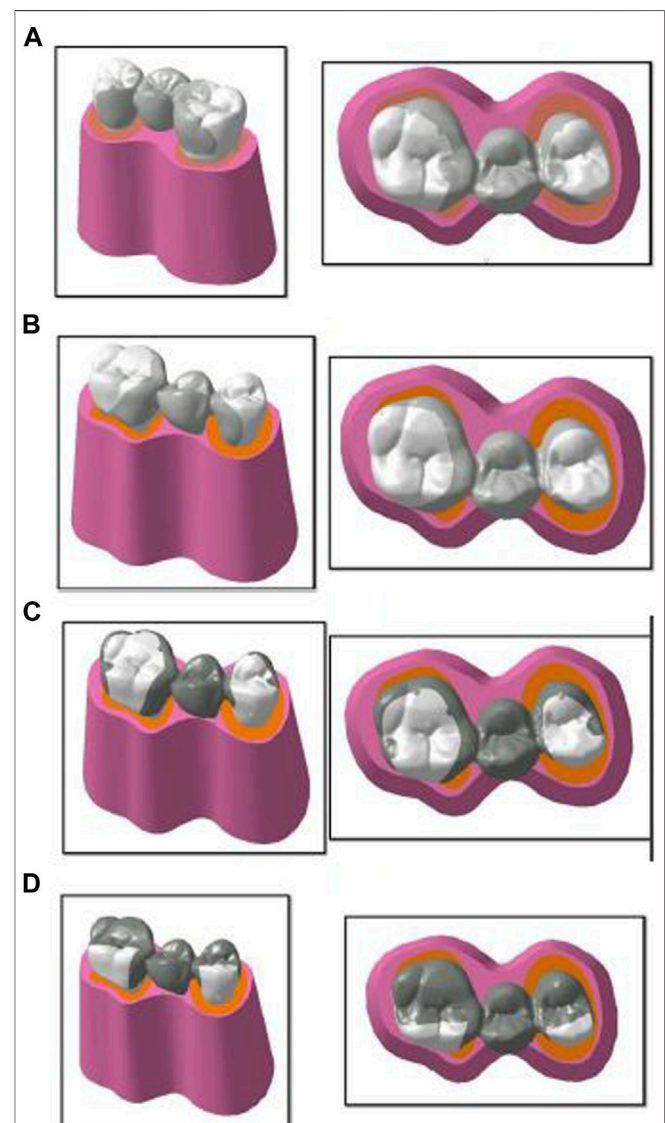


FIGURE 1 | Geometry creation of four designs: (A) design 1 with lingual wings and occlusal rests; (B) design 2 with wings and proximal slices; (C) design 3 with wings, rests, and grooves; and (D) design 4 with wings, rests, grooves, and occlusal coverage used for finite element analysis.

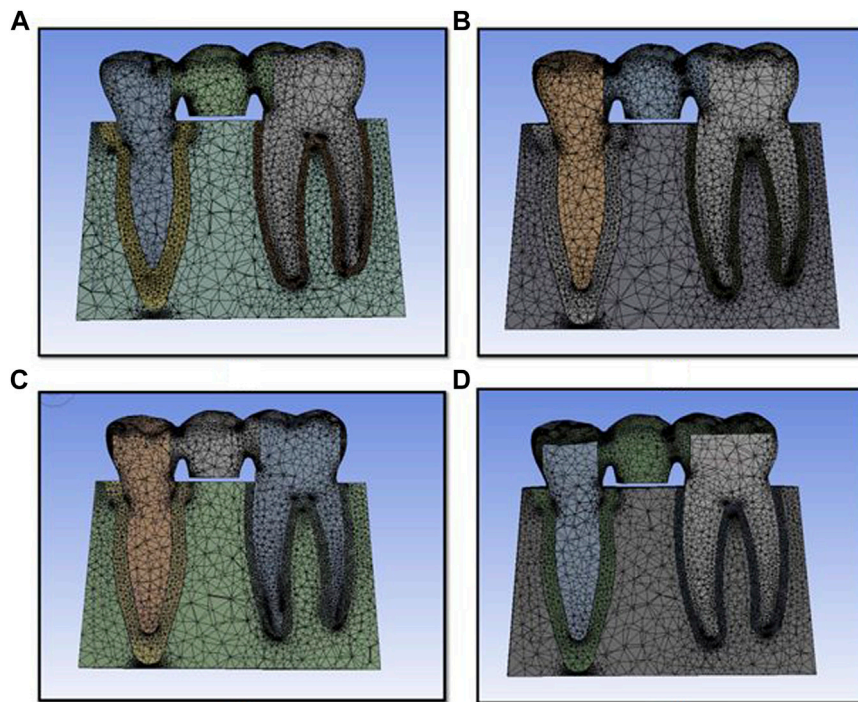


FIGURE 2 | Finite element model used for the study for design 1 (A), design 2 (B), design 3 (C), and design 4 (D).

2021), and among them, very few studies focused on the stress distribution of the components of RFPDs (Botelho, 2000; Chow et al., 2002; Zalkind et al., 2003). Understanding the mechanism of RFPD failures and improved knowledge of the biomechanical behavior of these restorations is obligatory (Botelho et al., 2014; Robati Anaraki et al., 2019; Esquivel-Upshaw et al., 2020). Hence, there is a need to evaluate stress among the components of RFPDs. Therefore, the study assessed stress concentration and distribution on the abutment, bone, and connector in four different designs of acid-etched RFPDs using FEA.

MATERIALS AND METHODS

A set of four models with four designs were prepared, in which the mandibular second premolar (pontic) was replaced using the mandibular first premolar and first molar as abutments. The abutments were prepared to receive the retainer of the RFPDs. These retainer designs incorporated additional features along with standard tooth preparation principles. Design 1 (Figure 1) included lingual wings and occlusal rests distally on the premolar and mesially on the molar. A tooth reduction of up to 1 mm was made for wing preparation. Occlusal rests of the depth of 1 mm, buccolingual width of 2.5 mm, and mesiodistal width of 1.5 mm were prepared. In design 2 (Figure 1B), proximal slices began as an extension of the lingual wing preparation with a supragingival chamfer margin 0.5 mm occlusal to the gingival margin terminating 1.5 mm short of the facio-proximal line angle, without undermining the facial

surface (Aversa et al., 2009). In design 3 (Figure 1C), along with the wings and proximal slice, grooves were added mid-lingually and proximally 1.5 mm short of the facio-proximal line angle, where the proximal slice preparation culminated. Grooves were prepared with a flat-end, tapered, fissured tungsten carbide bur up to a depth of 1 mm (Zalkind et al., 2003). In design 4 (Figure 1D), along with the wings, proximal slices, and grooves, the tooth had one occlusal coverage of 0.5 mm after a tooth preparation of 0.5 mm.

The lingual cusps were involved in the preparation. The prepared teeth with wax patterns of the four designs were scanned using a computerized tomography scan. The tooth profile and profile of the restorations were obtained. This model scanning was made in a Dicom format file and converted to CAD (computer-aided design) geometry. This model was imported into the SOLIDWORKS software (Infid of Enhancing Engineering, India), and 3D models of the components were created and further edited (Figures 2, 3). Next, the meshing of the model (Figure 2) was carried out and divided into finite elements after importing it into ANSYS-11 workbench software. After meshing the components and maintaining the mesh criterion, the boundary conditions were determined to define the relationships between elements (Figure 3).

Boundary constraints were applied onto the inferior margin of the mandible and the mesial and distal ends of the prosthesis. Without boundary constraints, the stresses applied to the model will act infinitely. The following assumptions were made: (1) the material was assumed to be linear elastic, (2) the load remained

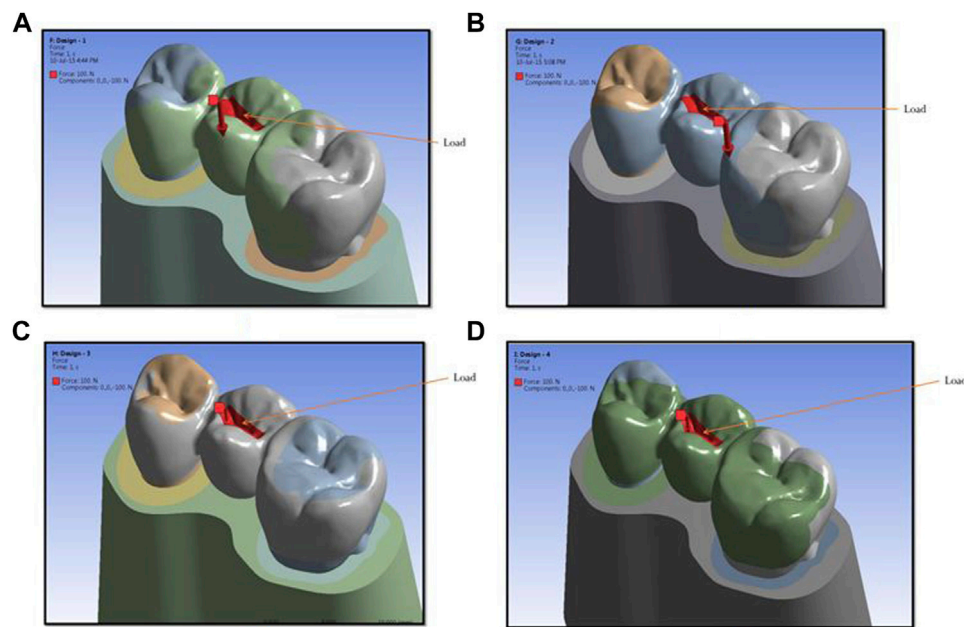


FIGURE 3 | Showing load areas for design 1 (A), design 2 (B), design 3 (C), and design 4 (D) used in the study.

TABLE 1 | Material properties used in the study.

Material	Component	Young's modulus (MPa)	Poisson's ratio
Dentin	Abutment	18,600	0.31
Bone	Cortical bone	15,000	0.3
Soft Bone	Cancellous Bone	1,500	0.3
Cobalt chromium alloy	Connector	218,000	0.3

constant concerning time, (3) other loads were neglected except for the applied load, (4) the boundary conditions do not change during loading, and (5) surface-to-surface contact between different parts is assumed to be of a “bonded” type. The contact area does not change during the analysis.

After meshing and maintaining the mesh criteria, material properties were applied to the model's various components. The corresponding properties of various materials were obtained from the literature (Table 1) (Chow et al., 2002). The component was then run to obtain the stresses and contact analysis of the structure and the partial dentures' respective components. After the analysis run was completed, the stresses in the system were visualized and noted down. A vertical load of 100 N was applied to the pontic's central groove (El Salam Shakal et al., 1997). Four types of analysis were conducted with a constant load (Figure 5). The model was fully constrained at the bottom of the abutment teeth. In post-processing, the stress concentration zones were analyzed and tabulated. The 3D model of the dental structure and prosthesis was generated using CATIA V5 package as per the given specifications. The model was imported into Ansys

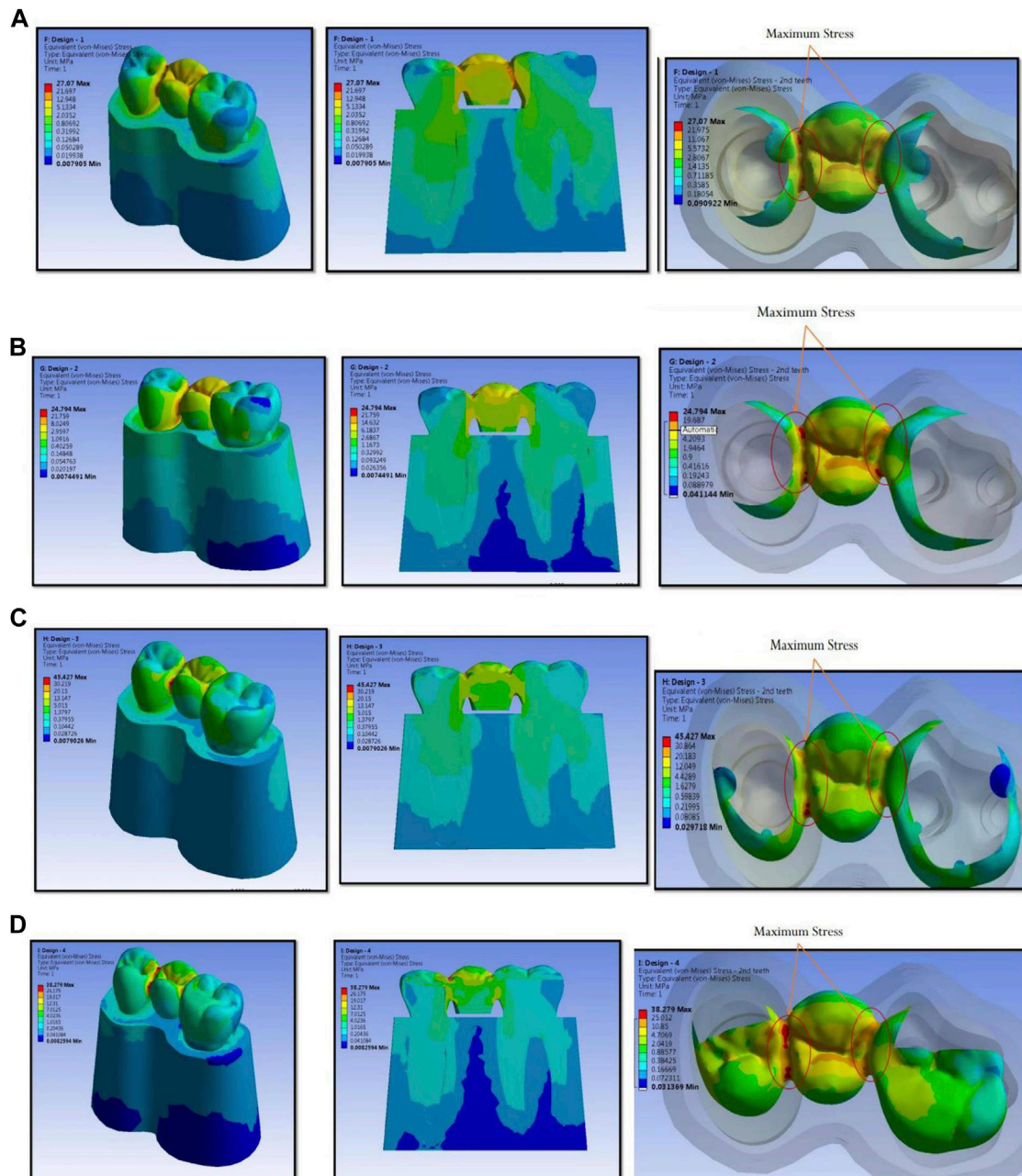
Workbench; the 3D component can mesh as a finite element body utilizing this software. Material properties are described as per the specifications, and the components were subjected to loading and boundary conditions. Static structural analysis was carried out to find stress and deformation in various components. The principal stress in megapascals (MPa) and displacement in millimeters (mm) as well as locations and magnitudes were identified and used to evaluate biomechanical behavior. Maximum principal stress describes the highest stress, and minimal stress describes the lowest stress and can be considered tensile stress.

RESULTS

The numerical analysis for Von Mises stresses occurring for the FEM models is summarized in Table 2. The maximum stress utilized for design 3 was the highest (45.427 MPa), followed by design 4 (38.279 MPa), design 1 (27.07 MPa), and design 2 (24.794 MPa). The maximum stress observed was in the prosthesis, and the magnitude among the study designs is

TABLE 2 | Comparison of stress distribution on the abutment, cortical bone, cancellous bone, and connector in all designs of resin-bonded fixed partial dentures.

Design	Abutment (MPa)	Cortical bone (MPa)	Cancellous bone (MPa)	Connector (MPa)
1	10.84	11.48	1.29	27.07
2	8.05	11.32	1.25	24.79
3	6.24	11.24	1.05	45.42
4	6.64	14.95	1.27	38.27

**FIGURE 4** | Maximum stress observed in prosthesis and the magnitude and stress concentration in prosthesis for design 1 (A), design 2 (B), design 3 (C), and design 4 (D) used in finite element analysis.

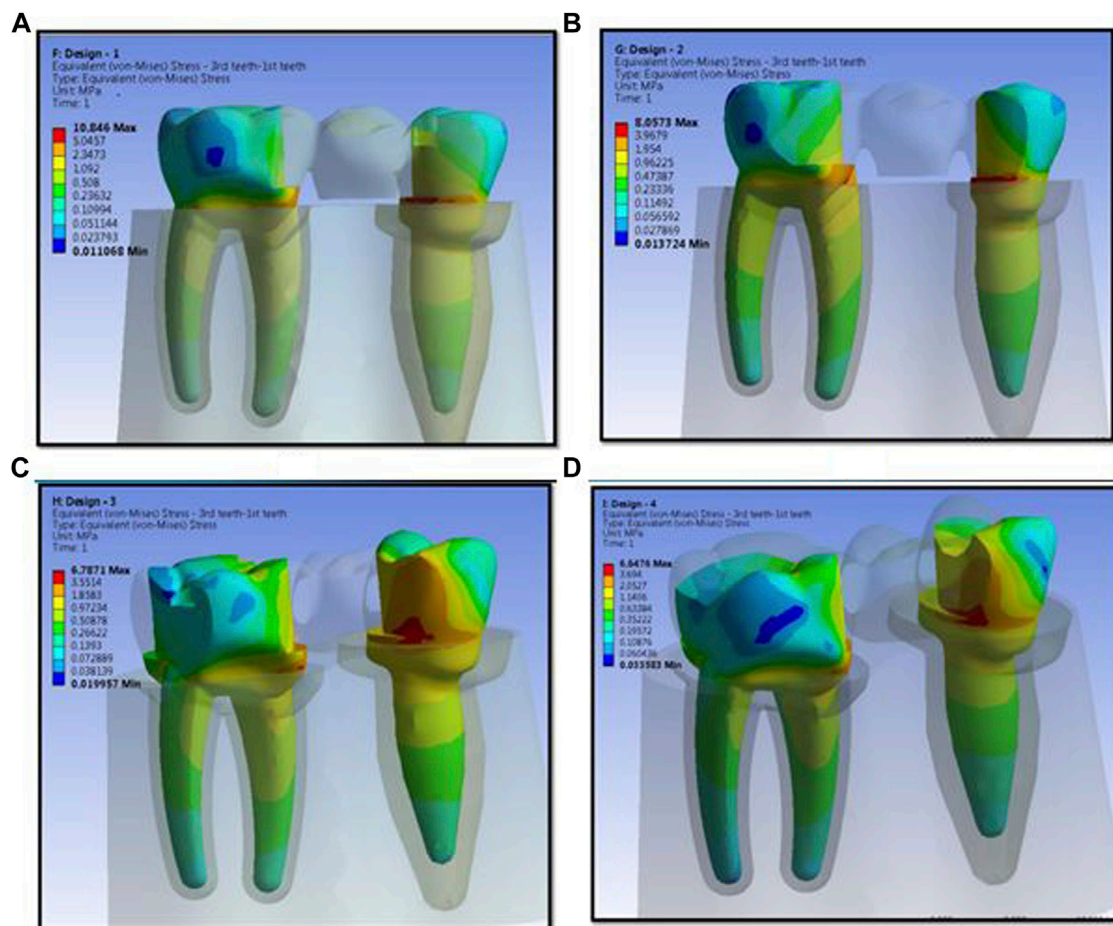


FIGURE 5 | Stress distribution on abutments for design 1 (A), design 2 (B), design 3 (C), and design 4 (D) used in finite element analysis.

shown in **Figure 4**. Design 3 showed the lowest stress on the abutment (6.7871 MPa); likewise, design 4 exhibited low stresses (6.6476 MPa), nearly the same as those on design 3. Both designs had more tooth surface coverage; hence, lower stresses acted on the abutment. Design 1 showed the highest stress (10.846 MPa) on the abutment among all four designs. The stress distribution on teeth is shown in **Figure 5**. It could be attributed to the rest as predominantly responsible for transferring stresses from the pontic to the abutment. Design 3 transferred the least amount of stress (11.24 MPa), while designs 1 (11.24 MPa), 2 (11.24 MPa), and 4 (14.95) transferred higher stresses onto the cortical bone (**Figure 6**). Similarly, design 3 transferred the least amount of stress (1.055 MPa), while designs 1 (1.29 MPa), 2 (1.25 MPa), and 4 transferred higher stresses (1.2717 MPa) onto the cancellous bone (**Figure 7**). The stresses acting on the connector were lowest in design 2 due to proximal extensions, which reduced the stress within the RBFPD. Design 2 (27.07 MPa) showed low stresses on the connector, almost comparable to design 1 (24.794 MPa). Higher stresses on the connector were observed in designs 3 and 4 due to the increased coverage area of the prosthesis on abutment teeth (**Figure 8**). Maximum deformation was observed in the

prosthesis, a magnitude less for design 4 (0.0029146 mm) followed by design 3 (0.0031592 mm), design 2 (0.00172 mm), and design 1 (0.001741 mm). The prosthesis had a larger share of the total load, resulting in stresses in these designs (**Figure 9**). The distribution stresses on various components of the study's different designs are shown in the scatter diagram (**Figure 10**).

DISCUSSION

RBFPDs were first described in the 1970s and have evolved significantly (Medina-Galvez et al., 2021). The development of resin cement has revolutionized prosthesis retention and bonding. RBFPDs are reversible and minimally invasive treatment options for prosthetic rehabilitation of single missing teeth (Aversa et al., 2009; Silva et al., 2009; Acharya et al., 2021). They also serve a masticatory and aesthetic function without compromising the abutment (Zalkind et al., 2003; Aversa et al., 2009; Silva et al., 2009; Anweigi et al., 2020). This is important for young patients who may have endodontic complications following extensive tooth preparation. Despite the advantages, the use of RBFPDs as definitive restorations

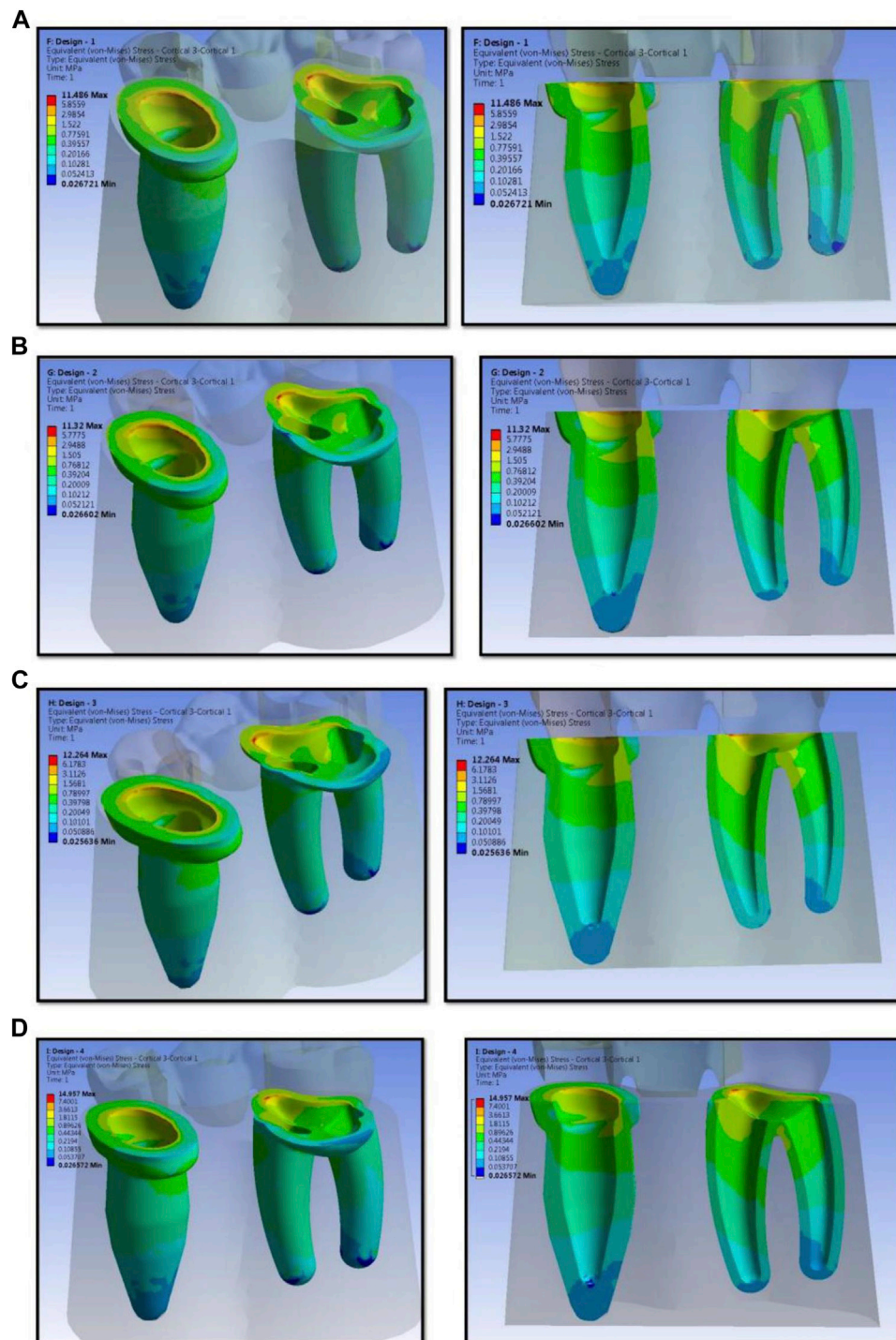


FIGURE 6 | Stress distribution on the different designs of resin-bonded fixed dental prosthesis on cortical bone for design 1 (A), design 2 (B), design 3 (C), and design 4 (D) used in finite element analysis.

remains controversial due to a lack of long-term prospective data on prosthetic success. A recent systematic review has estimated 5-year survival rates of 87.7% for resin-bonded prostheses and greater than 90% for conventional fixed prostheses depending on the design (Lin et al., 2003).

Although there is a lower than 94.5% success rate reported for implant-retained single crowns over the same 5-year follow-up, resin-bonded bridgework has the advantages of being less invasive and requiring a shorter total treatment time and less financial commitment. Since the components in fixed

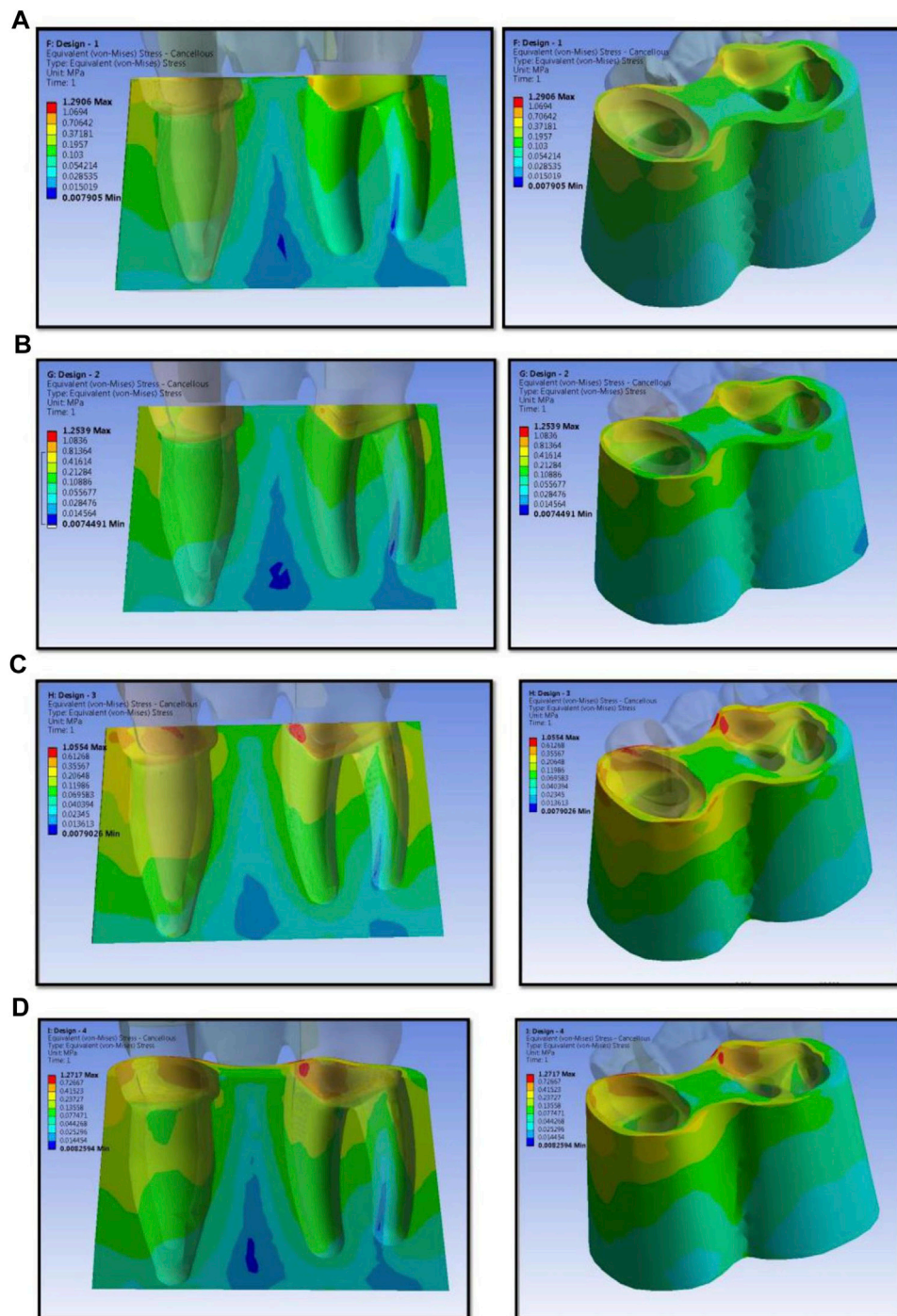


FIGURE 7 | Stress distribution on cancellous bone for design 1 (A), design 2 (B), design 3 (C), and design 4 (D) used in finite element analysis.

prosthesis–bone systems are complex geometrically, FEA is the most suitable tool for analyzing them (Borcić et al., 2007). A key factor for the success or failure of a dental prosthesis is how stresses are transferred to the surrounding bone. FEA helps us predict the pattern, concentration, and stresses acting on the prosthesis and surrounding tissues. This helps us determine the failure mechanisms of the prosthesis. Excessive stresses acting on

the surrounding bone and tissues cause tissue injury. The body then attempts to repair the injury and periodontium. This can occur if the forces are diminished or the tooth drifts away. The periodontium is remodeled to cushion its impact if the offending stress is chronic. This causes a widening of the periodontal ligament space due to the resorption of bone. It also results in angular bone defects without periodontal pockets and causes

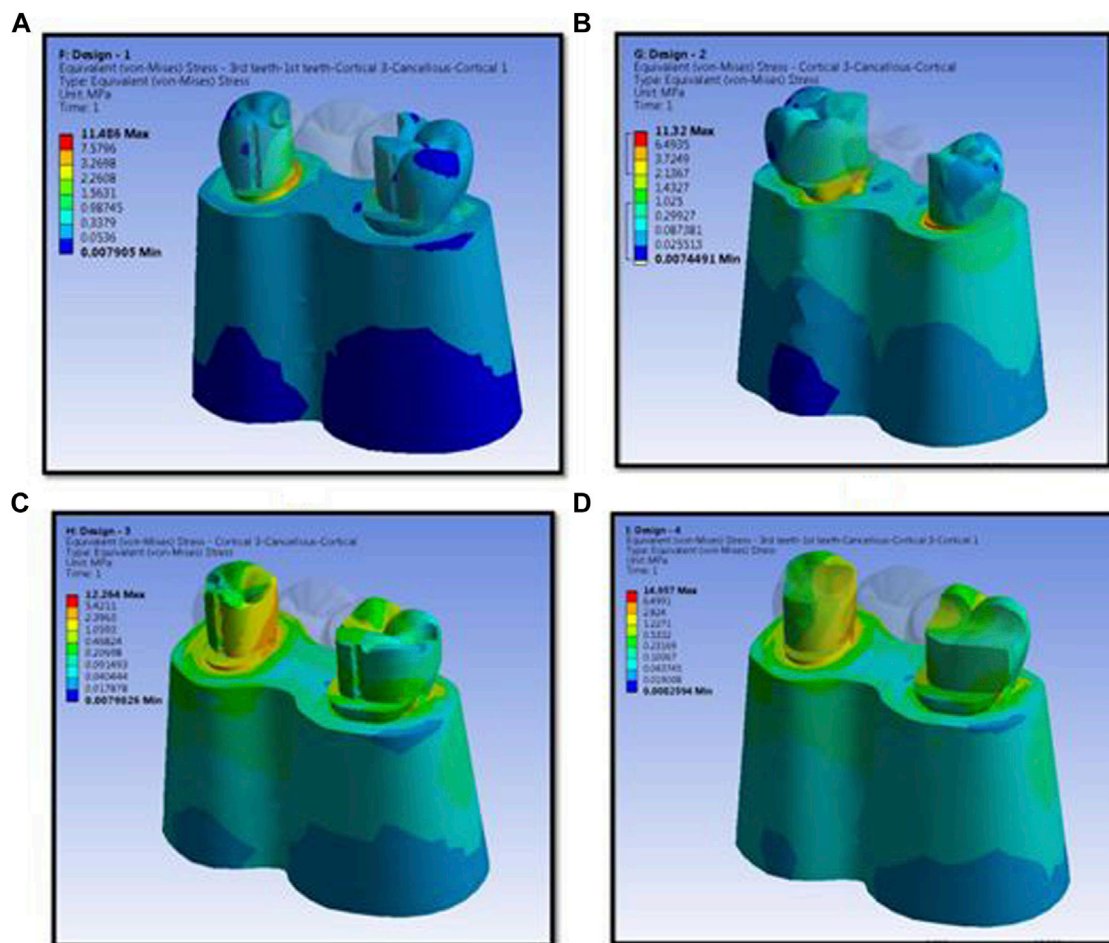


FIGURE 8 | Stress distribution in cortical bone, cancellous bone, and teeth for design 1 (A), design 2 (B), design 3 (C), and design 4 (D) used in finite element analysis.

mobility of teeth. Subsequently, it might lead to the restoration's failure due to the loss of the abutment tooth (Della Bona et al., 2013). Furthermore, undue stresses acting on the connector region can lead to fractures. The adequate thickness of the connector area is essential to prevent flexing and fracture, and a minimum thickness of 0.8 mm is recommended for fracture resistance (Pjetursson et al., 2007). The early design of the posterior Maryland Bridge included axial coverage and an occlusal rest. There was little proximal and lingual enamel preparation.

Posterior RBFPDs appeared to require a 180-degree-plus circumferential preparation of abutment teeth for predictable success (Toman et al., 2015). The design preparation was modified by incorporating mechanical retention features such as grooves for resistance. The L-shaped retainer covered one-half of the lingual cusps with a groove at the far side of the buccal line angle and another groove at the far opposite side to hold the abutment teeth firmly. Chow et al. presented an approach using a groove, a plate, and a strut, which involved minimal preparation of the posterior abutment to receive an RBFPD using a base metal alloy (Modi et al., 2015). Botelho (2000) recommended that the

major retainer has a wraparound configuration on at least three abutment surfaces or has strategically placed opposing axial grooves or slots for long-span prostheses to replace two or more missing teeth. Another report described a methodical preparation for posterior partial veneered restorations that provided proper posterior occlusal function and isolated the enamel's occlusal contact area to maintain the occlusion's vertical dimension (Saad et al., 1995).

A long-term follow-up indicated that abutment teeth mobility is one of the decisive prognostic factors for the success of RBFPDs (Farshad et al., 2013). Furthermore, it was reported that an RBFPD without any retentive preparation design failed significantly at a higher rate (Sichi et al., 2021). Saad et al. suggested that the addition of retentive grooves made a statistically significant difference in resistance to debonding forces (Saad et al., 1995). The results demonstrated that design modifications were necessary to improve clinical longevity. Therefore, the application of resin-bonded retainers with additional retentive structures, such as a pinhole and grooves in the anterior region, was recommended. In addition to this, the retainer thickness also affects the retention of the prosthesis.

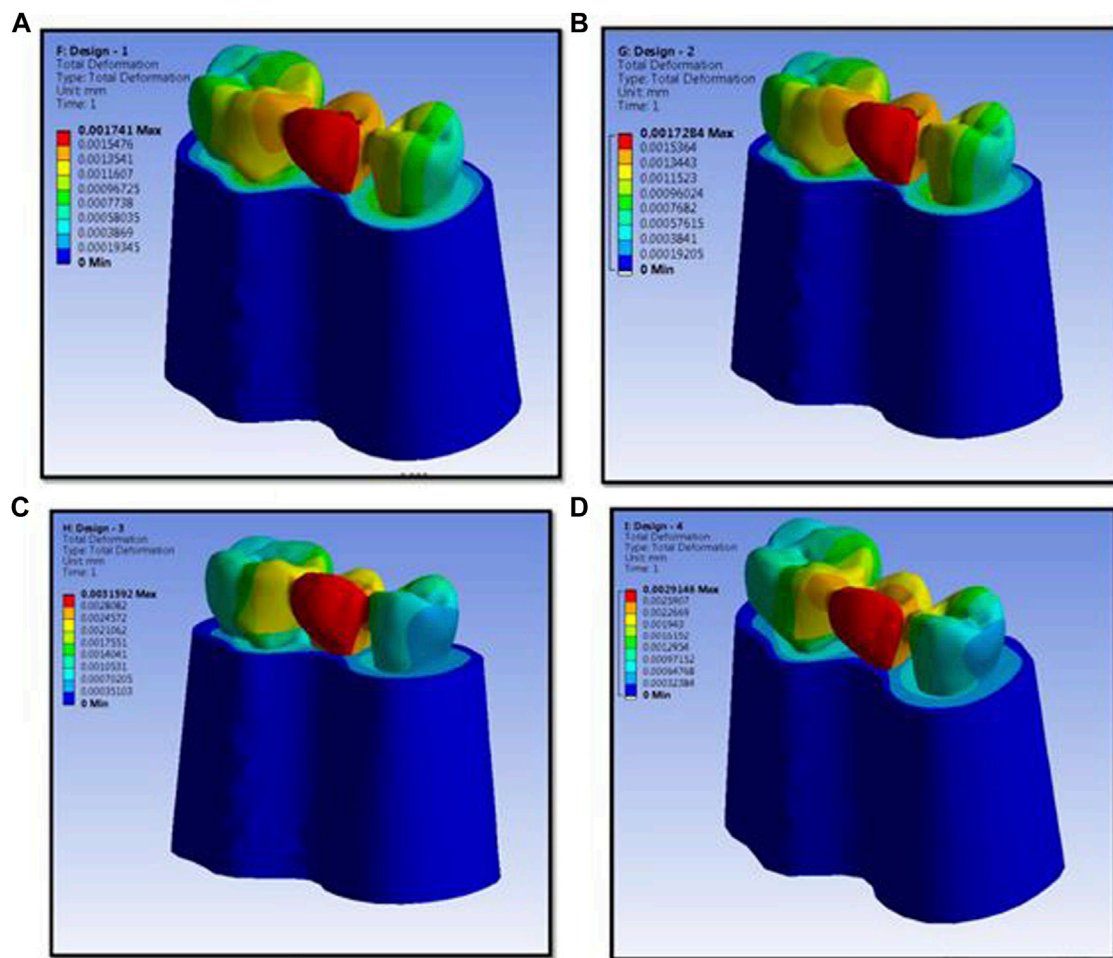
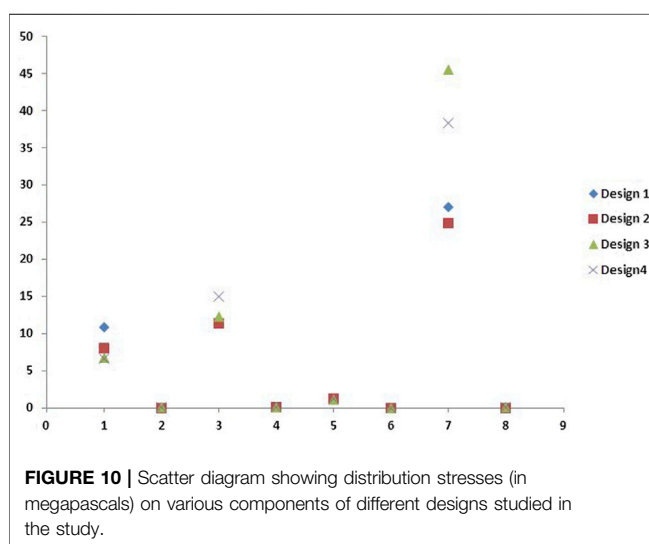


FIGURE 9 | Maximum deformation observed in prosthesis and the magnitude for design 1 (A), design 2 (B), design 3 (C), and design 4 (D) used in finite element analysis.



Chun et al. concluded that a minimum retainer thickness of 0.8 mm was required for long-term RBFPD success (Pjetursson et al., 2007). Very few studies have assessed stress acting on various designs of RBFPDs. The present study was aimed to evaluate a design that transmits less stress to the prosthesis and supporting structures. In the present study, four different RBFPD designs for tooth preparation included retentive features such as rests, grooves, and occlusal coverage. The tooth preparation for the retainers incorporated all design patterns currently used for etched-cast RBFPDs. Design 1 was the conventional RBFPD design with lingual reduction and occlusal rests. Design 2 combined slices, which gave proximal extensions for the RBFPDs. The proximal extensions reduced stress around the connector and the rest areas. Design 3 consisted of grooves in addition to the rests, wings, and slices. The grooves provided additional retention against displacing and rotational forces (Botelho, 2000). Proximal grooves compensate for the lack of proximal wraparound, limited by aesthetic requirements. Vertical

grooves were a particular feature that has been identified as reducing stresses on the cement bond and increasing resistance to debonding forces. The preparation involves irreversible damage to abutment teeth, and even when minimal preparation is intended, dentin exposure is likely during preparation. Design 4 added occlusal coverage to the features mentioned above. Occlusal coverage has improved the retention and resistance form of RBFPDs (Lin et al., 2005; Arora et al., 2014). In the present study, a vertical force of 100 N was applied to the pontic's natural groove, about one-sixth of the maximum biting force (El Salam Shakal et al., 1997; Zalkind et al., 2003). This region was chosen since it occludes with the stamp cusp of the opposing tooth. The resultant stresses acting on each area of the four models were assessed and tabulated. In all designs, the maximum stresses on the prosthesis were seen in the area around the connector. The maximum stresses were concentrated at the cervical margin of the abutment margin around the pontic on the teeth. It can be seen that stresses were highly concentrated near the connector but were relatively uniformly stressed throughout the occlusogingival direction away from the connector sites. Design 1 is the conventional design used by the majority of clinicians. Lesser stress concentration on the connector makes it less susceptible to fracture. Nevertheless, high stresses are transmitted onto the abutment and bone, which can be attributed to the rests of the design. Design 2 showed the least amount of stress on the connector, but owing to the high stresses transmitted onto the abutment and bone, it becomes a less-preferred design of RBFPDs. Design 3, despite the high stress within the connector, transmits the least amount of stress into the abutment and bone. As a result, there is less bone resorption and no harm to the supporting structures, resulting in the least likelihood of failure of RBFPD. The grooves included in the design increase the surface area present for bonding, adding to the retentive ability of the prosthesis (AlShaarani et al., 2019). These features ensure the clinical longevity of the prosthesis. Design 4 offers added coverage for the prosthesis but transmits high stresses to the abutment and bone. It is a nonconservative design of tooth preparation. Additionally, high stresses act on the connector, which may increase fracture probability in this region. These factors make design 4 unsuitable for RBFPDs.

A recent systematic review (Reddy et al., 2019) suggested that FEA analysis enhances the validity of the models. A Swedish study (Bakitian et al., 2020) recommended that the framework designs play a significant role in stress distribution. A Japanese study (Tsouknidas et al., 2020) reported that ceramic veneers could restore the biomechanical behavior of prepared anterior teeth. In the present study, stress load was evaluated on the connector, abutment, and bone of four different RBFPDs. Posterior teeth were used for evaluation in the present study. The authors found that the use of wings, rests, and grooves was ideal for tooth preparation to receive RBFPD; it was evident that this was a more conservative design than other designs studied. FEA was not a practical method of assessing the failure of the restorations, and many different clinical situations need to be considered. The properties of dentin were considered for the whole tooth, and the periodontal ligament's role was not considered a potential

limitation of the present study. The methodology of the present study would offer the possibility of stress analysis in the restorative material, primarily. A stress analysis was not carried out in the present study, and it was not our objective; hence, this is also considered a limitation.

The FEA can provide detailed quantitative data at any location within the mathematical model. Thus, FEA has become a valuable analytical tool in assessing various dentistry systems (Pjetursson et al., 2008). Keulemans et al. (2015) used five framework materials (zirconia, glass-ceramic, gold alloy, indirect fiber-reinforced composite, and direct fiber-reinforced composite). They reported that there were differences in biomechanical behavior between various RBFPDs. The authors concluded that an RBFPD made of FRC achieved promising stress distribution. These findings were not comparable with the present study since the study designs used in the present study were different from the designs used by Keulemans et al. (2015). Various researchers investigated anterior RBFPDs exceptionally with regard to design and loading. The use of RBFPDs in the posterior region is less predictable than in the anterior region because of occlusal forces. However, there is a lacuna in the published evidence assessing the factors associated with success in replacing teeth with RBFPDs in the posterior region (Keulemans et al., 2015; King et al., 2015).

In the present study, design 3 was found to have transmitted the least stress through and around the abutment teeth, and this results in lesser bone resorption around the abutment teeth. The study also found that the stress acting on the connector area was minimal in design 3. Reducing the stress acting in this region reduces the likelihood of fracture occurring in the restoration and increases the longevity of the restoration. Based on the above findings, design 3 is the design that should be advocated in clinical practice because it has better retention compared to other designs. The limitations of the present study include the following: (1) FEA was not a practical method for assessing the failure of the restorations, and many other clinical situations need to be considered; (2) the properties of dentin were considered for the whole tooth; and (3) the role of the periodontal ligament was not considered. The present study within these limitations established the RBFPDs in the posterior region by using FEA. Although stress concentrations often appear in FEA, the linear assumption used in a linear FEA does not precisely depict what is occurring in areas of stress. It is very unusual to fail as a fundamental component based on a stress concentration in a linear analysis.

CONCLUSION

Within the limitations of this study, it can be concluded that the design with wings, rests, and grooves is possibly the ideal and conservative design of tooth preparation for receiving a posterior RBFPD. The design with wings, rests, and grooves transmits less stress to the abutments and results in lesser bone resorption. It is most likely to be successful in clinical service, ensuring the longevity of the prosthesis.

DATA AVAILABILITY STATEMENT

The raw data supporting the conclusions of this article will be made available by the authors, without undue reservation.

AUTHOR CONTRIBUTIONS

Conceptualization, SS and PR; methodology, RM, SS, and PR; software, SS and SM; validation, SA, KL, VK, SM, and AJ; formal analysis, SM, VK, and AJ; investigation, SAS and PR; resources, RM, KL, and SA; data curation, ZA, AJ, and VK; writing—original draft preparation, SM and PR; writing—review and editing, SM, RM, and AJ; visualization, SS and VK; supervision, KL and SA; project administration, SS, KL, and SA; funding acquisition, SA. All

authors have read and agreed to the published version of the manuscript.

FUNDING

This research received funding from the Deanship of Scientific Research at Majmaah University, Al-Majmaah, Kingdom of Saudi Arabia under project No 1439–84.

ACKNOWLEDGMENTS

The authors would like to thank the Deanship of Scientific Research at Majmaah University, Al-Majmaah, Kingdom of Saudi Arabia, for supporting this project.

REFERENCES

- Acharya, P. H., Patel, V. V., Duseja, S. S., and Chauhan, V. R. (2021). Comparative Evaluation of Peri-Implant Stress Distribution in Implant Protected Occlusion and Cuspally Loaded Occlusion on a 3 Unit Implant Supported Fixed Partial Denture: A 3D Finite Element Analysis Study. *J. Adv. Prosthodont.* 13 (2), 79–88. doi:10.4047/jap.2021.13.2.79
- AlShaarani, F., Alaisami, R. M., Aljerf, L., Jamous, I. A., Elias, K., and Jaber, A. (2019). An Auxiliary Factor for Increasing the Retention of Short Abutments. *Heliyon* 5 (10), e02674. doi:10.1016/j.heliyon.2019.e02674
- Anweigi, L., Azam, A., Mata, C. d., AlMadi, E., Alsaleh, S., and Aldegheishem, A. (2020). Resin Bonded Bridges in Patients with Hypodontia: Clinical Performance over a 7 Year Observation Period. *Saudi dental J.* 32 (5), 255–261. doi:10.1016/j.sdentj.2019.10.011
- Arora, V., Sharma, M. C., and Dwivedi, R. (2014). Comparative Evaluation of Retentive Properties of Acid Etched Resin Bonded Fixed Partial Dentures. *Med. J. Armed Forces India* 70 (1), 53–57. doi:10.1016/j.mjafi.2013.03.011
- Aversa, R., Apicella, D., Perillo, L., Sorrentino, R., Zarone, F., Ferrari, M., et al. (2009). Non-linear Elastic Three-Dimensional Finite Element Analysis on the Effect of Endocrown Material Rigidity on Alveolar Bone Remodeling Process. *Dental Mater.* 25, 678–690. doi:10.1016/j.dental.2008.10.015
- Bakitarian, F., Papia, E., Larsson, C., and Vult von Steyern, P. (2020). Evaluation of Stress Distribution in Tooth-Supported Fixed Dental Prostheses Made of Translucent Zirconia with Variations in Framework Designs: A Three-Dimensional Finite Element Analysis. *J. Prosthodont.* 29 (4), 315–322. doi:10.1111/jopr.13146
- Borčić, J., Antonić, R., Urek, M. M., Petricević, N., Nola-Fuchs, P., Catić, A., et al. (2007). 3-D Stress Analysis in First Maxillary Premolar. *Coll. Antropol.* 31 (4), 1025–1029.
- Botelho, M. (2000). Design Principles for Cantilevered Resin-Bonded Fixed Partial Dentures. *Quintessence. Int.* 31 (9), 613–619.
- Botelho, M. G., Ma, G. J. K., Cheung, M. T. C., Law, W. Y. H., Tai, M. T., and Lam, W. Y. (2014). Long-term Clinical Evaluation of 211 Two-Unit Cantilevered Resin-Bonded Fixed Partial Dentures. *J. Dentistry* 42, 778–784. doi:10.1016/j.jdent.2014.02.004
- Chow, T. W., Chung, R. W. C., Chu, F. C. S., and Newsome, P. R. H. (2002). Tooth Preparations Designed for Posterior Resin-Bonded Fixed Partial Dentures: a Clinical Report. *The J. Prosthetic Dentistry* 88 (6), 561–564. doi:10.1067/jmpr.2002.129374
- Della Bona, A., Borba, M., Benetti, P., Duan, Y., and Griggs, J. A. (2013). Three-dimensional Finite Element Modelling of All-Ceramic Restorations Based on Micro-CT. *J. Dentistry* 41 (5), 412–419. doi:10.1016/j.jdent.2013.02.014
- El Salam Shakal, M. A., Pfeiffer, P., and Hilgers, R.-D. (1997). Effect of Tooth Preparation Design on Bond Strengths of Resin-Bonded Prostheses: a Pilot Study. *J. Prosthetic Dentistry* 77 (3), 243–249. doi:10.1016/s0022-3913(97)70180-x
- Esquivel-Upshaw, J. F., Mecholsky, J. J., Jr, Clark, A. E., Jenkins, R., Hsu, S. M., Neal, D., et al. (2020). Factors Influencing the Survival of Implant-Supported Ceramic-Ceramic Prostheses: A Randomized, Controlled Clinical Trial. *J. Dentistry* 103, 100017. doi:10.1016/j.jjodo.2020.100017
- Farshad, B., Ehsan, G., Mahmoud, S., Reza, K., and Mozhdeh, B. (2013). Evaluation of Resistance Form of Different Preparation Features on Mandibular Molars. *Indian J. Dent. Res.* 24 (2), 216–219. doi:10.4103/0970-9290.116686
- Keulemans, F., Shinya, A., Lassila, L. V., Vallittu, P. K., Kleverlaan, C. J., Feilzer, A. J., et al. (2015). Three-dimensional Finite Element Analysis of Anterior Two-Unit Cantilever Resin-Bonded Fixed Dental Prostheses. *ScientificWorldJournal* 2015, 864389. doi:10.1155/2015/864389
- King, P. A., Foster, L. V. V., Yates, R. J., Newcombe, R. G., and Garrett, M. J. (2015). Survival Characteristics of 771 Resin-Retained Bridges provided at a UK Dental Teaching Hospital. *Br. Dent. J.* 218, 423–428. doi:10.1038/sj.bdj.2015.250
- Lin, C.-L., Hsu, K.-W., and Wu, C.-H. (2005). Multi-factorial Retainer Design Analysis of Posterior Resin-Bonded Fixed Partial Dentures: a Finite Element Study. *J. Dentistry* 33 (9), 711–720. doi:10.1016/j.jdent.2005.01.009
- Lin, C. L., Lin, T. S., Hsu, K. W., Wu, C. H., and Chang, C. H. (2003). Numerical Investigation of Retainer Thickness Affecting Retention in Posterior Resin-bonded Prosthesis Using the Finite Element Method. *J. Chin. Inst. Eng.* 26, 781–789. doi:10.1080/02533839.2003.9670832
- Medina-Galvez, R., Cantó-Navés, O., Marimon, X., Cerrolaza, M., Ferrer, M., and Cabratosa-Termes, J. (2021). Bone Stress Evaluation with and without Cortical Bone Using Several Dental Restorative Materials Subjected to Impact Load: A Fully 3D Transient Finite-Element Study. *Materials* 14 (19), 5801. doi:10.3390/ma14195801
- Modi, R., Kohli, S., Rajeshwari, K., and Bhatia, S. (2015). A Three-Dimension Finite Element Analysis to Evaluate the Stress Distribution in Tooth Supported 5-unit Intermediate Abutment Prosthesis with Rigid and Nonrigid Connector. *Eur. J. Dent.* 09, 255–261. doi:10.4103/1305-7456.156847
- Pjetursson, B. E., Brägger, U., Lang, N. P., and Zwahlen, M. (2007). Comparison of Survival and Complication Rates of Tooth-Supported Fixed Dental Prostheses (FDPs) and Implant-Supported FDPs and Single Crowns (SCs). *Clin. Oral Implants Res.* 18 (Suppl. 3), 97–113. doi:10.1111/j.1600-0501.2007.01439.x
- Pjetursson, B. E., Tan, W. C., Tan, K., Brägger, U., Zwahlen, M., and Lang, N. P. (2008). A Systematic Review of the Survival and Complication Rates of Resin-Bonded Bridges after an Observation Period of at Least 5 Years. *Clin. Oral Implants Res.* 19, 131–141. doi:10.1111/j.1600-0501.2007.01527.x
- Reddy, M., Sundram, R., and Eid Abdemagyd, H. (2019). Application of Finite Element Model in Implant Dentistry: A Systematic Review. *J. Pharm. Bioall Sci.* 11 (Suppl. 2), 85–S91. doi:10.4103/JPBS.JPBS_296_18
- Robati Anaraki, M., Torab, A., and Mounesi Rad, T. (2019). Comparison of Stress in Implant-Supported Monolithic Zirconia Fixed Partial Dentures between Canine Guidance and Group Function Occlusal Patterns: A Finite Element Analysis. *J. Dent Res. Dent Clin. Dent Prospects* 13 (2), 90–97. doi:10.15171/joddd.2019.014

- Saad, A. A., Claffey, N., Byrne, D., and Hussey, D. (1995). Effects of Groove Placement on Retention/resistance of Maxillary Anterior Resin-Bonded Retainers. *J. Prosthetic Dentistry* 74 (2), 133–139. doi:10.1016/s0022-3913(05)80175-1
- Sichi, L. G. B., Pierre, F. Z., Arcila, L. V. C., de Andrade, G. S., Tribst, J. P. M., Ausiello, P., et al. (2021). Effect of Biologically Oriented Preparation Technique on the Stress Concentration of Endodontically Treated Upper Central Incisor Restored with Zirconia Crown: 3D-FEA. *Molecules* 26 (20), 6113. doi:10.3390/molecules26206113
- Silva, B. R., Silva, F. I., Jr., Moreira Neto, J. J., and Aguiar, A. S. (2009). Finite Element Analysis Application in Dentistry: Analysis of Scientific Production from 1999 to 2008. *Int. J. Dent.* 8, 197–201.
- Tanaka, C. B., Ballester, R. Y., De Souza, G. M., Zhang, Y., and Meira, J. B. C. (2019). Influence of Residual thermal Stresses on the Edge Chipping Resistance of PFM and Veneered Zirconia Structures: Experimental and FEA Study. *Dental Mater.* 35 (2), 344–355. doi:10.1016/j.dental.2018.11.034
- Tanoue, N. (2016). Longevity of Resin-Bonded Fixed Partial Dental Prostheses Made with Metal Alloys. *Clin. Oral Invest.* 20 (6), 1329–1336. doi:10.1007/s00784-015-1619-9
- Toman, M., Toksavul, S., Sabancı, S., Kıran, B., Dikici, S., Sarıkanat, M., et al. (2015). Three-dimensional Finite Element Analysis of Stress Distribution of Two-Retainer and Single-Retainer All-Ceramic Resin-Bonded Fixed Partial Dentures. *Quintessence. Int.* 46 (8), 691–696. doi:10.3290/j.qi.a34177
- Tsouknidas, A., Karaoglani, E., Michailidis, N., Kugiumtzis, D., Pissiotis, A., and Michalakakis, K. (2020). Influence of Preparation Depth and Design on Stress Distribution in Maxillary central Incisors Restored with Ceramic Veneers: A 3d Finite Element Analysis. *J. Prosthodont.* 29 (2), 151–160. doi:10.1111/jopr.13121
- Zalkind, M., Ever-Hadani, P., and Hochman, N. (2003). Resin-bonded Fixed Partial Denture Retention: a Retrospective 13-year Follow-Up. *J. Oral Rehabil.* 30 (10), 971–977. doi:10.1046/j.1365-2842.2003.01165.x

Conflict of Interest: The authors declare that the research was conducted in the absence of any commercial or financial relationships that could be construed as a potential conflict of interest.

Publisher's Note: All claims expressed in this article are solely those of the authors and do not necessarily represent those of their affiliated organizations, or those of the publisher, the editors, and the reviewers. Any product that may be evaluated in this article, or claim that may be made by its manufacturer, is not guaranteed or endorsed by the publisher.

Copyright © 2022 Shaikh, Rai, Aldhuwayhi, Mallineni, Lekha, Joseph, Kumari and Meshramkar. This is an open-access article distributed under the terms of the Creative Commons Attribution License (CC BY). The use, distribution or reproduction in other forums is permitted, provided the original author(s) and the copyright owner(s) are credited and that the original publication in this journal is cited, in accordance with accepted academic practice. No use, distribution or reproduction is permitted which does not comply with these terms.



Case Report: Combining Molar Interradicular Osteotomy With Immediate Implant Placement: A Three-Year Case-Series Study

Adel S. AlagI and Marwa Madi*

Periodontology Division, Preventative Dental Sciences Department, College of Dentistry, Imam Abdulrahman Bin Faisal University, Dammam, Saudi Arabia

OPEN ACCESS

Edited by:

Mohammad Khursheed Alam,
Al Jouf University, Saudi Arabia

Reviewed by:

Daniel Fernando Torassa,
National University of Cordoba,
Argentina
Lei Sui,
Tianjin Medical University, China

*Correspondence:

Marwa Madi
mimadi@iau.edu.sa

†ORCID:

Adel AlagI
orcid.org/0000-0001-6274-7677
Marwa Madi
orcid.org/0000-0002-3014-0405

Specialty section:

This article was submitted to
Biomaterials,
a section of the journal
Frontiers in Materials

Received: 04 March 2022

Accepted: 11 April 2022

Published: 12 May 2022

Citation:

AlagI AS and Madi M (2022) Case
Report: Combining Molar Interradicular
Osteotomy With Immediate Implant
Placement: A Three-Year Case-
Series Study.
Front. Mater. 9:889889.
doi: 10.3389/fmats.2022.889889

Background: Immediate implant placement in the area of multirooted molars includes many anatomical challenges, particularly with osteotomy preparation in the interradicular bone.

Methods: In this article, we are reporting ten cases in which implant beds were prepared before root extraction. After coronectomy, pre-extractive interradsular implant bed preparations were performed through the retained root complexes. A dimple in the roof of the furcation was created using a no. 8 round surgical bur. The osteotomies were then completed through the tooth's initially retained root complex in the regular sequence of drilling. Before implant placement, the remaining root segments were removed. The retained root parts guided the osteotomy drills and allowed for precise positioning and angulation of the implant bed preparation with respect to the emergence profile of the tooth.

Results: Data from a 3-year follow-up of the crestal bone showed good bone levels in relation to the implant platform.

Conclusion: The technique described permitted accurate implant placement in the prepared osteotomy, thus enabling immediate implant positioning in multirooted extraction sites.

Keywords: pre-extractive drilling, immediate implant, interradsular implant bed, clinical case, interradsular osteotomy

INTRODUCTION

Since the introduction of the immediate implant placement technique, placing implants in fresh extraction sockets became an acceptable procedure for more than two decades (Barone et al., 2015). Frequently, immediate implants are used for single-rooted teeth. In the case of immediate molar placement into molar sites, there are challenges involving site anatomy, occlusion, and biomechanical issues (Schropp and Isidor, 2008).

Immediate implants offer several advantages compared to the more conventional placement technique that requires 4 months following tooth extraction before implant installment (Bhola et al., 2008). Thus, significant reduction of the surgical phase coupled with a much shorter overall treatment time is achieved (Bhola et al., 2008). Today, immediate implants achieve long-term

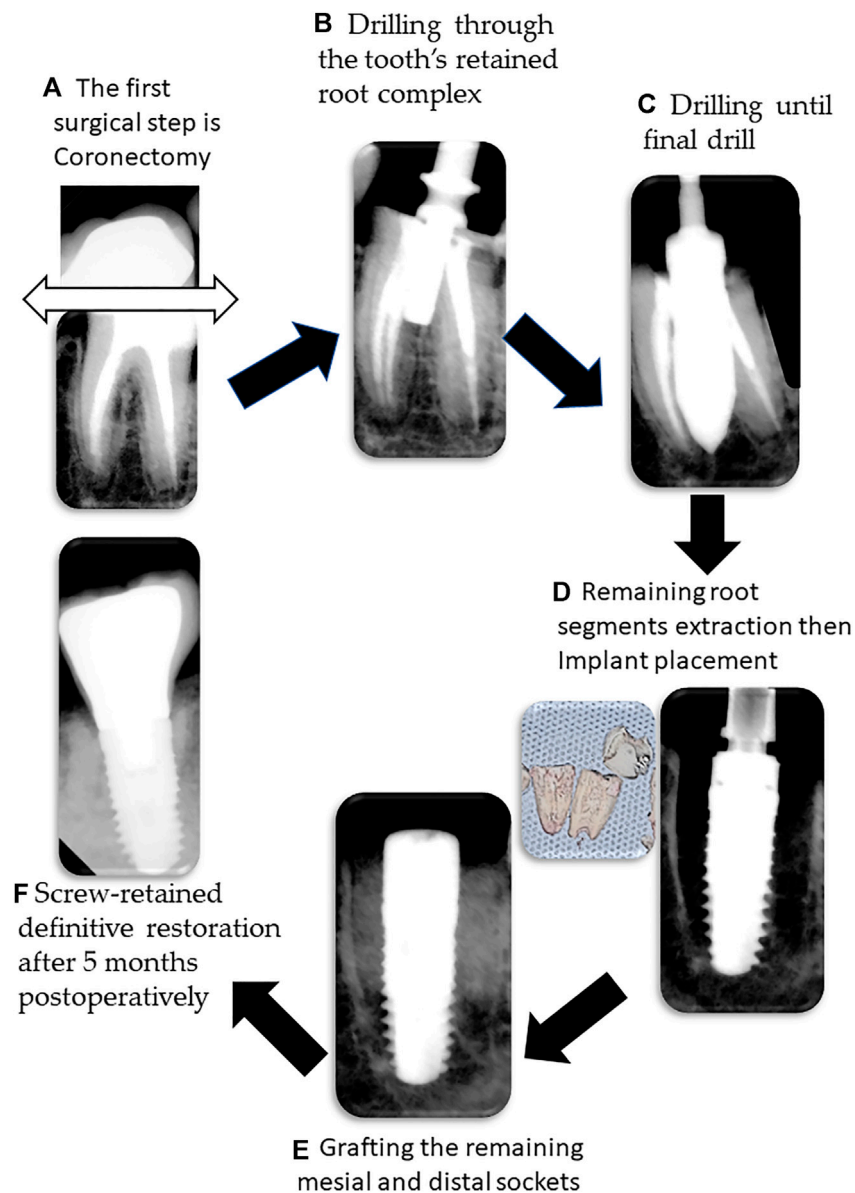


FIGURE 1 | Illustration of the surgical procedure steps. **(A)** Initial surgical is coronectomy using a high speed tapered diamond bur coronectomy; **(B)** after forming a dimple in the roof of the furcation, drilling through the tooth's retained root complex is performed; **(C)** final drilling is performed; **(D)** root separation is carried out and then the remaining root segments are extracted followed by implant placement; **(E)** bone graft is placed in the mesial and distal sockets; **(F)** after 5 months postoperatively, screw-retained definitive restoration is delivered.

survival rates comparable to those of delayed implants placed in healed sites with a two-stage surgical approach (Quirynen et al., 2007; Becker and Goldstein, 2008; Schropp and Isidor, 2008; Chen and Buser, 2009). These favorable outcomes are not only important for single-tooth replacement in the esthetic zone but also for implant placement in the molar regions (Atieh et al., 2010).

With respect to maxillary and mandibular molar regions, immediate implant placement entails a series of clinical challenges related to site-specific anatomical aspects, such as comparatively larger socket than implant size, root length,

height of the root trunk, and divergence of roots (Valenzuela et al., 2018).

It is essential to evaluate the anatomy of each patient's posterior mandible, including the variability in the position of the inferior alveolar canal and the submandibular fossa. This step is critical because of the potential high risk for inferior alveolar nerve injury and lingual plate perforation when attempting to achieve primary implant stability using native bone apical to the extraction socket (Greenstein and Tarnow, 2006).

In molar extraction sockets, achieving initial implant stability can be challenging due to the width of the alveolar socket, poor

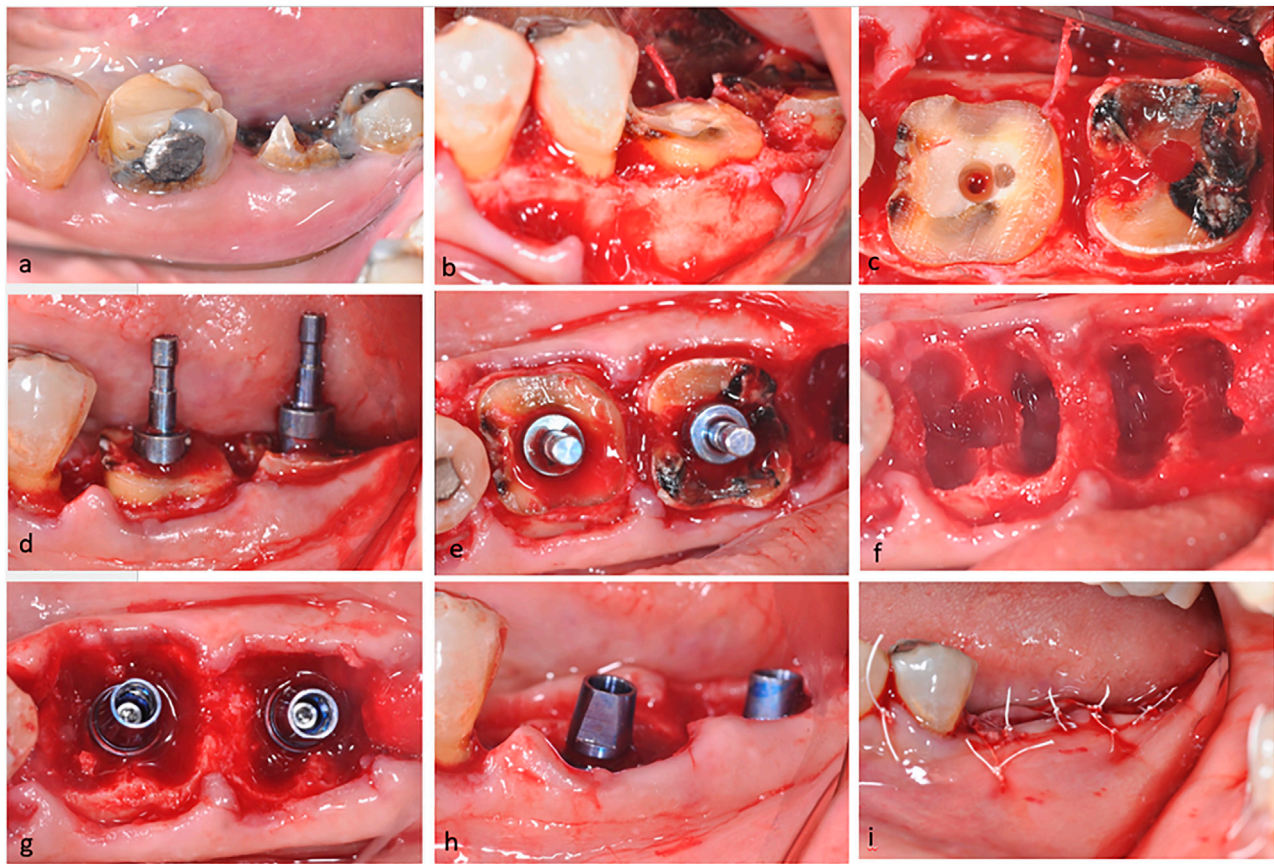


FIGURE 2 | Clinical photographs of the steps in this surgical procedure. **(A)** Preoperative lateral view of the mandibular left first and second molars, which were unrestorable; **(B)** clinical view showing flap reflection and coronectomy; **(C)** occlusal view showing the dimple created with a #8 round bur; **(D,E)** lateral and occlusal views showing parallel pins; **(F)** occlusal view showing the final osteotomy in each molar tooth; **(G,H)** occlusal and lateral views showing implant placement in the pre-extractive drill; and **(I)** immediate postoperative lateral view of surgical sites with primary soft tissue closure.

bone quality, and critical anatomical structures beyond the apices of molar roots, such as the inferior alveolar nerve. Consequently, consideration should be given to placing implants within the mandibular molar extraction socket itself (Cafiero et al., 2008).

The protocol of immediate implant placement offers several advantages, including a reduction in the number of the surgical procedures, favorable esthetics, preservation of bone height and width, improved quality of life, and increased patient comfort and satisfaction (Chen et al., 2004).

Placing implants in an ideal prosthetic position without compromising their primary stability remains a key goal. Thus, directing the initial osteotomy into the interradicular bone would be preferred. However, there are circumstances in which the drill may slip, resulting in implant placement within the confines of the residual extraction socket (Scarano, 2017). In this study, we present ten cases with three-year follow-up in which interradicular implant bed preparation was performed before root extraction; thus, the osteotomy drills would be stabilized and guided by the retained root aspects.

MATERIALS AND METHODS

The study population consisted of ten patients, eight females and two males, all of whom were non-smokers, and none reported any history of any systemic diseases or conditions that would preclude surgical implant placement and subsequent restoration. The patients' age ranged from 39 to 66 years.

All patients, after receiving a full description of the surgical procedure, signed informed consent in full accordance with the guidelines of the Helsinki World Medical Association Declaration and the revision of the 2013 Good Clinical Practice Guides, and ethical approval was obtained (IRB-2021-02-208).

Each patient had at least one molar tooth diagnosed as hopeless due to restorability or failed endodontic treatment (seven mandibular first molars, two mandibular second molars, and one maxillary first molar). These teeth were treatment-planned for extraction and immediate implant placement (Figure 2A, Figure 3A, Figure 4A,D). A Schematic presentation of the procedure is illustrated in Figure 1.

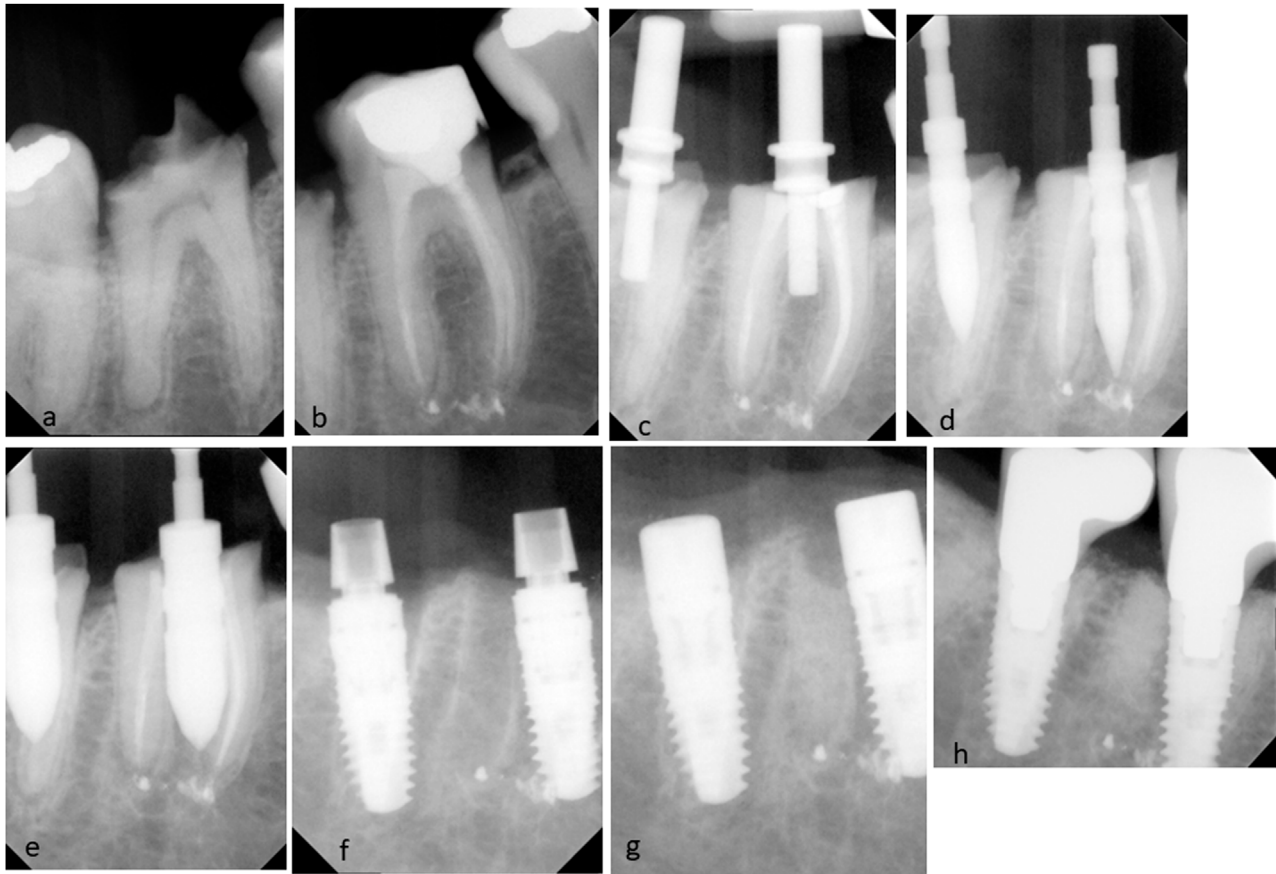


FIGURE 3 | Radiographic images of the surgical procedure. **(A,B)** Preoperative radiographs of mandibular left first and second molars; **(C)** pre-extractive interradiacal implant bed preparation. The parallel pins inserted in the initial osteotomy directly through each molar's initially retained root complex of the left first and second molars; **(D,E)** other osteotomy drills drilled directly through the root complex; **(F)** insertion of cylindrical screw-type implants after removal of the remaining roots; **(G)** healing abutments were placed and bone graft material filled the extraction socket around each implant; and **(H)** a periapical radiograph taken 6 months after placement of the definitive restorations.

The Surgical Phase

All procedures were performed under local anesthesia using lidocaine 2% 1:100,000 epinephrine. Mucoperiosteal flap was made with minimal soft tissue reflection, and coronectomy was accomplished using a high-speed tapered diamond bur (**Figures 1A** and **Figure 2B**). Pre-extractive interradiacal implant bed preparation was performed prior to root separation. A dimple in the roof of the furcation was created with a no. 8 round surgical bur to prevent skidding of the initial surgical drill (**Figure 2C**).

The osteotomies were performed directly through each tooth's retained root complex in the regular sequence of drilling starting with a point drill and finishing with the final drill before the roots were extracted and the implant was placed (**Figures 1B,C**).

The retained root components guided the osteotomy drills and aided precise positioning and angulation of the implant bed preparation with respect to the emergence profile of the tooth. The drilling depth was extended beyond the fundus of the socket in compliance with the preoperative radiographic assessment.

After completion of the drilling protocol, according to the manufacturer's instructions, the remaining root segments were separated. After root separation, periostomes were used to cut the periodontal ligament attachments to permit atraumatic extraction with the remaining root parts delicately removed using curved elevators (**Figures 2D–H** and **Figure 3C–E**).

For all cases, proper debridement of each socket was performed using a bone curette and saline irrigation. Screw-type dental implants D 4.5x L11 mm (Xive S Plus, Dentsply Sirona, United States, **Figure 1D**) were inserted in the interradiacal bone, and the implant shoulder of each implant was positioned at 1–2 mm apical to facial/buccal CEJ of adjacent teeth (**Figures 2H** and **Figure 3F**).

All 10 implants exhibited primary implant stability and were inserted under 35 NW torque. The gap around the implant and the mesial and distal sockets were completely packed with xenograft bone particles (**Figure 1E**) (NuOss cancellous bovine bone, 0.25–1 mm, ACE Surgical Supply Co., Massachusetts, United States) After inserting the bone graft material, the

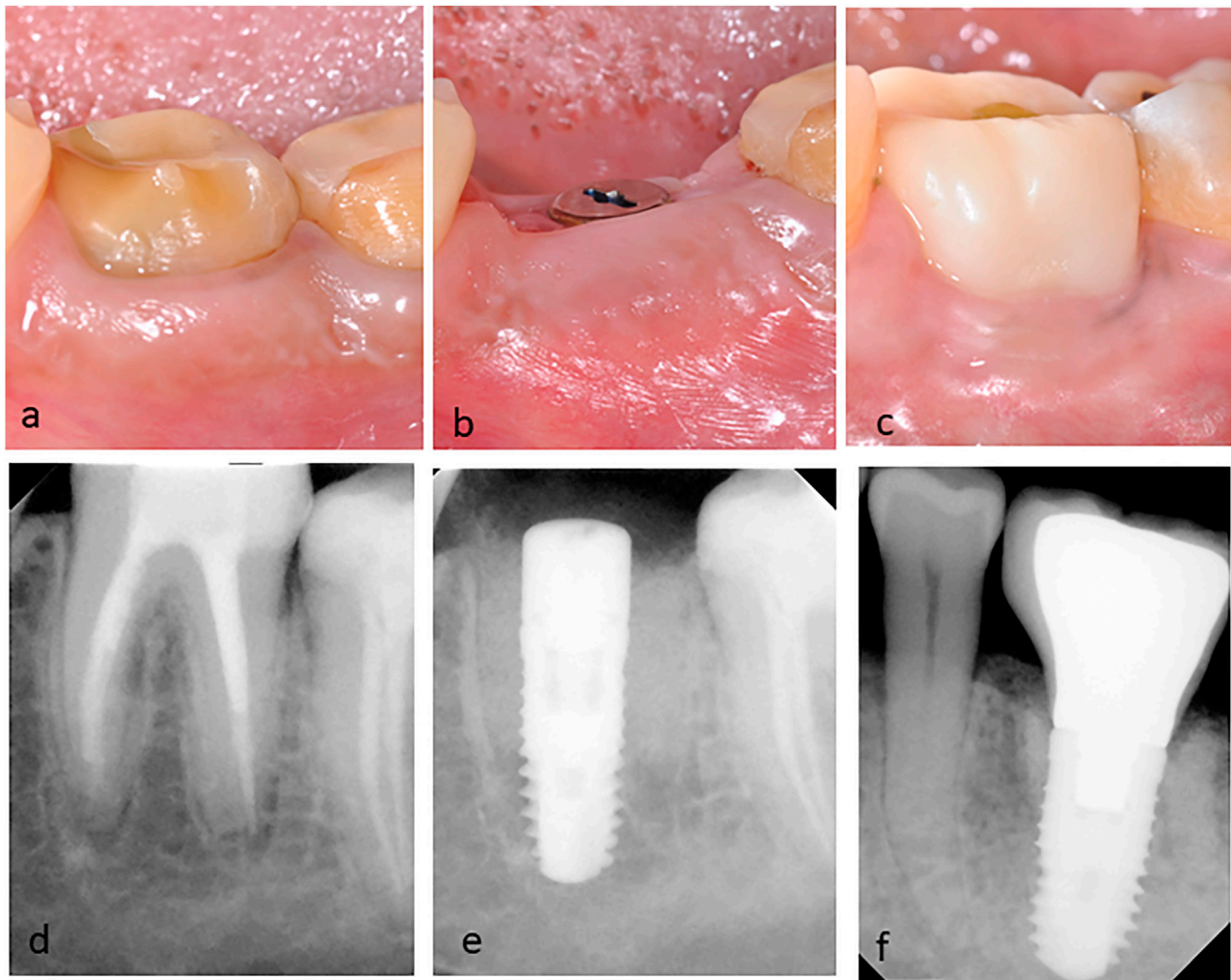


FIGURE 4 | Clinical and radiographic images of the mandibular left first molar with failed endodontic treatment. **(A)** Preoperative clinical lateral view; **(B)** postoperative clinical lateral views after 3 months of implant placement; **(C)** clinical picture of definitive porcelain fused to the metal screw-retained implant crown at three-year follow-up; **(D)** Preoperative periapical radiograph; **(E)** periapical radiographs of the implant after 3 months; and **(F)** radiographic image at three-year follow-up showing the marginal bone level.

extraction socket was covered with a resorbable collagen membrane (BioMend Membrane, Zimmer Biomet, Indiana, United States). The collagen membrane was stabilized, and each extraction socket was covered using horizontal mattress sutures using 3-0 Cytoplast™ non-absorbable PTFE sutures (Osteogenics, Lubbock, Texas, United States) (**Figure 1I**). Periapical radiographs were taken during the implant bed preparation and again immediately postoperative after completion of the surgical treatment (**Figure 3**).

The Postsurgical Phase

Healing was uneventful, and rinses were prescribed twice daily with 0.12% chlorhexidine digluconate (PerioAid®, Dentaaid, Barcelona, Spain) for 2 weeks along with ibuprofen 600 mg (Abbott Laboratories, United States) to manage any postoperative inflammation and discomfort or pain. Postsurgical instructions and oral hygiene measures were

explained to the patients. Sutures were removed 2 weeks after surgery.

Three months after implant placement, all patients were presented with healthy peri-implant tissues. A periapical radiograph was taken, and a second-stage surgery was performed by placing the healing abutment. The prosthetic treatment was initiated with provisional crown placement followed by placement of a screw-retained definitive restoration (**Figure 1F**). Annual radiographs were taken to evaluate the crestal bone level for each patient (**Figure 4**).

RESULTS

Healing was uneventful for all 10 patients with no complication during the follow-up period, thus giving a cumulative survival rate of 100% during the three-year follow-up period of this study.

The change in the marginal bone level was 0.11 ± 0.08 mm in all patients at the 3-year examination.

ImageJ software version 1.47 (Wayne Rasband, National Institutes of Health, United States) was used to measure the crestal bone loss on both the mesial and distal aspects of the implants. To set the scale for the measurements, the known implant width was used to calibrate the measurements. Then, a straight line was delineated from the implant platform to the alveolar crest on the mesial as well as the distal side. The average of both mesial and distal measurements was used to represent the bone level of each implant. (Figure 4F).

DISCUSSION

This study describes an alternative method of preparing osteotomy for immediate implant placement of multirooted molars. Drilling was performed prior to root separation, followed by root extraction and finally implant placement. Using this technique, surgeons are expected to receive better guidance during implant preparation. The osteotomy drills were stabilized and guided by the retained roots.

This form of osteotomy preparation can be less complicated and a useful modification of the standard surgical procedure to achieve more ideal implant positioning during immediate implant placement for a multirooted molar.

Immediate implant placement has become more popular among dentists providing implant dentistry treatment. However, still, primary implant stability and lack of micromovements are the two main factors necessary for achieving predictable high success of osseointegration (Albrektsson et al., 1981). Some advocate that the use of some specific implant surface treatment is able to reduce the healing time (Roccuzzo et al., 2001).

Optimal implant placement is more likely to be achieved using various technical approaches, such as radiographic templates or cone-beam computed tomography (CBCT) along with computer-assisted three-dimensional implant planning software programs.

In this study, sulcular incision was made around the mandibular molar to be extracted, and periosteal-releasing incisions were used for better flap adaptation following implant placement (Hamouda et al., 2015).

It is crucial to cover the surgical site and the peri-implant gap after immediate implant placement in order to achieve a successful grafting consolidation around the implant. Several recommendations have been published in the literature for the management of socket seals including the use of non-resorbable polytetrafluoroethylene (PTFE) membranes and resorbable collagen membranes for immediate implant placement (Hoffmann et al., 2008; Matarasso et al., 2009).

Hoffmann et al. (2008) used the non-resorbable polytetrafluoroethylene (PTFE) membranes to cover the socket with a significant regeneration of the volume of the socket, but the potential complications include exposure and dehiscence.

Urban et al. (2012) used the Ossix[®] cross-linked collagen membrane (Dentsply Sirona, York, Pennsylvania, United States), which is a resorbable collagen membrane, however, chemically

treated in order to prolong the period without resorption. The current implant survival rate was 100% with no failures observed during the three-year follow-up period, which was greater than the 95% survival rate reported by Hamouda et al. (2015).

In this study, drilling was initiated through the root trunk, after coronectomy and before root separation. Rebele et al. (2013) suggested using a sharp new drill to drill through the dentin and cementum at the furcation region. They also suggested that drilling through the dentin and retained root aspects appeared to be similar to drilling through tissues; however, it is slightly harder than dense cortical bone (Rebele et al., 2013).

In contrast, Hamouda et al. (2015), Scarano (2017), and Smith and Tarnow (2013) recommended drilling after root separation in order to make the drilling process easier as well as preventing dulling of the surgical drills.

In this study, immediate implant placement was achieved using a new pre-extraction implant bed preparation technique in ten patients. Prior to root separation, implants' osteotomies were prepared, then roots were separated, and implants were inserted. This allows for accurate implant placement in the drilled osteotomy, and also the remaining root segments would be partially luxated during the osteotomy drilling process.

The previous study (Valenzuela et al., 2018) mentioned that this alternative drilling method might result in a deficient implant insertion since it would modify the socket wall's morphology during the extraction procedure. Therefore, careful extraction using desmotomes or ultrasonic appliances should be conducted.

In order to avoid destroying the prepared implant bed and affecting the initial implant stability during the extraction operation, in this study, after osteotomy preparation, root separation was performed. Then, periostomes were used to sever the periodontal ligament surrounding the remaining roots. This eliminates the negative pressure present around the remaining roots as well as facilitates deeper insertion of the desmotomes and elevators to elevate the roots. Thus, atraumatic extraction operation was carried out to avoid altering the prepared implant bed.

This alternative drilling protocol will modify the socket wall's morphology during the extraction procedure, leading to a deficient implant insertion. Therefore, careful extraction using desmotomes or ultrasonic appliances is advised.

Similar to previous studies, Rebele et al. (2013), and Scarano (2017) recommended placing the implant after root extraction to minimize the complications encountered with extracting the remaining root segments.

In order to achieve initial implant stability, the implant should be placed in native apical and/or lateral bone to the extraction socket. Based on the anatomy of the tooth, the morphology of the extraction socket is determined. Accordingly, the tooth anatomy will have an influence on implant stability in the socket. Various parameters should be considered, including the width of the root at the cemento-enamel junction (CEJ), the length of the root, the degree of root divergence, and any anatomical limitations beyond the apices of the molar roots, such as the inferior alveolar nerve.

In this technique, the osteotomy was planned to engage the interradicular bone of the socket (type A and type B sockets) (Smith and Tarnow, 2013). Therefore, the presence of a sufficient

amount of septal bone that adequately supports circumferentially the implant facilitates achieving primary stability.

There is much debate in the literature as to the appropriate implant design to be used for immediate implantation in the mandibular molar region. Rebele et al. (2013) and Scarano (2017) used a cylindrical implant design, while Hamouda et al. (2015) and Rohra et al. (2017) preferred implants with a tapered design. In this study, the cylindrical body with a tapered end implant similar to that of Urban et al. (2012) was used. We observed a 100% implant success rate after 3 years as well as minimal marginal bone changes.

In the literature, there have been diverse approaches to combining immediate implant placement with regenerative procedures despite reports that regenerative treatments are not essential to achieve more successful healing or osseointegration for immediate implant (Botticelli et al., 2004; Lang et al., 2012).

Several grafting materials have been suggested in order to fill the mesial and distal bony sockets around immediate implants. Hayacibara et al. (2013), Tallarico et al. (2016), Scarano (2017) used bovine xenograft particles that showed marginal bone loss of approximately 1 mm compared to nongrafted implant sockets. According to Araújo et al. (2011,) the placement of deproteinized bovine bone mineral in a model of fresh extraction sockets enhanced hard tissue formation and improved marginal bone height.

Similar to the current study, a natural bovine porous bone mineral matrix was used with a 100% survival rate and no marginal bone loss after a three-year follow-up. The natural structure of this bone substitute is physically and chemically comparable to the mineralized matrix of human bone. The results of this study support the hypothesis that a low-resorption particulate graft should be used to the gap surrounding peri-implant in case of immediate implant placement to retain the surrounding bony walls and reduce the risk of marginal bone loss.

Immediate implant placement in the molar extraction site using the described technique would be indicated in extraction sites with sufficient root divergence in which primary stability can be achieved. Contraindications are tooth mobility, due to severed bone, presence of advanced furcation involvement, and unfavorable root position, such as fused roots and ankylosed roots (Tizcareño and Bravo-Flores, 2009; Rebele et al., 2013).

The strength of this technique is to provide guidance for the surgeon during immediate implant placement by using the tooth structure as a stent or guide. This technique may raise concerns regarding the possibility of a deleterious reaction caused by drill debris that has become lodged in the socket or within an

osteotomy. Accordingly, it is highly recommended that the site be thoroughly curetted prior to implant insertion. The limitation of this study is that it is a multiple case series of one technique, so a comparative study or clinical trial study would be recommended to further investigate the advantages of this technique. Also, more clinical parameters could be assessed in future studies.

CONCLUSION

The use of a modified pre-extractive interraderic implant bed preparation technique resulted in adequate primary implant stability and optimum implant location. After 3 years, implants placed using the pre-extraction interraderic implant bed preparation demonstrated a 100% success rate and less than 1 mm marginal bone loss (Hayacibara et al., 2013).

DATA AVAILABILITY STATEMENT

The raw data supporting the conclusions of this article will be made available by the authors upon request.

ETHICS STATEMENT

The studies involving human participants were reviewed and approved by the Institutional Review Board of IAU (IRB-2021-02-208). The patients/participants provided their written informed consent to participate in this study.

AUTHOR CONTRIBUTIONS

AA and MM: study concepts and study design. AA and MM: investigation, manuscript preparation, manuscript review, and manuscript editing. All authors approved the final manuscript for submission.

ACKNOWLEDGMENTS

Authors would like to acknowledge the assistance of W. Patrick Naylor, DDS, MPH, MS, for revising the manuscript and Rahaf Fahad Al Ghamdi for assisting in photography.

REFERENCES

- Albrektsson, T., Brånemark, P.-I., Hansson, H.-A., and Lindström, J. (1981). Osseointegrated Titanium Implants: Requirements for Ensuring a Long-Lasting, Direct Bone-To-Implant Anchorage in Man. *Acta Orthopaedica Scand.* 52 (2), 155–170. doi:10.3109/17453678108991776
- Araújo, M. G., Linder, E., and Lindhe, J. (2011). Bio-Oss Collagen in the Buccal gap at Immediate Implants: A 6-month Study in the Dog. *Clin. Oral Implants Res.* 22, 1–8. doi:10.1111/j.1600-0501.2010.01920.x
- Atieh, M. A., Payne, A. G., Duncan, W. J., de Silva, R. K., and Cullinan, M. P. (2010). Immediate Placement or Immediate Restoration/loading of Single Implants for Molar Tooth Replacement: A Systematic Review and Meta-Analysis. *Int. J. Oral Maxillofac. Implants* 25, 401–415.
- Barone, A., Toti, P., Quaranta, A., Derchi, G., and Covani, U. (2015). The Clinical Outcomes of Immediate versus Delayed Restoration Procedures on Immediate Implants: A Comparative Cohort Study for Single-Tooth Replacement. *Clin. Implant Dent Relat. Res.* 17, 1114–1126. doi:10.1111/cid.12225
- Becker, W., and Goldstein, M. (2008). Immediate Implant Placement: Treatment Planning and Surgical Steps for Successful Outcome. *Periodontol.* 2000 47, 79–89. doi:10.1111/j.1600-0757.2007.00242.x

- Bhola, M., Neely, A. L., and Kolhatkar, S. (2008). Immediate Implant Placement: Clinical Decisions, Advantages, and Disadvantages. *J. Prosthodont.* 17 (7), 576–581. doi:10.1111/j.1532-849x.2008.00359.x
- Botticelli, D., Berglundh, T., and Lindhe, J. (2004). Hard-tissue Alterations Following Immediate Implant Placement in Extraction Sites. *J. Clin. Periodontol.* 31, 820–828. doi:10.1111/j.1600-051x.2004.00565.x
- Cafiero, C., Annibaldi, S., Gherlone, E., Grassi, F. R., Gualini, F., Magliano, A., et al. (2008). Immediate Transmucosal Implant Placement in Molar Extraction Sites: A 12-month Prospective Multicenter Cohort Study. *Clin. Oral Implants Res.* 19 (5), 476–482. doi:10.1111/j.1600-0501.2008.01541.x
- Chen, S. T., and Buser, D. (2009). Clinical and Esthetic Outcomes of Implants Placed in Postextraction Sites. *Int. J. Oral Maxillofac. Implants* 24, 186–217.
- Chen, S. T., Wilson, T. G., and Hämmerle, C. H. (2004). Immediate or Early Placement of Implants Following Tooth Extraction: Review of Biologic Basis, Clinical Procedures, and Outcomes. *Int. J. Oral Maxillofac. Implants* 19, 12–25.
- Greenstein, G., and Tarnow, D. (2006). The Mental Foramen and Nerve: Clinical and Anatomical Factors Related to Dental Implant Placement: A Literature Review. *J. Periodontol.* 77 (12), 1933–1943. doi:10.1902/jop.2006.060197
- Hamouda, N. I., Mourad, S. I., El-Kenawy, M. H., and Maria, O. M. (2015). Immediate Implant Placement into Fresh Extraction Socket in the Mandibular Molar Sites: A Preliminary Study of a Modified Insertion Technique. *Clin. Implant Dentistry Relat. Res.* 17, e107–e116. doi:10.1111/cid.12135
- Hayacibara, R. M., Gonçalves, C. S., Garcez-Filho, J., Magro-Filho, O., Esper, H., and Hayacibara, M. F. (2013). The success Rate of Immediate Implant Placement of Mandibular Molars: A Clinical and Radiographic Retrospective Evaluation between 2 and 8 Years. *Clin. Oral Impl. Res.* 24 (7), 806–811. doi:10.1111/j.1600-0501.2012.02461.x
- Hoffmann, O., Bartee, B. K., Beaumont, C., Kasaj, A., Deli, G., and Zafiropoulos, G.-G. (2008). Alveolar Bone Preservation in Extraction Sockets Using Non-resorbable dPTFE Membranes: A Retrospective Non-randomized Study. *J. Periodontol.* 79 (8), 1355–1369. doi:10.1902/jop.2008.070502
- Lang, N. P., Pun, L., Lau, K. Y., Li, K. Y., and Wong, M. C. (2012). A Systematic Review on Survival and success Rates of Implants Placed Immediately into Fresh Extraction Sockets after at Least 1 Year. *Clin. Oral Implants Res.* 23 (5), 39–66. doi:10.1111/j.1600-0501.2011.02372.x
- Matarasso, S., Salvi, G. E., Siciliano, V. I., Cafiero, C., Blasi, A., and Lang, N. P. (2009). Dimensional ridge Alterations Following Immediate Implant Placement in Molar Extraction Sites: A Six-Month Prospective Cohort Study with Surgical Re-entry. *Clin. Oral Implants Res.* 20 (10), 1092–1098. doi:10.1111/j.1600-0501.2009.01803.x
- Quirynen, M., Van Assche, N., Botticelli, D., and Berglundh, T. (2007). How Does the Timing of Implant Placement to Extraction Affect Outcome? *Int. J. Oral Maxillofac. Implants* 22, 203–223.
- Rebele, S. F., Zuhr, O., and Hürzeler, M. B. (2013). Pre-extractive Interradicular Implant Bed Preparation: Case Presentations of a Novel Approach to Immediate Implant Placement at Multirooted Molar Sites. *Int. J. Periodontics Restorative Dent* 33 (1), 88–95. doi:10.11607/prd.1444
- Roccuzzo, M., Bunino, M., Prioglio, F., and Bianchi, S. D. (2001). Early Loading of Sandblasted and Acid-Etched (SLA) Implants: A Prospective Split-Mouth Comparative Study. *Clin. Oral Implants Res.* 12 (6), 572–578. doi:10.1034/j.1600-0501.2001.120604.x
- Rohra, D. E., Mistry, D. G., Joshi, D. T., and Khanvilkar, D. U. (2017). Implant Bed Preparation for Immediate Implantation in Molar Region: An Alternative Approach. *Iosr Jdms* 16 (05), 48–50. doi:10.9790/0853-1605064850
- Scarano, A. (2017). Traditional Postextractive Implant Site Preparation Compared with Pre-extractive Interradicular Implant Bed Preparation in the Mandibular Molar Region, Using an Ultrasonic Device: A Randomized Pilot Study. *Int. J. Oral Maxillofac. Implants* 32 (3), 655–660. doi:10.11607/jomi.5342
- Schropp, L., and Isidor, F. (2008). Timing of Implant Placement Relative to Tooth Extraction. *J. Oral Rehabil.* 35, 33–43. doi:10.1111/j.1365-2842.2007.01827.x
- Smith, R. B., and Tarnow, D. P. (2013). Classification of Molar Extraction Sites for Immediate Dental Implant Placement: Technical Note. *Int. J. Oral Maxillofac. Implants* 28 (3), 911–916. doi:10.11607/jomi.2627
- Tallarico, M., Khanari, E., Pisano, M., De Riu, G., Tullio, A., and Meloni, S. M. (2016). Single post-extractive Ultra-wide 7 mm-Diameter Implants versus Implants Placed in Molar Healed Sites after Socket Preservation for Molar Replacement: 6-month post-loading Results from A randomised Controlled Trial. *Eur. J. Oral Implantol.* 9 (3), 263–275.
- Tizcareño, M. H., and Bravo-Flores, C. (2009). Anatomically Guided Implant Site Preparation Technique at Molar Sites. *Implant Dentistry* 18 (5), 393–401. doi:10.1097/ID.0b013e3181b4b205
- Urban, T., Kostopoulos, L., and Wenzel, A. (2012). Immediate Implant Placement in Molar Regions: A 12-month Prospective, Randomized Follow-Up Study. *Clin. Oral Impl. Res.* 23 (12), 1389–1397. doi:10.1111/j.1600-0501.2011.02319.x
- Valenzuela, S., Olivares, J. M., Weiss, N., and Benadof, D. (2018). Immediate Implant Placement by Interradicular Bone Drilling before Molar Extraction: Clinical Case Report with One-Year Follow-Up. *Case Rep. Dentistry* 2018, 1–5. doi:10.1155/2018/6412826

Conflict of Interest: The authors declare that the research was conducted in the absence of any commercial or financial relationships that could be construed as a potential conflict of interest.

Publisher's Note: All claims expressed in this article are solely those of the authors and do not necessarily represent those of their affiliated organizations, or those of the publisher, the editors, and the reviewers. Any product that may be evaluated in this article, or claim that may be made by its manufacturer, is not guaranteed or endorsed by the publisher.

Copyright © 2022 Alagl and Madi. This is an open-access article distributed under the terms of the Creative Commons Attribution License (CC BY). The use, distribution or reproduction in other forums is permitted, provided the original author(s) and the copyright owner(s) are credited and that the original publication in this journal is cited, in accordance with accepted academic practice. No use, distribution or reproduction is permitted which does not comply with these terms.



Application of Amorphous Calcium Phosphate Agents in the Prevention and Treatment of Enamel Demineralization

Jiarong Yan^{1,2}, Hongye Yang^{1,3}, Ting Luo^{1,2}, Fang Hua^{1,2,4,5*} and Hong He^{1,2*}

¹The State Key Laboratory Breeding Base of Basic Science of Stomatology (Hubei-MOST) and Key Laboratory of Oral Biomedicine Ministry of Education, School and Hospital of Stomatology, Wuhan University, Wuhan, China, ²Department of Orthodontics, School and Hospital of Stomatology, Wuhan University, Wuhan, China, ³Department of Prosthodontics, School and Hospital of Stomatology, Wuhan University, Wuhan, China, ⁴Center for Evidence-Based Stomatology, School and Hospital of Stomatology, Wuhan University, Wuhan, China, ⁵Division of Dentistry, School of Medical Sciences, Faculty of Biology, Medicine and Health, University of Manchester, Manchester, United Kingdom

OPEN ACCESS

Edited by:

Kumar Chandan Srivastava,
Al Jouf University, Saudi Arabia

Reviewed by:

Shanshan Liu,
The first affiliated hospital of Bengbu
medical college, China

*Correspondence:

Fang Hua
hufang@whu.edu.cn
Hong He
drhehong@whu.edu.cn

Specialty section:

This article was submitted to
Biomaterials,
a section of the journal
Frontiers in Bioengineering and
Biotechnology

Received: 12 January 2022

Accepted: 15 April 2022

Published: 13 May 2022

Citation:

Yan J, Yang H, Luo T, Hua F and He H
(2022) Application of Amorphous
Calcium Phosphate Agents in the
Prevention and Treatment of
Enamel Demineralization.
Front. Bioeng. Biotechnol. 10:853436.
doi: 10.3389/fbioe.2022.853436

Enamel demineralization, as a type of frequently-occurring dental problem that affects both the health and aesthetics of patients, is a concern for both dental professionals and patients. The main chemical composition of the enamel, hydroxyapatite, is easy to be dissolved under acid attack, resulting in the occurrence of enamel demineralization. Among agents for the preventing or treatment of enamel demineralization, amorphous calcium phosphate (ACP) has gradually become a focus of research. Based on the nonclassical crystallization theory, ACP can induce the formation of enamel-like hydroxyapatite and thereby achieve enamel remineralization. However, ACP has poor stability and tends to turn into hydroxyapatite in an aqueous solution resulting in the loss of remineralization ability. Therefore, ACP needs to be stabilized in an amorphous state before application. Herein, ACP stabilizers, including amelogenin and its analogs, casein phosphopeptides, polymers like chitosan derivatives, carboxymethylated PAMAM and polyelectrolytes, together with their mechanisms for stabilizing ACP are briefly reviewed. Scientific evidence supporting the remineralization ability of these ACP agents are introduced. Limitations of existing research and further prospects of ACP agents for clinical translation are also discussed.

Keywords: enamel, demineralization, remineralization, amorphous calcium phosphate, hydroxyapatite

INTRODUCTION

Enamel demineralization is one of the most common dental problems which could appear as white spot lesions (WSLs) in the early stage and even progress into cavities if effective interventions are not taken in time (Julien et al., 2013). In the normal oral environment, hydroxyapatite on the enamel surface contacts saliva and maintains the balance of dissolution and redeposition (Sollböhrer et al., 1995; Featherstone, 2004), hydroxyapatite could be dissolved into calcium and phosphorus ions while calcium and phosphorus ions in saliva could crystallize directionally and orderly, forming the enamel-like hydroxyapatite structure on the surface of the enamel (Dorozhkin, 1997). When the oral hygiene condition is poor, plaque biofilms form and adhere onto the enamel surface decomposing sugars, producing organic acids,

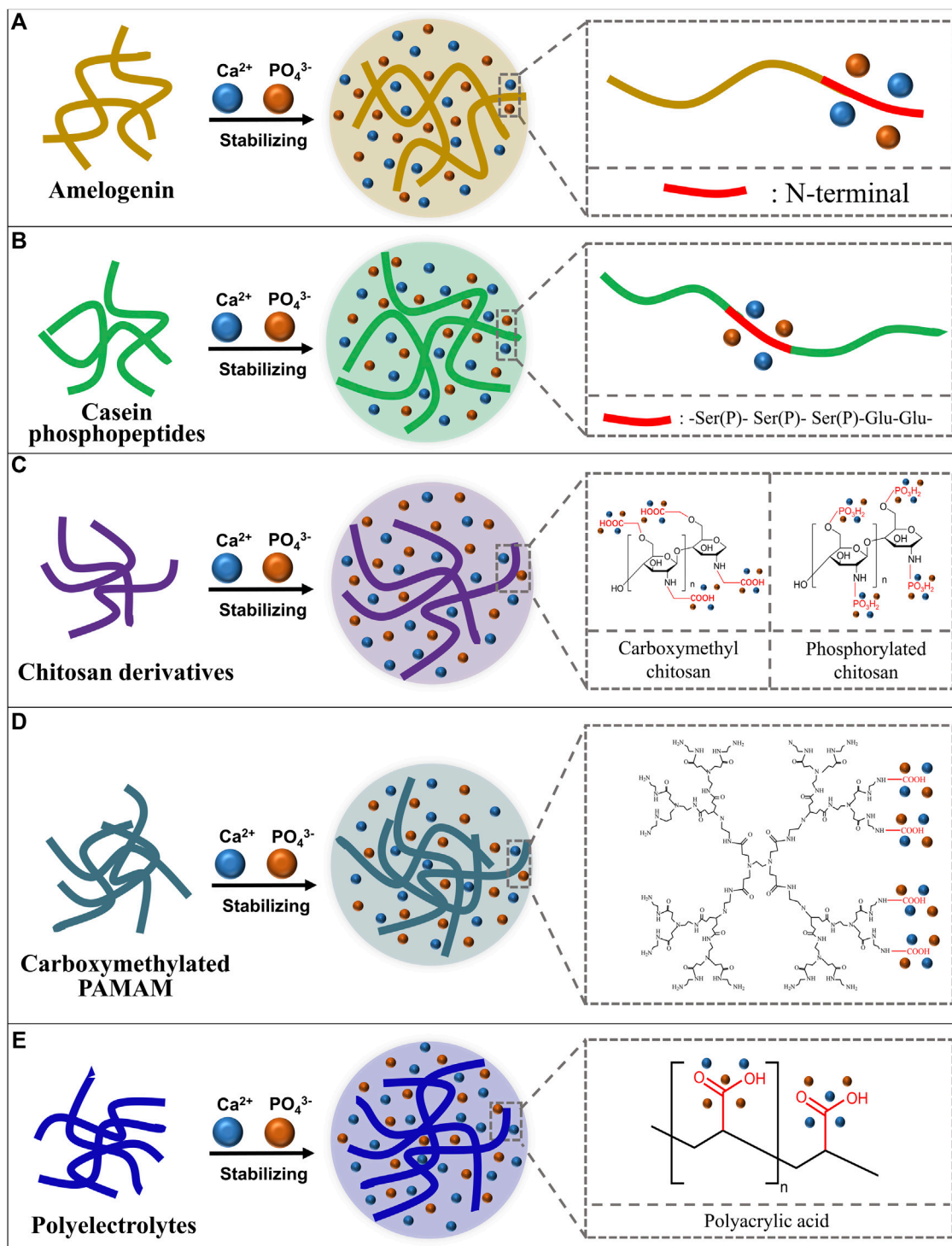


FIGURE 1 | Schematic diagram of ACP stabilizers and how they stabilize the ACP. **(A)** Amelogenin stabilizes calcium and phosphorus ions with its N-terminal; **(B)** Casein phosphopeptides stabilize calcium and phosphorus ions with the -Ser(P)- Ser(P)- Ser(P)-Glu-Glu- sequence; **(C)** Chitosan derivatives stabilize calcium and phosphorus ions with functional groups; **(D)** Carboxymethylated poly-amidoamine (PAMAM) stabilizes calcium and phosphorus ions with carboxyl groups; **(E)** Polyelectrolytes stabilize calcium and phosphorus ions with functional groups.

and resulting in an acidic pH environment around the enamel. Under this circumstance, the dissolution-redeposition balance of hydroxyapatite is broken. The dissolution of hydroxyapatite

occurs faster than the deposition of calcium and phosphorus ions, which eventually leads to the occurrence of enamel demineralization.

Based on the etiology of enamel demineralization, the strategies to prevent or treat enamel demineralization include: 1) Using antibacterial agents such as mouthwash or toothpaste containing antibacterial drugs (Hefti and Huber, 1987; Afennich et al., 2011; Hossainian et al., 2011; Rösing et al., 2017; Ahmed et al., 2019; Bijle et al., 2019; Guven et al., 2019; Karadağhoğlu et al., 2019; Shang et al., 2020) which could inhibit the accumulation and adhesion of cariogenic bacteria on the enamel surface to reduce the acid production from plaque biofilms; 2) Using fluorinated agents such as fluoride mouthwash (Chow et al., 2000; Songsiripraduboon et al., 2014; Larsson et al., 2020) and fluoride varnish (Gontijo et al., 2007; Marinho, 2009; Perrini et al., 2016), which could not only inhibit cariogenic bacteria but release fluorine, co-crystallize with calcium and phosphorus ions to form fluorapatite on the enamel surface (Margolis and Murphy, 1986; Zandim-Barcelos et al., 2011).

In addition to the above strategies, the enamel biomimetic remineralization strategy, which bases on the natural enamel crystallization process (Cölfen and Mann, 2003), is being studied extensively due to its biomimetic mineralization capability (Chen et al., 2015; Wang et al., 2017). According to the nonclassical crystallization theory, the crystallization processes of natural enamel could be interpreted as the following steps: 1) Calcium and phosphorus ions aggregating together to form amorphous calcium phosphate (ACP); 2) Amelogenin stabilizing ACP into clusters; 3) ACP then directionally arranging to form bundles of hydroxyapatite, then gradually forming enamel crystal, and finally forming enamel prism (Beniash et al., 2009; Yang et al., 2010; Kwak et al., 2016). To mimic the crystallization process of natural enamel and to achieve remineralization of demineralized enamel, ACP needs to be stabilized and then crystallizes directionally and orderly to form the enamel-like hydroxyapatite. In this review, we mainly focused on how different agents stabilize ACP and their remineralization effects on enamel demineralization.

AMELOGENIN AND ITS ANALOGS

Amelogenin (Amel) plays an important role in the formation of natural enamel (Wright et al., 2011; Moradian-Oldak, 2012; Ruan and Moradian-Oldak, 2015). Amelogenin could interact with calcium and phosphorus ions through the tyrosine enrichment segment on its N-terminal and stabilize calcium and phosphorus ions to an amorphous state (Figure 1A). The C-terminal of Amel could guide ACP to crystallize into hydroxyapatite directionally (Tsiourvas et al., 2015). There are studies using chitosan to load amelogenin and form the chitosan-amelogenin gel (CS-Amel gel) and using this gel system for reconstruction of demineralized enamel. The CS-Amel gel could stabilize calcium and phosphorus ions into ACP, guide ACP to form the enamel-like crystals which bind closely with natural enamel crystals (Ruan et al., 2013; Ruan et al., 2014). In addition to the direct application of amelogenin, there are studies focused on the

remineralization effect of amelogenin analogs. Zhong et al., 2021 self-assembled the N-terminal tyrosine segment of amelogenin to form leucine-rich amelogenin peptide (LRAP) and evaluated the stabilizing and directional guiding abilities of LRAP to calcium and phosphorus ions in mineralizing solutions. LRAP could stabilize calcium and phosphorus ions into ACP effectively and guide ACP to grow along its C-axis into bundles of hydroxyapatite crystals. Wang combined a phase conversion lyase (PTL) which mimics the function of the N-terminal of amelogenin with a synthetic peptide chain which has the function of the C-terminal of amelogenin to form amyloid amelogenin analog (PTL/C-AMG) (Wang Y et al., 2020). The PTL/C-AMG could combine calcium and phosphorus ions to form hydroxyapatite and promote the extension growth of hydroxyapatite crystals on the surface of natural enamel and eventually forms a highly ordered hydroxyapatite structure with mechanical properties similar to that of natural enamel. Lv and colleagues synthesized a short-chain polypeptide (QP5) based on the amino sequence of amelogenin and proved the stabilizing ability of QP5 to calcium and phosphorus ions. They verified the remineralization ability of QP5 to initial enamel demineralization in an *in vitro* enamel demineralization model and further confirmed its remineralization ability and potential for clinical transformation in a rat caries model (Lv et al., 2015; Han et al., 2017).

CASEIN PHOSPHOPEPTIDES

Casein phosphopeptides (CPP) are casein extracts from milk which could markedly increase the apparent solubility of calcium phosphate ions by forming ACP (Reeves and Latour, 1958). Researchers found that the main active sequence of CPP, the phosphoserine - glutamate cluster (-Ser(P)- Ser(P)- Ser(P)-Glu-Glu-), could stabilize calcium and phosphate ions and form the CPP stabilized ACP complex (CPP-ACP) (Adamson and Reynolds, 1996) to avoid the spontaneously crystallizing, phase conversing and precipitating of calcium and phosphorus ion (Shen et al., 2001) (Figure 1B). Reynolds soaked artificially demineralized enamel in CPP-ACP solution and found that CPP-ACP could remineralize the subsurface demineralization of enamel effectively. The mechanism may be that CPP can maintain a high concentration of calcium and phosphorus ions in the solution to infiltrate into the subsurface lesion area to achieve efficient enamel remineralization (Reynolds, 1997). The team further validated the preventive effect of CPP-ACP on enamel demineralization in a rat caries model (Reynolds et al., 1995). With the U.S. Food and Drug Administration and other regulatory agencies confirming the biosafety of CPP-ACP (Cochrane et al., 2010), CPP-ACP is added into oral health care products such as Tooth Mousse (GC, Tokyo, Japan) (Rees et al., 2007) and Tooth Mousse Plus (CPP-ACPF, GC, Tokyo, Japan) (Hamba et al., 2011; Bataineh et al., 2017; Olgen et al., 2021). These agents have been gradually used in clinical practice and have been studied in a number of clinical trials

(Sitthisettapong et al., 2015; Güçlü et al., 2016; Munjal et al., 2016; Thierens et al., 2019). However, the remineralization ability of CPP-ACP and CPP-ACPF for WSLs remains unknown. Researchers suggested that CPP-ACP and CPP-ACPF may have the ability to prevent and treat WSLs, but their effects are not significantly greater than using fluoride agent alone (Pithon et al., 2019; Wang D et al., 2020). In addition, casein related allergy in certain populations also limits the clinical use of CPP-ACP and CPP-ACPF.

POLYMERS

In addition to the aforementioned amelogenin and its analogs and CPP, some kinds of polymers can also stabilize calcium and phosphate ions, including chitosan derivatives, poly-amidoamine and polyelectrolytes.

Chitosan Derivatives

Chitosan derivatives, such as carboxymethyl chitosan (CMC) and phosphorylated chitosan (Pchi) could bind calcium ions through chelation reaction of carboxyl groups and calcium ions and then bind phosphate ions to form ACP (**Figure 1C**). The recrystallization of demineralization enamel is realized by the ordered crystallization of ACP to form enamel-like hydroxyapatite crystals (Zhang et al., 2014; Zhang et al., 2018). Zhu combined carboxymethyl chitosan (CMC) and lysozyme (LYZ) to stabilize ACP and formed the CMC/LYZ-ACP nano-gel, which can regenerate prism-like remineralized enamel layer on the surface of eroded enamel to realize the remineralization (Zhu et al., 2021). Song successively added CaCl_2 and K_2HPO_4 into Pchi solution to construct the Pchi-ACP nano-complex. X-ray diffraction and selective electron diffraction results confirmed the amorphous state of the nano-complex. And the results of scanning electron microscopy and micro-CT proved that the Pchi-ACP nano-complex could realize the remineralization of demineralized enamel (Song et al., 2021).

Poly-Amidoamine

Poly-amidoamine (PAMAM) was first synthesized by Tomalia in the 1980s (Tomalia et al., 1985). PAMAM contains a large number of amide groups that have the similar function to peptide bonds so that PAMAM could simulate functions of a variety of proteins and peptides (Svenson and Tomalia, 2012). PAMAM can have mineralization property through the modification of carboxyl groups. The carboxyl-modified PAMAM (PAMAM-COOH) could combine calcium ions through carboxyl groups and further attract phosphate ions to stabilize calcium and phosphate ions into ACP (Khopade et al., 2002; Zhou et al., 2007; Zhou et al., 2013) (**Figure 1D**). ACP could form enamel-like hydroxyapatite orderly on the surface of demineralized enamel through the crystallization guidance of PAMAM-COOH (Chen et al., 2013). Another study found that PAMAM-COOH can induce calcium and phosphorus ions to grow and

crystallize along the z-axis on the surface of demineralized enamel, and the microhardness of the remineralized enamel is comparable to that of the natural enamel (Chen M et al., 2014).

Polyelectrolytes

Polyelectrolytes are a class of polymorphs with ionizable units, which could ionize into charged polymorphs and counter-ions with opposite charge in aqueous solution (Koetz and Kosmella, 2007) such as polyacrylic acid (PAA), polyallylamine (PAH), polyaspartic acid (PASP), et al. PAA has rich carboxyl groups to combine with calcium ions to form the $-\text{COO}^-/\text{Ca}^{2+}$ structure (Huang et al., 2008), so that PAA can stabilize ACP (Gower, 2008; Dey et al., 2010) (**Figure 1E**). Qi added calcium and phosphorus ions into the PAA solution to construct the PAA-ACP complex and verified the stability of the PAA-ACP complex by solution turbidity analysis and dynamic light scattering. Scanning electron microscopy, transmission electron microscopy, infrared spectroscopy and X-ray diffraction analyses proved the remineralization ability of PAA-ACP (Qi et al., 2018). Our group used PAA to stabilize amorphous calcium phosphate, and then loaded PAA-ACP with aminoated mesoporous silicon nanoparticle (aMSN) to form the PAA-ACP@aMSN delivery system. The PAA-ACP@aMSN was proved to have the ability to promote enamel remineralization and surface microhardness analysis and X-ray diffraction analysis showed that the remineralization layer induced by PAA-ACP@aMSN had comparable mechanical property and crystal texture to natural enamel (Hua et al., 2020). PAA-ACP could also act as a dental adhesive filler to endow adhesives with enamel remineralization ability (Wang et al., 2018). Other polyelectrolytes like polyallylamine (Niu et al., 2017; Yang et al., 2017), polyaspartic acid (Zhou, et al., 2021), polyglutamic acid (Sikirić, et al., 2009; Terauchi, et al., 2019) could also stabilize calcium and phosphorus ions but the treatment or prevention effect of these polyelectrolyte-stabilized ACPs for enamel demineralization remains to be further investigated.

ACP PARTICLES

As a kind of amorphous substance, ACP is easy to spontaneously transform into apatite crystal in an aqueous solution from the thermodynamics point of view (Eanes et al., 1965; Chow et al., 1998). Therefore, in addition to the application of stabilizers to stabilize ACP in an amorphous state, another way to stabilize ACP is to store the prepared ACP in an anhydrous dry granular state to form ACP particles. Since the 1990s, ACP particle has been gradually used as a bioactive additive in the studies of tooth remineralization (Skrtec and Eanes, 1996). ACP particle could act as a bioactive filler of dental filling resin to endow the filling resin with the ability of continuous releasing of calcium and phosphorus ions to promote the formation of hydroxyapatite (Skrtec et al., 2004). However, the uncontrollable agglomeration of ACP particles in the resin affects the mechanical properties of resin such as

TABLE 1 | Comparison of the remineralization performance of ACP agents with other products.

Authors	Study type	Agents	Interventions	Evaluation methods	Results	Conclusions
Aras et al. (2020)	<i>In vitro</i>	Fluoride gel, CPP-ACP, CPP-ACPF, NovaMin-Fluoride, Xylitol-HAP-Fluoride, Ozone-Fluoride	Following manufacturer's instructions for 30 days	DIAGNOdent	There were significant differences in the scores before and after the remineralization procedure in all experimental groups. CPP-ACPF provided significantly more remineralization than other experimental groups.	Remineralization of demineralized areas was achieved in all experimental groups. The highest degree of remineralization according to the DIAGNOdent scores before and after the procedure was observed in the CPP-ACPF group.
Farzanegan et al. (2018)	<i>In vitro</i>	0.05% NaF and 0.05% ACP solution	1 min/day for 10 weeks	Microhardness tester	Microhardness of samples in NaF and ACP groups both had significantly improved after the treatment. No significant differences were found neither between the fluoride and ACP, nor the fluoride and control groups.	Both 0.05% NaF solution and 0.05% ACP solution enhanced the enamel microhardness and are suitable for treatment of white spot lesions.
Farzanegan et al. (2019)	<i>In vitro</i>	0.05% ACP, 0.5% ACP and 0.05% fluoride solutions	1 min/day for 10 weeks	Colorimeter	There was no significant difference among 0.05% ACP, 0.5% ACP and 0.05% fluoride solutions. And a significant difference was noted between these solutions and distilled water.	ACP is as effective as fluoride in the color improvement of WSLs.
(Oliveira et al. (2014)	<i>In vitro</i>	CPP-ACP, CPP-ACPF, 1.1% NaF dentifrice	Following manufacturer's instructions for 30 days	QLF	1.1% NaF dentifrice showed greater remineralization than CPP-ACP and CPP-ACPF.	The 1.1% NaF dentifrice demonstrated overall greater remineralization ability.
Behrouzi et al. (2020)	<i>In vitro</i>	CPP-ACPF, Remin Pro	Following manufacturer's instructions for 20 weeks	Microhardness tester	The hardness of samples in CPP-ACPF and Remin Pro groups significantly increased, but there was no statistical difference between CPP-ACPF and Remin Pro groups.	CPP-ACPF and Remin Pro can efficiently increase the hardness of incipient enamel lesions.
Yadav et al. (2019)	<i>In vitro</i>	Bio-minF, CPP-ACPF	Twice a day, 4 min per time for 6 weeks	Spectrophotometer, DIAGNOdent	Bio-minF, and CPP-ACPF showed significant recovery of color change and fluorescence loss. Bio-minF had higher fluorescence recovery value than CPP-ACPF and showed similar color change value to CPP-ACPF.	Both Bio-minF and CPP-ACPF could remineralize artificial enamel caries and showed improvement in color change and fluorescence loss.
Kamath et al. (2017)	<i>In vitro</i>	Nano-HA, CPP-ACPF, TCP	3 min/day for 14 days	DIAGNOdent, SEM, EDX	SEM evaluation showed favorable surface change in all groups. DIAGNOdent and EDX readings were statistically nonsignificant among groups.	All agents showed comparable remineralization potential.
Tahmasbi et al. (2019)	<i>In vitro</i>	0.05% NaF, CPP-ACPF, Remin Pro paste	Once a day, 5 min per time for 14 days	Microhardness tester	0.05% NaF was more efficient than Remin Pro and CPP-ACPF. Remin Pro and CPP-ACPF were not significantly different from the control group.	NaF mouthwash had the greatest efficacy for prevention of enamel demineralization compared with Remin Pro and CPP-ACPF.

(Continued on following page)

TABLE 1 | (Continued) Comparison of the remineralization performance of ACP agents with other products.

Authors	Study type	Agents	Interventions	Evaluation methods	Results	Conclusions
Jo et al. (2014)	<i>In vitro</i>	1000ppm F, CPP-ACP, and fTCP containing toothpaste	Twice a day for 2 weeks	QLF-D Biluminator	Fluorescence greatly increased in the fTCP and CPP-ACP groups compared with the fluoride and control groups.	fTCP and CPP-ACP seem to be more effective in reducing WSLs than 1000 ppm F containing toothpastes.
Bhadoria et al. (2020)	<i>In vitro</i>	CPP-ACPF, fTCP	Twice a day, 2 min per time for 10 days	Microhardness tester	fTCP shows significantly higher increase in mean microhardness when compared to CPP-ACPF and control group.	f-TCP showed comparatively more remineralization potential than CPP-ACPF.
Brochner et al. (2011)	RCT	CPP-ACP and fluoride containing toothpaste	Once a day for 4 weeks	QLF	A statistically significant regression of the WSL was disclosed in both study groups compared to baseline, but there was no difference between the groups.	The application of CPP-ACP could result in a reduced area of the lesions after 4 weeks but the improvement was however not superior to “natural” regression with daily use of fluoride toothpaste.
Huang et al. (2013)	RCT	CPP-ACPF and PreviDent fluoride varnish	CPP-ACPF group: twice a day for 8 weeks; Varnish group: a single application at the start of the study.	Visual assessment	The mean improvements assessed by the professional panel were 21%, 29%, and 27% in the CPP-ACPF, fluoride varnish, and control groups, respectively.	CPP-ACPF and PreviDent fluoride varnish do not appear to be more effective than normal home care for improving the appearance of white spot lesions over an 8-week period.
Akin and Basciftci, (2020)	Clinical controlled trial	0.025% NaF rinse and CPP-ACP	Following manufacturer's instructions after brushing teeth with F containing toothpaste for 6 months	Image processing with AutoCAD for quantitative analysis	The area of the white spot lesions decreased significantly in all groups. The success rate of CPP-ACP was significantly higher than that of NaF.	The use of CPP-ACP can be more beneficial than fluoride rinse for postorthodontic Remineralization.
Singh et al. (2016)	RCT	Fluoride toothpaste, fluoride varnish with fluoride toothpaste, CPP-ACP with fluoride toothpaste,	Subjects were advised to brush twice daily with fluoride toothpaste for 1, 3, 6 months. varnish application: a single application at the start of the study. CPP-ACP application: twice daily after brushing teeth	DIAGNOdent, Visual assessment	The mean visual and DIAGNOdent scores at various time intervals of observations were decreased more when fluoride varnish and CPP-ACP were used in addition to daily use of fluoride toothpaste, but the differences were not statistically significant.	The use of fluoride varnish and CPP-ACP in addition to twice daily use of fluoride toothpaste had no additional benefit in the remineralization of post-orthodontic WSLs.

CPP-ACP, casein phosphopeptide- amorphous calcium phosphate; CPP-ACPF, casein phosphopeptide- amorphous calcium phosphate with fluoride; HAP, hydroxyapatite; QLF, quantitative light-induced fluorescence; TCP, tricalcium phosphate; SEM, scanning electron microscope; EDX, energy dispersive X-ray; fTCP, fluoride tricalcium phosphate; RCT, randomized controlled trial.

bonding strength and bending strength, so that ACP particles are only suitable for materials with low requirements on mechanical properties, such as pit and fissure sealant (Skrtic et al., 2004; Dunn, 2007). In 2011, Xu synthesized nano ACP (NACP) by spray drying method for the first time and mixed it into dental resin as filler. The NACP modified dental resin could release calcium and phosphorus ions in an acidic environment, and the mechanical properties of the resin are even better than commercial dental resin materials (Xu et al., 2011). Since then, a large number of studies added NACP to dental materials such as orthodontic bonding resins, sealants, resin-modified glass ions and other materials, and verified their calcium and

phosphorus ion release ability and enamel remineralization ability (Chen C et al., 2014; Ma et al., 2017; Liu et al., 2018; Xie et al., 2019; Gao et al., 2020; Ibrahim et al., 2020).

ACP AGENTS VERSUS OTHER REMINERALIZATION AGENTS

In addition to ACP agents, there are many other enamel remineralization agents such as fluorine containing agents, hydroxyapatite preparations and tricalcium phosphate. *In vitro* and

in vivo studies have been conducted to compare the remineralization performance of ACP agents and other agents (Table 1). However, the conclusion varied among these studies. Some studies found that ACP agents have better remineralization effect than other agents, while others suggested that the remineralization effect of ACP agents is similar to or no better than other agents. Whether the ACP agents have better remineralization properties than other agents needs to be further investigated in the future research.

DISCUSSION

ACP agents have outstanding preventive and therapeutic capacity to enamel demineralization due to their ability to form the enamel-like hydroxyapatite on the surface of demineralized enamel (Kwak et al., 2016). However, Since ACP is easy to agglomerate and is unstable in an aqueous solution (Chow et al., 1998), the main challenge in applying the ACP for enamel remineralization is its stabilization. Many different materials that could stabilize calcium and phosphorus ions, including amelogenin and its analogs (Tsiourvas et al., 2015; Wang Y et al., 2020), casein phosphopeptides (Cross et al., 2005), polymers like chitosan derivatives (Zhu et al., 2021), carboxymethylated PAMAM (Chen et al., 2013) and polyelectrolytes (Hua et al., 2020), have been used in studies to stabilize calcium and phosphorus ions into ACP. Another strategy is to store the ACP in a water-free state so that ACP particles and NACP particles are formed (Betts et al., 1975; Xu et al., 2011). The remineralization abilities of these ACP agents have been confirmed in previous studies. However, except for CPP-ACP and CPP-ACPF which has been commercialized (Reise et al., 2021), most of the other ACP agents are still at *in vitro* experimental stage. It is still uncertain whether these ACP agents can achieve the remineralization of demineralized enamel *in vivo*. In addition, most of the studies evaluated the remineralization ability of ACP agents by measuring the hardness recovery of demineralized enamel (Gokkaya et al., 2020), observing the mineral deposition on demineralized enamel (Hua et al., 2020), or measuring the lesion depth (Soares-Yoshikawa et al., 2021). None of the above-mentioned evaluation methods can directly confirm whether ACP agents could form the enamel-like hydroxyapatite. The biomimetic remineralization ability of ACP agents needs further investigation. To further promote the translation of ACP agents into clinical application, basic studies with adequate evaluation methods as well as relevant *in vivo* studies are still needed. In addition, whether ACP agents have better remineralization effects compared to other agents remains to be further explored.

ACP complexes are in the amorphous state of the liquid phase (Chen et al., 2013; Niu et al., 2017; Qi et al., 2018; Song et al., 2021), and ACP particles (Skrtic et al., 2004; Xu et al., 2011) are solid powders. Neither the liquid nor the solid form is convenient for storage and direct application in the oral environment. Studies has been conducted to address the storage and application challenges of ACP agents:

- 1) Mouthwash. Studies used carriers like chitosan (Ruan et al., 2013) and carboxymethyl chitosan (Zhu et al., 2021) to load ACP agents and these delivery systems can be applied in the oral environment in the form of mouthwash.

- 2) Toothpaste and tooth desensitizer. Another form of application of the ACP agents is to make them into pastes. Our group used mesoporous silicon nanoparticles to load ACP agents to achieve the enrichment and storage of ACP and this delivery system can be applied as the filler of toothpaste (Hua et al., 2020). CPP-ACP agents can be used as desensitizers in the form of pastes (Pei et al., 2013; Chandavarkar and Ram, 2015; Yang et al., 2018).
- 3) Resin product. Particulate forms of ACP have been incorporated into resin products, like adhesives (Wang et al., 2018), pit and fissure sealants (Utneja et al., 2018), varnishes (Schemehorn et al., 2011) to achieve convenient applications that do not depend on patient compliance.

Mouthwash form of the ACP agent is convenient to use, but the relatively low concentration of ACP and its inability to persist on the enamel surface for long periods lead to the limited effectiveness of ACP agents to enamel remineralization. The paste-like application form could effectively enhance the concentration of ACP and could maintain a high concentration of ACP on the enamel surface during application, but like mouthwash, it still has a short duration of hydroxyapatite formation due to the effect of saliva flushing. ACP agents modified resin products can release ACP on the enamel surface for a long period thus achieving the long-term prevention or treatment of enamel demineralization. However, the effect of ACP agent incorporation on the performance of these products like mechanical performance and biocompatibility needs further exploration. And the long-term stability of the ACP release from these products should be considered in future studies.

CONCLUSION

Herein we summarize the strategies of stabilizing ACP. Calcium and phosphorus ions can be stabilized to the ACP state using a variety of methods, but the preventive and therapeutic effects of these ACP agents on enamel demineralization still await further investigation. There are three main forms of storage and application of ACP agents, namely mouthwash, toothpaste/tooth desensitizer, resin product. However, due to the shortcomings of the above-mentioned forms of ACP agents, more easy-to-use and long-lasting forms of ACP agents remain to be further explored.

AUTHOR CONTRIBUTIONS

JY drafted the manuscript. HY and TL revised the manuscript. FH and HH designed the work and revised the manuscript. All authors approved the final version to be published.

FUNDING

This work was financially supported by the National Natural Science Foundation of China (No. 81901044), Chinese Stomatological Association COS Basic Research Fund (No. COS-B2021-08), and Wuhan Young and Middle-aged Medical Talents Training Program (No. (2019)87).

REFERENCES

- Adamson, N. J., and Reynolds, E. C. (1996). Characterization of Casein Phosphopeptides Prepared Using Alcalase: Determination of Enzyme Specificity. *Enzyme Microb. Technol.* 19, 202–207. doi:10.1016/0141-0229(95)00232-4
- Afennich, F., Slot, D., Hossainian, N., and Van der Weijden, G. (2011). The Effect of Hexetidine Mouthwash on the Prevention of Plaque and Gingival Inflammation: a Systematic Review. *Int. J. Dent. Hyg.* 9, 182–190. doi:10.1111/j.1601-5037.2010.00478.x
- Ahmed, F., Prashanth, S., Sindhu, K., Nayak, A., and Chaturvedi, S. (2019). Antimicrobial Efficacy of Nanosilver and Chitosan against Streptococcus Mutans, as an Ingredient of Toothpaste Formulation: An *In Vitro* Study. *J. Indian. Soc. Pedod. Prev. Dent.* 37, 46–54. doi:10.4103/jisppd.jisppd_239_18
- Akin, M., and Basciftci, F. A. (2012). Can White Spot Lesions Be Treated Effectively? *Angle Orthod.* 82 (5), 770–775. doi:10.2319/090711.578.1
- Aras, A., Celenk, S., and Atas, O. (2020). Comparison of Traditional and Novel Remineralization Agents: A Laser Fluorescence Study. *J. Oral Health Oral Epidemiol.* 9 (1), 38–44. doi:10.22122/johoe.v9i1.1063
- Bataineh, M., Malinowski, M., Duggal, M. S., and Tahmassebi, J. F. (2017). Comparison of the Newer Preventive Therapies on Remineralisation of Enamel *In Vitro*. *J. Dent.* 66, 37–44. doi:10.1016/j.jdent.2017.08.013
- Behrouzi, P., Heshmat, H., Hoorizad Ganjkar, M., Tabatabaei, S. F., and Kharazifard, M. J. (2020). Effect of Two Methods of Remineralization and Resin Infiltration on Surface Hardness of Artificially Induced Enamel Lesions. *J. Dent. (Shiraz)* 21 (1), 12–17. doi:10.30476/dentjods.2019.77864
- Beniash, E., Metzler, R. A., Lam, R. S. K., and Gilbert, P. U. P. A. (2009). Transient Amorphous Calcium Phosphate in Forming Enamel. *J. Struct. Biol.* 166, 133–143. doi:10.1016/j.jsb.2009.02.001
- Betts, F., Blumenthal, N. C., Posner, A. S., Becker, G. L., and Lehninger, A. L. (1975). Atomic Structure of Intracellular Amorphous Calcium Phosphate Deposits. *Proc. Natl. Acad. Sci. U.S.A.* 72, 2088–2090. doi:10.1073/pnas.72.6.2088
- Bhadoria, N., Gunwal, M. K., Kukreja, R., Maran, S., Devendrappa, S. N., and Singla, S. (2020). An *In Vitro* Evaluation of Remineralization Potential of Functionalized Tricalcium Phosphate Paste and CPP-ACPF on Artificial White Spot Lesion in Primary and Permanent Enamel. *Int. J. Clin. Pediatr. Dent.* 13 (6), 579–584. doi:10.5005/jp-journals-10005-1813
- Bijle, M. N. A., Ekambaram, M., Lo, E. C. M., and Yiu, C. K. Y. (2019). The Combined Antimicrobial Effect of Arginine and Fluoride Toothpaste. *Sci. Rep.* 9, 8405. doi:10.1038/s41598-019-44612-6
- Bröchner, A., Christensen, C., Kristensen, B., Tranæus, S., Karlsson, L., and Sonnesen, L. (2011). Treatment of Post-orthodontic White Spot Lesions with Casein Phosphopeptide-Stabilised Amorphous Calcium Phosphate. *Clin. Oral. Investig.* 15 (3), 369–373. doi:10.1007/s00784-010-0401-2
- Chandavarkar, S. M., and Ram, S. M. (2015). A Comparative Evaluation of the Effect of Dentin Desensitizers on the Retention of Complete Cast Metal Crowns. *Contemp. Clin. Dent.* 6, S45–S50. doi:10.4103/0976-237x.152937
- Chen, L., Liang, K., Li, J., Wu, D., Zhou, X., and Li, J. (2013). Regeneration of Biomimetic Hydroxyapatite on Etched Human Enamel by Anionic PAMAM Template *In Vitro*. *Arch. Oral. Biol.* 58, 975–980. doi:10.1016/j.archoralbio.2013.03.008
- Chen, Z., Cao, S., Wang, H., Li, Y., Kishen, A., Deng, X., et al. (2015). Biomimetic Remineralization of Demineralized Dentine Using Scaffold of CMC/ACP Nanocomplexes in an *In Vitro* Tooth Model of Deep Caries. *PLoS. One.* 10, e0116553. doi:10.1371/journal.pone.0116553
- Chen, C., Weir, M., Cheng, L., Lin, N., Lin-Gibson, S., Chow, L., et al. (2014). Antibacterial Activity and Ion Release of Bonding Agent Containing Amorphous Calcium Phosphate Nanoparticles. *Dent. Mat.* 30, 891–901. doi:10.1016/j.dental.2014.05.025
- Chen, M., Yang, J., Li, J., Liang, K., He, L., Lin, Z., et al. (2014). Modulated Regeneration of Acid-Etched Human Tooth Enamel by a Functionalized Dendrimer that Is an Analog of Amelogenin. *Acta. Biomater.* 10, 4437–4446. doi:10.1016/j.actbio.2014.05.016
- Chow, L. C., Takagi, S., Carey, C. M., and Sieck, B. A. (2000). Remineralization Effects of a Two-Solution Fluoride Mouthrinse: an *In Situ* Study. *J. Dent. Res.* 79, 991–995. doi:10.1177/00220345000790041601
- Chow, L. C., Takagi, S., and Vogel, G. L. (1998). Amorphous Calcium Phosphate: the Content of Bone. *J. Dent. Res.* 77, 6. doi:10.1177/00220345980770010901
- Cochrane, N. J., Cai, F., Huq, N. L., Burrow, M. F., and Reynolds, E. C. (2010). New Approaches to Enhanced Remineralization of Tooth Enamel. *J. Dent. Res.* 89 (11), 1187–1197. doi:10.1177/0022034510376046
- Cölfen, H., and Mann, S. (2003). Higher-Order Organization by Mesoscale Self-Assembly and Transformation of Hybrid Nanostructures. *Angew. Chem. Int. Ed. Engl.* 42, 2350–2365. doi:10.1002/anie.200200562
- Cross, K. J., Huq, N. L., Palamara, J. E., Perich, J. W., and Reynolds, E. C. (2005). Physicochemical Characterization of Casein Phosphopeptide-Amorphous Calcium Phosphate Nanocomplexes. *J. Biol. Chem.* 280, 15362–15369. doi:10.1074/jbc.M413504200
- Dey, A., Bomans, P. H., Müller, F. A., Will, J., Frederik, P. M., de With, G., et al. (2010). The Role of Prenucleation Clusters in Surface-Induced Calcium Phosphate Crystallization. *Nat. Mat.* 9, 1010–1014. doi:10.1038/nmat2900
- Dorozhkin, S. (1997). Surface Reactions of Apatite Dissolution. *J. Colloid. Interface. Sci.* 191, 489–497. doi:10.1006/jcis.1997.4942
- Dunn, W. (2007). Shear Bond Strength of an Amorphous Calcium-Phosphate-Containing Orthodontic Resin Cement. *Am. J. Orthod. Dentofac. Orthop.* 131, 243–247. doi:10.1016/j.ajodo.2005.04.046
- Eanes, E. D., Gillesen, I. H., and Posner, A. S. (1965). Intermediate States in the Precipitation of Hydroxyapatite. *Nature* 208, 365–367. doi:10.1038/208365a0
- Farzanegan, F., Ameri, H., Miri Soleiman, I., Khodaverdi, E., and Rangrazi, A. (2018). An *In Vitro* Study on the Effect of Amorphous Calcium Phosphate and Fluoride Solutions on Color Improvement of White Spot Lesions. *Dent. J. (Basel)* 6 (3). doi:10.3390/dj6030024
- Farzanegan, F., Morteza-Saadat-Mostafavi, S., Ameri, H., and Khaki, H. (2019). Effects of Fluoride versus Amorphous Calcium Phosphate Solutions on Enamel Microhardness of White Spot Lesions: An *In-Vitro* Study. *J. Clin. Exp. Dent.* 11 (3), e219–e224. doi:10.4317/jced.54448
- Featherstone, J. (2004). The Continuum of Dental Caries—Evidence for a Dynamic Disease Process. *J. Dent. Res.* 83, C39–C42. doi:10.1177/154405910408301S08
- Gao, Y., Liang, K., Weir, M. D., Gao, J., Imazato, S., Tay, F. R., et al. (2020). Enamel Remineralization via Poly(amido Amine) and Adhesive Resin Containing Calcium Phosphate Nanoparticles. *J. Dent.* 64, 58–67. doi:10.1016/j.jdent.2019.103262
- Gokkaya, B., Ozbek, N., Guler, Z., Akman, S., Sarac, A. S., and Kargul, B. (2020). Effect of a Single Application of CPP-ACPF Varnish on the Prevention of Erosive Tooth Wear: An AAS, AFM and SMH Study. *Oral. Health. Prev. Dent.* 18, 311–318. doi:10.3290/j.ohpd.a43365
- Gontijo, L., Cruz, R. d. A., and Brandao, P. R. G. (2007). Dental Enamel Around Fixed Orthodontic Appliances after Fluoride Varnish Application. *Braz. Dent. J.* 18, 49–53. doi:10.1590/s0103-64402007000100011
- Gower, L. (2008). Biomimetic Model Systems for Investigating the Amorphous Precursor Pathway and its Role in Biomineralization. *Chem. Rev.* 108, 4551–4627. doi:10.1021/cr800443h
- Güçlü, Z. A., Alaçam, A., and Coleman, N. J. (2016). A 12-Week Assessment of the Treatment of White Spot Lesions with CPP-ACP Paste And/or Fluoride Varnish. *Biomed. Res. Int.* 2016, 8357621. doi:10.1155/2016/8357621
- Guyen, Y., Ustun, N., Tuna, E. B., and Aktoren, O. (2019). Antimicrobial Effect of Newly Formulated Toothpastes and a Mouthrinse on Specific Microorganisms: An *In Vitro* Study. *Eur. J. Dent.* 13, 172–177. doi:10.1055/s-0039-1695655
- Hamba, H., Nikaido, T., Inoue, G., Sadr, A., and Tagami, J. (2011). Effects of CPP-ACP with Sodium Fluoride on Inhibition of Bovine Enamel Demineralization: A Quantitative Assessment Using Micro-computed Tomography. *J. Dent.* 39, 405–413. doi:10.1016/j.jdent.2011.03.005
- Han, S., Fan, Y., Zhou, Z., Tu, H., Li, D., Lv, X., et al. (2017). Promotion of Enamel Caries Remineralization by an Amelogenin-Derived Peptide in a Rat Model. *Arch. Oral. Biol.* 73, 66–71. doi:10.1016/j.archoralbio.2016.09.009
- Hefti, A. F., and Huber, B. (1987). The Effect on Early Plaque Formation, Gingivitis and Salivary Bacterial Counts of Mouthwashes Containing Hexetidine/zinc, Aminefluoride/tin or Chlorhexidine. *J. Clin. Periodontol.* 14, 515–518. doi:10.1111/j.1600-051x.1987.tb00992.x
- Hossainian, N., Slot, D. E., Afennich, F., and Van der Weijden, G. A. (2011). The Effects of Hydrogen Peroxide Mouthwashes on the Prevention of Plaque and Gingival Inflammation: a Systematic Review. *Int. J. Dent. Hyg.* 9, 171–181. doi:10.1111/j.1601-5037.2010.00492.x
- Hua, F., Yan, J., Zhao, S., Yang, H., and He, H. (2020). *In Vitro* remineralization of Enamel White Spot Lesions with a Carrier-Based Amorphous Calcium Phosphate Delivery System. *Clin. Oral. Investig.* 24, 2079–2089. doi:10.1007/s00784-019-03073-x

- Huang, G. J., Roloff-Chiang, B., Mills, B. E., Shalchi, S., Spiekerman, C., Korpak, A. M., et al. (2013). Effectiveness of MI Paste Plus and PreviDent Fluoride Varnish for Treatment of White Spot Lesions: a Randomized Controlled Trial. *Am. J. Orthod. Dentofac. Orthop.* 143 (1), 31–41. doi:10.1016/j.jado.2012.09.007
- Huang, S.-C., Naka, K., and Chujo, Y. (2008). Effect of Molecular Weights of Poly(acrylic Acid) on Crystallization of Calcium Carbonate by the Delayed Addition Method. *Polym. J.* 40, 154–162. doi:10.1295/polymj.PJ2007162
- Ibrahim, M. S., Balhaddad, A. A., Garcia, I. M., Collares, F. M., Weir, M. D., Xu, H. H. K., et al. (2020). pH-Responsive Calcium and Phosphate-Ion Releasing Antibacterial Sealants on Carious Enamel Lesions *In Vitro*. *J. Dent.* 97, 103323. doi:10.1016/j.jdent.2020.103323
- Jo, S. Y., Chong, H. J., Lee, E. H., Chang, N. Y., Chae, J. M., Cho, J. H., et al. (2014). Effects of Various Toothpastes on Remineralization of White Spot Lesions. *Korean. J. Orthod.* 44 (3), 113–118. doi:10.4041/kjod.2014.44.3.113
- Julien, K., Buschang, P., and Campbell, P. (2013). Prevalence of White Spot Lesion Formation during Orthodontic Treatment. *Angle. Orthod.* 83, 641–647. doi:10.2319/071712-584.1
- Kamath, P., Nayak, R., Kamath, S. U., and Pai, D. (2017). A Comparative Evaluation of the Remineralization Potential of Three Commercially Available Remineralizing Agents on White Spot Lesions in Primary Teeth: An *In Vitro* Study. *J. Indian. Soc. Pedod. Prev. Dent.* 35 (3), 229–237. doi:10.4103/JISPPD.JISPPD_242_16
- Karadağlıoğlu, Ö., Ulusoy, N., Başer, K. H. C., Hanoğlu, A., and Şık, İ. (2019). Antibacterial Activities of Herbal Toothpastes Combined with Essential Oils against *Streptococcus Mutans*. *Pathogens* 8, 20. doi:10.3390/pathogens8010020
- Khopade, A., Khopade, S., and Jain, N. (2002). Development of Hemoglobin Aquasomes from Spherical Hydroxyapatite Cores Precipitated in the Presence of Half-Generation Poly(Amidoamine) Dendrimer. *Int. J. Pharm.* 241, 145–154. doi:10.1016/S0378-5173(02)00235-1
- Koetz, J., and Kosmella, S. (2007). *Polyelectrolytes and Nanoparticle*. Berlin: Springer Press.
- Kwak, S.-Y., Yamakoshi, Y., Simmer, J., and Margolis, H. C. (2016). MMP20 Proteolysis of Native Amelogenin Regulates Mineralization *In Vitro*. *J. Dent. Res.* 95, 1511–1517. doi:10.1177/0022034516662814
- Larsson, K., Stime, A., Hansen, L., Birkhed, D., and Ericson, D. (2020). Salivary Fluoride Concentration and Retention after Rinsing with 0.05 and 0.2% Sodium Fluoride (NaF) Compared with a New High F Rinse Containing 0.32% NaF. *Acta. Odontol. Scand.* 78, 609–613. doi:10.1080/00016357.2020.1800085
- Liu, Y., Zhang, L., Niu, L. N., Yu, T., Xu, H. H. K., Weir, M. D., et al. (2018). Antibacterial and Remineralizing Orthodontic Adhesive Containing Quaternary Ammonium Resin Monomer and Amorphous Calcium Phosphate Nanoparticles. *J. Dent.* 72, 53–63. doi:10.1016/j.jdent.2018.03.004
- Lv, X., Yang, Y., Han, S., Li, D., Tu, H., Li, W., et al. (2015). Potential of an Amelogenin Based Peptide in Promoting Remineralization of Initial Enamel Caries. *Arch. Oral. Biol.* 60, 1482–1487. doi:10.1016/j.archoralbio.2015.07.010
- Ma, Y., Zhang, N., Weir, M. D., Bai, Y., and Xu, H. H. K. (2017). Novel Multifunctional Dental Cement to Prevent Enamel Demineralization Near Orthodontic Brackets. *J. Dent.* 64, 58–67. doi:10.1016/j.jdent.2017.06.004
- Margolis, H., and Murphy, B. (1986). Effect of Low Levels of Fluoride in Solution on Enamel Demineralization *In Vitro*. *J. Dent. Res.* 65, 23–29. doi:10.1177/00220345860650010301
- Marinho, V. C. C. (2009). Cochrane Reviews of Randomized Trials of Fluoride Therapies for Preventing Dental Caries. *Eur. Arch. Paediatr. Dent.* 10, 183–191. doi:10.1007/bf03262681
- Moradian-Oldak, J. (2012). Protein-mediated Enamel Mineralization. *Front. Biosci.* 17, 1996–2023. doi:10.2741/4034
- Munjal, D., Garg, S., Dhindsa, A., Sidhu, G. K., and Sethi, H. S. (2016). Assessment of White Spot Lesions and In-Vivo Evaluation of the Effect of CPP-ACP on White Spot Lesions in Permanent Molars of Children. *J. Clin. Diagn. Res.* 10 (5), ZC149–ZC154. doi:10.7860/jcdr/2016/19458.7896
- Niu, L. N., Jee, S. E., Jiao, K., Tonggu, L., Li, M., Wang, L., et al. (2017). Collagen Intrafibrillar Mineralization as a Result of the Balance between Osmotic Equilibrium and Electroneutrality. *Nat. Mat.* 16, 370–378. doi:10.1038/nmat4789
- Olgen, I. C., Sonmez, H., and Bezgin, T. (2021). Effects of Different Remineralization Agents on MIH Defects: a Randomized Clinical Study. *Clin. Oral. Investig.* doi:10.1007/s00784-021-04305-9
- Oliveira, G. M., Ritter, A. V., Heymann, H. O., Swift, E., Jr., Donovan, T., Brock, G., et al. (2014). Remineralization Effect of CPP-ACP and Fluoride for White Spot Lesions *In Vitro*. *J. Dent.* 42 (12), 1592–1602. doi:10.1016/j.jdent.2014.09.004
- Pei, D., Liu, S., Huang, C., Du, X., Yang, H., and Wang, Y. (2013). Effect of Pretreatment with Calcium-Containing Desensitizer on the Dentine Bonding of Mild Self-Etch Adhesives. *Eur. J. Oral. Sci.* 121, 204–210. doi:10.1111/eos.12047
- Perrini, F., Lombardo, L., Arreghini, A., Medori, S., and Siciliani, G. (2016). Caries Prevention during Orthodontic Treatment: In-Vivo Assessment of High-Fluoride Varnish to Prevent White Spot Lesions. *Am. J. Orthod. Dentofac. Orthop.* 149, 238–243. doi:10.1016/j.jado.2015.07.039
- Pithon, M. M., Baião, F. S., Sant'Anna, L. I. D., Tanaka, O. M., and Cople-Maia, L. (2019). Effectiveness of Casein Phosphopeptide-Amorphous Calcium Phosphate-Containing Products in the Prevention and Treatment of White Spot Lesions in Orthodontic Patients: A Systematic Review. *J. Invest. Clin. Dent.* 10 (2), e12391. doi:10.1111/jicd.12391
- Qi, Y., Ye, Z., Fok, A., Holmes, B. N., Espanol, M., Ginebra, M. P., et al. (2018). Effects of Molecular Weight and Concentration of Poly(Acrylic Acid) on Biomimetic Mineralization of Collagen. *ACS. Biomater. Sci. Eng.* 4, 2758–2766. doi:10.1021/acsbomaterials.8b00512
- Rees, J., Loyn, T., and Chadwick, B. (2007). Pronamel and Tooth Mousse: an Initial Assessment of Erosion Prevention *In Vitro*. *J. Dent.* 35, 355–357. doi:10.1016/j.jdent.2006.10.005
- Reeves, R. E., and Latour, N. G. (1958). Calcium Phosphate Sequestering Phosphopeptide from Casein. *Science* 128, 472. doi:10.1126/science.128.3322.472
- Reise, M., Kranz, S., Heyder, M., Jandt, K. D., and Sigusch, B. W. (2021). Effectiveness of Casein Phosphopeptide-Amorphous Calcium Phosphate (CPP-ACP) Compared to Fluoride Products in an In-Vitro Demineralization Model. *Mater. (Basel)* 14, 5974. doi:10.3390/ma14205974
- Reynolds, E. C., Cain, C. J., Webber, F. L., Black, C. L., Riley, P. F., Johnson, I. H., et al. (1995). Anticariogenicity of Calcium Phosphate Complexes of Tryptic Casein Phosphopeptides in the Rat. *J. Dent. Res.* 74, 1272–1279. doi:10.1177/00220345950740060601
- Reynolds, E. C. (1997). Remineralization of Enamel Subsurface Lesions by Casein Phosphopeptide-Stabilized Calcium Phosphate Solutions. *J. Dent. Res.* 76, 1587–1595. doi:10.1177/00220345970760091101
- Rösing, C. K., Cavagni, J., Gaio, E. J., Muniz, F., Ranzan, N., Oballe, H. J. R., et al. (2017). Efficacy of Two Mouthwashes with Cetylpyridinium Chloride: a Controlled Randomized Clinical Trial. *Braz. Oral. Res.* 31, e47. doi:10.1590/1807-3107BOR-2017.vol31.0047
- Ruan, Q., and Moradian-Oldak, J. (2015). Amelogenin and Enamel Biomimetics. *J. Mat. Chem. B* 3, 3112–3129. doi:10.1039/C5TB00163C
- Ruan, Q., Siddiqah, N., Li, X., Nutt, S., and Moradian-Oldak, J. (2014). Amelogenin-chitosan Matrix for Human Enamel Regrowth: Effects of Viscosity and Supersaturation Degree. *Connect. Tissue. Res.* 55, 150–154. doi:10.3109/03008207.2014.923856
- Ruan, Q., Zhang, Y., Yang, X., Nutt, S., and Moradian-Oldak, J. (2013). An Amelogenin-Chitosan Matrix Promotes Assembly of an Enamel-like Layer with a Dense Interface. *Acta. Biomater.* 9, 7289–7297. doi:10.1016/j.actbio.2013.04.004
- Schemehorn, B. R., Wood, G. D., McHale, W., and Winston, A. E. (2011). Comparison of Fluoride Uptake Into Tooth Enamel From Two Fluoride Varnishes Containing Different Calcium Phosphate Sources. *J. Clin. Dent.* 22 (2), 51–54.
- Shang, Q., Gao, Y., Qin, T., Wang, S., Shi, Y., and Chen, T. (2020). Interaction of Oral and Toothbrush Microbiota Affects Oral Cavity Health. *Front. Cell. Infect. Microbiol.* 10, 17. doi:10.3389/fcimb.2020.00017
- Shen, P., Cai, F., Nowicki, A., Vincent, J., and Reynolds, E. C. (2001). Remineralization of Enamel Subsurface Lesions by Sugar-free Chewing Gum Containing Casein Phosphopeptide-Amorphous Calcium Phosphate. *J. Dent. Res.* 80, 2066–2070. doi:10.1177/00220345010800120801
- Sikirić, M. D., Gergely, C., Elkaim, R., Wachtel, E., Cuisinier, F. J., and Füredi-Milhofer, H. (2009). Biomimetic Organic-Inorganic Nanocomposite Coatings for Titanium Implants. *J. Biomed. Mat. Res.* A 89, 759–771. doi:10.1002/jbm.a.32021
- Singh, S., Singh, S. P., Goyal, A., Utreja, A. K., and Jena, A. K. (2016). Effects of Various Remineralizing Agents on the Outcome of Post-orthodontic White Spot Lesions (WSLs): a Clinical Trial. *Prog. Orthod.* 17 (1), 25. doi:10.1186/s40510-016-0138-9
- Singla, S., Maran, S., Bhadoria, N., Gunwal, M. K., Kukreja, R., and Devendrappa, S. N. (2020). An *In Vitro* Evaluation of Remineralization Potential of Functionalized Tricalcium Phosphate Paste and CPP-ACPF on Artificial White Spot Lesion in Primary and Permanent Enamel. *Int. J. Clin. Pediatr. Dent.* 13 (6), 579–584. doi:10.5005/jp-journals-10005-1813
- Sithissetapong, T., Doi, T., Nishida, Y., Kambara, M., and Phantumvanit, P. (2015). Effect of CPP-ACP Paste on Enamel Carious Lesion of Primary Upper

- Anterior Teeth Assessed by Quantitative Light-Induced Fluorescence: A One-Year Clinical Trial. *Caries. Res.* 49 (4), 434–441. doi:10.1159/000434728
- Skrtec, D., Antonucci, J. M., Eanes, E. D., and Eidelman, N. (2004). Dental Composites Based on Hybrid and Surface-Modified Amorphous Calcium Phosphates. *Biomaterials* 25, 1141–1150. doi:10.1016/j.biomaterials.2003.08.001
- Skrtec, D., and Eanes, E. (1996). Improved Properties of Amorphous Calcium Phosphate Fillers in Remineralizing Resin Composites. *Dent. Mat.* 12, 295–301. doi:10.1016/S0109-5641(96)80037-6
- Soares-Yoshikawa, A. L., Varanda, T., Iwamoto, A. S., Kantovitz, K. R., Puppini-Rontani, R. M., and Pascon, F. M. (2021). Fluoride Release and Remineralizing Potential of Varnishes in Early Caries Lesions in Primary Teeth. *Microsc. Res. Tech.* 84, 1012–1021. doi:10.1002/jemt.23662
- Sollböhmer, O., May, K. P., and Anders, M. (1995). Force Microscopical Investigation of Human Teeth in Liquid. *Thin. Solid. Films.* 264, 176–183. doi:10.1016/0040-6090(95)05847-8
- Song, J., Li, T., Gao, J., Li, C., Jiang, S., and Zhang, X. (2021). Building an Aprismatic Enamel-like Layer on a Demineralized Enamel Surface by Using Carboxymethyl Chitosan and Lysozyme-Encapsulated Amorphous Calcium Phosphate Nanogels. *J. Dent.* 107, 103599. doi:10.1016/j.jdent.2021.103599
- Songsirpraduboon, S., Hamba, H., Trairatvorakul, C., and Tagami, J. (2014). Sodium Fluoride Mouthrinse Used Twice Daily Increased Incipient Caries Lesion Remineralization in an *In Situ* Model. *J. Dent.* 42, 271–278. doi:10.1016/j.jdent.2013.12.012
- Svenson, S., and Tomalia, D. A. (2012). Dendrimers in Biomedical Applications—Reflections on the Field. *Adv. Drug. Deliv. Rev.* 64, 102–115. doi:10.1016/j.addr.2005.09.018
- Tahmasbi, S., Mousavi, S., Behroozibakhsh, M., and Badiie, M. (2019). Prevention of White Spot Lesions Using Three Remineralizing Agents: An *In Vitro* Comparative Study. *J. Dent. Res. Dent. Clin. Dent. Prospects.* 13 (1), 36–42. doi:10.15171/joddd.2019.006
- Terauchi, M., Tamura, A., Tonegawa, A., Yamaguchi, S., Yoda, T., and Yui, N. (2019). Polyelectrolyte Complexes between Polycarboxylates and BMP-2 for Enhancing Osteogenic Differentiation: Effect of Chemical Structure of Polycarboxylates. *Polym. (Basel)* 11, 1327. doi:10.3390/polym11081327
- Thierens, L. A. M., Moerman, S., Elst, C. V., Vercruysee, C., Maes, P., Temmerman, L., et al. (2019). The *In Vitro* Remineralizing Effect of CPP-ACP and CPP-ACPF after 6 and 12 Weeks on Initial Caries Lesion. *J. Appl. Oral. Sci.* 27, e20180589. doi:10.1590/1678-7757-2018-0589
- Tomalia, D. A., Baker, H., Dewald, J., Hall, M., Kallos, G., Martin, S., et al. (1985). A New Class of Polymers: Starburst-Dendritic Macromolecules. *Poly. J.* 17, 117–132. doi:10.1295/polymj.17.117
- Tsiourvas, D., Tsetsekou, A., Kammenou, M.-I., and Boukos, N. (2015). Biomimetic Synthesis of Ribbon-like Hydroxyapatite Employing Poly(l-Arginine). *Mat. Sci. Eng. C. Mat. Biol. Appl.* 58, 1225–1231. doi:10.1016/j.msec.2015.09.076
- Utneja, S., Talwar, S., Nawal, R. R., Sapra, S., Mittal, M., Rajain, A., et al. (2018). Evaluation of Remineralization Potential and Mechanical Properties of Pit and Fissure Sealants Fortified with Nano-Hydroxyapatite and Nano-Amorphous Calcium Phosphate Fillers: An *In Vitro* Study. *J. Conserv. Dent.* 21, 681–690. doi:10.4103/jcd.jcd_31_18
- Wang, D., Deng, J., Deng, X., Fang, C., Zhang, X., and Yang, P. (2020). Controlling Enamel Remineralization by Amyloid-like Amelogenin Mimics. *Adv. Mat.* 32, 2002080. doi:10.1002/adma.202002080
- Wang, H., Xiao, Z., Yang, J., Lu, D., Kishen, A., Li, Y., et al. (2017). Oriented and Ordered Biomimetic Remineralization of the Surface of Demineralized Dental Enamel Using HAP@ACP Nanoparticles Guided by Glycine. *Sci. Rep.* 7, 40701. doi:10.1038/srep40701
- Wang, Y., Hua, F., and Jiang, H. (2020). CPP-ACP May Be Effective, but Not Significantly Greater Than Using Fluorides Alone, in Preventing and Treating White Spot Lesions Around Orthodontic Brackets. *J. Evid. Based. Dent. Pract.* 20 (1), 101416. doi:10.1016/j.jebdp.2020.101416
- Wang, Z., Ouyang, Y., Wu, Z., Zhang, L., Changyu, S., Fan, J., et al. (2018). A Novel Fluorescent Adhesive-Assisted Biomimetic Mineralization. *Nanoscale* 18, 18980–18987. doi:10.1039/C8NR02078G
- Wright, J. T., Li, Y., Suggs, C., Kuehl, M. A., Kulkarni, A. B., and Gibson, C. W. (2011). The Role of Amelogenin during Enamel-Crystallite Growth and Organization *In Vivo*. *Eur. J. Oral. Sci.* 119 (Suppl. 1), 65–69. doi:10.1111/j.1600-0722.2011.00883.x
- Xie, X., Wang, L., Xing, D., Qi, M., Li, X., Sun, J., et al. (2019). Novel Rechargeable Calcium Phosphate Nanoparticle-Filled Dental Cement. *Dent. Mat. J.* 38, 1–10. doi:10.4012/dmj.2017-420
- Xu, H. H., Moreau, J. L., Sun, L., and Chow, L. C. (2011). Nanocomposite Containing Amorphous Calcium Phosphate Nanoparticles for Caries Inhibition. *Dent. Mat.* 27, 762–769. doi:10.1016/j.dental.2011.03.016
- Yadav, P., Desai, H., Patel, K., Patel, N., and Iyengar, S. (2019). A Comparative Quantitative & Qualitative Assessment in Orthodontic Treatment of White Spot Lesion Treated with 3 Different Commercially Available Materials - *In Vitro* Study. *J. Clin. Exp. Dent.* 11 (9), e776–e782. doi:10.4317/jced.56044
- Yang, H., Chen, Z., Yan, H., and Huang, C. (2018). Effects of Calcium-Containing Desensitizers on the Bonding Stability of an Etch-And-Rinse Adhesive against Long-Term Water Storage and pH Cycling. *Dent. Mat. J.* 37, 122–129. doi:10.4012/dmj.2017-006
- Yang, H., Niu, L., Sun, J. L., Huang, X., Pei, D., Cui, H., et al. (2017). Biodegradable Mesoporous Delivery System for Biomimetic Mineralization Precursors. *Int. J. Nanomed.* 12, 839–854. doi:10.2147/IJN.S128792
- Yang, X., Wang, L., Qin, Y., Sun, Z., Henneman, Z. J., Moradian-Oldak, J., et al. (2010). How Amelogenin Orchestrates the Organization of Hierarchical Elongated Microstructures of Apatite. *J. Phys. Chem. B* 114, 2293–2300. doi:10.1021/jp910219s
- Zandim-Barcelos, D., Tschoppe, P., Sampaio, J., and Kielbassa, A. (2011). Effect of Saliva Substitutes in Combination with Fluorides on Remineralization of Subsurface Dentin Lesions. *Support. Care. Cancer.* 19, 1143–1149. doi:10.1007/s00520-010-0924-8
- Zhang, J., Lynch, R., Watson, T., and Banerjee, A. (2018). Remineralisation of Enamel White Spot Lesions Pre-treated with Chitosan in the Presence of Salivary Pellicle. *J. Dent.* 72, 21–28. doi:10.1016/j.jdent.2018.02.004
- Zhang, X., Li, Y., Sun, X., Kishen, A., Deng, X., Yang, X., et al. (2014). Biomimetic Remineralization of Demineralized Enamel with Nano-Complexes of Phosphorylated Chitosan and Amorphous Calcium Phosphate. *J. Mat. Sci. Mat. Med.* 25, 2619–2628. doi:10.1007/s10856-014-5285-2
- Zhong, X., Lai, T. T., Chen, L., and Tian, K. (2021). Self-assembly and Mineralization of Full-Length Human Amelogenin and its Functional Fragments *In Vitro*. *West. China. J. Stomatol.* 32, 2002080. doi:10.7518/hxkq.2021.04.007
- Zhou, Y., Yang, J., Lin, Z., Li, J., Liang, K., Yuan, H., et al. (2013). Triclosan-loaded Poly(amido Amine) Dendrimer for Simultaneous Treatment and Remineralization of Human Dentine. *Colloids. Surf. B. Biointerfaces.* 115, 237–243. doi:10.1016/j.colsurfb.2013.11.045
- Zhou, Z. H., Zhou, P. L., Yang, S. P., Yu, X. B., and Yang, L. Z. (2007). Controllable Synthesis of Hydroxyapatite Nanocrystals via a Dendrimer-Assisted Hydrothermal Process. *Mat. Res. Bull.* 42, 1611–1618. doi:10.1016/j.materresbull.2006.11.041
- Zhou, Z., Zhang, L., Li, J., Shi, Y., Wu, Z., Zheng, H., et al. (2021). Polyelectrolyte-calcium Complexes as a Pre-precursor Induce Biomimetic Mineralization of Collagen. *Nanoscale* 13, 953–967. doi:10.1039/d0nr05640e
- Zhu, Y., Yan, J., Mujtaba, B. M., Li, Y., Wei, H., and Huang, S. (2021). The Dual Anti-caries Effect of Carboxymethyl Chitosan Nanogel Loaded with Chimeric Lysin ClyR and Amorphous Calcium Phosphate. *Eur. J. Oral. Sci.* 129, e12784. doi:10.1111/eos.12784

Conflict of Interest: The authors declare that the research was conducted in the absence of any commercial or financial relationships that could be construed as a potential conflict of interest.

Publisher's Note: All claims expressed in this article are solely those of the authors and do not necessarily represent those of their affiliated organizations, or those of the publisher, the editors and the reviewers. Any product that may be evaluated in this article, or claim that may be made by its manufacturer, is not guaranteed or endorsed by the publisher.

Copyright © 2022 Yan, Yang, Luo, Hua and He. This is an open-access article distributed under the terms of the Creative Commons Attribution License (CC BY). The use, distribution or reproduction in other forums is permitted, provided the original author(s) and the copyright owner(s) are credited and that the original publication in this journal is cited, in accordance with accepted academic practice. No use, distribution or reproduction is permitted which does not comply with these terms.



Zinc Oxide Nanoparticles: A Review on Its Applications in Dentistry

C Pushpalatha¹, Jithya Suresh¹, VS Gayathri¹, SV Sowmya², Dominic Augustine², Ahmed Alamoudi³, Bassam Zidane⁴, Nassreen Hassan Mohammad Albar⁵ and Shankargouda Patil^{6*}

¹Department of Pedodontics and Preventive Dentistry, Faculty of Dental Sciences, M.S. Ramaiah University of Applied Sciences, Bangalore, India, ²Department of Oral Pathology & Microbiology, Faculty of Dental Sciences, M.S. Ramaiah University of Applied Sciences, Bangalore, India, ³Oral Biology Department, Faculty of Dentistry, King Abdulaziz University, Jeddah, Saudi Arabia, ⁴Restorative Dentistry Department, Faculty of Dentistry, King Abdulaziz University, Jeddah, Saudi Arabia, ⁵Department of Restorative Dental Science, College of Dentistry, Shwajra Campus, Jazan University, Jazan, Saudi Arabia, ⁶Department of Maxillofacial Surgery and Diagnostic Sciences, Division of Oral Pathology, College of Dentistry, Shwajra Campus, Jazan University, Jazan, Saudi Arabia

OPEN ACCESS

Edited by:

Kumar Chandan Srivastava,
Al Jouf University, Saudi Arabia

Reviewed by:

Tarek El-Bialy,
University of Alberta, Canada
Reji Mathew,
Midwestern University, United States

*Correspondence:

Shankargouda Patil
dr.ravipatil@gmail.com

Specialty section:

This article was submitted to
Biomaterials,
a section of the journal
Frontiers in Bioengineering and
Biotechnology

Received: 11 April 2022

Accepted: 28 April 2022

Published: 19 May 2022

Citation:

Pushpalatha C, Suresh J, Gayathri VS, Sowmya SV, Augustine D, Alamoudi A, Zidane B, Mohammad Albar NH and Patil S (2022) Zinc Oxide Nanoparticles: A Review on Its Applications in Dentistry. *Front. Bioeng. Biotechnol.* 10:917990. doi: 10.3389/fbioe.2022.917990

Nanotechnology in modern material science is a research hot spot due to its ability to provide novel applications in the field of dentistry. Zinc Oxide Nanoparticles (ZnO NPs) are metal oxide nanoparticles that open new opportunities for biomedical applications that range from diagnosis to treatment. The domains of these nanoparticles are wide and diverse and include the effects brought about due to the anti-microbial, regenerative, and mechanical properties. The applications include enhancing the anti-bacterial properties of existing restorative materials, as an anti-sensitivity agent in toothpastes, as an anti-microbial and anti-fungal agent against pathogenic oral microflora, as a dental implant coating, to improve the anti-fungal effect of denture bases in rehabilitative dentistry, remineralizing cervical dentinal lesions, increasing the stability of local drug delivery agents and other applications.

Keywords: zinc oxide nanoparticles, biomedical application, nanodentistry, dental applications, restorative material

1 INTRODUCTION

Nanotechnology, wherein matter is manipulated on a molecular scale, has revolutionized modern dentistry. “Nanodentistry” is the amalgamation of nanotechnology and dentistry and provides the scope for the formulation of innovative materials that can have many potential applications in clinical practice. The nano size confers a larger surface area, allows the controlled synthesis and is also capable of altering the desired physical and chemical properties that enables them for unique interactions with biomolecules. They also have a higher percentage of surface atoms, which maximized their ability due to an increase in surface reactivity (Rasmussen et al., 2010).

Zinc is an essential trace element which is found in the muscle, bone, skin and also in the hard tissues of the tooth. Zinc Oxide Nanoparticle (ZnO NP) is a white colored odorless powder and has a molecular weight of 81.38 g/mol. FDA considers it as a generally recognized as safe (GRAS) substance. Its extensive applications in dentistry are credited to the unique optical, magnetic, morphological, electrical, catalytic, mechanical, and photochemical properties which can be easily altered as per the requirements: by modifying the size, doping with supplementary compounds, or adjusting the conditions of synthesis. As the size of the particles decrease, the desirable characteristics improve (Baek et al., 2012).

TABLE 1 | Studies focussing on the Applications of ZnO NPs in dentistry.

SI No.	Modification	Effect	Author
1	Dental resin composite containing ZnO NP	Inhibition of adhesion of <i>S. mutans</i>	Wang et al. (2019)
2	Flowable resin composite with ZnO NP	Decreased microleakage	Teymoornezhad et al. (2016)
3	Flowable resin composite with ZnO NP	Decreased microleakage	Hojati et al. (2013)
4	ZnO NP + resin-based dental composites	Anti-bacterial activity against <i>S. sobrinus</i>	Aydin Sevinç and Hanley, 2010)
5	ZnO NP	Anti-bacterial activity against <i>S. mutans</i> and <i>Lactobacillus</i>	Kasraei et al. (2014)
6	ZnO NP and GIC	Anti-bacterial activity against <i>S. mutans</i>	Vanajassun et al. (2014)
7	ZnO NP added into dental adhesive systems	Improved anti-microbial properties	Saffarpour et al. (2016)
8	ZnO NP added into dental adhesive systems	Improved anti-microbial properties	Jowkar et al. (2018)
9	ZnO NP added into dental adhesive systems	Improved anti-microbial properties	Gutiérrez et al. (2019)
10	ZnO NP used as interim cements	Anti-bacterial activity against <i>S. mutans</i>	Andrade et al. (2018)
11	ZnO NP	Anti-bacterial activity against <i>E. coli</i>	Liu et al. (2009)
12	Combination of ZnO NP and EDTA solution as irrigant	Enhanced fracture resistance of roots	Jowkar et al. (2020)
13	Addition of ZnO NP, calcium hydroxide NPs and chlorhexidine as intracanal medicament	Anti-bacterial activity against <i>E. faecalis</i>	Aguar et al. (2015)
14	ZnO NP as sealer	Enhanced sealing with remineralization of radicular dentin	Toledano et al. (2020)
15	ZnO NP as nanosealer	Reduction in apical microleakage	Javidi et al. (2014)
16	ZnO NP	Improved penetration depth into dentinal tubules	Elkateb et al. (2015)
17	ZnONP added into gutta percha cones	Enhanced anti-bacterial activity against <i>S. aureus</i> and <i>E. faecalis</i> , excellent hermetic seal	Alves et al. (2018)
18	ZnO NP in Zinc-Bioglass	Induce differentiation of hDPSCs	Huang et al. (2017)
19	ZnO NP in Zinc-Bioglass and Calcium Phosphate Cement	Promotion of odontogenic differentiation and angiogenesis	Zhang et al. (2015)
20	ZnO NP containing composite membranes of PCL/GEL	Anti-bacterial activity against <i>S. aureus</i>	ZnO NP + composite membranes of PCL/GEL
21	ZnO NP containing electrospun membranes of PCL/GEL	Anti-bacterial activity against <i>P. gingivalis</i> and <i>F. nucleatum</i>	ZnO NP + electrospun membranes of PCL/GEL
22	ZnO NP and serum albumin microspheres with minocycline	Enhanced anti-microbial spectrum, pH-responsiveness, sustained release, tissue-repairing and adhesion and enhanced controlled drug delivery	ZnO NP + serum albumin microspheres containing minocycline
23	ZnO NP added into PMMA in denture bases	Anti-fungal effect against <i>C. albicans</i>	Cierech et al. (2019)
24	ZnO NP incorporated into Auto-polymerized acrylic resins	Improvement of flexural strength	Kati. (2019)
25	ZnO NP added into Tissue conditioner	Anti-fungal effect	Homsiang et al. (2020)
26	Combination of ZnONP, chitosan and Ag NP	Anti-microbial effect against <i>C. albicans</i> , <i>S. mutans</i> , <i>P. aeruginosa</i> and <i>E. faecalis</i>	Mousavi et al. (2020)
27	ZnO NP in silicone prosthesis	Improved colour stability	Charoenkijjajorn and Sanohkan. (2020)
28	ZnO NP coating in NiTi wires	Reduction in the frictional forces, enhanced corrosion resistance and anti-bacterial effect against <i>S. mutans</i>	Kachoei et al. (2016)
29	ZnO NP and chitosan NPs in resin-based dental composite bonding agents	Anti-bacterial activity against <i>S. mutans</i> , <i>S. sanguis</i> and <i>L. acidophilus</i>	Mirhashemi et al. (2013)
30	ZnO NP	Anti-fungal effect against <i>C. albicans</i> (oral thrush)	Abd et al. (2015)
31	ZnO NPs and Ag NPs	Enhanced anti-bacterial effect in human and artificial saliva	Pokrowiecki et al. (2019)
32	ZnO NPs	Anti-fungal effect on <i>Aspergillus niger</i> and <i>C. albicans</i>	Pillai et al. (2020)
33	ZnO NPs	Enhanced sensitivity to <i>E. coli</i> , <i>P. aeruginosa</i> and Methicillin Resistant <i>S. aureus</i>	Ali et al. (2016)
34	Combination of ZnO NPs, Quercetin, Ceftriaxone, Ampicillin, Naringin and Amphotericin B	Enhanced drug efficacy against Methicillin resistant <i>S. aureus</i> , <i>S. pneumoniae</i> and <i>S. pyogenes</i> , <i>E. coli</i> , <i>S. marcescens</i> and <i>P. aeruginosa</i>	Akbar et al. (2021)
35	ZnO NPs	Detect low-level expression of biomarkers, preferential cytotoxicity against cancer cells, induce ROS.	Rasmussen et al. (2010)
36	ZnO NPs and PEG	Enhanced anti-bacterial activity against <i>E. coli</i> and <i>S. aureus</i> , low concentration cytotoxic action against cancer cells	Nair et al. (2008)
37	ZnO NPs and daunorubicin for UV irradiation	Synergistic cytotoxic effects on leukemic cells	Guo et al. (2008)
38	ZnO NPs	Dental wastewater purification treatment	Gu et al. (2020)
39	ZnO NPs	Purification of wastewater	Spoială et al. (2021)
40	ZnO NPs on implant surface	Enhanced proliferation of osteoblasts, anti-bacterial effect against <i>S. aureus</i>	Memarzadeh et al. (2015)
41	ZnO NPs on implant surface	Anti-bacterial effect against <i>S. mutans</i>	Abdulkareem et al. (2015)
42	ZnO NPs on implant surface	Anti-bacterial effect against <i>S. mutans</i>	Kulshrestha et al. (2014)
43	ZnO NPs incorporated into dentifrice	Inhibition of dentin demineralization and enhanced anti-microbial effects	Khan et al. (2020)
44	ZnO NPs nanogels	Promote dentin mineralization	Toledano et al. (2019)
45	ZnO NPs	Dentinal tubule occlusion	Toledano-Osorio et al. (2018)

In the present, ZnO NPs are being investigated as associates of anti-microbial agents which are one of the most important reasons for its use. A recent theory that explains this is the “Trojan Horse effect”, which states that the acidic lysosomal environment promotes nanoparticle degradation, that in turn brings about conversion of core metals to ions and the release of substances that are toxic and in turn interrupt cell reproduction. Other mechanisms of their anti-microbial action are by locally changing the microenvironments near the microbes and by producing reactive oxygen species (ROS) or by increasing solubility of these nanoparticles. This can induce interplay with -SH group of the enzymes in the microbes and cause malfunction of organelles causing denaturation of the proteins and resulting in damage to DNA. This in turn alters the DNA replication of the microorganisms. Another possible anti-microbial mechanism is by the release of H_2O_2 (Şuhani et al., 2018) and by the displacement of Magnesium ions which interferes with the metabolism of the bacteria. The enhanced effect against microbes is attributed to the increased ratio of surface/volume. Hence, the incorporation of ZnO NPs in dental restorative materials, luting materials, tissue conditioners, intracanal medicaments, irrigants, adhesives and other materials can have beneficial anti-microbial effects.

Further research is also being done on this nanoparticle, due to the unlimited fields of application such as regarding its anti-inflammatory activity in response to pathogens, its anti-demineralizing and remineralizing effect on the hard tissues of the tooth, its potential as an anti-cancer agent and many others (Carrouel et al., 2020; Wiesmann et al., 2020). ZnO NPs hence have widespread applications in the field of restorative dentistry, endodontics, regenerative endodontics, prosthetic dentistry, orthodontics, preventive dentistry, implantology and periodontology (Moradpoor et al., 2021). Although ZnO NPs are considered to be a biologically safe material that does not exhibit cell toxicity, however, further research into the regulatory and safety concerns in oral care products on long term use must be discussed, questioned and further researched upon. Majority of the research regarding these NPs are limited to *in-vitro* studies and few animal studies. Therefore, further investigations and clinical trials must be carried out in order to utilize it to its full potential.

2 APPLICATIONS OF ZINC OXIDE NANOPARTICLES IN DENTISTRY

Zinc Oxide Nanoparticles have a wide range of applications in the various branches of dentistry, such as in the field of restorative dentistry, endodontics, regenerative endodontics, periodontics, prosthodontics, orthodontics, oral medicine, cancer diagnosis, dental implantology, preventive dentistry and biomedical waste management. The research performed using these nanoparticles are summarized in **Table 1** and **Figure 1**.

2.1 Restorative Dentistry

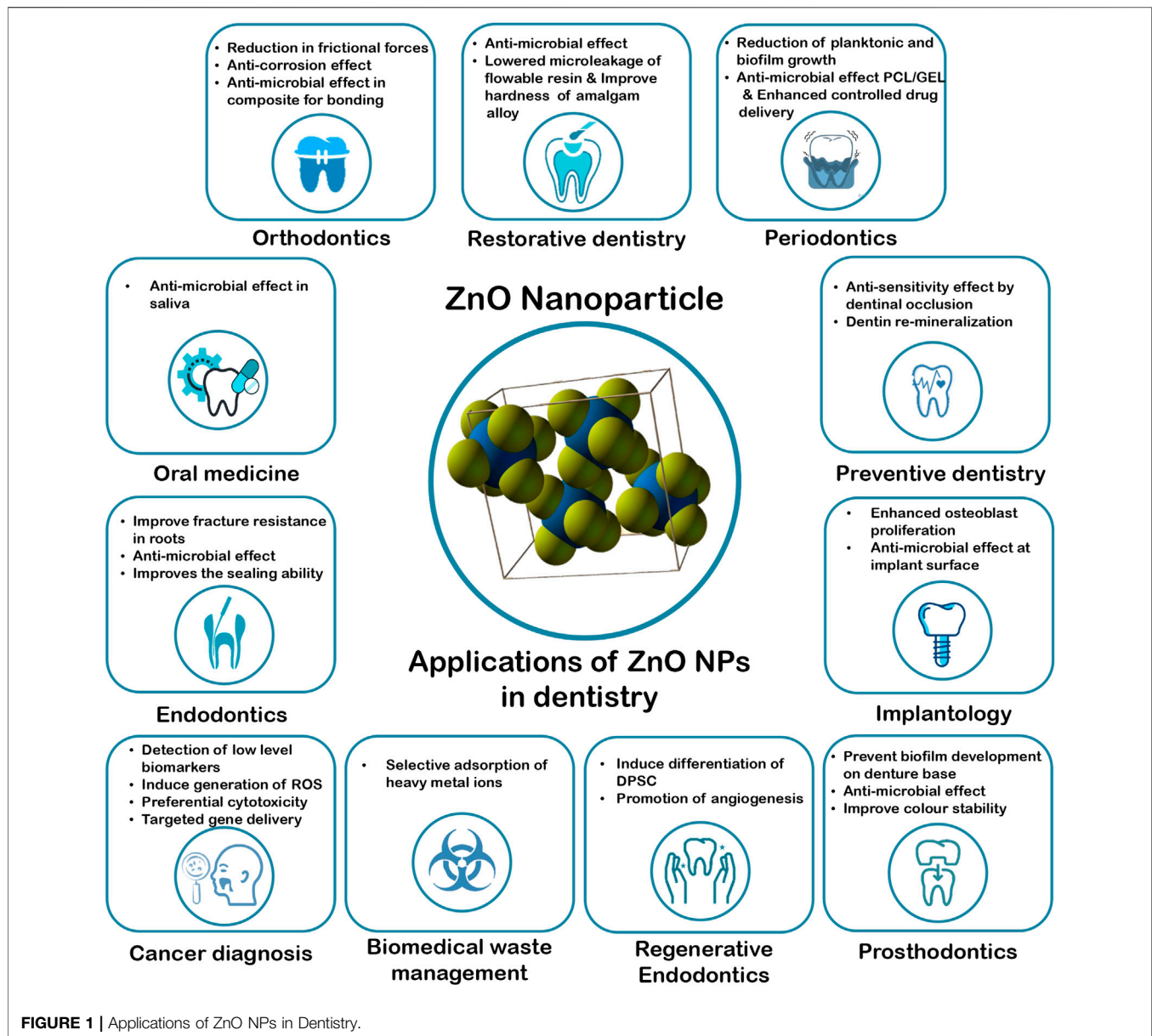
ZnO NPs have been found to improve the mechanical and anti-bacterial properties of dental restorative materials. According to a

study by Wang et al., it was reported that when ZnO NPs were incorporated in dental resin composites, there was inhibition in the growth and adhesion of *S. mutans*, and in small amounts did not affect the mechanical properties. This is extremely beneficial in not only in the prevention of secondary caries but also in the interception of bulk fracture of the material (Wang et al., 2019). Similarly, in a study done by Teymoornezhad et al., it was reported that incorporation of 3% ZnO NPs on flowable resin composite lowered the microleakage (Teymoornezhad et al., 2016). A comparable outcome was reported in the study by Hojati et al. (2013), on flowable resin composite (Tavassoli Hojati et al., 2013). When 10% ZnO NPs was added to resin-based dental composites, it showed anti-bacterial effectiveness against *S. Sobrinus* (Aydin Sevinç and Hanley 2010). These NPs were also found to exhibit anti-bacterial activity against *S. mutans* and *Lactobacillus* (Kasraei et al., 2014). ZnO NPs when incorporated in Glass Ionomer Cement (GIC) was also found to significantly improve the anti-bacterial properties against *S. mutans* without altering the mechanical properties (Vanajassun et al., 2014).

In various studies, it has been reported that incorporation of ZnO NPs into dental adhesive systems significantly improved the anti-microbial properties without affecting the bond strength adversely (Saffarpour et al., 2016; Jowkar et al., 2018; Gutiérrez et al., 2019). Zinc particles have proven to produce a strong bond at the interface of the dentin and resin by bringing about a decrease in the degeneration of collagen. The hardness of amalgam alloy was found to increase in proportion with the percentage loading of ZnO NPs (Yahya et al., 2013).

ZnO NPs when added to interim cements also exhibited anti-bacterial activity against *S. mutans* (Andrade et al., 2018). ZnO NPs were found to alter the lipid and protein contents of the cell membranes of *E. coli*, which caused distortion leading to leakage of cellular components, ultimately resulting in death (Liu et al., 2009). These properties are extremely beneficial in preventing the occurrence of secondary caries.

However, it was reported that the addition of 1% and 2% by weight of ZnO NPs into GIC did not exhibit anti-microbial activity against strains of *S. mutans*. This might be attributed to the inherent anti-bacterial property of the cement (Garcia et al., 2017). The incorporation of nano-spherical and nano-flower ZnO NPs to GIC was found to decrease the surface hardness, without affecting the flexural strength while incorporation of nano-rod ZnO NPs had no effect on the mechanical properties (Panahandeh et al., 2018). In another study done by Wang et al., it was reported that with the increase in the quantity of ZnO NPs, there was a decrease in the mechanical properties of dental composite resins, with the exception of flexural strength, which may be attributed to the agglomeration of the nanoparticles (Wang et al., 2019). In a systematic review by Arun et al., on the anti-bacterial properties of composite material incorporated with ZnO NPs, it was concluded that the material is unlikely to present a clinical advantage due to the short lifetime of anti-bacterial properties and the poor results against multi-species biofilms (Arun et al., 2021).



2.2 Endodontics

The applications of ZnO NPs in endodontics are diverse. In a study by Jowkar et al., When incorporated in EDTA solution for irrigation, the fracture resistance of the roots was enhanced (Jowkar et al., 2020a). In a study done by Aguiar et al., it was reported that these NPs promoted alkalization and action against *E. faecalis* when used as an intracanal medicament along with calcium hydroxide NPs and chlorhexidine (Aguiar et al., 2015). ZnO NPs when used as a sealer after endodontic therapy was found to exhibit excellent sealing efficacy along with remineralization of the radicular dentin thereby strengthening the tooth (Toledano et al., 2020). It was also reported that ZnO NPs brought about a reduction in the apical microleakage when used as a nano-sealer in endodontics (Javidi et al., 2014). It also significantly improved the

penetration depth into the dentinal tubules (Elkateb et al., 2015). Pristine gutta percha cones that were pre-treated argon plasma treatment and coated with ZnO NPs were found to exhibit antibacterial activity against *S. aureus* and *E. faecalis* which provides an excellent hermetic seal thereby reducing chances of reinfection and subsequent endodontic failure (Alves et al., 2018).

However, a study done by Jowkar et al., showed that push-out bond strength of the fiber posts did not improve on the addition of ZnO NPs (Jowkar et al., 2020b). When incorporated into Portland cement (PC) along with ZrO_2 , it was found not to impede with the anti-biofilm activity and to provide radiopacity to the cement. Also, the presence of ZnO NPs significantly reduced the compressive strength of the material (Guerreiro-Tanomaru et al., 2014).

2.3 Regenerative Endodontics

Incorporation of these NPs along with SiO₂, Na₂O, CaO and P₂O₅ to formulate Zinc-Bioglass, was reported to induce the differentiation of human Dental Pulp Stem Cells (hDPSCs) by bringing about an increase in the ALP activity (Huang et al., 2017). Similarly, it was reported that Zinc-Bioglass when incorporated with Calcium Phosphate Cement brought about odontogenic differentiation and also promoted angiogenesis by activating the Wnt, integrin, NF-κB, and MAPK pathways (Zhang et al., 2015). These play a pivotal role in the regeneration of the dentin-pulp tissues.

2.4 Periodontics

In the field of periodontal regeneration using guided tissue regeneration, the loading of ZnO NPs into composite membranes of polycaprolactone (PCL) and gelatin (GEL) which were electrospun, brought about reduction in the planktonic and the biofilm growth of the *S. aureus* significantly. These local anti-bacterial properties brought about enhancement in the clinical prognosis of treatments (Prado-Prone et al., 2020). Similarly, when ZnO NPs were incorporated in electrospun membranes made of PCL and PCL/GEL, it showed anti-bacterial activity against *P. gingivalis* and *F. nucleatum* species which in turn brought about an enhanced and better predictable periodontal regeneration (Münchow et al., 2015). ZnO NPs and serum albumin microspheres containing minocycline when incorporated in a Carbopol hydrogel exhibited enhancement of properties such as the anti-microbial spectrum, pH-responsiveness, sustained release, tissue-repairing and adhesion, and also enhanced controlled drug delivery that can increase stability of the drug (Mou et al., 2019).

2.5 Prosthodontics

The incorporation of ZnO NPs into the PMMA in denture bases was found to prevent biofilm development by *C. albicans* without exerting a cytotoxic effect on the host cells. Further research can advocate its application as a novel denture base material (Cierech et al., 2019). ZnO NPs in concentrations of 1wt% and 2wt% when incorporated in auto-polymerized acrylic resins was found to improve the flexural strength significantly (Kati 2019). In a study wherein 15 wt% ZnO NPs were incorporated into the tissue conditioner was also found to exhibit an anti-fungal effect (Homsiang et al., 2020). In another study, it was assessed that ZnO NPs along with chitosan and Silver NPs in the concentration of 2.5% inhibited the growth of *C. albicans*, and at a concentration of 5% inhibited the growth of *S. mutans*, *P. aeruginosa* and *E. faecalis* (Mousavi et al., 2020). The incorporation of 1.5% of ZnO NPs was found to improve the colour stability of silicone prosthesis (Charoenkijjajorn and Sanohkan 2020).

2.6 Orthodontics

Nanoparticles have been used in orthodontics to improve the quality of orthodontic treatment either in the form of nano-coated archwires, orthodontic adhesives, and orthodontic brackets (Tahmasbi et al., 2019; Moradpoor et al., 2021). The zinc oxide nanoparticles coated orthodontic appliances minimise

bacterial adhesion and enamel demineralization due to its antimicrobial and remineralization potential. Even attempts are made to add ZNO NPs into both orthodontic attachments and bonding materials since they provide a platform for bacterial attachment (Jatania and Shivalinga 2014; Riad et al., 2015; Reddy et al., 2016; Tahmasbi et al., 2019).

It was reported that coating of the NiTi wires with ZnO NPs brought about reduction in the frictional forces by 21% and exhibited anti-bacterial activity against *S. mutans*. It was also reported that ZnO NPs exhibited anti-corrosion effect that enhanced the corrosion resistance properties in the orthodontic wires (Kachoei et al., 2016). When a mixture of 10% weight each of ZnO NPs and chitosan NPs was incorporated into are resin-based dental composite bonding agents for the placement of brackets, it exhibited anti-bacterial activity against *S. mutans*, *S. sanguis* and *L. acidophilus*. This can significantly bring about reduction in the incidence of white-spot lesions during orthodontic therapy (Mirhashemi et al., 2013). Another study investigated that ZNO and CuO NPs coated orthodontic brackets showed better antibacterial activity against *S. mutans*, thus reducing the incidence of dental caries (Ramazanzadeh et al., 2015). It has been reported that when both orthodontic wires and brackets were coated with ZnO NPs the antibacterial potential against *S. mutans* was enhanced and reduced the frictional forces of coated wires (Behroozian et al., 2016). Similarly the stainless steel wires and orthodontic brackets coated with chitosan NPs or ZnO NPs reduced the friction between orthodontic brackets and a Stainless steel wire thus enhances the anchorage control and root resorption risk (Elhelbawy and Ellaithy 2021). Europium ions doped ZnO NPs were incorporated has orthodontic nanoadhesive enhanced the visibility of material for thorough removal of orthodontic adhesive after completion of treatment (Yamagata et al., 2012). It has been reported that orthodontic adhesive with less titanium dioxide, zinc oxide, and silver NPs causes bracket failure because the combination reduces shear bond strength (Reddy et al., 2016). The addition of ZnO to a light cure resin modified GIC as an orthodontic bonding agent improved the original compound's antimicrobial, physical, and flexural properties (Nuri Sari et al., 2015). Hence ZnO NPs have the potential to be widely used in orthodontic applications to improve treatment outcomes, including increased strength of materials and reduced bacterial count around the orthodontic appliance.

2.7 Oral Medicine

ZnO NPs have an inhibitory effect on *C. albicans* in saliva and hence can be used in the treatment of oral thrush, starting from a concentration of 0.05 mg/ml. It was also reported that ZnO NPs along with Silver NPs exhibited enhanced anti-bacterial effect in human and artificial saliva, which can have widespread applications in clinical scenarios (Pokrowiecki et al., 2019). ZnO NPs which are biosynthesized from *Beta vulgaris* was found to exhibit anti-fungal effect on pathogens such as *Aspergillus niger* and *C. albicans* (Pillai et al., 2020). ZnO NPs that are synthesized from Aloe vera leaf extract have been demonstrated to exhibit pronounced sensitivity to *E. coli*, *P. aeruginosa* and Methicillin Resistant *S. aureus*, and hence can

be considered as a promising candidate for nano-antibiotics, which deals with the enhancement of the effect against the bacterial strains that are resilient to conventional antibiotics (Ali et al., 2016). These NPs when conjugated with drugs such as Quercetin, Ceftriaxone, Ampicillin, Naringin and Amphotericin B showed enhanced drug efficacy against Methicillin resistant *S. aureus*, *S. pneumoniae*, *S. pyogenes*, *E. coli*, *Serratia marcescens* and *P. aeruginosa*. Hence, they provide a propitious approach in the combat against disease resistant pathogens (Akbar et al., 2021).

2.8 Cancer Diagnosis

ZnO NPs can be implicated in the diagnosis of cancers as it is proven to detect low-level expression of biomarkers which are used for early cancer detection. *In vitro*, it exhibits an inherent preferential cytotoxicity against cancer cells. It also possesses the ability to induce the generation of Reactive Oxygen Species (ROS) due to its semiconductor properties, as the electrons within the NPs can react with O₂ or hydroxyl ions or water after migrating to the surface to form superoxide and hydroxyl radicals (Manthe et al., 2010). These can set about cell death when the anti-oxidative capacity of the cell is exceeded. Research is being carried out on the utilization of ZnO NPs for gene silencing and targeted gene delivery, which can be utilized to combat cancer (Rasmussen et al., 2010). ZnO NPs that were coated with polyethylene glycol (PEG) were found to exhibit enhanced anti-bacterial activity against *E. coli* and *S. aureus* by bringing about damage to the cell membrane. They were also found to exhibit a low concentration threshold for cytotoxic action, with a which is due to the upregulation of the Fas ligand on the cell membrane which brings about apoptosis of the cancer cells (Nair et al., 2008). ZnO NPs also exhibits an efficient role in non-surgical tumor ablation method used in cancer therapy. It was demonstrated that ZnO NPs when combined with anti-cancer drug daunorubicin, along with Ultra Violet irradiation, exhibited synergistic cytotoxic effects on the leukemic cells (Guo et al., 2008).

2.9 Biomedical Waste Management

The ZnO NPs are found to selectively remove heavy metal ions such as Chromium by adsorption by virtue of their hydroxyl ions. It can therefore be used in dental waste water purification treatment as a green pollutant-diminishing strategy (Gu et al., 2020). Other studies have proven the efficacy of ZnO NPs which can be used in nano-composite membranes used for the purification of water. This is due to its antibacterial activity against *S. aureus* and the favourable photocatalytic activity, which enhances the adsorption of organic pollutants, pesticides and microbes that are found in the wastewater rendering it safe (Spoială et al., 2021).

2.10 Implantology

Chemical modifications of dental implant surfaces with ZnO NPs, which are effective antimicrobial agents, have been carried out in order to reduce the risk of dental implant failure and improve osteointegration. On coating the implant surface with ZnO NPs, the underlying osteoblast cells exhibited an enhanced proliferation after 5 and 10 days. They also exhibited antimicrobial properties against *S. aureus*. These properties are

useful to promote bone growth and in the inhibition of infection at the implant site (Memarzadeh et al., 2015). Similar results were reported in studies by Abdulkareem et al. and Kulshrestha et al., on the effect of ZnO NPs against *S. mutans* biofilm on dental implant surfaces (Kulshrestha et al., 2014; Abdulkareem et al., 2015). According to the findings, ZnO bio-functionalized thin films containing DMP1 peptides can improve the physicochemical, osteogenic, apatite nucleation and corrosion resistance properties of this material suggesting promising applications in dental implant (Trino et al., 2018).

Titanium (Ti)-zinc (Zn)-oxide nanocomposite-(nC) thin films were co-sputtered to strengthen the cohesiveness of metallic fixtures with bone. The developed thin film also exhibited strong antibacterial activity against *S. aureus* and *E. coli* (Goel et al., 2019). Modified titanium implant materials developed using N-halamine and ZnO nanoparticles demonstrated remarkable antibacterial activity against *P. aeruginosa*, *E. coli*, and *S. aureus* without using antibiotics (Li et al., 2017). Titanium implants with coatings of Poly (lactic-co-glycolic acid)/Silver/ZnO nanorods demonstrated long-lasting antibacterial activity against *S. aureus* and *E. coli*, as well as excellent cytocompatibility and biocompatibility (Xiang et al., 2017).

2.11 Preventive Dentistry

ZnO NPs incorporated in a dentifrice was found to cause dentinal tubule occlusion. These can also be incorporated as preservatives in dentifrices as it not only brings about inhibition of dentin demineralization but also exhibits enhanced anti-microbial effects (Khan et al., 2020). Its incorporation and in nanogels and application on eroded cervical dentin, was found to promote dentin mineralization (Toledano et al., 2019). These can be utilized in achieving an anti-sensitivity effect. Studies have shown that dentin which is treated with ZnO NPs exhibited greater ability to produce dentinal tubule occlusion which makes it an effective agent in the treatment of dentinal hypersensitivity [67]. The ZnO NPs treated dentin was found to have higher levels of proteoglycans that act as bonding agents between the HAp crystals and collagen network. Further, they enhance the release small integrin-binding ligand N-linked glycoproteins and small leucine-rich proteoglycans from dentin through Matrix Metalloproteinase-3 activity. These proteins take part in the mineralization of dentin, and the immobilized phosphorylated proteins induce formation of mineral. Zinc NPs also reduces the collagen degradation which is mediated by Matrix Metalloproteinase-3 in dentin that is partially demineralized and hence promotes dentin re-mineralization (Toledano-Osorio et al., 2018; Toledano et al., 2019).

3 CONCLUSION

Nano-dentistry has opened a new standpoint for revolution in oral care and portrays a growing field with the capability to address the new and improved applications in dentistry. ZnO NPs have a broad spectrum of applications the various fields of dentistry such as restorative dentistry, endodontics, regenerative endodontics, periodontology, prosthodontics, orthodontics, implantology, preventive dentistry among other fields. The use

of ZnO NPs represents a broadening horizon for the diagnosis, treatment, and prevention of various oral conditions, and in enhancing the characteristics of existing dental materials. It is hence crucial to strengthen the symbiosis between clinicians and materials scientists as nano-dentistry is still technology driven, with many roadblocks ahead. However, most of the research is still in the development pipeline and for realizing the complete *in vivo* potential in dentistry, further research that focus on its clinical implications should be carried out.

AUTHOR CONTRIBUTIONS

PC: Conceptualization, Resources, Data Curation, Original Draft Preparation, Supervision. GS: Conceptualization,

Resources, Data Curation, Original Draft Preparation. SV: Original Draft Preparation, Review & Editing, Visualization. DA: Original Draft Preparation, Review & Editing, Visualization. AA: Review & Editing, Visualization, Supervision. BZ: Review & Editing, Visualization, Supervision. NA: Review & Editing, Visualization, Supervision. SP: Original Draft Preparation, Review & Editing, Visualization, Supervision. All authors agree to be accountable for the content of the work.

ACKNOWLEDGMENTS

The authors thank MS Ramaiah University of Applied Sciences for the support.

REFERENCES

- Abdulkareem, E. H., Memarzadeh, K., Allaker, R. P., Huang, J., Pratten, J., and Spratt, D. (2015). Anti-biofilm Activity of Zinc Oxide and Hydroxyapatite Nanoparticles as Dental Implant Coating Materials. *J. Dent.* 43, 1462–1469. doi:10.1016/j.jdent.2015.10.010
- Aguiar, A. S., Guerreiro-Tanamaru, J. M., Faria, G., Leonardo, R. T., and Tanomaru-Filho, M. (2015). *J. Contemp. Dent. P. R.* 16, 624–629.
- Akbar, N., Aslam, Z., Siddiqui, R., Shah, M. R., and Khan, N. A. (2021). Zinc Oxide Nanoparticles Conjugated with Clinically-Approved Medicines as Potential Antibacterial Molecules. *Amb. Expr.* 11, 104. doi:10.1186/s13568-021-01261-1
- Ali, K., Dwivedi, S., Azam, A., Saquib, Q., Al-Said, M. S., Alkhedhairi, A. A., et al. (2016). Aloe Vera Extract Functionalized Zinc Oxide Nanoparticles as Nanoantibiotics against Multi-Drug Resistant Clinical Bacterial Isolates. *J. Colloid Interface Sci.* 472, 145–156. doi:10.1016/j.jcis.2016.03.021
- Alves, M. J., Grenho, L., Lopes, C., Borges, J., Vaz, F., Vaz, I. P., et al. (2018). Antibacterial Effect and Biocompatibility of a Novel Nanostructured ZnO-Coated Gutta-Percha Cone for Improved Endodontic Treatment. *Mater. Sci. Eng. C* 92, 840–848. doi:10.1016/j.msec.2018.07.045
- Andrade, V., Martínez, A., Rojas, N., Bello-Toledo, H., Flores, P., Sánchez-Sanhueza, G., et al. (2018). *J. Prosthet. Dent.* 119, 862–e1. doi:10.1016/j.prosdent.2017.09.015
- Arun, D., Adikari Mudiyansele, D., Gulam Mohamed, R., Liddell, M., Monsur Hassan, N. M., and Sharma, D. (2021). *Materials* 14, 40.
- Aydin Sevinç, B., and Hanley, L. (2010). *J. Biomed. Mat. Res. B Appl. Biomater.* 94, 22–31.
- Baek, M., Chung, H.-E., Yu, J., Lee, J.-A., Kim, T.-H., Oh, J.-M., et al. (2012). *Int. J. Nanomedicine* 7, 3081.
- Behroozian, A., Kachoei, M., Khatamian, M., and Divband, B. (2016). The Effect of ZnO Nanoparticle Coating on the Frictional resistance between Orthodontic Wires and Ceramic Brackets. *J. Dent. Res. Dent. Clin. Dent. Prospects* 10 (2), 106–111. doi:10.15171/joddd.2016.017
- Carrouel, F., Viennot, S., Ottolenghi, L., Gaillard, C., and Bourgeois, D. (2020). Nanoparticles as Anti-microbial, Anti-inflammatory, and Remineralizing Agents in Oral Care Cosmetics: a Review of the Current Situation. *Nanomaterials* 10 (1), 140. doi:10.3390/nano10010140
- Charoenkijakorn, D., and Sanohkan, S. (2020). The Effect of Nano Zinc Oxide Particles on Color Stability of MDX4-4210 Silicone Prostheses. *Eur. J. Dent.* 14, 525–532. doi:10.1055/s-0040-1713058
- Cierech, M., Wojnarowicz, J., Kolenda, A., Krawczyk-Balska, A., Prochwicz, E., Woźniak, B., et al. (2019). Zinc Oxide Nanoparticles Cytotoxicity and Release from Newly Formed PMMA-ZnO Nanocomposites Designed for Denture Bases. *Nanomaterials* 9, 1318. doi:10.3390/nano9091318
- Elhelbawy, N., and Ellaithy, M. (2021). Comparative Evaluation of Stainless-Steel Wires and Brackets Coated with Nanoparticles of Chitosan or Zinc Oxide upon Friction: An *In Vitro* Study. *Int. Orthod.* 19 (2), 274–280. doi:10.1016/j.ortho.2021.01.009
- Elkateb, W., Massoud, A., and Mokhless, N. (2015). *Trans. Shalaby*, 11.
- Garcia, P. P. N. S., Cardia, M. F. B., Francisconi, R. S., Dovigo, L. N., Spolidório, D. M. P., de Souza Rastelli, A. N., et al. (2017). Antibacterial Activity of Glass Ionomer Cement Modified by Zinc Oxide Nanoparticles. *Microsc. Res. Tech.* 80, 456–461. doi:10.1002/jemt.22814
- Goel, S., Dubey, P., Ray, S., Jayaganthan, R., Pant, A. B., and Chandra, R. (2019). Co-sputtered Antibacterial and Biocompatible Nanocomposite Titania-Zinc Oxide Thin Films on Si Substrates for Dental Implant Applications. *Mater. Technol.* 34 (1), 32–42. doi:10.1080/10667857.2018.1488924
- Gu, M., Hao, L., Wang, Y., Li, X., Chen, Y., Li, W., et al. (2020). The Selective Heavy Metal Ions Adsorption of Zinc Oxide Nanoparticles from Dental Wastewater. *Chem. Phys.* 534, 110750. doi:10.1016/j.chemphys.2020.110750
- Guerreiro-Tanamaru, J. M., Trindade-Junior, A., Cesar Costa, B., da Silva, G. F., Drullis Cifali, L., Basso Bernardi, M. L., et al. (2014). *Sci. World J.* 2014. doi:10.1155/2014/975213
- Guo, D., Wu, C., Jiang, H., Li, Q., Wang, X., and Chen, B. (2008). Synergistic Cytotoxic Effect of Different Sized ZnO Nanoparticles and Daunorubicin against Leukemia Cancer Cells under UV Irradiation. *J. Photochem. Photobiol. B Biol.* 93, 119–126. doi:10.1016/j.jphotobiol.2008.07.009
- Gutiérrez, M. F., Alegria-Acevedo, L. F., Méndez-Bauer, L., Bermudez, J., Dávila-Sánchez, A., Buvinic, S., et al. (2019). *J. Dent.* 82, 45–55.
- Homsiang, W., Kamonkhanitkul, K., Arksornnukit, M., and Takahashi, H. (2020). *Dent. Mat. J.*
- Huang, M., Hill, R. G., and Rawlinson, S. C. F. (2017). Zinc Bioglasses Regulate Mineralization in Human Dental Pulp Stem Cells. *Dent. Mater.* 33, 543–552. doi:10.1016/j.dental.2017.03.011
- Jatania, A., and Shivalinga, B. M. (2014). An *In Vitro* Study to Evaluate the Effects of Addition of Zinc Oxide to an Orthodontic Bonding Agent. *Eur. J. Dent.* 08 (01), 112–117. doi:10.4103/1305-7456.126262
- Javidi, M., Zarei, M., Naghavi, N., Mortazavi, M., and Nejat, A. H. (2014). *Contemp. Clin. Dent.* 5, 20.
- Jowkar, Z., Farpour, N., Koohpeima, F., Mokhtari, M. J., and Shafiei, F. (2018). *J. Contemp. Dent. P. R.* 19, 1404–1411.
- Jowkar, Z., Hamidi, S. A., Shafiei, F., and Ghahramani, Y. (2020). The Effect of Silver, Zinc Oxide, and Titanium Dioxide Nanoparticles Used as Final Irrigation Solutions on the Fracture Resistance of Root-Filled Teeth. *Cide* Vol. 12, 141–148. doi:10.2147/ccide.s253251
- Jowkar, Z., Omid, Y., and Shafiei, F. (2020). *J. Clin. Exp. Dent.* 12, e249.
- Kachoei, M., Nourian, A., Divband, B., Kachoei, Z., and Shirazi, S. (2016). Zinc-oxide Nanocoating for Improvement of the Antibacterial and Frictional Behavior of Nickel-Titanium Alloy. *Nanomedicine* 11, 2511–2527. doi:10.2217/nnm-2016-0171
- Kasraei, S., Sami, L., Hendi, S., AliKhani, M.-Y., Rezaei-Soufi, L., and Khamverdi, Z. (2014). Antibacterial Properties of Composite Resins Incorporating Silver and Zinc Oxide Nanoparticles on *Streptococcus mutans* and *Lactobacillus*. *Restor. Dent. Endod.* 39, 109–114. doi:10.5395/rde.2014.39.2.109
- Kati, F. A. (2019). Effect of the Incorporation of Zinc Oxide Nanoparticles on the Flexural Strength of Auto-Polymerized Acrylic Resins. *J. Oral Res.* 8, 37–41. doi:10.17126/joralres.2019.010

- Khan, A. S., Farooq, I., Alakrawi, K. M., Khalid, H., Saadi, O. W., and Hakeem, A. S. (2020). Dentin Tubule Occlusion Potential of Novel Dentifrices Having Fluoride Containing Bioactive Glass and Zinc Oxide Nanoparticles. *Med. Princ. Pract.* 29, 338–346. doi:10.1159/000503706
- Kulshrestha, S., Khan, S., Meena, R., Singh, B. R., and Khan, A. U. (2014). A Graphene/zinc Oxide Nanocomposite Film Protects Dental Implant Surfaces against cariogenic *Streptococcus Mutans*. *Biofouling* 30, 1281–1294. doi:10.1080/08927014.2014.983093
- Li, Y., Liu, X., Tan, L., Cui, Z., Yang, X., Yeung, K. W. K., et al. (2017). Construction of N-Halamine Labeled Silica/zinc Oxide Hybrid Nanoparticles for Enhancing Antibacterial Ability of Ti Implants. *Mater. Sci. Eng. C* 76, 50–58. doi:10.1016/j.msec.2017.02.160
- Liu, Y., He, L., Mustapha, A., Li, H., Hu, Z. Q., and Lin, M. (2009). Antibacterial Activities of Zinc Oxide Nanoparticles against *Escherichia coli* O157:H7. *J. Appl. Microbiol.* 107, 1193–1201. doi:10.1111/j.1365-2672.2009.04303.x
- Manthe, R. L., Foy, S. P., Krishnamurthy, N., Sharma, B., and Labhasetwar, V. (2010). Tumor Ablation and Nanotechnology. *Mol. Pharm.* 7, 1880–1898. doi:10.1021/mp1001944
- Memarzadeh, K., Sharili, A. S., Huang, J., Rawlinson, S. C. F., and Allaker, R. P. (2015). Nanoparticulate Zinc Oxide as a Coating Material for Orthopedic and Dental Implants. *J. Biomed. Mat. Res.* 103, 981–989. doi:10.1002/jbm.a.35241
- Mirhashemi, A., Bahador, A., Kassaei, M., Daryakenari, G., Ahmad-Akhoundi, M., and Sodagar, A. (2013). *J. Med. Bacteriol.* 2, 1–10.
- Moradpoor, H., Safaei, M., Mozaffari, H. R., Sharifi, R., Imani, M. M., Golshah, A., et al. (2021). An Overview of Recent Progress in Dental Applications of Zinc Oxide Nanoparticles. *RSC Adv.* 11 (34), 21189–21206. doi:10.1039/d0ra10789a
- Mou, J., Liu, Z., Liu, J., Lu, J., Zhu, W., and Pei, D. (2019). Hydrogel Containing Minocycline and Zinc Oxide-Loaded Serum Albumin Nanoparticle for Periodontitis Application: Preparation, Characterization and Evaluation. *Drug Deliv.* 26, 179–187. doi:10.1080/10717544.2019.1571121
- Mousavi, S. A., Ghotaslou, R., Khorramdel, A., Akbarzadeh, A., and Aeinfar, A. (2020). *Ir. J. Med. Sci.*
- Münchow, E. A., Albuquerque, M. T. P., Zero, B., Kamocki, K., Piva, E., Gregory, R. L., et al. (2015). *Dent. Mat.* 31, 1038–1051.
- Nair, S., Sasidharan, A., Divya Rani, V. V., Menon, D., Nair, S., Manzoor, K., et al. (2008). Role of Size Scale of ZnO Nanoparticles and Microparticles on Toxicity toward Bacteria and Osteoblast Cancer Cells. *J. Mater. Sci. Mater. Med.* 20, 235–241. doi:10.1007/s10856-008-3548-5
- Nuri Sari, M., Rahmani, N., Araghbidi Kashani, M., Eslami Amirabadi, G., Akbari Sari, A., and Seyedtabaie, E. (2015). Effect of Incorporation of Nano-Hydroxyapatite and Nano-Zinc Oxide in Resin Modified Glass Ionomer Cement on Metal Bracket Debonding. *J. Islamic Dent. Assoc. Iran* 27 (2), 70–76.
- Panahandeh, N., Torabzadeh, H., Aghaee, M., Hasani, E., and Safa, S. (2018). *J. Conserv. Dent.* JCD 21, 130.
- Pillai, A. M., Sivasankarapillai, V. S., Rahdar, A., Joseph, J., Sadeghfard, F., Anuf, A. R., et al. (2020). Green Synthesis and Characterization of Zinc Oxide Nanoparticles with Antibacterial and Antifungal Activity. *J. Mol. Struct.* 1211, 128107. doi:10.1016/j.molstruc.2020.128107
- Pokrowiecki, R., Wojnarowicz, J., Zareba, T., Koltsov, I., Lojkowski, W., Tyski, S., et al. (2019). Nanoparticles and Human Saliva: A Step towards Drug Delivery Systems for Dental and Craniofacial Biomaterials. *Ijn* 14, 9235–9257. doi:10.2147/ijn.s221608
- Prado-Prone, G., Silva-Bermudez, P., Bazzar, M., Focarete, M. L., Rodil, S. E., Vidal-Gutiérrez, X., et al. (2020). Antibacterial Composite Membranes of Polycaprolactone/gelatin Loaded with Zinc Oxide Nanoparticles for Guided Tissue Regeneration. *Biomed. Mat.* 15, 035006. doi:10.1088/1748-605x/ab70ef
- Ramazanazadeh, B., Jahanbin, A., Yaghoubi, M., Shahtahmassbi, N., Ghazvini, K., Shakeri, M., et al. (2015). Comparison of Antibacterial Effects of ZnO and CuO Nanoparticles Coated Brackets against *Streptococcus Mutans*. *J. Dent. (Shiraz)* 16 (3), 200–205.
- Rasmussen, J. W., Martinez, E., Louka, P., and Wingett, D. G. (2010). Zinc Oxide Nanoparticles for Selective Destruction of Tumor Cells and Potential for Drug Delivery Applications. *Expert Opin. Drug Deliv.* 7, 1063–1077. doi:10.1517/17425247.2010.502560
- Reddy, A. K., Kambalyal, P. B., Patil, S. R., Vankhre, M., Khan, M. Y., and Kumar, T. R. (2016). Comparative Evaluation and Influence on Shear Bond Strength of Incorporating Silver, Zinc Oxide, and Titanium Dioxide Nanoparticles in Orthodontic Adhesive. *J. Orthod. Sci.* 5 (4), 127–131. doi:10.4103/2278-0203.192115
- Riad, M., Harhash, A. Y., Elhiny, O. A., and Salem, G. A. (2015). Evaluation of the Shear Bond Strength of Orthodontic Adhesive System Containing Antimicrobial Silver Nano Particles on Bonding of Metal Brackets to Enamel. *Life Sci. J.* 12 (12), 27–34.
- Saffarpour, M., Rahmani, M., Tahriri, M., and Peymani, A. (2016). Antimicrobial and Bond Strength Properties of a Dental Adhesive Containing Zinc Oxide Nanoparticles. *Braz. J. Oral Sci.* 15, 66–69. doi:10.20396/bjos.v15i1.8647127
- Spoială, A., Ilie, C.-I., Truşcă, R.-D., Oprea, O.-C., Surdu, V.-A., ŞtefanVasile, B., et al. (2021). *Mat. Basel Switz.* 14, 4747.
- Şuhani, M. F., Băciuş, G., Băciuş, M., Şuhani, R., and Bran, S. (2018). *Clujul Med.* 91, 274.
- Tahmasbi, S., Mohamadian, F., Hosseini, S., and Eftekhar, L. (2019). A Review on the Applications of Nanotechnology in Orthodontics. *Nanomedicine J.* 6 (1), 11–18.
- Tavassoli Hojati, S., Alaghemand, H., Hamze, F., Ahmadian Babaki, F., Rajab-Nia, R., Rezvani, M. B., et al. (2013). Antibacterial, Physical and Mechanical Properties of Flowable Resin Composites Containing Zinc Oxide Nanoparticles. *Dent. Mater.* 29, 495–505. doi:10.1016/j.dental.2013.03.011
- Teymoornezhad, K., Alaghemand, H., Daryakenari, G., Khafri, S., and Tabari, M. (2016). Evaluating the Microshear Bond Strength and Microleakage of Flowable Composites Containing Zinc Oxide Nano-Particles. *Electron. Physician* 8, 3289–3295. doi:10.19082/3289
- Toledano, M., Cabello, I., Osorio, E., Aguilera, F. S., Medina-Castillo, A. L., Toledano-Osorio, M., et al. (2019). Zn-containing Polymer Nanogels Promote Cervical Dentin Remineralization. *Clin. Oral Invest.* 23, 1197–1208. doi:10.1007/s00784-018-2548-1
- Toledano, M., Osorio, E., Aguilera, F. S., Muñoz-Soto, E., Toledano-Osorio, M., López-López, M. T., et al. (2020). Polymeric Nanoparticles for Endodontic Therapy. *J. Mech. Behav. Biomed. Mater.* 103, 103606. doi:10.1016/j.jmbbm.2019.103606
- Toledano-Osorio, M., Osorio, E., Aguilera, F. S., Luis Medina-Castillo, A., Toledano, M., and Osorio, R. (2018). Improved Reactive Nanoparticles to Treat Dentin Hypersensitivity. *Acta Biomater.* 72, 371–380. doi:10.1016/j.actbio.2018.03.033
- Trino, L. D., Albano, L. G. S., Bronze-Uhle, E. S., George, A., Mathew, M. T., and Lisboa-Filho, P. N. (2018). Physicochemical, Osteogenic and Corrosion Properties of Bio-Functionalized ZnO Thin Films: Potential Material for Biomedical Applications. *Ceram. Int.* 44 (17), 21004–21014. doi:10.1016/j.ceramint.2018.08.136
- Vanajassun, P. P., Nivedhitha, M. S., Nishad, N. T., and Soman, D. (2014). *Adv. Hum. Biol.* 4, 31.
- Wang, Y., Hua, H., Li, W., Wang, R., Jiang, X., and Zhu, M. (2019). Strong Antibacterial Dental Resin Composites Containing Cellulose Nanocrystal/zinc Oxide Nanohybrids. *J. Dent.* 80, 23–29. doi:10.1016/j.jdent.2018.11.002
- Wiesmann, N., Tremel, W., and Brieger, J. (2020). Zinc Oxide Nanoparticles for Therapeutic Purposes in Cancer Medicine. *J. Mat. Chem. B* 8 (23), 4973–4989. doi:10.1039/d0tb00739k
- Xiang, Y., Li, J., Liu, X., Cui, Z., Yang, X., Yeung, K. W. K., et al. (2017). Construction of Poly(lactic-Co-Glycolic acid)/ZnO nanorods/Ag Nanoparticles Hybrid Coating on Ti Implants for Enhanced Antibacterial Activity and Biocompatibility. *Mater. Sci. Eng. C* 79, 629–637. doi:10.1016/j.msec.2017.05.115
- Yahya, N., Puspitasari, P., and Latiff, N. R. A. (2013). Hardness Improvement of Dental Amalgam Using Zinc Oxide and Aluminum Oxide Nanoparticles. *Charact. Dev. Biosyst. Biomater.*, 9–32. doi:10.1007/978-3-642-31470-4_2
- Yamagata, S., Hamba, Y., Nakanishi, K., Abe, S., Akasaka, T., Ushijima, N., et al. (2012). Introduction of Rare-Earth-Element-Containing ZnO Nanoparticles into Orthodontic Adhesives. *Nano Biomed.* 4 (1), 11–17.

Zhang, J., Park, Y.-D., Bae, W.-J., El-Fiqi, A., Shin, S.-H., Lee, E.-J., et al. (2015). Effects of Bioactive Cements Incorporating Zinc-Bioglass Nanoparticles on Odontogenic and Angiogenic Potential of Human Dental Pulp Cells. *J. Biomater. Appl.* 29, 954–964. doi:10.1177/0885328214550896

Conflict of Interest: The authors declare that the research was conducted in the absence of any commercial or financial relationships that could be construed as a potential conflict of interest.

Publisher's Note: All claims expressed in this article are solely those of the authors and do not necessarily represent those of their affiliated organizations, or those of

the publisher, the editors and the reviewers. Any product that may be evaluated in this article, or claim that may be made by its manufacturer, is not guaranteed or endorsed by the publisher.

Copyright © 2022 Pushpalatha, Suresh, Gayathri, Sowmya, Augustine, Alamoudi, Zidane, Mohammad Albar and Patil. This is an open-access article distributed under the terms of the Creative Commons Attribution License (CC BY). The use, distribution or reproduction in other forums is permitted, provided the original author(s) and the copyright owner(s) are credited and that the original publication in this journal is cited, in accordance with accepted academic practice. No use, distribution or reproduction is permitted which does not comply with these terms.



Impact of Frontier Development of Alveolar Bone Grafting on Orthodontic Tooth Movement

Yilan Miao^{1†}, Yu-Cheng Chang^{2†}, Nipul Tanna³, Nicolette Almer³, Chun-Hsi Chung³, Min Zou^{4,5,6}, Zhong Zheng^{7,8*} and Chenshuang Li^{3*}

¹School of Dental Medicine, University of Pennsylvania, Philadelphia, PA, United States, ²Department of Periodontics, School of Dental Medicine, University of Pennsylvania, Philadelphia, PA, United States, ³Department of Orthodontics, School of Dental Medicine, University of Pennsylvania, Philadelphia, PA, United States, ⁴Key Laboratory of Shanxi Province for Craniofacial Precision Medicine Research, College of Stomatology, Xi'an Jiaotong University, Xi'an, China, ⁵Clinical Research Center of Shanxi Province for Dental and Maxillofacial Diseases, College of Stomatology, Xi'an Jiaotong University, Xi'an, China, ⁶Department of Orthodontics, College of Stomatology, Xi'an Jiaotong University, Xi'an, China, ⁷David Geffen School of Medicine, University of California, Los Angeles, Los Angeles, CA, United States, ⁸School of Dentistry, University of California, Los Angeles, Los Angeles, CA, United States

OPEN ACCESS

Edited by:

Mohammad Khurshed Alam,
Al Jouf University, Saudi Arabia

Reviewed by:

Tarek El-Bialy,
University of Alberta, Canada

*Correspondence:

Zhong Zheng
zzheng@dentistry.ucla.edu
Chenshuang Li
lichens@upenn.edu

[†]These two authors have contributed
equally to this work and share the first
authorship

Specialty section:

This article was submitted to
Biomaterials,
a section of the journal
Frontiers in Bioengineering and
Biotechnology

Received: 04 February 2022

Accepted: 13 June 2022

Published: 30 June 2022

Citation:

Miao Y, Chang Y-C, Tanna N, Almer N,
Chung C-H, Zou M, Zheng Z and Li C
(2022) Impact of Frontier Development
of Alveolar Bone Grafting on
Orthodontic Tooth Movement.
Front. Bioeng. Biotechnol. 10:869191.
doi: 10.3389/fbioe.2022.869191

Sufficient alveolar bone is a safeguard for achieving desired outcomes in orthodontic treatment. Moving a tooth into an alveolar bony defect may result in a periodontal defect or worse—tooth loss. Therefore, when facing a pathologic situation such as periodontal bone loss, alveolar clefts, long-term tooth loss, trauma, and thin phenotype, bone grafting is often necessary to augment bone for orthodontic treatment purposes. Currently, diverse bone grafts are used in clinical practice, but no single grafting material shows absolutely superior results over the others. All available materials demonstrate pros and cons, most notably donor morbidity and adverse effects on orthodontic treatment. Here, we review newly developed graft materials that are still in the pre-clinical stage, as well as new combinations of existing materials, by highlighting their effects on alveolar bone regeneration and orthodontic tooth movement. In addition, novel manufacturing techniques, such as bioprinting, will be discussed. This mini-review article will provide state-of-the-art information to assist clinicians in selecting grafting material(s) that enhance alveolar bone augmentation while avoiding unfavorable side effects during orthodontic treatment.

Keywords: orthodontic tooth movement, alveolar bone graft, novel material, BMP-2, platelet-rich fibrin (PRF), bioactive glass, stem cell

INTRODUCTION

To avoid fenestrations or dehiscences during orthodontic tooth movement, it is critical for alveolar bone to possess adequate contour, thickness, and quality (Atwood and Coy, 1971; Abrams et al., 1987; Seifi and Ghoraishian, 2012). Orthodontically moving teeth into a region with reduced alveolar bone can worsen the periodontal status, slow down tooth movement, and cause root resorption or even tooth loss (Reichert et al., 2010). Clinical scenarios such as severe periodontitis, congenital alveolar clefts, long-term tooth loss, and trauma can induce alveolar bone loss (McAllister and Haghighat, 2007). Thus, augmentation of insufficient bone volume is often indicated prior to the initiation of orthodontic treatment.

In addition, patients with a thin phenotype have narrow alveolar bone support, which significantly limits the range of orthodontic tooth movement. To address this issue, the

TABLE 1 | The alveolar bone regeneration efficiency and the orthodontic implications of the alveolar bone grafting materials.

Materials	References	Combinatory Materials	Type of Study	Alveolar Bone Regeneration Efficiency		Side Effects			Impact on Orthodontics	
				Volume	Cellular Activity	Inflammation	Pain	Graft Failure	Tooth Movement Rate	Adverse Effect
BMP2	Kawamoto et al. (2002)	poly [D,L-(lactide-co-glycolide)]/gelatin sponge complex	Animal study (dog)	Significantly greater regenerated bone than spongiosa autograft	More osteoinductive activity associated with rhBMP2	N/A	N/A	N/A	Both rhBMP2 and spongiosa groups showed similar responses to orthodontic force as normal alveolar bone	Root resorption on pressure side with rhBMP2
	Hammoudeh et al. (2017)	DBM scaffold	Clinical study (secondary alveolar cleft repair)	Comparable bone regrowth and density as autologous iliac crest bone graft	N/A	Self-limited facial swelling, minor wound dehiscence	Improved without intervention	No increase in serious adverse events compared to iliac bone graft	Similar spontaneous canine eruption rate was observed among rhBMP2 and iliac crest bone groups	N/A
	Chandra et al. (2019)	N/A	Clinical study (PAOO)	A highly significant increase in bone density compared to conventional corticotomy procedure	BMP-2 stimulates recruitment and differentiation of osteoclasts	No significant difference on wound healing	No significant difference on pain scores	N/A	Reduced orthodontic treatment time	N/A
	Jiang et al. (2020)	BMP2-functionalized BioCaP granules	Animal study (dogs)	Compared to bovine xenograft: 1.25-fold enhanced bone formation, 1.42-fold more graft resorption, 1.36-fold higher bone density	BMP mediated osteogenesis-angiogenesis coupling	Reduced inflammation compared to bovine xenograft	Not observed	N/A	Slightly reduced orthodontic tooth movement rate but statistically not significant compared to bovine xenograft	Less root resorption and reduced periodontal probing depth compared to bovine xenograft
β -TCP	de Ruiter et al. (2011)	N/A	Animal study (goats)	More bone ingrowth than autografted iliac bone grafts, but the difference was not significant	No significant difference between β -TCP and iliac bone groups	No significant difference	N/A	N/A	No difference in orthodontic tooth movement between β -TCP and iliac bone	Minor degree of apical root resorption, analogous with human situation
	Klein et al. (2019)	N/A	Animal study (mice)	β -TCP and long bone allograft both induce normal bone healing, similarly to non-grafted normally healing sites	Increased osteoclast recruitment induced by β -TCP at the early stages of healing compared to allograft using long bones	No adverse inflammatory response	Not observed	Not observed	β -TCP and allograft both slowed orthodontic movement compared to control without grafting; no difference in orthodontic movement between β -TCP and allografts	N/A
Bioactive glasses	El Shazley et al. (2016)	N/A	Clinical study (extraction socket preservation)	TAMP grafted sockets healed with vertical trabeculae and large vascularized marrow spaces; better	TAMP scaffolds enhanced the recruitment of stem cells from grafted sockets	N/A	N/A	Not observed	N/A	N/A

(Continued on following page)

TABLE 1 | (Continued) The alveolar bone regeneration efficiency and the orthodontic implications of the alveolar bone grafting materials.

Materials	References	Combinatory Materials	Type of Study	Alveolar Bone Regeneration Efficiency		Side Effects			Impact on Orthodontics	
				Volume	Cellular Activity	Inflammation	Pain	Graft Failure	Tooth Movement Rate	Adverse Effect
	Shoreibah et al. (2012)	N/A	Clinical study (PAOO)	preservation of socket contour Significantly higher bone density was observed with bioactive glasses compared to the control group without grafting	Bioactive glass particles attract osteoprogenitor cells and osteoblasts	N/A	N/A	N/A	Significant reduction in total treatment time compared to the control group without grafting	No statistical difference on root resorption; absence of any significant apical root resorption
	Bahammam, (2016)	N/A	Clinical study (PAOO)	Lower bone density than bovine xenograft but not statistically significant. Both bioactive glass and bovine xenograft showed significantly greater density than the control group without grafting	Bioactive glass has homeostatic properties and demonstrated both osteoprotection and osteoconduction	Not observed	Not observed	Not observed	No difference was observed among bioactive glass, bovine xenograft, and control (no graft) groups	No significant difference in root length in all bioactive glass, bovine, and control (no graft) groups
PRF	Tehranchi et al. (2018)	N/A	Clinical study (extraction socket preservation)	Significantly higher bone density than control group without grafting	PRF contains various growth factors, cytokines, and enzymes	N/A	15% of patients reported severe post-injection pain	N/A	PRF accelerated orthodontic tooth movement, particularly in extraction cases	N/A
	Sar et al. (2019)	N/A	Animal study (rabbits)	N/A	PRF membrane alone led to an almost 3 times higher osteoblast cell count and almost 2.5 times higher blood vessel count when compared to the untreated control	Not observed	Not observed	N/A	PRF accelerated tooth movement	No orthodontic-related discomfort was observed
BM-MSCs	Tanimoto et al. (2015)	N/A	Animal study (dogs)	Radiopaque newly formed bone was observed with periodontal ligament space using MSCs, whereas the bone on carbonated hydroxyapatite control group is immature	MSCs exert new bone formation by osteogenic differentiation and induce capillary vessels	N/A	N/A	N/A	No difference in amount of tooth movement compared to carbonated hydroxyapatite for control; MSCs exhibit consistent tooth movement rate but control group did not	Not observed

rhBMP-2: recombinant human bone morphogenetic protein-2; DBM: demineralized bone matrix; PAOO: periodontally accelerated osteogenic orthodontics; β -TCP: beta tricalcium phosphate; TAMP scaffold: tailored amorphous multiporous scaffold; PRF: platelet-rich fibrin; BM-MSC: bone marrow-derived mesenchymal stromal cells; OTM: orthodontic tooth movement.

periodontally accelerated osteogenic orthodontics (PAOO) technique has been developed to broaden the biological range of orthodontic treatment by adding bone grafting material to the alveolar cortical surface (Wilcko et al., 2008). Pre-orthodontic bone grafting can also promote easier and less detrimental tooth movement through primary woven bone (Diedrich, 1996). Ideally, bone graft materials for orthodontic treatment should protect the teeth from complications and enhance the alveolar bone phenotype.

Based on where bone grafts are sourced, they may be categorized as autografts, allografts, xenografts, or synthetics. Autografts prevail amongst these categories in the maxillofacial region and are the current gold standard as they [1] consist of an abundance of spongy bone that is close to the alveolar bone structure, [2] display osteoconductive and osteoinductive potential (Boyne and Sands, 1972; Enemark et al., 1987; Ozaki and Buchman, 1998), and [3] promote periodontal regeneration (Ivanovic et al., 2014) without significantly unfavorable sequelae when teeth are orthodontically moved into grafted areas (Lu et al., 2021). However, the drawbacks of autografts are substantial, including but not limited to inadequate availability, expensive cost, mismatched size, and inevitable additional surgery for autograft harvest (Sharif et al., 2016). These limitations lend support to the use of substitute graft materials.

Allografts, such as decalcified freeze-dried bone allogeneic grafts (DFDBA) and freeze-dried bone allogeneic grafts (FDBA), are orthodontic-friendly (Lu et al., 2021); however, their osteoinductive potency is not conclusive (Schwartz et al., 1998). Xenografts, such as Bio-Oss® and Gen-Tech®, are the most common alveolar grafting materials for clinical use. They are successful when used for alveolar bone augmentation (da Silva et al., 2020), but can severely impair orthodontic treatment and cause substantial root resorption when teeth are moved into the grafted region (Lu et al., 2021). Although synthetic bone grafts, such as NanoBone® and BoneCeramic®, also promote bone augmentation, major adverse effects (namely root resorption and gingival invagination) make them an unfavorable choice for pre-orthodontic alveolar bone grafting (Lu et al., 2021). Therefore, there is an emerging need for new grafting materials to be not only osteoinductive and osteoconductive but also supportive of highly active bone metabolism during orthodontic tooth movement without adverse effects.

In this review, we highlight recent research advances in novel alveolar graft materials, as well as new combinations of previously developed materials, with a focus on orthodontic applications supported by pre-clinical and clinical evidence (Table 1).

OSTEOINDUCTIVE GROWTH FACTOR BONE MORPHOGENETIC PROTEIN 2 (BMP2)

Growth factors, cytokines, and chemokines that potentially enhance osteoblast proliferation and function as well as facilitate orthodontic tooth movement have been investigated for use as bone graft materials. For example, recombinant human

BMP2 (rhBMP2), a potent osteogenic growth factor, is currently the only Food and Drug Administration (FDA)-approved osteoinductive growth factor for bone graft substitutes (James et al., 2016). In the alveolar region, animal studies show that rhBMP2 with a poly [D,L-(lactide-co-glycolide)]/gelatin sponge complex has superior osteoinductive activity compared to spongiosa from the tibia, and the newly generated bone in both groups shows a similar histological response to orthodontic force as that of normal alveolar bone (Kawamoto et al., 2002). However, root resorption was observed over the 6-months course of tooth movement when the rhBMP2-based graft was used, while no significant resorption was observed in the autograft and control groups (Kawamoto et al., 2002). Moreover, Hammoudeh's group showed comparable bone regrowth and density values following secondary alveolar cleft repair in humans using a rhBMP2/DBM scaffold with an autologous iliac bone graft (Hammoudeh et al., 2017; Liang et al., 2017). The spontaneous canine eruption rate was similar among different grafting groups (Hammoudeh et al., 2017). In addition, applying rhBMP2 during PAOO procedures increased bone density around corticotomy sites and shortened orthodontic treatment time compared to conventional corticotomy alone (Chandra et al., 2019).

It is worth noting that although the osteoinductive activity of rhBMP2 increases with dose (El Bialy et al., 2017), high-dose rhBMP2 may not be favorable for orthodontic tooth movement. Kawamoto et al. found that high-dose rhBMP2 delays bone remodeling compared to low-dose rhBMP2 (Kawamoto et al., 2003). Moreover, high-dose rhBMP2 induces root resorption, while low-dose rhBMP2 causes only partial cementum resorption on the pressure side (Kawamoto et al., 2003).

To minimize the adverse effects of high-dose rhBMP2 while reducing the cost of this expensive material, rhBMP2-functionalized biomimetic calcium phosphate (BioCap) granules have been developed to achieve controlled and sustained rhBMP2 release. BioCap granules robustly enhanced bone regeneration and graft degradation over deproteinized bovine bone in an animal study (Jiang et al., 2020). In addition, due to its low immunogenicity and high angiogenic potency, BioCap graft reduces inflammation and periodontal probing depth during orthodontic treatment, while only slightly reducing the rate of orthodontic tooth movement (Jiang et al., 2020).

A synergistic effect was observed when rhBMP2 and vascular endothelial growth factor (VEGF) were used together to enhance bone generation around implant sites via an insoluble collagenous bone matrix (Schorn et al., 2017). In this combination, VEGF promotes angiogenesis and enhances osteoblastic differentiation, thereby facilitating craniofacial ossification (Duan et al., 2016), while the matrix acts as a scaffold for migrating osteoblasts. This combination product can reduce surgery time and minimize donor site morbidity while maintaining bone stability, as little resorption was observed over time (Schorn et al., 2017).

Despite its advantages, clinical complications such as significant postoperative facial swelling were observed in patients grafted with rhBMP2 (Hammoudeh et al., 2017).

Along with increasing clinical use of rhBMP2 in orthopedics, a growing side-effect profile has emerged, including postoperative inflammation, ectopic bone formation, osteoclast-mediated bone resorption, and inappropriate adipogenesis (James et al., 2016). BMP2 has also been associated with osteosarcoma growth (Tian et al., 2019); this complication has cast doubt on its application after tumor resection. Safe application of rhBMP2 therefore remains an inherent issue to conquer.

SYNTHETIC INORGANIC MATERIALS

Unlike autografts, allografts, and xenografts, synthetic materials are free from cross-infection and disease transmission and are not associated with donor site sacrifice. However, synthetic materials, particularly inorganic ones, are often osteoconductive without any osteoinductive or osteogenic potential. β -tricalcium phosphate (β -TCP), hydroxyapatite, and bioactive glasses are the most commonly used inorganic graft materials in periodontal regeneration (Sheikh et al., 2017).

β -tricalcium Phosphate (β -TCP)

TCPs were the first generation of calcium compounds used as bone grafts (Bohner et al., 2020). They are osteoconductive and have a similar composition to bone minerals. TCP has two crystallographic forms, α -TCP and β -TCP (Bohner et al., 2020), with the latter exhibiting good biocompatibility and osteoconductivity. As a graft material for alveolar cleft repair in animals, β -TCP promotes bone regeneration as effectively as autologous iliac crest bone (de Ruiter et al., 2011) and allograft from long bones (Klein et al., 2019). Moreover, no difference in orthodontic movement is observed between β -TCP and autograft (de Ruiter et al., 2011) or allograft (Klein et al., 2019). Since β -TCP shows no significant adverse effects on tooth movement in grafted sites, it is a promising material for further clinical investigation.

Bioactive Glasses

First introduced as a bone graft in early 1970, biocompatible tissue-bonding bioactive glasses are another synthesized inorganic graft material that has received clinical attention. After implantation, a hydroxycarbonate apatite layer and silicon-rich gel layer form on the surface of the bioactive glass. The roles of these layers are to attach to the surrounding bone and attract osteoprogenitor cells and osteoblasts, respectively (Hench, 1991). The composition of a particular bioactive glass (i.e. a combination of silicon dioxide, calcium oxide, sodium oxide, and phosphorus pentoxide) will determine its bioactivity (Shue et al., 2012). For instance, increasing silicon dioxide, decreasing alkali, and supplementing aluminum oxide modulates the durability and water resistance of bioactive glass, thereby altering its reliability and success (Pereira et al., 1994).

Different types of bioactive glass have been tested for alveolar bone grafting and novel modifications have been developed to improve biocompatibility of the material. For example, a novel bioactive glass scaffold, tailored amorphous multiporous (TAMP), was introduced in 2016 for extraction socket

preservation (El Shazley et al., 2016). Distinct from non-grafted sockets that showed corticalization after healing, the TAMP-grafted sockets healed with vertical trabeculae and large vascularized marrow spaces (El Shazley et al., 2016). Better preservation of socket contour was also observed with TAMP grafts (El Shazley et al., 2016). In addition, GlassBONE™ (Noraker, France), a synthetic resorbable bioactive glass 45S5 ceramic, has been successfully used for alveolar cleft reconstruction, with satisfactory healing found in two-thirds of tested patients (Graillon et al., 2018).

When bioactive glass is grafted, a significant increase in bone density is noted 6 months after the cessation of tooth movement; this finding may be attributed to the beneficial effects of alkalization on collagen synthesis and hydroxyapatite formation (Shoreibah et al., 2012). In addition, a marked reduction in orthodontic treatment duration was associated with bioactive glass grafting. Periodontal health was also enhanced with negligible apical root resorption and improved probing depth (Shoreibah et al., 2012). Although bioactive glass does not provide the same level of bone density as bovine-derived xenograft, both materials decrease the duration of orthodontic treatment and reduce the risk of root resorption (Bahammam, 2016).

Bioactive glass has also been applied with other grafting materials. For example, a case report from 2000 described how grafting a DFDBA-granular bioactive glass (1:1) mixture in the buccal aspect of the edentulous cleft region of a patient with cleft lip and palate resulted in good bone regeneration and successful orthodontic tooth movement into the grafted site (Yilmaz et al., 2000). However, these results should be interpreted with caution as they are derived from a single case report.

PLATELET-RICH FIBRIN (PRF)

Endogenous biomaterials have been developed to overcome the limitations associated with current clinical approaches for autografting. PRF is a cost-effective material (Miron and Choukroun, 2017) that is increasingly being used for regenerative dentistry, specifically next-generation autologous platelet therapy (Liu et al., 2019). PRF contains stem cells, growth factors, and cytokines and is obtained through a minimally invasive procedure that centrifuges whole blood without additives (Choukroun et al., 2006). It can modulate inflammation and enhance the healing process, thereby promoting the regenerative capacity of the periosteum (Miron and Choukroun, 2017). In addition, its dense, protein-rich fibrin mesh functions as a three-dimensional fibrous scaffold for cell migration and a retainer for sustained growth factor release (Karimi and Rockwell, 2019).

Both animal (Sar et al., 2019) and clinical studies (Tehranchi et al., 2018) show that PRF significantly accelerates alveolar bone turnover and orthodontic tooth movement, especially at the beginning of orthodontic treatment (Tehranchi et al., 2018). However, 15% of grafted patients experience severe pain attributable to PRF application (Tehranchi et al., 2018), highlighting the need for further investigation. Although the

clinical applications of PRF in regenerative dentistry have grown in recent years (Miron and Choukroun, 2017), its application in orthodontics is limited. It is largely unknown if the content variation of PRF from different patients or the same patient at different health statuses will impact its outcome as a graft in orthodontic treatment. Additionally, since PRF contains donor cells, it is not suitable to be used as an allograft. Its usage as an autograft material is also limited by availability when extracted from the patient's blood (Choukroun et al., 2006).

PLURI AND MULTIPOTENT CELLS

Over the last few decades, multiple pluri- and multi-potent cells have been explored for use in bone augmentation (Li C. et al., 2021; Holly et al., 2021). Bone marrow is the main source of MSCs for clinical applications; in fact, bone marrow-derived mesenchymal stromal cells (BM-MSCs) were the first MSCs to be discovered (Strioga et al., 2012). Compared to iliac crest bone grafts, resorbable collagen sponges combined with BM-MSCs provide similar bone healing results in the closure of alveolar cleft defects with reduced donor site morbidity and decreased donor site pain intensity and frequency (Gimbel et al., 2007).

Recently, successful bone regeneration has been reported using autogenous BM-MSCs in a dog model of an artificial alveolar cleft. In this study, new bone formation was achieved, thereby allowing orthodontic tooth movement beyond the anatomical limit (Tanimoto et al., 2015). Furthermore, a consistent rate of orthodontic tooth movement was observed in the experimental group compared to varied rates in the control group (Tanimoto et al., 2015), suggesting that MSCs in bone graft materials may have a modulatory effect on the bone remodeling process during orthodontic treatment. In alignment with this observation, the expression of RANKL, a molecule that regulates osteoclastic differentiation, was significantly increased in BM-MSCs under compressive stress (Wang et al., 2021). This finding suggests that BM-MSCs may accelerate tooth movement by expressing cytokines that promote osteoclastogenesis.

Due to ease of accessibility, dental-derived MSCs have gained attention in the past few years and have entered clinical trials (Paz et al., 2018). First isolated from the dental pulp of extracted third molars, dental-derived MSCs have now been purified from various dental tissues, including pulp tissue of permanent teeth and exfoliated deciduous teeth, apical papilla, periodontal ligament, gingiva, dental follicle, tooth germ, and alveolar bone (Gan et al., 2020). Dental-derived MSCs not only display the same characteristics as BM-MSCs but also possess immunomodulatory and anti-inflammatory advantages in the local dental tissue environment (Spagnuolo et al., 2018). Tanikawa *et al.* utilized autologous deciduous dental pulp stem cells for maxillary alveolar reconstruction and achieved progressive alveolar bone union without grafting site complications in cleft lip and palate patients (Tanikawa et al., 2020). Previous studies have also suggested that gingival-derived MSCs have great potential for repairing alveolar bone defects (Gao and Cao, 2020; Kandam et al., 2021). However, the impact of dental-derived MSCs on orthodontic tooth movement is not yet well understood.

MATERIALS WITH 3D PRINTED SCAFFOLDS

Conventional bone grafts, such as allografts and xenografts, often fail to provide the support necessary to maintain the desired generated tissue volume, especially under the mechanical forces in the oral cavity (Seciu et al., 2019). This is particularly challenging for vertical bone augmentation or personalized esthetic bone reconstruction, where highly tailored bone contours and structural stability are required. To overcome this obstacle, materials with three-dimensional architecture mimicking the anatomical and histological arrangement of natural bone have been developed (Kim et al., 2010).

Recent advances in microfabrication, particularly 3D bio-printing, support the construction of complex structures from bioactive/biodegradable materials, including polymers, bioceramics, and composites [as reviewed in (Asa'ad et al., 2016)]. In a recent study, a 3D-printed calcium phosphate scaffold was fabricated according to the geometry of artificial alveolar clefts in rats and showed promising scaffolding and osteoconductive properties (Korn et al., 2020). A 3D-printed custom hydroxyapatite/TCP graft supplied with rhBMP2 also achieved bone regeneration to the same level of rhBMP2-coupled deproteinized bovine bone material (Bio-Oss®) (Ryu et al., 2021). Although the exact mechanism of how 3D-printed scaffolds benefit orthodontic tooth movement remains unmapped, evidence suggests that grafting with 3D-printed scaffolds may offer enhanced orthodontic outcomes.

CONCLUSION AND FUTURE DIRECTIONS

Optimizing esthetics, providing functional and comfortable occlusion, and improving overall health are all goals of successful orthodontic treatment, for which preservation of the alveolar bone is a crucial limiting factor. Most materials reviewed in this article mediate accelerated orthodontic tooth movement and thus can reduce treatment duration and cost. These features are particularly attractive to patients facing extended treatment times, such as those in need of tooth extractions and additional periodontal support. Although a quantitative report is not currently realistic due to the limited available research to date, qualitatively analyzing pre-clinical novel materials will provide insight for their future usage in regenerative orthodontics. High-quality randomized controlled trials with larger sample sizes and longer follow-up periods are nevertheless warranted for translating these novel biological concepts into clinical practice. In our opinion, future exploration should also aim to reveal the potential long-term complications of these materials, as well as their impacts on growth and development in adolescents.

A rising number of reports suggest that adjunct treatments can support grafting and have the potential to improve orthodontic treatment. For example, the possibility of vibration accelerating orthodontic tooth movement has been a hot study topic over the last decade (Telatar and Gungor, 2021; Mayama et al., 2022). At the same time, studies have shown that high-frequency vibration treatment increases osteogenic differentiation of human BM-

MSCs *in vitro* (Pre et al., 2013) and low-level mechanical vibration stimulates osteogenesis and osteointegration of porous titanium implants in the repair of long bone defects (Jing et al., 2015). In addition, low-intensity pulsed ultrasound (LIPUS) has been proven to accelerate new alveolar bone formation in a periodontal injury animal model (Wang et al., 2018) and enhance BM-MSCs-based periodontal regenerative therapies (Wang et al., 2022). Moreover, LIPUS can shorten the overall duration of orthodontic treatment (Kaur and El-Bialy, 2020) and minimize orthodontically-induced tooth root resorption (El-Bialy et al., 2020). Last but not least, laser photobiomodulation in combination with PRF demonstrated better bone healing than PRF alone in an iliac crest critical-sized bone defect sheep model (Surmeli Baran et al., 2021). Photobiomodulation was also found to enhance bone formation of hydroxyapatite biomaterial in the dental alveolus in an experimental extraction rat model (Dalapria et al., 2022). On the other hand, the effects of photobiomodulation on orthodontic treatment have started to attract attention (Li J. et al., 2021; Yavagal et al., 2021). In all, a detailed assessment of the influence of adjunct treatments with different grafting materials on orthodontic tooth movement is warranted to further optimize treatment outcomes.

REFERENCES

- Abrams, H., Kopczyk, R. A., and Kaplan, A. L. (1987). Incidence of Anterior Ridge Deformities in Partially Edentulous Patients. *J. Prosthet. Dent.* 57 (2), 191–194. doi:10.1016/0022-3913(87)90145-4
- Asaad, F., Pagni, G., Pilipchuk, S. P., Gianni, A. B., Giannobile, W. V., and Rasperini, G. (2016). 3D-Printed Scaffolds and Biomaterials: Review of Alveolar Bone Augmentation and Periodontal Regeneration Applications. *Int. J. Dent.* 2016, 1–15. doi:10.1155/2016/1239842
- Atwood, D. A., and Coy, W. A. (1971). Clinical, Cephalometric, and Densitometric Study of Reduction of Residual Ridges. *J. Prosthet. Dent.* 26 (3), 280–295. doi:10.1016/0022-3913(71)90070-9
- Bahammam, M. A. (2016). Effectiveness of Bovine-Derived Xenograft versus Bioactive Glass with Periodontally Accelerated Osteogenic Orthodontics in Adults: a Randomized, Controlled Clinical Trial. *BMC Oral Health* 16 (1), 126. doi:10.1186/s12903-016-0321-x
- Bohner, M., Santoni, B. L. G., and Döbelin, N. (2020). β -Tricalcium Phosphate for Bone Substitution: Synthesis and Properties. *Acta Biomater.* 113, 23–41. doi:10.1016/j.actbio.2020.06.022
- Boyne, P. J., and Sands, N. R. (1972). Secondary Bone Grafting of Residual Alveolar and Palatal Clefts. *J. Oral Surg.* 30 (2), 87–92.
- Chandra, R., Rachala, M., Madhavi, K., Kambalyal, P., Reddy, A., and Ali, M. (2019). Periodontally Accelerated Osteogenic Orthodontics Combined with Recombinant Human Bone Morphogenetic Protein-2: An Outcome Assessment. *J. Indian Soc. Periodontol.* 23 (3), 257–263. doi:10.4103/jisp.jisp_612_18
- Choukroun, J., Diss, A., Simonpieri, A., Girard, M.-O., Schoeffler, C., Dohan, S. L., et al. (2006). Platelet-rich Fibrin (PRF): a Second-Generation Platelet Concentrate. Part IV: Clinical Effects on Tissue Healing. *Oral Surg. Oral Med. Oral Pathology, Oral Radiology, Endodontology* 101 (3), e56–e60. doi:10.1016/j.tripleo.2005.07.011
- de Ruiter, R., Meijer, G., Dormaar, T., Janssen, N., van der Bilt, A., Slootweg, P., et al. (2011). β -TCP versus Autologous Bone for Repair of Alveolar Clefts in a Goat Model. *Cleft Palate-Craniofacial J.* 48 (6), 654–662. doi:10.1597/09-219
- da Silva, H. F., Goulart, D. R., Sverzut, A. T., Olate, S., and de Moraes, M. (2020). Comparison of Two Anorganic Bovine Bone in Maxillary Sinus Lift: a Split-

AUTHOR CONTRIBUTIONS

YM, writing—original draft preparation, review and editing. Y-CC, NT, C-HC, NA, MZ, and ZZ, writing—review and editing. CL, conceptualization, writing—review and editing, funding acquisition. All authors have read and agreed to the published version of the manuscript.

FUNDING

This study was supported by the American Academy of Periodontology Foundation Teaching Fellowship and Schoenleber Pilot Grant, University of Pennsylvania for Y-CC; and the American Association of Orthodontists Foundation (AAOF) Orthodontic Faculty Development Fellowship Award, American Association of Orthodontists (AAO) Full-Time Faculty Fellowship Award, University of Pennsylvania School of Dental Medicine Joseph and Josephine Rabinowitz Award for Excellence in Research, and J. Henry O'Hern Jr Pilot Grant from the Department of Orthodontics, University of Pennsylvania School of Dental Medicine for CL.

- Mouth Study with Clinical, Radiographical, and Histomorphometrical Analysis. *Int. J. Implant Dent.* 6 (1), 17. doi:10.1186/s40729-020-00214-w
- Dalapria, V., Marcos, R. L., Bussadori, S. K., Anselmo, G., Benetti, C., da Silva Santana, A. C. A., et al. (2022). LED Photobiomodulation Therapy Combined with Biomaterial as a Scaffold Promotes Better Bone Quality in the Dental Alveolus in an Experimental Extraction Model. *Lasers Med. Sci.* 37 (3), 1583–1592. doi:10.1007/s10103-021-03407-w
- Diedrich, P. R. (1996). Guided Tissue Regeneration Associated with Orthodontic Therapy. *Seminars Orthod.* 2 (1), 39–45. doi:10.1016/s1073-8746(96)80038-7
- Duan, X., Bradbury, S. R., Olsen, B. R., and Berendsen, A. D. (2016). VEGF Stimulates Intramembranous Bone Formation during Craniofacial Skeletal Development. *Matrix Biol.* 52–54, 127–140. doi:10.1016/j.matbio.2016.02.005
- El Bialy, I., Iskoot, W., and Reza Nejadnik, M. (2017). Formulation, Delivery and Stability of Bone Morphogenetic Proteins for Effective Bone Regeneration. *Pharm. Res.* 34 (6), 1152–1170. doi:10.1007/s11095-017-2147-x
- El Shazley, N., Hamdy, A., El-Eneen, H. A., El Backly, R. M., Saad, M. M., Essam, W., et al. (2016). Bioglass in Alveolar Bone Regeneration in Orthodontic Patients. *JDR Clin. Transl. Res.* 1 (3), 244–255. doi:10.1177/2380084416660672
- El-Bialy, T., Farouk, K., Carlyle, T. D., Wiltshire, W., Drummond, R., Dumore, T., et al. (2020). Effect of Low Intensity Pulsed Ultrasound (LIPUS) on Tooth Movement and Root Resorption: A Prospective Multi-Center Randomized Controlled Trial. *Jcm* 9 (3), 804. doi:10.3390/jcm9030804
- Enemark, H., Sindet-Pedersen, S., and Bundgaard, M. (1987). Long-term Results after Secondary Bone Grafting of Alveolar Clefts. *J. Oral Maxillofac. Surg.* 45 (11), 913–918. doi:10.1016/0278-2391(87)90439-3
- Gan, L., Liu, Y., Cui, D., Pan, Y., Zheng, L., and Wan, M. (2020). Dental Tissue-Derived Human Mesenchymal Stem Cells and Their Potential in Therapeutic Application. *Stem Cells Int.* 2020, 1–17. doi:10.1155/2020/8864572
- Gao, X., and Cao, Z. (2020). Gingiva-derived Mesenchymal Stem Cells and Their Potential Applications in Oral and Maxillofacial Diseases. *Cscr* 15 (1), 43–53. doi:10.2174/1574888X14666191107100311
- Gimbel, M., Ashley, R. K., Sisodia, M., Gabbay, J. S., Wasson, K. L., Heller, J., et al. (2007). Repair of Alveolar Cleft Defects. *J. Craniofac Surg.* 18 (4), 895–901. doi:10.1097/scs.0b013e3180a771af
- Graillon, N., Degardin, N., Foletti, J. M., Seiler, M., Alessandrini, M., and Gallucci, A. (2018). Bioactive Glass 45S5 Ceramic for Alveolar Cleft Reconstruction, about 58 Cases. *J. Cranio-Maxillofacial Surg.* 46 (10), 1772–1776. doi:10.1016/j.jcms.2018.07.016

- Hammoudeh, J. A., Fahradyan, A., Gould, D. J., Liang, F., Imahiyebo, T., Urbinelli, L., et al. (2017). A Comparative Analysis of Recombinant Human Bone Morphogenetic Protein-2 with a Demineralized Bone Matrix versus Iliac Crest Bone Graft for Secondary Alveolar Bone Grafts in Patients with Cleft Lip and Palate. *Plastic Reconstr. Surg.* 140 (2), 318e–325e. doi:10.1097/PRS.0000000000003519
- Hench, L. L. (1991). Bioceramics: from Concept to Clinic. *J Am. Ceram. Soc.* 74 (7), 1487–1510. doi:10.1111/j.1151-2916.1991.tb07132.x
- Holly, D., Klein, M., Mazreku, M., Zamborsky, R., Polak, Š., Danišovič, L., et al. (2021). Stem Cells and Their Derivatives-Implications for Alveolar Bone Regeneration: A Comprehensive Review. *Ijms* 22 (21), 11746. doi:10.3390/ijms222111746
- Ivanovic, A., Nikou, G., Miron, R. J., Nikolidakis, D., and Sculean, A. (2014). Which Biomaterials May Promote Periodontal Regeneration in Intra-bony Periodontal Defects? A Systematic Review of Preclinical Studies. *Quintessence Int.* 45 (5), 385–395. doi:10.3290/j.qi.a31538
- James, A. W., LaChaud, G., Shen, J., Asatrian, G., Nguyen, V., Zhang, X., et al. (2016). A Review of the Clinical Side Effects of Bone Morphogenetic Protein-2. *Tissue Eng. Part B Rev.* 22 (4), 284–297. doi:10.1089/ten.TEB.2015.0357
- Jiang, S., Liu, T., Wu, G., Li, W., Feng, X., Pathak, J. L., et al. (2020). BMP2-Functionalized Biomimetic Calcium Phosphate Graft Promotes Alveolar Defect Healing during Orthodontic Tooth Movement in Beagle Dogs. *Front. Bioeng. Biotechnol.* 8, 517. doi:10.3389/fbioe.2020.00517
- Jing, D., Tong, S., Zhai, M., Li, X., Cai, J., Wu, Y., et al. (2015). Effect of Low-Level Mechanical Vibration on Osteogenesis and Osseointegration of Porous Titanium Implants in the Repair of Long Bone Defects. *Sci. Rep.* 5, 17134. doi:10.1038/srep17134
- Kandalam, U., Kawai, T., Ravindran, G., Brockman, R., Romero, J., Munro, M., et al. (2021). Predifferentiated Gingival Stem Cell-Induced Bone Regeneration in Rat Alveolar Bone Defect Model. *Tissue Eng. Part A* 27 (5-6), 424–436. doi:10.1089/ten.TEA.2020.0052
- Karimi, K., and Rockwell, H. (2019). The Benefits of Platelet-Rich Fibrin. *Facial Plastic Surg. Clin. N. Am.* 27 (3), 331–340. doi:10.1016/j.fsc.2019.03.005
- Kaur, H., and El-Bialy, T. (2020). Shortening of Overall Orthodontic Treatment Duration with Low-Intensity Pulsed Ultrasound (LIPUS). *Jcm* 9 (5), 1303. doi:10.3390/jcm9051303
- Kawamoto, T., Motohashi, N., Kitamura, A., Baba, Y., Suzuki, S., and Kuroda, T. (2003). Experimental Tooth Movement into Bone Induced by Recombinant Human Bone Morphogenetic Protein-2. *Cleft Palate-Craniofacial J.* 40 (5), 538–543. doi:10.1597/1545-1569_2003_040_0538_etmibi_2.0.co_210.1597/1545-1569(2003)040<0538:etmibi>2.0.co;2
- Kawamoto, T., Motohashi, N., Kitamura, A., Baba, Y., Takahashi, K., Suzuki, S., et al. (2002). A Histological Study on Experimental Tooth Movement into Bone Induced by Recombinant Human Bone Morphogenetic Protein-2 in Beagle Dogs. *Cleft Palate-Craniofacial J.* 39 (4), 439–448. doi:10.1597/1545-1569_2002_039_0439_ahsoet_2.0.co_2
- Kim, K., Lee, C. H., Kim, B. K., and Mao, J. J. (2010). Anatomically Shaped Tooth and Periodontal Regeneration by Cell Homing. *J. Dent. Res.* 89 (8), 842–847. doi:10.1177/0022034510370803
- Klein, Y., Kunthawong, N., Fleissig, O., Casap, N., Polak, D., and Chaushu, S. (2020). The Impact of Alloplast and Allograft on Bone Homeostasis: Orthodontic Tooth Movement into Regenerated Bone. *J. Periodontol.* 91, 1067–1075. doi:10.1002/JPER.19-0145
- Korn, P., Ahlfeld, T., Lahmeyer, F., Kilian, D., Sembdner, P., Stelzer, R., et al. (2020). 3D Printing of Bone Grafts for Cleft Alveolar Osteoplasty - In Vivo Evaluation in a Preclinical Model. *Front. Bioeng. Biotechnol.* 8, 217. doi:10.3389/fbioe.2020.00217
- Li, C., Mills, Z., and Zheng, Z. (2021a). Novel Cell Sources for Bone Regeneration. *MedComm* 2 (2), 145–174. doi:10.1002/mco2.51
- Li, J., Ge, X., Guan, H., Jia, L., Chang, W., and Ma, W. (2021b). The Effectiveness of Photobiomodulation on Accelerating Tooth Movement in Orthodontics: A Systematic Review and Meta-Analysis. *Photobiomodulation, Photomed. Laser Surg.* 39 (4), 232–244. doi:10.1089/photob.2020.4954
- Liang, F., Yen, S. L.-K., Imahiyebo, T., Sanborn, L., Yen, L., Yen, D., et al. (2017). Three-Dimensional Cone Beam Computed Tomography Volumetric Outcomes of rhBMP-2/Demineralized Bone Matrix versus Iliac Crest Bone Graft for Alveolar Cleft Reconstruction. *Plastic Reconstr. Surg.* 140 (4), 767–774. doi:10.1097/PRS.0000000000003686
- Liu, Y., Sun, X., Yu, J., Wang, J., Zhai, P., Chen, S., et al. (2019). Platelet-rich Fibrin as a Bone Graft Material in Oral and Maxillofacial Bone Regeneration: Classification and Summary for Better Application. *BioMed Res. Int.* 2019, 3295756. doi:10.1155/2019/3295756
- Lu, J., Wang, Z., Zhang, H., Xu, W., Zhang, C., Yang, Y., et al. (2022). Bone Graft Materials for Alveolar Bone Defects in Orthodontic Tooth Movement. *Tissue Eng. Part B Rev.* 28, 35–51. doi:10.1089/ten.TEB.2020.0212
- Mayama, A., Seiryu, M., and Takano-Yamamoto, T. (2022). Effect of Vibration on Orthodontic Tooth Movement in a Double Blind Prospective Randomized Controlled Trial. *Sci. Rep.* 12 (1), 1288. doi:10.1038/s41598-022-05395-5
- McAllister, B. S., and Haghighat, K. (2007). Bone Augmentation Techniques. *J. Periodontology* 78 (3), 377–396. doi:10.1902/jop.2007.060048
- Miron, R. J., and Choukroun, J. (2017). *Platelet Rich Fibrin in Regenerative Dentistry: Biological Background and Clinical Indications*. Hoboken, NJ: John Wiley & Sons, Inc.
- Ozaki, W., and Buchman, S. R. (1998). Volume Maintenance of Onlay Bone Grafts in the Craniofacial Skeleton: Micro-architecture versus Embryologic Origin. *Plastic Reconstr. Surg.* 102 (2), 291–299. doi:10.1097/00006534-199808000-00001
- Paz, A. G., Maghaireh, H., and Mangano, F. G. (2018). Stem Cells in Dentistry: Types of Intra- and Extraoral Tissue-Derived Stem Cells and Clinical Applications. *Stem Cells Int.* 2018, 1–14. doi:10.1155/2018/4313610
- Pereira, M. M., Clark, A. E., and Hench, L. L. (1994). Calcium Phosphate Formation on Sol-Gel-Derived Bioactive Glasses in Vitro. *J. Biomed. Mat. Res.* 28 (6), 693–698. doi:10.1002/jbm.820280606
- Prè, D., Ceccarelli, G., Visai, L., Benedetti, L., Imbriani, M., Cusella De Angelis, M. G., et al. (2013). High-Frequency Vibration Treatment of Human Bone Marrow Stromal Cells Increases Differentiation toward Bone Tissue. *Bone Marrow Res.* 2013, 1–13. doi:10.1155/2013/803450
- Reichert, C., Götz, W., Smeets, R., Wenghöfer, M., and Jäger, A. (2010). The Impact of Nonautogenous Bone Graft on Orthodontic Treatment. *Quintessence Int.* 41 (8), 665–672.
- Ryu, J.-I., Yang, B.-E., Yi, S.-M., Choi, H.-G., On, S.-W., Hong, S.-J., et al. (2021). Bone Regeneration of a 3D-Printed Alloplastic and Particulate Xenogenic Graft with rhBMP-2. *Ijms* 22 (22), 12518. doi:10.3390/ijms222212518
- Sar, C., Akdeniz, S. S., Arman Ozcipcici, A., Helvacioğlu, F., and Bacanlı, D. (2019). Histological Evaluation of Combined Platelet-Rich Fibrin Membrane and Piezo-Incision Application in Orthodontic Tooth Movement. *Int. J. Oral Maxillofac. Surg.* 48 (10), 1380–1385. doi:10.1016/j.ijom.2019.04.001
- Schorn, L., Sproll, C., Ommerborn, M., Naujoks, C., Kübler, N. R., and Depprich, R. (2017). Vertical Bone Regeneration Using rhBMP-2 and VEGF. *Head. Face Med.* 13 (1), 11. doi:10.1186/s13005-017-0146-0
- Schwartz, Z., Somers, A., Mellonig, J. T., Carnes, D. L., Jr., Dean, D. D., Cochran, D. L., et al. (1998). Ability of Commercial Demineralized Freeze-Dried Bone Allograft to Induce New Bone Formation Is Dependent on Donor Age but Not Gender. *J. Periodontology* 69 (4), 470–478. doi:10.1902/jop.1998.69.4.470
- Seciu, A.-M., Craciunescu, O., Stanciu, A.-M., and Zarnescu, O. (2019). Tailored Biomaterials for Therapeutic Strategies Applied in Periodontal Tissue Engineering. *Stem cells Dev.* 28 (15), 963–973. doi:10.1089/scd.2019.0016
- Seifi, M., and Ghorashian, S. (2012). Determination of Orthodontic Tooth Movement and Tissue Reaction Following Demineralized Freeze-Dried Bone Allograft Grafting Intervention. *Dent. Res. J.* 9 (2), 203–208. doi:10.4103/1735-3327.95237
- Sharif, F., Ur Rehman, I., Muhammad, N., and MacNeil, S. (2016). Dental Materials for Cleft Palate Repair. *Mater. Sci. Eng. C* 61, 1018–1028. doi:10.1016/j.msec.2015.12.019
- Sheikh, Z., Hamdan, N., Ikeda, Y., Grynps, M., Ganss, B., and Glogauer, M. (2017). Natural Graft Tissues and Synthetic Biomaterials for Periodontal and Alveolar Bone Reconstructive Applications: a Review. *Biomater. Res.* 21, 9. doi:10.1186/s40824-017-0095-5
- Shoreibah, E. A., Ibrahim, S. A., Attia, M. S., and Diab, M. M. (2012). Clinical and Radiographic Evaluation of Bone Grafting in Corticotomy-Facilitated Orthodontics in Adults. *J. Int. Acad. Periodontol.* 14 (4), 105–113.
- Shue, L., Yufeng, Z., and Mony, U. (2012). Biomaterials for Periodontal Regeneration. *Biomater* 2 (4), 271–277. doi:10.4161/biom.22948
- Spagnuolo, G., Codispoti, B., Marrelli, M., Rengo, C., Rengo, S., and Tatullo, M. (2018). Commitment of Oral-Derived Stem Cells in Dental and Maxillofacial Applications. *Dent. J.* 6 (4), 72. doi:10.3390/dj6040072

- Strioga, M., Viswanathan, S., Darinskas, A., Slaby, O., and Michalek, J. (2012). Same or Not the Same? Comparison of Adipose Tissue-Derived versus Bone Marrow-Derived Mesenchymal Stem and Stromal Cells. *Stem Cells Dev.* 21 (14), 2724–2752. doi:10.1089/scd.2011.0722
- Surmeli Baran, S., Temmerman, A., Salimov, F., Ucak Turer, O., Sapmaz, T., Haytac, M. C., et al. (2021). The Effects of Photobiomodulation on Leukocyte and Platelet-Rich Fibrin as Barrier Membrane on Bone Regeneration: An Experimental Animal Study. *Photobiomodulation, Photomed. Laser Surg.* 39 (4), 245–253. doi:10.1089/photob.2020.4943
- Tanikawa, D. Y. S., Pinheiro, C. C. G., Almeida, M. C. A., Oliveira, C. R. G. C. M., Coudry, R. d. A., Rocha, D. L., et al. (2020). Deciduous Dental Pulp Stem Cells for Maxillary Alveolar Reconstruction in Cleft Lip and Palate Patients. *Stem Cells Int.* 2020, 1–9. doi:10.1155/2020/6234167
- Tanimoto, K., Sumi, K., Yoshioka, M., Oki, N., Tanne, Y., Awada, T., et al. (2015). Experimental Tooth Movement into New Bone Area Regenerated by Use of Bone Marrow-Derived Mesenchymal Stem Cells. *Cleft Palate-Craniofacial J.* 52 (4), 386–394. doi:10.1597/12-232
- Tehranchi, A., Behnia, H., Pourdanesh, F., Behnia, P., Pinto, N., and Younessian, F. (2018). The Effect of Autologous Leukocyte Platelet Rich Fibrin on the Rate of Orthodontic Tooth Movement: A Prospective Randomized Clinical Trial. *Eur. J. Dent.* 12 (3), 350–357. doi:10.4103/ejd.ejd_424_17
- Telatar, B. C., and Gungor, A. Y. (2021). Effectiveness of Vibrational Forces on Orthodontic Treatment. *J. Orofac. Orthop.* 82 (5), 288–294. doi:10.1007/s00056-020-00257-z
- Tian, H., Zhou, T., Chen, H., Li, C., Jiang, Z., Lao, L., et al. (2019). Bone Morphogenetic Protein-2 Promotes Osteosarcoma Growth by Promoting Epithelial-mesenchymal Transition (EMT) through the Wnt/ β -catenin Signaling Pathway. *J. Orthop. Res.* 37 (7), 1638–1648. doi:10.1002/jor.24244
- Wang, J., Jiao, D., Huang, X., and Bai, Y. (2021). Osteoclastic Effects of mBMMSCs under Compressive Pressure during Orthodontic Tooth Movement. *Stem Cell. Res. Ther.* 12 (1), 148. doi:10.1186/s13287-021-02220-0
- Wang, Y., Li, J., Zhou, J., Qiu, Y., and Song, J. (2022). Low-intensity Pulsed Ultrasound Enhances Bone Marrow-Derived Stem Cells-Based Periodontal Regenerative Therapies. *Ultrasonics* 121, 106678. doi:10.1016/j.ultras.2021.106678
- Wang, Y., Qiu, Y., Li, J., Zhao, C., and Song, J. (2018). Low-intensity Pulsed Ultrasound Promotes Alveolar Bone Regeneration in a Periodontal Injury Model. *Ultrasonics* 90, 166–172. doi:10.1016/j.ultras.2018.06.015
- Wilcko, M. T., Wilcko, W. M., and Bissada, N. F. (2008). An Evidence-Based Analysis of Periodontally Accelerated Orthodontic and Osteogenic Techniques: A Synthesis of Scientific Perspectives. *Seminars Orthod.* 14 (4), 305–316. doi:10.1053/j.sodo.2008.07.007
- Yavagal, C. M., Matondkar, S. P., and Yavagal, P. C. (2021). Efficacy of Laser Photobiomodulation in Accelerating Orthodontic Tooth Movement in Children: A Systematic Review with Meta-Analysis. *Int. J. Clin. Pediatr. Dent.* 14 (Suppl. 1), S91–S97. doi:10.5005/jp-journals-10005-1964
- Yilmaz, S., Kiliç, A. R., Keles, A., and Efeoglu, E. (2000). Reconstruction of an Alveolar Cleft for Orthodontic Tooth Movement. *Am. J. Orthod. Dentofac. Orthop.* 117 (2), 156–163. doi:10.1016/s0889-5406(00)70226-5

Conflict of Interest: The authors declare that the research was conducted in the absence of any commercial or financial relationships that could be construed as a potential conflict of interest.

Publisher's Note: All claims expressed in this article are solely those of the authors and do not necessarily represent those of their affiliated organizations, or those of the publisher, the editors and the reviewers. Any product that may be evaluated in this article, or claim that may be made by its manufacturer, is not guaranteed or endorsed by the publisher.

Copyright © 2022 Miao, Chang, Tanna, Almer, Chung, Zou, Zheng and Li. This is an open-access article distributed under the terms of the Creative Commons Attribution License (CC BY). The use, distribution or reproduction in other forums is permitted, provided the original author(s) and the copyright owner(s) are credited and that the original publication in this journal is cited, in accordance with accepted academic practice. No use, distribution or reproduction is permitted which does not comply with these terms.



The Anticariogenic Efficacy of Nano Silver Fluoride

C. Pushpalatha¹, K. V. Bharkhavy¹, Arshiya Shakir¹, Dominic Augustine², S. V. Sowmya², Hammam Ahmed Bahammam³, Sarah Ahmed Bahammam⁴, Nassreen Hassan Mohammad Albar⁵, Bassam Zidane⁶ and Shankargouda Patil^{7*}

¹Department of Pedodontics and Preventive Dentistry, Faculty of Dental Sciences, M.S. Ramaiah University of Applied Sciences, Bangalore, India, ²Department of Oral Pathology and Microbiology, Faculty of Dental Sciences, M.S. Ramaiah University of Applied Sciences, Bangalore, India, ³Department of Pediatric Dentistry, College of Dentistry, King Abdulaziz University, Jeddah, Saudi Arabia, ⁴Department of Pediatric Dentistry and Orthodontics, College of Dentistry, Taibah University, Medina, Saudi Arabia, ⁵Restorative Department, Jazan University, Jazan, Saudi Arabia, ⁶Restorative Dentistry Department, King Abdulaziz University, Jeddah, Saudi Arabia, ⁷Department of Maxillofacial Surgery and Diagnostic Sciences, Division of Oral Pathology, College of Dentistry, Jazan University, Jazan, Saudi Arabia

OPEN ACCESS

Edited by:

Kumar Chandan Srivastava,
Al Jouf University, Saudi Arabia

Reviewed by:

Agnese D'Agostino,
Politecnico di Milano, Italy
Tarek El-Bialy,
University of Alberta, Canada

*Correspondence:

Shankargouda Patil
dr.ravipatil@gmail.com
orcid.org/0000-0001-7246-5497

Specialty section:

This article was submitted to
Biomaterials,
a section of the journal
Frontiers in Bioengineering and
Biotechnology

Received: 28 April 2022

Accepted: 08 June 2022

Published: 01 July 2022

Citation:

Pushpalatha C, Bharkhavy KV, Shakir A, Augustine D, Sowmya SV, Bahammam HA, Bahammam SA, Mohammad Albar NH, Zidane B and Patil S (2022) The Anticariogenic Efficacy of Nano Silver Fluoride. *Front. Bioeng. Biotechnol.* 10:931327. doi: 10.3389/fbioe.2022.931327

Dental caries is a common chronic disease, and anyone can be at threat of it throughout their lifespan. In school-aged children, dental caries is the most frequent disease related with oral health. Contemporary dental caries management focuses on non-restorative, non-invasive, and micro-invasive therapeutic techniques that effectively eliminate the caries progression at the lesion level and decrease the loss of healthy tooth structure. One of these strategies is to use caries apprehending agents with antibacterial and remineralizing characteristics. Due to recent regulatory approval in the United States, the use of silver diamine fluoride (SDF) for the therapy of dental caries has received substantial interest. SDF has successfully prevented and reversed both primary tooth caries and permanent teeth root caries. Even though SDF is an effective anti-caries agent, but it is associated with certain drawbacks like gum irritation, metallic taste, and irreversible dark stains on applying on cavities. As an alternative agent Nano Silver Fluoride (NSF) is preferable because it performs like SDF without tooth staining. It has comparable preventive and antibacterial activities as SDF. Further, it is ergonomic, economic and safe in children and adults. The current article aims to highlight the superior properties of NSF as a better anti-caries agent outstripping the limitations of discoloration of SDF.

Keywords: nano silver fluoride, silver diamine fluoride, anticaries agent, varnish, colloid

INTRODUCTION

Dental caries is a challenge since it is pervasive among children and has a detrimental influence on their quality of life. Dental caries is a worldwide public health concern that is consistently surveyed and reported in several countries. In 2020, the worldwide prevalence rate of dental caries in primary and permanent teeth was 46.2% and 53.8%, respectively, which was regarded as excessive (Kazeminia et al., 2020). A complicated interplay between acid-producing tooth-adherent bacteria and fermentable carbohydrates causes the dental caries. The acids in dental plaque may demineralize enamel and dentin in fissures and smooth surfaces of teeth over time. The so-called white spot lesion is the first visible symptom of dental caries. If demineralization continues, the white spot's surfaces will cavitate, resulting in a cavity. White spot lesions may remineralize and not progress if the demineralization environment is decreased or removed. Therefore, effective measures should be

undertaken to improve the condition described above, as well as to reconfigure and manage at all levels (Kazeminia et al., 2020). To achieve the objective of minimizing dental caries, it is necessary to seek for effective treatment and preventive treatment strategies. SDF has been used globally to combat dental caries in children, especially 38% solution. The presence of 38% SDF may decrease the demineralization of dentine and enamel and hinder the growth of cariogenic bacteria. Additionally, it prevents collagen breakdown in demineralized dentin (Mei et al., 2013a). SDF has a preventive impact on the complete dentition when just applied on carious anterior teeth and also proved successful in preventing cavities in permanent teeth (Chu et al., 2002; Mei et al., 2013a). Hence SDF therapy is considered as an indispensable component of caries prevention. According to published scientific clinical cases involving more than 4,000 young children globally, there is currently no indication of fatality or systemic detrimental consequences. SDF comprises approximately 24% and 28% (w/v) silver and 5%–6% (w/v) fluoride (Mei et al., 2013b). Oral exposure to one drop of SDF would result in a lower fluoride ion concentration than a 0.25 ml application of fluoride varnish (Crystal et al., 2017). Despite the benefits of SDF, there are disadvantages like as tooth discoloration, ulceration, and staining of tissues (Targino et al., 2014). These side effects instigated the researchers to find a material of equal efficacy while not compromising the esthetics. The application of nanoscience and technology in dentistry resulted in the emergence of Nano Silver Fluoride as a new anti-caries agent. Targino et al. (2014) first made NSF by chemically reducing silver nitrate, using chitosan as carrier and fluoride as stabilizing agent, while Haghgoo et al. (2014) made a varnish by mixing nanosilver with sodium fluoride varnish. Colloidal solution and varnish were the two most widely studied types of NSF. This novel anti-caries agent is safe for humans to use and has exceptionally significant antibacterial activity against Mutans streptococci and Lactobacilli, the primary microorganisms implicated in the formation of dental caries. The main composition of NSF proposed by Targino et al. (2014), was silver nanoparticles (376.5 µg/ml), chitosan (28,585 µg/ml), and sodium fluoride (5,028.3 µg/ml). The synergic components present in NSF formulation such as chitosan, AgNPs, and fluoride demonstrates that they are effective in caries prevention. The chitosan added into the formulation acts as stabilizing agent of the colloid with both antibacterial and anti-demineralizing effect. Fluoride incorporated into NSF also inhibits enamel mineral loss and has shown substantial capacity to suppress bacterial biofilm growth by its anti-adherence as well as anticariogenic activity. Silver is commonly used in the form of nitrates to achieve antibacterial effects. But when AgNPs are used, the surface area accessible for exposure to the microbial community is significantly increased. The antimicrobial effectiveness of nano silver particles is inversely related to their size. Sodium borohydride is frequently added as a reducing agent in preparing NSF formulations. In 2014, Haghgoo et al. (2014) prepared 5% NSF which was composed of Silver nanoparticle powder and polyvinyl pyridoline as a dispersant. It contained 22,600 ppm of slow release Sodium fluoride varnish stored in

light proof brown bottle. Some researchers have used thiolated polyethylene glycol (PEG) as a reducing and capping agent in the formulation instead of sodium borohydride to lessen its toxicity. The PEG-coated AgNPs added into formulation enhances AgNPs stability even at high ionic concentrations. This modified formulation was shown to be less hazardous and less likely to oxidize (Zhao et al., 2020). NSF is available in the form of a yellow solution that has been shown to be stable over a three-year period. This material is both ecofriendly and affordable. The aim of this literature review is to present a brief narrative review of the existing literature on the anticariogenic efficacy of Nano Silver Fluoride.

ANTICARIOGENIC ACTION OF NANO SILVER FLUORIDE

Anticariogenic action of NSF is associated with several processes, including reduced demineralization, accelerated remineralization, interference with pellicle and plaque development, and suppression of bacterial growth and metabolism. The cumulative effect of Chitosan, Silver nanoparticles, and Sodium fluoride added to the Nano Silver Fluoride formulation is responsible for the NSF anticariogenic action. The NSF colloidal formulation inhibits cariogenic biofilm formation, has antibacterial properties, and helps to remineralize teeth (Waikhom et al., 2022; Ahmed et al., 2019; Vieira Costa e Silva et al., 2018; dos Santos et al., 2014; dos Santos Junior et al., 2017). The anticariogenic effects of NSF have been surveyed through *in-vitro* and *in-vivo* studies against cariogenic microorganisms, as well as its remineralizing capability in both animal and human models which are discussed in the following headings.

Anti-Bacterial Effect of Nano Silver Fluoride

Studies reports that NSF is an excellent oral antibacterial agent because it is effective against cariogenic pathogens, primarily *Streptococcus mutans*, and also inhibits oral biofilm formation (Vieira Costa e Silva et al., 2018; Ahmed et al., 2019; Waikhom et al., 2022). Silver nanomaterials incorporated into NSF formulation are mainly necessary for the antibacterial property. The antibacterial activity of silver nanoparticles against *Streptococcus mutans* is 25 times stronger than chlorhexidine, particularly at diameters between 80 and 100 nm, while cytotoxicity has been found to rise at dimensions smaller than 20 nm (dos Santos Junior et al., 2017). Few studies have found AgNPs in NSF formulations with diameters of ranging from 2.56 ± 0.43 nm, 3.2 ± 1.2 nm and 5.9 ± 3.8 nm to favour antibacterial activity against *Streptococcus mutans* (Targino et al., 2014; dos Santos et al., 2014; Zhao et al., 2020). Studies reports that Silver nanoparticles (AgNPs) exhibits the antibacterial action by different mechanism. One such mechanism is by interrupting the bacterial cell wall and membrane integrity, encouraging the cell membrane permeability and loss of cell constituents, and ultimately inducing cell death (Shrivastava et al., 2007). AgNPs can inhibit the respiratory cascade by combining the sulfhydryl,

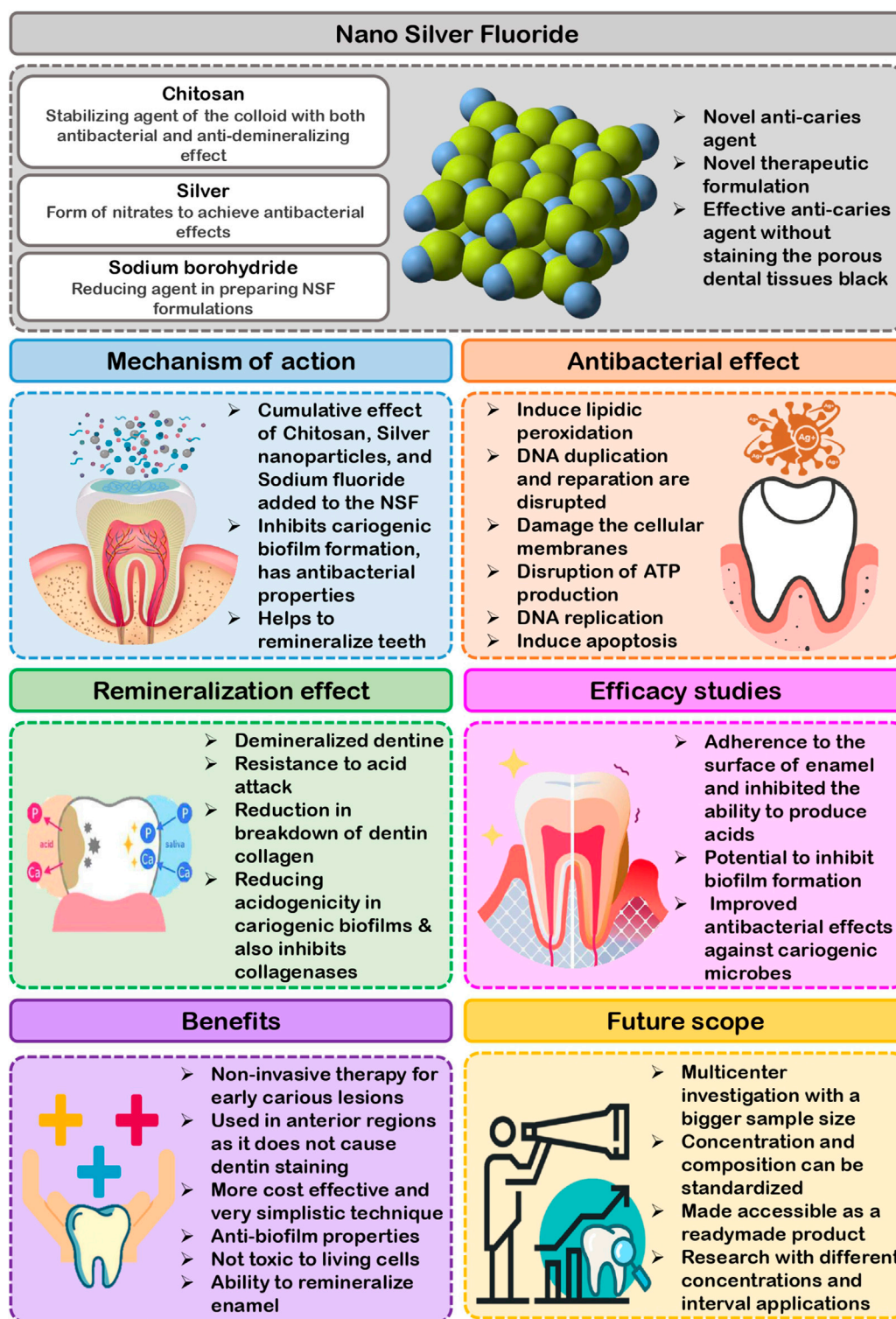


FIGURE 1 | Highlights on Nano Silver Fluoride.

causing lipid peroxidation, oxidative damage to DNA and proteins, and ultimately cell death (Hamed et al., 2017). AgNPs has a potential to attach to sulphur and phosphorous

groups in DNA, resulting in DNA damage, aggregation, and disruption of transcription and translation (Durán et al., 2010). AgNPs promote dephosphorylation of phosphotyrosines,

therefore interfering with cell signal transmission and thus damaging the cells (Shrivastava et al., 2007). When AgNPs are subjected to aerobic conditions, Ag⁺ may be released from the particles' surface. The released Ag⁺ exerts powerful antimicrobial effects by direct interaction with the cell membrane and bacterial cell wall components, which is one of the most important mechanisms of AgNPs toxicity (**Figure 1**) (Xiu et al., 2012). Kim suggests that the production of free radicals by AgNPs could be assumed as one more way for AgNPs biocidal action (Kim et al., 2007). According to electron spin resonance spectroscopy study, when AgNPs come into contact with bacteria, they produce free radicals, which can damage the cellular membranes and make it porous, ultimately resulting in cell death (Sharma et al., 2018). According to Morone's research, the antibacterial activity of silver nanoparticles is size sensitive, with nanoparticles in the 1–10 nm range being more effective (Morones et al., 2005; Martínez-Castañón et al., 2008). Due to the fact that contact area and surface energy are inversely proportional to size, the smaller the silver nanoparticle, the greater its antibacterial activity. The antibacterial action of Chitosan, a potential agent used in the NSF formulation with polycation, is soluble in aqueous solutions of small organic acids like acetic acid and lactic acid and it can be linked in the mere existence of polyvalent anions like phosphates. This chitosan during cellular adherence process inhibits *Streptococcus mutans* and demonstrated significant antibacterial and plaque reduction activity at subsequent phases of accumulation, indicating that chitosan is effective in preventing dental caries (Hamed et al., 2017). Fluoride present in NSF formulation is effective at controlling cariogenic biofilms and reduces bacterial extracellular polysaccharide formation significantly. They are indeed effective at reducing acidogenicity in cariogenic biofilms and also inhibit collagenases, which slows the breakdown of dentin collagen (Gao et al., 2016).

Remineralization of Enamel Carious Lesion by Nano Silver Fluoride

Fluoride added into the NSF formulation is mainly necessary for remineralizing early enamel carious lesion. Fluoride prevents caries largely through topical processes, such as preventing dental mineral dissolution by adsorbing onto crystal surfaces, encouraging remineralization at the crystal surfaces, and forming a fluorapatite coating that is acid resistant. The caries preventive effect of fluoride ions by its potency to establish the balance between demineralization and remineralization is crucial followed by the mitigation in the solubility of calcium hydroxyapatite (Oliveira et al., 2019). Silver nanoparticles can infiltrate into demineralized area and precipitate at that particular site resulting in an increase in the enamel hardness and resistance to acid attack (Rosenblatt et al., 2009). Chitosan, which is present in NSF formulations, has the potential to prevent tooth enamel demineralization by interfering with the release of enamel mineral elements. As a result, researchers suggested using nano silver fluoride containing silver NPs, Fluoride and chitosan is effective in enamel and dentin remineralization. Using optical coherence tomography and the microhardness

test, researchers have found that nano silver fluoride seems to have a remineralizing effect on enamel caries. In addition, a clinical study revealed that nano silver fluoride is almost as efficient as silver diamine fluoride in preventing caries (Nozari et al., 2017; Teixeira et al., 2018; Silva et al., 2019). Another study also suggested that NSF could halt active dentine caries without causing tooth discoloration (Tirupathi et al., 2019). The silver and fluoride concentrations used in Dos Santos Jr.'s study were approximately 400 ppm and 2,275 ppm, respectively for remineralizing the demineralized dentine (dos Santos Junior et al., 2017).

THERAPEUTIC USE OF NANO SILVER FLUORIDE IN DENTAL CARIES MANAGEMENT

NSF is an anticaries agent that, when administered to enamel or dentin caries lesions, provides a non-invasive approach for caries arrest and treatment. Traditional dental therapy for the management of carious lesions may be time consuming and costly, and in some situations may not be practical owing to inability to afford or tolerate invasive treatment. NSF application is affordable, non-invasive and non-toxic and hence most communities can afford it. The treatment approach is very simple; just two drops may be administered yearly to children without any risk. According to studies, NSF formulation is as effective as SDF in preventing and arresting dental caries (Nagireddy et al., 2019). NSF was compared to conventional antibacterial materials and SDF for its antibacterial efficiency against *Streptococcus mutans*, and it was found that NSF had lower Minimum Inhibitory Concentration (MIC) and Minimum Bactericidal Concentration (MBC) values than Chlorhexidine and SDF. As a result, lower NSF concentrations may be as effective as conventional products (Teixeira et al., 2018; Ahmed et al., 2019). Furthermore, NSF interfered with *Streptococcus mutans* adherence to the surface of enamel and inhibited the ability of *Streptococcus mutans* to produce acids more than Sodium Fluoride (Martínez-Castañón et al., 2008). Multidrug-resistant bacteria could be controlled by silver nanoparticles–fluoride colloids, which pose no significant hazard to human health. Nano-silver has a potential to inhibit biofilm formation by restricting biofilm-forming bacteria's development. According to research, Nano-silver in varnishes has been found to have improved antibacterial effects against cariogenic microbes such *Streptococcus mutans* and *Streptococcus salivarius* (Di Giulio et al., 2013). NSF has been identified as an effective *Streptococcus mutans* biofilm inhibitor since it can lower the CFU counts (Teixeira et al., 2018; Vieira Costa e Silva et al., 2018; Espíndola-Castro et al., 2020a). As a result, the NSF formulation may be a more biocompatible antibacterial agent for *Streptococcus mutans*.

In-vitro studies have also proven that NSF has the greatest remineralization effect when compared against Nanohydroxyapatite serum and Fluoride varnish (Nozari et al., 2017). In a study analyzing the remineralization potential using Optical Coherence Tomography (OCT) assay found that NSF

TABLE 1 | Studies related to anti-microbial activity of NSF against cariogenic pathogens.

Author	Pathogens studied	Comparator	Tests done	Research findings
Teixeira et al. (2018)	<i>Streptococcus mutans</i>	NaF toothpaste	Microdilution tests, Anti-adherence and anti-acid effects	NSF had a MIC of 30 ppm against <i>Streptococcus mutans</i> . NSF-containing dentifrices outperformed NaF-containing dentifrices in inhibiting bacterial attachment to the tooth surface (MIC of NaF dentifrice 180 ppm). NSF-containing dentifrices were able to avoid the pH drop
Vieira Costa e Silva et al. (2018)	<i>Streptococcus mutans</i>	NaF and Deionized water	Enamel adhesion and acid production	When compared to the negative control, NaF (positive control) and NSF were helpful at averting pH reduction, with NSF outperforming both the positive and negative controls
Haghighi et al. (2014)	<i>Streptococcus mutans</i> and <i>Streptococcus salivarius</i>	Different concentrations of NSF (0.1%, 0.5%, 1%, 2.5%, and 5%)	Bacteria per millimeter	<i>Streptococcus mutans</i> and <i>Streptococcus salivarius</i> were both vulnerable to nanosilver varnish, with <i>Streptococcus salivarius</i> being more susceptible than <i>Streptococcus mutans</i> . In the presence of varnishes containing 1% nanosilver or higher, the population of microorganisms was reduced
Soekanto et al. (2017)	<i>Streptococcus mutans</i> and <i>Enterococcus faecalis</i>	Propolis fluoride and SDF	MIC, MBC	PPF had a 3% MIC for <i>Streptococcus mutans</i> and a 10% minimum bactericidal concentration (MBC). PPF had a MIC of 6% for <i>Enterobacter faecalis</i> . NSF's MIC and MBC for <i>Streptococcus mutans</i> were 3.16% and 4.16%, respectively. For <i>Enterobacter faecalis</i> , the NSF MIC was 3.16%, whereas the MBC was 4.16%. Apparently NSF and PPF reduced biofilm development in a dose-dependent manner
Sayed et al. (2020)	<i>Streptococcus mutans</i> and <i>Streptococcus salivarius</i>	NaF varnish	Agar diffusion test	When the concentration of NSF was raised, the mean value of inhibition zone size (mm) rose. As the concentration of NSF was increased, the mean value of the inhibitory zone (mm) for <i>Streptococcus salivarius</i> decreased. In both bacterial strains, traditional fluoride varnish had no inhibitory zones
Gultom et al. (2019)	<i>Streptococcus mutans</i> and <i>Enterobacter faecalis</i>	SDF	Viability of Biofilm in various stages of maturation	NSF was comparable with Silver Diamine Fluoride in inhibiting formation of <i>Enterobacter faecalis</i> and <i>Streptococcus mutans</i> biofilm

outperforms NaF and has established that silver nanoparticles added to NaF for enamel remineralization of primary dentition may augment fluoride performance because of their antibacterial effect (Vieira Costa e Silva et al., 2018). Further, NSF with 600 and 1,500 ppm were shown to create very little dentin staining than commercially available SDF in a digital spectrophotometric investigation comparing dentine staining induced by NSF and SDF (Espíndola-Castro et al., 2020a). Hence NSF may be a plausible substitute to SDF because it does not compromise esthetics. Moreover, NSF preparations maintain the collagen morphology and can induce mostly intrafibrillar mineral deposition with little extrafibrillar precipitation, characteristic of biomimetic remineralization and does not cause dentin discoloration while SDF caused a change in collagen morphology because of its high pH and dentin staining (Sayed et al., 2020).

According to Asmaa Aly Abo El Soud (2020), Nano silver fluoride (NSF) is more efficient than Silver Diamine Fluoride (SDF) on demineralized enamel surfaces of human premolars extracted for orthodontic reasons (Abo El Soud et al., 2020). NSF boosts remineralization by improving the intensity and quality of apatite crystal components. Nanosilver remineralized deciduous

dental enamel and improved bactericidal activity without darkening the demineralized teeth with one exposure per year. In comparison to the usual sealant, AgNPs added to the sealant improved remineralization in permanent first molars' and nano silver-based fluoride varnish preparation formulation were compared in an *in-vitro* study done by Targino et al. They found that antimicrobial efficacy of Nano silver based fluoride varnish formulation was superior to SDF. However, the cytotoxicity of Nano silver-based fluoride varnish preparation was lower than silver diamine fluoride (Targino et al., 2014). NSF at 10,147 ppm was not found to be as effective as sodium fluoride varnish (22,600 ppm) and SDF (44,800 ppm) on surface microhardness of enamel with artificial caries lesions (Akyildiz and Sönmez, 2019). The remineralization effectiveness of NSF in solution form was greater with increased surface microhardness values after enamel remineralization in comparison with NaF varnish and nano-Hydroxyapatite Serum group (Nozari et al., 2017). Zhao et al. (2020) suggested that NSF formulation containing 2.5% NaF and PEG-AgNPs had same remineralizing potential of dentinal caries in comparison to 12% SDF.

TABLE 2 | Studies related to remineralization potential of NSF for caries prevention.

Author, Year	Samples	Experimental group	Control group	Tests done	Research findings
Zhao et al. (2020)	Third molars	1%–12% SDF, 2%–2.5% NaF + AgNps	Deionized water	SEM, Micro CT	NSF and NaF proved equally successful in remineralizing enamel, with a statistically significant difference (p 0.001) when compared to deionized water, but no distinction is made between them
Teixeira et al. (2018)	Deciduous teeth	NSF NaF	Deionized water	Vickers microhardness, OCT	There is no statistically significant difference in VHN between the NSF and NaF dentifrices. OCT analysis demonstrates that the NaF and NSF dentifrices behave similarly
Nozari et al. (2017)	Primary anterior teeth	Group 1: 5% NaF varnish Group 2: n-HAP serum Group 3: NSF	Group 4: no agent	Vickers microhardness Atomic Force microscopy	NSF is perhaps the most effective in remineralization. In terms of remineralizing early caries, both NaF varnish and n-HAP serum performed similarly
Silva et al. (2019)	Human teeth	Group 1: NSF Group 2: NaF	No agent	Optic coherence Tomography, Vickers microhardness, Fluorescence spectroscopy	The extinction coefficients of the NaF and nanosilver fluoride groups were similar, but the negative group had a lower extinction coefficient
Ata (2019)	Premolars	Group 1: Control Group 2: NSF Group 3: N-HAP Group 4: CPP-ACP paste	No treatment	Vickers Microhardness	The highest SMH values were observed in NSF group (mean: 238.84 ± 20.31)
Nanda and Naik (2020)	Premolars	Group 3: NSF + GIC Group 4: NSF + composite	Group 1: GIC Group 2: Composite	Vickers microhardness	The mean microhardness value of GIC and composite groups pretreated with NSF was more than the non-treated group, indicating lesser demineralization
Akyildiz and Sönmez (2019)	Sound Third molars	NSF group Sodium Fluoride group SDF group	No treatment	Vickers Microhardness, SEM images	NSF group showed maximum mineral deposit on enamel surface
El-Desouky et al. (2021)	Primary teeth	NSF group (Ia) Fluoride Varnish Group (IIa)	No treatment (Ib, IIb)	Vickers Microhardness, Polarized Light microscopy	Both NSF and Fluoride varnish is equally effective

TABLE 3 | *In-Vivo* randomized controlled studies related to NSF for caries management.

Author, Year	Study sample	Comparison	Research findings
Arnaud et al. (2021)	337 children aged between 5 and 7 years	NSF 600—Intervention and NSF 400—Positive control	When compared to NSF 400 (56.5%), NSF 600 had a greater performance level in preventing caries (72.7%, $p = 0.025$)
Freire et al. (2017)	12 school children of both genders, between 7 and 8 years	NSF- Experimental group Saline- Control group	In comparison to the other groups, NSF had lower CFU numbers. <i>Streptococcus mutans</i> growth in enamel treated with NSF is reduced
Nagireddy et al. (2019)	100 deciduous molars from 60 children	NSF- Experimental group Saline- Control group	After 7 days, 78% of teeth in the NSF group exhibited arrest of dentine caries, whereas 72.91% showed arrested caries after 5 months and 65.21% after 12 months
Tirupathi et al. (2019)	159 active dentinal carious lesions in primary molars (from 50 children)	5% Nano-silver fluoride varnish - Experimental group SDF—Control group	Success rate of 77% at the end of twelve-month follow up with Nano-silver fluoride varnish
Butrón-Téllez Girón et al. (2017)	22 children aged from 1 to 6 years	Experimental group- Fluoride varnish added with 0.1% AgNPs Control group- Commercial fluoride varnish	Teeth that had been lacquered with AgNPs showed a lower mean fluorescence intensity than those that had been painted with commercial varnish
dos Santos et al. (2014)	Primary teeth (130) in children	NSF—Experimental group Water- Control group	72.7% of the NSF group had halted decay, whereas 27.4% of the control group had 66.7% of lesions treated with NSF were still arrested after a year
Al-Nerabieah et al. (2020)	63 preschoolers with 164 active lesions	Combination of Nano-Silver Fluoride and Green Tea Extract (NSF-GTE) with SDF	At the end of 6 months, NSF-GTE and SDF had total arrest rates of 67.4% and 796

In underdeveloped countries, Nano Silver Fluoride (NSF) was a successful agent for preventing and reversing dental caries, but its influence on caries must be examined using alternate evaluation methods as well. The dental biofilm adhered to enamel treated with NSF had decreased numbers of *Streptococcus mutans* viability (absorbance) and colony forming units (CFU), and there was also a substantial distinction between the OHI-S mean values at baseline in a pilot randomised double blind crossover clinical study to evaluate the antimicrobial properties of NSF in 12 school children with their teeth treated with NSF in the experimental group and saline in the control group. Nanosilver fluoride was shown to be an efficient dental biofilm suppressor since it lowered *Streptococcus mutans* CFU counts and absorbance values, had no impact on biofilm pH, and decreased OHI-S values (Freire et al., 2017). Another study conducted in 130 decayed deciduous teeth of children treated with NSF and control (water), 81% of teeth in the NSF group had halted carious lesions on day 7, 72.7% after 5 months and 66.7% of lesions were still arrested after a year, whereas the control group had 0%, 27.4% and 34.7% respectively (dos Santos et al., 2014). In yet another study conducted in 22 children aged 1–6 years with white spot lesions detected by baseline DIAGNOdent values were treated with the fluoride plus 0.1% AgNPs and the children in control group were treated with commercial fluoride varnish once a week for a 3 weeks and after 3 months follow-up DIAGNOdent measurements were taken and it was found that teeth coated with AgNPs varnish exhibited lower mean fluorescence intensity than those treated generic varnish, indicating that dental remineralization was higher in this group (Butrón-Téllez Girón et al., 2017). Tirupathi et al. tested the therapeutic caries arresting potency of a prepared 5% silver nanoparticles introduced Sodium fluoride (NSF) varnish with commercially available thirty eight percent SDF in 159 primary molars in 50 children for a year and showed similar number of active and arrested caries. In primary molars, the authors discovered that a 5% NSSF therapy administered yearly is superior to or similar to a 38% SDF treatment in preventing dentinal caries (Tirupathi et al., 2019). In one of the double blinded randomized controlled trial done to compare the efficacy of different concentrations of NSF it was disclosed that higher concentrations of AgNPs in NSF attributed to the superior antibacterial efficacy. NSF when administered straight to dentinal caries, resulted in stoppage of cavities in 65.21% of teeth, and hence provides a minimally invasive approach for decay stoppage and cure (Nagireddy et al., 2019). Hence, from these in-vivo investigations, it can be concluded that NSF application can prevent tooth caries in around 65%–70% of instances, with no significant difference between NSF and SDF and has comparable clinical effectiveness as SDF in reducing the advancement of dentinal carious lesions in primary posterior teeth when applied once a year. In-vitro comparison of different fluoride-based varnishes such as SDF, NSF and propolis fluoride showed significantly increased level of calcium, phosphate, and fluoride ions on the treated human dentin discs surface. This suggests that NSF is a promising anticariogenic agent (Soekanto et al., 2017).

Table 1 highlights the *in-vitro* research and clinical trials exploring at NSF's antibacterial impact, whereas **Table 2** provides *in-vitro* and *in-vivo* remineralizing potential studies for caries management. **Table 3** overviews *in-vivo* randomized controlled studies using NSF for caries management.

BENEFITS OF NANO SILVER FLUORIDE

NSF can be used with minimal armamentarium even in peripheral community treatment camps. Since NSF is a non-invasive treatment for the management of early carious lesions, it will not create uncooperative behavior in very young children. It is safe to use in the anterior teeth without fear of tooth discoloration. NSF formulations do not oxidize when it comes in contact with the oxygen of the medium, hence is stable. There was no colour change noticed over time because of size of the AgNPs. Espíndola-Castro *et al* reported that yellowish stains are noticed after 2 weeks of NSF application mainly due the chitosan present in the formulation. However, these stains can be easily removed by gauze or by tooth brushing (Espíndola-Castro et al., 2020b). It does not irritate soft tissues since it has a lower pH and is more biocompatible. NSF is more cost effective than SDF and do not have metallic taste (Yin et al., 2020). Also, it has a very simple technique of application which can be learned by paramedical staffs at a Primary Health Center who can provide this treatment under a Dentist's supervision. Nano silver particles have the ability to remineralize enamel, particularly in deciduous teeth even at a lower concentration. It is bactericidal to wide range of organisms like *Streptococcus mutans*, *Enterococcus faecalis*, and *Escherichia coli*. It has anti-biofilm properties as well. Nano silver fluoride is not toxic to living cells since majority of NSF formulations are prepared at a very low concentration (Akyildiz and Sönmez, 2019).

FUTURE SCOPE

To generalize the results, a multicenter investigation with a bigger sample size may be done. NSF concentration and composition can be standardized and made accessible as a readymade product. Primary health care personnel can be taught how to use NSF on children with high caries risk and from underserved populations. Research with different concentrations and frequencies of applications with larger sample size can be conducted to determine the best protocol for Nano-Silver Fluoride with natural extract application. Future *in vitro* and *in vivo* research can be conducted by integrating NSF into dental restorative materials to provide both antibacterial and remineralization advantages in a single material. This unique dental restorative material may prevent secondary caries, which is one of the most significant shortcomings in conventional restorative materials. Since NSF has excellent antibacterial property against wide range of pathogens it may be used in periodontal therapy to prevent and treat periodontal infections.

CONCLUSION

NSF is an economic, ergonomic, non-invasive agent that is safer in children and adults. Also, it is biocompatible, non-discoloring, non-caustic and more efficient than the conventional fluorides and SDF. NSF can be used to treat decayed primary teeth in underdeveloped countries since it is simple, cheap, and does not require a sensitive application method. Thus, NSF is a better anticaries agent outstripping the limitations of SDF.

AUTHOR CONTRIBUTIONS

CP: Conceptualization, resources, data curation, original draft preparation, and supervision. KB: Conceptualization, resources, data curation, and original draft preparation. AS:

REFERENCES

- Abo El Soud, A. A., Elsaied, H. A., and Omar, S. M. M. (2020). Comparative Evaluation of the Effects of Silver Diamine Fluoride (Commercial and Lab Prepared) versus Nano Silver Fluoride on Demineralized Human Enamel Surfaces (*In Vitro* Study). *Egypt. Dent. J. (Oral Med. X-Ray, Oral Biol. Oral Pathology)* 66, 153–163. doi:10.21608/edj.2020.77529
- Ahmed, F., Prashanth, S., Sindhu, K., Nayak, A., and Chaturvedi, S. (2019). Antimicrobial Efficacy of Nanosilver and Chitosan against *Streptococcus Mutans*, as an Ingredient of Toothpaste Formulation: An *In Vitro* Study. *J. Indian Soc. Pedod. Prev. Dent.* 37 (1), 46. doi:10.4103/jisppd.jisppd_239_18
- Akyildiz, M., and Sönmez, I. S. (2019). Comparison of Remineralising Potential of Nano Silver Fluoride, Silver Diamine Fluoride and Sodium Fluoride Varnish on Artificial Caries: an *In Vitro* Study. *Oral Health Prev. Dent.* 17 (5), 469–477. doi:10.3290/j.ohpd.a42739
- Al-Nerabieah, Z., Arrag, E. A., Comisi, J. C., and Rajab, A. (2020). Effectiveness of a Novel Nano-Silver Fluoride with Green Tea Extract Compared with Silver Diamine Fluoride: A Randomized, Controlled, Non-inferiority Trial. *Ijdos* 7, 753–761. doi:10.19070/2377-8075-20000148
- Arnaud, M., Junior, P. C., Lima, M. G., e Silva, A. V., Araujo, J. T., Gallembek, A., et al. (2021). Nano-silver Fluoride at Higher Concentration for Caries Arrest in Primary Molars: A Randomized Controlled Trial. *Int. J. Clin. Pediatr. Dent.* 14 (2), 207–211. doi:10.5005/jp-journals-10005-1920
- Ata, M. S. (2019). Influence of Nano-Silver Fluoride, Nano-Hydroxyapatite and Casein Phosphopeptide-Amorphous Calcium Phosphate on Microhardness of Bleached Enamel: *In-Vitro* Study. *Tanta Dent. J.* 16 (1), 25. doi:10.4103/tjdtj_29_18
- Butrón-Téllez Girón, C., Mariel-Cárdenas, J., Pierdant-Pérez, M., Hernández-Sierra, J. F., Morales-Sánchez, J. E., and Ruiz, F. (2017). Effectiveness of a Combined Silver Nanoparticles/fluoride Varnish in Dental Remineralization in Children: *In Vivo* Study. *Superf. vacío* 30 (2), 21–24. doi:10.47566/2017_syv30_1-020021
- Chu, C. H., Lo, E. C. M., and Lin, H. C. (2002). Effectiveness of Silver Diamine Fluoride and Sodium Fluoride Varnish in Arresting Dentin Caries in Chinese Pre-school Children. *J. Dent. Res.* 81 (11), 767–770. doi:10.1177/154405910208101109
- Crystal, Y. O., Marghalani, A. A., Ureles, S. D., Wright, J. T., Sulyanto, R., Divaris, K., et al. (2017). Use of Silver Diamine Fluoride for Dental Caries Management in Children and Adolescents, Including Those with Special Health Care Needs. *Pediatr. Dent.* 39 (5), 135–145.
- Di Giulio, M., Di Bartolomeo, S., Di Campli, E., Sancilio, S., Marsich, E., Travan, A., et al. (2013). The Effect of a Silver Nanoparticle Polysaccharide System on *Streptococcal* and *Saliva-Derived* Biofilms. *Ijms* 14 (7), 13615–13625. doi:10.3390/ijms140713615
- dos Santos Junior, V. E., Targino, A. G. R., Flores, M. A. P., Rodríguez-Díaz, J. M., Teixeira, J. A., Heimer, M. V., et al. (2017). Antimicrobial Activity of Silver Conceptualization, resources, data curation, and original draft preparation. DA: Original draft preparation, review and editing, visualization. SS: Original draft preparation, review and editing, visualization. HB: Review and editing, visualization, supervision. SB: Review and editing, visualization, supervision. NA: Review and Editing, visualization, supervision. BZ: Review and editing, visualization, supervision. SP: Original draft preparation, review and editing, visualization, supervision. All authors agree to be accountable for the content of the work.
- Nanoparticle Colloids of Different Sizes and Shapes against *Streptococcus Mutans*. *Res. Chem. Intermed.* 43 (10), 5889–5899. doi:10.1007/s11164-017-2969-5
- dos Santos, V. E., Jr, Filho, A. V., Ribeiro Targino, A. G., Pelagio Flores, M. A., Galembeck, A., Caldas, A. F., Jr, et al. (2014). A New "Silver-Bullet" to Treat Caries in Children - Nano Silver Fluoride: A Randomised Clinical Trial. *J. Dent.* 42 (8), 945–951. doi:10.1016/j.jdent.2014.05.017
- Durán, N., Marcato, P. D., Conti, R. D., Alves, O. L., Costa, F., and Brocchi, M. (2010). Potential Use of Silver Nanoparticles on Pathogenic Bacteria, Their Toxicity and Possible Mechanisms of Action. *J. Braz. Chem. Soc.* 21 (6), 949–959. doi:10.1590/S0103-50532010000600002
- El-Desouky, D., Hanno, A., Dowidar, K., Hamza, S. A., and El-Desouky, L. M. (2021). Evaluation of the Anticariogenic Effect of Nano Silver Fluoride on Demineralization of Enamel in Primary Teeth (An *In Vitro* Study). *Alexandria Dent. J.* 46 (2), 153–159. doi:10.21608/adjalexu.2020.20537.1017
- Espíndola-Castro, L. F., Rosenblatt, A., Galembeck, A., and Monteiro, G. (2020). Dentin Staining Caused by Nano-Silver Fluoride: a Comparative Study. *Oper. Dent.* 45 (4), 435–441. doi:10.2341/19-109-L
- Espíndola-Castro, L. F., Rosenblatt, A., Galembeck, A., and Monteiro, G. (2020). Dentin Staining Caused by Nano-Silver Fluoride: a Comparative Study. *Oper. Dent.* 45 (4), 435–441. doi:10.2341/19-109-L
- Freire, P. L. L., Albuquerque, A. J. R., Sampaio, F. C., Galembeck, A., Flores, M. A. P., Stamford, T. C. M., et al. (2017). AgNPs: The New Allies against *S. Mutans* Biofilm - A Pilot Clinical Trial and Microbiological Assay. *Braz. Dent. J.* 28, 417–422. doi:10.1590/0103-6440201600994
- Gao, S., Zhang, S., Mei, M. L., Lo, E. C., and Chu, C. H. (2016). Caries Remineralisation and Arresting Effect in Children by Professionally Applied Fluoride Treatment - a Systematic Review. *BMC oral health* 16 (1), 12–19. doi:10.1186/s12903-016-0171-6
- Gultom, F. P., Khoirunnisa, N., Sahlan, M., and Soekanto, S. A. (2019). Evaluation of the Potential of Nano Silver Fluoride against *Streptococcus Mutans* and *Enterobacter Faecalis* in Various Stages of Biofilm Maturation, AIP Conference Proceedings, Melville, USA (College Park, Maryland).
- Haghgoo, R., Saderi, H., Eskandari, M., Haghshenas, H., and Rezvani, M. (2014). Evaluation of the Antimicrobial Effect of Conventional and Nanosilver-Containing Varnishes on Oral *Streptococci*. *J. Dent. (Shiraz)* 15 (2), 57–62.
- Hamed, S., Emara, M., Shawky, R. M., El-domany, R. A., and Youssef, T. (2017). Silver Nanoparticles: Antimicrobial Activity, Cytotoxicity, and Synergism with N-Acetyl Cysteine. *J. Basic Microbiol.* 57 (8), 659–668. doi:10.1002/jobm.201700087
- Kazemina, M., Abdi, A., Vaisi-Raygani, A., Jalali, R., Shohaimi, S., Daneshkhah, A., et al. (2020). The Effect of Lavender (*Lavandula Stoechas* L.) on Reducing Labor Pain: A Systematic Review and Meta-Analysis. *Evidence-Based Complementary Altern. Med.* 2020 (1), 1–11. doi:10.1155/2020/4384350
- Kim, J. S., Kuk, E., Yu, K. N., Kim, J.-H., Park, S. J., Lee, H. J., et al. (2007). Antimicrobial Effects of Silver Nanoparticles. *Nanomedicine Nanotechnol. Biol. Med.* 3, 95–101. doi:10.1016/j.nano.2006.12.001

- Liu, B. Y., Lo, E. C. M., Chu, C. H., and Lin, H. C. (2012). Randomized Trial on Fluorides and Sealants for Fissure Caries Prevention. *J. Dent. Res.* 91 (8), 753–758. doi:10.1177/0022034512452278
- Martínez-Castañón, G. A., Nino-Martínez, N., Martínez-Gutiérrez, F., Martínez-Mendoza, J. R., and Ruiz, F. (2008). Synthesis and Antibacterial Activity of Silver Nanoparticles with Different Sizes. *J. nanoparticle Res.* 10 (8), 1343–1348. doi:10.1007/s11051-008-9428-6
- Mei, M. L., Chu, C. H., Lo, E. C. M., and Samaranayake, L. P. (2013). Fluoride and Silver Concentrations of Silver Diammine Fluoride Solutions for Dental Use. *Int. J. Paediatr. Dent.* 23 (4), 279–285. doi:10.1111/ipd.12005
- Mei, M. L., Ito, L., Cao, Y., Li, Q. L., Lo, E. C. M., and Chu, C. H. (2013). Inhibitory Effect of Silver Diamine Fluoride on Dentine Demineralisation and Collagen Degradation. *J. Dent.* 41 (9), 809–817. doi:10.1016/j.jdent.2013.06.009
- Morones, J. R., Elechiguerra, J. L., Camacho, A., Holt, K., Kouri, J. B., Ramírez, J. T., et al. (2005). The Bactericidal Effect of Silver Nanoparticles. *Nanotechnology* 16, 2346–2353. doi:10.1088/0957-4484/16/10/059
- Nagireddy, V. R., Reddy, D., Kondamadugu, S., Puppala, N., Mareddy, A., and Chris, A. (2019). Nanosilver Fluoride-A Paradigm Shift for Arrest in Dental Caries in Primary Teeth of Schoolchildren: A Randomized Controlled Clinical Trial. *Int. J. Clin. Pediatr. Dent.* 12 (6), 484–490. doi:10.5005/jp-journals-10005-1703
- Nanda, K. J., and Naik, S. (2020). An *In-Vitro* Comparative Evaluation of Pre-treatment with Nano-Silver Fluoride on Inhibiting Secondary Caries at Tooth Restoration Interface. *Cureus* 12 (5), e7934. doi:10.7759/cureus.7934
- Nozari, A., Ajami, S., Rafiei, A., and Niazi, E. (2017). Impact of Nano Hydroxyapatite, Nano Silver Fluoride and Sodium Fluoride Varnish on Primary Teeth Enamel Remineralization: an *In Vitro* Study. *J. Clin. Diagn. Res.* 11 (9), ZC97. doi:10.7860/JCDR/2017/30108.10694
- Oliveira, B. H., Rajendra, A., Veitz-Keenan, A., and Niederman, R. (2019). The Effect of Silver Diamine Fluoride in Preventing Caries in the Primary Dentition: a Systematic Review and Meta-Analysis. *Caries Res.* 53 (1), 24–32. doi:10.1159/000488686
- Rosenblatt, A., Stamford, T., and Niederman, R. (2009). Oral Health Care in Disadvantaged Communities' Oral Health Care in Disadvantaged Communities, 1999. *J. Dent. Res.* 88 (2), 116–125.
- Sayed, M., Hiraishi, N., Matin, K., Abdou, A., Burrow, M. F., and Tagami, J. (2020). Effect of Silver-Containing Agents on the Ultra-structural Morphology of Dentinal Collagen. *Dent. Mater.* 36 (7), 936–944. doi:10.1016/j.dental.2020.04.028
- Sharma, G., Nam, J.-S., Sharma, A., and Lee, S.-S. (2018). Antimicrobial Potential of Silver Nanoparticles Synthesized Using Medicinal Herb Coptidis Rhizome. *Molecules* 23 (9), 2268. doi:10.3390/molecules23092268
- Shrivastava, S., Bera, T., Roy, A., Singh, G., Ramachandrarao, P., and Dash, D. (2007). Characterization of Enhanced Antibacterial Effects of Novel Silver Nanoparticles. *Nanotechnology* 18 (22), 225103. doi:10.1088/0957-4484/18/22/225103
- Silva, A. V. C., Teixeira, J. D. A., Melo, P. C. D., Lima, M. G. D. S., Mota, C. C. B. D. O., Lins, E. C. C., et al. (2019). Remineralizing Potential of Nano-Silver-Fluoride for Tooth Enamel: an Optical Coherence Tomography Analysis. *Pesqui. Bras. em Odontopediatria Clínica Integr.* 19. doi:10.4034/pboci.2019.191.50
- Soekanto, S. A., Rosithahakiki, N., Sastradipura, D. F. S., and Sahlan, M. (2017). Comparison of the Potency of Several Fluoride-Based Varnishes as an Anticariogenic on Calcium, Phosphate, and Fluoride Ion Levels. *Int. J. Appl. Pharm.* 9, 55–59. doi:10.22159/IJAP.2017.V9S2.14
- Targino, A. G. R., Flores, M. A. P., dos Santos Junior, V. E., de Godoy Bené Bezerra, F., de Luna Freire, H., Galembeck, A., et al. (2014). An Innovative Approach to Treating Dental Decay in Children. A New Anti-caries Agent. *J. Mater. Sci. Mater. Med.* 25 (8), 2041–2047. doi:10.1007/s10856-014-5221-5
- Teixeira, J. A., Santos Júnior, V. E. D., Melo Júnior, P. C. D., Arnaud, M., Lima, M. G., Flores, M. A. P., et al. (2018). Effects of a New Nano-Silver Fluoride-Containing Dentifrice on Demineralization of Enamel and streptococcus Mutans Adhesion and Acidogenicity. *Int. J. Dent.* 2018, 1351925. doi:10.1155/2018/1351925
- Tirupathi, S., Svsg, N., Rajasekhar, S., and Nuvvula, S. (2019). Comparative Cariostatic Efficacy of a Novel Nano-Silver Fluoride Varnish with 38% Silver Diamine Fluoride Varnish a Double-Blind Randomized Clinical Trial. *J. Clin. Exp. Dent.* 11 (2), e105–e112. doi:10.4317/jced.54995
- Vieira Costa e Silva, A., Teixeira, J. A., Mota, C. C. B. O., Clayton Cabral Correia Lins, E., Correia de Melo Júnior, P., de Souza Lima, M. G., et al. (2018). *In Vitro* morphological, Optical and Microbiological Evaluation of Nanosilver Fluoride in the Remineralization of Deciduous Teeth Enamel. *Nanotechnol. Rev.* 7 (6), 509–520. doi:10.1515/ntrev-2018-0083
- Waikhom, N., Agarwal, N., Jabin, Z., and Anand, A. (2022). Antimicrobial Effectiveness of Nano Silver Fluoride Varnish in Reducing Streptococcus Mutans in Saliva and Plaque Biofilm when Compared with Chlorhexidine and Sodium Fluoride Varnishes. *J. Clin. Exp. Dent.* 14 (4), e321–e328. doi:10.4317/jced.59093
- Xiu, Z.-m., Zhang, Q.-b., Puppala, H. L., Colvin, V. L., and Alvarez, P. J. J. (2012). Negligible Particle-specific Antibacterial Activity of Silver Nanoparticles. *Nano Lett.* 12 (8), 4271–4275. doi:10.1021/nl301934w
- Yin, I. X., Zhao, I. S., Mei, M. L., Lo, E. C. M., Tang, J., Li, Q., et al. (2020). Synthesis and Characterization of Fluoridated Silver Nanoparticles and Their Potential as a Non-staining Anti-caries Agent. *Ijn* 15, 3207–3215. doi:10.2147/ijn.s243202
- Zhao, I. S., Yin, I. X., Mei, M. L., Lo, E. C. M., Tang, J., Li, Q., et al. (2020). Remineralising Dentine Caries Using Sodium Fluoride with Silver Nanoparticles: An *In Vitro* Study. *Ijn* 15, 2829–2839. doi:10.2147/ijn.s247550

Conflict of Interest: The authors declare that the research was conducted in the absence of any commercial or financial relationships that could be construed as a potential conflict of interest.

Publisher's Note: All claims expressed in this article are solely those of the authors and do not necessarily represent those of their affiliated organizations, or those of the publisher, the editors and the reviewers. Any product that may be evaluated in this article, or claim that may be made by its manufacturer, is not guaranteed or endorsed by the publisher.

Copyright © 2022 Pushpalatha, Bharkhavy, Shakir, Augustine, Sowmya, Bahammam, Bahammam, Mohammad Albar, Zidane and Patil. This is an open-access article distributed under the terms of the Creative Commons Attribution License (CC BY). The use, distribution or reproduction in other forums is permitted, provided the original author(s) and the copyright owner(s) are credited and that the original publication in this journal is cited, in accordance with accepted academic practice. No use, distribution or reproduction is permitted which does not comply with these terms.



Modified Mineral Trioxide Aggregate—A Versatile Dental Material: An Insight on Applications and Newer Advancements

C. Pushpalatha¹, Vismaya Dhareshwar¹, S. V. Sowmya², Dominic Augustine², Thilla Sekar Vinothkumar^{3,4}, Apathsakayan Renugalakshmi⁵, Amal Shaiban⁶, Ateet Kakti⁷, Shilpa H. Bhandi^{8,9}, Alok Dubey¹⁰, Amulya V. Rai¹ and Shankargouda Patil^{11,12*}

OPEN ACCESS

Edited by:

Kumar Chandan Srivastava,
Al Jouf University, Saudi Arabia

Reviewed by:

Hector Flores,
Autonomous University of San Luis
Potosí, Mexico
Shivaranjany Sivakumar,
Mahsa University, Malaysia

*Correspondence:

Shankargouda Patil
dr.ravipatil@gmail.com
orcid.org/0000-0001-7246-5497

Specialty section:

This article was submitted to
Biomaterials,
a section of the journal
Frontiers in Bioengineering and
Biotechnology

Received: 11 May 2022

Accepted: 24 June 2022

Published: 09 August 2022

Citation:

Pushpalatha C, Dhareshwar V,
Sowmya SV, Augustine D,
Vinothkumar TS, Renugalakshmi A,
Shaiban A, Kakti A, Bhandi SH,
Dubey A, Rai AV and Patil S (2022)
Modified Mineral Trioxide
Aggregate—A Versatile Dental
Material: An Insight on Applications
and Newer Advancements.
Front. Bioeng. Biotechnol. 10:941826.
doi: 10.3389/fbioe.2022.941826

¹Department of Pedodontics and Preventive Dentistry, Faculty of Dental Sciences, M.S. Ramaiah University of Applied Sciences, Bangalore, India, ²Department of Oral Pathology and Microbiology, Faculty of Dental Sciences, M.S. Ramaiah University of Applied Sciences, Bangalore, India, ³Department of Restorative Dental Science, Division of Operative Dentistry, College of Dentistry, Jazan University, Jazan, Saudi Arabia, ⁴Department of Conservative Dentistry and Endodontics, Saveetha Dental College, Saveetha Institute of Medical and Technical Sciences, Chennai, India, ⁵Department of Preventive Dental Sciences, Division of Pedodontics, College of Dentistry, Jazan University, Jazan, Saudi Arabia, ⁶Department of Endodontics, College of Dentistry, King Khalid University, Abha, Saudi Arabia, ⁷Department of Pediatric Dentistry, Preventive Division, Riyadh Elm University, Riyadh, Saudi Arabia, ⁸Department of Restorative Dental Science, Division of Operative Dentistry, College of Dentistry, Jazan University, Jazan, Saudi Arabia, ⁹Department of Cariology, Saveetha Dental College and Hospitals, Saveetha Institute of Medical and Technical Sciences, Saveetha University, Chennai, India, ¹⁰Department of Preventive Dental Sciences, Division of Pedodontics, College of Dentistry, Jazan University, Jazan, Saudi Arabia, ¹¹Department of Maxillofacial Surgery and Diagnostic Sciences, Division of Oral Pathology, College of Dentistry, Jazan University, Jazan, Saudi Arabia, ¹²Centre of Molecular Medicine and Diagnostics (COMManD), Saveetha Dental College and Hospitals, Saveetha Institute of Medical and Technical Sciences, Saveetha University, Chennai, India

Mineral Trioxide Aggregate (MTA) has been a material of revolution in the field of dentistry since its introduction in the 1990s. It is being extensively used for perforation repairs, apexification, root-end filling, obturation, tooth fracture repair, regenerative procedures, apexogenesis, pulpotomies, and as a pulp-capping material because of its desired features such as biocompatibility, bioactivity, hydrophilicity, sealing ability, and low solubility. Even though its application is wide, it has its own drawbacks that prevent it from reaching its full potential as a comprehensive replacement material, including a long setting time, discoloration, mud-like consistency, and poor handling characteristics. MTA is a material of research interest currently, and many ongoing studies are still in process. In this review, the newer advancements of this versatile material by modification of its physical, chemical, and biological properties, such as change in its setting time, addressing the discoloration issue, inclusion of antimicrobial property, improved strength, regenerative ability, and biocompatibility will be discussed. Hence, it is important to have knowledge of the traditional and newer advancements of MTA to fulfill the shortcomings associated with the material.

Keywords: Mineral Trioxide Aggregate, MTA, Modified MTA, Drug Delivery, Discoloration

INTRODUCTION

The practice of endodontic treatment has changed significantly over the past 200 years, with considerable advancements in technology and techniques. The conventional approach has undergone various changes, owing to rising patient demand for tooth preservation and improvements in material science and novel technology. Mineral Trioxide Aggregate (MTA) is a potent material in endodontics that has changed the prognosis of patients with the worst clinical condition of their teeth (Kaur et al., 2017). Despite the fact that the oral environment is typically damp, all dental products perform best in a dry environment. MTA is a Product developed using Portland cement and bismuth oxide (Camilleri, 2015).

The MTA was designed for certain clinical applications where maintaining a dry field is problematic, such as retrograde endodontic filling and the repair of perforated areas. Extended usage includes apexification, dressing over pulpotomies (PP), as a pulp-capping (PC) material, and sealer cement. The versatile nature of the MTA's application demanded the necessity for new preparations that included additives with cement, which is an original or combination of radiopacifiers. These modifications are intended to improve the material's properties and functionality (Figure1).

MTA is composed of Portland cement with bismuth oxide and gypsum. Calcium, silicon, and aluminum are the other constituents of cement. Tricalcium and dicalcium silicates and tricalcium aluminate are the primary component (Figure2). MTA is made of 50–75% calcium oxide (CaO) and 15–25% silicon dioxide (SiO₂) by weight. They make up 70–95% of cement (Camilleri, 2015). When the aforementioned raw ingredients are combined, then tricalcium silicate, dicalcium silicate, tricalcium aluminate, and tetracalcium aluminoferrite are formed. MTA is Type 1 Portland cement (American Society for Testing Materials), with a fineness (Blaine number) ranging from 4,500 to 4,600 cm²/g. For easier dental radiographic diagnosis, bismuth oxide is added to the cement (Camilleri, 2008).

X-ray diffraction analysis is used to determine the phases formed in MTA. Tricalcium silicate, dicalcium silicate, and bismuth oxide exhibited peaks in unhydrated MTA. Other phases, such as dicalcium silicate and tricalcium aluminate, are present in trace amounts (Camilleri, 2015). The original Portland cement formulation was replaced with tricalcium silicate to avoid the inclusion of an aluminum phase and to eliminate trace elements. Bismuth oxide was replaced with alternative radiopacifiers. Because of its many functions, MTA can come into contact with a range of oral environmental factors, including blood, saliva, tissue fluids, dental restorative materials, tooth structure, and even air. The quality and setting of the material are affected under these conditions (Tawil et al., 2015).

The setting time, mechanical properties, discoloration, manipulation, and mud-like consistency of cements have been a major technical concern of traditional MTA for a long time. More recently, these practical issues have emerged as a key source of concern for applications in the field of dentistry, particularly when it comes to the setting time, which should be maintained to a minimum. The goal of this review is to use an evidence-based dental approach to systematically evaluate the literature of modified MTA in order to overcome these shortcomings when compared to commercially available MTA.

HISTORY

Portland cement was first used in dental literature in 1878 by Dr. Witte in Germany, who published a case report on utilizing the material to plug root canals. Joseph Aspdin, an Englishman, invented Portland cement in 1824. Over a century later, Dr. Mahmoud Torabinejad and his co-inventor, Dean White, received two US patents for MTA.

MTA was originally published in the dental literature in 1993 and was approved by the FDA in 1998. In 1998, Dentsply, Tulsa Dental, Johnson City, TN, United States, commercialized the original MTA as ProRoot MTA. The

Modified Mineral Trioxide Aggregate – A Versatile Dental Material

- Novel biomaterials
- Versatile nature
- Maintaining a dry field is problematic
- The repair of perforation area



MTA

- 50-75 % calcium oxide (CaO) and 15-25 % silicon dioxide (SiO₂)
- Modifications are intended to improve the material's properties and functionality

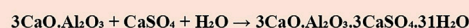
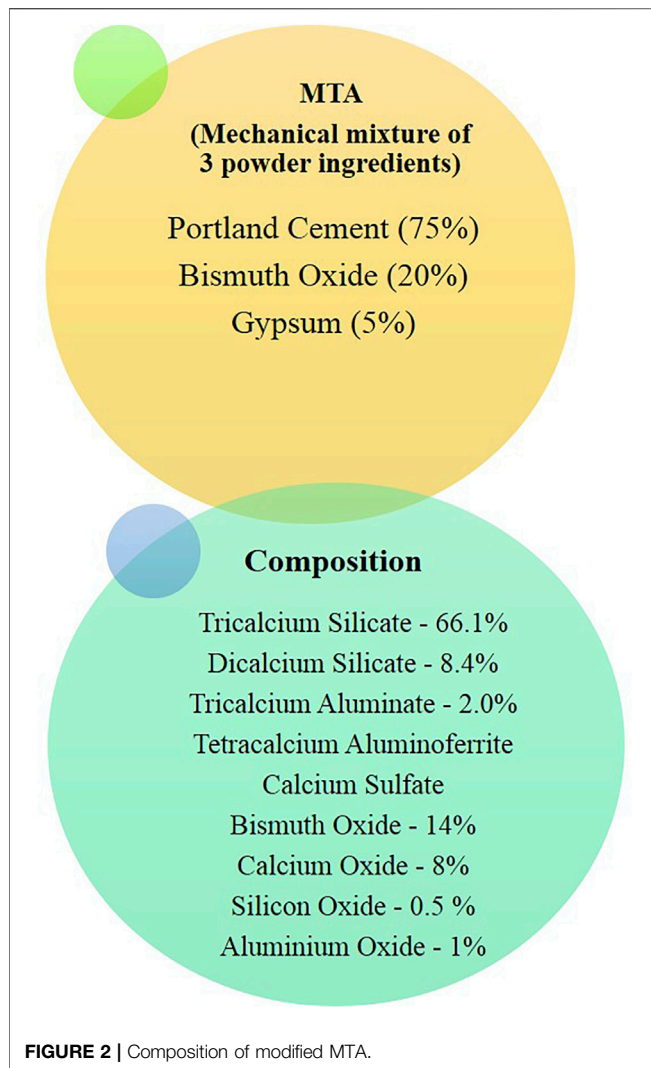


FIGURE 1 | Properties that make modified MTA a versatile dental material.



“Tooth-colored ProRoot MTA” was first introduced in 2002 and was later patented. ProRoot MTA gray and white versions had comparable compositions, while the tooth-colored versions use white Portland cement, which has less iron content.

Following the ProRoot, Dentsply introduced more MTA formulations. MTA Angelus (Angelus, Londrina, Brazil/Clinician’s Choice, New Milford, CT) was first introduced in Brazil in 2001 and acquired FDA approval in 2011, allowing it to be sold in the United States (Tawil et al., 2015). Angelus was the first to introduce it, and it included both gray and white formulations. Bismuth oxide with Portland cement was used in MTA Angelus. It contained different amounts of tricalcium and dicalcium silicate than ProRoot MTA and other cements (Camilleri, 2008). According to the manufacturer, the absence of gypsum decreased the material’s setting time. Hence, MTA Angelus was found to set in less than 50 min, compared to that of ProRoot MTA, which has been claimed to take over 2 h to set (Camilleri, 2015). When compared to ProRoot MTA, MTA Angelus had a lower level of bismuth oxide, which explains the reduced radiopacity of the material. The first MTA products

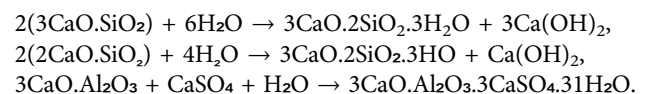
were gray, and this formulation was the focus of much of the early research. The white form of MTA was introduced to the market in 2002 in response to staining problems raised when MTA residues were left in the clinical crown (Tawil et al., 2015).

Next, MTA Plus was introduced by Avalon Biomed, a firm based in the United States. The specific surface area of MTA Plus is 1.537 m²/g, which is larger than the other MTAs’ values. Because the specific surface area is greater, more surface is available for the cement reaction, resulting in a faster reaction rate. Using the Brunauer–Emmett–Teller (BET) gas adsorption method, ProRoot MTA and MTA Angelus were shown to have a similar fineness of 1 m²/g (Camilleri, 2015).

The categorization of calcium silicate (CS)-based materials has been proposed based on chemistry (Zafar et al., 2020) (Table 1). Despite numerous studies on the various materials available for the procedure, no material has yet been discovered that meets all of the criteria for an ideal material, such as biocompatibility, apical seal, and microleakage, and research is still ongoing.

Setting Reaction of MTA

MTA, being hydrophilic, requires moisture to set. Therefore, it is unhindered by blood or water, as moisture is required for a better setting of the material. The required hydration for setting is provided by a moist cotton pellet placed temporarily (until the next appointment) in indirect contact and/or on the surrounding tissues. The hydration reaction during setting occurs between tricalcium silicate and dicalcium silicate to form calcium hydroxide and calcium silicate hydrate gel, producing an alkaline pH. The released calcium ions diffuse through the dentinal tubules and increase their concentration over time as the material sets. The setting reaction of MTA is shown in the following reaction (Camilleri, 2015).



CHALLENGES ATTRIBUTED TO MTA USAGE IN CLINICAL SETTINGS

Evidence-based practice is essential for dental practitioners in the new millennium. MTA is a biomaterial that has a significant impact in the dental field. Though MTA has a wide range of applications, it has limitations like discoloration, mud-like consistency, long setting time, leakage, solubility, and difficulty in manipulation that hinder it from achieving its full potential. Evidence-based practitioners who desire to adopt the most recent and best available evidence into their practices are sometimes perplexed by MTA research’s exponential expansion since 1993, which has resulted in the existence of various modified materials and multiple randomized clinical trials with inhomogeneous findings.

Modifications to MTA and items with different compositions but comparable applications are addressed here in order to assist dentists in selecting the proper material for fixing difficult

TABLE 1 | Classification of MTA as bioactive materials (Zafar et al., 2020).

Generation	Bio-active materials
First-generation	Gray MTA White MTA
Second-generation	Modifications to MTA MTA Angelus
Third-generation	Endo CPM (cement/Portland modified) iRootSP (also retailed as EndoSequence BC and SmartPaste Bio) MTA Obtura Tech Biosealer Endo <ul style="list-style-type: none"> • New endodontic cement/calcium-enriched mixture • Bioaggregate • Biodentine • Ortho MTA • MTA Plus • Generex A and Generex B
Fourth-generation	Hybrid cements <ul style="list-style-type: none"> • Calcium phosphate/calcium silicate/bismutite cement • NRC (incorporating HEMA (2-hydroxyethyl methacrylate)) • MTA with 4-META/MMA- TBB (4-methacryloxyethyl trimellitateanhydride in methyl methacrylate initiated by tri-n-butyl borane) • Light-cured cements including TheraCal LC

instances with maximum competence. Many researchers suggested that changes to MTA and the introduction of new biomaterials for use in perforation repair, root-end filling, pulp capping, and other procedures necessitated testing for biocompatibility, cytotoxicity, genotoxicity, sealing ability, inductivity or conductivity of hard tissue formation, and insolubility before recommending them for clinical use. In the following text, the shortcomings of MTA and its modified aspects are discussed (Figure3).

Discoloration

Tooth discoloration has been linked to bismuth oxide and calcium silicate (Parirokh and Torabinejad, 2010a; Krastl et al., 2013). The usage of both gray MTA (GMTA) and white MTA (WMTA) has also been linked to tooth discoloration. Reports indicate that gray MTA, white MTA Angelus, and white ProRoot MTA have strong staining potential, whereas Retro MTA, MM-MTA, and MTA Ledermix have least staining potential (Możyńska et al., 2017). Some clinical cases report dark discolorations of the teeth and gums after the MTA use (Karabucak et al., 2005; Berger et al., 2014; D'mello and Moloney, 2017). Tooth discoloration was also observed after using MTA in primary molars for pulpotomy. Nearly 60% of the cases have been reported with tooth discoloration (Naik and Hegde, 2005; Belobrov and Parashos, 2011).

GMTA caused clinically noticeable crown discoloration after 1 month, whereas the total color change caused by WMTA exceeded the perceptible threshold for the human eye after 3 months, implying that GMTA should be avoided in the esthetic zone and WMTA should be used with caution when filling pulp chambers with the materials (Camilleri, 2015). WMTA samples showed discoloration 3 days after inserting the material into a mold that was in contact with

phosphate buffer solution (PBS). The reason for discoloration is debatable, linked mainly to interaction between bismuth oxide and the collagen of the tooth tissue and sodium hypochlorite, which is usually used in root canal therapy. When Boutsoukis et al. studied the removal efficiency of MTA as a root canal filler material in 2008, they detected deep root discoloration in the majority of the specimens filled with Angelus gray MTA (AWMTA). Arsenic present in many Portland cements and MTA can present discoloration. Iron and manganese have also been proposed as possible causes of discoloration (Boutsoukis et al., 2008). In a 2005 study on arsenic release from MTA, Duarte et al. found that the amount of arsenic emitted from MTA is extremely low. The presence of ferric oxides in MTA and their stabilising effect on arsenic in this material, as well as MTA's insolubility and use of modest doses of MTA for therapeutic purposes, may limit arsenic release into tissue fluids, which could cause toxicity (Duarte et al., 2005). However, the solubility of some Portland cements and the release of arsenic from these materials have raised concerns. A comparative study was carried out to evaluate the tooth discoloration using calcium-enriched mixture cement, Portland cement, and MTA mixed with propylene glycol (MTA-PG) in comparison to WMTA. The results showed that after 6 months, Portland cement had the most discoloration and MTA and MTA-PG had the least discoloration effect (Salem-Milani et al., 2017).

Difficulty in Manipulation of MTA

MTA is a difficult cement to handle due to its granular consistency (Kogan et al., 2006), reduced setting time (Camilleri et al., 2005), and initial looseness of the material (Fridland and Rosado, 2003; Kogan et al., 2006; Coomaraswamy et al., 2007). When the mixture begins to dry, it loses its cohesiveness and becomes very difficult to handle the cement (Lee, 2000). The consistency of the freshly mixed material, which is commonly described as gritty or sandy, is another issue with the original MTA formulation. The original formulation is hand spatulated, making distribution to the surgical site challenging. To make handling easier, Teflon sleeves and pluggers particularly intended for placing MTA, mainly developed carriers for dispersing MTA, and scooping MTA out of grooves in a plastic block have all been employed. In one study, the hand and ultrasonic installation of varying thicknesses of MTA in high density polyethylene (HDPE) tubes were compared. Radiographic and microscopic analyses revealed that the manual method produced superior adaptation with fewer voids than the ultrasonic method for all thicknesses (Parirokh and Torabinejad, 2010b).

Complexity as an Obturating Material

MTA could provide significant benefits like superior physiochemical and bioactive properties, when used as a root canal obturation material. MTA is an effective obturating material for retreatment; obturation is combined with root-end resection, apexification, internal resorption,



FIGURE 3 | Pitfalls of modified MTA.

dens in dente, and in conventional endodontic therapy. Obturating with MTA enhances the prognosis and retention of the natural teeth in both conventional and complex therapies.

Although MTA presents significant advantages, it has some disadvantages when used as obturating material. GMTA can discolor teeth if it is placed in the coronal part or near the cemento-enamel junction (CEJ) in anterior teeth. This is due to the reduction of ferrous ions (FeO) in the dentinal tubules, which may increase over time (Asgary et al., 2005). It could be a significant issue in anterior aesthetics without PFM restorations and if ceramic crowns and veneers are not properly opaqued in the laboratory. Obturation of MTA in case of curved canals after placement is challenging for curing and removal of the material. Hence, MTA obturation is considered as a permanent filling material and therefore treated in the possible event of failure by surgical resection of the root end. Another relatively insignificant disadvantage is

ProRoot MTA that has slow setting time and might take 2.5–4.0 h to set and 21 days to cure completely. Restoration using MTA in the curved canal should be considered a permanent filling for root canal obturation. The difficulty in obturating curved root canals, the potential for discoloration, and the extended setting time are all disadvantages of utilizing MTA as a root canal filling material (Torabinejad et al., 1995; Boutsoukakis et al., 2008; Mathew et al., 2021).

Long Setting Time

GMTA's initial and final setting times are much longer than that of WMTA. The lower amounts of sulfur and tricalcium aluminate in WMTA account for the longer setting time when compared to Portland cement (Parirokh and Torabinejad, 2010b). One of the reasons why MTA should not be implemented in a single visit is its extended setting time. In comparison to other retrograde filling materials such as amalgam, Super-EBA, and Intermediate restorative material, MTA has a longer setting time (2 h and

45 min). MTA is unsuitable for most clinical applications due to its extended setting time. Different powder-to-water ratios are common in clinical practice because the quantity given is rarely used in a single application and have an impact on MTA's characteristics, resulting in a prolonged setting time (Camilleri, 2015). This has been mentioned as one of the material's flaws. According to researchers, WMTA has a much shorter setting time than GMTA. When samples are maintained under dry conditions, they affect MTA setting time and bacterial leakage. MTA should not be placed in one visit without external moisture since two-sided hydration results in greater flexural strength than one-sided hydration (Parirokh and Torabinejad, 2010b).

Washout Effect

One of MTA's disadvantages is washout or the tendency of freshly made cement paste to breakdown when it comes into contact with blood or other fluids. When cleaning an osteotomy site, a root-end filling material can washout, resulting in a weakened root-end seal and its consequences. It has been demonstrated that adding carboxymethyl chitosan or gelatin to cement based on calcium silicates (the primary components of Portland cement in MTA) improves washout resistance (Kim et al., 2011; Formosa et al., 2013).

Solubility

MTA's solubility is a point of contention among researchers. MTA solubility is found to be minimal or non-existent in most investigations. However, a long-term study, which found enhanced solubility, suggests that the powder-to-water ratio may alter the degree of solubility. MTA porosity and solubility increase with larger water-to-powder ratios. More water would boost calcium release from MTA, according to the authors. Another factor contributing to MTA's insolubility is the presence of bismuth oxide, which is insoluble in water (Parirokh and Torabinejad, 2010b).

Affordability of the Material

MTA is a dental material that has a variety of endodontic uses. According to a study, MTA is commonly used in postgraduate endodontic training programs in the United Kingdom, and its expensive cost is seen as the main barrier to its utilization. In the United Kingdom study, nearly half of the respondents said they wanted more information on how to utilize MTA in clinical practice. In case of direct pulp capping MTA is found to be more cost effective than calcium hydroxide. According to consultant pediatric dentist surveys, the majority of pediatric dentists do not use MTA due to its high cost (Ha et al., 2016).

MTA MODIFICATIONS WITH IMPROVED CHARACTERISTICS AND APPLICATIONS

Despite the fact that MTA is a hydraulic material, it is never exposed to water in clinical dentistry. The substance has been recommended for usage as a filling material for root ends, as well as for repair in perforation areas, apexification, pulpotomy treatments, and for pulp capping. MTA has recently been

introduced as a sealant for root canals. The generation of by products, that is, calcium hydroxide and the hydraulic nature of MTA, is responsible for all of its beneficial properties (Camilleri, 2015). MTA interacts with a variety of environments depending on the material application. When MTA is employed for repair of the perforation area, as a material for root-end filling, and to a lesser extent, in the case of direct pulp capping (DPC), blood comes into contact with it. Blood obstructs the hydration of the material and lowers MTA microhardness (Camilleri, 2015). Material characteristics and failure to set are also influenced by tissue fluids, including serum.

The mixing and administration technique is the key problem in the clinical setting with initial MTA preparation (Camilleri, 2015). MTA is traditionally blended by manipulating the powder on a mixing pad by combining the solid and liquid components. Alternative techniques for mixing, such as the use of an amalgamator, have also been studied. There is a widely held idea among researchers about powder and cement that is the surface area and initial setting time are inversely proportional. In other words, as the surface area of the powder increases, the likelihood of the particles reacting with water increases, resulting in a faster hydration process and a shorter initial setting time.

MTA Modification to Improve Setting Time

Another clinical problem is the setting time of the initial MTA formulation, which was reported to be greater than 3 h (Camilleri, 2015). When the material is utilized for root-end filling and repair of the perforation area, a long setting time is not a concern. When utilized as a PC or as a dressing over PP, however, faster setting time is required. A huge number of reports have surfaced involving the addition or substitution of various chemicals to the mixing liquid for water. The most common compounds are CaCl_2 , $\text{Ca}(\text{NO}_3)_2$ /nitrate, and $\text{Ca}(\text{HOO})_2$. These additives are frequently used in the building industry to help Portland cement set faster. Setting accelerators affect both tricalcium silicate and tricalcium aluminate's setting reactions. Mechanically mixed MTA uses the CaCl_2 accelerator and has a faster setting time.

A study conducted by Saghiri et al., in 2020 on the evaluation of mechanical activation and chemical synthesis for particle size modification of WMTA showed that the use of the finer particle size in WMTA reduced the initial setting time that had previously been mentioned as a major drawback. When data from milling for 10 and 30 min was compared, 10 min was regarded as the optimal milling time for the powder (Saghiri et al., 2020). Further grinding resulted in a considerable increase in the surface area based on the Scanning Electron Microscope (SEM) particle size test. There was also a minor reduction in the setting time. The results showed that when compared to milling and control groups, the sol-gel approach produced finer powder with a smaller range of particles and normal powder particle distribution, resulting in higher compressive strength, pH, and calcium release rate of the powder (Saghiri et al., 2020). Both modification procedures had a considerable impact on powder quality, although the effect of the sol-gel process was significantly greater than milling, according to statistical analysis. The sol-gel method's result was found to be finer, with a shorter distribution

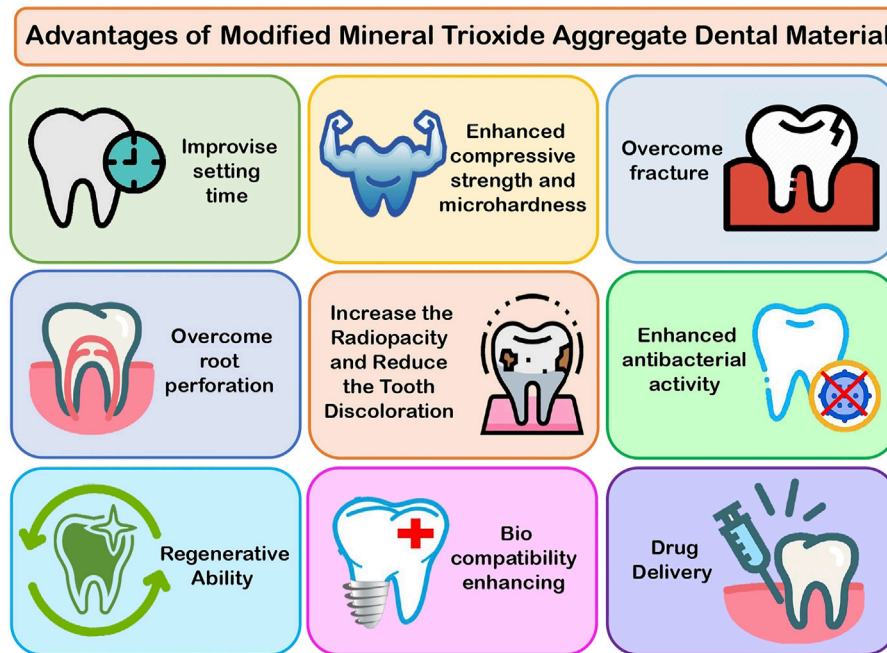


FIGURE 4 | Advantages of modified MTA.

range and more homogeneous particles, than the other groups. As a result, both approaches investigated increased the surface area. Mechanical activation, on the other hand, was not as successful as the sol–gel technique in lowering the initial setting time (Saghiri et al., 2020). Furthermore, the sol–gel technique produced finer particles with a narrower size distribution range.

According to a study conducted by Kharouf et al., in 2021 titled “Tannic acid speeds up the setting of MTA cement and improves its surface and bulk properties.” Tannic acid (TA) can deposit on the grains’ surfaces (calcium oxide, calcium silicates, and trisilicates) and it can also be incorporated between the grains to change the porosity of the composite. The fact that the grains are coated with a polyphenol-based coating results in a much smaller pH increase when the cement is placed in water, which could also explain the cement’s faster setting kinetics. The presence of TA on the grain surface and in the pores explains the increase in compressive stiffness and stress in the dry state because TA molecules form strong intramolecular hydrogen bonds and hydrogen bonds/ionic interactions with the grain surface. As a result, adding TA to MTA cements reduces the setting time and grain size of the resulting cement while increasing the hydrophilicity of the composite materials (Kharouf et al., 2021).

Modified MTA With Enhanced Compressive Strength and Microhardness

A study conducted by Eskandarinezhad et al., in 2021 on the effects of hydroxyapatite (HA) and zinc oxide (ZnO)

nanoparticles on compressive strength of WMTA showed that the compressive strength of MTA was unaffected by HA or ZnO nanoparticles (Figure 4). As a result of the advantages of these nanoparticles, they can be used in cases where compressive strength is important, such as the repair of furcal perforations, pulp capping, and apexogenesis, or in cases where compressive strength is not important, such as the apical plug and as a retrograde material in surgery (Eskandarinezhad et al., 2020).

Kucukyildiz et al. conducted an *in-vitro* comparison of the physical, chemical, and mechanical properties of graphene nanoplatelet (GNP) with Angelus MTA. According to the Fourier transform infrared spectroscopy (FTIR) analysis, adding GNP to MTA did not change the binding structure of the material’s atoms. According to energy dispersive X-ray spectroscopy (EDX) analysis, adding GNP to MTA did not change the crystal structure of the material but did result in an increase in the carbon ratio. By adding GNP to pulp capping materials to enhance hard tissue formation potential, the material’s microhardness can be increased, providing superior resilience under permanent restoration. The particle size of the MTA material is reduced, and its microhardness is increased as a result of adding GNP to the material; thus, GNP contributes to the MTA material’s strength. *In vivo* and *in vitro* research studies are needed to see how the GNP addition affects the biological effect on pulp (Kucukyildiz et al., 2021).

Modification of MTA to Overcome Fracture

Endodontically treated teeth were long thought to be more susceptible to fracture than healthy teeth. This is because endodontic procedures can cause chemical and structural

changes in the root canal dentin, making the tooth vulnerable to vertical root fracture (VRF). A variety of factors influence the brittleness of endodontically treated teeth. The use of root canal filler material to fortify the remaining tooth structure is one method of preventing VRF in endodontically treated teeth. Despite their poor adherence to the dentinal walls of the root canal system, gutta-percha and sealers have remained the standard of care for obturating root canals in endodontics (Fridland and Rosado, 2003). MTA has been proposed as having the ability to form a tighter seal with root dentin walls than many other available materials (Camilleri, 2015). Ballal et al. conducted a study to compare the fracture resistance of teeth obturated with two different types of MTA, ProRoot MTA and OrthoMTA and discovered that teeth obturated with OrthoMTA III had significantly higher fracture resistance than teeth obturated with ProRoot MTA. The difference in setting mechanisms could explain OrthoMTA III's superior performance and pH neutralization during the reaction. As a result, enough H₂O is produced to supply humidity to the dentin *via* dentinal tubules (Ballal et al., 2020).

The toughness of dentin is substantially higher in a hydrated state than in a dehydrated state. Another factor contributing to OrthoMTA III's higher fracture resistance when compared to control and groups of ProRoot MTA is the interfacial adhesion between RC dentin walls and MTA. However, when compared to ProRoot MTA, the precipitate was more visible in the OrthoMTA III group. The toughness of dentin is substantially higher in a hydrated state than in a dehydrated state. Another factor contributing to OrthoMTA III's higher fracture resistance when compared to control and groups of ProRoot MTA is the interfacial adhesion between RC dentin walls and MTA. Under current conditions, OrthoMTA III had a stronger biomineralization impact. Stronger interfacial bonding may be induced by this improved biomineralization impact. Within the dentinal tubules, petals-like precipitate are formed in the experimental groups. However, when compared to ProRoot MTA, the precipitate was more visible in the OrthoMTA III group. A study conducted by Żuk-Grajewska et al., in 2020 on the fracture resistance of MTA mixed with PBS in human roots filled with and without CaOH pre-medication showed that even when short-term calcium hydroxide pre-medication was utilized, MTA mixed with Ca and Mg free phosphate-buffered saline had a considerable strengthening impact on the fracture resistance of structurally weak roots. When MTA was mixed with water and pre-treated with calcium hydroxide for 2 or 12 weeks, the strengthening effect on human roots was lost (Żuk-Grajewska et al., 2021).

Modification of MTA to Minimize Root Perforation

Root perforations are openings in the external root surfaces that allow communication between the root canal system and the root surface. It can be considered as pathogenic if it arises from defects in the resorptive area or caries, although the majority of them are because of iatrogenic causes during and after RC procedures. Perforations in the roots are one of the reasons for failure in

endodontics, and if they are not detected and corrected promptly, they can result in the loss of the affected teeth. MTA has several desirable properties for endodontic repair, including strong sealing ability, biocompatibility, antibacterial properties, and hydrophilic behavior (Shin et al., 2021).

A study conducted by Adl et al., in 2019 on evaluation of the absence and presence of blood contamination, dislodgement resistance in a new pozzolan-containing calcium silicate-based substance when compared to ProRoot MTA and Biodentine showed that higher bond strength was seen in Biodentine and ProRoot MTA than in EndoSeal MTA (Adl et al., 2019). This result could be explained by the fact that pozzolan-based materials have a much lower releasing ability of Ca/P ratio and calcium of the apatite-like crystalline precipitate when compared to other calcium silicate cements. This viewpoint is supported by the fact that the concentration of accessible ions influences the nucleation and growth of the apatite layer, suggesting that they may be superior alternatives for furcal perforation repair (Shin et al., 2021). The final restoration should be placed within 7 days while using ProRoot MTA.

MTA Modification to Improve Radiopacity and Reduce Tooth Discoloration

Bismuth oxide, the radiopacifying agent in MTA, becomes unstable when it interacts with strong oxidizing agents such as sodium hypochlorite or amino acids found in dentin collagen, resulting in tooth discoloration. Tooth discoloration occurs when this cement is used for additional treatment techniques such as vital pulp therapy, sealing root canal perforations, and root resorptions.

In a study conducted in 2020 by Bolhari et al. to evaluate the characteristics of different environmental conditions of MTA mixed with ZnO, it was discovered that the addition of 5% ZnO prevented tooth discoloration and decreased the compressive strength of both MTA Angelus and ProRoot MTA cement significantly in all exposure settings. Zinc hydroxide creates an impenetrable barrier around tricalcium silicate, preventing hydration of the cement. Because the composition and hydration of Portland cement and MTA are similar, this negative effect may occur in MTA as well, resulting in a reduction in compressive strength values. ZnO had no effect on the microhardness of these cements and was discovered on the surface of the cements to which it was added. Although adding 5% ZnO to MTA prevents tooth discoloration, it has a negative impact on the hydration and compressive strength of the tested cements but has no effect on the surface microhardness of Angelus and ProRoot MTA (Bolhari et al., 2020).

A study conducted by Peng et al., in 2021 on the spray pyrolysis of Zr-doped Bi₂O₃ radiopacifier on MTA showed bismuth oxide (Bi₂O₃) and zirconium (Zr)-doped Bi₂O₃ compounds were almost spherically produced. The particles had a tiny agglomeration on their surface, with the bigger particles (about 2 µm) having a small number of microscopic particles (0.5 µm) on their surface. Radiopacifiers made by spray pyrolysis had a faster setting time than those made by the sol-gel method. Furthermore, when compared to Bi₂O₃ and other ratios of Zr-doped Bi₂O₃ mixed

with Portland cement, Bi_2O_3 with 15 mol% Zr doping had significantly better radiopacity and mechanical strength under X-ray excitation. The results support the use of Zr-doped Bi_2O_3 as a novel radiopacifier in future dental filling and pulp-capping applications *via* spray pyrolysis. Future research should concentrate on the effects of Zr in conjunction with Portland cement and the impact of tooth discoloration (Peng et al., 2021).

Modification of MTA With Enhanced Antibacterial Activity

The success of endodontic treatment is intimately linked to the control of bacterial infection in the root canal. Various studies have linked five– seven bacterial species to root canal infection, with *Porphyromonas gingivalis*, *Porphyromonas endodontalis*, and *Enterococcus faecalis* being the most often isolated bacterial species from pulpitis. Apical periodontitis is linked to *Enterococcus faecalis* in RC-treated teeth, whereas *Porphyromonas endodontalis* and *Porphyromonas gingivalis* are related to the infection of the root canal (RC) (Shin et al., 2021). Because the root canal system is anatomically complex, the complete elimination of pathogenic microorganisms in the root canal is challenging.

A study conducted by Shin et al., in 2020 evaluated the antibacterial activity of a mixture of MTA and nitric oxide (NO)-releasing molecules against bacteria like *Enterococcus faecalis* and *Porphyromonas endodontalis* and the physical features of MTA and MTA-NO mixture to determine the efficacy of these techniques. When a NO-releasing molecule, such as diethylenetriamine-NO (DETA-NO), is mixed with powder of MTA, NO gets released quickly from DETA-NO before the mixture sets or during the initial phase, but the process slows down after the mixture sets (Shin et al., 2021). As a result, the high concentration of NO and mineral oxide and the mixture of MTA and NO had significant antibacterial action in the early stages and proved useful in eliminating oral microorganisms. Furthermore, bone formation and wound healing following endodontic treatment is due to NO released from the mixture at a low concentration.

Modification of MTA With Regenerative Ability

Calcium silicate-based materials (CSBMs) have been used in a variety of endodontic procedures, including regenerative endodontics, root-end closure, vital pulp therapy, and perforation repair. These bioactive compounds have the ability to stimulate stem cell proliferation and differentiation into odontogenic/osteogenic cells. MTA, the first CSBM produced, was widely used in endodontic procedures. Angiogenesis is required for the mineralization of stem cells and the formation of extracellular matrix to recruit stem cells for oxygen and nutrient provision. Previous research has shown that angiogenic signaling molecules can aid stem cell proliferation and differentiation. Despite its high clinical success rate, a study discovered that MTA has decreased proangiogenic activity, which may influence the first cell-material contact and regeneration qualities (Almehari et al., 2021).

To improve the angiogenic properties, a study was conducted by Almehari et al., in 2021 to evaluate the additive effect of iloprost on the biological properties of MTA on mesenchymal stem cells. On day 7, MTA reduced cell viability. This result was explained by iloprost's capacity to upregulate the proangiogenic factors and initiate proliferation of cells. In addition, MTA's setting time, which is longer, may have also allowed for a more regulated and gradual release of iloprost. The cell morphological alterations on the material surfaces revealed human bone marrow-derived mesenchymal stem cells (hMSCs) had less spread of cells on the dentin disc, which was consistent with the assay of cell viability (Almehari et al., 2021). The appearance of cells that were round on the material surface could be due to the leak of compounds, which influenced interaction between the cell and materials. On days 7 and 14, however, the substrate's surface was covered with flat cells, demonstrating that the materials were biocompatible. hMSC migration throughout the first 24 h, resulting in a nearly 50% reduction in cell migration. When compared to MTA alone, iloprost had no effect on cell migration, which could be related to the grown cells due to the 2D environment. The results revealed that markers of osteogenic expression were dramatically elevated in MTA-iloprost-treated cells when compared to MTA-treated cells. This could be due to iloprost's elevation of VEGF, which causes the production of osteogenic and odontogenic markers. Thus, adding iloprost to MTA increased the cell vitality and differentiation of osteogenic potential capability of mesenchymal stem cells, suggesting that it could be used as a biomaterial in the future.

A study conducted by Tien et al., in 2021 on additive manufacturing of caffeic acid-inspired MTA/poly-caprolactone scaffold for regulating vascular induction and osteogenic regeneration of dental pulp stem cells showed that the physicochemical and biological responses were caused by the surfaces of the various scaffolds that had been coated with caffeic acid (CA). The CA 20 scaffold not only had strong mechanical strength but also had apatite precipitate immersed in stimulated body fluid, indicating that this was the ideal physical and chemical microenvironment for human dental pulp stem cell (hDPSC) activities (Tien et al., 2021). Cell adhesion, proliferation, and osteogenic differentiation were all improved when the MTA scaffold was coated with a CA concentration of 20 mg/ml. Furthermore, VEGF adsorption resulted in an increase in CA coating on hDPSC osteogenesis differentiation. Most notably, *in vivo*, the MTA scaffold with CA covering demonstrated good bone regeneration. Furthermore, the CA 20 scaffold appeared to have better osteogenesis ability than the CA 0 scaffold, as determined by CT and histological analyses. These results could be related to the CA coating's augmentation of bone-like apatite production and VEGF adsorption. Because CA is a bioinspired polymer, it can be used as a highly functional bioactive covering for various scaffolds in bone tissue creation and other biomedical applications. A study conducted by Ghasemi et al. (2021) on the effect of Ze–Ag–Zn on MTA on the odontogenic activity of hDPSCs showed that the incorporation of Ze–Ag–Zn particles into AMTA had no effect on the material's biomineralization ability, and further research is

needed to assess the underlying molecular interaction between HDPSCs and these types of particles, based on the findings of previous studies and their limitations.

A study conducted by Lim et al., in 2021 on *in vitro* evaluation of the mineralization and biocompatibility potential of MTA that included CaF_2 showed that the addition of more than 5% calcium fluoride (CaF_2) could be considered to increase pulp cell regeneration ability without compromising physical properties. However, clinical circumstances such as long-term irritation and inflammation following pulp contact may result in a different outcome (Lim et al., 2021).

Matrix metalloproteinases (MMPs), enzymes involved in bone remodeling, cells generated by osteoclasts, and other cells such as fibroblasts and macrophages, are all known to play a role in the restoration of the dental matrix. The main components of the extracellular matrix (ECM) act as metalloproteinases' primary substrates. The MMP-induced catalysis causes structural changes in the matrix. MMPs have been found to perform a variety of roles, including regulating cell activity and participating in inflammatory reactions. MMPs have been shown to play an important regulatory role in cell differentiation and migration, growth factors, angiogenesis, and inflammation development.

Modified MTA That Accelerates Biocompatibility

The introduction of tricalcium silicate materials that are resin modified has resulted in the development of a command cure material that may be used for PC. Resins improve the flow of material, making it acceptable for use as a sealer for RC. The liquid water mixing has been replaced by a variety of resins. As a result of these improvements, MTA that is light activated and MTA that is resin modified have been developed for the use in RC sealing cements. A variety of resin systems have been examined. The most common are light-curing systems, containing Bis-GMA and a resin that is biocompatible and contains HEMA, TEGDMA, camphorquinone, and EDMAB, with or without polyacrylic co-maleic acid, Bis-TEGDMA, Bis-GMA, PMDM, and HEMA (Camilleri, 2015).

TheraCal is a tricalcium silicate compound that is light curable and is used for PC. Environmental circumstances and fluid availability have an impact on TheraCal hydration. In reality, the restricted fluid availability limits material hydration when employed as a pulp-capping material. TheraCal's ability to release calcium is controversial; in a study, it was shown to be comparable to CaOH , but later studies showed no calcium generated, and leaching of the calcium ion was found to be extremely low. When extracts of TheraCal came into contact with pulp cells, they were found to be cytotoxic. Angelus sells Fillapex of MTA is a modified MTA-based resin. MTA is a salicylate resin, and additional ingredients make up this mixture (Camilleri, 2015).

The inclusion of polymers that are soluble in water showed that in prototype materials it can improve material flow. ProRoot Endo Sealer is a commercially available product that contains particles that make up the cement suspended in a polymer that is

soluble in water. At low water/cement ratios, the polymer that is soluble in water puts the cement particles on charge. The resultant charged particles repel each other, resulting in less flocculation and enhanced flow of material. Another soluble polymer, propylene glycol, has been utilized to increase MTA flow.

In a study conducted by Toida et al., in 2021 on pulp response to capping material flow that is phosphorylated pullulan-based in MTA (MTAPPL), it was shown that the group had reduced inflammatory cell infiltration, whereas the Nex-Cem MTA (NX) and Dycal (DY) groups had more inflammatory cells with infiltration of polymorphonuclear leucocytes at the exposed site of pulp (Kim et al., 2011). According to the findings, MTAPPL had lower inflammatory responses than the other experimental groups at all time points. The study also revealed that with the exception of the DY group, the deposition of tissue that was mineralized was seen in the MTAPPL, NX, and TheraCal LC (TH) groups. This finding can improve the sealing ability, inhibit bacterial leakage, and boost the reparative capacity of pulp cells by depositing calcium phosphate minerals along the dentin-material contact. After 70 days, the MTAPPL, TH, and NX groups showed more mineralized tissue formation than the DY group. Tubular dentin grew under the osteodentin and was also identified as layers of odontoblast that were well arranged with odontoblast-like cells. There were no tunnel defects in any groups. However, some pulp-like tissue was found at the tissue barrier that was mineralized in the MTAPPL group. This could be due to the faster formation of mineralized tissue. MTAPPL's ability to adhere to human dentin was compared to NX, TH, and DY. There was no separation between MTAPPL and dentin in the experiment, even under the high-vacuum conditions of the SEM sample chamber, indicating that it has outstanding sealing ability as a pulp-capping material. On the other hand, NX, TH, and DY did not stick well to dentin and demonstrated separation from dentin interface. Leakage and bacterial infection may occur as a result of these holes. As a result, MTAPPL biomaterials have good dentin sealing ability and pulpal responsiveness (Toida et al., 2021). MMP-2 and MMP-9 protein expressions in cultured monocytes/macrophages are unaffected by MTA Repair HP, according to a study conducted by Barczak et al. (2021) to investigate the MTA Repair HP formula's effect on the inflammation process, involving the tooth and periodontal tissues using the THP-1 monocyte/macrophage model with biomaterial applied in direct contact with the cells. A study conducted by Tabari et al., in 2020 on an animal study on the biocompatibility of MTA mixed with different accelerators showed the inflammatory response diminished over time for all of the accelerators, that is, sodium hypochlorite (Na_2HPO_4), citric acid, and calcium lactate gluconate (CLG) studied in this investigation. The inflammatory responses caused by MTA combined with 0.1 percent citric acid and MTA mixed with 15 percent Na_2HPO_4 were equivalent to those induced by MTA mixed with pure water, according to the findings of this investigation. Despite the lack of substantial differences in histological reactions between control MTA and MTA mixed with CLG, the latter cement elicited a moderate-to-severe

TABLE 2 | Summary of studies relevant to modifications of MTA.

Author and year	Agents incorporated	Properties modified	Result
Saghiri et al. (2020), Duarte et al. (2005)	Particle size modification of WMTA using the sol-gel method	Setting time	<ul style="list-style-type: none"> Reduction in the setting time Higher compressive strength Increased the surface area
Kharouf et al. (2021), Salem-Milani et al. (2017)	Incorporation of tannic acid	Setting time	<ul style="list-style-type: none"> Strong intramolecular hydrogen bonds Increase in compressive stiffness and peak compressive stress in the dry state Reduces the setting time and grain size Increases composite materials' hydrophilicity
Eskandarinezhad et al. (2021), Kogan et al. (2006)	Hydroxyapatite (HA) and ZnO nanoparticles in WMTA	Compressive strength	<ul style="list-style-type: none"> Compressive strength of MTA was unaffected by HA or ZnO nanoparticles
Kucukyildiz et al. (2020), Camilleri et al. (2005)	Graphene nanoplatelet in Angelus MTA	Microhardness	<ul style="list-style-type: none"> No modification in the binding structure of the material's atoms observed No change in crystal structure noticed Increase in microhardness and strength
Ballal et al. (2020), Fridland and Rosado, (2003)	Ortho MTA III	Fracture resistance	<ul style="list-style-type: none"> Superior resilience under permanent restoration Higher fracture resistance Superior performance and neutralization of elevated pH during the reaction Stronger biomineralization Higher compressive and flexural strengths than ProRoot MTA
Žuk-Grajewska et al. (2020), Coomaraswamy et al. (2007)	MTA mixed with PBS in human roots filled with and without CaOH pre-medication	Fracture resistance	<ul style="list-style-type: none"> MTA mixed with Ca and Mg free phosphate-buffered saline had a strengthening impact on the fracture resistance
Adl et al. (2019), Parirokh and Torabinejad, (2010b)	New pozzolan-containing calcium silicate-based material	Dislodgement resistance	<ul style="list-style-type: none"> Higher bond strength
Bolhari et al. (2020), Asgary et al. (2005)	MTA mixed with different concentration of ZnO	Tooth discoloration	<ul style="list-style-type: none"> 5% ZnO prevented tooth from discoloration Reduction in compressive strength Negative impacts on the hydration
Peng et al. (2021), Torabinejad et al. (1995)	Spray pyrolysis of zirconium-doped bismuth oxide radiopacifier	Radiopacity	<ul style="list-style-type: none"> Faster setting time BizO₃ with 15 mol% Zr doping exhibited significantly better radiopacity Increased mechanical strength
Shin et al. (2021), Lee, (2000)	Mixture of MTA and NO-releasing molecule	Antibacterial activity	<ul style="list-style-type: none"> Significant antibacterial action in the early stages and useful in eliminating oral microorganisms Bone formation and wound healing property
Almeshari et al. (2021), Boutsoukis et al. (2008)	Additive effect of iloprost with MTA	Regenerative ability	<ul style="list-style-type: none"> Capacity to upregulate the proangiogenic factors and initiate proliferation of cell Biocompatible Marker of osteogenic expression dramatically elevated in MTA-iloprost-treated cells MTA increased the cell vitality and differentiation of osteogenic potential capability
Tien et al. (2021), Mathew et al. (2021)	Caffeic acid-inspired MTA	Regenerative ability	<ul style="list-style-type: none"> Strong mechanical strength Ideal physical and chemical microenvironment for hDPSC activities Cell adhesion, proliferation, and osteogenic differentiation improved Improved osteogenesis differentiation Good bone regeneration
Ghasemi et al. (2021), Formosa et al. (2013)	Ze-Ag-Zn to MTA	Regenerative ability	<ul style="list-style-type: none"> No effect on the material's biomineralization Further research is needed to assess the underlying molecular interaction
Lim et al. (2021), Kim et al. (2011)	Addition of calcium fluoride to MTA	Mineralization	<ul style="list-style-type: none"> Increase pulp cell regeneration
Toida et al. (2021), Ha et al. (2016)	Addition of phosphorylated pullulan and TheraCal in MTA	Biocompatibility	<ul style="list-style-type: none"> Reduced inflammatory cell infiltration Deposition of tissue that was mineralized was seen Improve the sealing ability, inhibit bacterial leakage, and boost the reparative capacity of pulp cells Mineralized tissue formation Layers of odontoblast seen
Barczak et al. (2021), Saghiri et al. (2020)	MTA Repair HP with application of the THP-1 monocyte/macrophage model	Biocompatibility	<ul style="list-style-type: none"> Protein expression in cultured monocytes/macrophages is unaffected by MTA Repair HP

(Continued on following page)

TABLE 2 | (Continued) Summary of studies relevant to modifications of MTA.

Author and year	Agents incorporated	Properties modified	Result
Tabari et al. (2020), Kharouf et al. (2021)	MTA mixed with different accelerators such as sodium hypochlorite, citric acid, calcium lactate gluconate	Biocompatibility	<ul style="list-style-type: none"> • Inflammatory responses of sodium hypochlorite and citric acid was similar to conventional MTA • Calcium Lactate Gluconate elicited moderate-to-severe inflammatory response
Almeshari et al. (2021), Boutsioukis et al. (2008)	MTA with iloprost	Biocompatibility	<ul style="list-style-type: none"> • Showed biocompatibility and the development of hard tissue • It upregulates the mRNA expression of vascular endothelial growth factor, fibroblast growth factor-2, and platelet-derived growth factor in human dental pulp stem cells
Kim et al. (2021), Eskandarinezhad et al. (2020)	MTA with elastin-like polypeptide	Biocompatibility	<ul style="list-style-type: none"> • Better in binding strength to dentin and flow rate • Same or better quality of sealer in terms of dentinal tubule penetration and washout resistance
Bohns et al. (2020), Kucukyildiz et al. (2021)	Incorporation of amoxicillin-loaded microspheres in MTA	Drug delivery	<ul style="list-style-type: none"> • Delayed release with minimal impact on the material's physical and mechanical properties
Almeida et al. (2018), Ballal et al. (2020)	MTA-based endodontic sealer with calcium aluminate (C3A) and silver-containing C3A particles	Antibiofilm	<ul style="list-style-type: none"> • Antibiofilm effect was improved in the presence of C3A particles, while the biofilm inhibition was lower in the presence of Ag • Physicochemical properties of the modified MTA-based sealer were similar to the commercial material • Significant increase in Ca^{+2} release
Hernandez-Delgadillo et al. (2017), Żuk-Grajewska et al. (2021)	MTA mixed with bismuth lipophilic nanoparticles (BisBAL NPs)	Antibiofilm and antimicrobial	<ul style="list-style-type: none"> • MTA-BisBAL NPs inhibited the growth of <i>Enterococcus faecalis</i>, <i>Escherichia coli</i>, and <i>Candida albicans</i>, and also detached the biofilm of fluorescent <i>Enterococcus faecalis</i> after 24 h of treatment • Cytotoxicity was not observed when MTA-BisBAL NPs was added on human gingival fibroblasts
Nagas et al. (2016), Shin et al. (2021)	Mixing alkaline resistant(AR) glass fibers in ProRoot MTA	Fracture resistance	<ul style="list-style-type: none"> • Highest fracture strength • Higher diametral tensile strength and compressive strength
Marciano et al. (2019), Adl et al. (2019)	Mixing MTA Angelus with aluminum fluoride	Tooth discoloration	<ul style="list-style-type: none"> • Did not significantly alter the radiopacity, setting time, and volume change • pH and calcium ion release significantly increased • Prevented discoloration • Did not interfere in inflammatory response
Siboni et al. (2017), Bolhari et al. (2020)	Incorporation of povidine and polycarbonate	Radiopacity	<ul style="list-style-type: none"> • Had bioactivity with calcium release • Strong alkalizing activity and apatite-forming ability • Adequate radiopacity
Dianat et al. (2017), Peng et al. (2021)	MTA with methyl cellulose as liquid	Mechanical properties	<ul style="list-style-type: none"> • Using methyl cellulose as the hydrating liquid enhance some mechanical properties but does not compromise pH of white ProRoot MTA

inflammatory response on the 7th day after implantation (Tabari et al., 2020).

In another study, pulpal response to the combined use of mineral trioxide aggregate and iloprost for direct pulp capping, conducted by Adl et al., in 2021 found that when used as pulp-capping materials, iloprost, MTA, and MTA-iloprost all produced positive results. All materials demonstrated biocompatibility and the formation of hard tissue. Because it increases the mRNA expression of VEGF, fibroblast growth factor-2, and platelet-derived growth factor in human dental pulp stem cells (Adl et al., 2019). As a result, the combination of MTA and iloprost may have a little therapeutic value. A study conducted by Kim et al., in 2020 on the investigation of properties of an unique experimental elastin-like polypeptide-based MTA as an endodontic sealer showed that the experimental elastin-like polypeptide (ELP)-based MTA sealer performed better in binding strength to dentin and flow rate than the other experimental

groups at a 0.4 L/P ratio (Kim et al., 2021). In addition, when compared to commercial MTA sealers, it has the same or better quality in terms of dentinal tubule penetration and outstanding washout resistance. As a result, if additional research and clinical trials confirm its qualities, the ELP-based MTA sealer may be approved for clinical use. Incorporating V125E8 a 125 times-repeated structure of a valine–proline–glycine–valine–glycine unit with eight glutamates added on the C-terminus into MTA could be a promising way to develop functionally advanced bioactive sealers for endodontic therapy and regenerative endodontics.

Modified MTA as a Drug Delivery

MM-MTA is manufactured by Micro-Mega (Besancon, Cedex, France), and it uses MTA capsules that can be blended using an amalgamator. The MM-MTA delivery system has the advantage of including a delivery method comparable to glass ionomer cements.

The compressive strength of the set material was proven to be increased, but the efficiency of mechanical mixing remains unknown. Another study found that mixing different processes had no significant effect on the resulting MTA mixtures, despite increased material microhardness (Camilleri, 2015). Incorporation of amoxicillin-loaded microspheres in MTA cement: an *in vitro* study, conducted by Bohns et al., in 2020, demonstrated the development of bioactive cement using polymeric microspheres to provide antibiotics with delayed release as a viable drug delivery mechanism for treating local tooth infections. The synthesis result is simple, repeatable, and extremely reliable. The use of polymeric microspheres at a concentration of 5% results in delayed release with a minimal impact on the physical and mechanical properties of the material. Limiting the release of antibiotics administered at local infection sites could have applications in dental materials that come into close contact with tooth tissues (Bohns et al., 2020). **Table 2** summarizes the changes made to the MTA to address flaws of conventional MTA.

CONCLUSION

MTA's introduction was recognized as a watershed moment in material science, and its properties have since been improved to maximize its benefits. It is the most widely used endodontic material by dentists because it has been demonstrated to be effective in a variety of clinical settings. However, this substance has always had a few limitations that have prompted researchers all over the world to look for alternatives. The majority of newer formulations contain additives that improve material properties. With the recent

introduction of new, improved MTA products, novel tricalcium silicate-based materials have surpassed MTA's major applications. MTA-based materials are still widely used due to their outstanding properties and regeneration capacity. Although more long-term research is needed to confirm this concept, the novel materials could still be viewed as a possible alternative to MTA.

AUTHOR CONTRIBUTIONS

PC: conceptualization, resources, data curation, original draft preparation, and supervision. VD: conceptualization, resources, data curation, and original draft preparation. SS: original draft preparation, review and editing, and visualization. DA: original draft preparation, review and editing, and visualization. TV: original draft preparation, review and editing, and visualization. AR: review and editing and visualization. AS: review and editing and visualization. AK: review and editing and visualization. SB: review and editing and visualization. AD: review and editing and visualization. AR: review and editing and visualization. SP: review and editing, visualization, and supervision. All authors agree to be accountable for the content of the work.

ACKNOWLEDGMENTS

The authors thank MS Ramaiah University of Applied Sciences for the support.

REFERENCES

- Adl, A., Sadat Shojae, N., and Pourhatami, N. (2019). Evaluation of the Dislodgement Resistance of a Newpozzolan-Based Cement (EndoSeal MTA) Compared to ProRoot MTA and Biodentine in the Presence and Absence of Blood. *Scanning* 2019, 3863069. doi:10.1155/2019/3863069
- Almeida, L. H. S., Moraes, R. R., Morgental, R. D., Cava, S. S., Rosa, W. L. O., Rodrigues, P., et al. (2018). Synthesis of Silver-Containing Calcium Aluminate Particles and Their Effects on a MTA-Based Endodontic Sealer. *Dent. Mater.* 34 (8), e214–e223. doi:10.1016/j.dental.2018.05.011
- Almeshari, A., Elsafadi, M., Almadhari, R., Mahmood, A., Alsubait, S., and Aksel, H. (2021). The Additive Effect of Iloprost on the Biological Properties of Mineral Trioxide Aggregate on Mesenchymal Stem Cells. *J. Dent. Sci.* 17, 225–232. doi:10.1016/j.jds.2021.03.018
- Asgary, S., Parirokh, M., Eghbal, M., and Brink, F. (2005). Chemical Differences between White and Gray Mineral Trioxide Aggregate. *J. Endod.* 31, 101–103. doi:10.1097/01.don.0000133156.85164.b2
- Ballal, N. V., Rao, S., Yoo, J., Ginjupalli, K., Toledano, M., Al-Haj Husain, N., et al. (2020). Fracture Resistance of Teeth Obturated with Two Different Types of Mineral Trioxide Aggregate Cements. *Braz. Dent. Sci.* 23 (3), 1–9. doi:10.14295/bds.2020.v23i3.2000
- Barczak, K., Palczewska-Komsa, M., Lipski, M., Chlubek, D., Buczkowska-Radlińska, J., and Baranowska-Bosiacka, I. (2021). The Influence of New Silicate Cement Mineral Trioxide Aggregate (MTA Repair HP) on Metalloproteinase MMP-2 and MMP-9 Expression in Cultured THP-1 Macrophages. *Int. J. Mol. Sci.* 22 (1), 295. doi:10.3390/ijms22010295
- Belobrov, I., and Parashos, P. (2011). Treatment of Tooth Discoloration after the Use of White Mineral Trioxide Aggregate. *J. Endod.* 37 (7), 1017–1020. doi:10.1016/j.joen.2011.04.003
- Berger, T., Baratz, A., and Gutmann, J. (2014). *In Vitro* investigations into the Etiology of Mineral Trioxide Tooth Staining. *J. Conserv. Dent.* 17 (6), 526. doi:10.4103/0972-0707.144584
- Bohns, F. R., Leitune, V. C. B., Garcia, I. M., Genari, B., Dornelles, N. B., Guterres, S. S., et al. (2020). Incorporation of Amoxicillin-Loaded Microspheres in Mineral Trioxide Aggregate Cement: an *In Vitro* Study. *Restor. Dent. Endod.* 45 (4), e50. doi:10.5395/rde.2020.45.e50
- Bolhari, B., Meraji, N., Rezazadeh Sefideh, M., and Pedram, P. (2020). Evaluation of the Properties of Mineral Trioxide Aggregate Mixed with Zinc Oxide Exposed to Different Environmental Conditions. *Bioact. Mater.* 5 (3), 516–521. doi:10.1016/j.bioactmat.2020.04.001
- Boutsoukis, C., Noura, G., and Lambrianidis, T. (2008). *Ex Vivo* study of the Efficiency of Two Techniques for the Removal of Mineral Trioxide Aggregate Used as a Root Canal Filling Material. *J. Endod.* 34, 1239–1242. doi:10.1016/j.joen.2008.07.018
- Camilleri, J. (2015). Mineral Trioxide Aggregate: Present and Future Developments. *Endod. Top.* 32 (1), 31–46. doi:10.1111/etp.12073
- Camilleri, J., Montesin, F. E., Di Silvio, L., and Pitt Ford, T. R. (2005). The Chemical Constitution and Biocompatibility of Accelerated Portland Cement for Endodontic Use. *Int. Endod. J.* 38 (11), 834–842. doi:10.1111/j.1365-2591.2005.01028.x
- Camilleri, J. (2008). The Chemical Composition of Mineral Trioxide Aggregate. *J. Conserv. Dent.* 11, 141–143. doi:10.4103/0972-0707.48834
- Coomaraswamy, K., Lumley, P., and Hofmann, M. (2007). Effect of Bismuth Oxide Radioopacifier Content on the Material Properties of an Endodontic Portland

- Cement-Based (MTA-like) System. *J. Endod.* 33 (3), 295–298. doi:10.1016/j.joen.2006.11.018
- D'mello, G., and Moloney, L. (2017). Management of Coronal Discolouration Following a Regenerative Endodontic Procedure in a Maxillary Incisor. *Aust. Dent. J.* 62 (1), 111–116. doi:10.1111/adj.12462
- Dianat, O., Naseri, M., and Tabatabaei, S. F. (2017). Evaluation of Properties of Mineral Trioxide Aggregate with Methyl Cellulose as Liquid. *J. Dent. (Tehran)* 14 (1), 7–12.
- Duarte, M. A. H., de Oliveira Demarchi, A. C. C., Yamashita, J. C., Kuga, M. C., and de Campos Fraga, S. (2005). Arsenic Release provided by MTA and Portland Cement. *Oral Surg. Oral Med. Oral Pathology, Oral Radiology, Endodontology* 99 (5), 648–650. doi:10.1016/j.tripleo.2004.09.015
- Eskandarinezhad, M., Ghodrati, M., Pournaghi Azar, F., Jafari, F., Samadi Pakchin, P., Abdollahi, A. A., et al. (2020). Effect of Incorporating Hydroxyapatite and Zinc Oxide Nanoparticles on the Compressive Strength of White Mineral Trioxide Aggregate. *J. Dent. (Shiraz)* 21 (4), 300–306. doi:10.30476/DENTJODS.2020.82963.1034
- Formosa, L. M., Mallia, B., and Camilleri, J. (2013). A Quantitative Method for Determining the Antiwashout Characteristics of Cement-Based Dental Materials Including Mineral Trioxide Aggregate. *Int. Endod. J.* 46 (2), 179–186. doi:10.1111/j.1365-2591.2012.02108.x
- Fridland, M., and Rosado, R. (2003). Mineral Trioxide Aggregate (MTA) Solubility and Porosity with Different Water-To-Powder Ratios. *J. Endod.* 29 (12), 814–817. doi:10.1097/00004770-200312000-00007
- Ghasemi, N., Salarinasab, S., Rahbarghazi, R., Sedghi, S., and Davoudi, P. (2021). Effect of Incorporation of Zeolite Containing Silver-Zinc Nanoparticles into Mineral Trioxide Aggregate on Odontogenic Activity of Human Dental Pulp Stem Cells. *J. Dent. (Shiraz)* 22 (3), 187–192. doi:10.30476/DENTJODS.2020.86183.1172
- Ha, W. N., Duckmanton, P., Kahler, B., and Walsh, L. J. (2016). A Survey of Various Endodontic Procedures Related to Mineral Trioxide Aggregate Usage by Members of the Australian Society of Endodontology. *Aust. Endod. J.* 42 (3), 132–138. doi:10.1111/aej.12170
- Hernandez-Delgadillo, R., Del Angel-Mosqueda, C., Solís-Soto, J. M., Munguia-Moreno, S., Pineda-Aguilar, N., Sánchez-Nájera, R. I., et al. (2017). Antimicrobial and Antibiofilm Activities of MTA Supplemented with Bismuth Lipophilic Nanoparticles. *Dent. Mater J.* 36, 503–510. doi:10.4012/dmj.2016-259
- Karabucak, B., Li, D., Lim, J., and Iqbal, M. (2005). Vital Pulp Therapy with Mineral Trioxide Aggregate. *Dent. Traumatol.* 21 (4), 240–243. doi:10.1111/j.1600-9657.2005.00306.x
- Kaur, M., Singh, H., Dhillon, J. S., Batra, M., and Saini, M. (2017). MTA versus Biodentine: Review of Literature with a Comparative Analysis. *J. Clin. Diagn Res.* 11 (8), ZG01. doi:10.7860/JCDR/2017/25840.10374
- Kharouf, N., Zghal, J., Addiego, F., Gabelout, M., Jmal, H., Haikel, Y., et al. (2021). Tannic Acid Speeds up the Setting of Mineral Trioxide Aggregate Cements and Improves its Surface and Bulk Properties. *J. Colloid Interface Sci.* 589, 318–326. doi:10.1016/j.jcis.2020.12.115
- Kim, H. J., Jang, J. H., and Kim, S. Y. (2021). Investigation of Characteristics as Endodontic Sealer of Novel Experimental Elastin-like Polypeptide-Based Mineral Trioxide Aggregate. *Sci. Rep.* 11 (1), 1–8. doi:10.1038/s41598-021-90033-9
- Kim, Y., Lee, C.-Y., Kim, E., and Jung, I.-Y. (2011). Failure of Orthograde MTA Filling: MTA Wash-Out? *J. Korean Acad. Conserv. Dent.* 36 (6), 510–514. doi:10.5395/jkacd.2011.36.6.510
- Kogan, P., He, J., Glickman, G. N., and Watanabe, I. (2006). The Effects of Various Additives on Setting Properties of MTA. *J. Endod.* 32 (6), 569–572. doi:10.1016/j.joen.2005.08.006
- Krastl, G., Allgayer, N., Lenherr, P., Filippi, A., Taneja, P., and Weiger, R. (2013). Tooth Discoloration Induced by Endodontic Materials: a Literature Review. *Dent. Traumatol.* 29 (1), 2–7. doi:10.1111/j.1600-9657.2012.01141.x
- Kucukyildiz, E. N., Dayi, B., Altin, S., and Yigit, O. (2021). *In Vitro* comparison of Physical, Chemical, and Mechanical Properties of Graphene Nanoplatelet Added Angelus Mineral Trioxide Aggregate to Pure Angelus Mineral Trioxide Aggregate and Calcium Hydroxide. *Microsc. Res. Tech.* 84 (5), 929–942. doi:10.1002/jemt.23654
- Lee, E. (2000). A New Mineral Trioxide Aggregate Root-End Filling Technique. *J. Endod.* 26, 764–765. doi:10.1097/00004770-200012000-00027
- Lim, M., Song, M., Hong, C. U., and Cho, Y. B. (2021). The Biocompatibility and Mineralization Potential of Mineral Trioxide Aggregate Containing Calcium Fluoride—An *In Vitro* Study. *J. Dent. Sci.* 16, 1080–1086. doi:10.1016/j.jds.2021.04.019
- Marciano, M. A., Camilleri, J., Lucateli, R. L., Costa, R. M., Matsumoto, M. A., and Duarte, M. A. H. (2019). Physical, Chemical, and Biological Properties of White MTA with Additions of ALF3. *Clin. Oral Invest* 23 (1), 33–41. doi:10.1007/s00784-018-2383-4
- Mathew, A. I., Lee, S. C., Rossi-Fedele, G., Bogen, G., Nagendrababu, V., and Ha, W. N. (2021). Comparative Evaluation of Mineral Trioxide Aggregate Obturation Using Four Different Techniques—A Laboratory Study. *Materials* 14 (11), 3126. doi:10.3390/ma14113126
- Mozyńska, J., Metlerski, M., Lipski, M., and Nowicka, A. (2017). Tooth Discoloration Induced by Different Calcium Silicate-Based Cements: A Systematic Review of *In Vitro* Studies. *J. Endod.* 43 (10), 593–1601. doi:10.1016/j.joen.2017.04.002
- Nagas, E., Cehreli, Z. C., Uyanik, O., Vallittu, P. K., and Lassila, L. V. J. (2016). Reinforcing Effect of Glass Fiber-Incorporated ProRoot MTA and Biodentine as Intraorifice Barriers. *J. Endod.* 42 (11), 1673–1676. doi:10.1016/j.joen.2016.08.002
- Naik, S., and Hegde, A. H. (2005). Mineral Trioxide Aggregate as a Pulpotomy Agent in Primary Molars: an *In Vivo* Study. *J. Indian Soc. Pedod. Prev. Dent.* 23 (1), 13–16. doi:10.4103/0970-4388.16020
- Parirokh, M., and Torabinejad, M. (2010). Mineral Trioxide Aggregate: A Comprehensive Literature Review-Part I: Chemical, Physical, and Antibacterial Properties. *J. Endod.* 36 (1), 16–27. doi:10.1016/j.joen.2009.09.006
- Parirokh, M., and Torabinejad, M. (2010). Mineral Trioxide Aggregate: A Comprehensive Literature Review-Part III: Clinical Applications, Drawbacks, and Mechanism of Action. *J. Endod.* 36 (3), 400–413. doi:10.1016/j.joen.2009.09.009
- Peng, T.-Y., Chen, M.-S., Chen, Y.-Y., Chen, Y.-J., Chen, C.-Y., Fang, A., et al. (2021). Impact of Zr-Doped Bi2O3 Radiopacifier by Spray Pyrolysis on Mineral Trioxide Aggregate. *Materials* 14 (2), 453. doi:10.3390/ma14020453
- Saghiri, M. A., Kazerani, H., Morgano, S. M., and Gutmann, J. L. (2020). Evaluation of Mechanical Activation and Chemical Synthesis for Particle Size Modification of White Mineral Trioxide Aggregate. *Eur. Endod. J.* 5 (2), 128–133. doi:10.14744/eej.2020.84803
- Salem-Milani, A., Ghasemi, S., Rahimi, S., Ardalan-Abdollahi, A., and Asghari-Jafarabadi, M. (2017). The Discoloration Effect of White Mineral Trioxide Aggregate (WMTA), Calcium Enriched Mixture (CEM), and Portland Cement (PC) on Human Teeth. *J. Clin. Exp. Dent.* 9 (12), e1397. doi:10.4317/jced.54075
- Shin, J.-H., Ryu, J. J., and Lee, S.-H. (2021). Antimicrobial Activity and Biocompatibility of the Mixture of Mineral Trioxide Aggregate and Nitric Oxide-Releasing Compound. *J. Dent. Sci.* 16 (1), 29–36. doi:10.1016/j.jds.2020.07.018
- Siboni, F., Taddei, P., Zamparini, F., Prati, C., and Gandolfi, M. G. (2017). Properties of BioRoot RCS, a Tricalcium Silicate Endodontic Sealer Modified with Povidone and Polycarboxylate. *Int. Endod. J.* 50, e120–e136. doi:10.1111/iej.12856
- Tabari, M., Seyed Majidi, M., Hamzeh, M., and Ghoreishi, S. (2020). Biocompatibility of Mineral Trioxide Aggregate Mixed with Different Accelerators: an Animal Study. *J. Dent. (Shiraz)* 21 (1), 48–55. doi:10.30476/DENTJODS.2019.77826.0
- Tawil, P. Z., Duggan, D. J., and Galicia, J. C. (2015). MTA: a Clinical Review. *Compend. continuing Educ. Dent. (Jamesburg, N. J.)* 36 (4), 247.
- Tien, N., Lee, J.-J., Jr, Lee, A. K.-X., Lin, Y.-H., Chen, J.-X., Kuo, T.-Y., et al. (2021). Additive Manufacturing of Caffeic Acid-Inspired Mineral Trioxide Aggregate/ Poly-ε-Caprolactone Scaffold for Regulating Vascular Induction and Osteogenic Regeneration of Dental Pulp Stem Cells. *Cells* 10 (11), 2911. doi:10.3390/cells10112911
- Toida, Y., Kawano, S., Islam, R., Jiale, F., Chowdhury, A. A., Hoshika, S., et al. (2021). Pulpal Response to Mineral Trioxide Aggregate Containing Phosphorylated Pullulan-Based Capping Material. *Dent. Mater. J.* 41, 126–133. doi:10.4012/dmj.2021-153

- Torabinejad, M., Hong, C., McDonald, F., and Pittford, T. (1995). Physical and Chemical Properties of a New Root-End Filling Material. *J. Endod.* 21 (7), 349–353. doi:10.1016/s0099-2399(06)80967-2
- Zafar, K., Jamal, S., and Ghafoor, R. (2020). Bio-active Cements-Mineral Trioxide Aggregate Based Calcium Silicate Materials: a Narrative Review. *J. Pak Med. Assoc.* 70 (3), 497–504. doi:10.5455/JPMA.16942
- Żuk-Grajewska, E., Saunders, W. P., and Chadwick, R. G. (2021). Fracture Resistance of Human Roots Filled with Mineral Trioxide Aggregate Mixed with Phosphate-Buffered Saline, with and without Calcium Hydroxide Pre-medication. *Int. Endod. J.* 54 (3), 439–453. doi:10.1111/iej.13426

Conflict of Interest: The authors declare that the research was conducted in the absence of any commercial or financial relationships that could be construed as a potential conflict of interest.

Publisher's Note: All claims expressed in this article are solely those of the authors and do not necessarily represent those of their affiliated organizations, or those of the publisher, the editors, and the reviewers. Any product that may be evaluated in this article, or claim that may be made by its manufacturer, is not guaranteed or endorsed by the publisher.

Copyright © 2022 Pushpalatha, Dhareshwar, Sowmya, Augustine, Vinothkumar, Renugalakshmi, Shaiban, Kakti, Bhandi, Dubey, Rai and Patil. This is an open-access article distributed under the terms of the Creative Commons Attribution License (CC BY). The use, distribution or reproduction in other forums is permitted, provided the original author(s) and the copyright owner(s) are credited and that the original publication in this journal is cited, in accordance with accepted academic practice. No use, distribution or reproduction is permitted which does not comply with these terms.

Frontiers in Bioengineering and Biotechnology

Accelerates the development of therapies,
devices, and technologies to improve our lives

A multidisciplinary journal that accelerates the
development of biological therapies, devices,
processes and technologies to improve our lives
by bridging the gap between discoveries and their
application.

Discover the latest Research Topics

[See more →](#)

Frontiers

Avenue du Tribunal-Fédéral 34
1005 Lausanne, Switzerland
frontiersin.org

Contact us

+41 (0)21 510 17 00
frontiersin.org/about/contact



Frontiers in
Bioengineering
and Biotechnology

